

**U.S. DEPARTMENT OF THE INTERIOR  
U.S. GEOLOGICAL SURVEY**

**Evaluation of Metallic Mineral Resources and their Geologic  
Controls in the East Mojave National Scenic Area,  
San Bernardino County, California**

*by*

**U.S. Geological Survey**

**1991**

**Open-File Report 91-427**

This report is preliminary and has not been reviewed for conformity with U.S. Geological Survey editorial standards or with the North American Stratigraphic Code. Any use of trade, product or firm names is for descriptive purposes only and does not imply endorsement by the U.S. Government.

## CONTENTS

---

	<u>Page</u>
Executive summary .....	1
Introduction .....	2
General geologic setting .....	5
Proterozoic rocks and their mineralization.....	7
Early Proterozoic.....	7
Middle and Late Proterozoic.....	10
Granite.....	10
Diabase .....	11
Evidence of Proterozoic mineralization.....	11
Latest Proterozoic and Paleozoic strata .....	13
Overview.....	13
Summary of rock sequences.....	14
Mesozoic rocks .....	15
Triassic plutons .....	15
Triassic sedimentary rocks.....	15
Triassic and(or) Jurassic volcanic and hypabyssal rocks .....	15
Jurassic and Cretaceous plutonic rocks: Introduction.....	17
Jurassic plutonic rocks.....	17
Late Jurassic dikes .....	18
Cretaceous plutonic rocks .....	19
Tertiary rocks .....	21
Introduction.....	21
Van Winkle Mountain and vicinity .....	23
Hackberry Mountain, Woods Mountains, and Wild Horse Mesa .....	23
Piute Range, Castle Mountains, and Castle Peaks .....	24
Cima volcanic field .....	25
Tertiary and Quaternary deposits .....	25
Development of pediment domes.....	27
Geophysics.....	30
Gravity survey .....	31
Magnetic survey.....	32
Discussion of gravity and magnetic anomalies.....	33

Ivanpah Valley and New York Mountains .....	33
Lanfair Valley and Piute Range.....	34
Mid Hills, Providence, and South Providence Mountains .....	35
Granite Mountains.....	36
Old Dad Mountain and Kelso Mountains.....	37
Clark Mountain Range.....	38
Woods Mountains Caldera.....	40
Aerial gamma-ray surveys .....	40
Landsat Thematic Mapper (TM) surveys.....	43
Geochemistry .....	47
RASS, PLUTO, and NURE data bases.....	47
Sample types.....	48
Evaluation of data .....	49
Data coverage .....	51
Geochemical evaluation.....	51
Soda Mountains.....	53
Little Cowhole Mountain.....	54
Cowhole Mountain .....	55
Cinder Cone area.....	55
Marl Mountains .....	58
Old Dad Mountain .....	59
Kelso Mountains.....	61
Bristol Mountains.....	61
Clark Mountain Range .....	62
Mescal Range.....	63
Ivanpah Mountains .....	64
Cima Dome .....	65
New York Mountains .....	66
Mid Hills.....	67
Providence Mountains.....	67
Granite Mountains .....	69
Van Winkle Mountain .....	70
Grotto Hills.....	70
Pinto Mountain.....	70
Table Mountain.....	71
Woods Mountains .....	71

Hackberry Mountain.....	71
Vontrigger Hills.....	73
Piute Range.....	74
Castle Mountains.....	75
Homer Mountain.....	75
U.S. Bureau of Mines data base .....	76
Assembly of data base .....	76
Frequency distributions of elements .....	78
Nonparametric correlations.....	80
Associations using factor analysis.....	81
Evaluation of metallic mineral resources in the EMNSA .....	84
Introduction.....	84
Definitions .....	89
Delineation of areas permissive and favorable for undiscovered metallic mineral resources.....	92
Proterozoic deposits .....	96
Carbonatite-related, rare-earth element--Shonkinitic, carbonatite, and associated rock types in the Mountain Pass Area .....	96
Carbonatite-related, rare-earth element in the EMNSA .....	103
Known occurrences .....	103
Permissive terranes .....	103
Favorable tracts .....	103
Other types of deposits .....	104
Volcanogenic massive sulfide deposits in Arizona and Nevada.....	104
Volcanogenic massive sulfide deposits in the EMNSA .....	104
Granite-related U, Th, and REE deposits in Alaska and elsewhere.....	105
Granite-related U, Th, and REE deposits in the EMNSA.....	106
Vein deposits and skarn deposits in the EMNSA .....	107
Platinum-group occurrences associated with ultramafic rocks in Nevada and Arizona.....	108
Platinum-group occurrences associated with ultramafic rocks in the EMNSA	109
Mesozoic deposits .....	109
Breccia pipe and related deposits .....	109
Gold breccia pipe .....	109
Silver-copper brecciated dolostone .....	113
Tungsten veins .....	114

Fluorite veins.....	115
Known occurrences .....	117
Permissive terrane and favorable tract.....	117
Porphyry molybdenum deposit, low fluorine.....	118
Classification of the deposits .....	118
Big Hunch molybdenum system.....	119
Known occurrences .....	123
Permissive terrane .....	123
Favorable tract.....	124
Porphyry copper and porphyry copper, skarn-related.....	124
Known occurrences .....	124
Permissive terranes and favorable tract.....	124
Skarn.....	125
Known occurrences .....	126
Permissive terranes and favorable tracts .....	128
Polymetallic replacement, distal disseminated Au-Ag, and vein magnesite .....	129
Known occurrences .....	129
Permissive terranes and favorable tracts .....	130
Polymetallic vein, polymetallic fault, and gold-silver, quartz-pyrite vein .....	130
Known occurrences .....	130
Permissive terranes and favorable tracts .....	132
Tertiary deposits .....	133
Volcanic-hosted epithermal gold deposits .....	133
Known occurrences .....	133
Permissive terranes .....	135
Favorable tracts .....	136
Speculative associations.....	136
Summary .....	139
References cited .....	142

## TABLES

[All tables at the end of text]

1.	Listing of the estimated average concentrations of potassium, uranium, and thorium for various geologic units in the East Mojave National Scenic Area. . . . .	171
2.	Summary of resultant colors of alteration minerals and vegetation on a color-ratio composite image prepared with TM channels 5/7 in red, TM channels 3/1 in green, and TM channels 3/4 in blue. . . . .	172
3.	Listing of areas in the East Mojave National Scenic Area, Calif., with references to interpretive geochemical reports and releases of raw geochemical data. . . . .	173
4.	Analyses of select rock samples from some mineralized areas in the East Mojave National Scenic Area, California. Analysis numbers same as table 5. . . . .	174
5.	Descriptions of select rock samples collected from some mineralized occurrences in the East Mojave National Scenic Area, California. . . . .	176
6.	Geochemical statistics for selected elements in samples of stream sediment, heavy-mineral concentrate, rock, and soil from the East Mojave National Scenic Area and surrounding area from 34°30' to 35°40' north latitude and 114°45' to 116°15' west longitude, Calif., and Nev. . . . .	179
7.	Summary of geochemical anomalies in the East Mojave National Scenic Area, Calif. . . . .	182
8.	Types and numbers of mineral occurrences identified as being present in the East Mojave National Scenic Area as of February, 1991. . . . .	184
9.	Summary statistics for 20 elements in 1,050 samples of rock analyzed from the East Mojave National Scenic Area. . . . .	185
10.	Array of Spearman correlation coefficients for 1,050 rock samples from the East Mojave National Scenic Area. . . . .	186
11.	Characteristics of permissive terranes and favorable tracts for Proterozoic carbonatite-related, rare-earth-element deposits; Mesozoic gold-bearing breccia pipes; Mesozoic stockwork molybdenum systems and other types of deposits in the East Mojave National Scenic Area, Calif. . . . .	187
12.	Analyses of rocks in the general area of the Big Hunch, New York Mountains, stockwork molybdenum system. . . . .	188
13.	Chemical analyses of 97 rocks reported by the U.S. Bureau of Mines (1990a) from 47 mineralized sites designated as gold-silver, quartz-pyrite veins. . . . .	190

## ILLUSTRATIONS

[Plates are in pocket]

- Plate 1. Preliminary geologic map of the East Mojave National Scenic Area, California.
2. Locations of identified mineral occurrences in the East Mojave National Scenic Area, California, classified as to type of occurrence.
3. Estimated extent of pediments and adjacent areas of thin alluvial cover, including generalized lithological content of piedmont deposits and inferred thickness of Cenozoic cover in the East Mojave National Scenic Area, California.
4. Isostatic residual gravity map of the East Mojave National Scenic Area, California.
5. Aeromagnetic map of the East Mojave National Scenic Area, California.
6. Localities of rock samples analyzed by the U.S. Bureau of Mines (1990a) and shown to contain in excess of 500 ppb gold in the East Mojave National Scenic Area, California.

## FIGURES

Figure	1. Location map of the study area of the East Mojave National Scenic Area, San Bernardino County, California.....	<b>191</b>
	2. Map of the East Mojave National Scenic Area showing locations of some of the major mountain ranges.....	<b>192</b>
	3. Schematic tectonic map of southeastern California and adjoining regions showing relations among major structural and paleogeographic elements.....	<b>193</b>
	4. Generalized geologic map of the East Mojave National Scenic area.....	<b>194</b>
	5. Geologic sketch map of the north-central part of the East Mojave National Scenic Area showing the distribution of the various phases of the Teutonia Batholith. ....	<b>195</b>
	6. Satellite image of the Providence Mountains and adjacent piedmonts, East Mojave National Scenic Area, California (Landsat 4 Thematic Mapper scene 40149-17441, 12 December 1984 (path 39, row 36)).....	<b>196</b>
	7. Generalized map of the Cima volcanic field showing the locations of major pediment domes. ....	<b>197</b>
	8. Index map showing the $1^{\circ} \times 2^{\circ}$ quadrangles in the general area of the East Mojave National Scenic Area from which the NURE aerial gamma-ray data were taken for this study. ....	<b>198</b>

9. Contoured plots of percent potassium , thorium as parts per million equivalent , and uranium as parts per million equivalent .....	199
10. Color-ratio composite produced by digital image processing of a quarter Landsat Thematic Mapper scene that includes a large part of the East Mojave National Scenic Area.....	202
11. Spectra of highly altered dacite-rhyolite samples collected at Hart Mine, Castle Mountains.....	203
12. Spectra of weathered sample of quartz monzonite and of altered samples, including gossan, all collected at Hidden Hill Mine site. ....	204
13. Spectra of monzogranite including altered sample collected at open shaft, in general area of Tungsten Flats.....	206
14. Spectrum of highly altered Rock Springs monzodiorite sample. Mafic minerals have been altered to nontronite, which dominates the spectrum .....	207
15. Spectra of dolomitic marble and of garnet-calc-silicate rock derived from the Moenkopi Formation collected near skarn deposit.....	208
16. Spectra of monzogranite samples , one altered, collected from road cut in New York Mountains.....	209
17. Spectra of altered quartz monzonite collected at the Big Horn Mine.....	210
18. Spectra of Tertiary rocks collected north of Hackberry Mountain. ....	211
19. Spectrum of dacite collected in Piute Hills, near old Mohave road. ....	212
20. Spectrum of Proterozoic quartz diorite weathered surface, collected near True Blue Mine. Sample does not appear to be altered.....	213
21. Spectrum of rhyolite ash flow tuff, which appears to be slightly altered; collected near Hole-in-the-Wall campground.....	214
22. Spectrum of granite unit collected at Granite Pass. ....	215
23. Map of the East Mojave National Scenic Area, Calif., showing geographic areas discussed in section on geochemistry of RASS, PLUTO, and NURE data bases.....	216
24. Sampling sites for RASS and PLUTO stream-sediment samples from the East Mojave National Scenic Area, Calif. ....	217
25. Sampling sites for RASS and PLUTO heavy-mineral-concentrate samples from the East Mojave National Scenic Area, Calif.....	218
26. Sampling sites for RASS and PLUTO rock samples from the East Mojave National Scenic Area, Calif.....	219
27. Sampling sites for NURE stream-sediment and soil samples from the East Mojave National Scenic Area, Calif.....	220

28. Distribution of anomalous and high concentrations of Cu, Pb, Zn, and Ag in RASS and PLUTO stream-sediment samples from the East Mojave National Scenic Area, Calif.....	221
29. Distribution of anomalous and high concentrations of Cu, Pb, Zn, and Ag in RASS and PLUTO heavy-mineral-concentrate samples from the East Mojave National Scenic Area, Calif.....	222
30. Distribution of anomalous and high concentrations of Cu, Pb, Zn, and Ag in RASS and PLUTO rock samples from the East Mojave National Scenic Area, Calif. ....	223
31. Distribution of anomalous concentrations of Au, As, Sb, and Bi in RASS and PLUTO heavy-mineral-concentrate samples from the East Mojave National Scenic Area, Calif.....	224
32. Distribution of anomalous concentrations of Au, As, Sb, and Bi in RASS and PLUTO rock samples from the East Mojave National Scenic Area, Calif. ....	225
33. Distribution of anomalous and high concentration of Ba, Mn, Co, and B in RASS and PLUTO stream-sediment samples from the East Mojave National Scenic Area, Calif. ....	226
34. Distribution of anomalous and high concentrations of Ba, Mn, Co, and B in RASS and PLUTO heavy-mineral-concentrate samples from the East Mojave National Scenic Area, Calif.....	227
35. Distribution of anomalous and high concentrations of Ba, Mn, Co, and B in RASS and PLUTO rock samples from the East Mojave National Scenic Area, Calif. ....	228
36. Distributon of anomalous and high concentrations of Sn, Mo, W, and Be in RASS and PLUTO stream-sediment samples from the East Mojave National Scenic Area, Calif. ....	229
37. Distribution of anomalous and high concentrations of Sn, Mo, W, and Be in RASS and PLUTO heavy-mineral-concentrate samples from the East Mojave National Scenic Area, Calif.....	230
38. Distribution of anomalous and high concentrations of Sn, Mo, W, and Be in RASS and PLUTO rock samples from the East Mojave National Scenic Area, Calif. ....	231
39. Distribution of anomalous and high concentrations of Th, Nb, and La in RASS and PLUTO heavy-mineral-concentrate samples from the East Mojave National Scenic Area, Calif. ....	232

40. Distribution of anomalous and high concentration of Th, Nb, and La in RASS and PLUTO rock samples from the East Mojave National Scenic Area, Calif.	233
41. Distribution of anomalous and high concentrations of U, Th, and La in NURE stream-sediment and soil samples from the East Mojave National Scenic Area, Calif.	234
42. Distribution of anomalous and high concentrations of Ce, Nd, Sm, and Eu in PLUTO heavy-mineral concentrate samples from the East Mojave National Scenic Area, Calif.	235
43. Distribution of anomalous and high concentration of Ce, Nd, Sm, and Eu in PLUTO rock samples from the East Mojave National Scenic Area, Calif. ...	236
44. Distribution of anomalous and high concentrations of Ce, Sm, and Eu in NURE stream-sediment and soil samples from the East Mojave National Scenic Area, Calif.	237
45. Distribution of anomalous and high concentrations of Tb, Dy, and Yb in PLUTO heavy-mineral-concentrate samples from the East Mojave National Scenic Area, Calif.	238
46. Distribution of anomalous and high concentrations of Tb, Dy, and Yb in PLUTO rock samples from the East Mojave National Scenic Area, Calif.....	239
47. Distribution of anomalous and high concentrations of Tb, Dy, Yb, and Lu in NURE stream-sediment and soil samples from the East Mojave National Scenic Area, Calif. ....	240
48. Plots showing frequency distribution for Au, Ag, As, Ba, Ce, Co, Cr, Cs, Fe, La, Mo, Ni, Sb, Sc, Sm, Ta, Th, U, W, and Zn in rocks from the East Mojave National Scenic Area analyzed by the U.S. Bureau of Mines (1990a).	241
49. Concentrations of gold, silver, arsenic, antimony, molybdenum, and zinc in mineralized rocks analyzed by the U.S. Bureau of Mines (1990a), grouped by deposit type in the East Mojave National Scenic Area.....	251
50. Scatter plots for gold versus silver, gold versus iron , lanthanum versus samarium, silver versus antimony, cobalt versus iron, and barium versus uranium, for 1,050 rocks from the East Mojave National Scenic Area analyzed by the U.S. Bureau of Mines (1990a). ....	255
51. Plot showing antimony compared with arsenic in 131 samples containing greater than 200 ppm antimony selected from the 1,050 rock-data base from the East Mojave National Scenic Area .....	261

52. Possible linkages among some types of mineral occurrences in the East Mojave National Scenic Area associated with felsic intrusive rocks.....	263
53. Graph showing number of mines in the East Mojave National Scenic Area plotted against the year of their last recorded production. ....	264
54. Mineral land classification diagram adopted by the State of California showing a diagrammatic relationship of mineral-resource-zone categories to the resource-reserve classification system.....	265
55. Sketch map showing major permissive terranes and favorable tracts for (1) Proterozoic carbonatite-related, REE occurrences; (2) Mesozoic gold-bearing breccia pipes; (3) Mesozoic tungsten veins; and (4) Mesozoic stockwork molybdenum systems in the East Mojave National Scenic Area. ....	266
56. Sketch map showing major permissive terranes and favorable tracts for (1) Mesozoic mineralized skarns of all types and iron skarns in particular; (2) Mesozoic porphyry copper and porphyry copper, skarn-related systems; (3) Mesozoic polymetallic replacement occurrences; and (4) Tertiary volcanic hosted, epithermal gold-silver occurrences in the East Mojave National Scenic Area. ....	267
57. Geologic sketch map of the area surrounding the gold-bearing, Cretaceous breccia pipes at the Colosseum Mine in the north-central part of the East Mojave National Scenic Area. ....	268
58. Metal zoning in the northeast part of the Clark Mountain Mining District, north-central East Mojave National Scenic Area.....	269
59. Scanning electron micrographs of a selected sample from the gold-bearing breccia pipe at the Colosseum Mine. ....	270
60. Schematic representation in cross-section of the displacement to the west of the silver-copper brecciated dolostone vein-type occurrences from their initial positions at the top of the gold-bearing breccia pipes at the Colosseum Mine. ....	275
61. Schematic diagrams showing relations of gouge within a fault zone.....	276
62. Cross section through the Coeur d'Alene Mine, Idaho, showing complex anastomosing pattern of traces of fault found in 200-ft intervals of underground mine workings. ....	277
63. Schematic cross-section showing the relationship of sediment-hosted gold deposits on the fringes of base- and precious-metal mining districts.....	278

## EXECUTIVE SUMMARY

Large areas of the East Mojave National Scenic Area (EMNSA) contain indications of metallic mineralization of various types that are younger than the rocks that host them. These metallic indications can be classified into approximately 20 specific types of metallic occurrences that are known to show extremely wide-ranging grades and tonnages. Among the types of metallic occurrences recognized are polymetallic vein; low-sulfide, gold-quartz vein; polymetallic replacement; gold breccia pipe; gold-silver, quartz-pyrite vein; polymetallic fault and skarn; copper, zinc-lead, tungsten, tin-tungsten, and iron skarn; porphyry molybdenum-copper; and epithermal quartz-adularia (alunite) gold. Most of the approximately 700 individual mineral occurrences known have been extensively prospected for more than a century, and at least 15 percent of them have been credited with some production, mostly of minor quantities of metal. Nonetheless, it is possible that economically significant concentrations of some metals remain to be discovered in the EMNSA, or that some known occurrences will become economic in the future. In recent years gold ore bodies at three relatively large deposits in the EMNSA (Castle Mountain, Colosseum, Morning Star) have been brought into production, and their current combined gold production and reserves are much greater than that of all the preceding discoveries of gold. This is partly a reflection of the present availability of heap-leaching extraction methods. Some of the mountain ranges that have widespread metallic occurrences and show geochemical anomalies in various sample media are the Providence Mountains, Clark Mountain Range, Ivanpah Mountains, and the New York Mountains. In addition, the general area of Hackberry Mountain lacks abundant metallic occurrences although it is included in a tract judged to be favorable for the discovery of epithermal, volcanic-hosted gold deposits. These five mountain ranges make up a broad, roughly north-south trending region in the central part of the EMNSA. Much less endowed with known occurrences of all of the various types of deposits considered above are the Granite Mountains, the central parts of the Piute Range, the Fenner Valley area, the general area of Cima Dome, Old Dad Mountain area and areas west to Soda Lake, and the Cima volcanic field. These areas lie in the western and eastern parts of the EMNSA.

We have made some judgments concerning the gravel-covered areas in the EMNSA, including the areal extent of pediment surfaces apparently covered only by thin veneers of gravel. But there are few data available to us for most of the covered areas. The presence of mineralized rocks, the type of mineral occurrence, and the extent and intensity of the mineralized rocks in the covered areas are essentially unknown. Most covered epigenetic mineral deposits do not respond to the standard geophysical methods evaluated in this study, particularly at the broad spacing of our data-collection points.

Restricting estimates concerning the presence of undiscovered metal resources in the EMNSA only to many of the currently known types of occurrences would yield small estimates for the volumes of many metals that might be exploited there at some future date, provided that tonnages of most previously discovered deposits in the EMNSA are indicative of the tonnages of deposits still to be discovered. Metals from any newly discovered base-metal deposit of the types presently known in the EMNSA probably would be insignificant from the standpoint of national needs. For example, copper from a newly discovered skarn deposit in the EMNSA would have roughly a 50 percent chance of being in excess of approximately 10,000 tonnes contained copper. In 1989, domestic production of copper amounted to 1,500,000 tonnes of copper.

Based on the geologic environments of large recently discovered deposits of gold in the EMNSA, however, some parts of the EMNSA appear to include mineralized environments capable of hosting significant undiscovered gold and silver resources. In addition, the widespread distribution in many parts of the EMNSA of geochemically anomalous samples and numerous mineral occurrences, many of which are associated with the emplacement of igneous rock (including copper skarn, lead-zinc skarn, tin-tungsten skarn, polymetallic vein, gold-silver quartz-pyrite vein, low-fluorine porphyry molybdenum, gold breccia pipe, volcanic-hosted gold), indicates metallogenic environments in those parts of the EMNSA that may be the sites of additional future discoveries of types of mineral deposits that are not now recognized.

## INTRODUCTION

The East Mojave National Scenic Area (EMNSA), designated on January 13, 1981 (46 Federal Register 3994) by the Secretary of Interior and modified on August 9, 1983 (48 Federal Register 36,210), encompasses approximately 1.5 million acres of federal, state, and private land in the Mojave Desert of southern California. The lands are in northeastern San Bernardino County, adjacent to the Nevada border, and about halfway between Las Vegas and Barstow (fig. 1).

The EMNSA is part of the California Desert Conservation Area that in total comprises about 25 million acres in southern California. Established by Congress in 1976 under Section 601 of the Federal Land Policy and Management Act, about half of the Conservation Area is public land administered by the Bureau of Land Management (BLM). BLM completed a comprehensive plan for multiple use of the entire area in 1980. Numerous sites considered by BLM to be Areas of Critical Environmental Concern are scattered throughout the conservation area and several are within the EMNSA.

In 1986 the California Desert Protection Act was first introduced in Congress by California's Senator Alan Cranston and Representative Mel Levine. Under this Act, recently reintroduced in the 102nd Congress as Senate Bill 21 on January 14, 1991, approximately 4.5 million acres of the

Conservation Area, including the EMNSA, would be transferred to the National Park Service and attain National Park status. The California Desert Protection Act of 1991, House Resolution 2929, sponsored by Representatives Mel Levine, Richard H. Lehman, and George Miller, was introduced in July, 1991. This Resolution designates 77 areas, totaling approximately 4.4 million acres, to be part of the National Wilderness Preservation System. Under this Resolution, the approximately 1.5 million acres of the EMNSA would be designated a National Monument and would include 700,000 acres of Wilderness. As proposed in House Resolution 2929, withdrawal of the lands as a National Monument would permit mining only on existing, valid mining claims and would preclude any further entry under the mining laws of the United States. On July 26, 1991, President George Bush recommended, under a proposed California Public Lands Wilderness Act, that approximately 2.24 million acres in 62 areas in California be added to the National Wilderness Protection System. This latter recommendation has been put forward in the House of Representatives as House Resolution 3066, sponsored by Jerry Lewis, William M. Thomas, Al McCandless, and Duncan L. Hunter. Most of the 62 areas are in the southern California desert, and six of them (CDCA--239,--250, --256,--262,--263, and--266) are in the EMNSA. In order that the available mineral-resource data base be as complete as possible before the bills are considered for action by Congress, this report presents an evaluation of known and unknown mineral resources of the EMNSA by the U.S. Geological Survey as a consequent progression of investigations by the U.S. Bureau of Land Management (1980; 1982) and recently completed studies by the U.S. Bureau of Mines (1990a; Schantz and others, 1990). As pointed out by Weldin (1991), a few parts of the California Desert Conservation Area, generally outside the EMNSA, are among the most highly mineralized regions in the nation.

The EMNSA includes the following units of the California Desert Conservation Area, all of which were initially considered BLM Wilderness Study Areas:

CDCA--227	Clark Mountain
CDCA--235A	Shadow Valley
CDCA--237	Magee-Atkins
CDCA--237A	Deer Spring
CDCA--237B	Valley View
CDCA--238A	Teutonia Peak
CDCA--238B	Cima Dome
CDCA--239	Cinder Cones
CDCA--243	Old Dad Mountain
CDCA--244	Rainbow Wells
CDCA--245	Eight-Mile Tank
CDCA--249	Kelso Mountains

CDCA--250 (part)	Kelso Dunes
CDCA--256 (part)	Bristol-Granite Mountains
CDCA--262	South Providence Mountains
CDCA--263	Providence Mountains
CDCA--264	Mid Hills
CDCA--265	New York Mountains
CDCA--266	Castle Peaks
CDCA--267	Fort Piute
CDCA--270	Table Mountain
CDCA--271	Woods Mountains
CDCA--272	Signal Hill

After preliminary examination of these lands with respect to the extent of their existing use and state of degradation, BLM recommended the following as "suitable" for designation as wilderness:

CDCA--237A
CDCA--239
CDCA--250 (part)
CDCA--256 (part)
CDCA--262
CDCA--263
CDCA--266
CDCA--267

The known mineral resources of these eight areas, as well as of all others so recommended within the California Desert Conservation Area, were examined by the U.S. Geological Survey and the U.S. Bureau of Mines. A Mineral Summary was prepared as Background Data for the California Desert Protection Act of 1987 (v. 1-2, U.S. Department of Interior, U.S. Bureau of Mines and U.S. Geological Survey, May, 1988). These studies were, necessarily, cursory and recommended additional investigations prior to any land-use decisions, particularly where substantial mineral resources were identified.

This report presents an evaluation of the potential for discovery of additional metallic mineral resources specifically within the EMNSA, based on geologic analysis that has included field work, primarily by other geologists during their assembly of a regional geologic map. Those geologic investigations also included study of the mineral resources of many individual areas within the EMNSA. Known mineral occurrences are classified by deposit type insofar as possible, and tracts of ground that are permissive geologically for additional discoveries of such deposits are outlined, with discussion of the characteristics of the types of mineral deposits and degree of favorability where we judge the information suitable for us to make such evaluations. The section below titled

"Evaluation of Metallic Mineral Resources In the EMNSA" includes definitions of many terms, such as mineral occurrence and mineral deposit, used throughout the report.

This report was assembled under the Southern California mineral-resource framework and assessment project, supervised by Richard M. Tosdal of the Menlo Park, Calif., Section of the Western Mineral Resources Branch, in response to a request from the National Mineral Resource Assessment Program (NAMRAP), currently chaired by Joseph A. Briskey, Jr., Reston, Va. Specific contributions to the report include the following: (1) machine-generated plots of mineral deposits and files of geochemical data by Kenneth R. Bishop; (2) description of Early Proterozoic geology and metallogeny by Clay M. Conway; (3) areas of pediment and thin alluvial cover and local provenance of alluvial materials by John C. Dohrenwend; (4) Latest Proterozoic, Paleozoic, and Mesozoic geology and the geology of carbonatite-related, rare-earth element (REE) deposits in the general area of Mountain Pass by Gordon B. Haxel; (5) discussion of gravity and magnetic surveys by John D. Hendricks; (6) introductory remarks and the geology of gold breccia pipes and their related veins by Carroll Ann Hodges; (7) inferred isopachs showing depths to basement rocks in the valley-fill areas by Robert C. Jachens; (8) machine-generated geologic map of the EMNSA by Robert J. Miller and David M. Miller; (9) geology of Tertiary rocks by Robert J. Miller; (10) implications of aerial gamma-surveys by Joseph S. Duval; (11) Landsat thematic mapper surveys by Marguerite J. Kingston, Shirley L. Simpson, and Marty Power; (12) discussion of geochemical surveys by Gary A. Nowlan; (13) descriptive geology of epithermal, volcanic-hosted gold deposits by James J. Rytuba; (14) various other aspects concerning the evaluation of metallic mineral resources by Richard M. Tosdal and Ted G. Theodore; (15) delineation of permissive terranes and favorable tracts by most of the above-named individuals; and (16) preparation of many of the illustrations by Diana L. Mangan. All of the contributors responded admirably and in a timely manner to the schedule requirement of this report. The U.S. Geological Survey wishes to express its appreciation to the personnel of the U.S. Bureau of Mines for providing copies of their field examinations in the EMNSA (U.S. Bureau of Mines, 1990a; Schantz and others, 1990) as soon as they were available. In particular, we wish to thank Linda R. Gray of the Western Field Operations Center, Spokane, Wash., of the U.S. Bureau of Mines for providing us with the machine-readable files and paper copies of the above reports.

## GENERAL GEOLOGIC SETTING

The EMNSA lies in the northeastern Mojave Desert (figs. 2, 3), a large physiographic province in southern California that is defined by its Neogene geologic history. The desert physiography consists of ranges that are separated by basins either filled by alluvial material or underlain at shallow depths by pediments. In the EMNSA some ranges attain elevations greater than 7,000 ft,

some 5,000 ft above the alluvial valley floors; extensive range-fringing pediments are present and some spectacular pediment domes are developed.

The diverse geologic history of the EMNSA spans at least 1,760 million years (m.y.). The oldest rocks are Early Proterozoic gneisses that underlie much of the northern part of the area. These rocks underwent regional metamorphism at high metamorphic grades at about 1,700 million years (Ma), and were subsequently intruded by granitic rocks from about 1,695 to 1,650 Ma, and intruded again at about 1,400 Ma by granitic rocks and at 1,100 Ma by diabase. Unique carbonatites and alkaline igneous rocks compose a part of the 1,400 Ma-intrusive episode. Latest Proterozoic, Paleozoic, and Early Mesozoic sedimentary strata were deposited unconformably across the Proterozoic gneissic and granitic rocks (fig. 3). These sedimentary rocks formed in marine and, less commonly, continental environments along the western edge of the North America craton and represent the transition from the cratonal sedimentary sequence on the southeast to a miogeoclinal sequence on the northwest.

Beginning in the mid-Mesozoic, widespread magmatism affected the region (fig. 3). Triassic volcanic rocks, locally present in several ranges in the western part of the EMNSA, represent the oldest products of this magmatism. Jurassic volcanism and plutonism produced rocks with slight alkalic affinities that lie along the eastern edge of the magmatic arc of that age. Subsequent plutonism in the Cretaceous is characterized by rocks of calc-alkaline affinities, typical of batholithic rocks within the cores of continental magmatic arcs. During the middle to late Mesozoic, the interior of the Cordillera underwent shortening along the fold and thrust belt. Thrust slices within this belt in the EMNSA involve the cratonal Proterozoic basement and locally some of the Mesozoic plutonic rocks.

A period of tectonic quiescence characterized the region in the early Cenozoic. In the Miocene, volcanism became widespread along the southern and eastern parts of the EMNSA and possibly elsewhere. Significant extensional deformation occurred in the Miocene in areas largely just outside of and in northern parts of the EMNSA, along the lower Colorado River to the east, and in the central Mojave Desert to the southwest (fig. 3). This deformation is characterized by the structural superposition of intensely-faulted, upper-crustal rocks on top of middle-crustal rocks along regionally subhorizontal detachment faults, several of which project underneath the rocks exposed in the EMNSA. The EMNSA, however, apparently escaped much of this intense extensional deformation. High-angle faults cut several of the ranges, and many of them possibly have undergone several ages of movements ranging back to Mesozoic time. Some faults are of local importance to the physiographic development of the ranges and basins, and in places, seem to have controlled the emplacement of various kinds of ore bodies.

In the late Miocene, extensive erosion produced broad pediment domes in the northwestern part of the area. Alkali basaltic volcanism followed pediment formation in the late Miocene and

Pliocene. Erosion during the Quaternary has continued to degrade the pediment domes and mountain ranges and to supply sediment to the valleys.

## PROTEROZOIC ROCKS AND THEIR MINERALIZATION

### Early Proterozoic

Early Proterozoic rocks in the EMNSA constitute a third or more of the area of bedrock exposure (pl. 1; fig. 4). These rocks received very little attention until the past few years. Prior to the recent studies, the most extensive regional mapping was by Hewett (1956), who mapped the northern three-fourths of the EMNSA at 1:125,000 and who included all the Proterozoic rocks either in a gneiss and granite unit or in a syenite and shonkinite unit. The latter unit, which includes small bodies at Mountain Pass, is described below. Hewett gave brief descriptions of the Proterozoic rocks at various localities. Other mapping studies of the area through the 1970s (northern Providence Mountains, Hazzard, 1954; Mountain Pass area of Clark Range, Olson and others, 1954; Clark Range, Clary, 1967; Clark Range and Ivanpah Mountains, Burchfiel and Davis, 1971; McCullough Range, Bingler and Bonham, 1972; Old Dad Mountain, Dunne, 1977) generally show only one or few map units for Early Proterozoic rocks and give similarly sketchy lithologic and petrographic descriptions. These early studies provided little information on Early Proterozoic structures, relative age relations of rock types, conditions of metamorphism, or petrologic characteristics. Reviews of the east Mojave Desert region (Miller, 1946; McCulloh, 1954; Burchfiel and Davis, 1981) emphasized the paucity of data on the Early Proterozoic rocks and the need for further research. Reconnaissance geochronologic studies (Wasserburg and others, 1959; Silver and others, 1961; Lanphere, 1964) established that the crystalline Proterozoic rocks in the Death Valley and eastern Mojave Desert regions were approximately 1.7 to 1.6 billion years old (Ga).

Geologic mapping and geochronologic, isotopic, and petrologic studies during the 1980s focused on the Early Proterozoic crystalline complex of the eastern Mojave Desert region and have led to major advances in understanding the Early Proterozoic crustal evolution of this region and the southwestern United States. Geologic mapping in the study area and nearby areas (New York Mountains, Miller and others, 1986; Providence Mountains, Goldfarb and others, 1988; Turtle Mountains, Howard and others, 1988; McCullough Range, Anderson and others, 1985) locally has resulted in the extensive subdivision of the Early Proterozoic rocks. Moreover, Wooden and Miller (1990) summarized the Proterozoic evolution of this part of the Mojave Desert.

The Early Proterozoic rocks of the EMNSA consist of high-grade tectonized supracrustal and plutonic rocks intruded by younger plutonic rocks deformed in a subsequent Early Proterozoic orogenic event. Recent petrologic studies (Elliot, 1986; Elliot and others, 1986; Thomas and others, 1988; Young and others, 1989; Young, 1989) have shown that supracrustal rocks of the New York Mountains and McCullough Range underwent granulite facies metamorphism at low pressure. Protoliths for the gneisses are variable, including a range of sedimentary, volcanic, and plutonic rock types (DeWitt and others, 1984, 1989; Miller and others, 1986; Wooden and Miller, 1990; Nielson and others, 1987; Hewett, 1956; Hazzard and Dosch, 1937; Anderson and others, 1985; Bender and Miller, 1987; Goldfarb and others, 1988). Interpreted sedimentary rock types are fine-grained aluminous and quartz-rich rocks such as shale and siltstone, immature sandstone, volcaniclastic sandstone, and less common quartzite. Volcanic protoliths are most commonly of felsic compositions, dacites and rhyodacite, though locally there appears to have been sparse to abundant mafic and ultramafic rocks within the rock sequences. Some of the interpreted volcanic rocks could have been intrusive, rather than extrusive in origin. This is apparently the case in the Providence Mountains and Mid Hills, where a bimodal suite of felsic and mafic gneisses could, based upon the available compositional data, represent volcanic rocks, intrusive rocks, or immature clastic sedimentary rocks such as graywacke, or some a combination of them all (Wooden and Miller, 1990). Metamorphosed plutons range from gabbroic to granitic compositions for the 1,760-1,730-Ma suite of metamorphosed plutons; the post 1,730-Ma suite is mostly granite. Those igneous rocks of intermediate composition are apparently most abundant (Wooden and Miller, 1990).

The EMNSA and nearby areas in southeastern California, southern Nevada, and northwestern Arizona are underlain by Early Proterozoic crust (Mojave crustal province of Wooden and Miller, 1990) that is isotopically and chronologically anomalous compared to Early Proterozoic crust throughout the rest of the western United States. Neodymium crust-formation model ages of 2.0 to 2.3 Ga in the Mojave crustal province suggested to Bennett and DePaolo (1984, 1987) that this terrane formed from the mantle at 2.0 to 2.3 Ga or that the terrane formed at approximately 1.9 to 1.65 Ga and incorporated a significant component of Archean crust. Because of the general lack of crystallization in the 2.3 to 2.0 Ga range, Bennett and DePaolo (1987) preferred the latter interpretation and furthermore suggested that this terrane was transported on a left-lateral fault at least 400 km from the north where it formed against and incorporated Archean crust. Lead isotope characteristics (Wooden and others, 1988; Wooden and Miller, 1990) require that the Mojave crustal province incorporated lead from an Archean reservoir; lead in ~1.7-Ga-rocks is more radiogenic than expected if it were derived directly from the mantle. The Nd model ages coupled with U-Pb zircon data suggest 1.7 to 2.2 Ga as the likely age for an event in which Archean clastic material, probably from the Wyoming Province, was subducted allowing addition of radiogenic

lead into the mantle from which the Mojave crustal province was derived (Wooden and Miller, 1990). Wooden and Miller suggest that the formation cycle of the crust started about 2.2 Ga.

New U-Pb zircon data which constrain these crust-formation models come mostly from the New York and Ivanpah Mountains (Wooden and Miller, 1990). The oldest ages reported from the Mojave crustal block are between 2.09 to 2.30 Ga, based on the  $^{207}\text{Pb}^*/^{206}\text{Pb}^*$  ages of zircons from altered siliceous volcanic(?) rock in the Turtle Mountains, approximately 50 km south-southeast of the EMNSA. Uranium-lead ages for these same zircons range from 1.77 to 2.15 Ga. Migmatitic banded gneiss in the New York and eastern Ivanpah Mountains (pl. 1) give  $^{207}\text{Pb}^*/^{206}\text{Pb}^*$  ages that range from 1.70 to 1.97 Ga. Discordant and complicated U-Pb data on these rocks suggest that zircon growth may have occurred more than 2.0 Ga ago and again at about 1,705 Ma during the Ivanpah orogeny, a regional metamorphic event as high as granulite facies. Wooden and Miller (1990) suggest that the protolith of the gneiss was likely a mixed supracrustal sequence of volcanic and associated immature sedimentary rocks. A minimum age for rocks of sedimentary protolith is 1.76 Ga, the age of a gabbro-diorite-granite plutonic suite that intrudes the layered gneiss in the Ivanpah Mountains; a source region must contain rocks at least 1.97 Ga. Volcanic rocks are constrained by the isotopic data to be at least 1.97 Ga and possibly as old as 2.3 to 2.4 Ga.

The layered gneiss and 1,760-Ma-plutonic suite in the New York and Ivanpah Mountains, and plutons (1,734 and 1,726 Ma) that intruded gneiss and schist in the Old Woman and Piute Mountains, both south of the EMNSA, were all deformed and metamorphosed during the Ivanpah orogeny between 1,710 and 1,700 Ma (Wooden and Miller, 1990). Metamorphism was at granulite grade in the McCullough, New York, Ivanpah, and Providence Mountains and at upper amphibolite grade in the Old Woman, Piute, and other mountain ranges south of the study area (Thomas and others, 1988; Wooden and Miller, 1990). Granitic augen gneiss and gneissic granite in the New York Mountains and McCullough Range and other ranges in the east Mojave area are from 1,708 to 1,713 Ma (Wooden and Miller, 1990; DeWitt and others, 1984). They are pre- to syntectonic and place an upper limit on the age of the Ivanpah orogeny. A post-tectonic suite of granitic to dioritic plutons in the eastern Mojave Desert region has U-Pb zircon ages from 1,660 to 1,690 Ma (Wooden and Miller, 1990). Some of these plutons contain deformational fabrics indicating a second orogenic event following the Ivanpah orogeny. The widespread "postorogenic" plutons are generally alkali-calcic. They have recently been studied geochemically and compared with granites of similar age in Arizona (Anderson and others, 1990; Miller and Wooden, 1988; Bender and others, 1988; Orrell and others, 1987).

## Middle and Late Proterozoic

### Granite

Several areas in the north-central part of the EMNSA are underlain by distinctive granitoid rocks approximately 1.4 Ga in age (pl. 1). The largest mass crops out at Mountain Pass, and four others are present south of I-15. Similar granites are widespread elsewhere in southern California, in central and southern Arizona, and in southern Nevada. Most of the following descriptions apply to the entire suite in the southwest (Anderson and Bender, 1989; Anderson, 1989). These rocks are commonly called "anorogenic," as their emplacement was generally not associated with regional or, commonly, even local deformation.

The Middle Proterozoic granites are generally coarse-grained and characterized by large, conspicuous phenocrysts of K-feldspar. Most of the granites are monzogranite or syenogranite, although some plutons include subordinate or minor granodiorite, quartz monzodiorite, and (or) quartz monzonite. Common accessory and minor minerals include biotite, hornblende or muscovite, fluorapatite, zircon, and magnetite.

Compositionally, the 1.4 Ga granitoid suite ranges from approximately 60 to 75 weight percent  $\text{SiO}_2$ , and is rather potassic. Compared with more typical calc-alkaline granitoids, the Middle Proterozoic granites have high  $\text{Fe}/\text{Mg}$  and low  $\text{Ca}$ ,  $\text{Mg}$ , and  $\text{Sr}$ . The magmas that crystallized to form the 1.4 Ga plutons were generally, with local exceptions, poor in exsolved fluids, as indicated by the paucity of aplites, pegmatites, and hydrothermal alteration; and characterized commonly by coarsely crystalline porphyritic fabrics (Anderson and Bender, 1989). The most mafic granitoids are locally charnockitic.

The 1.4 Ga granitoid suite ranges in alumina saturation from moderately peraluminous to weakly metaluminous. Most or all of the occurrences within the EMNSA are metaluminous. These peraluminous and metaluminous types of granite have somewhat different assemblages of accessory minerals. The metaluminous granites lack primary muscovite whereas the peraluminous granites lack hornblende. Both types carry biotite. Sphene is common only in metaluminous granites; monazite takes its place in the peraluminous granites, which lack fluorite, except in highly differentiated granites (for example, at Prescott, Ariz.).

Highly evolved members of the 1.4 Ga granitoid suite are enriched in  $\text{Rb}$ ,  $\text{Th}$ , and  $\text{U}$ ; and depleted in  $\text{Ba}$  and  $\text{Sr}$ . The granite in the Marble Mountains, south of the EMNSA has exceptionally high thorium: 163 ppm, mean of 5 samples (the average upper crustal abundance of thorium is 11 ppm) (Anderson and Bender, 1989, table 2b). Middle Proterozoic igneous rocks of the Mountain Pass area are described more fully in a section below.

## Diabase

Small diabase dikes thought to be of Late Proterozoic age are present locally in the eastern parts of the EMNSA (D.M. Miller, oral commun., 1990; C.M. Conway, unpub. data, 1990). All of these occurrences are too small to show at the scale of the geologic map (pl. 1). These diabases are part of a suite emplaced about 1,100 Ma throughout much of the southwestern United States (Howard, 1991; Hammond, 1991). Widespread large dikes are present in the southern Death Valley and Kingston Range region within 25 km north-northwest of the EMNSA (Wright, 1968; Wright and others, 1976). Small dikes are present in numerous ranges of the eastern Mojave Desert south of the EMNSA (Howard, 1991). The diabase dikes are ophitic and typically altered, mostly deuterically.

Dikes observed in the northern part of the New York Mountains dip steeply to the northeast and strike northwest where they are undeformed and may post-date mineralized veins in brecciated Early Proterozoic gneiss. No systematic study has been done on the diabase dikes in the EMNSA.

## Evidence of Proterozoic Mineralization

Hewitt (1956) noted that, although many mineral occurrences are hosted by Early Proterozoic gneiss in the eastern Mojave Desert region, the major periods of ore deposition were Mesozoic and late Tertiary. He furthermore concluded that there is no clear evidence for widespread Early Proterozoic mineralization in the area. There is, however, limited evidence for some minor mineralization of Proterozoic age, in addition to the rare-earth element deposits associated with the 1,400-Ma carbonatite at Mountain Pass. This deposit is discussed more fully in a subsequent section.

Minor rare-earth elements and thorium have been mined from pegmatite in the New York Mountains (Miller and others, 1986). Similar pegmatites are common within the Early Proterozoic gneiss terrane throughout the northern EMNSA and have been interpreted to be the source of most of the anomalous concentrations of these elements in stream sediment geochemical data (see below; Miller and others, 1986). Volborth (1962) suggested that these allanite-bearing pegmatites are related genetically to Mountain Pass-type syenite-carbonatite, but the field evidence of Miller and others (1986) indicates the pegmatites are older, presumably Early Proterozoic, and therefore unrelated to a Middle Proterozoic carbonatite system.

The polymetallic skarn (copper, lead, zinc, and iron) at the Butcher Knife Mine, located in the Mid Hills (SE 1/4 SE 5, T.13 N., R. 15 E. and map no. 414 of U.S Bureau of Mines (1990a) has been inferred to be of Proterozoic age (Ntiamoah-Agyakwa, 1987), because the intensity of overall skarn development at the mine apparently increases toward strongly foliated mafic dikes that are

inferred to be of Proterozoic age. The mafic dikes share the same fabric with the surrounding gneiss into which the dike intruded. Skarn mineralization is in places confined along a minor fault and subsidiary splays for a strike length of about 80 m. The best developed garnet-bearing skarn lies in the Proterozoic gneiss, which is in contact with a highly-brecciated limestone. The gneiss and the brecciated limestone form a roof pendant to the Cretaceous Mid Hills Adamellite of the Teutonia batholith of Beckerman and others (1982); only the gneiss is in contact with the granitic rocks. Ntiamoah-Agyakwa (1987) interpreted the 15-m wide foliated Proterozoic(?) mafic dike that lies along the contact between the gneiss and limestone to be the apparent source of the skarn-forming fluids. As is evident, the basis for assigning a Proterozoic age to the skarn is not conclusive as the mafic dike is not dated and Early Proterozoic limestones are not known throughout the region (C.M. Conway, unpub. mapping, 1990). It is possible however, that there are two ages of skarn mineralization here, one in the Proterozoic followed by tectonic juxtaposition of the Paleozoic(?) limestone against the gneiss, after which a second episode of skarn mineralization along the fault contact formed from fluids derived from the subjacent Cretaceous Mid Hills Adamelite.

There are some additional suggestions of apparently minor Proterozoic mineralization elsewhere in the Ivanpah Mountains. At Mineral Spring, in the SW 1/4 sec. 2, T. 15 N., R. 14 E., southeast of Mineral Hill, intensely fractured rocks of the Early Proterozoic undivided migmatite, granitoid gneiss, and granitoids map unit (Xg1, pl. 1) are cut by numerous quartz-galena-chalcopyrite veins. Most of the quartz is of a milky-white variety in hand sample, and generally shows variable amounts of staining by secondary copper minerals. The bulk of the mineralization seems to have been concentrated along a 1- to 2-m wide zone that contains abundant gossan along its trace of N. 10° E., with a 25° W. dip. These veins are foliated and concordant with the fabric of the surrounding gneisses. Some of the veins have highly deformed, schistose selvages of brown carbonate-rich material along their margins, together with, in places, some formerly clay-rich zones now recrystallized to white mica. Thus, the veins are definitely part of the metamorphic complex. However, the presence of some jasperoidal-appearing material along the structure, in marked contrast to the milky-white vein quartz, and the subsequent brecciation and neomineralization along the structure suggests that there have been multiple episodes of mineralization in the general area, presumably in the Mesozoic. We very tentatively assign the deformed quartz-galena-chalcopyrite veins to an Early Proterozoic mineralization event related to the widespread magmatic rocks of this age in the immediately surrounding area. Some of the Paleozoic carbonate rocks in the Ivanpah and Clark Mountain Range also show development of a ductile fabric, developed presumably from the regional Mesozoic thrusting in the region (Burchfiel and Davis, 1981). Thus, the veins in the general area of Mineral Spring could also be Mesozoic in age.

Intrusion of diabase dikes in the southern Death Valley and Kingston Ranges resulted in formation of talc deposits by contact metamorphism of a carbonate member of the Crystal Spring Formation of the Middle Proterozoic Pahrump Group (Wright, 1968). The region between the southern Panamint Range and the Kingston range contains 29 deposits that produced 1,200,000 tons of talc ore. Talc and clay mines are present within a few km of the northern boundary of the EMNSA in the Halloran Hills. Whether these mines are associated with diabase is unknown. Asbestos, iron, and uranium deposits in the Middle Proterozoic Apache Group in central Arizona were formed by processes related to the emplacement of very large diabase sills (Wrucke and others, 1986).

Mineral deposits in both the Death Valley and central Arizona regions were controlled by the nature of the intruded sedimentary rocks. Host rocks suitable to the formation of such ore deposits, notably the Pahrump Group, are virtually absent in the EMNSA. This and the near absence of diabase sills suggests there is little if any potential for mineral deposits associated with diabase in the study area.

## LATEST PROTEROZOIC AND PALEOZOIC STRATA

### Overview

Latest Proterozoic and Paleozoic strata in the EMNSA were deposited upon a substrate consisting of Early Proterozoic gneissic and granitoid rocks (Wooden and Miller, 1990) and Middle Proterozoic granite (Anderson and Bender, 1989) as described above. These strata are exposed in small areas of several ranges in the EMNSA: Clark Mountain Range, the Providence Mountains, Old Dad Mountain, New York Mountains, Ivanpah Mountains, Cowhole Mountains, and Cima Dome (pl. 1). A few even smaller bodies of metasedimentary rocks, most commonly marble or calcsilicate hornfels, of probable Paleozoic age are scattered throughout the EMNSA (for example, Miller and others, 1985; DeWitt and others, 1984; Howard and others, 1987). These small bodies typically are roof pendants in Jurassic or Cretaceous plutons or slivers within fault zones (fig. 4).

Two northeast-trending boundaries or transitions between the Late Proterozoic to Paleozoic miogeocline on the west and the North American craton on the east pass through the central part of the Mojave Desert (fig. 3); the inferred boundary between the North American craton and the Late Proterozoic clastic rocks passes through the EMNSA and that for the Paleozoic carbonate rocks passes to the west of the EMNSA (Stewart and Poole, 1975; Burchfiel and Davis, 1981). Thus, the latest Proterozoic to Paleozoic strata in the EMNSA are basically cratonal and relatively thin.

Latest Proterozoic strata in the Clark Mountain Range, Providence Mountains and at Old Dad Mountain are transitional to the miogeocline but they are overlain by cratonal early Paleozoic strata. The autochthonous latest Proterozoic rocks in the Clark Mountain Range and Ivanpah Mountains are miogeoclinal (Burchfiel and Davis, 1981). The paleogeographic position of the late Paleozoic rocks is obscure owing to generally incomplete preservation or exposure (Burchfiel and Davis, 1981).

### Summary of Rock Sequences

The most complete and best preserved sequences of the latest Proterozoic to Paleozoic rocks are in the Providence Mountains (Hazzard, 1954). These rocks are only locally metamorphosed, notably where they are intruded by Mesozoic plutons. The section rests unconformably on Early Proterozoic gneiss, and is approximately 2,700 m thick (Hazzard, 1954). The lower part of the section consists of latest Proterozoic to Late Cambrian quartzite, dolomite, limestone, siltstone, and shale. The upper part comprises Devonian to Permian units that contain limestone and subordinate chert, sandstone, and shale. Ordovician and Silurian strata are absent, as they are in all cratonal sections in the southwestern United States. Latest Proterozoic to Paleozoic stratigraphic units in the Providence Mountains have been correlated both with units in the Death Valley region to the north and units in the western Grand Canyon region to the east (Stewart, 1970; Stone and others, 1983; Goldfarb and others, 1988).

In the Old Dad Mountain area, Paleozoic rocks and conformably underlying latest Proterozoic strata are strongly structurally disrupted but not highly metamorphosed. The section is generally similar to that in the Providence Mountains (Dunne, 1977).

Paleozoic rocks in the central New York Mountains are preserved as roof pendants in a batholith of Cretaceous granitic rocks. Most of the strata have been converted to marbles, calcsilicate hornfels, or pelitic hornfels. They also have been affected by multiple episodes of Mesozoic folding and thrust faulting. Despite the metamorphism and deformation these rocks have undergone, a stratigraphic section generally similar to that in the Providence Mountains can be recognized or reconstructed (Burchfiel and Davis, 1977). The chief difference is that latest Proterozoic strata are absent; the lowest Cambrian unit rests unconformably on Early Proterozoic gneiss.

Latest Proterozoic and Paleozoic strata in the central part of the Ivanpah Mountains are included in the generalized regional descriptions given by Hewett (1956), and subsequent detailed information shows that they are similar to and continuous with rocks in the Clark Mountain Range and Mescal Range (Burchfiel and Davis, 1971).

In the area of the Clark Mountain Range, cratonal and miogeoclinal sequences are tectonically juxtaposed (Burchfiel and Davis, 1971). The autochthonous and parautochthonous Paleozoic strata are cratonal, whereas the overlying thrust sheets carry latest Proterozoic and Paleozoic rocks of transitional to miogeoclinal facies. Low grade metamorphism is locally developed.

## **MESOZOIC ROCKS**

### **Triassic Plutons**

Triassic plutonic rocks are widely scattered in regions surrounding the EMNSA (Barth and others, 1991; Miller, 1978). In the Clark Mountain area, several small dioritic stocks intrude Paleozoic strata, and one of these bodies has yielded K-Ar hornblende ages of 190 and 200 Ma (Burchfiel and Davis, 1971; Mueller and others, 1979). These are presumably minimum ages; the stocks may be Triassic. No Triassic U-Pb ages have been reported for plutons in the EMNSA, but as more U-Pb ages are determined, Triassic plutons may be discovered. A dioritic orthogneiss unit in the Granite Mountains (Howard and others, 1987), previously thought to be Triassic is now known to be Jurassic (D.M. Miller, oral commun., 1991).

### **Triassic Sedimentary Rocks**

In all of the above-mentioned ranges of the EMNSA that contain latest Proterozoic and Paleozoic sequences, these strata are conformably overlain by reddish sandstone, limestone, and shaly limestone, or their metamorphosed equivalents. These rocks are correlated with the Early to Middle Triassic Moenkopi Formation (Walker, 1987). In the Providence Mountains, this unit is approximately 300 m thick and contains Early Triassic fossils.

In the Mescal Range, a unit of sandstone, shale, and limestone stratigraphically above the Moenkopi Formation and below a Jurassic sandstone unit is correlated with the Late Triassic Chinle Formation by Hewett (1956). This correlation is questioned by Marzolf (1983). Possible Chinle-correlative rocks have not been reported elsewhere in the EMNSA.

### **Triassic and (or) Jurassic Volcanic and Hypabyssal Rocks**

Several ranges within the EMNSA contain volcanic and volcaniclastic rocks, intercalated sedimentary rocks, and related hypabyssal rocks of Triassic and (or) Jurassic age. Stratigraphic sequences, in varying degrees of preservation, are exposed in four areas: the Mescal Range, the Old Dad Mountain–Cow Hole Mountains–Soda Mountains area, the New York Mountains, and the Providence Mountains. In a few other areas, metamorphosed or hydrothermally altered Triassic

and(or) Jurassic volcanic, hypabyssal, and sedimentary rocks are present as small pendants in Jurassic or Cretaceous plutons, or as slivers in fault zones. Among these small relicts, Jurassic rocks are probably more common than Triassic rocks. Owing to common metamorphism or alteration, and to lack of study, little is known about the petrology and geochemistry of Triassic and Jurassic volcanic rocks in the EMNSA.

In the Mescal Range, a unit of crossbedded arenitic sandstone (see below) approximately 250 m thick is overlain by a unit, approximately 200 m thick, of dacitic flow breccias and lava flows (Hewett, 1956). These volcanic rocks have not been studied in detail. They are probably Jurassic, based upon correlation with similar rocks in the Cow Hole Mountains. The sandstone unit contains dinosaur tracks, the only dinosaur tracks known in California (Reynolds, 1983).

A diverse volcanic and sedimentary sequence of rocks, more than 3 km thick, in Old Dad Mountain and the Cow Hole Mountains consists of interbedded intermediate to silicic lava flows and flow breccias, quartz arenite, sandstone and siltstone, sedimentary breccia and megabreccia, silicic ignimbrite, and other minor rock types (Busby-Spera, 1988; Busby-Spera and others, 1989; Marzolf, 1983; 1988; 1991). U-Pb zircon ages of some of the volcanic rocks indicate that this sequence is approximately 170 Ma, which is Middle Jurassic according to current geologic time scales (Harland and others, 1989). A generally similar sequence of rocks is present in the Soda Mountains, near the west edge of the EMNSA (Grose, 1959).

The quartz arenite units in the Mescal Range, Old Dad Mountain, and Cowhole Mountains are in part eolian. Until recently, these quartz arenites were generally correlated with the Early Jurassic (Peterson and Pipiringos, 1979) eolian Aztec Sandstone of the southern Great Basin and Navajo Sandstone of the Colorado Plateau. However, the U-Pb ages cited above indicate that the Jurassic quartz arenites in the EMNSA probably correlate with the Carmel Formation or the Entrada Sandstone of the Colorado Plateau.

In the Providence Mountains, intermediate to silicic volcanic, volcaniclastic, and hypabyssal rocks, in part intensely altered, have been mapped by Miller and others (1985) and Goldfarb and others (1988). The hypabyssal rocks typically have granitic textures. These igneous rocks in part overlie the Moenkopi Formation, and are probably Triassic and(or) Jurassic in age (Walker, 1987). In some places, the volcanic rocks contain intercalated conglomerate and siltstone.

In the New York Mountains, a sequence of metamorphosed volcanic rocks approximately 250 m thick overlies the Moenkopi Formation, and is in turn overlain by a metasedimentary unit approximately 70 m thick (Burchfiel and Davis, 1977). The volcanic rocks are silicic in composition, include breccia or conglomerate, and contain subordinate intercalated metasiltstone and, near the base of the unit, metaconglomerate. The metasedimentary unit comprises siltstone, conglomerate, and tuffaceous sandstone and siltstone. The conglomerate beds contain clasts derived from the underlying volcanic unit. These two units could be either Triassic or Jurassic in

age; the latter is perhaps more likely. The metavolcanic rocks are generally schistose or mylonitic. Metasedimentary lithologies range from argillite to schist. Both the volcanic and sedimentary units in the New York Mountains contain metamorphic biotite.

### **Jurassic and Cretaceous Plutonic Rocks: Introduction**

Plutons known to be of Jurassic age or of Cretaceous age, based upon U-Pb geochronology, are common in the EMNSA (pl. 1; fig. 4). Other plutons are definitely or almost certainly Mesozoic, but it is uncertain whether they are Jurassic or Cretaceous. The Jurassic and Cretaceous plutons and ranges in which they crop out within the EMNSA are too numerous to list or describe individually. Rather, the descriptions below focus upon typical or relatively well-studied plutons, and upon features of special interest.

Both the Jurassic and the Cretaceous plutons within the EMNSA are small parts of magmatic belts that extend through much of the southern Cordillera and are oblique to one another (Miller and Barton, 1990; Fox and Miller, 1990; Tosdal and others, 1990).

Known Jurassic plutons and Cretaceous plutons in the EMNSA region are generally different in petrology and geochemistry. Miller and others (1982) and Fox and Miller (1990) have summarized the characteristics of Jurassic and Cretaceous plutonic rocks in the Bristol Lake region, which includes the Granite Mountains, southern Providence Mountains, and Colton Hills in the southwestern corner of the EMNSA. The Cretaceous granitoids are characterized by relatively low color index, white to buff or flesh-colored feldspars, and absence of clots of mafic minerals. In contrast, the Jurassic granitoids commonly are more heterogeneous, contain less quartz, more commonly are conspicuously sphene-bearing, and are more potassic, have higher color index, contain lavender, grey, or pinkish alkali feldspar, and contain clots of mafic minerals. In some places, Jurassic plutons are associated with magnetite skarn deposits or zones of extensive albitization. For some Mesozoic plutons for which U-Pb ages have not been determined, a reasonable inference as to a Jurassic or a Cretaceous age of emplacement can thus be made from the overall composition of the plutons. Such estimates are probably most applicable to granodiorite and granite compositions, and have a lower probability of being correct for dioritic or gabbroic rocks. In this report, we follow the IUGS classification scheme (Streckeisen and others, 1973) adopted for plutonic igneous rocks.

#### **Jurassic Plutonic Rocks**

The most thoroughly studied Jurassic plutonic rocks in the region of the EMNSA are those in the area of the southern Bristol Mountains, southern Providence Mountains, and Colton Hills (Fox and Miller, 1990). Widespread emplacement of Jurassic plutons followed by approximately 50 m.y. the emplacement of scattered Triassic plutons in the Mojave Desert region (Tosdal and others,

1990; Anderson and others, 1991). Three types of Jurassic plutonic rocks are common: mafic rocks, intermediate to silicic mixed or heterogeneous rocks, and leucocratic monzogranite (pl. 1). The mafic rocks are generally the oldest and the leucocratic rocks the youngest.

Compositionally, the mafic rocks include fine- to coarse-grained gabbro, diorite, monzodiorite, and quartz monzodiorite; common mafic minerals include clinopyroxene, hornblende, and biotite. Generally, the mafic rocks have  $\text{SiO}_2$  contents of 49 to 60 percent; are subalkaline and metaluminous; and have relatively high abundances of large-ion lithophile elements (LILE), for example commonly as much as  $\approx 3$  percent  $\text{K}_2\text{O}$  and  $\approx 1,000$  ppm Ba.

The mixed intrusive rocks are by far the most abundant. They are markedly heterogeneous, ranging from fine-grained equigranular to coarsely porphyritic, and continuously from quartz monzodiorite to syenogranite and syenite. A number of phases or facies or subgroups occur, typically with gradational contacts. Chemically, the mixed intrusive rocks have a wide range of  $\text{SiO}_2$  contents: 52 to 74 percent; are subalkaline to, less commonly, alkaline; and metaluminous to weakly peraluminous. Some rocks are potassic, with  $\text{K}_2\text{O}/\text{Na}_2\text{O} \approx 2$ . Ba abundances are as great as 2,000 to 4,000 ppm in some of the mafic and intermediate rocks.

The monzogranite is the most homogeneous of the three rock types. It comprises fine- to medium-grained leucocratic biotite monzogranite, locally with minor muscovite. It is subalkaline and generally moderately peraluminous. Trace-element abundances are unremarkable.

Many of the Jurassic plutonic rocks in the EMNSA are strongly altered. In the southernmost Providence Mountains and the southern Bristol Mountains, the rocks have undergone widespread albitization, characterized by replacement of potassium feldspar by albite (Fox, 1989; Fox and Miller, 1990). Intense albitization is present as linear white zones in otherwise normally mesocratic rocks. Less intense albitization produces mottled patches or spots. Chemically, albitization is characterized by doubling of  $\text{Na}_2\text{O}$  content and nearly complete loss of  $\text{K}_2\text{O}$  (typically from 6 percent to  $<1$  percent). Accompanying changes in Fe, Mg, and Ca depend upon the extent of chloritization of mafic phases. Aluminum, Ti, Zr, Y, and REE are generally immobile on a hand-specimen scale during alteration.

The few U-Pb ages that have been determined for Jurassic plutons in or near the EMNSA are typically  $\approx 165$  to 160 Ma (see summaries by Fox and Miller, 1990; Tosdal and others, 1989).

#### **Late Jurassic Dikes**

In the southern Providence Mountains and Colton Hills, swarms of Late Jurassic intermediate to silicic dikes intrude Jurassic plutons and are themselves intruded by Cretaceous plutons (Fox and Miller, 1990). The dikes range from dacite porphyry to aphanitic rhyodacite to aplite. Similar dikes are known in a few other places within the EMNSA. Similar and possibly related swarms of Late Jurassic mafic or intermediate to silicic dikes are widespread in eastern California and

southwestern Arizona (Chen and Moore, 1979; Hopson, 1988; Powell, 1981; Karish and others, 1987; Haxel and others, 1988; Tosdal and others, 1990). Some of the apparently Jurassic dikes that crop out in the Providence Mountains have been correlated by James (1989) with the approximately 150 Ma Independence dike swarm of eastern California. James (1989) suggests that the more than 500 km long dike swarm may be related to continental-scale arc-normal extension, changes in plate motions, or a combination of oblique subduction with left-lateral shear.

### Cretaceous Plutonic Rocks

The most thoroughly studied Cretaceous plutonic rocks of the EMNSA are those of the Teutonia batholith (Beckerman and others, 1982). Beckerman and others (1982) state that the Teutonia batholith is Jurassic and Cretaceous, based chiefly upon K-Ar cooling ages that provide minimum emplacement ages. They divided the batholith into seven plutons or units, with a large area of granitic rocks in Halloran Hills area (DeWitt and others, 1984) undivided and undescribed (fig. 5). One pluton is Jurassic, the Ivanpah Granite (pl. 1). The other six plutons, which constitute most of the batholith, are Cretaceous. Miller and others (1986) report a preliminary U-Pb zircon age of 93 Ma (determined by E. DeWitt) for the Mid Hills Adamellite, which makes up much of the New York Mountains and Mid Hills. Fox and Miller (1990), who had access to additional unpublished U-Pb ages, included the Teutonia batholith among Cretaceous units. "Teutonia batholith" thus should be redefined to exclude the coincidentally spatially associated Jurassic Ivanpah Granite; this revised usage is followed in the summary below.

The six major plutons that constitute the Teutonia batholith crop out chiefly in the New York Mountains and Mid Hills, and the Cima Dome-Wildcat Butte-Marl Mountains area (pl. 1). Five of the six plutons are fairly large, with exposed areas  $\approx$ 50 to 200 km<sup>2</sup>. The sixth pluton forms a subcircular outcrop area only  $\approx$ 2 km in diameter.

The five relatively large plutons of the Teutonia batholith range in composition from quartz diorite and monzodiorite through granodiorite through monzogranite to syenogranite. Quartz-poor modal compositions (quartz monzodiorite, quartz monzonite, quartz syenite) are present only in the Rock Spring Monzodiorite. Other rocks are medium- to coarse-grained; some plutons or facies within plutons are equigranular, whereas others have alkali feldspar phenocrysts. Biotite is ubiquitous; hornblende is common to absent; one pluton locally contains a little primary muscovite. Three of the five plutons are leucocratic, with color indices less than 5.

The sixth, small pluton (Black Canyon Hornblende Gabbro, unit Kbc, pl. 1) comprises compositionally and texturally variable hornblende-rich mesocratic to melanocratic gabbro. Magnetite content is high: average 6.5 volume percent. This pluton intrudes two of the larger, granitic plutons.

Chemically, the six plutons of the Teutonia batholith form a broadly calc-alkaline series. The hornblende gabbro contains 43 to 49 percent SiO<sub>2</sub>; the other five plutons range to 68 to 77 percent SiO<sub>2</sub>. The granitoid plutons generally straddle the boundary between metaluminous and peraluminous compositions. Moderately or strongly peraluminous granites are absent. Abundances of Ba, Sr, and Rb (the only trace elements analyzed) are generally normal and unremarkable for granitic rocks.

Geobarometric data indicate that the Rock Spring Monzodiorite phase of the Teutonia batholith of Beckerman and others (1982) was emplaced at pressures of <1 to 3 kb (Anderson and others, 1988; 1991), corresponding to upper-crustal depths of approximately <3 to 10 km. Present exposures provide a tilted view of the batholith: the shallowest plutons, emplaced at pressures of approximately 0.5 kb, are on the north and the deepest plutons, emplaced at approximately 3 kb, are to the south (J.L. Anderson, oral commun., 1990). The Teutonia batholith is among the shallowest of the Mesozoic plutonic complexes in the Mojave Desert region studied by Anderson and others (1988; 1991): pressure estimates for ten other complexes range from 2 to 3 kb to 7 to 9 kb. These pressure data conflict with geologic evidence that the roof of the batholith is exposed in the south, which should therefore be the shallowest part of the batholith (Goldfarb and others, 1988).

For the EMNSA region as a whole, Cretaceous plutons generally have U-Pb zircon ages in the ranges 99 to 95 Ma and 75 to 70 Ma (Wright and others, 1987; Fox and Miller, 1990, citing J.L. Wooden and E. DeWitt, oral commun., 1987). The approximately 70-Ma Late Cretaceous plutons crop out in the Granite Mountains, at Homer Mountain, and in the Fenner Hills. In the Granite Mountains, a suite of Cretaceous igneous rocks includes a granodiorite pluton, a zoned pluton, and granite, aplite and pegmatite dikes (Howard and others, 1987). The granodiorite pluton makes up most of the western Granite Mountains (pl. 1), and a larger zoned pluton makes up the southeastern part. Magmatic biotite from the zoned pluton yielded presumed emplacement K-Ar ages of 70.9 to 74.5 Ma (Howard and others, 1987). These Cretaceous plutons in the EMNSA apparently were emplaced more or less at the same time as the culmination of compressional deformational events along the Cordilleran thrust belt (Miller and Barton, 1990).

Some Mesozoic deformational features of regional extent crop out in the western and north-central parts of the EMNSA. These deformational features are reflections of compressional tectonism shown by brittle-style thrust plates developed in the foreland of the Cordilleran thrust belt and ductile-style thrust nappes in southeastern California and Arizona (Howard and others, 1980; Burchfiel and Davis, 1981; Snee and Miller, 1988; Miller and Barton, 1990).

Middle Triassic through Early Jurassic generally east-directed thrust faults are present in the Cowhole Mountains and the Clark Mountain Range (Burchfiel and Davis, 1981). In the Cowhole Mountains, metamorphosed Paleozoic rocks apparently have been thrust eastwards and are

overlapped unconformably by the Upper Triassic(?) to Lower Jurassic Aztec Sandstone. In the Clark Mountain Range, some east-vergent structures have been cut by plutons dated at 190 and 200 Ma (Burchfiel and Davis, 1981). There is also some evidence for latest Jurassic to Early Cretaceous crustal shortening in the Ivanpah Mountains where a deformed pluton is present in the hinge region of a large, east-verging fold that apparently has been associated with some thrusting during its development (Burchfiel and Davis, 1971, 1981).

## TERTIARY ROCKS

### Introduction

Following the cessation of crustal shortening and plutonism during the Late Cretaceous--early Tertiary, a quiescent period ensued which lasted until about early Miocene time. Very little tectonic or magmatic activity has been documented for the Mojave region during this time. The early to middle Miocene, however, was a period of intense volcanism and extensional faulting throughout much of the Mojave and Sonoran Desert region. Volcanism in the EMNSA during the Tertiary partly reflects continental-scale regression of calc-alkaline intermediate magmatism from the southeast to the northwest along a narrow arc (Eaton, 1984). As pointed out by Eaton (1984), this arc is envisioned as being a back-arc region in a predominantly continental crustal environment. Much of the eastern part of the area of the EMNSA represents a tectonic block that retained relative structural stability during a time when movement on low-angle normal or detachment faults resulted in significantly rotated and disrupted supracrustal sequences in many of the mountain ranges to the north, southwest, and east of the EMNSA (Hileman and others, 1990; McCurry and Hensel, 1988; Spencer, 1985; Reynolds and Nance, 1988; Burchfiel and Davis, 1988, Wilshire, 1988). Miocene extensional deformation has been described by Burchfiel and Davis (1988) in the Clark Mountain Range and in the Mesquite Mountains in the northern part of the EMNSA and in the Kingston Range to the northwest. Sedimentary and tectonic deposits also accumulated in a Miocene extensional basin that underlies part of the Shadow Valley area (Reynolds and Nance, 1988; Wilshire, 1988). Multiple detachment faults exposed on Homer Mountain (Spencer, 1985), immediately east of the EMNSA, roughly coincide with the western edge of the north-trending Colorado River extensional corridor that has been well-documented in many other reports. The region immediately to the south of the EMNSA, including the Old Woman, Piute, Little Piute, and Ship Mountains, underwent moderate extension during the Miocene (Hileman and others, 1990) and the central Mojave, from Barstow to near Baker, may have been extended highly in the early Miocene (Glazner and others, 1989). Glazner and O'Neil (1989) have determined a smooth,

eastward increase in initial whole-rock  $^{87}\text{Sr}/^{86}\text{Sr}$  ratios for silicic volcanic rocks in the Mojave Desert region of southern California. Initial whole-rock  $^{87}\text{Sr}/^{86}\text{Sr}$  ratios for these types of rocks in the Castle Mountains are reported by them to be in the 0.70526 to 0.70990 range. Glazner and O'Neil (1989) interpret the smoothness and lack of discontinuities in the eastward increase in initial whole-rock  $^{87}\text{Sr}/^{86}\text{Sr}$  ratios to reflect the absence of any broad zones of pre-Tertiary rifting or major faulting. The increase in these ratios must be due to an eastward increasing amount of crustal material incorporated into the magmas.

Broad areas in the northern parts of the EMNSA also were subjected to some moderate amounts of extension from the late Miocene to the Recent in association with the development of pediment domes (see below).

Economically the most significant Tertiary mineralization known to date (1991) in the EMNSA is associated spatially with volcanic rocks (see below). Nonetheless, there is evidence that some gold-bearing veins that thus far have yielded only small amounts of ore and are far removed from areas of extensive Tertiary volcanic rock may also be Tertiary in age and may be associated with Tertiary magmatism. Lange (1988) found that prominent geomorphic and structural features showing a N.  $20^{\circ}$  to  $40^{\circ}$  E. trend in the general area of the Telegraph Mine, in the north-central part of the EMNSA (U.S. Bureau of Mines, 1990a, map no. 121, pl. 1), acted as open conduits or as breccia-filled high permeability zones during mineralization dated isotopically at  $10.3 \pm 0.4$  Ma. There is no documented volcanism close to 10.3 Ma in the area of the Telegraph Mine; some andesite in the vicinity has been dated at 12.8 Ma, and the oldest alkaline basalts in the area are 7.5 Ma (H.G. Wilshire, written commun., 1991). Thus, there is the possibility that the 10.3-Ma date has been reset. Nonetheless, as Lange (1988) concluded, mineralization at the Telegraph Mine may be related to regional right-lateral, north-south shear stresses that, in turn, resulted in the opening of low-angle, en-echelon tension gashes. These mineralized tension gashes at the Telegraph Mine probably are related to post-20 Ma combined wrenching across the San Andreas, Death Valley, and Soda Avawatz fault zones. Although we assigned the mineralization at the Telegraph Mine to a gold-silver, quartz-pyrite type of occurrence, the mineralization there seems definitely to be of an epithermal variety, showing relatively high gold/silver ratios for the ores (Lange, 1988). Total production from the Telegraph Mine has been 2,178 tons of ore that included 2,178 oz gold; 5,423 oz silver; and 500 lb of copper with 1948 as the last year of recorded production (U.S. Bureau of Mines, 1990a). Hewett (1956) shows production from the Telegraph Mine to include a total of 2,548 oz gold. Drilling in 1968 sponsored by the Office of Mineral Exploration of the U.S. Geological Survey resulted in the blocking out of 72,750 tons at a grade of 0.5 oz Au/ton and 1.16 oz Ag/ton at the Telegraph Mine (U.S. Bureau of Mines, 1990a).

## **Van Winkle Mountain and Vicinity**

The oldest Tertiary volcanic and sedimentary rocks in region of the EMNSA are exposed in the Van Winkle Mountain, northernmost Clipper Mountains and Old Dad Mountains (pl. 1). In the Van Winkle Mountain, the sequence consists of tuff breccia, rhyodacite lava flows, air-fall and ash-flow tuff that conformably are capped by olivine basalt flows. These are correlative with sequences of rock exposed to the west in the Bristol Mountains (Miller and others, 1985). A distinctive sanidine-bearing rhyolite tuff present near the top of this sequence has been correlated with the Peach Springs Tuff of Young and Brennan (1974) by Glazner and others (1986). This regionally extensive ash-flow tuff sheet has been used as a chronostratigraphic marker in many of the mountain ranges in the eastern Mojave desert of California and in western Arizona. Ages for the tuff reported in the literature vary from 16 to 22 Ma. However, Nielson and others (1990) have established an age of  $18.5 \pm 0.2$  Ma for the emplacement of the unit. The older reported ages have been attributed by them to contamination by pre-Tertiary rock and the younger ages to alteration or incomplete argon extraction during the process of dating. The Peach Springs Tuff is exposed in discontinuous patches in the Old Dad Mountains, Piute Range, Castle Mountains, Mid Hills, Clipper Mountains, and on the east side of the Providence Mountains (pl. 1). In most of these ranges, however, the Peach Springs Tuff is present at or near the bottom of the Cenozoic stratigraphic sequence.

## **Hackberry Mountain, Woods Mountains, and Wild Horse Mesa**

The Hackberry and Woods Mountains are underlain by volcanic and sedimentary rocks, predominantly of middle Miocene age (pl. 1). These rocks rest unconformably on an erosional surface of pre-Tertiary crystalline basement that locally includes paleotopographic relief in excess of 300 m (Bonura, 1984). Rhyolite flows and domes, breccias, and tuffs on the eastern side of Hackberry Mountain and in the Vontrigger Hills have not been dated isotopically. A lacustrine unit of limestone, dolomite and minor sandstone overlies the silicic volcanic rocks, and contains vertebrate fossils of Barstovian to Calendonian age (McCurry, 1985). The relation of the lacustrine unit to the quartz latite-to-rhyolite flows, domes and pyroclastic rocks that comprise the main mass of Hackberry Mountain is unclear. Hackberry Mountain is capped by an ash-flow tuff which is also exposed in many of the nearly flat-lying mesas in the western Woods Mountains and eastern Providence Mountains. The tuff was originally termed the Hole-in-the-Wall Tuff but later changed to the Tuff of Wildhorse Mesa by McCurry (1988). It represents approximately  $80 \text{ km}^3$  of metaluminous to weakly peralkaline magma erupted at 15.8 Ma (McCurry, 1988). The eruption of this tuff apparently produced a shallow trap-door caldera roughly 10 km in diameter centered in

the eastern Woods Mountains (see section titled "Geophysics" below). Resurgent doming and eruption of rhyolitic flows and tuff largely filled the caldera. One of these flows has been dated isotopically at 14.8 Ma. The final eruptions in the area of Woods Mountains were basalt, basaltic andesite, and basanite flows, one of which has a whole rock K-Ar age of 10.3 Ma. Minor lacustrine and alluvial sediments are intercalated in the upper part of the volcanic sequences exposed there. Large magnitude aeromagnetic and gravity anomalies coincide with the caldera (see below). McCurry and Hensel (1988) suggested that the anomaly is probably due to an underlying pluton on the basis of geophysical modeling.

### **Piute Range, Castle Mountains, and Castle Peaks**

The sequences of Cenozoic rocks exposed in the Piute Range and in the Castle Peaks area are similar and have been correlated by Nielson and others (1987). The rocks of the Castle Mountains, although contemporaneous with rocks in the adjoining ranges, are dominated by a voluminous silicic volcanic center which thins rapidly east and west and apparently is not present in the Piute Range. Nielson and others (1987) have divided the rocks of the Piute Range into two map units. The lower unit consists of arkose and conglomerate present near the base of the exposed sequence. These sedimentary rocks contain clasts derived from underlying basement in the Piute Range and possibly also from basement rocks exposed in the New York Mountains. Basaltic andesite flows and breccias and some remnants of Peach Springs Tuff are intercalated with the sedimentary rocks at the north end of the range. The upper unit consists of mafic lava flows and breccias, rhyolitic lava flows and tuffs, and interbedded alluvial sediments. A white tuff in the middle of the upper unit may be correlative with a similar tuff described by Miller and others (1986) in the general area of Castle Peaks.

The lower part of the exposed sequences of Tertiary rock in the Castle Mountains is predominantly andesite with probable Peach Springs Tuff at the base, thereby allowing correlation of these rocks with those in much of the Piute Range. Capps and Moore (1991), however, consider the basal tuff to be older than the Peach Springs Tuff on the basis of the results of potassium-argon ages of approximately 22 Ma obtained from the unit in the Castle Mountains. The lower unit in the Castle Mountains, moreover, has been folded into a broad, northeast-trending anticline (Turner and others, 1983; Turner, 1985). As much as 350 m of rhyolite flows, tuffs and associated domes overlie the folded unit. The tuffs and rhyolites of this silicic center host most of the known mineralization in the Hart Mining District (see below). The aggregate thickness of these silicic rocks apparently decreases rapidly to the south and they are not considered by Nielson and others (1987) to underlie the volcanic rocks of the Piute Range as Turner (1985) has suggested. Geochronologic data reported by Ausburn (1988, 1991), Capps and Moore (1991), Linder (1988),

Nielson and others (1987), and Turner (1985) are somewhat inconsistent, but generally define a period of rhyolite, latite, and basalt volcanism from about 17 Ma to about 12-13 Ma. The mineralization probably accompanied rhyolite dome formation at about 15.5 Ma (Capps and Moore, 1991). An age of about 8 Ma (Nielson and others, 1987) on basalt from the Piute Range is the youngest age reported from the eastern part of the EMNSA.

### **Cima Volcanic Field**

The volcanic rocks of the Cima volcanic field consist of more than 50 basalt cinder cones and numerous associated lava flows that overlie as much as 300 m of variably tilted Tertiary sedimentary rocks. The sedimentary rocks were deposited nonconformably on, and derived from, Cretaceous and older crystalline rocks (Wilshire and others, 1987). Eruptions of basalt in the area west of Cima dome began as volcanism was waning elsewhere in the EMNSA (pl. 1). The majority of the flows associated with the Cima basalt field erupted between 7.6 Ma and the present, with an eruptive hiatus between 3 and 1 Ma (Wilshire, 1988). The age of the youngest flow has been estimated to be between 400 and about 120,000 yrs. (H.G. Wilshire, written commun., 1991). All of the basalts in the field are alkalic, hypersthene- or nepheline-normative hawaiites or basanites (Wilshire, 1987). Study of Nd, Sr, and Pb isotopic compositions of <1 Ma hawaiites from the Cima volcanic field suggest that they were derived from a mantle source (Farmer and others, 1991). Many of the flows contain mantle-derived xenoliths of spinel peridotite or pyroxenite. Lower crustal xenoliths are also present and are represented by both silica-saturated to silica-oversaturated and undersaturated lithologies. Wilshire and others (1991) have discussed the possible origins of various types of xenolith found in the Cima volcanic field.

### **TERTIARY AND QUATERNARY DEPOSITS**

Deposits of Tertiary and(or) Quaternary age in the EMNSA include landslide and sedimentary breccia deposits, gravel, playa and pluvial lake deposits, basalt cinder deposits, basalt lava flows, and basalt cones (pl. 1). Quaternary deposits include eolian sand, alluvial fan deposits, playa and pluvial lake deposits, basalt cinder deposits, basalt lava flows and vent basalt. The provenance and the apparent source regions for many of the alluvial fan deposits are indicated on plate 3.

General composition of piedmont deposits in the EMNSA are delineated on plate 3. This map was prepared from analysis of geometrically rectified Landsat Thematic Mapper image data processed by R.G. Blom and R.E. Crippen of the Jet Propulsion Laboratory, Pasadena, Calif. Mid-winter, low sun angle scenes were used to maximize topographic expression, resulting from increased topographic modulation of irradiance. The following data were used: Landsat 5, Path 39, Row 36 (Needles, Calif.) Quads 1 and 2 (acquired 12/12/84) and Landsat 5, Path 39, Row 35

(Las Vegas, Nev.) Quad 3 (acquired 1/10/85). Individual spectral bands were adjusted for path (atmospheric) radiance and sensor calibration. These data were then ratioed (3/1 to emphasize ferric iron variations, 5/4 to emphasize ferrous iron variations, and 5/7 to emphasize hydroxyl/carbonate variations), and the resulting band-ratioed images were scaled for approximately one percent saturation at range extremes. The achromatic component of the TM data was computed by averaging bands 3, 4, 5 and 7, edge enhanced with a high pass 5x5 box filter, and then merged by component multiplication with each of the three band-ratioed images. Ratioed bands were combined as false color composites where 5/7 is displayed as red, 5/4 is displayed as green, and 3/1 is displayed as blue. The resulting false color composite images maximize compositional discrimination while at the same time retaining topographic and structural information within the merged achromatic component.

Compositional boundaries in piedmont areas were delineated on the basis of abrupt changes in color and texture (pl. 3). Drainage divides within the ranges were mapped from 1:100,000-scale, 50 m contour maps. Compositional information was inferred from mapped bedrock lithologies exposed in these source areas (pl. 1). The most extensively exposed bedrock lithologies within a given upland source area were inferred to comprise the predominant lithologic component of surface deposits on the associated piedmont surface; these dominant lithologies are shown in boldface type. The false color composite image of the Providence Mountains (fig. 6) provides some notable contrasts in the lithologic components in the flanking, associated piedmont surface. This particular figure exemplifies well the spatial distribution of uniform color responses within the band-ratioed images used to delineate the compositional boundaries (compare fig. 6 and pl. 3).

Areas of pediments and thin (<100 m thick) Late Tertiary and Quaternary alluvial cover in the EMNSA are an integral component of plate 3. Range front-piedmont contacts were delineated on the basis of abrupt transitions between areas of little shadow and smooth texture (piedmonts) and areas of abundant shadow and coarse texture (uplands). These interpretations were supplemented by stereoscopic photogeologic observations made from high-altitude U-2 Color IR photography.

Areas of pediments and thin alluvial deposits, as much as 50-100 m thick, were estimated from interpretation of the distribution of planar areas of exposed bedrock, including in some areas deformed Tertiary sediments, and small prominent residual knobs (as inferred from the analysis of enhanced Thematic Mapper imagery, aerial photography, and available geologic mapping). These features are particularly abundant in the following areas (from north to south): intermontane valleys and piedmonts adjacent to the Halloran Hills, piedmont areas within and surrounding the Cima Volcanic Field and Cima Dome, the northern margin of Ivanpah Valley, intermontane valleys and piedmonts along the eastern flank of the Mid Hills, the piedmonts adjacent to the eastern and southern flanks of the Piute Range, the piedmonts surrounding the Woods Mountains, Hackberry Mountain, the Vontrigger Hills, and Homer Mountain, and the southern piedmont of the Granite

Mountains. Extensive areas of thick basin filling deposits are apparently limited to parts of Ivanpah Valley, Fenner Valley and the valley occupied by Kelso Wash (the area of the Devils Playground).

## DEVELOPMENT OF PEDIMENT DOMES

The largest and best developed pediment domes in the eastern Mojave Desert are in the EMNSA and form the crest of the Ivanpah Upland of Hewitt (1956), a broad irregular highland that forms the south and west flanks of Shadow Valley (fig. 7). This section of the report is presented here in a form modified somewhat from Dohrenwend (1988). More than 60 late Cenozoic lava flows of the Cima volcanic field cover large areas on the crests and flanks of these domes and record a 5-m.y. history of pediment-dome evolution in this area. Comparison of the relative positions of lava-flow-covered pediment remnants and modern pediment surfaces indicates that, since at least latest Miocene time, (1) downwasting has been the dominant mode of pediment modification, (2) downwasting rates have been highest in crestal areas, have progressively decreased downslope, and have been significantly influenced by general base-level differences, and (3) the general form of the pediment domes has changed little during the last 5 m.y. Moreover, the ages of the youngest rock units truncated by these pediments and the oldest lava flows which overlie them indicate that these pediment domes formed rapidly during a 3.5 m.y. interval of the late Miocene and have been a conspicuous landscape element in the general area of Shadow Valley since that time.

Eleven pediment domes have been more or less continuously evolving in the Ivanpah Upland over the past several million years, and the remnants of at least three other domes have been partly buried and preserved by lava flows of the Cima field (fig. 7). Although termed "domes", these landforms are more conical than domelike in overall form (Sharp, 1957) with slopes that typically vary by less than  $\pm 0.5$  degrees along any radial profile. The domes are low (0.1-0.4 km high), broad (5-16 km across), and therefore, gently sloping (1.5°-4.5°). Although in places interrupted by inselbergs, surfaces are generally smooth and regular; local relief is commonly less than 5 m. Locally, networks of shallow drainageways have incised these pediment surfaces into irregular patchworks of dissected and undissected areas. Undissected areas are mostly flat with anastomosing drainageways and indistinct interfluvia; dissected areas are scored by shallow, subparallel valleys separated by low rounded interfluvia.

These pediments have been the subject of several lengthy and detailed geomorphic analyses (Davis, 1933; Sharp, 1957; Warmke, 1969; Oberlander, 1974; and Dohrenwend and others, 1987). Davis (1933) speculated that Cima Dome, the largest of these domes (fig. 7), was formed primarily by the backwasting of bounding scarps on an upfaulted terrain of low relief. Sharp (1957)

explained Cima Dome and adjacent domes as the product of upwarping of an ancient erosion surface with subsequent erosional modification and regrading. Warnke (1969) argued that downcutting followed by lateral corrosion and backwasting were the most important processes of pedimentation and concluded that the combined presence of suitable rock types, granitic rocks and their sedimentary derivatives, and a temporary local base-level is the principal determinant of pediment formation in this area. Oberlander (1974) interpreted the present pediment domes as relict forms produced by erosional stripping of deeply weathered terrains developed during periods of greater effective moisture. Dohrenwend and others (1987) documented a latest Tertiary and Quaternary history of essentially continuous pediment downwasting when downwasting rates have been greatest in crestal areas and have progressively decreased downslope to mid-flank areas which have remained in a state of approximate topographic equilibrium.

As all of these workers have observed, the distribution of pediments in the Ivanpah Upland is largely controlled by lithology. Most pediment surfaces cut indiscriminantly across Mesozoic granitic rocks of the Teutonia batholith (pl. 1; see above) and Tertiary terrigenous clastic rocks, whereas inselbergs of Proterozoic metamorphic rocks stand as much as 250 m above these surfaces. At least three separate Cretaceous plutons probably are present within the area of the Cima volcanic field, and these rocks are intruded swarms of Tertiary dikes (Wilshire, 1988). The plutonic rocks are typically deeply weathered; low-energy seismic measurements (K.D. Mahrer, written commun., 1988) indicate pervasive subsurface weathering to depths in excess of 40 m. Tertiary sediments vary in composition from clastic materials derived mainly from Teutonia granitic sources to those derived mainly from Proterozoic metamorphic sources, including gneisses, carbonate, granitic and volcanic rocks. The rocks were deposited in several steep-sided basins and consist of gravel, fine grained sandstone, siltstone, claystone, generally near the base, coarse avalanche breccias, extremely coarse (boulders to 10 m) debris flow deposits, and, in places, gravity slide blocks as much as 0.5 km across of various breccias, including abundant clasts of dolomite. These rocks are locally significantly deformed, with dips as steep as 70° NE, SE, and SSE. Relief on their contact with the Cretaceous granitic rocks locally exceeds 150 m (Sharp, 1957; Wilshire and others, 1987). Lithologic, biostratigraphic and paleomagnetic correlations suggest a 18.5 to 9 Ma age for these rocks (Reynolds and Nance, 1988).

Potassium-argon ages indicate three principal periods of late Cenozoic volcanic activity in the Cima volcanic field (Dohrenwend and others, 1984; Turrin and others, 1984, 1985). The earliest period, dated between  $7.5 \pm 0.2$  and  $6.5 \pm 0.2$  Ma, is represented by one small, deeply eroded vent and flow complex in the southeast corner of the field. Lavas of the latest period, which spans the last 1.1 m.y. of Quaternary time, were confined to the southern part of the field and have flowed generally west and southwest toward Soda Lake Valley. An intermediate period, dated between

$5.1 \pm 0.2$  and  $3.3 \pm 0.1$  Ma, was the longest and most volumetric. Flows of this period form the northern part of the field and are the most significant lavas in the present discussion.

Flows of the intermediate period form mesa caprocks that preserve remnants of the pediment surfaces which flanked the west side of Shadow Valley in latest Miocene and early Pliocene time. North of Highway I-15, flows were erupted between  $5.1 \pm 0.2$  and  $4.2 \pm 0.2$  Ma from several vents. At least five flows moved down shallow valleys southwest toward Soda Lake Valley and northeast toward Shadow Valley. South of Highway I-15, more voluminous flows were erupted between  $4.8 \pm 0.2$  and  $3.3 \pm 0.1$  Ma from at least 16 vents. These flows, including several overlapping and superimposed lava sheets, were erupted near the crest of a large pediment dome. The lava sheets spread east and northeast across the dome's east flank toward Shadow Valley and south to southeast toward what is now the Quaternary part of the Cima field. In addition, several less extensive lavas flowed west and southwest toward Soda Lake Valley down valleys between several small pediment domes along the western edge of the field (pl. 1).

Comparison of differences in height between the late Tertiary pediment surfaces buried by these lava flows and adjacent modern pediment surfaces enables the reconstruction of a 5-m.y. history of pediment evolution in the Ivanpah Upland. Topographic relations demonstrate that the Cima lava flows have been erupted into a continually downwasting, erosional environment that has been active since before inception of the volcanism. Progressively younger flows have buried progressively lower surfaces so that each caprock-protected pediment remnant now stands at a height above the modern surfaces that is directly related to the age of its overlying basalt flow (Dohrenwend and others, 1987).

Average downwasting rates determined from the height differences between lava-flow-covered and modern surfaces are clearly related to distance from dome crests and to general base level elevations. On pediments sloping toward Soda Lake Valley, where basin floor elevation is about 280 m, average downwasting rates have ranged between 1.2 and  $2.8 \text{ cm}/10^3 \text{ yr}$  on upper flanks and between 0.0 and  $0.4 \text{ cm}/10^3 \text{ yr}$  in mid-flank areas. Lower flanks have probably aggraded to some extent (Dohrenwend and others, 1987). On pediments sloping towards Shadow Valley, where axial elevation is 1,100 to 1,200 m, average downwasting rates have ranged between 0.5 and  $0.9 \text{ cm}/10^3 \text{ yr}$  on upper flanks and between 0.0 and  $0.3 \text{ cm}/10^3 \text{ yr}$  in mid-flank areas. Thus pediment downwasting has been greatest in crestal and upper-flank areas and has progressively decreased downslope so that overall pediment degradation, in areas unprotected by resistant caprocks, has followed a general pattern of crestal lowering, upper-slope decline, and mid-slope stability. Also, as might be expected, average downwasting rates have been substantially greater on those pediments which drain westward to the relatively low basin floor of Soda Lake Valley than on those which drain eastward towards the much higher axis of Shadow Valley. However, even the most rapid of these rates indicate relatively little landscape change, no more than 50 m of

downwasting in crestal and upper slope areas and little to no change in mid-slope areas over the past 5 m.y.

Relations between pediment surfaces of the Ivanpah Upland, rock units truncated by these surfaces, and lava flows which overlie them indicate that these pediment domes formed rapidly during the late Miocene and have been a conspicuous landscape element in the Shadow Valley area since that time. Extensive pediment surfaces, capped by latest Miocene and early Pliocene lava flows, cut smoothly and uninterrupted across deeply weathered Cretaceous granitic rocks and both tilted and faulted late Miocene terrigenous clastic rocks. The oldest basalt flows that cap an extensive pediment surface have been dated by K-Ar analysis at  $5.1 \pm 0.2$  Ma (Turrin and others, 1985), and the age of the truncated terrigenous clastic rocks has been estimated on the basis of biostratigraphic and paleomagnetic correlations at approximately 11 Ma (Reynolds and Nance, 1988). Therefore, pediment formation occurred between 11 and 5 Ma. Moreover, limited occurrences of lava flows as old as  $7.5 \pm 0.2$  Ma that lie at or very close to the levels of both modern and remnant latest Miocene pediment surfaces suggest that these surfaces may have been in existence prior to 7.5 Ma. Thus, the pediment domes of the Ivanpah Upland probably formed within less than 3.5 m.y. (11-7.5 Ma) during the late Miocene.

For those few instances in the Basin and Range province where field relations have permitted estimates of average long-term rates of range-front retreat and pediment formation, estimates range up to a maximum of  $1 \text{ km}/10^6 \text{ yr}$  (Wallace, 1978; Menges and McFadden, 1981; Saunders and Young, 1983; Dohrenwend, 1987). However, formation of the large pediment domes of the Ivanpah Upland in the EMNSA by slope retreat would appear to require rates of at least 1.5 to perhaps as much as  $3.5 \text{ km}/10^6 \text{ yr}$ . Thus it would appear that either general slope-retreat proceeded at a significantly faster rate in this area than elsewhere in the Basin and Range province, or that some other process or combination of processes was responsible for the formation of these pediment domes.

There is no apparent mineralization associated with development of pediment domes in the EMNSA.

## GEOPHYSICS

Geophysical studies conducted within the EMNSA include gravity and aeromagnetic surveys on a regional scale, local electrical (induced polarization, telluric, and audio magnetotelluric) traverses, a limited number of heat flow measurements, and airborne radiometric measurements. Each of these methods has a particular application in assessing the mineral potential of the area.

In general, gravity anomalies, when analyzed for regions the size of the present study area, will yield information as to: (1) the rock-density distribution within the crust, (2) the isostatic state of

the region, and (3) when combined with other geophysical data, the nature of the lower crust and upper mantle. Although the isostatic state and nature of the lower crust and upper mantle are important in understanding the genesis of mineral deposits in a region, they do not have a direct application to the resource potential in the upper crust. In order to eliminate the gravitational effects arising from deep sources, the isostatic anomaly (Jachens and Griscom, 1982) will be used in describing gravity anomalies in the EMNSA.

In contrast to Bouguer gravity anomalies, magnetic anomalies, discussed herein, arise strictly from sources in the upper crust and in this part of the Basin and Range province, represent susceptibility contrasts less than about 15 km in depth. Magnetic variations primarily result from differences in magnetite content, and the inherent or remnant magnetization of a particular rock body. Analysis of the magnetic patterns in the study area are helpful in delineating buried contacts between varying rock units, the location and attitude of fault zones, the depth to basement beneath sedimentary cover, and, at least in one case, the presence of substantial iron and iron-related deposits.

Electrical traverses have been conducted in the Providence Mountains (Goldfarb and others, 1988; Miller and others, 1985) in order to delineate the extent of alteration and sulfide mineralization along the East Providence and Bighorn fault systems (pl. 1).

Heat flow measurements obtained within the EMNSA are part of a broad regional survey of the southern Basin and Range (J.H. Sass and others, unpub. data, 1990). When viewed over a large area, the EMNSA displays values in the range of about 80 to 100  $\text{mWm}^{-2}$  which are fairly typical of the region. Heat-flow measurements are important to an understanding of the thermal history of the region. However, currently available spacing of the individual measurements does not allow us to make direct comparisons with individual geologic features.

Airborne radiometric measurements were conducted throughout the region as part of the National Uranium Resource Evaluation Program (NURE). These measurements are sensitive to concentrations of uranium, potassium, and thorium. Results of this survey are discussed in a section below.

## Gravity Survey

Gravity data for the EMNSA and surrounding area were obtained from Snyder and others (1982), Miller and others (1986), and Mariano and others (1986). The observed gravity data were reduced to the free-air anomaly. Bouguer, curvature, and terrain corrections, using a density of  $2.67 \text{ gm/cm}^3$ , were added to obtain the complete Bouguer anomaly. In order to eliminate that part of the Bouguer field that arises from deep sources, a regional field was subtracted from the Bouguer anomaly using the method described by Jachens and Griscom (1982). The resulting

isostatic anomaly is shown on plate 4, and will be used below in the description of specific gravity features.

There is a relatively straightforward relation between the isostatic anomaly and rock-types as mapped within the study area (compare pls. 1 and 4). In general, isostatic "highs" are present in areas consisting predominantly of Proterozoic metamorphic rocks and Jurassic granitoids. Intermediate isostatic values are present in regions of Cretaceous plutonic rocks, whereas thick deposits of Tertiary volcanic rocks and Tertiary-Quaternary surficial deposits produce isostatic "lows". Density measurements presented by Miller and others (1986) and Wilshire and others (1987) indicate, from samples collected in the New York Mountains and Cinder Cones area, that Proterozoic schist and gneiss average  $2.674 (\pm 0.07)$  gm/cm<sup>3</sup>, Mesozoic intrusive rocks (adamellite or monzogranite, and granite)  $2.60 (\pm 0.02)$  gm/cm<sup>3</sup>, and unspecified Tertiary volcanic rocks show a wide range, averaging  $2.456 (\pm 0.40)$  gm/cm<sup>3</sup>. In addition, two samples of Proterozoic amphibolite have densities of 2.96 and 3.10 gm/cm<sup>3</sup>.

### Magnetic Survey

Data used to produce the aeromagnetic map (pl. 5) were collected during three separate surveys in California: (1) the Kingman-Trona area (U.S. Geological Survey, 1983), (2) the Needles  $1^\circ \times 2^\circ$  quadrangle (U.S. Geological Survey, 1981), and (3) that portion of the Kingman  $1^\circ \times 2^\circ$  quadrangle in Nevada (Oliver, 1986). In all of these surveys, a flight height of 1,000 ft (304 m) above average terrain was employed. Because of the irregularity of the local topography, however, the actual height above ground varied from about 400 ft (122 m) to 2,500 ft (762 m) (Miller and others, 1986). In the California surveys, flight-line spacing was 0.5 mi (0.8 km) whereas spacing averaged 1.0 mi (1.6 km) in Nevada. The California and Nevada surveys have been merged in order to eliminate any effects caused by the differing survey parameters. On plate 5 the standard (uniform) earth's magnetic field has been subtracted from the observed measurements to yield the residual magnetic field.

Cursory examination of plate 5 reveals that within the EMNSA there are regions that display diverse residual magnetic characteristics. These regions generally fall into three types of magnetic patterns: (1) low amplitude ( $>200$  nT), low gradient highs and lows, (2) intermediate to large amplitude (200-500 nT), intermediate gradient highs and lows, and (3) intermediate amplitude (100-300 nT), steep gradient complex anomalies. In the most general sense, these three anomaly patterns can be related to rock type or geologic environment. Type 1 patterns correspond to alluvial valleys and areas of predominantly Cretaceous granite; type 2 anomalies correlate with exposures of Proterozoic metamorphic rocks and Jurassic granitoids; and type 3 anomalies are present in areas including mostly Tertiary to Quaternary mafic to silicic lava flows, vents and

pyroclastic material. The magnetic signature of a region not only depends on the magnetic character of the rock but also the depth to the source. For example, in a deep basin the basement rocks may be quite magnetic but because of the increased distance between sensor and source and the nonmagnetic character of the intervening basin fill the amplitudes and gradients of anomalies will be reduced and the magnetic signature may be quite different from areas where similar source rocks are near the surface. Two isolated magnetic anomalies of particular note in the EMNSA are associated with the Vulcan iron-skarn deposit and the Woods Mountain caldera (McCurry, 1988) and are discussed in the following section.

## **Discussion of Gravity and Magnetic Anomalies**

Interpretation of the gravity and magnetic maps (pls. 4 and 5) are summarized from a series of relatively recent U.S. Geological Survey Wilderness Bulletins and Miscellaneous Field Studies Maps. Interpretations included in four additional geologic and geophysical studies pertaining to the region also contributed significantly to our own report (Carlisle and others, 1980; McCurry, 1988; Beckerman and others, 1982; DeWitt and others, 1984). Although these studies are for the most part not adjoining, they cover a large part of the area and the geophysical interpretations can be projected across intervening regions. In addition to this summary of previous work, a brief discussion of the gravity and magnetic characteristics of the southern Clark Mountain Range and Woods Mountains caldera is presented.

### **Ivanpah Valley and New York Mountains**

Isostatic gravity values in this region vary from a high of about -12 mGal over the central New York Mountains to a low of -40 mGal in the Ivanpah Valley. The highest values are associated with outcrops of Proterozoic schist and gneiss whereas the low values represent unconsolidated basin-fill material in Ivanpah Valley. The alluvial thickness in Ivanpah Valley is in excess of 6,500 ft (1,980 m) as shown by cuttings and drill hole logs from the Ivanpah Partnership "Ivanpah 13" (Hodgson, 1980). Carlisle and others (1980), from detailed gravity, magnetic and seismic surveys suggest that the maximum sediment thickness is about 8,000 ft (2,440 m), which is present on the east side of the valley. The north-northwest striking Ivanpah fault cuts across the valley from the vicinity of Mountain Pass to the general area of the Vanderbilt Mine (pl. 1). Seismic information provided by Carlisle and others (1980) suggest that vertical offset is approximately 1,200 ft (366 m) in the center of the valley near the Morningstar Road (pl. 1). The series of northwest striking faults in the area of the Vanderbilt Mine generally corresponds to a change in the type of basement rock from Proterozoic schist and gneiss on the northeast to the Cretaceous Mid Hills Adamellite on the southwest. This change is marked by a steep gravity gradient, decreasing to the southwest, with a variation of about 20 mGal. Gravity values also decrease toward the south and southeast

from the northern New York Mountains. This decrease is attributed to a southward thickening wedge of volcanic rock, gravel, and alluvium that cumulatively attain a thickness of a few thousand feet in Lanfair Valley (Miller and others, 1986). A gravity decrease that is present between the north-central part of the New York Mountains and the town of Nipton cannot be explained by examination of surface exposures. This decrease is probably due to an unexposed felsic intrusion of unknown age or even thrusting of Proterozoic rocks over Tertiary basin fill (Miller and others, 1986). However, Proterozoic rocks are not known to be thrust over Tertiary rocks in any of the mountain ranges of the EMNSA.

Magnetic anomaly values in this area range from highs of slightly more than +200 nT to lows in excess of -200 nT. Anomalies over Proterozoic rocks are broad with amplitudes ~100 nT. Three such positive anomalies are present in the Ivanpah Valley. Two, in the southwest and southeast part of the valley, are roughly circular and Carlisle and others (1980) suggest the tops of the sources are approximately 3,200 ft (975 m) below the surface which is beneath the basement-sediment interface. The third is a positive ridge trending north along the western side of the valley. Depth to source estimate for this anomaly is 5,700 ft (1,738 m) (Carlisle and others, 1980). The magnetic signature in areas of exposed Proterozoic rocks suggests that metamorphism or hydrothermal alteration has affected the magnetite content of the rocks (Miller and others, 1986). The positive anomalies in Ivanpah Valley may, therefore, represent relatively unaltered Proterozoic basement sources. Volcanic rocks exposed along the southeastern margin of the New York Mountains near Barnwell (pl. 1) produce high amplitude, short wavelength anomalies indicating the magnetic character of the rock. In the New York Mountains the change from Proterozoic schist and gneiss, on the northeast to Cretaceous adamellite on the southwest is noted by a down-to-the-northeast magnetic gradient. This change in magnetic level corresponds, but is opposite in sense, to the gravity gradient discussed earlier. This would imply that the Mid Hills Adamellite is less dense, but more magnetic, than the adjacent Proterozoic metamorphic rocks. The reduced magnetic character of the Proterozoic rocks may reflect extensive alteration of magnetite in these rocks.

#### **Lanfair Valley and Piute Range**

This area is characterized by large magnetic anomalies and a relatively flat isostatic gravity field. A northeast trending belt of positive magnetic anomalies extends from Fenner Valley on the southwest through the Vontrigger Hills and southern Piute Range terminating some 6 mi (10 km) east of the central Piute Range. An apparent westerly arm of this pattern connects the Grotto Hills and Lanfair Buttes region to the central part of this trend. These positive anomalies correlate well with outcrops of Proterozoic crystalline rocks. Southeast of this magnetic ridge is an area consisting primarily of Mesozoic granitic rocks in the Signal Hill and Homer Mountain areas. The

region here is characterized by a series of magnetic lows. The contact between these two units is largely concealed beneath volcanic and alluvial deposits of the southern Lanfair Valley and may correspond to the abrupt magnetic change between the magnetically high and low areas (Nielson and others, 1987). The northern Piute Range and Castle Mountains contain extensive volcanic vents and associated rocks and the magnetic field displays a number of sharp large amplitude highs and lows. In the vicinity of Hart Mine, near the northeast corner of the EMNSA, the magnetic field is fairly subdued, although this area also contains extensive volcanic material similar to that exposed in the Piute Range. The relatively smooth magnetic field here may represent a topographic effect, because the area is lower and not as rugged as the Piute Range; this results in a more constant survey height. Alternatively, there possibly may be an absence of highly magnetic volcanic vents in the immediate vicinity.

The isostatic gravity field in this region is relatively smooth, showing a general decrease into Lanfair Valley. A low closure of about 5 mGal, based on one station, over the Lanfair Buttes probably represents a sequence of alluvial and volcanic material as much as 1 km thick. A similar anomaly is present near the junction of Ivanpah and Hart Mine roads. Small gravity highs are present over the Vontrigger Hills and south of the Grotto Hills. These anomalies probably represent the thinning or absence of post-Cenozoic sedimentary or volcanic cover.

#### **Mid Hills, Providence, and South Providence Mountains**

In the New York Mountains and northern Mid Hills, between the Ivanpah and Cedar Canyon Roads, gravity and magnetic anomalies are relatively smooth and flat, thereby highlighting the overall uniform character of the Mid Hills Adamellite (pls. 4, 5). South of Cedar Canyon, however, both gravity and aeromagnetic maps show large changes and numerous closures, reflecting the mixture of these Proterozoic metamorphic rock, Mesozoic intrusions, Tertiary volcanic rocks, and Tertiary sedimentary rocks. A large (-400 nT) arcuate magnetic low extends from the Grotto Hills to the Cedar Canyon fault in the Mid Hills (pl. 5). This feature probably results from both a thickened Tertiary and (or) Quaternary volcanic and (or) sedimentary sequence and dipolar lows associated with positive anomalies to the south. A circular area, some 9 mi (15 km) in diameter, of relatively high magnetic values lies to the south of the above mentioned low. This region is characterized by outcrops of both Proterozoic and Mesozoic crystalline rocks and the high magnetic anomaly reflects the presence of these rocks at the surface. The westernmost peak in this high area of magnetic values is present over the Black Canyon Gabbro of Beckerman and others (1982) which is a circular Cretaceous plug of hornblende gabbro in the Mid Hills Adamellite, some 1.25 mi (2 km) in diameter. The gabbro here contains as much as 6.5 volume percent opaque minerals, primarily magnetite (Beckerman and others, 1982), resulting in the observed magnetic anomaly. A 5 to 10 mGal gravity anomaly corresponds to the large

magnetically high area. Gravity values in the central and northern Providence Mountains show a general decrease towards the northwest. This gradient probably reflects the general change in the types of rock in the basement from relatively dense Jurassic granitoids in the southeast to the Cretaceous Mid Hills Adamellite in the northwest (pl. 1).

The central and southern Providence Mountains are characterized by several large positive magnetic anomalies. The largest of these is associated with the Vulcan iron skarn deposit. This anomaly (3,500 nT) suggests a possible continuation of the ore body to the east (Goldfarb and others, 1988). Another large magnetic anomaly (~2,000 nT) some 6 mi (10 km) to the northeast may represent the presence of an iron skarn and(or) highly magnetic Jurassic granitoid body. Positive anomalies present in the southern part of the Woods Mountains suggest that the nonmagnetic tuff that makes-up the surfical exposures overlies magnetic basement of probable Jurassic age.

The East Providence fault strikes northerly along the east side of the range (pl. 1). In general, a series of magnetic lows correspond to the surface trace of the fault. Some of the lows are present over exposures of apparently nonmagnetic Paleozoic sedimentary rocks while others, present in areas of Proterozoic or Jurassic crystalline rock, may result from hydrothermal alteration of magnetic minerals along the fault. Steep down-to-the-west gravity and magnetic gradients are present 1 to 2 mi (1.6-3.2 km) into Kelso Wash along the west side of the Providence Mountains, suggesting that the east side of the valley is a pediment surface.

### Granite Mountains

Isostatic gravity values in this region vary from a high of about -10 mGal to a low of -25 mGal (pl. 4). A really corresponding magnetic values are in the range of >+200 to <-100 nT (pl. 5). Generally, the northern part of the range is characterized by a magnetic low and a positive gravity closure. The southern part of the range displays a gravity minimum and a variable, but generally high, magnetic anomaly. The division between these two geophysically distinct regions is marked by the concave-to-the-southeast striking Bull Canyon fault (pl. 1). Gravity and magnetic features of the region have been discussed by Howard and others (1987) and are therefore only summarized briefly here. The magnetic trough in the northern part of the range corresponds to the Bull Canyon fault and probably reflects topographic effects, low magnetic susceptibility of the unaltered plutonic rocks, and possibly alteration along the fault zone. Gravity anomalies indicate that the predominantly Jurassic basement rocks north of the fault are denser than the mostly Cretaceous granites that crop out to the south of the fault.

The west margin of the Granite Mountains is marked geomorphologically by Budweiser Wash and the corresponding Bristol Mountains fault (pl. 1). Steep gravity gradients here indicate that this fault is a major structure that juxtaposes less dense Tertiary volcanic rocks of the Old Dad

Mountains and some sedimentary rocks to the west with Mesozoic crystalline rocks of the mountains.

North and northwest of the Granite Mountains, in the alluvial plain of the Devils Playground, gravity values suggest that the thickness of sedimentary deposits is not greater than about 1,000 ft (305 m) and basement rocks here are probably Mesozoic granitoids. In the western part of this valley, a northwest-trending 300 nT magnetic ridge is present along the southwestern margin of the northern Bristol Mountains. This anomaly also roughly corresponds to the projection of the Bristol Mountains fault farther towards the southeast. The anomaly is fairly broad with subdued gradients suggesting that the source lies at some depth below the surface, possibly as much as ~1 mi (1.6 km). The source of this anomaly is not evident from surface observations and there is not a prominent associated gravity anomaly. Two possibilities for a source are extensive iron skarn mineralization or intrusion of Tertiary igneous rocks along the fault zone.

#### **Old Dad Mountain and Kelso Mountains**

Exposed in this area are a wide variety of rock types that include Proterozoic schist and gneiss, Paleozoic sedimentary rocks, Mesozoic granitoids, Tertiary volcanic rocks, and unconsolidated sediments (pl. 1). The gravity and magnetic patterns are equally complex. The northwest trending Old Dad Mountain is characterized by both gravity and magnetic highs of as much as 10 mGal and 400 nT, respectively (pls. 4, 5). Along the southwest margin of this range, the magnetic gradient is typical of a steeply dipping fault, although some of the gradient probably results from topographic differences. Both the gravity and magnetic anomalies appear to wrap around the southern end of Old Dad Mountain and the Kelso Mountains before dying out in Kelso Wash. A prominent arcuate magnetic and gravity trough is present over the Kelso Mountains. This anomaly separates the gravity and magnetic highs of Old Dad Mountain from an area of positive anomalies centered north of Kelso Peak. The northwest limb of the trough appears to continue for as much as 18 mi (30 km) and the northeast limb some 6 mi (10 km), merging with lows of Kelso Wash. Because the area of the trough is, for the most part, covered by alluvial deposits the source of the anomaly is not evident. If these features represent a fault or series of faults, extensive hydrothermal alteration has taken place along the fault zones and the concave area has been down-dropped; if the anomalies reflect an intrusive contact, alteration may have occurred along this contact and the rock in the concave area is less dense than the surrounding terrane.

Trending due north from Old Dad Mountain and the Kelso Mountains is a very prominent isostatic gravity lineation (pl. 4). Relief across this feature is about 10 mGal, down to the east. A somewhat similar north-northwest-trending gradient is noted along the northeast side of Shadow Valley. These two prominent anomalies intersect at the northern end of Shadow Valley. Dimensionally, the magnetic pattern is quite similar to the prominent gravity lineation, although the

area of the western gravity gradient is represented by a series of sharp magnetic highs and lows reflecting surficial Tertiary basaltic vents and associated volcanic rock. The gravity gradient along the northeastern edge of Shadow Valley has a corresponding magnetic gradient, although the sense of relief is opposite (i.e. the magnetic anomaly is down-to-the-northeast). The southern part of the area of the gravity low defined by these two linear anomalies includes extensive exposures of Cretaceous granite. One interpretation is that the granite extends northward beneath sedimentary cover and forms the floor of Shadow Valley. The gravity low therefore represents the combined effect of low-density alluvial valley fill and a relatively low density basement rock. Small outcrops of pre-Tertiary rocks have been noted in Shadow Valley (DeWitt and others, 1984). These have no corresponding gravity anomaly from which we surmise that the alluvial fill is relatively thin. The magnetic pattern within the valley shows little relief and is a relative high when compared to immediately adjacent terranes; this would be consistent with the above interpretation. A northwest trending magnetic gradient crosses the valley in the vicinity of Interstate Highway 15. This lineation may mark a lithologic change in the Cretaceous granitoid complex, or it may represent a subsurface fault with down-to-the-northeast displacement.

#### Clark Mountain Range

Lying between the Ivanpah and Shadow Valleys, the Clark Mountain Range is a structurally and lithologically complex block consisting of early Proterozoic metamorphic rocks, middle Proterozoic igneous intrusions, and Paleozoic to Mesozoic sedimentary units (pl. 1). The east side of the range is characterized by a structurally complex, diversity of Proterozoic metamorphic and igneous rocks, while the western part of the range is characterized by a relatively thick section of Phanerozoic sedimentary rocks that has been thrust over the basement complex. Geophysically, both gravity and magnetic anomalies indicate that the Proterozoic rocks continue to the east at shallow depths nearly to the center of Ivanpah Valley (pls. 4, 5). The trend of the anomalies in the western part of Ivanpah Valley is north-south which is at an angle of some 20° to the north-northwest structural grain of the surrounding region. In the western Clark Mountain Range, geophysical anomalies follow the regional structural trends.

Isostatic gravity values in this region vary from lows of about -40 mGal in the Ivanpah and Shadow Valleys to a high of approximately -10 mGal over the eastern range front near the intersection of Interstate Highway 15 and the Ivanpah Road. Gravity values show a gentle decrease westward across the range until sharp gradients associated with Shadow Valley are encountered. The apparent smoothness of the isostatic anomaly is in part due to the relatively wide spacing of gravity stations within the range. Small features, such as igneous dikes and plugs in the general area of Mountain Pass, cannot be detected with the available survey, even though large density contrasts may exist between rock units. Lower gravity values in the western part of the

Clark Mountain Range are due in part to the presence there of a sequence of Paleozoic sedimentary rock that may have a total thickness of as much as 1.5 mi (2.5 km).

The residual magnetic anomaly shows a large amount of relief within the Clark Mountain Range in contrast to the isostatic gravity. Although some of the magnetic variation may be due to topographic effects, a series of highs and lows in the southern part of the range cannot be accounted for by a varying distance between the aircraft and ground surface. Traversing from east to west across the southern part of the mountains, the broad magnetic high in western Ivanpah Valley probably represents a magnetite or pyrrhotite component of the Proterozoic basement there. This anomaly continues from the southern Ivanpah Valley northward, generally conforming to the shape of the margins of the valley. Immediately to the west of this high, there is an elongate magnetic low closure of  $\sim 80$  nT, which displays gradients similar to the above high. This low corresponds to the subsurface projection of the Ivanpah fault (Burchfiel and Davis, 1971) and may indicate the presence of hydrothermal alteration along the fault zone. A magnetic high extends from immediately northwest of Mountain Pass some 6 mi (10 km) to the south-southeast. Gradients associated with this anomaly suggest a shallow source and the anomaly appears to be related to a series of mid-Proterozoic ultrapotassic rock and carbonatite exposed in the area. These rocks are the host for the rare-earth deposits of Mountain Pass as described below. To the west of this magnetic ridge, there is a northwest-oriented low of about -100 nT. The location and trend of this anomaly appear to correspond to a series of thrust faults that crop out in the western Clark Mountain Range and Ivanpah Mountains, and the low may represent a thrust-stacking of Paleozoic sedimentary rocks on Proterozoic basement. A +200 nT magnetic anomaly is present in the southwestern Clark Mountain Range, Mescal Range, and Striped Mountain area. The source of this anomaly is not obvious from surface exposures; gradients, however, indicate that the top of the causative body cannot be much more than 1 mile (1.6 km) below the surface and is probably at the top of the Proterozoic basement. Several small outcrops of Mesozoic granitoids are present in this area (pl. 1). When combined, the above anomalies indicate a complex distribution of lithologies and magnetic properties in the southern Clark Mountain Range and northern Ivanpah Mountains. In contrast, the northern Clark Mountain Range is typified by gentle gravity and magnetic gradients, although the region is structurally complex. The gravity in the northern Clark Mountain Range consists of a gradient that extends southwestward from a high in the southern Spring Mountains to the low in Shadow Valley. A northwest-trending magnetic gradient in this area is present between positive anomalies in the western Ivanpah Valley and a series of lows along the western flank of the Clark Mountain Range.

### **Woods Mountains Caldera**

Two of the most prominent features on plates 4 and 5 are the negative gravity and magnetic anomalies associated with the late Tertiary Woods Mountains caldera (McCurry, 1988). Both anomalies are large amplitude, circular features with very steep gradients. These features are in sharp contrast to the surrounding gravity and magnetic fields. The gravity anomaly is approximately -30 mGal and some 8.7 mi (14 km) in diameter while the magnetic anomaly is ~-600 nT and about 5.5 mi (8.85 km) in diameter. Both of these features appear to be related to a caldera and(or) an underlying pluton. The presence of Jurassic granitoids within the boundaries of the gravity low, the fact that the anomalies are of differing lateral extent, and the fact that centers of the lows do not coincide (the magnetic center is offset some 1.9 mi (3 km) to the southwest) all indicate that the anomalies do not result strictly from a caldera infilling of low density and low susceptibility/low remnant magnetization pyroclastic material (pl. 1). The magnetic anomaly may represent the true size and geometry of the actual caldera which, as shown by McCurry (1988, figs. 1 and 2), is a "trap door" feature with the west and southwest parts downdropped more than the east parts resulting thereby in a west-dipping relatively smooth caldera floor. Structural relief along the western caldera margin may be in excess of 0.6 mi (1 km).

The associated gravity anomaly of the Woods Mountains caldera extends well beyond the surficial bounds of this feature (compare pls. 1 and 4). This indicates that a negative density contrast, that occupies an area larger than the surface expression, must be present in the subsurface. Positive magnetic anomalies are present peripheral to the magnetic low but are within the area of the negative gravity anomaly.

The gravity low probably represents the combined effect of an intrusion of a relatively low density granitic stock into Jurassic granitoids, and caldera formation and infilling with low density pyroclastic material and rhyolite. The silicic stock in this case would be circular and on the order of 8.7 mi (14 km) in diameter with steeply dipping sides. The magnetic low probably results from filling of the caldera by pyroclastic material and by nonmagnetic silicic lava. Positive magnetic anomalies peripheral to the magnetic low but within the gravity anomaly would reflect the presence of magnetic Jurassic granitoids left above the intrusion. These granitoids may have been remagnetized during the magmatic event.

### **Aerial Gamma-Ray Surveys**

Aerial gamma-ray surveys measure the gamma-ray flux produced by the radioactive decay of the naturally occurring elements potassium ( $^{40}\text{K}$ ), uranium ( $^{238}\text{U}$ ), and thorium ( $^{232}\text{Th}$ ) in the top few inches of rock or soil (Duval and others, 1971). If the gamma-ray system is properly calibrated (for example, see Grasty and Darnley, 1971), the data can be expressed in terms of the

estimated concentrations of the radioactive elements. Potassium data are usually expressed as concentrations in units of percent potassium (percent K), thorium as parts per million equivalent thorium (ppm eTh), and uranium as parts per million equivalent uranium (ppm eU). The term equivalent is used because the technique measures the gamma-ray flux from the decay of thallium ( $^{208}\text{TI}$ ) and bismuth ( $^{214}\text{Bi}$ ) which are decay products of  $^{232}\text{Th}$  and  $^{238}\text{U}$ , respectively, and because of the possibility of radioactive disequilibrium in the thorium and uranium decay series.

During the period 1975-1983, the U.S. Department of Energy carried out the National Uranium Resource Evaluation (NURE) Program which included aerial gamma-ray surveys of most of the conterminous United States. Figure 8 is an index map showing the  $1^{\circ}$  by  $2^{\circ}$  National Topographic Map Series (NTMS) quadrangles from which the data (U.S. Department of Energy, 1979a, b, c; 1980) were taken for this study. Although many of the airborne gamma-ray systems used to make these surveys were calibrated, many of the early surveys were done without calibration and were not converted to the concentrations of the radioactive elements. Detailed examinations of the digital data available on magnetic tape also showed that many of the "calibrated" surveys do not match the data from "calibrated" surveys of adjacent areas. For these reasons the data must be corrected to obtain a consistent data base. Duval and others (1989, 1990) discuss the types of corrections applied to the data and they also provide index maps that indicate the specific kinds of corrections applied to the data sets used in this work.

The NURE aerial gamma-ray data were collected by several private contractors using "high-sensitivity" gamma-ray systems. These systems used sodium iodide detector crystals with detector volumes of 2,000-3,300 in<sup>3</sup> (33-54 L). All of the systems included electronic navigation equipment, radar altimeters, magnetometers, and "upward-looking" gamma-ray detectors. The upward-looking detectors were partially shielded from radiation coming from the ground by placing them on top of the other detectors or by using lead. The purpose of the upward-looking detectors was to measure the amount of radiation from  $^{214}\text{Bi}$  in the atmosphere and to use that information to correct the estimated ground concentrations of  $^{238}\text{U}$ . The data were corrected by the contractors for background radiation due to aircraft contamination and cosmic rays, Compton scattering effects, altitude variations, and airborne  $^{214}\text{Bi}$ .

The gamma-ray surveys were flown at a nominal altitude of 400 ft (122 m) above the ground. The gamma-ray systems were calibrated using the calibration pads at Grand Junction, Colo. (Ward, 1978), and the dynamic test strip at Lake Mead, Ariz. (Geodata International, Inc., 1977). The nominal flight-line spacings for the surveys (fig. 9A-C) were 1 to 3 mi and included tie lines flown approximately perpendicular to the flight lines at intervals of 25 to 29 km.

Table 1 lists the estimated average concentrations of potassium, uranium, and thorium for some of the geologic units which crop out in the EMNSA. The values listed in table 1 were determined by inspection of gamma-ray profiles overlain on the geologic map (pl. 1) but not all of the geologic

units found in the study area are included in table 1 because of little or inadequate data over some units. Average potassium concentrations range from 0.5 to 3.5 percent K with the highest values (greater than 2.9 percent K) present with Jurassic quartz monzonite of Goldstone (map unit Jgo, pl. 1) and Ivanpah Granite (Jig), with Cretaceous Mid Hills Adamellite (Kmh), with Tertiary younger volcanic rocks (Tvl), Wild Horse Mesa Tuff (Tw), and Tortoise Shell Mountain Rhyolite (Tts), and with Proterozoic granitic rocks (Xg2). As pointed out by Beckerman and others (1982), the K<sub>2</sub>O contents, in percent, of the Mid Hills Adamellite and the Ivanpah Granite are commonly in the 3.5-4.8 and 5.0-9.0 range, respectively, and seemingly corroborate the K-values sensed remotely by the aerial gamma ray surveys. The lowest average potassium values (less than 1.0 percent K) coincide with Cambrian dolomite (Cd). Average uranium values range from 1.5 to 4.4 ppm eU with the highest values (greater than 3.5 ppm eU) present in Quaternary eolian sands (Qes<sub>2</sub>) and playa deposits (Qp), in younger Tertiary volcanic rocks (Tvl), dacite and rhyolite (Tdr), and Tortoise Shell Mountain Rhyolite (Tts), and in Mesozoic volcanic and sedimentary rocks (Mzv). The lowest average uranium values (less than 2 ppm eU) are present in Cambrian dolomite (Cd), in Late Proterozoic and Cambrian siliciclastic rocks (Czs), and in Jurassic felsic rocks of Colton Hills (Jfc). Average thorium values in table 1 range from 3.0 to 31.0 ppm eTh with the highest values (greater than 17 ppm eTh) present in Quaternary eolian sands (Qes<sub>2</sub>) and playa deposits (Qp), Tertiary dacite and rhyolite (Tdr), in Cretaceous Teutonia Adamellite (Kt), in Jurassic Ivanpah Granite (Jig), and in Proterozoic migmatite (Xm). The lowest average thorium values (less than 7 ppm eTh) are present in Quaternary eolian sands (Qes<sub>1</sub>), in Cambrian dolomite (Cd), in Late Proterozoic and Cambrian siliciclastic rocks (Czs), and in Jurassic Sands Granite (Js).

Anomalously high thorium values are present also at two locations not listed in table 1. These locations were not included in the table because the flight lines pass near the contacts between different geologic units and the data could not be positively assigned to a particular geologic unit. The first of these locations has a maximum value of 42 ppm eTh and the flight line passes over and near an outcrop of Middle Proterozoic granitic rocks approximately at 35°29' N. and 115° 32'W. This same location has high uranium values greater than 7 ppm eU and some potassium values greater than 4 percent K. The second area of similar thorium values is present in and near a patch of Jurassic Ivanpah Granite (Jig), approximately at 35°22' N. and 115°30' W. A similar anomalously high potassium value of greater than 5 percent K is present in a small mass of Jurassic quartz monzonite of Goldstone (Jgo) near 34°56' N. and 115°32' W. Contoured plots of K, eTh, and eU for the EMNSA and surrounding area are shown in figure 9A-C.

The ratios of K/eTh, eU/K, and eU/eTh were also calculated and examined for the existence of anomalies. A possibly anomalous value of K/eTh=0.72, indicative of a relatively enriched content of Th, is present in Early Proterozoic granitic rocks (Xg1) near 35°4' N. latitude and 115°7'30" W.

longitude. This possible anomaly is located in the vicinity of an occurrence of polymetallic veins. Similarly reduced K/eTh values ranging from 0.3 to 0.5 are also present over some of the Cretaceous Live Oak Granodiorite (Klo) near 35°17' N. and 115°16' W. This outcrop is known to have one tungsten skarn deposit (pl. 2). Limited amounts of data over a large mass of Jurassic quartz monzonite of Goldstone (Jgo) in the vicinity of 34°52' N. and 115°34' W. have K/eTh values in the range of 0.3 to 0.5. These values suggest that this mass has anomalous K/eTh values and it is known to host numerous mineral occurrences of various types (pl. 2). Other apparently anomalous K/eTh values ranging from 0.3 to 0.7 are present in Quaternary eolian sands (Qes1) near 34°55' N. and 115°44' W. The high values are caused by the low thorium content (about 4.4 ppm eTh) of the eolian sands.

Various eU/K and EU/eTh anomalies also are present in the EMNSA. One eU/K anomaly with values of 4.5 to 5.9 is present approximately at 36°54' N. and 115°36' W. This anomaly is apparently associated with Tertiary gravel (Tg) but its significance is unknown. Approximately at 34°56' N. and 135°34' W., a similar eU/K anomaly is present in Permian to Devonian limestone (PDI). At this location, the uranium concentration is a moderate value of about 2 ppm eU which suggests that the apparently anomalous value is likely to be characteristic of the limestone. Near 35°4' N. and 115°11' W., anomalies of eU/K=4.4 and eU/eTh=0.8 are present in Tertiary volcanic rocks (Tv1). The radioelement concentrations at the anomaly location are 1.5 percent K, 7 ppm eU, and 8 ppm eTh. The potassium and thorium values can be considered as moderate but the uranium value is relatively high and should be considered anomalous. Other high eU/K values ranging from 2.5 to 4.8 are present along a section of a north-south flight line at 115°32' W., from 35°25' N. to 35°29' N.; eU/eTh values as high as 1.4 are present at some places along the same section of flight line. This section of flight line crosses various rock types.

In conclusion, the NURE gamma-ray data available for the study area provide limited measurements of the potassium, uranium, and thorium concentrations of the various geologic units present on the surface. Some concentrations of potassium are consistent with known potassium contents of exposed plutonic rocks. The most prominent thorium anomalies are likely to be associated with the carbonatite-related, REE deposits at Mountain Pass, just outside the EMNSA. The ratio data also show a number of interesting anomalies and some of them may be related to mineral occurrences. A more detailed gamma-ray survey would provide more site-specific information that could then be more closely related to the geology and mineral occurrences.

### **Landsat Thematic Mapper (TM) Surveys**

As a part of this report, a quarter Landsat Thematic Mapper (TM) scene was processed to be used as a guide for mapping various lithologic units and to highlight the general distribution of

possible areas of hydrothermal alteration. For the preliminary results described in this section, a color ratio composite was produced by digital image processing and interpreted by inspection (fig. 10).

As described above, the EMNSA consists of a diverse group of sedimentary, metamorphic and volcanic rocks (pl. 1). Crystalline rocks include a variety of gneisses and schists along with marble and quartzite. The most widely distributed sedimentary unit is dolomite. Limestone, quartzite, and shale are also well exposed throughout the area of the EMNSA. Mesozoic rocks include andesitic to rhyolitic lava flows and some sandstone, and shale together with a wide variety of plutonic rocks that range from granite to diorite in composition and are cut extensively by narrow felsic and mafic dikes.

A TM scene recorded June 6, 1986 was selected for the study because the sun angle is highest at the time of the summer solstice, and shadowing in this area of high topographic relief is minimized. Landsat TM imagery has 30-m spatial resolution, six spectral bands in the visible and near infrared, and excellent radiometric and geometric characteristics:

TM Bands	Wavelength Coverage $\mu\text{m}$
1	0.45-0.52
2	0.52-0.60
3	0.63-0.69
4	0.76-0.90
5	1.55-1.75
6	Thermal IR, not used in this study
7	2.08-2.35

Color composite images display color variations that show differences in spectral radiance that is recorded by the Landsat Thematic Mapper from surface materials. Ratioing of selected channels minimizes the influence of topography and enhances spectral differences. Color compositing of three stretched ratios to form color-ratio composite (CRC) images of TM data allows the presence of specific minerals or mineral groups to be detected. This information is shown as certain colors on the color image. Rocks and soils that are mineralogically and spectrally similar may not be discriminated.

The CRC of the EMNSA was produced using ratios of TM channels 5:7 (red), 3:1 (green), and 3:4 (blue) according to the techniques of Knepper and Simpson (1991; fig. 10). The resulting colors, used for identification of minerals or mineral groups that may be associated with hydrothermal alteration, are summarized in table 2.

A working copy of a color versatec print was prepared from the CRC at a scale of 1:100,000 to overlay on various geophysical and geologic maps of the EMNSA. Nuances of color and tonal

differences, unfortunately, were lost in the color versatec paper copy necessitating reference to the original color transparency to better interpret the CRC.

In the CRC image, a contribution by a color filter indicates a high ratio value relative to other materials in the scene; thus red is due to high TM 5:7 values and represents vegetation which has a strong H<sub>2</sub>O absorption in the region of band 7. The TM 3:4 ratio expresses the increase in reflectance from the chlorophyll absorption band in TM 3 to the near-infrared reflectance plateau in TM channel 4, so that the blue color component is very low for vegetated areas. Carbonate minerals and hydroxyl-bearing minerals, such as muscovite, kaolinite or jarosite, which may be associated with hydrothermal alteration, should result in a magenta color because of the combination of high TM 5:7 (red) plus a moderate value for TM 3:4 for the blue component. However, most hydrothermally altered rocks which contain hydroxyl bearing minerals are also limonitic so that the magenta color usually designates only carbonate mineral-bearing units. TM 3:1 is coded green and defines ferric iron (limonite) bearing rock and soil. Yellow, the result of combining red and green, appears where TM 5:7 (red) is high due to the presence of carbonate or hydroxyl-bearing minerals, and where TM 3:1 (green) is high due to ferric iron-bearing minerals such as limonite. White areas indicate a high value in all three component ratios that is most indicative of the presence of many alteration minerals, especially jarosite, which strongly contributes to the overall radiance.

The detection of limonite has been traditionally important to remote sensing for hydrothermal alteration. As defined by Blanchard (1968), limonite is a general term for hydrous ferric iron oxides and hydroxides. These minerals absorb strongly in the visible region, near TM channels 1 and 4. Limonite may be associated with hydrothermally altered rocks as a result of weathering of pyrite or hematite or other iron-bearing minerals. Gossans typically have an intense ferric iron absorption. However, some limonite may also be disseminated in sedimentary, volcanic or metamorphic rocks and is unrelated to any epigenetic hydrothermal alteration. Field evaluation is needed to absolutely distinguish hydrothermally altered rocks from those that may only include some limonitic materials due to weathering of syngenetic iron-bearing minerals. For example, weathering of biotite and other mafic minerals in granite or metamorphic rock may produce hematite on some outcrops.

Laboratory spectral reflectance measurements of representative rock samples collected from the EMNSA were made using a Beckman UV5240 spectrophotometer, with HALON as a reflectance standard. Four to six representative rock samples were collected from outcrop for the laboratory measurements. Two or three spectral reflectance measurements were made on the weathered surface of each sample to assure that recorded measurements were consistent. The spectral curves were averaged for plotting. Some of these data, which measure spectral reflectance from 400 nm to 2,500 nm to encompass the wavelength range of the TM channels, are reproduced in figures 11

through 22. Note that many of the igneous rock samples are spectrally flat so that they will not show a distinctive color in the image. The red color response of overlying vegetation will mask these rocks and any derived soils. The altered samples, such as the rock spectra of figures 9 to 12 display deep absorption bands between 2,200 nm and 2,350 nm which correspond to TM band 7. Carbonate samples typically display absorption features from 2,331 nm to 2,335 nm, which also correspond to band 7.

The most obvious area of alteration in the EMNSA as defined by the CRC color assignments is in the Castle Mountains, which includes the Hart Mining District (fig. 10; pl. 2). Clusters of white pixels are surrounded by yellow and green pixels. Similar areas of alteration may be represented by the white-to-yellow clusters of pixels in the area of the southeastern Providence Mountains. Some of the areas correspond to workings at the Hidden Hill Mine, near the southern tip of these mountains; others have not been checked in the field. From the yellow to white colors on the CRC, there appear to be some areas of alteration within the south central Hackberry Mountain where Proterozoic granitoids are in contact with Tertiary volcanic rock (fig. 10; pl. 1). Some groups of yellow-white pixels correspond with the northern part of the Hackberry Mountain where field checking has confirmed alteration of the volcanic rocks. Another grouping of small numbers of alteration-related pixels is present in the Ivanpah Mountains where yellow to white colored pixels are displayed in the image on the southern and eastern slopes. This region includes the recently (1990) active Morning Star Mine (fig. 10; pl. 2). There are also small skarn deposits of various types (pl. 2) located at the contact of carbonate rocks with quartz monzonite on the western slopes of the Ivanpah Mountains and Mescal Range, and these correspond to pixels showing the yellow and white image pixels.

There are small clusters of yellow pixels spread throughout the alluvial areas. Many of these may correspond to areas of exposed soil where cattle have frequented wells. Some others seem to correspond to mine workings, as in the Tungsten Flat area of the Signal Hill Mining District (pl. 2). However, there is no widespread exposure of apparently altered rock at these localities.

The magenta color in the CRC in the area of the northeastern slope of the New York Mountains corresponds to outcrops of carbonate rocks that are intruded by granite. This area has also been the site of some skarn-type mineralization.

Granite outcrops in the Granite Mountains are present at low elevations as boulders and unvegetated talus and appear blue in the image. The fracture pattern typical for granite can be seen in the CRC, both at low and high elevations, but lichen cover at high elevations causes a red color response in the image (fig. 10).

Additional areas in the EMNSA that show a yellow to white color on the CRC need to be field checked in order to deny or confirm the presence of hydrothermal alteration. There may be other causes of the color responses in the CRC. Further processing of the TM data may reveal a more

direct correspondence with hydrothermal alteration on the ground and may also allow a better discrimination of the various rock types that crop out over the EMNSA.

## **GEOCHEMISTRY**

This section of the report is comprised of two parts. In the first part, the RASS, PLUTO, and NURE computerized data bases of the U.S. Geological Survey are examined, largely from the basis of regional geochemistry. In addition, some descriptions of a select number of mineral occurrences obtained during our investigation are included. Table 3 lists sources of data that have been released, and tables 4 and 5 respectively list geochemical data and sample descriptions from some select rocks collected by us from a small number of mineralized systems in the EMNSA. In the second part, we examine the implications of data obtained from analyses of 1,050 rocks by the U.S. Bureau of Mines (1990a) from various sites within the EMNSA; these samples are mostly mineralized or altered samples from mines and prospects.

### **RASS, PLUTO, AND NURE Data Bases**

The objective of the examination of RASS, PLUTO, and NURE data is to recognize geochemical patterns that might be related to mineralization. Application of the principles of mineral-deposit models (Cox and Singer, 1986) includes the recognition of characteristic geochemical signatures for each model. The regional geochemistry addresses geochemical signatures in terms of possible mineral deposits without regard to the size or grade of the deposits. The discussion of the geochemistry of each area includes some descriptions of known mineral occurrences and classifies them in terms of mineral deposit models.

Analytical data for the East Mojave National Scenic Area stored in the RASS, PLUTO, and NURE data bases were retrieved and examined using the STATPAC system (VanTrump and Miesch, 1977) of the U.S. Geological Survey. The RASS and PLUTO data bases contain data for rock, stream-sediment, heavy-mineral-concentrate, soil, and other types of geologic samples collected by the U.S. Geological Survey. They also contain data for other sample types such as water and vegetation. The NURE data base contains data for samples collected during the National Uranium Resource Evaluation Program of the U.S. Department of Energy (Cook and Fay, 1982).

The RASS and PLUTO data bases were designed and managed, respectively, by the Branch of Exploration Geochemistry and the Branch of Analytical Laboratories before the merger of the two branches into the Branch of Geochemistry in 1987. The two data bases are similar in content and characteristics, but major differences in operation have hindered merger into a single data base. In addition, the logistical problem of merging two large data bases is a major obstacle during a time of limited budgets. Since merger of the two branches into the Branch of Geochemistry, most new

data have gone into the PLUTO database. However, most of the data for the EMNSA were obtained before 1987 and therefore are resident in both RASS and PLUTO. Before the merger of the branches in 1987, RASS data tended to be from large mineral-resource evaluations of public lands or other large projects while the PLUTO data base tended to receive data from more specialized projects and from a wider variety of types of projects. Both the RASS and PLUTO data bases include systems of coding sample descriptions and other information; because of the general nature of the data going into the two systems, the RASS system of coding is simpler but less comprehensive than the PLUTO system. The PLUTO system of coding offers a great deal of flexibility and the opportunity to describe a sample quite precisely but is consequently more cumbersome. The two data bases may eventually be supplemented or replaced by a newer, state-of-the-art system.

The data for selected elements useful in mineral-resource evaluations were studied and map plots were produced. The data in the RASS, PLUTO, and NURE data bases are available to the public, but most of the data have not been released as published or open-file reports; table 3 lists sources of data that have been released.

#### Sample Types

Sieved stream-sediment samples, heavy-mineral-concentrate samples (panned from stream sediments in most cases), and rock samples were the sample media from the RASS and PLUTO data bases that were considered, because they were the most widely sampled media in the study area and are the standard sample media for mineral-resource evaluations by the U.S. Geological Survey. The PLUTO data base contained some samples with very approximate coordinates (rounded to one-half minute or more of latitude or longitude), and these samples were not considered in this study, thus ensuring that plotted localities are within about one-half mile of actual localities.

Standard coding in the RASS and PLUTO data bases does not always specify the size fraction analyzed for the stream-sediment samples. Examination of the original requests for analysis or consultation with the original investigators confirmed that the minus-80 mesh (<0.177 mm) fraction of each of the stream-sediment samples was the fraction analyzed.

Heavy-mineral-concentrate samples from the RASS data base are the nonmagnetic heavy fraction of stream sediments, except that 15 samples from the west side of the Ivanpah Mountains were panned from mine-dump material. The RASS concentrate samples were prepared by subjecting panned samples to a series of magnetic and heavy-liquid separations, resulting in samples consisting of nonmagnetic ore minerals and heavy accessory minerals such as sphene and zircon. The PLUTO heavy-mineral-concentrate samples were all derived from stream sediments; after panning, the highly magnetic minerals (mostly magnetite) were removed with a hand magnet

and the less magnetic fraction was ground and analyzed (Jean Juillard, oral commun., 1991). Because of the major difference in the processing of RASS and PLUTO heavy-mineral-concentrate samples, they were treated as different sample media in the data analysis; drastic differences in concentrations of common elements such as Fe, Ca, and Mn confirmed that the RASS and PLUTO concentrate samples should be treated as different sample media.

Of the 944 RASS and PLUTO rock samples, about 700 are specified by coding or by notes to be samples of mineralized or altered rock or are from faults. These 700 samples may be thought of as samples of the channels where mineralizing fluids passed. Coding for about 140 of the 944 samples does not indicate whether they are of economic significance; the range of concentrations for most elements in these approximately 140 samples is 1-2 orders of magnitude and the maximum concentrations indicate some samples may be mineralized. In any case, concentrations significantly above expected regional background are of interest, especially if several elements are anomalously high (geochemical signatures) in the same samples or same areas. When considered from the standpoint of mineralized rocks, the geochemical signature is more important than absolute concentrations, because there is usually no way of determining the exact nature of the sample or the intent of the sampler. For example, the sample may be from a highly mineralized vein, may be a composite of dump samples, or may be a sample of altered but not obviously mineralized rock. For this mineral-resource evaluation, data from all 944 rock samples were combined for data analysis and considered from the standpoint of mineralized rocks.

The NURE data consist of analyses of the 35- to 18-mesh (0.5 to 1.0 mm) fraction of stream sediments from the Kingman quadrangle and of the minus-100 mesh (0.149 mm) fraction of stream sediments and soils from the Needles, San Bernardino, and Trona quadrangles. The data also contain 13 playa sediments. Comparison of the minus-100 mesh stream-sediment and soil data showed that the two media could be combined into one dataset, and this was done. Comparison of data from the Kingman quadrangle (35-18 mesh) with data from the Needles-San Bernardino-Trona quadrangles (minus-100 mesh) showed biases in the means of the concentrations of as much as two to one for the nine elements included in this report and analyzed in samples from both areas (Ce, Dy, Eu, La, Lu, Sm, Th, U, and Yb). However, the bias was high for Ce, Dy, Eu, and Lu in Kingman samples and high for La, Sm, Th, U, and Yb in Needles-San Bernardino-Trona samples; therefore, the biases in the means are difficult to attribute to differences in sample grain size and may represent geologic differences or analytical biases.

#### Evaluation of Data

The standard method of analysis for RASS and PLUTO samples was semiquantitative, direct-current arc emission spectrography (Grimes and Marranzino, 1968; Myers and others, 1961); RASS samples were usually analyzed for 31 elements by this method while PLUTO samples were

analyzed for those 31 elements plus about 15 more, mostly rare earth elements (REE). RASS and PLUTO samples from some specific areas in the EMNSA were analyzed by atomic absorption and other methods; these additional analyses were examined but their usefulness is limited because of poor areal coverage.

Concentrations of elements determined by the emission spectrographic method are usually reported as six steps per order of magnitude that represent intervals of some power of 10 times 1.2 to 1.8, 1.8 to 2.6, 2.6 to 3.8, 3.8 to 5.6, 5.6 to 8.3, and 8.3 to 12 (Motooka and Grimes, 1976). For most samples in this report, those intervals are represented by the values 1.5, 2, 3, 5, 7, and 10, respectively (or powers of 10 of these numbers). For some samples the reported values are somewhat different but still represent approximately the same intervals. Upper and lower limits of determination (table 6) varied somewhat with method and with time during the approximately 6-year period when the samples were analyzed. These variations are reflected in table 6 by ranges of lower determination limits and by some maximum concentrations greater than the customary upper determination limits listed. The precision of the emission spectrographic method is approximately plus or minus one reporting interval at the 83 percent confidence level and plus or minus two reporting intervals at the 96 percent confidence level (Motooka and Grimes, 1976).

In the NURE program, stream-sediment and soil samples were routinely analyzed by neutron activation analysis for approximately 17 elements (Cook and Fay, 1982). These routine procedures did not include most of the elements that are generally of interest in mineral resource evaluations. The NURE program made extensive use of a supplemental package of analyses that includes most elements of interest in the search for hydrothermal ore deposits, but those supplemental analyses were performed only on samples from the Kingman quadrangle. In addition, there are many discrepancies between the digital NURE data base and the published reports concerning whether analyses, on the one hand, were performed and reported concentrations were less than the limits of determination, or whether analyses, on the other hand, were not performed. Therefore, the NURE data base is of limited usefulness for evaluations of elements that might be indicative of hydrothermal processes but is useful for evaluating the presence of U, Th, and REE. Coefficients of variation for three NURE stream-sediment or soil samples that were each analyzed by neutron activation analysis for various elements from 16 to 297 times ranged from 5.0 to 47.8 percent (Cook and Fay, 1982, table 2).

RASS and PLUTO 31-element emission spectrographic data for stream-sediment samples appeared to be compatible, and thus the two data bases were merged into one dataset for statistical evaluation and map plotting. RASS and PLUTO 31-element emission spectrographic data for rocks also appeared to be compatible, and they were also merged into a single dataset. The additional elements, mostly REE, analyzed by emission spectrography for PLUTO stream-sediment samples and rock were treated as separate datasets. Data for RASS and PLUTO

concentrate samples were treated as separate datasets because differences in sample preparation led to incompatible geochemical results.

#### **Data Coverage**

Figure 23 shows geographic areas covered by the geochemical datasets in and along the border of the EMNSA. This map is used as a base for other figures in this section of the report.

Sampling localities for the various sample media are shown in figures 24 to 27. Stream-sediment samples (fig. 24) were collected in almost all of the areas outlined on figure 23; sampling density is quite sparse except in areas in the Clark Mountain Range, the Ivanpah Mountains, and the Providence Mountains. PLUTO concentrate samples (fig. 25) are quite evenly but sparsely distributed throughout the area. RASS concentrate samples (fig. 25) are limited to several areas and sampling density is fairly adequate for geochemically characterizing those areas; the Providence Mountains were heavily sampled, allowing an excellent geochemical characterization of that area. Distribution of sampling sites of rocks (fig. 26) is spotty and is dominated by heavy sampling in the Providence Mountains. NURE samples (fig. 27) are distributed fairly uniformly, although somewhat sparsely.

#### **Geochemical Evaluation**

Symbol plots of selected elements in the various sample media were prepared in order to show geochemical trends in the EMNSA and adjacent areas. The selected elements were the possibly ore-related elements Ag, As, Au, B, Ba, Be, Bi, Co, Cu, Mn, Mo, Nb, Pb, Sb, Sn, Th, U, W, and Zn. Also included, because of the proximity of the Mountain Pass REE deposit, were the rare earth-elements La, Ce, Dy, Eu, Lu, Nd, Sm, Tb, and Yb.

Table 6 lists statistics for the selected elements based on samples from the EMNSA and the surrounding area from 34°30' to 35°45' North latitude and 114°45' to 116°15' West longitude. Threshold concentrations, defined as highest background concentrations, were selected by visual and statistical examination of the data, by observation of elemental concentrations near known mineralized areas, and by reference to published reports of specific geochemical studies of areas within the study area. The threshold concentrations listed in table 6 for the EMNSA are regional thresholds and do not take into account any variations in bedrock or other factors. Table 6 includes published threshold concentrations established for two wilderness study areas within the EMNSA (Goldfarb and others, 1988, table 3; Miller and others, 1985, tables 1,2); these are included for reference and illustrate how threshold concentrations vary with scale of the study, local bedrock-mineralization and the judgment of the individual investigator.

Because lower limits of determination for emission spectrographic techniques are high relative to average crustal abundances for some elements (Au, Ag, As, Sb, Bi, Th, and W), any detectable concentration for these elements is anomalous, depending on sample type; some of the rare earth

elements also fall in this category (Tb, Dy). For elements with a wide range of detectable concentrations, a "high" category is included and plotted on figures 28 to 47. Because some subjectivity is involved in establishing threshold concentrations, inclusion of a "high" category shows the appearances of geochemical patterns if slightly lower thresholds are chosen.

The high proportion of samples with anomalous concentrations of Ag, Ba, Cu, Mo, Pb, and Zn in rock and heavy-mineral-concentrate samples (table 6) is the result of the large number of samples collected in highly mineralized parts of the Providence Mountains.

Figures 28-47 show the map distributions of anomalous and high concentrations of elements in the various sample media. Each figure plots no more than four elements and these are represented by vertical, horizontal, and diagonal lines. Where any detectable concentration of a given element is anomalous, only the samples with anomalous concentrations are plotted; otherwise, anomalous concentrations and high concentrations are shown as lines of longer and shorter length, respectively.

Any geochemical evaluation of geologic terrane has to deal with the issue of determining which elemental concentrations are background and which are anomalous. This issue becomes more difficult when a wide range of rock types is present. For example, the average concentration of cobalt in mafic rocks is 48 ppm (parts per million), but in granites the average concentration is 1 ppm (Rose and others, 1979, p. 554). If high concentrations of cobalt are accompanied by high concentrations of other common constituents of mafic rocks, such as Ni and Cr, high concentrations of cobalt might be due to the presence of mafic rocks and therefore will probably not be anomalous. On the other hand, if high concentrations of cobalt are accompanied by high concentrations of base metals but not by Ni and Cr, then hydrothermal activity may be the reason for the high concentrations; cobalt is part of the geochemical signature for a number of mineral-deposit types (porphyry copper, for example) that are not associated with mafic rocks (Cox and Singer, 1986). Therefore, the recognition of geochemical signatures is an important part of this geochemical evaluation of the EMNSA in view of the wide range of bedrock types. The following suggestions as to permissive mineral-deposit types in each of the areas discussed are based on the general types of bedrock in a given area and the geochemical signature for the area.

A special problem in the identification of geochemical signatures in the EMNSA is that of the recognition of REE signatures inasmuch as the rare earths tend to be present together (Levinson, 1980, p. 868) whether in accessory minerals, such as apatite or monazite, or in economic deposits, such as at the Mountain Pass Mine. Also, REE tend to be present in high concentrations in granites of the EMNSA (D.M. Miller, written commun., 1991) and especially in syenite, also a fairly common rock type in the EMNSA. Thresholds for REE listed in table 6 were established based on concentrations in RASS-PLUTO stream-sediment and NURE sediment-soil samples collected within about 0.8 km of the Mountain Pass Mine and also 3.2 to 4.8 km away from the

mine but downstream. These samples showed an association of REE, Ba, and Sr, all components of the ore in the Mountain Pass Mine.

Based on mineral-deposit occurrences and on geologic studies of the EMNSA and surrounding areas, the EMNSA has potential for many types of mineral deposits, including porphyry Cu-Mo deposits, precious and base metals (polymetallic) in veins or replacement bodies, gold deposits of several types (Au breccia and volcanic-hosted Au), various types of mineralized skarn, and U-Th-Nb-REE-bearing carbonatites or pegmatites. Table 7 summarizes the geochemical results on an area-by-area basis. The areas are discussed in more detail below. The combined RASS and PLUTO stream-sediment datasets are referred to as stream-sediment samples, whereas the combined NURE stream-sediment and soil samples are referred to simply as NURE samples.

The following discussions of areas apply the qualitative terms "not," "weakly," "mildly," "moderately," or "highly" anomalous to each of the areas as a whole. These qualitative terms are based on the number and proportion of samples with anomalous concentrations, the number of elements present in anomalous concentrations, the intensity of the anomalous concentrations in individual samples, and the number of sample media with anomalous concentrations. A preponderance of high but not necessarily anomalous concentrations is the basis for regarding some areas as at least weakly anomalous (table 7) in terms of a given element. The rationale is that a mineralizing system at depth might result in what appears to be a high background; the geochemical signature then determines where the area falls on the scale between "not anomalous" and "highly anomalous." As always, the mineral resource potential of each area is determined by the geochemistry in conjunction with geologic, geophysical, and mineral-deposit studies and other evidence. As stated before, the geochemical signatures for each area are defined without regard to possible grade or tonnage.

Bedrock types in the following sections are listed according to relative abundance in each area. Elements are listed in the general order of those associated with various sulfide deposits, those associated with late-stage magmatic differentiates, and those elements that are part of the REE association; obviously, there is considerable overlap of these three associations.

#### Soda Mountains

Bedrock of the part of the Soda Mountains on the west border of the EMNSA (fig. 23) includes Jurassic and Cretaceous granitoid rocks and Mesozoic volcanic and sedimentary rocks (pl. 1). Some stream-sediment samples from the Soda Mountains have anomalous concentrations of Zn, B, Mo, and Sn. Concentrate samples contain anomalous concentrations of Cu, Ag, Zn, Mn, Pb, Au, Bi, Sn, Mo, Be, Th, Nb, La, Ce, Tb, Yb, and Dy. No rock samples were collected in the area. NURE samples have anomalous concentrations of Eu and Lu. The area is overall mildly

anomalous geochemically. Possible deposit types are porphyry Cu-Mo, polymetallic veins and replacement bodies, Cu or Pb-Zn skarns, and Th-Nb-REE bearing-pegmatite or carbonatite. The anomalous values of the Nb-REE elements in concentrate samples may have been derived from small outcrops of Proterozoic rock too small to show at the scale of our geologic map (pl. 1). Inasmuch as the Soda Mountains are outside the EMNSA, types of deposit are not shown on the compilation of the types of mineral deposits (pl. 2).

#### Little Cowhole Mountain

Jurassic or Cretaceous granitoid rocks of Cowhole Mountains and Cambrian dolomite are present in approximately equal amounts in the area of Little Cowhole Mountain (pl. 1). The granitoid rocks of Cowhole Mountains in places are cut by epidote-chlorite veins with or without quartz and pyrite, especially near their southwesternmost exposure in the Little Cowhole Mountains. Stream-sediment samples do not contain anomalous concentrations of any of the elements considered. Concentrate samples contain anomalous concentrations of Cu, Bi, Sn, Mo, Be, Th, and Tb. No rock samples were collected. The area is geochemically mildly anomalous. From the available geochemistry, possible deposit types are copper and tin skarns and Th-Be-REE-bearing pegmatites. Deposits known at Little Cowhole Mountain include the copper skarns at the Anthony prospects and at the El Lobo Mine (pl. 2). At the Anthony prospects (U.S. Bureau of Mines, 1990a, map no. 338, pl. 1), copper skarn is seemingly zoned mineralogically from tight, steeply dipping, in places well-bedded light-green pyroxene skarn to olive-green to -brown compact masses of approximately 100 percent andradite containing secondary copper minerals that replace chalcopyrite. Along the easternmost skarn at this locality, skarn is developed variably at least 500 m along the contact between granitoid of Cowhole Mountain and dolomite. The best concentration of secondary copper minerals are associated directly with the most intense retrograde alteration of andradite to epidote. The contact between granitoid of Cowhole Mountain in detail is quite irregular and the most continuously exposed pod of skarn has a width of approximately 100 to 150 m. In all, some skarn is exposed for more than 800 m along the contact. At the El Lobo Mine (U.S. Bureau of Mines, 1990a, map no. 339, pl. 1), extensive banded, brown-black garnet-pyroxene skarn in places is mantled by early-stage calc-silicate hornfels, and cut by K-feldspar-chalcedonic quartz-bearing veins that include diffuse boundaries that fade into the surrounding groundmass of calc-silicate hornfels. Medial portions of the mm- to cm-sized veins are occupied by irregular concentrations of apple-green epidote. In places, ovoid pods of garnet-pyroxene skarn are approximately 100 m wide. The bulk of the sulfides, mostly chalcopyrite, apparently are associated with epidote-altered garnet-pyroxene skarn. In addition, some coarsely crystalline sphalerite, in masses approximately 0.5 cm wide, is intergrown with epidote. The granitoid of

Cowhole Mountain, in the area immediate to the El Lobo Mine, is mostly a partly chloritized, hornblende diorite that includes less than 1 volume percent dispersed cubes of iron oxide that replace pyrite. One of the prospect pits at the El Lobo Mine shows intense development of siderite to be controlled strongly by minor structures striking north-south, and dipping approximately 40° west. Nonetheless, the overall concentration of secondary copper minerals in the general area is relatively weak.

#### Cowhole Mountain

Bedrock of Cowhole Mountain includes Jurassic or Cretaceous granitoid rocks, Jurassic quartz arenite, Mesozoic volcanic and sedimentary rocks, Cambrian dolomite, Devonian to Permian limestone, and Early Proterozoic gneiss and granitoid rocks (pl. 1). The only element present in anomalous concentrations in samples from Cowhole Mountain is Mo in the lone concentrate sample from the area. No rock samples were collected. The area is not geochemically anomalous, based on the RASS and PLUTO stream-sediment data sets and NURE samples. In addition to the polymetallic and iron skarn shown on plate 2 in the northern part of Cowhole Mountain (U.S. Bureau of Mines, 1990a, pl. 1, map nos. 343-344), the polymetallic skarn at the Mosaic Queen (no. 344) is the proximal occurrence in a genetic sense, of a fairly continuous zone of metallization that extends along a strike length of about 0.5 km in a northwest-southeast direction. At its southeasternmost end, unprospected metallization in places as much as 30 m wide is dominated by massive replacement of Cambrian dolomite and Devonian to Permian limestone by specularite associated with epidote. Some coarsely-crystalline specularite crystals are as much as 1 cm wide, and the specularite replacement bodies show very sharp contacts with fractured and altered limestone. The iron metallization becomes dominated by a magnetite-garnet-pyroxene skarn alteration somewhat to the south of the Mosaic Queen, and some pendants of limestone have been converted almost entirely to massive epidote that includes some disseminated, fine-grained crystals of specularite. At the Mosaic Queen sucrosic, gray-white marble weathers pinkish-tan and includes less than 5 volume percent calc-silicate minerals. Immediately above the major prospect pit there, magnetite-hematite is intergrown with olive-green to -brown massive garnet. Magnetite is definitely predominant over specularite. Samples analyzed by the U.S. Bureau of Mines (1990a) from this locality include as much as 3,900 ppm zinc, 2,600 ppm copper, and greater than 10,000 ppm lead.

#### Cinder Cone Area

Approximately equal map areas of Cretaceous adamellite and Pliocene and Pleistocene basalt lava flows dominate the Cinder Cone area due east of Baker in the northwest part of the EMNSA

(pl. 1). The Cinder Cone area, as defined for this section (fig. 23), includes the Halloran Hills. Lesser amounts of Early Proterozoic gneiss and granitoid rocks, at and to the east of Seventeen Mile Point, and Pliocene and Pleistocene basalt cinder deposits are also present. All sample media are represented in the samples collected in the Cinder Cone area. Many elements are present in anomalous concentrations in all sample media. Stream-sediment samples contain anomalous concentrations of Zn, Mo, Co, and B. Concentrate samples have anomalous concentrations of Cu, Mn, Ag, Zn, Co, Bi, Sn, Mo, Be, B, Th, Nb, Tb, and Yb. Rock samples have anomalous concentrations of Cu, Pb, Ag, Zn, As, Sb, Mn, Bi, Sn, Mo, and W. NURE samples contain anomalous concentrations of Th, Ce, and Eu. Possible deposit types, based on geochemistry, include porphyry Cu-Mo, polymetallic veins and replacement bodies, a variety of types of mineralized skarn, and Th-Nb-REE-bearing carbonatite and pegmatite. This large area is moderately anomalous based on the large number of elements present in anomalous concentrations even though the concentrations tend to be only weakly to moderately anomalous.

Types of deposits known in this general area include gold-silver quartz-pyrite veins, polymetallic veins, polymetallic fault, and polymetallic and tungsten skarn (pl. 2). Occurrences of polymetallic fault essentially are oxidized base- and precious-metal mineralized fault zones that include mostly fault gouge and breccia and lack well-developed concentrations of quartz and carbonate minerals as gangue. Most of these mineral occurrences are in the general area of Seventeen Mile Point and the Paymaster and Oro Fino Mines and these epigenetic occurrences are hosted by Early Proterozoic rocks. There is some likelihood that these areas may be parts of large slide blocks (H.G. Wilshire and J. Nielson, written commun., 1991). Approximately 50 percent of the occurrences have been classified as gold-silver quartz-pyrite veins. Generally, widely-spaced fractures showing northwesterly strikes are filled by brick-red iron oxides that locally include approximately 0.3-m-wide brecciated vein quartz. The attitudes of such mineralized fractures and veins are at very high angles to the metamorphic, ductile-style foliation in the enclosing gneiss and granitoid. At the main workings of the Paymaster Mine (U.S. Bureau of Mines, 1990a, map no. 353, pl. 1), there is a 1- to 2-m wide zone of brecciated gneiss and granitoid impregnated highly by vein quartz. Similarly, the zone impregnated by vein quartz, and presumably gold and silver, is at a high angle to the fabric of the enclosing metamorphic rocks. Some nearby veins pinch and swell, also at high angles to the metamorphic fabrics. At the Paymaster No. 3 Mine, mineralized gold-silver quartz-pyrite zones are as much as 2- to 3-m wide, have a N. 10° W. strike, and dip to the northeast. These zones extend at the surface as much as 50 m from the main portal.

Exposures near the central parts of sec. 22, T. 13 N., R. 10 E. contain epidotized granodiorite that may be the locus of emplacement of a widespread mineralized system that shows the general area of the gold-silver quartz-pyrite veins at the Paymaster Mine as a distal manifestation. In the

pediment area away from the major exposures of bedrock and approximately 0.8 km west of the Paymaster Mine, there are small pods of 1- to 2-m wide heavily epidotized granodiorite and possibly some hedenbergitic, calcic exoskarn, where the epidotized granodiorite is in contact with marble.

Gold-silver quartz-pyrite veins also appear to be the predominant type of deposit in the general area of the Oro Fino Mine, SE 1/4 sec. 23, T. 13 N., R. 10 E. Such veins have been emplaced along a west-northwest striking fault there that includes recrystallized, well-bedded marble and brecciated limestone in its hanging wall. The fault zone is at least 2 to 3 m wide, and shows ample evidence in outcrop of a brittle style of deformation; its dip is approximately 35° to 40° N. The brecciated limestone body is terminated to the east by another north-northeast striking fault that seems to have hosted the bulk of the mineralization explored in the workings. Near the head frame at these workings, very steeply dipping and shattered rocks crop out for distances as much as 5 to 6 m and have been explored by at least two shafts.

Some of the most intensely mineralized rock this area is in the immediate vicinity of the Oro Fino Mine and its nearby workings, in the SE 1/4 sec. 23, T. 13 N., R. 10 E. (U.S. Bureau of Mines, 1990a, map no. 356, pl. 1). This particular mine is designated incorrectly as the Brannigan Mine on the Old Dad Mountain, 15-minute quadrangle. At the Oro Fino Mine, a west-northwest striking mineralized fault includes recrystallized, well-bedded limestone and brecciated limestone in its hanging wall. Presumably these rocks are part of the Paleozoic sequence of rocks in the EMNSA, but they have not been mapped separately on the accompanying geologic map (pl. 1). The mineralized fault zone is 2- to 3-m wide, and dips 35° to 40° north, and includes gold-silver, quartz-pyrite-type veins along it. On the east, the limestone megabreccia in the hanging wall is bounded by a north-northeast-striking, mineralized structure that apparently hosted some of the most productive ore shoots at the mine and was explored by a major shaft and auxiliary levels. Heavily iron-oxide-stained quartz-pyrite veins show maroon- to brick-red colors, that grade into ochre-dominated colors. In the area of the main head frame, very steeply dipping shattered mineralized rocks along the north-northeast mineralized structure are as much as 5 to 6 m wide and explored by at least two shafts.

The workings of the Brannigan Mine are close to the SE corner of sec. 26 T., 13 N., R. 10 E., (U.S. Bureau of Mines, 1990a, map no. 362, pl. 1). Near these workings, some well-bedded quartzite includes a thin, quartz-pebble conglomerate at its base that lies unconformably on gneissic metaquartzite that presumably is Proterozoic in age. The quartzite is probably Late Proterozoic and Cambrian in age and is included with the Early Proterozoic gneiss unit on the geologic map of the EMNSA because of its limited areal extent (pl. 1). At the main workings of the Brannigan Mine (termed the Brannigan East by the U.S. Bureau of Mines (1990a), and subsequently reclaimed as the Rachele claim group), quartz-sulfide (pyrite) veins with or without chalcopyrite and tremolite

and(or) actinolite appear to have been the ore worked in the past. Some of these veins show altered, enclosing wall rocks that show a coarsely-crystalline dark green, possibly hedenbergitic pyroxene. Such zones of alteration and mineralization follow closely bands of dolomite in the Paleozoic rocks. A sample analyzed by the U.S. Bureau of Mines (1990a) from this locality included 8,750 ppb gold and 160 ppm silver to seemingly confirm thereby the high silver/gold ratio characteristic of many polymetallic veins in the EMNSA (see below).

In the Turquoise Mountain Mining District of the Halloran Hills, just outside the EMNSA, copper-molybdenum mineralization is reported to be related apparently to shallow-seated porphyritic intrusions (Hall, 1972). There is little known mineralization in Proterozoic rocks of this area. Mineralization at the Telegraph Mine (U.S. Bureau of Mines, 1990a; map no. 121, pl. 1), near the southeast end of the Halloran Hills, includes low-sulfide, vug filling quartz veins that are gold- and silver-bearing and that were emplaced approximately at 10 Ma (Lange, 1988). These veins cut the Cretaceous Teutonia Adamellite of Beckerman and others (1982) and they are classified by us as gold-silver, quartz-pyrite veins that are epithermal and wrench fault-related (see below). Early Proterozoic rocks in southeastern parts of the Halloran Hills lie within the Cinder Cones Wilderness Study Area where Wilshire and others (1987) found no evidence of mineralization. Wilshire and others (1987) assigned a low potential for gold and silver to areas underlain by Early Proterozoic rocks primarily because of their proximity to Cretaceous plutonic rocks, thought elsewhere in the region to be associated genetically with mineralization in Proterozoic wall rocks (Hewett, 1956). However, neither indications of mineralization in the vicinity of those contacts nor signs of prospecting were found by Wilshire and others (1987).

### Marl Mountains

Bedrock geology of the Marl Mountains, approximately 6 km northeast of Kelso Peak, is dominated by Cretaceous adamellite (pl. 1). Early Proterozoic gneiss and granitoid rocks are also present. Stream-sediment samples from the Marl Mountains have anomalous concentrations of Pb, Ag, Zn, and Mo. Concentrate samples have anomalous concentrations of Cu, Ag, Zn, Au, Bi, Sn, Mo, Th, La, Ce, Nd, Sm, Tb, Yb, and Dy. No rock samples from the Marl Mountains are available. NURE samples have anomalous concentrations of Th, La, Eu, and Dy. The area is moderately anomalous geochemically. Deposit types possible from these data include porphyry Cu-Mo, polymetallic veins and replacement bodies, and REE-Th-bearing carbonatite and pegmatite. Cretaceous adamellite in the Marl Mountains is known to include four polymetallic veins, five gold-silver quartz-pyrite veins, and one polymetallic fault (pl. 2).

## Old Dad Mountain

No single rock type dominates Old Dad Mountain and its surrounding area (pl. 1). The promontory at Old Dad Mountain itself is underlain by a resistant knob of limestone that is part of the Devonian to Permian limestone unit. Units present are Early Proterozoic gneiss and granitoid rocks, Devonian to Permian limestone, Jurassic granite, Mesozoic volcanic and sedimentary rocks, Late Proterozoic and Cambrian siliciclastic rocks, and Tertiary volcanic rocks. Dunne (1972, 1977) mapped the Old Dad Mountain area and included all Proterozoic rocks in a single metamorphic rock map unit; he provided scanty information on these rocks. Hewett (1956) reported the presence of granite, schist, and quartzite intruded by syenite dikes. Stream-sediment samples from Old Dad Mountain do not have anomalous concentrations of any of the elements considered. Concentrates have anomalous concentrations of Cu, Pb, Ag, Bi, Sn, Th, and Tb. Rocks have anomalous concentrations of Cu, Pb, Zn, Ag, Au, Co, Mo, Bi, B and Be. NURE samples have anomalous concentrations of Eu. The area is mildly anomalous geochemically. Porphyry Cu-Mo deposits, polymetallic vein or replacement bodies, mineralized skarn, pegmatites, or carbonatites may be present on the basis of the elemental concentrations above. The area in the vicinity of Old Dad Mountain under discussion here extends approximately 16 km in a northwest-southeast direction from south of Seventeen Mile Point to south of the Kelso Mountains (pl. 1). From northwest to southeast, the types of deposits in the vicinity of Old Dad Mountain include polymetallic faults at the Sweet (Reviella) claim group (U.S. Bureau of Mines, 1990a, map no. 366) and Lucky (ODM) claim group (map no. 368), some polymetallic veins also at the Lucky (ODM) claim group, and iron skarn at the Old Dad Mountain iron deposit (map no. 369) showing also some minor amounts of polymetallic vein present. In addition, there is copper- and zinc-bearing magnetite skarn at the Golden M (map no. 372) approximately 3 km southeast of the main promontory at Old Dad Mountain itself (pl. 2) that we classify as polymetallic skarn.

Although these four mineralized occurrences extend almost across the entire length of the Old Dad Mountain area, surface indications of alteration are confined to the general areas of the mineralized occurrences. However, alteration is well-exposed and widespread at one of the occurrences. At the Lucky (ODM) group of claims, a zone of chloritic alteration, as much as 150 m thick and containing abundant iron oxides (presumably after iron sulfide(s) of some type), is present in Cambrian and Late Proterozoic siliciclastic rocks (map unit CZs, pl. 1), that as mapped includes shattered and chloritized granodiorite. Some of this granodiorite contains fault zones filled by 0.3 m-wide ochre gossan. Recrystallized limestone, presumably part of map unit PDI and seemingly in tectonic contact with the siliciclastic rocks, overlies the siliciclastic rocks and, in places, is laced with iron-oxide strained fractures. Shattered siliciclastic rocks below the contact

show fairly abundant secondary copper minerals on their weathered surfaces together with some glassy-appearing, vein-type quartz. The exposed width of these shattered rocks showing signs of mineralization at this particular locality is as much as 150 m and the strike length is approximately 3.5 to 4 km. Some narrow, sulfide-impregnated rhyolite or rhyodacite, clay-altered dikes, that contain 5 to 15 volume percent phenocrystic quartz, have been emplaced into the shattered siliciclastic rocks and apparently are related genetically to the surrounding alteration. A select sample analyzed by the U.S. Bureau of Mines (1990a) from this locality includes about 500 ppb gold. In many gold-rich porphyry-type systems, 500 ppb is the concentration of gold in many of the ore zones (Sillitoe, 1979), and this value of gold in select samples is considered by many exploration geologists to constitute a threshold that warrants additional investigation. As a comparison, geochemical studies of the Kalamazoo porphyry copper deposit, Ariz., show that the ore there, not known particularly for its gold content, contains as much as 800 ppb gold along some extended intercepts of drill core (Chaffee, 1976). Much of the area of Old Dad Mountain is included within a tract permissive for the presence of iron skarn on the basis of fairly contiguous positive magnetic anomalies as we describe below. However, the alteration in the general area of the Lucky (ODM) group of claims suggests that other types of occurrences may be present, including porphyry gold and polymetallic replacement (see below), in addition to those already listed above.

At the Old Dad Mountain iron deposit, massive magnetite-hematite replacement bodies show knife-edge contacts with the surrounding coarsely crystalline, brecciated white marble. The U.S. Bureau of Mines (1990a) estimates 400,000 to 500,000 tons of magnetite-hematite-rich rock remain in place at this locality. Much of the magnetite is intergrown with actinolite, and seems to be related genetically to a highly schistose, chloritized granodiorite, not shown on plate 1 because of its relatively small size, that is cut by magnetite-actinolite-epidote veins. Blades of actinolite commonly are present in clusters as much as 2 to 4 cm wide. In addition, the schistose granodiorite shows some early-stage gray-green pyroxene hornfels near its contacts with limestone. The apparently richest pods of magnetite-bearing rock formed in limestone that crops out somewhat away from the actual contact with schistose granodiorite, perhaps as much as 5 to 10 m from the contact. Overall, the mineralization at this locality is associated with a low-sulfur-bearing environment, although minor amounts of secondary copper minerals, probably chrysocolla, are present in some of the pods of magnetite as alteration products of chalcopyrite.

At the Golden M polymetallic skarn occurrence, most mineralization is confined to an approximately 1-m wide minor fault zone that strikes about N. 40° E., dips 80° to 90° south and that separates a small mass of Proterozoic gneiss, included with undivided Mesozoic volcanic and sedimentary rocks (map unit MZv, pl. 1), from Permian to Devonian limestone (map unit PDI). The fault zone is at a high angle to foliation in the gneiss. Secondary copper minerals are present

in most masses of magnetite-epidote that form highly irregular replacement pods along a strike length of about 150 to 300 m. Some garnet skarn that is olive-green-brown in color shows impregnation by reticulated, mm-sized veinlets of magnetite. In addition, much of the limestone close to the workings (2 adits and an incline) is heavily stained by orange iron oxide(s) suggestive of impregnation by some iron sulfides. One of the samples analyzed by the U.S. Bureau of Mines (1990a) from this locality includes more than 500 ppb gold.

### Kelso Mountains

Bedrock of the Kelso Mountains includes Early Proterozoic gneiss and granitoid rocks, Late Proterozoic and Cambrian siliciclastic rocks and Cretaceous granitoid rocks (pl. 2). Concentrate samples have anomalous concentrations of Cu, Ag, Au, W, La, Ce, Nd, Sm, Tb, and Dy. NURE samples contain anomalous concentrations of La and Dy. There are no rock samples from the area in the data bases. The area is geochemically mildly anomalous overall. Mineralized skarns and REE-bearing pegmatite and carbonatite are possible deposit types. The Kelso Mountains are characterized by a REE geochemical signature, although the presence of Cu, Ag, and Au may be indicative of the presence of polymetallic veins. Types of mineral occurrences known in the general area of the Kelso Mountains include polymetallic fault, gold-silver quartz-pyrite vein, and polymetallic vein (pl. 2). Most of these occurrences, 12 in all, are associated spatially with Late Proterozoic and Cambrian siliciclastic rocks that crop out in the southeastern part of the Kelso Mountains (pl. 1). The two gold-silver quartz-pyrite veins known here crop out in areas underlain by Early Proterozoic gneiss and granitoid rock. These spatial associations between type of mineral occurrence and host rock suggest derivation of some of the gold and silver from Early Proterozoic gneiss and granitoid rock as we describe below. We presume the known mineralization in the general area of the Kelso Mountains to be related to Mesozoic magmatism. However, Jurassic or Cretaceous granitoid rock (pl. 1) that crops out in the southern part of the Kelso Mountain area is not known to host any metallic mineral occurrences. Analyses of mineralized rock from the area of the Kelso Mountains further suggests that overall intensity of precious-metal mineralization here is less than that found elsewhere in the EMNSA (U.S. Bureau of Mines, 1990a). Only two analyzed samples of mineralized rock contain more than 500 ppb gold at the 12 sites.

### Bristol Mountains

Bedrock of the Bristol Mountains at the edge of the EMNSA near its southwest corner and northwest of the Granite Mountains consists of Jurassic granitoid rocks. Stream-sediment samples in the Bristol Mountains contain anomalous concentrations of Mn, Pb, Zn, Sn, Mo and B. Concentrate samples contain anomalous concentrations of Cu, Mn, Ag, Zn, Be, Nb, La, Nd, Sm,

Eu, Yb, and Dy. NURE samples have anomalous concentrations of Yb and Eu. The data bases contain no rock data. The area geochemically is mildly to moderately anomalous overall. Skarn, polymetallic vein or replacement bodies, and REE-bearing carbonatite or pegmatite are possible deposit types. We have not classified or shown the distribution of the types of mineral occurrence present in the Bristol Mountains.

### Clark Mountain Range

Bedrock of the Clark Mountain Range includes Early Proterozoic granitoid rocks and gneiss, Late Proterozoic and Cambrian siliciclastic rocks, Cambrian dolomite, and Devonian to Permian limestone (pl. 1). The Clark Mountain Range is moderately to highly anomalous from a geochemical standpoint. Many elements are present in anomalous concentrations in all sample media (table 7). Present and past mining activities emphasize the anomalous geochemistry of the area. The presence of the Mountain Pass carbonatite-hosted REE deposit is reflected by anomalous concentrations of REE in concentrate and NURE samples. Other possible deposit types in the Clark Mountain Range include porphyry Cu-Mo, polymetallic vein and replacement bodies, skarn, and pegmatite, based on the anomalous metal concentrations. Types of mineral occurrences and deposits in the Clark Mountain Range include: (1) silver-copper veins in brecciated dolostone; (2) polymetallic veins; (3) gold breccia pipe at the Colosseum Mine (see below); (4) tungsten veins; (5) barite veins; (6) polymetallic replacement; (7) copper skarn; (8) zinc-lead skarn; (9) gold-silver quartz-pyrite vein; (10) placer gold-PGE; and (11) polymetallic skarn (pl. 2). As we describe below, many of these deposits and mineral occurrences apparently are linked genetically as exemplified by many occurrences that surround the gold breccia pipe at the Colosseum Mine (Sharp, 1984). Silver-copper brecciated dolostone, tungsten veins, and barite veins apparently are related to emplacement of the gold breccia pipe at the Colosseum Mine during the Cretaceous (see below). All of the tungsten vein occurrences are present on the east side of the range and they are hosted by Early Proterozoic younger granitoids (map unit Xg1, pl. 1). In addition, on the west side of the range, some of the polymetallic replacement deposits and occurrences are present in an environment distal to polymetallic, copper, and zinc-lead deposits and occurrences (pl. 2). Lastly, mineralization at the Conquistador No. 2 Mine (U.S. Bureau of Mines, 1990a, map no. 70, pl. 1) apparently is related to development of the metamorphic fabric in the enclosing Cambrian and Late Proterozoic siliciclastic rocks (pl. 1). At this locality, there are a series of shafts and approximately 15 trenches and shallow prospects that explore a N.  $35^{\circ}$  E.,  $35^{\circ}$  to  $45^{\circ}$ -north dipping vein exposed discontinuously along a strike length of about 300 m. Where well exposed in the shafts, individual veins commonly are as much as 1 m wide and they show bleaching of the surrounding siliciclastic rocks for distances of about 3 m on either side of the trace of the vein segments. Quartz in the

veins is milky-white in color and typically includes some iron oxides that replace pyrite, which at one time constituted probably as much as 2 volumes percent of the vein. The fabric of the vein quartz parallels the schistosity in the surrounding siliciclastic rock. Elsewhere in the general area of the Conquistador No. 2 Mine, wispy, apparently deformed, stringers of vein quartz cut across the well-developed slaty cleavage in the siliciclastic rocks. The occurrences at the Conquistador No. 2 Mine are one of the few places in the EMNSA where mineralization seems to be associated with the metamorphic deformation that has affected the rocks. Nonetheless, our cursory examination of exposures of the siliciclastic rock in the general area of the Conquistador No. 2 Mine suggests that this type or style of mineralization is fairly isolated. There is no widespread development of a pervasive low-sulfide, gold quartz type of vein mineralization, as we classify the Conquistador No. 2 Mine following the criteria of Cox and Singer (1986) for these types of deposit.

#### Mescal Range

Bedrock of the Mescal Range includes Cambrian dolomite, Late Proterozoic to Cambrian siliciclastic rocks, Jurassic sandstone, Devonian to Permian Limestone and Cretaceous granitoid rocks (pl. 1). Concentrations of Pb, Zn, and Tb are anomalous in concentrate samples. There are no rock samples from the area shown as Mescal Range on figure 23. Polymetallic veins or replacements are the most likely deposit types in the area in as much as Early Proterozoic rocks hosting REE-bearing pegmatite and carbonatite do not crop out in this area. Known deposits and occurrences in the general area of the Mescal Range are predominantly zinc-lead bearing. They include zinc-lead skarn (exemplified by the Mohawk Mine), polymetallic skarn, polymetallic replacement, and polymetallic vein, and they are concentrated especially in the general area of several small bodies of Cretaceous monzogranite that crop out near the west end of Mohawk Hill in the northwestern part of the area of the Mescal Range (pl. 2). In addition, there are a small number of gold-silver quartz-pyrite veins and one placer gold occurrence, the latter present in gravels near the Mohawk Mine. The widespread presence of zinc-lead-bearing types of deposit here contrasts markedly with the copper-bearing types, classified mostly as copper skarn (pl. 2), just to the north of Mohawk Hill in the general area of the Copperworld Mine. However, the predominance of zinc-lead types of occurrences here does not exclude the possibility of significant precious-metal deposits being present. There are some fairly widespread exposures of coarse-grained monzogranite porphyry that are intensely propylitically and argillitically altered in association with emplacement of pyritic-bearing quartz veins and stockworks in the southern part of the Mescal Range. These exposures of altered monzogranite, shown as map unit Kg1 on the geologic map of the EMNSA (pl. 1), are in the general area of the Iron Horse (Bonanza), Lead Lady, and Blue

Buzzard Mines (U.S. Bureau of Mines, 1990a, map nos. 144-146, pl. 1). The mostly polymetallic replacement-type mineralization at these three deposits appears to be related to the altered monzogranite. However, analyses by the U.S. Bureau of Mines (1990a) of mineralized rock from these three deposits all show gold concentrations of <500 ppb (pl. 6). Nonetheless, many jasperoids in the general area of these deposits include gold concentrations in excess of 1,000 ppb, and related targets are currently (1991) being drilled by the exploration group of Phelps Dodge Mining Co. (John D. Forrester, oral commun., 1991). Additional discussion concerning genetic linkages among types of deposits is included below.

#### Ivanpah Mountains

Bedrock of the Ivanpah Mountains includes Jurassic granite, Early Proterozoic granitoid rocks, gneiss, and migmatite, Devonian to Permian limestone, Late Proterozoic and Cambrian siliciclastic rocks, and Cambrian dolomite (pl. 1). Stream-sediment samples from the Ivanpah Mountains contain anomalous concentrations of Cu, Ag, Zn, Mo, Sn and W. The other sample media contain anomalous concentrations of many elements that suggest the presence of polymetallic veins or replacement bodies, porphyry Cu-Mo deposits, skarns, and carbonatites or pegmatites containing deposits of REE or Th. Concentrate samples have anomalous concentrations of Cu, Mn, Pb, Ag, Au, Co, Bi, Mo, W, Sn, Be, Th, La, Ce, Nd, Sm, Tb, and Dy. Rock samples have anomalous concentrations of Cu, Zn, Co, Mn, Pb, Ag, As, Sb, Ba, Bi, Sn, Mo, Be, and B. NURE samples contain anomalous concentrations of Th, U, La, Ce, Lu, Sm, Eu, Tb, Yb, and Dy. Overall the Ivanpah Mountains are geochemically moderately to highly anomalous. Thick sequences of Paleozoic carbonate rock are exposed prominently in the Striped Mountain block of the Ivanpah Mountains area (pl. 1). Deposit types in this block include tungsten skarn, polymetallic fault, polymetallic vein, copper skarn, and one unnamed occurrence of low-sulfide, gold-quartz vein in the Cambrian and Late Proterozoic siliciclastic rocks (U.S. Bureau of Mines, 1990a, map no. 16, pl. 1). At the latter locality, shattered rocks, approximately 1 m wide, show local emplacement of quartz-pyrite-minor chalcopyrite veins at a high angle to the regional attitude of foliation in the surrounding siliciclastic rock. However, the vein quartz is itself deformed and shows a foliated fabric including lineated margins lacking carbonate minerals in its selvages. Approximate attitude of the veins is N. 40° W., with a 55° S. dip. Jasperoid along a 2- to 3-m-wide steeply dipping fault that strikes N. 35° W., at the Express Mine (U.S. Bureau of Mines, 1990a, map no. 171, pl. 1) has been explored by a 10- to 12-m-wide open cut and is classified by us as a polymetallic fault (pl. 2). In addition, the area of Striped Mountain contains a vast resource of limestone, apparently including also a large proportion of paper-grade limestone (U.S. Bureau of Mines, 1990a).

The bulk of the mineralization in terms of numbers of occurrences is present in Jurassic granitoid rock as polymetallic veins, gold-silver quartz-pyrite veins, polymetallic faults, zinc-lead skarns in pendants too small to show at the scale of the geologic map, and one fluorite vein (pl. 2). The gold-silver quartz-pyrite veins show no apparent lateral zonation relative to the distribution of polymetallic veins in this general area. The tin (tungsten) skarn mineralization at the Evening Star Mine (U.S. Bureau of Mines, 1990a, map no. 193, pl. 1) apparently is related to emplacement of Jurassic granitoid rock, although the main mass of the Jurassic granitoid rock crops out approximately 1 to 5 km east of the workings at the Evening Star Mine (pl. 1). Narrow dikes at the Evening Star Mine and at the nearby Standard No. 2 Mine are similar lithologically to Jurassic granitoid rock east of these two occurrences. At the Evening Star Mine, chalcopyrite-bearing tremolite hornfels is present near the outer limits of skarn development and is mantled by a zone of recrystallized limestone that includes fine-grained crystals of magnetite and(or) pyrite. In places, the marble has been dolomitized as much as 10 m away from some zones of heavily sulfidized, structurally controlled skarn. To the south-southwest of the Evening Star Mine, Jurassic granitoid has been converted to an epidote endoskarn showing relict outlines of plagioclase. Magnetite is abundant in many of the pods of skarn at the Evening Star Mine, and the magnetite seems to be one of the earliest post-silicate phases to crystallize in the open space environment of the skarns there.

#### Cima Dome

Bedrock of the Cima Dome area includes two bodies of Cretaceous adamellite made up of the Teutonia Adamellite and the Kessler Springs Adamellite, both of Beckerman and others (1982) and an elongate, northwest-trending body of Jurassic granite (pl. 1). Geochemical samples in the area of Cima Dome are represented by only one sample, a rock that contains an anomalous concentration of the element Tb. There is only one known mineral occurrence in the area of Cima Dome; this occurrence is at the Teutonia Mine (U.S. Bureau of Mines, 1990a, map no. 210, pl. 1). At the Teutonia Mine, polymetallic-vein mineralization is concentrated along a N. 60° W.-striking zone in the Kessler Springs Adamellite of Beckerman and others (1982). Alteration in the area of the mine extends approximately 20 to 30 m from some of the major strands of vein exposed by several currently inaccessible shafts, and alteration consists mainly of conversion of plagioclase to clay minerals, possibly including some halloysite. Some 4- to 5-cm wide greasy-gray veins of quartz show early-stage sulfide(s), now oxidized to ochre-brown iron oxides, primarily along the walls of the veins but also including some late-stage sulfide(s) along the medial parts of the veins. A select sample of ore obtained from a dump at the Teutonia Mine was examined using the scanning electron microscope. Silver-bearing minerals identified include galena and argentite.

Contents of silver in galena are highly variable even at the scale of the several-hundred-micron-wide domains examined. Some silver-bearing galena, as narrow 5 mm-wide rims surrounding discontinuously much larger crystals of sphalerite, is confined to short segments of the rims. The remaining galena is apparently free of any detectable silver. Some of the tetrahedrite detected is argentiferous and it seems to be paragenetically intermediate between early-stage sphalerite and late-stage galena that is notably nonsilver bearing. Other minerals detected during the scanning electron microscope study are aurichalcite (ideally  $2(\text{Zn}, \text{Cu})\text{CO}_2 \cdot 3(\text{Zn}, \text{Cu})\text{OH}_2$ ), barite, possibly specular hematite, covellite, and argentite. Argentite is present as feathery 2 to 3 mm long crystals on the borders of irregularly shaped crystals of galena. The argentite is mantled by covellite in places. Overall, the locality shows relatively sparse concentrations of secondary copper minerals, including both malachite and chrysocolla. Although some veins also include iron-carbonate minerals in them, the veins overall still retain a high quartz/carbonate mineral ratio. No carbonate minerals were noted in the walls of the veins. In places, vein material is coxcombed, brecciated, and filled by jasperoidal material. We have classified the mineralization at the Teutonia Mine as a silver-rich variety of polymetallic vein. Production from the Teutonia Mine apparently includes approximately 1,500 oz silver during 1880 (U.S. Bureau of Mines, 1990a).

### New York Mountains

The New York Mountains include extensive areas of Cretaceous adamellite (namely, the Mid Hills Adamellite of Beckerman and others, 1982) and Early Proterozoic migmatite and granitoid rocks and lesser amounts of Tertiary basalt and andesite, Devonian to Permian limestone, Cretaceous granodiorite, Tertiary dacite flows, Mesozoic volcanic and sedimentary rocks, Triassic sedimentary rocks, Cambrian dolomite, and Miocene rhyolite ash-flow tuff (pl. 1). Numerous elements are present in anomalous concentrations in all sample media from the New York Mountains. Geochemically, the area is one of the most highly anomalous in the EMNSA. Stream-sediment samples contain anomalous concentrations of Cu, Mn, Pb, Ag, Zn, Mo, W, Co, B and Be. Concentrate samples have anomalous concentrations of Cu, Mn, Pb, Ag, Zn, Co, Ba, Bi, Sn, Mo, W, Be, B, Th, Nb, La, Ce, Nd, Sm, Eu, Tb, Yb, and Dy. Rock samples have anomalous concentrations of Cu, Pb, Ag, Zn, Au, As, Co, Sb, Ba, Bi, Sn, La, Mo, and B. NURE samples have anomalous concentrations of Th, U, La, Ce, Lu, Eu, and Yb. Possible deposit types are porphyry Cu-Mo, polymetallic vein and replacement bodies, disseminated Au, skarn of all types, and U-Th-Nb-bearing carbonatite and pegmatite. The Mid Hills adamellite of Beckerman and others (1982) hosts the Big Hunch stockwork molybdenum deposit (U.S. Bureau of Mines, 1990a, map no. 290, pl. 1; Ntiamoah-Agyakwa, 1987) that shows intensely developed quartz stockworks cropping out across an area of approximately  $5 \text{ km}^2$  near the southwest edge of the

New York Mountains (pl. 2). In addition, the New York Mountains include the following types of deposit: (1) polymetallic fault, gold-silver quartz-pyrite vein and polymetallic vein in Early Proterozoic migmatite; (2) copper skarn and polymetallic skarn in Permian to Devonian limestone; and (3) polymetallic vein, polymetallic fault, gold-silver quartz pyrite vein, and tungsten vein in the Mid Hills Adamellite of Beckerman and others (1982). The most intense concentration of mineral occurrences and deposits is present in the Early Proterozoic migmatite (pl. 2). Analyses of mineralized rock from a cluster of these occurrences and deposits, in an area of about 20 km<sup>2</sup> near the site of Vanderbilt, show gold concentrations higher than 500 ppb (pl. 6).

#### Mid Hills

Cretaceous Mid Hills Adamellite and Rock Springs Monzodiorite, both of Beckerman and others (1982), and Early Proterozoic granitoid rocks are the predominant rock types in the Mid Hills (pl. 1). Tertiary tuffs are also present. Stream-sediment samples from the Mid Hills contain anomalous concentrations of Zn, Mo, Be, and B. Concentrate samples contain anomalous concentrations of Mn, Ag, Ba, Bi, Mo, W, B, Th, Nb, La, Ce, and Nd. Rock samples contain anomalous concentrations of Cu, Mn, Pb, Ag, Bi, As, Ba, Co, W, Mo and Sn. NURE samples contain anomalous concentrations of Ce. Possible deposit types include porphyry Cu-Mo, polymetallic vein and replacement bodies, skarns, and REE-Th-Nb-bearing pegmatites and carbonatites. The area is mildly to moderately anomalous overall from a geochemical standpoint. The Mid Hills area includes some polymetallic vein, gold-silver quartz-pyrite vein, and polymetallic fault types of occurrences and deposits, together with a small number of polymetallic skarn and copper skarn occurrences hosted by pendants of Devonian to Permian limestone within the Mid Hills Adamellite of Beckerman and others (1982) (pl. 2). Most of these occurrences are present near the mapped outer limit of the Mid Hills Adamellite. Analyses of mineralized rock from several polymetallic vein and polymetallic fault-types of occurrences in the general area of the Gold Valley Mine (U.S. Bureau of Mines, 1990a, map no. 570, pl. 1) show gold concentrations in excess of 500 ppb (pl. 6). Although the Mid Hills Adamellite in places shows intense mineralization at the surface, large areas of this rock in the Mid Hills are unaltered.

#### Providence Mountains

Geology in the Providence Mountains is complicated by the presence of major faults that bound many of the map units (pl. 1). The area is dominated by Devonian to Permian limestone, Cambrian dolomite, and Jurassic granitoid rocks, including quartz monzonite of Goldstone and quartz syenite of Winston Basin, Early Proterozoic granitoid rocks, and Miocene rhyolite ash-flow tuff (pl. 1). There are also significant amounts of Cretaceous porphyritic monzogranite, Late

Proterozoic and Cambrian siliciclastic rocks, and Jurassic hypabyssal and metavolcanic rocks and diorite. The Providence Mountains are geochemically the most highly anomalous area in the EMNSA. They have been heavily sampled; map plots emphasize the anomalous nature of the area. All sample media contain anomalous concentrations of many elements. Stream-sediment samples contain anomalous concentrations of Cu, Mn, Pb, Ag, Zn, Co, Sn, Mo, Ba, Bi, and B. Concentrate samples have anomalous concentrations of Cu, Mn, Pb, Ag, Zn, Au, Ba, As, Co, Sb, Bi, Sn, Mo, W, B, Th, Nb, La, Ce, Nd, Sm, Eu, and Tb. Rock samples contain anomalous concentrations of Cu, Mn, Pb, Ag, Zn, Au, Ba, Co, Sb, As, Bi, Sn, Mo, W, Be, B, Th, Nb, Nd, Eu, Tb, Yb, La, Ce and Dy. NURE samples contain anomalous concentrations of Th, U, La, Lu, Sm, Eu, Yb, Ce and Dy. Possible deposit types in the Providence Mountains include porphyry Cu-Mo, polymetallic veins and replacement bodies, mineralized skarn of all types, disseminated Au, and REE-U-Th-Nb-bearing carbonatite and pegmatite.

Plate 2 shows the density and overall distribution of types of mineral occurrences in the Providence Mountains. That part of the northern Providence Mountains underlain by Early Proterozoic intermediate-age granitoids, mostly augen gneiss of granite and granodiorite composition, includes the most dense concentration of metallic mineral occurrences in the EMNSA. In this area, the metallic mineral occurrences seem to be preferentially concentrated in a broadly elongate, north-northeast trending zone centered along the trace of the East Providence fault (pl. 1). Polymetallic vein-, polymetallic fault-, and gold-silver, quartz-pyrite vein-types of occurrences are predominant. Near the center of this intensely mineralized area, there are also shown two occurrences of possible low-fluorine, stockwork molybdenum systems (pl. 2). These two possible stockwork molybdenum systems are in, and in the general area of Cretaceous intrusive breccia (map unit Kmh, pl. 1) at Globe Wash (Goldfarb and others, 1988). Goldfarb and others (1988) describe these molybdenum occurrences as follows. In upper Globe Wash, massive felsic dikes or sills and irregularly shaped, silica-cemented (collapse?) breccias are altered to quartz and sericite. Widespread propylitic alteration in Proterozoic gneiss becomes more pervasive and intense near mineralized zones. Sericitic alteration of wall rock is common along quartz veins. The SS No. 17 prospect contains visible grains of molybdenite (a select sample yielded 0.025 percent molybdenum) along with large pyrite crystals and native sulfur after pyrite, in massive, white radial and ring quartz dikes surrounding a felsic intrusive breccia. Another select sample of gossan from a minor fault in the general area of the SS No. 17 prospect includes approximately 0.06 weight percent molybdenum (table 4, analysis no. 46). The development of breccia in this general area may reflect explosive release of vapor concomitant with transition from a single phase to a two phase fluid regime. Several companies have explored this area since 1970 on the basis of evidence suggesting a molybdenum stockwork deposit at depth. The highest molybdenum concentrations were detected in chip samples collected near the SS Nos. 20-22, 27-29 Mine, South

(Star? Mine), which are near the center of the area of molybdenum exploration. Goldfarb and others (1988) further suggest that there is unknown potential for a molybdenum porphyry system in upper Globe Wash. Brecciated, porphyritic, leucocratic Cretaceous Mid Hills Adamellite intruding Proterozoic gneiss to the west of the East Providence fault zone shows extensive propylitic and argillic alteration, with local sericitic alteration and pyritization common near silicified breccia zones. One prospect pit contains molybdenite rosettes in white quartz veins of both ring and radial geometry; the veins have anomalous fluorine, lead, and zinc concentrations.

Although the age of mineralization of the polymetallic veins and other occurrences hosted by the Early Proterozoic intermediately-age granitoids has not been established, they may be related to, and zoned around, a large Cretaceous-age porphyry-type system centered on the molybdenite occurrences at Globe Wash described above. However, the lateral extent of the quartz stockworks at Globe Wash at the inferred center of the system is quite small compared to the areal size and intensity of quartz stockworks known in many other similar stockwork molybdenum systems (Theodore and Menzie, 1984; Theodore and others, 1991). In fact, at Globe Wash, brecciated fragments of sericitically altered granite have been flooded secondarily by quartz and some molybdenite (Goldfarb and others, 1988) across only a relatively small area in the bottom of Globe Wash. The vein quartz is not coextensive with the mapped Cretaceous granite (map unit Kmh, pl. 1). Therefore, we suggest that if this truly is the central part of a very large porphyry system, then the most heavily molybdenum- and(or) copper-mineralized parts would be at extreme depths below the surface.

## Granite Mountains

Bedrock of the Granite Mountains is dominated by Cretaceous granitoid rocks, mostly 70 to 75 Ma in age (pl. 1). Lesser amounts of Jurassic diorite and granitoid rocks are also present. Concentrate and rock samples have anomalous concentrations of many elements. Copper, Mn, Pb, Ag, Zn, Co, Ba, Bi, Sn, Mo, W, Be, Th, Nb, La, Ce, Nd, Tb, and Yb are present in anomalous concentrations in concentrate samples. Rock samples have anomalous concentrations of Cu, Mn, Ag, As, Pb, Co, Sn, Zn, Ba, Bi, Mo, B, Nb, Nd, Tb, Yb, Ce, and Dy. NURE samples contain anomalous concentrations of La, Sm, and Eu. The area is only mildly to moderately anomalous from a geochemical standpoint because, although many elements are present in anomalous concentrations, they are generally weakly anomalous or else a small proportion of samples from the area have anomalous concentrations of a given element. Porphyry Cu-Mo, polymetallic veins and replacements, and REE-Th-Nb-bearing pegmatites are possible deposit types based on the available geochemistry. There are only a small number of mineral occurrences in the Granite Mountains area (pl. 2). These include two polymetallic veins, one iron skarn, and

one gold-silver quartz-pyrite vein--all widely separated from one another and not showing any apparent zonal relations. Moreover, most of the exposed granitoid rocks in the Granite Mountains area are not altered visibly at the surface.

#### Van Winkle Mountain

Van Winkle Mountain, near the south-central edge of the EMNSA, is largely Miocene airfall tuff and lava flows (pl. 1). Miocene tuff breccia and Cretaceous monzogranite make-up small parts of the area. The only samples from the area shown as Van Winkle Mountain on figure 23 are two NURE samples. Lanthanum is the only element present in anomalous concentrations. The area is geochemically weakly anomalous, based on limited information. There are three mineral occurrences known in the area of Van Winkle Mountain (pl. 2). Only one of these has sufficient data available upon which to make a deposit-type classification, and that one occurrence has been classified as a polymetallic fault that cuts Miocene air-fall tuff and lava flows (map unit Tal, pl. 1).

#### Grotto Hills

The larger of the Grotto Hills, in Lanfair Valley in the east-central part of the EMNSA, is composed of Miocene shallow intrusive rocks and rhyolite, basalt, and dacite that crop out in an area of about 6 km<sup>2</sup> (pl. 1). The smaller, western hills are Cambrian dolomite and Devonian to Permian limestone in an area of about 0.5 km<sup>2</sup>. Stream-sediment samples from the Grotto Hills contain anomalous concentrations of Ag, Zn, and Mo. Concentrate samples contain anomalous concentrations of Cu, Mn, Zn, Co, and Mo. No rock samples were collected in the Grotto Hills. NURE samples from the area do not have anomalous concentrations of any element. Possible types of occurrences are polymetallic veins and replacements. The area is geochemically weakly anomalous. There are no mineral occurrences known in the Grotto Hills (pl. 2).

#### Pinto Mountain

Pinto Mountain is underlain mainly by Miocene rhyolite ash-flow tuff, but a small area of Cretaceous Mid Hills Adamellite of Beckerman and others (1982) is also present (pl. 1). The only anomalous concentrations from Pinto Mountain are Mo in concentrate samples and Eu in NURE samples. No rock samples in the RASS and PLUTO data bases were collected from the area. The area is not geochemically anomalous. There are no mineral occurrences known in the immediate area of Pinto Mountain (pl. 2).

### Table Mountain

Most of the Table Mountain area is Cretaceous granitoid rocks with small areas of Early Proterozoic granitoid rocks and Tertiary tuff (pl. 1). Zinc and Mo are present in anomalous concentrations in stream-sediment samples from Table Mountain. Concentrate samples contain anomalous concentrations of Ag. Rock samples contain anomalous concentrations of Cu, Pb, Ag, Sb, Sn, and Mo. NURE samples contain anomalous concentrations of Th, La, Ce, and Dy. The area is geochemically mildly anomalous. Possible deposit types suggested by the geochemical results include polymetallic veins and REE-Th-bearing pegmatites. Three mineral occurrences are present in the area of Table Mountain, and they consist of two polymetallic vein systems and one polymetallic fault (pl. 2), one of which is the site of an analyzed rock that contains more than 500 ppb gold (pl. 6; U.S. Bureau of Mines, 1990a).

### Woods Mountains

Bedrock of the Woods Mountains is dominated by Miocene rhyolite ash-flows and domes (pl. 1). Lesser areas of bedrock are composed of Miocene rhyolite lava flow and basalt flows. No rock samples represent the Woods Mountains in the data sets examined. Silver and La in concentrate samples, and Dy in NURE samples are the only anomalous element concentrations. The area is geochemically weakly anomalous. There are no metallic mineral occurrences known in the Woods Mountains area (pl. 2; U.S. Bureau of Mines, 1990a).

### Hackberry Mountain

Bedrock of Hackberry Mountain, in the east-central part of the EMNSA, is mostly Miocene volcanic rocks of rhyolite, basalt, and dacite (pl. 2). A small area of Early Proterozoic gneiss and granitoid rocks is also present. Stream-sediment samples from Hackberry Mountain contain anomalous concentrations of Ba. Concentrate samples have anomalous concentrations of Mn, Ag, Zn, Ba, and Mo. NURE samples contain anomalous concentrations of Ce, Eu, and Dy. No rock samples were collected. The area is geochemically mildly anomalous. Possible deposit types are polymetallic vein and faults, and REE-bearing pegmatite. Seven of 16 mineral occurrences known in the area of Hackberry Mountain have been classified as polymetallic fault (pl. 2). Most of these seven polymetallic faults are concentrated in a northeast-trending zone along the southeast flank of Hackberry Mountain. Analyses of mineralized rock from the seven polymetallic faults all contain less than 500 ppb gold (pl. 6; U.S. Bureau of Mines, 1990a). One sample from a locality classified as a polymetallic vein (U.S. Bureau of Mines, 1990a, map no. 600, pl. 1), however,

does contain more than 500 ppb gold. This particular locality is well south of the locus of most recent exploration activities by private industry (Gottlieb and Friberg, 1984). These activities center on widely dispersed silicification in the general area of the seven polymetallic faults described above. In addition, these seven occurrences coincide with (1) a magnetic low (pl. 5) suggestive of demagnetization resulting from hydrothermal alteration, and with (2) a coincident limonite and alteration anomaly detected by our analysis of the thematic mapper image (fig. 10; see above).

Our field examinations reveal the presence of abundant silicification along the southeast flank of Hackberry Mountain but none of this silicification apparently is comparable to the intensity of the pervasive silicification and stockwork veining described below in the general area of the Hart Mine. Most of the silicification at Hackberry Mountain is present in rhyolite flows or densely welded ash flows. In addition, there is pervasive bleaching of these rocks in association with the argillic alteration confined mostly along a northeast-trending zone on the southeast flank where the polymetallic faults are present. Our use of the term polymetallic to describe these mineralized faults is based primarily on the presence of elevated abundances of lead, arsenic, antimony, and some zinc in them. Approximately 3,800 lb production of lead is credited to the Dewey Mine, one of the seven occurrences classified as a polymetallic fault (U.S. Bureau of Mines, 1990a). Furthermore, Gottlieb and Friberg (1984) describe results of exploration activities as follows: \*\*\*. . . The Hackberry Mountain prospect is a late Tertiary disseminated precious metal deposit hosted by rhyolites and ash-flow tuffs. Geochemical and lithologic logging of four drill holes down to 900 ft show an upper unaltered zone down to 200 ft with occasional native Au in hematite-replaced sanidine. An altered zone extends to 800 ft, and an unaltered zone extends from 800 to 900 ft. The altered zone is mainly ash-flows and the unaltered zones are mainly rhyolite lava flows.

Surface and drill hole samples [in the Hackberry Mountain prospect] show varying degrees of alteration and mineralization. The ore consists of fine grained native Au surrounded by bladed stibnite, chalcedony and hematite. Argillic alteration is dominant, with lesser amounts of silicification. In the argillically altered rock the phenocrysts are altered to clay minerals, and the groundmass, which had devitrified to quartz and potassium feldspar prior to alteration, remains fresh. Silicified rocks are altered to quartz plus Fe and Mn oxides. Major element chemistry indicates Si and Mn increase in altered rocks, Al, Fe, and K remain constant, and Mg, Ti, Na, and Ca decrease. Ca is the best indicator of alteration. Minor element chemistry shows that Zn increases with alteration, Ba, Cr, and V remain constant, and Sr decreases. Sr, believed to be contained in plagioclase, is an accurate indication of alteration whereas Ba, contained in the more stable sanidine was not mobilized. Trace elements La, Y, and Yb remain constant with respect to alteration. Au varies from 0.001 to 0.088 oz/ton . . . \*\*\*

## Vontrigger Hills

Bedrock of the Vontrigger Hills in the southeast part of the EMNSA is mostly Early Proterozoic younger granitoid rocks, between 1,660 and 1,695 Ma, and migmatite (pl. 1). Small areas of Miocene volcanic rocks and Cretaceous granitoid rocks are found mainly in the western part of the area. Stream-sediment samples from the Vontrigger Hills do not contain anomalous concentrations of any elements and NURE samples have anomalous concentrations of only Eu. However, concentrate and rock samples have anomalous concentrations of many elements. Concentrate samples have anomalous concentrations of Cu, Mn, Ag, Zn, Ba, Mo, Nb, La, Ce, and Yb. Rock samples have anomalous concentrations of Cu, Mn, Pb, Zn, Ag, Sb, As, Bi, Mo, Be, B, and Nb. Therefore, the area is geochemically moderately anomalous overall. Possible deposit types include porphyry Cu-Mo, polymetallic veins and replacement bodies, and REE-Nb-bearing pegmatites.

Six mineral occurrences in the Vontrigger Hills include three polymetallic veins, two low-sulfide gold-quartz veins, and one polymetallic fault (pl. 2). All occurrences are far removed from the Cretaceous granitoid that crops out near the southwest end of the Vontrigger Hills (pl. 1), and all the occurrences are hosted by Early Proterozoic younger granitoids. Although the mineral occurrences are each represented by a single symbol on the map showing distribution of deposit types (pl. 2), mineralization is extremely widespread at some of the localities such as that in the general area of the Rattlesnake Mine (U.S. Bureau of Mines, 1990a, map no. 592, pl. 1). Near the Rattlesnake Mine main workings, there are numerous prospect pits, shafts, and a partially reclaimed open cut, approximately 100 m wide, that apparently all follow favorable indications of gold mineralization of various attitudes and types in an area of about 3 km<sup>2</sup>. Much of the gold mineralization initially exploited at the Rattlesnake Mine, classified as polymetallic veins, is along a 10-m-wide zone of intensely silicified and highly fractured, foliated Early Proterozoic younger granitoid rock. This mineralized zone has a strike of about N. 70° W., and is present at the northern edge of what appears to be a porphyritic monzogranite of undetermined extent and not shown on plate 1. In addition, there are numerous unmineralized porphyritic granite dikes, containing potassium feldspar phenocrysts, that cut the Early Proterozoic younger granitoid rock. In the general area of the open cut, the mineralization apparently exploited consists of gold-bearing quartz veins that are hosted by Early Proterozoic younger granitoid rock.

At the True Blue Mine, near the Bobcat Hills part of the area at the Vontrigger Hills (U.S. Bureau of Mines, 1990a, map no. 588, pl. 1), discontinuous, narrow stringers of vein quartz in places partly fill open cavities developed in Early Proterozoic younger granitoid rock and elsewhere. The open cavities are lined by chrysocolla, azurite, and iron oxide that replace pyrite.

Typically these veins are 1 to 2 cm wide and approximately 10 to 16 cm long; they cut the foliation in the surrounding Early Proterozoic younger granitoid rock at high angles.

### Piute Range

The southern part of the Piute Range is dominated by Cretaceous granitoid rocks, but also contains substantial areas of Early Proterozoic younger granitoid rocks and Miocene basalt flows (pl. 1). The middle and northern parts of the range are almost exclusively Miocene dacite to andesite flows, domes, and breccias, but also contain small areas of underlying Middle Proterozoic granitoid rocks, Miocene welded ash-flow tuff, and Early Proterozoic younger granitoid rocks. Stream-sediment samples from the southern and middle parts of the Piute Range contain anomalous concentrations of Zn, Co, Mo, Be, and B. Stream-sediment samples from the northern part of the range do not have anomalous concentrations of any element. Concentrate samples from the southern and middle parts of the range have anomalous concentrations of Cu, Pb, Zn, Ag, Ba, B, Bi, Sn, W, Be, Mo, La, Sm, and Tb. Rock samples from the southern part of the range contain anomalous concentrations of Cu, Pb, Ag, Zn, Au, Sb, Bi, Mo, and W. NURE samples from the southern part of the range have anomalous concentrations of Th. Rock and concentrate samples from the northern part of the range contain anomalous concentrations of Be. Concentrate samples from the northern part of the range also have anomalous concentrations of Sn. NURE samples from the north part of the range contain anomalous concentrations of La, Ce, Lu, Sm, Eu, Yb and Dy. Overall, the Piute Range is geochemically moderately to highly anomalous. Possible deposit types include porphyry Cu-Mo, polymetallic veins and replacement bodies, disseminated Au, and REE-bearing carbonatite or pegmatite. There are no mineral occurrences reported by the U.S. Bureau of Mines (1990a) in the northern and central part of the Piute Range. Much of this part of the range includes relatively thick sequences of Miocene dacite to andesite flows, domes and breccias (pl. 1). However, there are numerous prospects and previously mined areas in the southern part of the range, particularly to the west-northwest of Signal Hill and to the east-northeast of Billie Mountain (pl. 2). This area is known as Tungsten Flat or the Signal Hill Mining District and includes only a small number of tungsten vein localities and several polymetallic vein localities plotted on the deposit-type map. However, the overall concentration of prospects and other workings of various types is extensively developed in an area of about 6 to 7 km<sup>2</sup> that contains widespread exposure of Cretaceous granitoid rock. Wolframite-bearing quartz veins typically are 1 to 2 m wide, strike N. 20° W., and dip steeply to the northeast; these veins are concentrated mostly in the northern part of the district. They are generally discontinuous and have been extensively explored along strike lengths as much as 100 m. Secondary copper minerals are common in many of the workings. Intense clay alteration is confined to rocks generally within 5 to

7 m adjacent to the veins. The Leiser Ray Mine, near the south end of the mining district shows elevated abundances of galena and chalcopyrite relative to occurrences at the north end of the district, and is a polymetallic vein-type occurrence that has a past production of 15,130 lb copper, 1,660 lb lead, 1,178 oz silver, and 26.69 oz gold (U.S. Bureau of Mines, 1990a). The main vein at the Leiser Ray Mine probably was discovered prior to 1891 (Hewett, 1956). The metal zonation in the Tungsten Flat Mining District seems to show polymetallic on the south, including mostly silver at the Leiser Ray Mine, distal to tungsten on the north. Hewett (1956, pl. 2) shows that the mineralization in the Tungsten Flat Mining District lies astride the projected east-northeast trend of the hinge line of the Piute anticline.

### Castle Mountains

Bedrock of the Castle Mountains is mainly Miocene dacite and rhyolite in the form of shallow intrusions and extrusive domes, flows, and breccia (pl. 1). Smaller areas of bedrock are composed of Early Proterozoic migmatite, Miocene basalt and andesite lava flows and rhyolite ash-flow tuffs. Stream-sediment samples from the Castle Mountains contain anomalous concentrations of Mn, Pb, Zn, Co, and Mo. Concentrate samples have anomalous concentrations of Cu, Mn, Zn, Ba, Co, Bi, Mo, B, Th, La, Ce, Nd, Sm, Eu, Yb, and Dy. Manganese, Ag, Sb, Pb, Ba, Mo, Be, B, Nb, Ce, Eu and Tb are present in anomalous concentrations in rock samples. NURE samples contain anomalous concentrations of Dy and Eu. The Castle Mountains are geochemically moderately to highly anomalous. Possible deposit types include porphyry Cu-Mo, polymetallic vein and replacement bodies, disseminated Au, and REE-Th-Nb-bearing carbonatite and pegmatite. The Castle Mountains include the economically significant epithermal quartz-alunite, quartz-adularia gold deposits at the Hart Mine, hosted by Tertiary volcanic rocks (pls. 1, 2). As we describe below, these deposits constitute one of the largest economic reserves of mineable gold known to date in southern California.

### Homer Mountain

Bedrock of Homer Mountain, at the east edge of the EMNSA, is composed of Early Proterozoic granitoid rocks (pl. 1). Stream-sediment samples from Homer Mountain contain anomalous concentrations of Ag, Zn, Mo, Be, and B. Concentrate samples have anomalous concentrations of Zn, Sn, and Mo. The only element present in anomalous concentrations in rock samples is Nb. NURE samples have anomalous concentrations of Lu, Sm, Eu and Dy. The area is geochemically mildly anomalous. Possible deposit types include polymetallic vein and REE-Nb-bearing pegmatite. Inasmuch as the area of Homer Mountain is outside the EMNSA, we have not included discussion of its mineral occurrences.

## U.S. Bureau of Mines Data Base

### Assembly of Data Base

In this section of this report, we examine some of the metallic mineral-resource implications of geochemical data obtained by the U.S. Bureau of Mines (1990a, table 2A and B) on 1,050 rocks analyzed from the EMNSA. These rock samples are classified as chip, random chip, grab, and select by the U.S. Bureau of Mines (1990a, table A-1). The chip samples, those rock chips taken in a regular series continuously along a line across a mineralized zone or other exposure, contain the most information for determination of the presence or absence of metal concentrations in a volume of rock. Select samples, those pieces of rock generally judged to be most representative of the best mineralized parts of a mineralized vein or exposure, are typically used as a first approximation to determine the presence or absence of a particular minor metal or metals in a mineralized system; for example, gold in a sample of sulfidized skarn. Most of these rock samples are from mineralized occurrences known within the EMNSA; approximately 98 percent of the rock samples can be assigned to mineralized sites, or their immediate vicinity, classified by us as belonging to a particular type of deposit model (table 8). As such, the analyses that compose this data base provide sampling across the EMNSA of many of the various types of mineral deposits which are known to be present there. These samples yield data that can be used to determine local geochemical thresholds to be expected for various metals and suites of metals present in various systems, to determine zonal relations of metals among genetically linked types of deposits, and to determine metal associations in variously grouped samples of the data base. Most samples that make-up the data base are from the mesothermal environment which is widespread in the EMNSA (see above). Only seven samples of the 1,050 in the data base are from sites that have been assigned by us as belonging to an epithermal, quartz-alunite or quartz-adularia, gold-type system that is volcanic-hosted and Tertiary in age. The overwhelming bulk of the samples are associated with Mesozoic metallogenic environments. However, the data base does not include any samples from the Providence Mountains in the south-central part of the EMNSA (pl. 6). As described above, these mountains contain some of the most widely distributed and intensely concentrated mineral occurrences, mined and unmined (U.S. Bureau of Mines, 1990a), in the EMNSA. In the Providence Mountains, there are approximately 200 mineralized sites that have been examined and described by the U.S. Bureau of Mines (1990a; Moyle and others, 1986) and by the U.S. Geological Survey and the U.S. Bureau of Mines (Goldfarb and others, 1988) in an area of about 250 km<sup>2</sup>. Most of these mineralized sites are polymetallic veins (pl. 2). In the Providence Mountains Wilderness Study Area, past production has been recorded from 13 nonferrous metallic lode deposits, with the largest production from the Bonanza King Mine during 1901-1960

(Goldfarb and others, 1988, table 1). The Bonanza King Mine yielded 5,302+ tons of ore that included 56.57 oz gold, 82,272 oz silver, 913 lb copper, 69,275 lb lead, and 2,312 lb zinc. Production recorded from the remaining 12 mines is minimal. The Vulcan Mine produced 2.6 million tons iron ore from an iron skarn from 1942 to 1947 (Goldfarb and others, 1988; Moyle and others, 1986). The distribution of the sampling sites is an important point that must be kept in mind during the discussion below of various subsets of the data base.

Although the report by the U.S. Bureau of Mines (1990a) includes analyses for 33 elements, we have selected 20 elements (Au, Ag, As, Ba, Ce, Co, Cr, Cs, Fe, La, Mo, Ni, Sb, Sc, Sm, Ta, Th, U, W, and Zn) upon which to base our statistical calculations described below. These studies are primarily an attempt to determine elemental associations in the sampled mineral deposits and mineral occurrences. One cannot make any inference about sizes of known or unknown deposits from the presence of a particular element, regardless of its concentration and its association with other elements, in a small number of samples from a site. As noted by Barton (1986), "the presence of a given element seldom if ever proves the existence of an ore deposit." As indicated in table 9, many of the 20 elements selected include large numbers of undetermined concentrations; primarily the undetermined values of elemental concentration are less than some threshold. In fact, detection thresholds for individual elements vary highly among the samples for many of the reported analyses. For example, there are 56 different detection thresholds for gold in the <2 to <49,000 ppb range. However, 158 of 253 samples reported as containing gold concentrations at less-than-detection thresholds have a detection threshold of 2 ppb. In order to (1) study elemental inter-relations in the 20 element-by-1,050 rock matrix, and (2) maximize the number of samples for which there are supposedly valid values available, we substituted each concentration reported as "less-than" a particular value with a concentration that is 50 percent of the value of the most sensitive detection level for the entire data base. A completely filled matrix is required for sampling adequacy by some of the correlation techniques using principal components factor analysis we describe below. Following the procedures outlined above, we were able to assemble a completely filled composite 20-element-by-1,050-sample geochemical matrix. Only one "greater than" value was substituted from the raw data reported by the U.S. Bureau of Mines (1990a). This reported concentration, >10,000 ppm arsenic, was substituted with a value of 10,000 ppm arsenic in the geochemical matrix we composited.

Some important elements from an economic resource standpoint, such as copper and lead, are present in a wide variety of geologic environments in the EMNSA but are judged not to be suitably represented in the raw data matrix. Such a judgment reflects primarily the large number of samples for which there are unreported concentrations for these elements. Among the 1,050 rock samples, copper concentrations are not available for 485 samples (U.S. Bureau of Mines, 1990a). In addition, another 113 samples show copper concentrations in excess of the uppermost reporting

limit (10,000 ppm). With regard to lead, 563 samples show no reported values, and 76 samples contain lead concentrations higher than the uppermost reporting limit (10,000 ppm). Therefore, we do not examine copper or lead relations to the 20 elements listed above.

Some of the elements we chose to include in the matrix, nonetheless, do show a high percentage of "less than" values relative to the 1,050 rock samples analyzed. Included among these are the following elements, with the number of "less thans" shown parenthetically after each element: silver (481), cerium (402), cobalt (642), cesium (549), nickel (801), tantalum (687), and zinc (477). However, a very high percentage of the reported "less than" concentrations in the raw geochemical data matrix (U.S. Bureau of Mines, 1990a, table 2A and B) for each of the seven elements above are at the most sensitive detection threshold. For example, detection thresholds are 2 ppm silver for 468 of the 481 analyses shown on table 9 as having a "less than" value in the raw data matrix. Therefore, a replacement value of 1 ppm silver for each of the 481 analyses should not distort the resulting matrix significantly. In addition, the presence of cobalt, currently a metal considered to have strategic importance, in highly anomalous concentrations at several localities in the EMNSA (U.S. Bureau of Mines, 1990a), is considered by us to be fairly important from a geochemical standpoint and we chose to examine its relations to other elements and to type of deposit in the EMNSA even though "less than" concentrations are more than 60 percent of the total number of cobalt concentrations reported (table 9; U.S. Bureau of Mines, 1990a). The most sensitive detection threshold for cobalt was 5 ppm, and 609 of the 642 "less than" values are reported to be <5 ppm (U.S. Bureau of Mines, 1990a).

#### Frequency Distributions of Elements

Frequency distributions of the untransformed geochemical data obtained by the U.S. Bureau of Mines (1990a, table 2A and B) are strongly skewed positively; that is, the most frequently occurring values are in the lowermost ranges of the reported concentrations with long "tails" in distribution of elemental concentrations toward high values. They are thus strongly nonnormal in overall distribution. To perform standard statistical calculations, the geochemical data in the composited 20 element-by-1,050 sample matrix were transformed by common logarithms to approximate thereby a closer fit to lognormality. Figure 48 shows frequency diagrams for the transformed data of the 20 elements. We should emphasize again that these data represent samples obtained from a wide variety of geologic environments and types of deposits in the EMNSA outside the general area of the Providence Mountains (see above). Somewhat more deposit-type specific relations among elemental suites are included below in the descriptions of several of the deposits present in the EMNSA. Tests of kurtosis and skewness values (table 9), frequently used measures of goodness-of-fit for normality, at the 95 percent confidence level show all 20 of the elemental distributions tested in the log-transformed data set deviate from lognormality. Positive

values of skewness indicate that the right "tail" of the distribution is longer than the left "tail", as is also readily apparent in the plotted histograms (fig. 48). Kurtosis refers to relationships among the peak, the center, and the tails of a distribution; for example, a deviation from normality that might be due to an extremely flat peak with relatively flat tails. A zero value of both kurtosis and skewness indicates a distribution that is normal. Among the 20 elements tested, visual inspection of the log-transformed distributions for iron and uranium show them to have the closest approaches to normality; antimony also approaches a normal distribution (fig. 48). Certainly, the fact that the original data represent a compositing of geochemical information from a wide variety of deposit types that show wide-ranging concentrations of elements together with a censoring of the data for many elements because of thresholds of detection higher than the actual distribution, all have contributed to yield the elemental distributions found. Nonetheless, distribution of gold values in the geochemical data matrix shows that approximately 200 of the 1,050 rocks analyzed from the EMNSA by the U.S. Bureau of Mines (1990a) include concentrations of gold higher than, or equal to, 500 ppb--a value considered by many exploration geologists as suggestive for ensuing evaluations in mesothermal geologic environments (see above). Similar conclusions were reached by the U.S. Bureau of Mines (1990a). In light of questions that might be raised concerning correlation calculations employing statistical methods that require normal distributions in the sampled population, nonparametric Spearman correlations were calculated below for the 20 elements transformed by logarithms to the base 10.

The distribution of concentrations of gold, silver, arsenic, antimony, molybdenum, and zinc in the 20-element-by-1,050 rock matrix by deposit type for 12 of the 20 types of deposit we recognize in the EMNSA is shown graphically on figure 49A-F. Most of the samples that show elevated concentrations of gold are from mineralized occurrences classified as polymetallic vein, polymetallic fault, and gold-silver, quartz-pyrite vein (fig. 49A). The number of samples analyzed for each of these three types of deposits are 286, 75, and 97, respectively. Silver is concentrated especially in the silver-copper brecciated dolostone type of vein occurrence that is distal to, and related genetically to, emplacement of the gold breccia pipes at the Colosseum Mine (fig. 49B; Sharp, 1984; see below). Arsenic apparently is most strongly concentrated in polymetallic veins, and to a somewhat lesser degree, in the polymetallic replacement deposits (fig. 49C). Concentrations of high values of antimony in the data base commonly are in silver-copper brecciated dolostone, lead-zinc skarn, and, much less so, polymetallic vein (fig. 49D). However, we have only seven analyses available from the lead-zinc skarn environment. High values of molybdenum are present in polymetallic veins, polymetallic replacement, and in two of the three samples analyzed from the known stockwork molybdenum Big Hunch system in the EMNSA. Additional analyses of rock from the Big Hunch system are reported below in the section describing the mineralization there in somewhat greater detail. Furthermore, as we noted above,

the U.S. Bureau of Mines (1990a) data base we refer to in this part of the report does not include samples from the Providence Mountains that have been demonstrated to show some elevated abundances of molybdenum at Globe Wash (see above; Moyle and others, 1986). Lastly, high concentrations of zinc are fairly common in the 20-element-by-1,050 rock geochemical matrix in those samples obtained from the polymetallic replacement occurrences, polymetallic veins, and copper skarns (fig. 49E).

#### Nonparametric Correlations

A nonparametric correlation statistic for all trace-element pairs available for the 20-element data set was calculated as Spearman's  $r$  (Davis, 1986), where  $r=1 - [6\sum(RX-RY)^2 / (n(n^2-1)]$ , and RX and RY are the two sets of rankings with n being the number of trace-element pairs. Each value is ranked and corrections made for tied observations. Results of the calculation for  $r$  are given in table 10, and scatter plots for gold compared with silver and iron are given in figure 50A-B. Gold shows the strongest positive Spearman correlation coefficients for silver and iron, 0.323 and 0.319 respectively in the 1,050-sample data base. Such relatively reduced values of Spearman correlation coefficients for gold to other elements in the data set are probably a result of the presence of gold in a large number of types of deposits in the EMNSA as described above. Gold is known to be present in the following types of deposit in the EMNSA (table 8): polymetallic vein; low sulfide, Au-quartz vein; polymetallic replacement; polymetallic replacement; distal disseminated Au-Ag; Au-breccia pipe; Ag-Cu brecciated dolostone; Ag-Ag, quartz-pyrite vein; polymetallic fault; polymetallic skarn; W skarn; Sn(W) skarn; and Cu skarn. Gold shows a somewhat enhanced association for silver, 0.4 Spearman correlation coefficients in a 97-sample subset composited from 47 localities of gold-silver quartz-pyrite vein occurrences in the EMNSA. A stepwise regression analysis (Davis, 1986) shows that only about 10 percent of the variance in the log values of gold can be predicted from the log values of iron alone in the 1,050-sample data base. Similarly, stepwise regression analysis including log values for silver, barium, chromium, iron, antimony, scandium, tantalum, and uranium accounts for about 31 percent of the variance of the log values of gold in the 1,050-sample data base--reflecting primarily the geologic inhomogeneity of the data. Plots showing strong, positive associations between element pairs in the data set are exemplified by samarium-lanthanum (0.896), antimony-silver (0.552), and iron-cobalt (0.691); values of the correlation coefficients are shown parenthetically (fig. 50C-E; table 10). Finally, a plot of barium versus uranium provides an example of an elemental association in the 1,050-sample data set that is extremely weak (fig. 50E; 0.001 Spearman correlation coefficient, table 10). In all of these plots (fig. 50), most of the samples for which we substituted values at the detection threshold are readily apparent.

### Associations Using Factor Analysis

Principal components factor analysis, another multivariate statistical approach (Klovan, 1968; Davis, 1986), was used in an attempt to detect additional, geologically significant elemental associations that may not have been resolved through the use of correlation coefficients. Our preliminary tests involved utilization of various other standard manipulations of the 20 element-by-1,050 sample data set as we described above (table 9). Based upon our knowledge of the geologic environments sampled in the EMNSA, we concluded that the data set should primarily reflect contributions from the Proterozoic environment and the Mesozoic mesothermal environment. A simple factor analysis using two factors provides the following high loadings for the geochemical data:

Factor 1: Ce, Th, Sc, Sm, Cs, Ta, Ba

Factor 2: Fe, Co, Zn, U

Factor 2 in this simple model also includes some moderate loadings for gold, arsenic, molybdenum and nickel. Therefore, in an attempt to resolve further the elemental associations masked by the simple two-factor model, we examined the data set using more than two factors. Of the options attempted, a relatively complex factor analysis using eight factors provides a geologically reasonable discrimination of the variances among the geochemical data. The R-mode principal components analysis, using an orthogonal transformation solution and emphasizing interrelationships among elements under consideration, reveals the following high, positive loadings among elements in the eight-factor model, listed in order of decreasing loadings, with notably lower elemental loadings in each factor shown parenthetically:

Factor 1: La, Sm, Th, Ce, Sc, Ta, Ba, Cs

Factor 2: Co, Fe, (Sc)

Factor 3. Sb, As, Ag, Zn, (Mo)

Factor 4: Au, Ag

Factor 5: W, (Cs)

Factor 6: Ni

Factor 7: U, (Ta)

Factor 8: Cr, Mo, Ba

These loadings, or measures of the degree of intercorrelation among the grouped elements (Klovan, 1968), are considered to be firmly established statistically because total matrix sampling adequacy has a value of 0.868, and thus meets minimum mathematical expectations of partial correlations tending toward zero (Kaiser, 1970). For the eight-factor model adopted, calculated communalities suggest that anywhere from approximately 62 percent (Cs) to approximately 93

percent (W) of any elemental variance in the 20-element-by-1,050 sample data set is predictable from the remaining 19 other elements.

Elemental associations in the eight-factor model suggest dominance in their loadings by several geologic processes or environments:

Factor 1: Jurassic and Proterozoic igneous rocks

Factor 2: Selected skarns and polymetallic veins

Factor 3: Gold breccia pipe and distal occurrences; selected skarns; polymetallic veins and replacements

Factor 4: All deposit types in Mesozoic mesothermal environment

Factor 5: Tungsten vein and tungsten skarn

Factor 6: Iron skarn and polymetallic vein

Factor 7: Mesozoic polymetallic veins and skarns; Jurassic igneous rocks

Factor 8: Polymetallic vein, fluorite veins, stockwork molybdenum occurrences

As pointed out in the geochemistry subsection above entitled "Evaluation of Data," the EMNSA resides in a broad geologic province that apparently contains widespread elevated abundances of rare-earth elements in rocks of highly diverse ages. As shown, many unaltered samples of Proterozoic and Jurassic granites are modestly enriched in La, Ce, Nd, Sn, Th, and several other elements (D.M. Miller, written commun., 1991). Therefore, the high loadings of many of these elements in Factor 1 must reflect their elevated abundances in Jurassic and Proterozoic granites in the EMNSA. In addition, the high loading of uranium and, to somewhat lesser degree, tantalum in Factor 7 must also be at least a partial reflection of their modest but persistent elevated presence in Jurassic granites. Uranium is present in some unaltered samples of Jurassic granite in concentrations of as much as 20 ppm.

From the 1,050-sample data base, we assembled a smaller one that included all samples showing cobalt concentrations greater than or equal to 50 ppm, and then examined elemental relations in it to establish deposit types associated with high loadings of cobalt and its associated elements (Factor 2). Sixty-four of 89 samples in this data base are from a geologic environment dominated by development of skarn (copper skarn, polymetallic skarn, iron skarn, tin-tungsten skarn, tungsten skarn, or zinc-lead skarn) and polymetallic-vein types of deposits. The highest concentration of cobalt detected is 859 ppm (U.S. Bureau of Mines, 1990a). Other types of deposit that include high concentrations of cobalt are gold-silver quartz-pyrite veins (two samples contain 799 and 460 ppm cobalt); polymetallic faults; vein barite; polymetallic replacement; and, finally, four samples from localities that cannot be classified by us into types of deposit based on the information available. Furthermore, cobalt in the 89-sample data base shows relatively weak overall Spearman correlation coefficients for other metals, the three highest being for nickel, cesium, and uranium in the 0.22-0.27 range. From the relations above, therefore, mesothermal

environments in the EMNSA that include the above-listed types of deposits can be considered at least as permissive hosts for significant concentrations of cobalt. The known occurrences of these types of deposit in the EMNSA are shown on plate 2, and additional discussion of the types of deposits and their permissive areas and favorable tracts is included below.

A 131-sample data base, including all samples containing more than 200 ppm antimony from the U.S. Bureau of Mines (1990a), was also prepared to evaluate Factor 3 loadings listed above. Fifty-five of the 131 samples are from vein occurrences distal to the Colosseum gold breccia pipe and genetically related to it (Sharp, 1984); 42 of these antimony-enriched samples are from sites included by us with the silver-copper brecciated dolostone type of vein occurrence (see below). In addition, some selected deposits of skarn, polymetallic vein, and polymetallic replacement also show abundances of antimony greater than 200 ppm elsewhere in the EMNSA (fig. 49D). In the 131 samples, antimony shows the highest positive correlation coefficients with silver, arsenic and gold; figure 51 is a plot of antimony versus arsenic for the 131 samples. Although we are not able to evaluate statistically relations of copper and lead because of the large number of qualified values for these elements in the data base as we described above, copper and lead in the silver-copper brecciated dolostones marginal to the gold-bearing breccia pipes at the Colosseum Mine are uniformly high (see below; U.S. Bureau of Mines, 1990a). If data were available for copper and lead, these elements undoubtedly would make up a strong component of Factor 3. The presence of elevated concentrations of antimony, arsenic, and some gold in silver-copper brecciated dolostones in the Clark Mountain Range might be used as a favorable geochemical signature for gold-bearing breccia pipes at depth. In addition, the silver-to-gold ratio in silver-copper brecciated dolostone distal to the Colosseum Mine is typically higher than 1,000 (see below).

Factor 4 shows high loading for gold and silver. Our evaluation of the 197 samples in the data base that contain abundances of gold in excess of 500 ppb indicates that there appears to be no type of metallic mineral deposit in the Mesozoic mesothermal environment of the EMNSA that one might exclude from being deposition sites of significant gold (pl. 6). By far, the most abundant deposit type whose samples contain gold in excess of 500 ppb is polymetallic vein, reflecting thereby its predominance in the EMNSA (table 8). A select sample from the polymetallic veins at the Big Horn Mine near the south end of the Providence Mountains includes 25,000 ppb gold (table 4, analysis no. 15). In addition, skarns of all types show some analyses carrying at least 500 ppb gold corroborating apparently the conclusions of Theodore and others (1991) that all types of skarns are at minimum permissive sites of enhanced gold deposition (see below).

Although Factor 6 shows a high loading only for nickel, the number of samples containing elevated concentrations of nickel is quite low. Only 31 of the 1,050 samples analyzed by the U.S. Bureau of Mines (1990a) contain higher than 100 ppm nickel, and only two of these are in excess of 500 ppm. These two samples are from mineralized sites classified as polymetallic vein (U.S.

Bureau of Mines, 1990a, map no. 282) and iron skarn at the Old Dad Mountain deposit (map no. 369). Eleven of the 31 samples analyzed and shown to contain more than 100 ppm nickel are from polymetallic veins. In addition, three of the silver-copper brecciated dolostone occurrences that are distal, in a petrogenetic sense, to the gold breccia pipes at the Colosseum Mine also contain some rock whose nickel contents are greater than 100 ppm.

Factor 7 shows a high loading for uranium and a moderate loading for tantalum. Only 18 samples analyzed by the U.S. Bureau of Mines (1990a) contain in excess of 50 ppm uranium, and eight of these are from mineralized sites classified as some type of metallized skarn of which four are iron skarn. The highest content of uranium found (1,590 ppm) in the EMNSA is from the general area of the REE-bearing carbonatites at the Esperanza group of claims in the northern part of the Ivanpah Mountains (U.S. Bureau of Mines, 1990a, map no. 156, pl. 1). Some polymetallic veins also contain high concentrations of uranium elsewhere in the EMNSA.

## **EVALUATION OF METALLIC MINERAL RESOURCES IN THE EMNSA**

### **Introduction**

Evaluation of metallic mineral resources to be described below primarily addresses known occurrences in the EMNSA, but also includes some discussion of additional types of metallic mineral deposits judged by us to be permissive in the various metallogenic terranes outlined for the EMNSA. We define our usage of the terms "occurrence" and "deposit" together with some other relevant expressions below. Furthermore, some of the industrial minerals (e.g., fluorite, magnesite, and barite) have also been incorporated into some of the discussions below because of their intimate petrogenetic association with many of the metal-bearing systems. A total of approximately 15 person-weeks were spent during 1990 in the EMNSA by 10 geologists to gather information first hand for this report. Because of the short time-frame requested, we have had to rely heavily on recently completed geologic investigations by others in the region (Goldfarb and others, 1988; Miller and others, 1984; 1985; Wooden and Miller, 1990; Wooden and others, 1988). In addition, studies by the U.S. Bureau of Mines (1990a; Schantz and others, 1990) and the California Department of Conservation, Division of Mines and Geology (exemplified by Kohler, 1984) provide the major inventories of metallic minerals available to us for the EMNSA; this inventory was supplemented where appropriate by information contained in records of the Mineral Resources Data System (MRDS) of the U.S. Geological Survey and by data made available from the files of several major mining companies that have been active at various times in the EMNSA during the last 20 years. In addition, the U.S. Bureau of Land Management (1980) analyzed some 29 resource areas, totaling 7.59 million acres of the entire CDCA (and including all

of the EMNSA), and classified the land with respect to its potential for energy resources and mineral resources. As classified by them, the Clark Mountain Range, Mescal Range, Ivanpah Mountains, Hackberry Mountain, and Castle Mountains include areas favorable for future discovery of locatable mineral deposits. The New York Mountains, Mid Hills, Providence Mountains, Granite Mountains, and all ranges west of Kelso were classified as areas having unqualified or unknown potential.

Our evaluation generally follows the first two parts of a three-part methodology initially developed for the Alaska Mineral Resource Assessment Program (AMRAP) of the U.S. Geological Survey, which in effect is a methodology based on analogy (see Harris, 1984). This methodology in its entirety consists of (1) delineating areas or domains of coherent geology that are consistent with the geology associated with a particular type or types of metalliferous deposits elsewhere, (2) building grade and tonnage models that describe the types of deposits recognized, and (3) estimating the numbers of undiscovered deposits (Singer, 1975, 1990, 1991; Singer and Cox, 1988; Menzie and Singer, 1990). Mineral deposits and occurrences listed and described by the U.S. Bureau of Mines (1990a) in the EMNSA were classified into about 20 types of metallic mineral occurrences after first examining a select number of these occurrences in the field to (1) confirm their classification(s), and (2) ascertain any mining district-wide characteristics pertinent to the overall evaluation (table 8). The types of models assigned to the occurrences in the EMNSA generally follow the models for ore deposits in Cox and Singer (1986). The existence of fairly up-to-date compilations of grade and tonnage models (Cox and Singer, 1986; Bliss, 1991; Singer, 1990, 1991; and many others) allows us to forego this aspect of the evaluation, and to compare instead the grades and tonnages of the various kinds of deposits in the EMNSA with similar deposits elsewhere. However, throughout the discussions below, we emphasize the possibility of district-scale, petrogenetic linkages among many of individual types of metallic mineral occurrences (fig. 52). Many of these litho-tectonic linkages are well-established in a large number of mining districts elsewhere and they are presented here in graphic form to emphasize that the presence of one type of mineral deposit or mineral occurrence can be used potentially as an indicator of many other types of deposit or occurrences in the surrounding, similar geologic environment. However, the presence of one type of deposit or occurrence does not mean that some other sought-for occurrence will necessarily also be present. In addition, we do not mean to imply that all the examples of mineral occurrences from the EMNSA shown on figure 52 are linked temporally and genetically. For example, the Jurassic Vulcan iron skarn deposit is not linked genetically to the apparently Cretaceous-age Big Hunch stockwork molybdenum system. Instead, the presence of magnetite skarn in stockwork molybdenum systems elsewhere suggests to us that the presence of a stockwork molybdenum system in the EMNSA demonstrates an environment

permissive for iron skarn, and, conversely, the presence of iron skarn in the EMNSA suggests that stockwork systems are also permissive.

There are many well-documented genetic linkages among metal deposits. One of the best examples of linkages among deposits in a mining district in the Cordillera of western North America is that at Bingham Canyon, Utah (Einaudi, 1982, fig. 7.14A). At Bingham Canyon, igneous rocks and their immediately surrounding sedimentary rocks in the core of the porphyry system contain two zones of disseminated metal: (1) copper plus molybdenum, and (2) copper. In places, this proximal zone is followed outwards by copper skarn. Distal to these are the lead-zinc-silver ores (polymetallic replacement deposits of our terminology), which are as much as 3 km from the outcrops of the central Middle Tertiary, genetically related monzogranite. By 1976, the Bingham Mining District yielded 1.3 billion tons of ore averaging 0.85 weight percent Cu (Einaudi, 1982). The mining district historically has also been a major producer of gold: up to 1986 more than 19 million oz Au were produced from lode and placer deposits (Tooker, 1990). Spatial linkages between skarn ores and disseminated porphyry-hosted ores at Yerington, Nev., Christmas, Ariz., and Ely, Nev., also are depicted graphically by Einaudi (1982). In addition, two sediment-hosted gold deposits (Mel-Co and Barney's Canyon) have fairly recently been discovered 5 and 8 km respectively from the outcrop of the central stock at Bingham Canyon (Sillitoe and Bonham, 1990). These two deposits are also considered to be related genetically to the emplacement of the central copper- and molybdenum-bearing ores in the core of the mining district. Mineable oxide reserves at the Barneys Canyon deposit are 10 million tonnes (at an average grade of 0.046 oz Au/t) and, at the Mel-Co deposit, they are 3.1 million tonnes (at an average grade of 0.07 oz Au/t) (Gunter and others, 1990). Finally, the characteristics of gold skarn, another type of deposit that may be linked genetically to porphyry-type ores in these types of magmatic-hydrothermal systems is discussed by Theodore and others (1991). Another example of district-wide linkages is the zonation among various ore bodies and their Ag:Au ratios in the Leadville Mining District, Colo., as discussed in detail by Thompson (1990).

Emplacement of many of the individual epigenetic metallic occurrences and deposits in the EMNSA should not be viewed as isolated events in time and (or) space. The zonal arrangement of silver-copper brecciated dolostone, tungsten, and fluorite veins that surround a centrally located gold-bearing breccia pipe at the Colosseum Mine in the EMNSA provides an excellent example of such linkages (Sharp, 1984; see below). In addition, we discuss several other types of deposits that are not currently (1991), and we cannot emphasize currently too strongly, known to be present in the EMNSA, but may be found there at some time in the future because they are known elsewhere in geologic environments similar to those in the EMNSA. In 1980, new exploration techniques, concepts, and field investigations resulted in the recognition of several mineral environments in the CDCA that prior to that time were unsuspected of being present there (U.S.

Bureau of Land Management, 1980). We do not herein attempt to estimate numbers of undiscovered metallic mineral deposits in the EMNSA as has been done elsewhere (Richter and others, 1975; Singer and others, 1983; Peterson and others, 1983). However, a quantitative assessment for some types of deposits in the EMNSA by others in the U.S. Geological Survey is expected to be completed sometime late in 1991 or early in 1992. Although we have been able to assign with variable degrees of certainty model types to 587 of the 701 mineral occurrences identified by the U.S. Bureau of Mines (1990a) in the EMNSA (table 8), we in fact have very limited first-hand knowledge for example, about (1) the character and intensity of alteration marginal to the occurrences, (2) the distribution of deposit-scale anomalous elements and elemental ratios, and (3) the intensity and preferred orientation(s) of fracture patterns that may or may not surround the identified deposits and occurrences. These types of data are critical for understanding the extent of the penetration of epigenetic, mineralizing fluids into the rocks surrounding any occurrence of metals, and, as a corollary, whether or not that particular occurrence of metal is one part of a much larger system as we describe below for the veins that surround the Colosseum Mine. Our evaluation assumes that many metalliferous concentrations (occurrences or deposits, as we define below) cannot be treated as isolated occurrences exclusive of other types of deposits as presently recognized in much of the economic geology literature. Indeed, many of the types of models listed by Cox and Singer (1986) can be linked genetically into a continuum of deposits as we have described, whose sites of eventual deposition are controlled both laterally and vertically by various physico-chemical processes, including depth below the paleosurface and separation of a vapor phase from the metal-bearing fluids. Furthermore, B.A. Berger (written commun., 1988) emphasized the dynamic nature of the evolution of many epithermal metalliferous systems: "... we are using models [currently] as rigid static entities in combination with other geological variables in the assessment process. From my limited perspective, models of epithermal systems are not independent from dynamic geologic processes such as the tectonic evolution of a region, changes in climate through time, and evolving landscape . . . we must look for ways to portray epithermal systems in a less rigid framework . . . and to apply them in a more dynamic way." Lastly, we emphasize that (1) exploration methodologies are evolving continually (see Baily, 1981), and that (2) quantitative model-based assessments can be made only for those types of mineral deposits that are currently recognized and for which grade-tonnage distributions are available. Any assessment for Proterozoic, carbonatite-related rare-earth deposits prior to discovery of the deposits at Mountain Pass would not have resulted in an accurate characterization of the geology of the EMNSA for these types of deposit. Such model-based, rather than target-based, quantitative assessments of many geologic terranes, which show signs of widespread mineralization and which are likely to be explored further at some future time, would most likely yield estimates of metal endowment that would be lower than the actual endowment.

Several examples from north-central Nevada emphasize this last point dramatically. Prior to discovery and recognition of the sedimentary rock-hosted gold-silver deposits near Carlin, Nev., in the early 1960's, no one could have properly assessed the surrounding geologic terranes as favorable or permissive for the presence of large gold-silver deposits. Many of these sedimentary-rock hosted gold-silver deposits are now known to be world class in size and grade (Bagby and Berger, 1985; Bagby and others, 1986; Berger, 1986). The sedimentary-rock hosted gold deposits at Getchell, Nevada, were discovered in the 1940s (Joralemon, 1951), but the true nature of the deposits was not recognized until much later (see Bagby and Cline, 1991). As pointed out by Roberts (1986), one of his previous papers (Roberts, 1960) defined some mineral belts in north-central Nevada and noted that many of the then known, apparently small, mineral deposits including gold in placers, are localized along traces of the margins of windows in the regionally extensive Roberts Mountains thrust. The spatial association between the trace of the Roberts Mountains thrust and the mineral deposits provided the geologic basis upon which private industry could then focus its exploration efforts. In another example, the Fortitude gold skarn deposit in the Battle Mountain Mining District, Nev., was not discovered until 1981, some 115 years after the district was first organized (Wotruba and others, 1986; Roberts and Arnold, 1965). Prior to start up of mining operations in 1985, the Lower Fortitude gold-skarn orebody contained 5.1 million tonnes of ore at a grade of 10.45 g/t Au; 27.8 g/t Ag; and 0.2 weight percent Cu (Theodore and others, 1991). In fact, there were no skarns in outcrop anywhere in the immediate area of the Fortitude deposit prior to its exposure during open-pit operations.

As with all applied exploration methodologies, actual discoveries of economic concentrations of metals are substantially limited compared to the number of claim groups commonly examined. Peters (1978) introduced the concept of "teaser districts" as those areas that include an abundance of small mines and (or) prospects that draw an inordinate amount of exploration effort before eventual rejection by some exploration group. There are two possibilities in such "teaser districts". On the one hand, the absence of some fundamental geologic condition from the ore-forming process apparently precludes accumulation of metals into a mineable concentration; the process may never have attained that particular intensity required to affect a volume of rock sufficient for an orebody (Peters, 1978). On the other hand, the major orebody may still be there somewhere in the "teaser district", but may be found only by a redirection of geologic concepts by the exploration team, a reassessment of economics in the district, or by the application of newly developed exploration tools and concepts.

An assessment of the EMNSA based on potential exploration targets (Menzie and Singer, 1990) for a particular metal or groups of closely related metals can lead to the recognition of new models and, necessarily, to a delineation of geologic terranes permissive for those new models. However, the cost of implementing state-of-the-art geochemical and geophysical techniques in a

program to determine potential exploration targets in the 1.5 million acres of the EMNSA would be exorbitant, especially when one considers that geochemical expenditures higher than approximately \$20,000 per 640 acres are fairly commonplace in private industry.

Lode metal mines apparently were first discovered in 1861 in the mountain ranges that were subsequently included in the EMNSA (Hewett, 1956). These discoveries were followed shortly by others in the Ivanpah Mountains during 1865, and, in that same year, the Clark Mountain Mining District was organized. First shipments of ore from the Copper World Mine took place during 1869, and in fact, many of the small lode mines that historically have shown sporadic production in the intervening years were discovered between 1865 and 1892 (Hewett, 1956). Subsequently, the region again was explored extensively for tungsten, zinc, and lead from 1915-1918 during World War I. However, many of the mines in the EMNSA ceased production at the end of World War I and apparently never produced again (fig. 53). The data for figure 53 were obtained from U.S. Bureau of Mines (1990a). Many other mines in the EMNSA, mostly gold producers, ceased production in 1941 with promulgation of the government order that closed down domestic mining of gold at the outset of World War II (see Shawe, 1988).

## Definitions

This part of the report follows closely the overall organization of one prepared recently by John and others (1991) for the Reno, Nev.,  $1^{\circ} \times 2^{\circ}$  resource-evaluation study currently underway by the U.S. Geological Survey. In the present report we adapt somewhat the definitions put forth by Cox and others (1986) for the terms "ore deposit", "mineral deposit", and "mineral occurrence". Specifically, a "mineral occurrence" is "a concentration of a mineral . . . that is considered valuable by someone somewhere, or that is of scientific or technical interest". However, use of this definition does not imply endorsement of economic value by the U.S. Geological Survey for the mineral occurrences considered in this report. A "mineral deposit" is "a mineral occurrence of sufficient size and grade that it might, under the most favorable of circumstances, be considered to have economic potential, a necessary corollary being that drilling has tested the system to the point that a grade and tonnage can be assigned to the volume of rock with some level of confidence. An "ore deposit" is "a mineral deposit that has been tested and is known to be of sufficient size, grade, and accessibility to be producible to yield a profit" according to Cox and others (1986). The inclusion of a concept of "profit" in this description put forth by Cox and others (1986) and many others is somewhat unfortunate in that it leads to contradictions when applied to estimates of speculative resources present in a given area (H.G. Wilshire and Jane Nielson, written commun., 1991). Certainly we can envision that national needs might require extraction of some metals under circumstances that do not yield a profit. If we were to attempt some estimate of the numbers

of a particular type of deposit present in a region or present in a favorable area for that deposit, then all existing occurrences, regardless of size and prior mining history, would have to be treated as unknowns if either the grade or the tonnage at the site were not available to us. An ore deposit is the economic, measured and demonstrated, identified resource part of the resource-reserve classification scheme adopted by the U.S. Bureau of Mines and U.S. Geological Survey (1980). Furthermore, the grade and tonnage of an ore deposit is not necessarily the same as the "geologic resource" of the deposit. The "geologic resource" is the grade or tonnage of the mineralized volume of rock that has not been constrained by economic-limiting factors such as topography or site location; the mineralized volume of rock is commonly broken down by variable grades, that includes the ore deposit itself (see Peters, 1978). As pointed out by Bailly (1981), there are five major factors involved in the determination as to whether or not a deposit becomes an economic reserve: (1) existence of the deposit; (2) extractability of the elements of value from the deposit; (3) availability of energy and materials for extraction of the elements of value; (4) acceptable environmental requirements, and (5) favorable economics for a potential mining operation at the site of the deposit. In the EMNSA, recent exploration activities have resulted in discovery of several gold-silver deposits for which both grade and tonnage data have not been released and are considered proprietary by the holder of the claims. In addition, only preliminary grade and tonnage figures are available to us for the Big Hunch stockwork molybdenum system in the New York Mountains (see below), although the extent of this large mineralized system has been known widely since the 1970s and an, in place, geologic resource of approximately 800,000,000 pounds molybdenum has been estimated (U.S. Bureau of Mines, 1990a).

Mineral occurrences, mineral deposits, and ore deposits are classified further into various types on the basis of descriptive mineral deposit models contained primarily in Cox and Singer (1986) as we described above, but included below are additional references as well to particular types of other deposits that are not contained in Cox and Singer (1986). These include gold-bearing breccia pipe, gold skarn, gold-silver quartz-pyrite veins and several others. The mineral deposit models are based on groups of mineral deposits that have in common both a relatively wide variety and a large number of attributes and have formed in a common geologic environment. Table 8 lists mineral occurrences identified in the EMNSA by model type and the appropriate references to descriptive models for these deposit types. Some of the deposit types assigned to a given category include a small number of occurrences and deposits that diverge widely from the age and mode of emplacement of the rest of that particular category. For example, although most gold-silver, quartz-pyrite veins presumably are Mesozoic in age and are related apparently to the mesothermal batholithic environment in the EMNSA, we include some deposits of different age and origin, such as those at the Telegraph Mine, under this same category. Mineralization at the Telegraph Mine apparently is Tertiary in age and seems to be associated with wrench fault-related tectonism

(Lange, 1988). We have not subdivided this category of gold-silver, quartz-pyrite veins further in our study because the geologic information is not available to us upon which we might make a valid judgment about age and tectonic environment for the 79 gold-silver, quartz-pyrite veins other than those at the Telegraph Mine studied by Lange (1988).

Grade and tonnage frequency distribution models contain data on the shape of curves for grades and tonnages for groups of mineral deposits from which grades and (or) tonnages at various percentiles may be extracted. They are useful in quantitative resource assessments (Singer, 1990; 1991) by providing information about the potential metal content of undiscovered deposits within a tract of land permissive for a given type or model, and are used in economic analyses of these resources, provided that (1) estimates may be made with some confidence concerning the number of individual deposits that may be present within that given tract of land (see above), and further provided, that (2) any undiscovered deposits would show grade and tonnages that are within the limits of the grades and tonnages of the ore-deposit model under consideration. Typically, grade and tonnage models are frequency cumulations based on average grades of each metal or mineral commodity for an individual deposit and the associated tonnage based on the total of past production, reserves, and resources at the lowest possible cutoff grade (Singer, 1990). However, appropriate care must be exercised in the accumulation of data for a grade and tonnage model because of the strong possibility of the significant distortion of the grade and (or) tonnage curves if one mixes unlike data such as production data and geologic resource data. In addition, data from geologically mixed populations of deposits can result in distorted grade and tonnage distribution curves. Furthermore, prior production data may be influenced heavily by topography in the general area of a deposit that is being exploited presently or has been exploited completely in the past. Ideally, a "geologic" resource and not an "economic" one should make up the individual grade and tonnage data points along the entire distribution curve of a grade-tonnage model. However, such information may not be available in the geologic literature for many already mined out deposits. Grade and tonnage distribution models currently are usually developed simultaneously by many workers as part of the descriptive aspects of the models (Cox and Singer, 1986). When there are sufficient grade and tonnage data available to build a model, the grade and tonnage data can help refine descriptive mineral deposit models (Singer, 1990; 1991). Singer (1990; 1991) discusses in detail the formulation of grade and tonnage models and some of the problems associated with their development and use. With regard to the EMNSA, one major shortcoming of present grade and tonnage models involves the bulk mineable, volcanic-hosted gold-silver deposits (John and others, 1991) such as are present in the Castle Mountains. A lack of sufficient grade and tonnage data for these types of deposits has resulted in retention by Cox and Singer (1986) of an artificial division of volcanic-hosted deposits into Comstock (adularia-sericite), quartz alunite (acid-sulfate), and hot spring types with all bulk mineable, volcanic-hosted gold-

silver deposits currently classified as hot spring deposits (D.A. Singer, oral commun., 1990). In a genetic sense, hot spring deposits are necessarily shallow level end members of adularia-sericite and quartz-alunite deposits as described by Berger and Henley (1989), and with continued discoveries of adularia-sericite and quartz-alunite mineralized systems, hot spring deposits will probably cease to have a separate grade and tonnage model (John and others, 1991).

## **Delineation of Areas Permissive and Favorable for Undiscovered Metalliferous Mineral Resources**

Several sections below present the characteristics of various metalliferous mineral deposits in the EMNSA, and in addition, delineate those areas where the geology is permissive for as yet undiscovered mineral occurrences. For many mineral occurrences identified in the EMNSA, we briefly describe notable characteristics and cite herein known deposits of that particular type in the EMNSA. We then describe criteria we used to delineate areas that may contain undiscovered occurrences and briefly describe the geologic characteristics of these areas. Two types of areas that may contain undiscovered mineral occurrences are delineated for many models types: permissive terranes and favorable tracts (Menzie and Singer, 1990). Permissive terranes are areas that might contain a certain type of mineral occurrence. Any geologic terrane in the EMNSA that is geologically similar to a terrane elsewhere that contains mineralization is considered permissive for the same type of mineralization whether there are signs of mineralization or not. Some of the permissive areas are very broadly outlined because their geologic environments conducive to the hosting of mineral occurrences in the EMNSA are wide ranging. For some types of mineral systems we cannot demonstrate that a particular type of mineral occurrence actually is present within the area shown as permissive for that occurrence type. Favorable tracts are domains within permissive terranes, and the favorable tracts are known to the authors to contain some positive indications that a mineralized system, generally irrespective of overall size or grade, is present or that mineralizing processes have occurred. For example, the presence of some known mined deposits and some mineral occurrences, hydrothermal alteration known to be restricted to a certain type of mineralized system, and plutons of an age and chemical signature that are associated with known mineralized systems elsewhere are all considered characteristics for the potential presence of that type of mineralized system in an area. Because positive indications that some type of ore-forming processes have occurred are required to designate an area as favorable for a certain type of mineralized system or mineral deposit model, favorable tracts are commonly of a much smaller areal extent than permissive areas and are more likely in the judgment of the persons making the mineral evaluation to contain undiscovered mineral resources of that model type. In all likelihood, many areas judged to be favorable have already been considered as such by exploration geologists

in private industry. The absence of any recent discoveries of major mineral occurrences in those areas designated as favorable may be interpreted to indicate a diminished likelihood for the presence of any future additional discoveries of the model of mineral occurrence in question. However, many ore deposit models are not being sought as viable targets at all times, and we do not have available the complete history of exploration for the favorable areas we outline. We cannot make any quantitative judgments concerning probabilities of discoveries in favorable areas versus probabilities of discoveries in the enclosing permissive terrane. Nonetheless, there are some mineral occurrences in the EMNSA that we have judged to constitute an exception to the above-stated rules for delineating a favorable tract within a permissive terrane for a given type of deposit. As we have described above, we judge the quartz-molybdenite vein occurrence at Globe Wash not to merit classification of a surrounding tract favorable for the presence of a large stockwork molybdenum system(s) at depth. By definition, permissive terranes must include all favorable tracts. Thus, these definitions of permissive terrane and favorable tract constitute a two-fold classification that has also been followed in a study currently in preparation that deals with metallic mineral resources of Nevada (Cox and others, 1991). We have not attempted to refine the outlined permissive terranes by deleting parts that can be confidently described as barren of a particular type of mineral occurrence (see Menzie and Singer, 1990) primarily because we do not have available to us the needed complete exploration histories and results of detailed studies in the various mountain ranges of the EMNSA. However, the permissive-and-favorable classification scheme of mineral resources is not the only one in use. As pointed out by Gair (1989b), an assessment of the mineral-resource potential of an area is an evaluation of the possibility or likelihood that such resources are present in an area; the assessment may or may not include some quantitative measures of the probability of the presence of a given type of mineral occurrence. Gair (1989b) and his associates proceed to attach a subjective classification scheme for various degrees of favorability for the presence of mineral resources that include high, moderate, low, and nil categories. We have chosen not to qualify further the permissive terranes and favorable tracts we outline below in the EMNSA, because we lack the information needed to differentiate confidently among the above-listed categories.

We emphasize, however, that we do not presume to have in hand all available positive indications of mineral occurrences even for those mineral-occurrences types known to us throughout the EMNSA, primarily because of inherent conditions that limited severely data gathering for the present investigation. Furthermore, the permissive terranes and favorable tracts are presented below only for some of the currently recognized ore-deposit models, including on the one hand those that are described formally in the economic geologic literature together with their grade-tonnage distributions and, on the other hand, some additional models that have not been formally described or are in the process of being described; for example, porphyry gold (see

Rytuba and Cox, 1991). Yet, some categories of mineral-occurrence models can provide viable exploration targets in certain permissive terranes. Descriptions by Hewett (1931) of unoxidized gold- and pyrite-bearing porphyry that is sericitized at the Red Cloud Mine in the Goodsprings Mining District, Nevada, about 13 km from the California-Nevada stateline, indicate that a porphyry gold-type of mineralized system should at least be considered as being permissive in intrusive rocks of similar age in the EMNSA. The methodology outlined above, however, cannot consider any types of mineral occurrences that are currently unrecognized as constituting a separate model.

The two-fold permissive area and favorable tract land-classification scheme we use herein for the various types of metal-bearing, mineral models is somewhat analogous to the scheme adopted recently by the State of California, as exemplified in its Mineral Land Classification Diagram (fig. 54; D.O. Shumway, written commun., 1991). As we use the term "permissive terrane", it includes both of their sections, Areas of Identified Mineral Resource Significance and Areas of Undetermined Mineral Resource Significance of the Mineral Land Classification Diagram. Our "favorable tract" is roughly equivalent to their Areas of Identified Mineral Resource Significance and the area of Known Mineral Occurrence (MRZ-3a) (fig. 54).

Geophysical methods described above that estimate depth to bedrock in those parts of the EMNSA covered by valley-fill deposits were used to place limits on extension of permissive terranes and favorable tracts from the mountain ranges into the valleys. We have used a 500 m depth-to bedrock limit to bound the permissive terranes and (or) favorable tracts in the valleys where the bedrock is covered by mostly unconsolidated Tertiary and (or) Quaternary deposits (pl. 3). This depth limit is somewhat arbitrary (for comparison, a recently completed 1:1,000,000 state-wide assessment for Nevada used a 1 km depth limit; Blakely and Jachens, 1990), but we believe that extrapolation of bedrock to depths greater than 500 m is subject to such uncertainties in the EMNSA as to have no scientific merit at the working scale of our assessment (1:100,000). Also, under present economic conditions, blind exploration for mineral deposits only very rarely exceeds 200 m depths, although exploration may extend to much greater depths than these in areas of known mineralization or altered rock, and in areas where specific geophysical targets are calculated to be at great depths.

For evaluation of deposits hosted by Mesozoic and older rocks, a map showing isopachs or depth contours to Mesozoic bedrock was constructed using procedures described by Jachens and Moring (1990) and using some of the data they acquired for partly contiguous regions in Nevada. This map was then modified to reflect the detailed geology available in those areas where lack of gravity stations resulted in a spurious placement of the 500-m-depth contour line (pl. 3). As described by Jachens and Moring (1990), there are several uncertainties associated with the depth to Mesozoic and older bedrock contours, and the 500 m isopach probably is less accurate than the

1 km isopach for the Cenozoic basin fill used in the study of the entire state of Nevada (R.C. Jachens, oral commun., 1990). Thus, the extent of permissive terranes and favorable tracts buried beneath Cenozoic, nonmagnetic (that is, nonvolcanic) sequences of rock shown on figures 55 and 56 should be viewed with extreme caution and regarded only as a first-cut estimate.

Thickness of nonmagnetic late Cenozoic basin fill also was semi-quantitatively estimated using aeromagnetic data collected by the National Uranium Resource Evaluation (NURE) program over the EMNSA. The NURE data were collected along east-west flightlines flown approximately 5 km apart and 120 m above the ground. These data were analyzed using both qualitative and quantitative techniques by J.D. Hendricks to produce a map showing areas of shallow magnetic sources (approximately <1 km depth to magnetic source) in the EMNSA. The map showing shallow magnetic sources, when combined with the available geologic map (pl. 1) and a depth to mostly Mesozoic and older basement rocks map allows separation of areas of thick (>0.5-1.0 km), nonmagnetic Cenozoic deposits (valley-fill sediments) from areas of shallow basin fill. Areas are thus outlined to show the subsurface extent of shallow basin fill and may be considered to be within permissive terranes for the presence of certain types of mineral occurrence based on the extrapolation of permissive terranes from adjacent exposed bedrock (pl. 3).

In the following discussion, mineral occurrences are separated by age into three groups: occurrences that may have formed during the Proterozoic, those that may have formed during the Mesozoic, and deposits that may have formed during the Cenozoic. Some deposit types may have formed repeatedly during both the Mesozoic and Cenozoic (such as mineralized faults and polymetallic vein deposits). Such deposit types are discussed in detail only with the age group in which they are most closely allied, generally the Mesozoic, even though the characteristics of known deposits elsewhere in the Mesozoic and Tertiary and the distribution of permissive terranes and favorable tracts for these deposits in the EMNSA may be somewhat different. In addition, Proterozoic rare-earth ore deposits at Mountain Pass are associated with carbonatite and alkalic intrusions and are currently (1991) in production; they are discussed below in some detail because they are present in 1.4 Ga-age rocks just outside the north-central boundary of the EMNSA (fig. 7). Furthermore, near Mountain Pass but inside the EMNSA, there is one breccia pipe-related gold deposit at the Colosseum Mine, also currently in production, apparently associated with Mesozoic felsic intrusions near the east flank of the Clark Mountain Range. Rocks that are similar in age to these two mineralized systems are present elsewhere in the EMNSA.

## Proterozoic Deposits

### Carbonatite-related, Rare-Earth-Element--Shonkinitic, Carbonatite, and Associated Rock Types in the Mountain Pass Area

The rare earth element (REE) deposit at Mountain Pass just outside the EMNSA is the most important Proterozoic deposit in the immediate area of the EMNSA (fig. 7), and it is contained within the largest body of Middle Proterozoic granitoids and carbonatite shown on plate 1. This carbonatite is in turn related to Middle Proterozoic shonkinitic, syenite, and potassic granite (Olson and others, 1954; Olson and Pray 1954; Crow, 1984; DeWitt and others, 1987; Heinrich 1966, p. 354-360; Woyski 1980). These silicate rock types can be collectively referred to as ultrapotassic rocks (Castor and others, 1989). This section of the report briefly summarizes the geologic setting, physical configuration, petrology, geochemistry, and REE mineralization of the ultrapotassic rocks and carbonatite of the Mountain Pass area.

The ultrapotassic rocks and carbonatite of the Mountain Pass area are present within a strip of Proterozoic rocks, approximately 60 km long, that extends from the northeastern Ivanpah Mountains, east of Kokowee Peak, north-northwestward to Mesquite Pass (Hewitt, 1956). The strip is composed of Early Proterozoic,  $\approx$ 1,700 Ma (DeWitt, 1987; Wooden and Miller, 1990), gneisses and granitic simple pegmatites unrelated to the Middle Proterozoic ultrapotassic rocks and carbonatite, which intrude the older rocks. The strip of Proterozoic rocks is autochthonous, and is bounded on the west by a high-angle fault and an early Mesozoic thrust fault, and on the east by the Ivanpah Valley and another high-angle fault (Burchfiel and Davis, 1981). All of the Proterozoic rocks are cut by andesite and rhyolite dikes, most likely of Tertiary age.

Within this strip of Proterozoic crystalline rocks, the ultrapotassic rocks and carbonatite are restricted to an area extending from approximately 2 km northwest of the Mountain Pass deposit to approximately 9 to 13 km southeast of the deposit. This belt of ultrapotassic rocks and carbonatite is truncated on the north by a high-angle transverse fault (Olson and others, 1954, pl. 1), although small bodies are scattered east of the fault (D.M. Miller, oral commun. 1991). To the southeast, the abundance of ultrapotassic rocks and carbonatite decreases gradually, and apparently does not extend from the general area of Mineral Spring across Ivanpah Valley, based on our interpretation of the presence of rocks of the Teutonia batholith of Beckerman and others (1982) in this region (see below).

The ultrapotassic rocks form several hundred thin dikes and seven larger intrusive bodies. Most of the larger dikes dip moderately to steeply southwestward. The dikes are approximately 0.3 to 10 m wide, and some individual dikes are as much as 1,100 m long. The large intrusive bodies are

ovoid to irregular in map pattern, and range from 200 to 1,800 m in maximum exposed dimension. The largest of these bodies lies north of the Mountain Pass deposit.

Carbonatite forms about 200 small dikes and one large intrusive body. Most of the dikes are approximately 0.3 to 2 m thick. The carbonatite dikes are rather variable in orientation. The dikes intrude both Early Proterozoic gneiss and the Middle Proterozoic shonkinite. A few of these tabular carbonate bodies may be veins rather than dikes.

The single large carbonatite body, called the Sulfide Queen carbonatite, strikes approximately north-south, has a strike length of approximately 700 m, dips approximately 40° west, and is roughly 70 m thick (Barnum, 1989). Its principal map dimensions are approximately 700 m by 200 m. The carbonatite intrusion is irregular, showing (1) apophyses that extend into the enclosing Early Proterozoic gneiss, (2) satellite carbonatite intrusions as much as 60 m in length along the margin, and (3) inclusions of gneiss and shonkinite as much as 50 m long within the marginal parts of the carbonatite.

Carbonatite is considerably less widespread than the ultrapotassic rocks. Most of the carbonatite dikes are present within a belt extending approximately 2 km north from the southern end of the Sulfide Queen carbonatite body. Only a few small carbonatite dikes are present as scattered outcrops south of Interstate 15. Most of these dikes south of Interstate 15 are in close proximity to the small (nondike) shonkinite intrusions; some of the carbonatite dikes parallel shonkinite dikes.

The general intrusive sequence of rock types in the Mountain Pass area is, from oldest to youngest (Olson and others, 1954): (1) the main shonkinite bodies, (2) mesosyenite, (3) syenite, (4) quartz syenite, (5) potassic granite, (6) shonkinite or minette dikes, and finally (7) carbonatite bodies, including dikes and the Sulfide Queen intrusion.

The following summary of the petrology of the ultrapotassic rocks and carbonatite of the Mountain Pass area is derived largely from the detailed descriptions provided by Olson and others (1954; see also DeWitt, 1987). Although Olson and others (1954, p. 59-63) essentially recognized the igneous character and origin of the carbonatite at Mountain Pass from field, regional, petrologic, and geochemical evidence, they conservatively referred to it as "carbonate rock". All subsequent workers have simply treated the carbonatite as an intrusive igneous rock.

The main shonkinite bodies are typically medium- to coarse-grained, equigranular, and mesocratic to melanocratic composed of subequal proportions of grayish-red microcline, green augite, and black biotite, with subordinate amphibole. Microperthitic albite is common within the microcline, but discrete grains of plagioclase typically constitute only 1 to 3 volume percent of the shonkinite. Other accessory minerals include various combinations of apatite (typically 2-4 volume percent), Fe-Ti oxides, sphene, zircon, epidote, olivine, and, rarely, pseudoleucite(?). The pyroxenes are augite and aegirine-augite. Amphiboles are hornblende and (or) sodic amphibole; commonly both are present. The sodic amphibole is riebeckite and (or) arfvedsonite. Textures are

hypidiomorphic-granular or poikilitic with microcline enclosing biotite, augite, apatite, and other minerals.

With decreasing pyroxene and biotite and increasing alkali feldspar, shonkinite grades into syenite. Typical syenite contains approximately 80 to 85 percent alkali feldspar-orthoclase and(or) microcline, commonly perthitic; 5 percent plagioclase; less than 5 percent quartz; and 10 to 15 percent biotite, amphibole, and, less commonly, augite or aegirine-augite. Common accessory minerals include hematite, apatite, sphene, zircon, rutile, and allanite. Much of the syenite is coarse-grained and equigranular; some contains orthoclase phenocrysts; textures are hypidiomorphic-granular. Mafic (augite- and biotite-rich) syenites generally have mafic phenocrysts. In leucosyenite, biotite is the sole mafic mineral. Some syenites contain hornblende, others sodic amphibole. Late crocidolite (fibrous or asbestosform sodic amphibole) replaces other mafic minerals and forms veinlets.

Quartz syenites, gradational in character between syenite and granite, are petrographically similar to syenite, but contain 5 to 10 percent modal quartz.

The granites of the Mountain Pass area are fine- to coarse-grained, and commonly have pinkish alkali feldspar phenocrysts. The granites typically are composed mostly of K-feldspar, with  $\leq 10$  percent plagioclase and 10 to 40 percent quartz. Color index is  $< 5$  percent; mafic minerals are biotite, hornblende, and sodic amphibole. Accessory minerals include Fe-Ti oxides, zircon, apatite, sphene, monazite, metamict thorite (?), allanite, epidote, and fluorite.

The late shonkinite dikes are fine-grained and they resemble and can alternatively be termed minette. They consist of K-feldspar, biotite or phlogopite, augite or aegirine-augite, and hornblende; and accessory minerals quartz, apatite, sphene, Fe-Ti oxides, calcite, and fluorite. Biotite and(or) phlogopite, the dominant mafic mineral, forms both phenocrysts and is in the groundmass. Some rocks also contain phenocrysts of pyroxene and(or) hornblende.

In one area north of the Mountain Pass deposit, there are biotite-rich dikes composed of biotite (phlogopite?) and aegirine, with subordinate or minor feldspar and calcite.

One large mass, the Sulfide Queen intrusive body, a number of smaller masses, and many dikes of carbonatite are present in the Mountain Pass area. The following summary focuses upon the Sulfide Queen body, which Olson and others (1954; see also Heinrich, 1966; Woolley and Kempe, 1989) divided into three map units (oldest to youngest): ferruginous dolomite carbonatite (beforsite); barite-calcite carbonatite (sövite), and silicified carbonatite. These three types are mutually intergradational, and each has several textural and compositional variants. The following descriptions are of the principal varieties.

The dolomite carbonatite is fine-grained and consists of dolomite, barite, and monazite, with accessory calcite, magnetite, and pyrite. Some rocks also contain bastnaesite  $[(Ce,La)(CO_3)F]$  and

parisite  $[(Ce,La)_2Ca(CO_3)_3F_2]$ . Local additional accessory minerals include thorite(?), apatite, aegirine, and phlogopite.

Barite-calcite carbonatite is the most abundant rock type within the Sulfide Queen carbonatite body. This sövite consists of 40 to 75 percent calcite, 15 to 50 percent barite, and 5 to 15 percent bastnaesite. Common accessory minerals include crocidolite, chlorite, phlogopite, apatite, thorite(?), allanite, zircon, galena (Mitchell, 1973), hematite, magnetite, and pyrite. The rock typically has a fine-grained groundmass surrounding subhedral barite phenocrysts 1 to 4 cm across.

The silicified carbonatite is texturally similar to the barite-calcite carbonatite, but has abundant quartz and correspondingly lower abundance of calcite. The silicified carbonatite consists of bastnaesite, barite, and quartz; with subordinate or accessory calcite, monazite, hematite and goethite, sericite, galena, and pseudomorphs of hematite after pyrite. Bastnaesite content is as much as 60 percent. Quartz forms both euhedral crystals and subsequently crystallized chalcedonic veins or layers.

All three types of carbonatite within the Sulfide Queen carbonatite body are cut by fractures, veins, and shear zones coated or filled with crocidolite, chlorite, iron oxides, or other minerals. Supergene minerals include iron oxides, Pb or Cu carbonates, quartz, and wulfenite.

Fenetization (alkali metasomatism) is widespread in and around the ultrapotassic rocks and carbonatite. Alteration minerals include microcline, albite, riebeckite (including crocidolite), aegirine, chlorite, phlogopite, barite, calcite, iron oxides, sericite, and quartz. Some, and possibly much, of the fenetization is associated with carbonatite intrusions.

Twenty analyses of ultrapotassic silicate rocks from the Mountain Pass area have been published (Olson and others, 1954, table 3; Crow, 1984, table 2). Only nine of these samples have both major- and trace-element data. Watson and others (1974) present partial averages of 95 major-element analyses of ultrapotassic rocks and phlogopite-carbonate dikes. Unfortunately, no carbonatite analyses have been published (except for the phlogopite-carbonate dike average, with 44 percent  $SiO_2$ ). A synthetic glass produced experimentally by Jones and Wyllie (1983) to approximate the composition of Mountain Pass sövite contains approximately 45 percent  $CaO$ , 7 percent  $BaO$ , and 18 percent  $La_2O_3$ . Mountain Pass carbonatite has initial  $^{87}Sr/^{86}Sr = 0.7044$  (Powell and others, 1966).

The shonkinites (including shonkinitic dikes) contain 47 to 50 percent  $SiO_2$ , 6 to 9 percent  $K_2O$ , and  $\leq 1.5$  percent  $Na_2O$ ; and have high mg numbers: 0.72 to 0.82. The syenitic and granitic rocks range from 54 to 71 percent  $SiO_2$ , with 6 to 12 percent  $K_2O$  and <1 to 4 percent  $Na_2O$ .  $K_2O/Na_2O$  ranges from 2 to 16. Ten of the fourteen samples analysed for major elements (Crow, 1984) and five of the six average compositions (Watson and others, 1974) have  $K_2O/Na_2O > 3$ ,

and thus qualify as ultrapotassic (Bergman, 1987). Alkali systematics of some of the syenites and granites may have been modified by fenetization.

The ultrapotassic rocks have large or very large abundances of large-ion-lithophile elements (LILE) and somewhat elevated abundances of many high-field-strength elements (HFSE). Barium is quite high: 5,600 to 9,500 ppm in shonkinite and 2,300 to 5,700 ppm in syenites and granites. Rubidium contents also are high: 240 to 720 ppm. The high concentrations of potassium have already been described. All of the syenite and granite samples have >100 ppm thorium. Tantalum and hafnium contents are also high, typically several times greater than average upper crustal abundances (Taylor and McLennan, 1985; table 2.15).

The ultrapotassic rocks have high abundances of light-rare earth elements (LREE) but unexceptional contents of heavy rare earth elements (HREE). In the shonkinite, mean abundances of La and Ce are 330 and 720 ppm, respectively. The shonkinites have very steep chondrite-normalized REE spectra, with  $La_{cn}=600$  to 1,800 and  $Yb_{cn}=10$ . Europium anomalies are small or nil. The syenite and granite REE patterns are similar but somewhat less steep, and have slightly lower abundances and no significant Eu anomalies.

The Mountain Pass carbonatite is “one of the most unusual of all carbonatites...” (Heinrich, 1966). Mountain Pass is distinguished by comparatively high barite and bastnaesite content, and low content of silicate minerals, apatite, and magnetite; exceptionally high abundance of LREE; absence of enrichment in niobium and tantalum; and association with potassic, silica-saturated or silica-oversaturated progenitors. Most carbonatites are genetically associated with sodic, silica-undersaturated rocks, such as nephelinites and ijolites (=mesocratic nepheline-clinopyroxene plutonic rock).

Crow (1984) concluded that the shonkinite and syenite, and possibly the granite (Crow, oral commun., 1987, quoted by DeWitt, 1987, p. 54), are comagmatic and related by fractional crystallization. His preferred model involves generation of a parental shonkinitic melt by 1 percent melting of REE-enriched mantle garnet peridotite, followed by 20 percent fractional crystallization of shonkinite to produce syenite.

Its field relations and extraordinary composition leave little or no doubt as to the igneous nature of the Mountain Pass carbonatite. This is further supported by experiments conducted by Jones and Wyllie (1983, p. 1723): “The results from our synthetic rare earth carbonate mixture indicate that the addition of  $H_2O$  is all that is required to permit the analogous carbonatite at Mountain Pass, California to exist as a liquid magma at a low pressure and at a temperature near 650° C”. Additional experiments are consistent with a magmatic origin for the bastnaesite in the Mountain Pass carbonatite (Wyllie, 1989).

No systematic study of the petrology and origin of the Mountain Pass carbonatite has been published. In general, the origin of carbonatites is controversial (Gittins, 1989; Le Bas, 1987;

Twyman and Gittins, 1987; Hall, 1987; Kjarsgaard and Hamilton, 1989; Hamilton and others, 1989). Among the key facts to be explained are the frequent association of carbonatites with nephelinitic rocks and the very large concentrations of certain incompatible elements, notably LREE and Nb, in most carbonatites. Three possibilities are commonly entertained (Gittins, 1989): (1) fractionation from mantle-derived 'carbonated nephelinite' to produce carbonatite; (2) immiscible separation of a carbonatitic liquid and a nephelinitic or phonolitic silicate liquid from a mantle-derived parent; and (3) direct melting of carbonated metasomatised mantle peridotite, to produce separate carbonatitic and silicate magmas. The first possibility is implausible, as 'carbonated nephelinite' magma apparently does not exist in nature, and it is unlikely that fractional crystallization could generate the high REE and Nb abundances that generally characterize carbonatites. However, as described above, Mountain Pass is characterized by an absence of an enrichment in Nb compared to many other carbonatite-hosted REE deposits.

Applicability of either of the remaining hypotheses to Mountain Pass is uncertain. A model for the origin of the Mountain Pass carbonatite presumably will be exceptional, as Mountain Pass's association with potassic rather than sodic silicate rocks and its extraordinary content of LREE and paucity of Nb are exceptional.

The close spatial association of the Sulfide Queen carbonatite intrusion with the largest of the shonkinite-syenite intrusions certainly suggests a close genetic link. Such a genetic link could be compatible with separation of the carbonatite and shonkinite by liquid immiscibility; or with separate but related genesis of the carbonatitic and shonkinitic magmas in the mantle, followed by ascent of the two magmas through the same crustal conduits.

Lanphere (1964) obtained K-Ar and Rb-Sr dates of 1,380 to 1,440 Ma for biotite from shonkinite at Mountain Pass. DeWitt and others (1987) summarize U-Th-Pb and  $^{40}\text{Ar}/^{39}\text{Ar}$  geochronologic data. Apatite from the shonkinite has a U-Pb age of 1,410 Ma. Phlogopite from the shonkinite and arfvedsonite from the syenite have  $^{40}\text{Ar}/^{39}\text{Ar}$  plateau dates 1,400 to 1,403 Ma. Monazites from the carbonatite have Th to Pb ages of 1,375 Ma. Bastnaesite and parisite from the carbonatite have complex systematics suggesting post-emplacement migration of Pb. Thus, the ultrapotassic rocks and carbonatite in the Mountain Pass area are  $\approx$ 1,400 Ma.

Castor and others (1989) state that 1,400 Ma ultrapotassic intrusive rocks form a north-south trending zone at least 130 km long in southeastern California. However, they do not specify the localities that make up this zone. Mountain Pass is obviously one of them. Ultrapotassic and related rocks also are present in the Piute Mountains, approximately 90 km south-southeast of Mountain Pass (Gleason and others, 1988; Gleason, 1988). In the Piute Mountains, a small 1,400 Ma pluton of shonkinite, syenite, and alkali granite contains rocks that are potassic to ultrapotassic, and generally have high abundances of LILE and, to a lesser extent, HFSE.

REE production at the Mountain Pass deposit is from the Sulfide Queen carbonatite body. Textural relations indicate that REE mineralization is dominantly primary or magmatic; only a small portion is hydrothermal (Mariano, 1989a). Bastnaesite and parisite are the chief ore minerals. Subordinate REE minerals in the deposit (R.L. Scherer, written commun., 1980) include monazite, synchisite  $[(Ce,La)Ca(CO_3)_2F]$ , sahamalite  $[(Mg, Fe)(Ce,La)_2(CO_3)_4]$ ; a mineral first discovered at Mountain Pass: Jaffe and others, 1953], and allanite.

Mountain Pass bastnaesite is extremely LREE enriched:  $La_{cn} \approx 7 \times 10^5$ ,  $Yb_{cn} \approx 20$  (Mariano, 1989b). In other terms: in Mountain Pass bastnaesite, Yb is enriched over average continental upper crust by a factor of only  $\approx 2$ , whereas La is enriched by a factor of  $\approx 8,000$ .

Typical Mountain Pass REE ore contains approximately 40 percent calcite, 25 percent barite and (or) celestite, 10 percent strontianite, and 12 percent bastnaesite (Barnum, 1989). The proportion (in percent) of the REE in average ore is:

La	33
Ce	49
Pr	4
Nd	13
Sm	0.5
Eu	0.1
Gd	0.2
Tb + Y	0.1
$\Sigma$ other HREE	0.2

These proportions are determined chiefly by the even-odd atomic number alternation of terrestrial (and chondritic) REE abundances and the extremely LREE-enriched character of the bastnaesite.

According to Barnum (1989), average bastnaesite ore reserves at Mountain Pass contain approximately 9 percent lanthanides, and the Mountain Pass ore body has 31 million tons of proven and probable reserves, based upon a 5 percent cutoff lanthanide grade. Mariano (1989a, table 7.1; 1989b, p. 331) provides similar estimates: 40 or 31 million tons of 8 or 9 percent  $REE_2O_3$  (the former figures are as of the end of 1986; the latter figures are with a 5 percent cutoff grade).

Until recently, Mountain Pass was the world's major source of LREE. Its reported reserves are approximately 2.7 million tons of  $REE_2O_3$ . However, the Bayan Obo, Mongolia Fe-Nb-REE deposit, with estimated reserves of 37 million tons of  $REE_2O_3$ , is the largest known REE deposit (Mariano, 1989b; Ontoyev, 1990). As this deposit is so large, China has approximately 75 percent of the world reserves of REE (O'Driscoll, 1988). The Bayan Obo deposit is advantageous in its comparatively high contents of Eu and Sm, two of the less abundant and more valuable REE. In

1986, production of REE from the United States, largely from Mountain Pass, and from China were approximately equal. In 1989, U.S. production was 14,000 metric tonnes of  $\text{REE}_2\text{O}_3$  derived from bastnaesite, presumably mostly from Mountain Pass; total Chinese production was 20,000 metric tonnes (Hedrick, 1990).

Although Mountain Pass will no longer dominate the world's LREE supply (unless supply from China were disrupted), it will continue to be a major source of LREE for the foreseeable future.

### **Carbonatite-related, Rare-Earth-Element in the EMNSA**

#### **Known Occurrences**

Although four occurrences in the EMNSA are assigned by us provisionally to carbonatite-related, REE-type systems (U.S. Bureau of Mines, 1990a, map nos. 48, 156, 351, and 358), only one of these (map no. 156) is known definitely to be associated with carbonatite and related types of rock. The other three may owe their reported elevated abundances of REE to Proterozoic quartz-bearing pegmatite and thus they may not have the resource implications we ascribe to the Esperanza Group of claims at map no. 156. In the general area of the Esperanza Group of claims, which in part apparently extend 0.4 km inside the boundary of the EMNSA near Mineral Spring of the northeastern Ivanpah Mountains (pl. 2), small bodies of carbonatite and related ultrapotassic rocks crop out widely in an area of possibly as much as 5 to 6  $\text{km}^2$ .

#### **Permissive terrane**

We believe that the geologic terrane in the EMNSA permissive for Middle Proterozoic, carbonatite-related REE deposits and(or) occurrences includes all areas underlain by or shallowly underlain by rocks that are Early Proterozoic in age (pl. 1).

#### **Favorable tract**

We show one tract favorable for the presence of additional discoveries of carbonatite-related REE deposits in and just outside the EMNSA (fig. 55). This tract is elongated and aligned in a northwest-southeast direction; it extends from the general area of the Mountain Pass REE deposit on the northwest to the general area of the Esperanza Group of claims on the southeast. Criteria used to delineate the favorable tract boundaries are listed on table 11, and primarily reflect the known presence of REE-bearing carbonatite and ultrapotassic rock in numerous exposures of small bodies throughout the area delineated. According to the U.S. Bureau of Land Management

(1982), drilling in the southeasternmost of this outlined area favorable for REE deposits has resulted in discovery of "substantial resources of rare earth and thorium mineralization."

#### Other Types of Deposits

##### Volcanogenic Massive Sulfide Deposits in Arizona and Nevada

Massive sulfide deposits are known in the Early Proterozoic rocks of Arizona (Anderson and Guilbert, 1979; Donnelly and Conway, 1988; DeWitt, 1991), including several in western Arizona (Stensrud and More, 1980; Conway and others, 1986; Conway, 1986; Conway and others, 1991) that are within the Mojave crustal province (Wooden and others, 1988; Wooden and Miller, 1990). The massive sulfide deposits in western Arizona range in size from small deposits of 1.6 thousand tons to as much as 1.5 million tons of Cu-Pb-Zn-Ag-Au ore (summarized in DeWitt, 1991). The larger deposits, such as those located around Bagdad, Ariz., are comparable to a median-sized massive sulfide deposit, based upon compiled grades and tonnages from throughout the world (Singer and Mosier, 1986). In central Arizona, The Early Proterozoic United Verde deposit at Jerome is a giant deposit of similar grade and tonnage to some of the largest deposits in the world (Singer and Mosier, 1986; DeWitt, 1991). The deposit at Jerome is associated with a sequence of Early Proterozoic rocks different in age and lithology from those found in western Arizona (DeWitt, 1991) and in the EMNSA.

Massive sulfide deposits are mainly of three types: (1) Cyprus-type deposits, found in marine mafic volcanic settings that also contain an ophiolite assemblage; (2) Besshi-type deposits, found in sedimentary sequences consisting of clastic terrigenous rocks and tholeiitic to andesitic tuff; and (3) Kuroko-type deposits, associated with marine rhyolite and dacite and subordinate basalt and sedimentary rocks (Cox and Singer, 1986; see also Sangster, 1980). Distinctive alteration patterns characterized by magnesium metasomatism and exhalative silica deposits are associated with many of the deposits (Franklin and others, 1981). Where metamorphosed, the alteration sequences are converted to chlorite, and cordierite-anthophyllite assemblages, and to quartzite, respectively.

##### Volcanogenic Massive Sulfide Deposits in the EMNSA

Although no volcanogenic massive sulfide deposits of any type are known in EMNSA, or for that matter anywhere in southern California, certain features characteristic of these deposits have been described in the geologic province that includes the EMNSA. For example, massive sulfide deposits of varying size and the presence of widespread Mg-metasomatism in the Early Proterozoic gneisses of the Mojave crustal province in western Arizona suggest that this terrane may contain more deposits of this type. In addition, possible protoliths for bimodal felsic gneiss-amphibolite

sequences in the Providence Mountains include volcanic rocks (Wooden and Miller, 1990), although these sequences have subsequently been interpreted to have plutonic protoliths (D.M. Miller, oral commun., 1991). Furthermore, cordierite-anthophyllite rocks are reported as small pods in Early Proterozoic gneiss in the Old Woman Mountains, to the immediate south of EMNSA. Other occurrences of similar rocks are known farther to the west (Powell, 1981). Some 95 km to the south of EMNSA in the Turtle Mountains, Howard and others (1988) suggest the possibility of volcanogenic mineralization of Early Proterozoic age at the Virginia May Mine. There, the mineral occurrence contains spinel which, as a zinc-bearing variety, is common to metamorphosed Besshi-type massive sulfide deposits (Sheridan and Raymond, 1982). All these features, although not associated with known occurrences or past producing mines of any size, do suggest that the possibility for volcanogenic massive sulfide deposits in EMNSA must be entertained and can not be dismissed. DeWitt and others (1989) recognized this possibility and argued for the potential of Besshi-type, sedimentary-hosted massive sulfide deposits in the McCullough Mountains, to the immediate north of the EMNSA.

In light of the many uncertainties concerning the possibility of volcanogenic massive sulfide deposits in the EMNSA, we delineate no permissive terranes or favorable tracts for these types of deposit in the EMNSA.

#### Granite-related U-, Th, and REE Deposits in Alaska and Elsewhere

The predominant ore mineral in those granitic rocks favorable for the presence of uranium deposits is uraninite ( $\text{UO}_2$ ). Ballhorn (1989) recognizes three types of granite worldwide that have been shown to host uranium deposits: (1) metaluminous anorogenic granite of alaskitic composition exemplified by those at Rossing, Namibia, whose ore is related primarily to magmatic differentiation; (2) peraluminous granite, exemplified by the Mississippian-to-Permian in age, mostly two mica granites in the Central Massif, France; and (3) alkaline granite, exemplified by the Jurassic granite at Bokan Mountain, Alaska. Uranium-enriched rocks associated with the last two types of granite apparently are related to circulation of mostly sub-solidus, hydrothermal fluids and to some minor amounts of early-stage processes of magmatic differentiation. Nokleberg and others (1987) have designated uranium-bearing granites in Alaska to be included within a felsic plutonic uranium type of deposit, and they describe this deposit-type as follows. Felsic plutonic uranium deposits in Alaska consist of disseminated uranium minerals, thorium minerals, and REE-minerals in fissure veins and in alkalic granite dikes in or along the margins of alkalic and peralkaline granitic plutons, or in granitic plutons, including granite, alkalic granite, granodiorite, syenite, and monzonite. The ore-forming environment is mainly the margins of epizonal to mesozonal granitic plutons. Ore minerals in the deposits include allanite, thorite, uraninite,

bastnaesite, monazite, uranothorianite, and xenotime, sometimes with galena and fluorite. Notable examples are the Roy Creek (Mount Prindle) deposit in east-central Alaska, and the Bokan Mountain deposits in southeastern Alaska.

#### Granite-related U-, Th, and REE deposits in the EMNSA

Early and Middle Proterozoic rocks in the EMNSA are notably enriched in large-ion lithophile and high-field-strength elements, including U, Th, and REE (Miller and others, 1986; Wooden and Miller, 1990). Despite this enrichment, mineral occurrences containing these elements are rare with the exception of the Mountain Pass carbonatite described previously. There are, however, allanite-bearing pegmatites intruding Early Proterozoic gneiss in the New York Mountains which carry Th and REE concentrations that are above normal levels for this region (Miller and others, 1986). Because of these few occurrences and the general enrichment in U, Th, and REE in the EMNSA, the potential for deposits associated with the granitic rocks needs to be evaluated. It should be noted here that Jurassic granitoids also are enriched in large-ion lithophile and high-field strength elements (Fox and Miller, 1990) and some of the following discussion pertains to rocks of this age.

Geochemical studies at the mining-district scale of the levels of overall enrichment(s) of uranium in rock associated with granite-related uranium deposits provide a base to which we may compare apparent uranium concentrations found in the EMNSA by airborne radiometric surveys described above. Maximum concentrations of fairly widespread uranium detected in the EMNSA are slightly over 5 ppm (fig. 9C). Most of the areas showing these highest concentrations of uranium contain exposure of Proterozoic rock and locally Jurassic rocks. In a comparative study of uranium concentrations in uranium-mineralized and barren peraluminous two-mica granitoids, Friedrich and Cuney (1989) find that 62 unaltered samples of coarse-grained granite in the massif of St. Sylvestre have an average uranium content of 22 ppm; 45 fine-grained samples contain an average content of approximately 17 ppm. The St. Sylvestre granitoid massif contains a proved resource of 38,000 tonnes uranium. In marked contrast, 90 unaltered peraluminous granitoid samples from the barren Manaslu massif in Tibet contain an average content of 9 ppm uranium. Therefore, the 5 ppm-maximum uranium contents over broad regions of the EMNSA suggest that we are not dealing with a province wherein one would expect development of significant granite-related uranium deposits. Ballhorn (1989) notes that approximately 90 percent of the outcrops sampled within terranes judged to be favorable for the three types of granite-related uranium deposits he recognizes and we list above, show concentrations of approximately 10 to 20 ppm uranium. Such large volumes of uranium-enriched rock provide the source(s) of the uranium for

subsequent leaching and concentration by oxidizing and CO<sub>2</sub>-enriched, largely subsolidus fluids (Friedrich and Cuney, 1989).

The conclusions above do not preclude the possibility of there being some small, high grade occurrences of uranium in select areas in the EMNSA. Figure 48R shows the distribution of uranium concentrations in 1,050 samples analyzed from the EMNSA (U.S. Bureau of Mines, 1990a). The two highest concentrations of uranium found during this sampling program are 1,570 and 1,590 ppm; the former from the polymetallic vein at the Mammoth Mine (map no. 3, U.S. Bureau of Mines, 1990a) and the latter from the Esperanza group of claims (map no. 156), which are clustered in the general area of some carbonatite-related REE occurrences near Minerals Spring, in the Ivanpah Mountains. Both of the highly uranium-enriched occurrences yield significant responses when examined by hand-held scintillometers, and both of these occurrences are in areas showing widespread outcrops of Proterozoic rock. In addition, the Esperanza group of claims is within the favorable tract we delimit above for the presence of carbonatite-related REE deposits that extends from northwest of the REE deposits at Mountain Pass to the trace of the 500-m depth-to-basement contour southeast of Mineral Spring.

#### **Vein Deposits and Skarn Deposits in the EMNSA**

As discussed above, Hewett (1956) suggested that certain base- and precious-metal vein deposits in the area of the EMNSA might be of Proterozoic age. Preliminary investigations in an area east of the Albermanle Mine in the New York Mountains suggests the possibility that polymetallic veins there predate intrusion of Middle Proterozoic diabase dikes. The time of emplacement of many veins examined by us in Early Proterozoic rocks of the EMNSA can only be constrained to post-date deformation of the foliated host rocks. Thus only the possibility remains that some vein deposits might be as old as Early Proterozoic. Nothing was noted in the literature or during the bulk of our reconnaissance field investigations of the Early Proterozoic rocks to suggest that the majority of veins predated deformation or were formed during either of the orogenic events. The presence of a ductile deformed, metamorphic fabric in some polymetallic veins in the general area of Mineral Spring, Ivanpah Mountains, can be used as evidence to support emplacement during the Proterozoic. Furthermore, as we describe above, polymetallic skarn at the Butcher Knife Mine in the New York Mountains may also be Proterozoic in age (Ntiamoah-Agyakwa, 1987).

Tungsten veins of Early Proterozoic age are an additional type of vein deposit that may be found in EMNSA, although occurrences of these deposits are not presently known in the ENMSA. The possibility of veins of this type in the EMNSA is based on the association of tungsten-bearing veins with Early Proterozoic two-mica granite in the Hualapai Mountains, Arizona, located some

50 km to the southeast of EMNSA. Tungsten is present there as wolframite in veins. The 1,680- to 1,690-Ma granite in the Hualapai Mountains is considered to be part of the widespread, post-orogenic Early Proterozoic granites (Chamberlain and Bowring, 1990; Conway and others, 1991) that crop out in western Arizona and southern California. They are alkali-calcic in composition and have associated deposits or contain anomalous concentrations of tungsten, tin, beryllium, niobium, lanthanum, and yttrium (Conway, 1991). These granites are also found in the region of EMNSA (Bender and others, 1988; Anderson and others, 1990, Miller and Wooden, 1988).

#### Platinum-group Occurrences Associated with Ultramafic Rocks in Nevada and Arizona

Small exposures of ultramafic rock are reported in Early Proterozoic rocks in the McCullough Mountains and New York Mountains and elsewhere in Nevada and Arizona, and some of these exposures are associated with somewhat elevated abundances of platinum-group elements. Ultramafic rocks are known in nearby Early Proterozoic sequences in the Gold Butte area of southern Nevada (Volborth, 1962; Dexter and others, 1983), Lost Basin, northwestern Arizona (Page and others, 1986; Theodore and others, 1987a), and near Bagdad, Arizona (Floyd Gray, oral commun., 1988; C.M. Conway, unpub. data, 1990). Recently, anomalous concentrations of platinum were reported by Lechler (1988) at the Gingerload prospect in the Crescent Peak Mining District, Nev. The Crescent Peak Mining District is located at the north edge of the New York Mountains, approximately 11 km north of Castle Peaks, which are in the EMNSA. In the Crescent Peak Mining District, a silicified Early Proterozoic granitoid, has probably been mineralized by Cretaceous granite (D.M. Miller, written commun., 1991). The Gingerload prospect is a Pb-Zn-Cu-Ag-Au polymetallic vein (Lechler, 1988).

## Platinum-group Occurrences Associated with Ultramafic Rocks in the EMNSA

There are no known platinum-group mineral occurrences in the EMNSA. Some small exposures of metamorphosed Early Proterozoic ultramafic rocks in the Ivanpah Mountains in the EMNSA contain as much as 22 weight percent MgO (Wooden and Miller, 1990). However, there are no platinum-group analyses of these rocks available. There may be some potential for copper, cobalt, chromium, and platinum-group elements associated with such rocks in the EMNSA as Alaskan platinum-group-element-type or zoned ultramafic chromium-platinum-type occurrences (Page and Gray, 1986). These Early Proterozoic ultramafic rocks in the EMNSA should be studied geochemically to evaluate this potential.

## Mesozoic Deposits

### Breccia Pipe and Related Deposits

#### Gold Breccia Pipe

The Colosseum Mine, in the Clark Mountain Mining District north of Mountain Pass (pl.2), is historically the largest gold producer within the EMNSA, and currently (1991), the largest metals mine in operation, producing about 70,000 oz of gold and 30,000 oz of silver per year. Mining operations at the Morning Star Mine were on standby during April 1991, although gold continued to be produced from a 2 million-ton heap-leach pad at the property (Keith Jones, Vanderbilt Gold Corp., oral commun., 1991). Some ore apparently is also being shipped from several other small operations in the EMNSA, but gold production from them is minor. The Clark Mountain Mining District includes the Mountain Pass REE deposit previously described above, just outside the EMNSA boundary, and numerous abandoned copper, fluorite, and tungsten mines and prospects.

The Colosseum gold deposit, investigated in detail by Sharp (1984), is in a breccia pipe complex consisting of two connected felsite breccia pipes and outlying felsite dikes in a horst block of Proterozoic younger undivided granitoids (unit Xg, pl. 1). The ore is primarily free gold and disseminated auriferous pyrite. Surrounding related mineralization includes vein silver-copper in brecciated dolostone, tungsten, and fluorite, described below. Production, initially begun in 1929, was shut down in 1939, but the mine was reopened in 1987 as an open pit operation. According to the U.S. Bureau of Mines (1990a), ore reserves in 1989 were estimated at 10.5 million tons averaging 0.062 oz gold per ton. About 7 years of mine life were left, as of February, 1990, at a production rate of 70,000 oz/yr and gold price of \$400/oz. The following descriptive summary of the deposit is taken from Sharp (1984).

Breccia-pipe gold has not been defined formally as a deposit type (Cox and Singer, 1986), and thus characteristics of the Colosseum ore body cannot readily be compared with those of other deposits assigned to this specific type, although descriptions of some individual breccia-pipe gold deposits are available (Baker and Andrew, 1991). Sillitoe (1991) includes the Colosseum deposit with six other breccia pipe-hosted gold deposits he described. The overall range in contained gold as a geologic resource in those seven gold-bearing breccia pipes is 9-101 tonnes, and the mean content of gold in them is about 44 tonnes. Thus, the Colosseum Mine, which has been shown to contain about 20 tonnes gold, is one of the smaller of such systems known.

The Clark Mountain Mining District is in the southernmost tip of the 800-km-long Cordilleran fold and thrust belt, active tectonically from Permian through Cretaceous time (pl. 2). Three major northwest-trending thrust faults transect the region and, together, account for a total west-to-east displacement of 64 to 80 km (Burchfiel and Davis, 1971). Hewett (1956) estimated that, originally, 7,000 to 10,000 m of Paleozoic sedimentary rocks were thrust over the Proterozoic granitoids that now constitute the horst block in which the breccia pipes occur (fig. 57). Thrusting was followed by the high-angle Clark Mountain and Ivanpah normal faults that offset the region during basin-and-range deformation. Only about 500 m of Paleozoic carbonate rocks are exposed presently in the downdropped block to the west. The mineralized breccia pipes, dated at approximately 100 Ma (Sharp, 1984) were intruded after thrusting but before normal faulting that produced the basin/range horst-and-graben structures during the late Tertiary, as interpreted by Sharp (1984).

The breccia pipes, associated with felsite dikes, are exposed as resistant knobs in the Proterozoic gneisses. They are each about 170 x 235 m across at the surface, elongate northeast-southwest and connected by a narrow dike. The pipes represent multiphase breccia events, including significant collapse, and the lithologies within them indicate the composition of the overlying Paleozoic sedimentary rocks and the height of stoping during the development of the breccia. Overlying rocks included the Cambrian Tapeats Sandstone, Cambrian Bright Angel Shale, and Upper Cambrian to Devonian dolomite units. The Colosseum ore body is in the west pipe, but both pipes are mineralized. Each pipe consists of early felsite disrupted by later igneous breccia; however, the western pipe contains in addition abundant clasts of the structurally higher Paleozoic rocks that had been thrust over the Proterozoic rocks prior to onset of breccia-pipe emplacement. The abundance of sedimentary rocks as clasts indicates that the western pipe stoped through the Tapeats Sandstone and Bright Angel Shale well into the overlying dolomite, whereas the eastern pipe, predominantly containing basement rock and felsite igneous breccia, did not invade the Paleozoic sedimentary rocks significantly. Height above the current surface subjected to stoping was at least 430 to 460 m. Gold is disseminated in breccia and closely associated with pyrite, commonly filling fractures in pyrite. Highest concentrations of gold are in the western pipe

where pyrite has replaced carbonate breccia fragments, greatly increasing the overall concentration of sulfides.

Metal zoning in this part of the Clark Mountain Mining District is apparently related spatially and genetically to breccia-pipe mineralization (fig. 58). The gold zone is restricted to a circular area around the breccia pipes, plus a crescent-shaped area west of and bounded by the Clark Mountain normal fault. Within the breccia pipes, gold is associated mainly with sulfide minerals, primarily pyrite, whereas outside the pipes, gold is a constituent of quartz-barite and quartz-pyrite veins and veinlets that form a complex network surrounding felsite dikes. Silver is present predominantly in a broadly concentric zone west of, and bounded by the Keystone thrust; the veins comprise the Ivanpah Mining District, which had significant production into the early parts of the 20th century. Tungsten is found predominantly in a broad northwest-trending belt, intersecting a part of the gold zone and bounded on the west by the Clark Mountain fault. Field inspection of the regional distribution of tungsten veins suggests that some of the tungsten veins in the Proterozoic granitoids may not be related to the emplacement of the gold-bearing breccia pipe at the Colosseum Mine (pl. 2), inasmuch as known tungsten veins are present in Proterozoic granitoids as much as 6.5 km southeast of the Colosseum Mine. According to Sharp (1984), however, felsite dikes related to the emplacement of the breccia pipes extend from Clark Mountain to Mountain Pass, a distance of 11 km. Within the gold zone, tungsten is present as wolframite and scheelite in Proterozoic rock. Fluorite is in veins and shear zones associated with the Keystone and Mesquite Pass thrust faults west of the silver zone.

Sharp (1984) attributed these spatial relations to development of a single hydrothermal system initially stacked vertically, but subsequently displaced by gravity gliding (detachment faulting) on the then extant Keystone thrust and by high-angle normal faulting on the Clark Mountain fault. Epithermal vein silver, originally highest in the system, is now juxtaposed horizontally with the deeper gold-rich breccia pipe complex. Thus, the district zoning from west to east represents the displaced slices of once-vertical zones, with vein silver in the silver-copper brecciated dolostone occurrences at the top (fig. 58).

Felsite is the oldest rock in the breccia pipe at  $99.8\text{--}102\pm4$  Ma (K-Ar dates by Geochron Laboratories, Sharp, 1984), and consists of equal parts of quartz, K-feldspar, and sericite, plus secondary siderite; carbonate content is about 6 volume percent. The second phase of intrusion caused brecciation of the felsite, producing the igneous breccia consisting mainly of felsite matrix with minor quartzite, granite, gneiss, and andesite clasts. A third phase occurred in the west pipe producing collapse rubble breccia that is the most intensely mineralized rock of the entire complex. Dolomite breccia fragments are replaced by disseminated pyrite, accompanied by sphalerite, siderite, and chalcopyrite hosting gold and silver. As of 1984, commercial values of disseminated gold had been found as deep as 170 m below the surface.

According to Sharp (1984), the breccia pipes were emplaced by fluidization, with carbon dioxide the dominant fluidizing agent. Carbonate content increases with each stage of fluidization and intrusion (6 volume percent in the felsite, 20 volume percent in the igneous breccia, 30 volume percent in the rubble breccia), indicating increasing amounts of carbonate rock were assimilated by the intrusion and were incorporated into the breccias as the breccias reached progressively higher levels of stoping into the Upper Cambrian to Devonian dolomite.

Gold mineralization in the breccia pipes is present in an irregular vertical cylinder surrounding a barren core (Sharp, 1984). Depth of oxidation is about 100 m and degree of oxidation is about 80 percent. Supergene enrichment, however, is of no mineralogic or economic importance. The barren core in the interior of the rubble breccia pipe is void of gold but contains minor to major amounts of pyrite, zinc, and copper in well-silicified impervious rock. Late gold-bearing fluids were unable to percolate through this impermeable unit to reach the favored sulfide sites for gold deposition. Gold content varies directly with depth, and gold is commonly alloyed with silver (as electrum) as fracture fillings in pyrite or along grain boundaries. According to Sharp (1984), gold:silver ratios averaged 1.5 to 1 in marked contrast to the gold:silver ratios found in the surrounding vein deposits (see below). Gangue minerals in order of decreasing abundance are siderite, goethite, quartz, and sericite.

Pyrite is the most susceptible host for precipitation of gold, apparently because of its ease of fracturing (Sharp, 1984). There are four principal vein types: quartz-pyrite, quartz-barite, calcite-barite, and calcite-dolomite, plus occasional veins of an unknown source and genetic significance; they contain lead, antimony, tungsten, and zinc with minor silver.

According to Sharp (1984) mineral paragenesis and sequence of events are as follows: (1) early coarse, barren pyrite and minor quartz; (2) coarse, second-stage pyrite with included gold, chalcopyrite, sphalerite, bornite(?), and pyrrhotite; (3) shattering and fracturing of coarse pyrite; (4) major phase of gold mineralization, intruding fractures and interstices in pyrite, accompanied by sphalerite, chalcopyrite, and galena; (5) fine-grained, barren pyrite; (6) siderite replacement and flooding of the breccia matrix; and (7) localized veining by quartz and fine-grained pyrite. Gold is disseminated throughout the deposit; electrum mineralization was later parogenetically than the main-stage sulfide mineralization.

Two examples of gold included by pyrite were identified in scanning electron (SEM)

micrographs obtained from one polished thin section of felsite breccia from the Colosseum Mine (fig. 59A-D). The largest grain (about 7-8 microns, fig. 59B, C) was clearly deposited along a fracture, possibly representing the major gold-mineralizing phase (stage 4 above) of Sharp's (1984) paragenetic sequence. The smaller grain (about 4 microns, fig. 59D) may represent the second phase (stage 2 above) of included gold, associated with pyrrhotite. SEM examination also revealed grains of monazite and other rare-earth-element minerals localized in cracks between euhedral pyrite crystals (fig. 59E, F). Additional minerals identified within pyrite include bismuth and silver tellurides (fig. 59G), possibly resorbed chalcopyrite, pyrrhotite, and sphalerite (fig. 59H), sphalerite with euhedral pyrite inclusions and prominent replacement rim of covellite surrounded by feldspar (fig. 59I), and small grains of wolframite (fig. 59A).

#### Silver-Copper Brecciated Dolostone

Silver veins in the Ivanpah zone of the Clark Mountain Mining District are categorized as silver-copper brecciated dolostone; they are peripheral to the gold breccia pipes of the Colosseum ore body in Proterozoic rocks to the east (pl. 2). The veins are restricted to Upper Cambrian-Devonian dolomite, downdropped to the west from its earlier overthrust position above the Proterozoic rocks (pl. 1).

According to the U.S. Bureau of Mines (1990a), the veins are present in fractured, sheared, and brecciated zones in gray-yellow dolostone. Ore mineralization is reported as stromeyerite, ideally  $(\text{CuAg})_2 \text{S}$ , in pods and blebs, with minor azurite and malachite, and a gangue of calcite-dolomite and quartz (Hewett, 1956). Most of the individual vein systems strike northwest and dip steeply northeast. More than 4 million dollars in silver was produced from the Clark Mountain Mining District in the late 1800s, primarily from the Beatrice, Monitor, Stonewall, and Lizzie Bullock Mines (Sharp, 1984); production from the Monitor Mine continued up to 1942.

The U.S. Bureau of Mines (1990a) analyzed 92 samples from these deposits. Maximum silver content was 3,080 ppm, and maximum gold, 946 ppb. In 32 of these samples, copper was well over 1,000 ppm and >10,000 ppm in 11 of them. For 47 samples with gold >1 ppb and silver >1 ppm, the average Ag:Au ratio was 4,660. This ratio is notably high and contrasts with the Ag:Au ratio of approximately 0.67 at the Colosseum gold deposit. Lead content was >10,000 ppm in 4 samples but 1,000 ppm or greater in 32 samples. Zinc showed >10,000 ppm in only 3 samples and >1,000 ppm in 18 samples.

Sharp (1984) developed an intriguing hypothesis for the origin of the Ivanpah silver deposits, relating them genetically to the gold mineralization of the Colosseum breccia pipe. By this hypothesis, silver-bearing hydrothermal fluids accompanying the felsite breccias rose through the

Proterozoic granitoid rocks, in which the gold ore bodies are now present, into the overthrust Paleozoic sedimentary rocks. They stoped upward well into the Cambrian-Devonian dolomite units; height of stoping is demonstrated by the presence of abundant carbonate fragments within the Colosseum breccia pipe. Mesothermal gold mineralization is richest in this pipe because of selective massive replacement of carbonate minerals by sulfide minerals. Epithermal vein silver, however, emplaced in the overlying dolomite, was subsequently downdropped to the west along high-angle normal faulting and low-angle detachment fault(s) during a post-mineral extensional event localized along a pre-existing thrust plane. Thus, the breccia pipe was effectively decapitated, spatially juxtaposing the silver-copper occurrences in the dolomite on the west with the gold mineralization in lower parts of the pipe to the east (fig. 60). The mineral zoning and fault pattern as described by Sharp (1984) fit this explanation.

Although not exact analogues, the silver-copper deposits in the Ivanpah Mining District exhibit some characteristics of polymetallic veins and polymetallic replacement occurrences, which generally are related to igneous intrusions of felsic composition (Cox and Singer, 1986). They are particularly common in areas of high permeability, such as breccia veins and pipes, and may form replacement bodies in carbonate rocks. If the analogy of the Ivanpah silver veins with the polymetallic vein, grade-tonnage model is correct, some conclusions may be drawn regarding the probability of discovery of additional economic ore bodies of this model type. Grade-tonnage models based on data from 75 deposits in the United States and Canada classified as polymetallic veins indicate a 90 percent chance that any newly discovered deposit will contain at least a few hundred tonnes of ore, at average silver grades of approximately 140 g/tonne. Only a 10 percent chance exists that that a new deposit will contain as much as 200,000 tonnes of ore, at grades as high as 4,700 g/tonne silver. The median tonnage for these 75 deposits is 7,600 tonnes and the median grade is 820 g/tonne silver. These values indicate that a deposit yet to be discovered has a 50 percent chance of containing as much tonnage at a grade of just over 800 g/tonne silver. It seems unlikely that economic, large-tonnage deposits of a type similar to the silver veins of the Ivanpah Mining District are likely to be discovered in the EMNSA.

#### Tungsten Veins

Tungsten is present in veins and skarns within the EMNSA. Veins are primarily in Proterozoic schist and gneiss and localized in a northwest trending belt south of and overlapping the gold and silver zones of the Ivanpah/Colosseum breccia pipes (pl. 2). Other small occurrences are present in presumably 70-Ma Cretaceous monzogranites, mostly in the Signal Hill Mining District near the south end of the Paiute Range (area VI, fig. 55). According to the U.S. Bureau of Mines (1990a), the Mojave Tungsten Mine, south of the Colosseum Mine, produced 64,000 lb of 60 percent WO<sub>3</sub>

concentrates in 1915 and 1916; elsewhere, production has been minor or nil, although one sample (from the Old Boy prospect, 35°00'N., 115°02'W.) analyzed by the U.S. Bureau of Mines (1990a) contains 25,900 ppm tungsten.

Tungsten veins in both the Ivanpah/Colosseum District and the Cretaceous intrusive bodies farther south are in fault and shear zones that strike generally northwest. Tungsten mineralization most commonly consists mainly of wolframite present with vein quartz; scheelite is present in some veins. At the Mojave Mine, gold, silver, pyrite, azurite, and malachite, in a gangue of quartz and subsidiary calcite, are accessory to the iron-manganese and calcium tungstates. Limonite is common in some veins. Consistent detection of tungsten in veins within the Upper Cambrian to Devonian dolomite as well as in quartz veins of the Proterozoic granitoids prompted extension of the tungsten zone around the Colosseum breccia pipes west of the Keystone and Clark Mountain faults (fig. 58; Sharp, 1984).

Sharp (1984) concluded that the tungsten mineralization surrounding the Colosseum Mine was genetically related to the breccia pipe complex. Tungsten was deposited in a zone both vertically and laterally intermediate between mesothermal gold and epithermal silver.

The descriptive model of tungsten veins by Cox and Bagby (1986) fits closely with characteristics of the tungsten veins in the EMNSA. Such deposits typically contain wolframite and base-metal sulfides in quartz veins associated with granitoid rocks emplaced in sedimentary or metamorphic rocks. The deposits consist generally of swarms of parallel veins. Grade/tonnage models based on data from 16 deposits worldwide indicate that a 90 percent chance exists for any new discovery to contain at least 45,000 tons of ore at a grade of 0.6 percent  $WO_3$ , whereas only a 10 percent chance exists for a new deposit to contain as much as 7,000,000 tons at grades as high as 1.4 percent  $WO_3$ , provided that there is an independence between grade and tonnage. A probability of 50 percent applies to discovery of a deposit as large as 560,000 tons at grades as high as 0.9 percent  $WO_3$  (Jones and Menzie, 1986a).

#### Fluorite Veins

Fluorite veins are present at scattered localities in the EMNSA, most notably throughout the entire Clark Mountain Mining District (Sharp, 1984) where the mineralization is in low-angle shears and fractures parallel to the Keystone and Mesquite Pass thrust zones (fig. 58). In this northernmost part of the EMNSA, veins commonly contain varying amounts of pyrite, copper carbonate minerals, silver, and tungsten, all of which are associated also with the Colosseum breccia pipe gold mineralization. Because fluorite is much more broadly distributed than the mineralized zones adjacent to the breccia pipes, it is not clear that the fluorite is similarly related genetically (see above).

According to the U.S. Bureau of Mines (1990a), minor fluorite production occurred only at the Pacific and Juniper Mines, and there has been none since 1961. At the Pacific Mine, about 3.2 km southwest of the Colosseum ore body, fluorite is "concentrated in zones at least 6 ft thick along low-angle, north-striking, west-dipping thrust faults," within Upper Cambrian to Devonian dolomite. It also is present in high-angle shear zones together with quartz, sericite, limonite, stibnite, and copper minerals. Analyses of eleven samples showed metal contents as high as 122,000 ppm antimony, 367 ppm molybdenum, 592 ppm silver, 190 ppm tungsten, and 56,300 ppm zinc. One sample contained 3.07 weight percent copper and 26.1 weight percent lead, and 3 others contained 3.68 weight percent, 3.94 weight percent, and 5.26 weight percent fluorine, respectively. The U.S. Bureau of Mines (1990a) concluded from these analyses that "significant resources exist" at the Pacific Mine. At the Juniper Mine, about 1.6 km south of the Pacific Mine, massive purple and green fluorite is present in sheared, brecciated zones 2 m thick or more within surrounding carbonate rock. The zones are partly silicified, with minor amounts of limonite and copper carbonate minerals. Based on sample analyses, the U.S. Bureau of Mines (1990a) estimates resources of 300,000 tons containing 20 to 30 weight percent fluorite, 3 weight percent copper, and 10 troy oz/ton Ag. The fluorite veins at both the Pacific and Juniper Mines are associated with polymetallic veins, as are a number of fluorite prospects in the area. Scattered fluorite veins also are present in shear zones in Proterozoic granite gneiss near the Albemarle Mine in the northeast corner of the EMNSA in the Castle Peaks Wilderness Study Area (Miller and others, 1986). Production was insignificant from these veins, but 15 samples analyzed ranged from 1 percent to 59 percent fluorine (U.S. Bureau of Mines, 1990a). Miller and others (1986) did not identify any potential for development of resources there. Additionally, fluorite veins are present in dolomite near the contact with the Mid Hills Adamellite, associated with the Big Hunch molybdenite system in the southern New York Mountains (pl. 2). Select samples of mineralized Mid Hills Adamellite in the general area of the Giant Ledge Mine (U.S. Bureau of Mines, 1990a, map no. 296) show flooding by fluorite to as much as 20 volume percent. Polymetallic veins that cut the Mid Hills Adamellite at this locality in Caruthers Canyon also show assemblages of galena, chalcopyrite, quartz, pyrite, fluorite, and white mica. In the southern Providence Mountains, the Golden Nugget deposit includes blue and green fluorite veins in association with quartz and polymetallic veins in fault and shear breccia zones. Production from this deposit has been nil, but the U.S. Bureau of Mines (1990a) analyzed 111 grab, host, vein, chip, and dump samples, of which 15 contained lead, from 100 to 620 ppm, 25 contained zinc, from 26 to 600 ppm, 89 contained copper, from 20 to 990 ppm, 56 contained molybdenum, from 6 to 270 ppm, 61 contained gold, from a trace to 2.83 troy oz/ton, 59 contained silver, from a trace to 1.4 oz/ton, and 7 chip samples contained 0.08 to 25 weight percent fluorine. If the Golden Nugget prospect is developed for other metals, fluorite could be a possible by-product.

No descriptive or grade-tonnage model exists in Cox and Singer (1986) for fluorite veins. If, however, future production of fluorite in the EMNSA is contingent upon development of associated polymetallic veins, the probability is not high that large tonnage economic ore bodies of that type remain to be discovered in the EMNSA, based on statistics of the grade-tonnage model for polymetallic veins (Cox and Singer, 1986).

### Known Occurrences

In the EMNSA (pl. 2; see above), the only known occurrence of gold-bearing breccia pipes is at the Colosseum Mine. Silver-copper brecciated dolostone is present in a broad area, generally west of the ores at the Colosseum Mine, in Paleozoic rock sequences (pl. 1). The silver-copper brecciated dolostone mineralization presumably developed at the same time the ores at the Colosseum Mine were emplaced and forms a halo of petrogenetically-linked deposits. Tungsten veins are present in Proterozoic granitoids in and around the general area of gold ores at the Colosseum Mine (pl. 2); most of them are presumably linked to the emplacement of the gold-bearing breccia pipe (Sharp, 1984), but some may not be related to the pipe development during the Cretaceous (see above). In addition, there are scattered occurrences of tungsten veins elsewhere in the EMNSA, including widespread veins in the Signal Mining District near the south end of the Piute Range (pl. 2; see above), and minor occurrences hosted by the Mid Hills Adamellite. Vein-type fluorite is associated with the Colosseum breccia pipes (see above), in Paleozoic sequences of carbonate rock west of the Colosseum Mine (pl. 2), and also is present in scattered localities elsewhere (see above).

### Permissive Terrane and Favorable Tract

We believe that a permissive terrane and a favorable tract for gold-bearing breccia pipes are largely coextensive and are defined in the northern part of the EMNSA by the outer limit of silver-copper brecciated dolostone occurrences in Paleozoic rock and the outer limit of tungsten veins in Proterozoic younger granitoid (pl. 2; fig. 55). The terrane outlined for gold-bearing breccia pipes is also shown as being both permissive and favorable for tungsten veins as is another small area near the south end of the Paiute Range (fig. 55).

We show no permissive terranes or favorable tracts specifically for silver-copper brecciated dolostones or fluorite veins in the EMNSA. Inasmuch as silver-copper brecciated dolostones are probably related to Mesozoic magmatism, the vast expanse of Mesozoic igneous rocks in the EMNSA makes all of the carbonate sequences exposed there permissive hosts largely coextensive with the permissive terranes shown below for skarn.

Geologic factors controlling ore deposition at the Colosseum gold mine include the presence of Proterozoic crystalline host rock overlain by reactive carbonate sequences at the time of emplacement of a CO<sub>2</sub>-rich magmatic-hydrothermal system during the Cretaceous. Exposure of the mesothermal gold-bearing ores adjacent to the epithermal silver veins of the Ivanpah zone was dependent on a complex sequence of tectonic and erosional events, according to Sharp (1984). The vein-silver is the downfaulted top of the Clark Mountain breccia-pipe system, emplaced adjacent to the Colosseum ore zone as a result of vertical uplift and tilting of the Proterozoic basement. This was then followed by detachment faulting that decapitated the breccia pipe and juxtaposed the vertically stacked precious-metal zones. The west breccia pipe was particularly favorable to ore mineralization because it stopped high into Upper Cambrian to Devonian dolomite and includes large volumes of carbonate fragments within the breccia. This reactive rock was susceptible to replacement by pyrite, whose low strength and brittle character fractured in response to continued brittle-style strain, thereby providing a receptive host for late gold-mineralizing fluids (Sharp, 1984).

#### **Porphyry Molybdenum Deposit, Low Fluorine**

#### **Classification of the Deposits**

The Big Hunch system in the southwestern part of the New York Mountains in the EMNSA is an example of a number of relatively recently reclassified molybdenum deposits and molybdenum-enriched systems that are associated with Jurassic to Pliocene calc-alkaline magmatic arcs in the western North America Cordillera (this section of the report is modified from Theodore and others, 1991a). In addition, several molybdenum-enriched porphyry systems of Paleozoic age (Schmidt, 1978), and presumed Paleozoic age (Ayuso and Shank, 1983), crop out in eastern North America and bear many similarities to the ones in western North America. Such stockwork molybdenum systems generally have low fluorine contents relative to deposits of the better known Climax type (Theodore and Menzie, 1984). The fluorine-deficient porphyry molybdenum systems previously have been included in different ways in the several classifications of porphyry molybdenum deposits (Woodcock and Hollister, 1978; Sillitoe, 1980; Mutschler and others, 1981; White and others, 1981; Cox and Singer, 1986). Guilbert and Park (1986) considered the low-fluorine stockwork molybdenite deposits as a subset of porphyry base-metal systems. The one striking characteristic of all these systems is their minor-element signature, especially when compared to the better known stockwork molybdenum systems exemplified by the one at Climax, Colo. (see Westra and Keith, 1981; White and others, 1981). Thompson (1982), in a further modification of the classification scheme for stockwork molybdenum deposits, suggested that alkali-calcic and the alkali molybdenum stockwork deposits of Westra and Keith (1981) be subdivided into a

monzonite-syenite subtype and into a leucogranite subtype. The Climax-type systems are characterized by highly differentiated high-silica rhyolite magmas that are enriched in fluorine (locally as much as 2-3 weight percent), niobium, rubidium, molybdenum, tin, and tungsten and are nearly depleted in copper and strontium (Ludington, 1981). The Climax-type systems are present in rifted cratons whereas the relatively low-fluorine, or quartz monzonite-type systems are related to continental margins.

Fluorine-deficient porphyry molybdenum systems generally show overall fluorine contents of less than 0.1 weight percent, and many of these systems also include significant concentrations of copper and silver (Czechura, 1983); some include significant tungsten and gold (Theodore and others, 1991a; Theodore and Menzie, 1984). At Buckingham, Nev., gold skarns at the Surprise Mine and at the Carissa Mine probably are temporally and genetically related to the Buckingham stockwork molybdenum system (Schmidt and others, 1988). Westra and Keith (1981, fig. 9) showed a continuity of hypogene copper and molybdenum grades between porphyry copper deposits and fluorine-deficient porphyry molybdenum deposits.

Fluorine-deficient porphyry molybdenum systems, which are widespread throughout the geologic provinces of the Cordillera, are present in magmatic arcs that generally parallel the Mesozoic batholiths. In the Basin and Range province, several Late Cretaceous-age deposits in Nevada (Buckingham, Hall, Pine Nut) and many other prospects are related to small granitic bodies peripheral to the Sierra Nevada batholith. These prospects include the Magruder Mountain (Sylvania), Nev., and, in the EMNSA, the Big Hunch, Calif., systems, both of which may have been emplaced sometime in the Mesozoic (see below).

Grade and tonnage distribution plots for 33 fluorine-deficient and nine Climax-type stockwork molybdenum systems reveal some significant differences between these two types of deposit. The most pronounced difference between fluorine-deficient and Climax-type stockwork molybdenum deposits is their grades; median grade for the fluorine-deficient type is 0.084 percent Mo and for the Climax-type is 0.19 percent Mo. The median tonnages for fluorine-deficient and Climax-type systems apparently are 93 million tonnes and 230 million tonnes, respectively. From data plots for the fluorine-deficient molybdenum stockwork systems, one might estimate that roughly 10 percent (0.1) of such undiscovered systems in the Cordillera of western North America would include tonnages greater than 630 million tonnes. Last, tonnage and grade for the fluorine-deficient molybdenum stockwork deposits are independent statistically (Theodore and Menzie, 1984).

#### Big Hunch Molybdenum System

Most of this section of the report dealing with the Big Hunch molybdenum system is taken from Ntiamoah-Agyakwa (1987). The Big Hunch system is an extremely large system that is

inferred to encompass approximately 1.8 billion tons of mineralized rock with an estimated grade of approximately 0.025 weight percent molybdenum (U.S. Bureau of Mines, 1990a). As such, the grade for the Big Hunch system is about one-half the median grade for the deposits of this class of deposit reported by Theodore and Menzie (1984). The main center of alteration associated with this system is the Big Hunch Mine area (Secs. 34 and 35, T. 13 N., R. 15 E.). A second center east of the Lighthouse Mine (secs. 35 and 36; T. 13 N., R. 15 E.) is much less well-developed. The best developed alteration zones are quartz, phyllitic (quartz-sericite) and argillic. No propylitic stage of alteration has been observed. A questionable potassic stage is poorly represented by erratic relict K-feldspar stable assemblages. Intensity of silicification declines away from the core of the system and concentrations of sericite and clay minerals increase successively. Ore mineralogy is simple, consisting chiefly of pyrite, chalcopyrite, sphalerite, galena, and molybdenite with minor amounts of magnetite, specularite, bornite, and wolframite-heubnerite. We studied two select samples of diamond drill core from DDH York no. 9 at depths of approximately 68 m below the surface using the scanning electron microscope. The purpose of this admittedly cursory examination was to determine the mineral phase(s) that hosts the bulk of the silver in the system. Silver was not detected during any of the spot analyses of the polished surfaces. However, we did determine that many of the quartz-molybdenite veins in the Big Hunch system also contain tetrahedrite, and some minor amounts of galena as minute blebs in stout crystals of pyrite. None of the tetrahedrite was found to contain detectable silver, as is common in many low-fluorine stockwork molybdenum systems elsewhere (Theodore and Menzie, 1984). In places, tetrahedrite seems to predate paragenetically the crystallization of minor amounts of sphalerite. In addition, some tetrahedrite in close proximity to chalcopyrite shows notable concentrations of arsenic and some zinc. Growth zones of tetrahedrite against quartz suggest that some of the earliest crystallized tetrahedrite is more arsenian than the latest crystallized varieties. Fluorite is ubiquitous. Although the presence of fluorite in the Big Hunch system rightly suggests highly elevated concentrations of fluorine during the metallogenesis here, the overall abundance of fluorine in these types of systems is still less than that found in the much higher grade, and rift-related Climax-type systems (White and others, 1981; Westra and Keith, 1981; Theodore and Menzie, 1984).

The surface and vertical extent of the Big Hunch system was established by Ntiamoah-Agyakwa (1987) from surface mapping on a scale of 1:4,800 and data from over 2,000 m of drill cores representing nine drill holes. All holes were drilled from the surface and went through the mineralized zones. The Big Hunch system is semi-elliptical: in detail, it is a hook-shaped (pseudoannular) compound system made-up of two nested concentric patterns. It measures about 3.2 x 4 km. The larger outer system is incomplete, cut off on the west by the Cliff Canyon fault and on the north by an ENE-striking fault (pl. 1). The exposed vertical extent of the system is about 250 m, from 5,700 ft to 6,500 ft in elevation. The west surface of the central stockwork apparently dips about 35° SW under the Cliff Canyon fault. This suggests to Ntiamoah-Agyakwa

(1987) that the southern portion of the Cliff Canyon fault is a normal fault with the downthrown side to the west.

In the Big Hunch molybdenum system, quartz-sericite alteration is not only the most conspicuous, but also the best-developed alteration product in the Mid Hills Adamellite which hosts the system (Ntiamoah-Agyakwa, 1987). This type of alteration is characterized by a preponderance of quartz veins with sericite selvages. Pyrite is not ubiquitous in this alteration; fluorite is commonly present. Muscovite is characteristically coarse-grained. Development of the quartz-sericite veins apparently took place during three episodes, the second of which seems to have been the episode during which the bulk of the molybdenite was introduced. The second episode of silicification also involved intense hydroxyl metasomatism. Clay minerals and fine-grained hydrothermal quartz are replaced by quartz veins. This second generation quartz is massive, compact, milky quartz. In most cases, veining is episodic, resulting in rhythmic bands of quartz and sulfides and(or) oxides. In its most advanced stage, silicification is the most destructive event, obliterating most of the earlier stages of alteration. In areas where development stages can be traced, such as at Lecyr Well, (T. 14 N., R. 16 E., sec. 21), alteration proceeds from closely-spaced fractures to quartz veins with sericite selvages. Influx of altering fluids depended on either the extent of fracturing or permeability of the initial argillized host. Where extensive microfracturing preceeded fluid influx, the product is near complete silicification. Fluorite, molybdenite or pyrite may accompany this second stage. In some cases, orthoclase-microcline veins developed.

Although the geochemistry of the Big Hunch molybdenum system has been described by Ntiamoah-Agyakwa (1987) and the U.S. Bureau of Mines (1990a), additional analyses of 36 rocks in the general area of the system are shown in table 12. The overall intensity of fluorine metasomation (as fluorite and micas mostly in veins, see above) and the sporadic intensity of molybdenum introduction is shown by the data. Furthermore, the large number of samples showing fluorine abundances greater than 1,000 ppm, together with their locations throughout an area of approximately  $5 \text{ km}^2$ , emphasize that the emplacement of this system during the Late Cretaceous has affected significantly a very large volume of rocks.

Potassic alteration is either very weakly developed or absent from the Big Hunch molybdenum system in contrast to the extent of potassic alteration at other stockwork molybdenum systems (Ntiamoah-Agyakwa, 1987). Secondary biotite was noted only in a 1 m section in hole 9. Here, it is poorly developed at a depth of about 3 m as a thin vein about 0.1 mm wide. Pervasive argillic alteration is cross cut by 1- to 2-mm wide sericite veinlets and 0.1 mm fine-grained, amorphous biotite microveins. Biotite in the original porphyritic to equigranular adamellite is in varying stages of degradation. Primary magmatic orthoclase is still preserved. This unique assemblage may be a localized product and not system wide. Potassic alteration, as defined for porphyry coppers and

molybdenum deposits (Einaudi and Burt, 1982; Hollister, 1978) is thus not represented. The following observations support such a conclusion: (a) the orthoclase vein described above is pegmatitic, at least 2 cm across, and cuts a quartz-sericite alteration in which the original orthoclase phenocrysts have been partially or completely replaced; (b) contrary to occurrences in classical porphyry systems, both orthoclase and biotite veins are paragenetically younger than argillic and phyllitic alteration; (c) the paragenetic assemblages in other drill holes involved either complete disappearance of both potassium-rich minerals (K-feldspar and biotite) or preservation of original primary granitic mineralogy.

There is no correspondence at the regional scale between density of deposits or occurrences and intensity or overall volume of metal introduced. As described above, the subeconomic (at 1991 market conditions), Big Hunch molybdenum system hosts one of the largest concentrations of metal known to-date in the EMNSA. However, the grade of this type of molybdenum system is the limiting factor that finds many of such systems in the western Cordilleran of the United States economically marginal at best. Nonetheless, there is some zoning of types of veins marginal to the Big Hunch system. As pointed out by Ntiamoah-Agyakwa (1987), some of the more important polymetallic vein occurrences in the general area of the Big Hunch System include Lighthouse (Dorr?, Cu-W), Giant Ledge (Pb-Cu with Ag), and Sagamore (Cu-Pb with Zn, Ag and W). Smaller prospects include Garvanza (Cu-W), Hard Cash (Cu-Zn-F, W?), Lecyr Well (Cu, Zn-Mo?), and Live Oak (Cu-Zn with W). Thus, this area of the New York Mountains is classified by Ntiamoah-Agyakwa (1987) as a polymetallic Mo-Cu-W porphyry center with varying amounts of silver, lead, and zinc in its surrounding veins.

Potassium-argon dates were obtained by Ntiamoah-Agyakwa (1987) on six samples spatially and(or) temporally associated with emplacement of the Big Hunch molybdenum system. The six dates obtained cluster into two groups: 67 to 71 Ma and 59 to 66 Ma, the short time interval between the two clusters suggested to Ntiamoah-Agyakwa (1987) that all samples dated are part of one continuous process during Late Cretaceous magmatism event associated with emplacement of the Mid Hills Adamellite. However, U-Pb data for zircons from this body indicate that it crystallized about 93 Ma (E. DeWitt, oral commun., 1985). The Late Cretaceous ages ascribed to the alteration associated with the Big Hunch system in the area of Fourth of July Canyon by Ntiamoah-Agyakwa (1987) have been verified by others (69 Ma on biotite in sericitized rock, D.M. Miller, written commun., 1991; 69 to 88 Ma on biotite, Beckerman and others, 1982). Thus, there was either polyphase emplacement of the Mid Hills Adamellite over approximately 25 m.y. or the alteration and emplacement of the Big Hunch system was related to a Late Cretaceous hydrothermal event discrete from the Mid Hills Adamellite.

## Known Occurrences

The presence of molybdenum in the general area of the New York Mountains has been known since the 1950s (Ntiamoah-Agyakwa, 1987), and nearby relatively small veins have achieved some production of note in the general area of the Big Hunch system. As indicated by the maps showing our classification of deposit types in the EMNSA, there is in fact only a small number of vein-type occurrences in the general area of the Big Hunch (pl. 2). The petrogenetic linkage of polymetallic veins and other types of deposits to low-fluorine, porphyry molybdenum systems is indicated schematically on figure 52. We cannot preclude the possibility that there are linkages elsewhere in the EMNSA, outside the general area of the Big Hunch system, between polymetallic veins and some buried porphyry molybdenum system. A corollary from this schematic linkage is the fact that one does not need to observe enhanced abundances of molybdenum and fluorine to indicate possible presence of a porphyry molybdenum system at depth, although fluorine and molybdenum anomalies might be additional positive signatures. A number of samples analyzed from polymetallic veins in the EMNSA by the U.S. Bureau of Mines (1990a) have been shown to include more than 500 ppm molybdenum (fig. 51E). The pervasive character of veining, fractures, and alteration patterns, if present, are the diagnostic features one must first consider before making a qualified judgment about the potential presence of a porphyry system, either a molybdenum one, or a copper-molybdenum one.

## Permissive Terranes

We delineate one terrane as being permissive for stockwork molybdenum systems in the EMNSA (fig. 55). This terrane follows generally the inferred and mapped outline of the Mid Hills Adamellite. As such, the localities of possible stockwork molybdenum mineralization at Globe Canyon are also included within this permissive terrane. The mineralization at Globe Canyon apparently is associated spatially with two small outlines of the Mid Hills Adamellite that crop out approximately 0.5 km south of the main mass of the body (pl. 1). We exclude Jurassic plutonic rocks from the permissive terrane for stockwork molybdenum systems primarily because most contain relatively reduced contents of silica relative to those stockwork molybdenum systems known elsewhere in the Cordillera of western North America. The Jurassic plutonic rocks in the EMNSA as a group apparently are not that highly evolved. In addition, we have chosen to exclude all Cretaceous plutons other than the Mid Hill Adamellite either because of their low silica chemical composition or because of the absence of a widespread composite mode of emplacement. The Rock Springs Monzodiorite of Beckerman and others (1982) generally has an overall low silica content (54-64 weight percent) compared with igneous rocks associated with most of these types

of molybdenum systems; it is essentially a porphyritic, compositionally variable rock that includes mostly monzodiorite, quartz monzodiorite, and some quartz monzonite (pl. 1). Estimates of 0 to 3 kb pressures of emplacement for the Teutonia batholith by Anderson and others (1988, 1991) were obtained from the Kessler Springs Adamellite, the Mid Hills Adamellite, and the Rock Springs Monzodiorite. The 3 kb pressures of the Rock Springs Monzodiorite suggest that its currently exposed levels may be well below those depths commonly ascribed to most porphyry systems, molybdenum and copper-molybdenum, in the southwestern United States. The Kessler Springs Adamellite is seemingly shallow seated (0-0.5 kb; Andersen and others, 1991), but it apparently shows minimal evidence of a wide-ranging, composite nature for its emplacement mode, as does the Teutonia Adamellite phase of the batholith (D.M. Miller, oral commun., 1991).

#### Favorable Tract

We delineate a relatively small area in the general area of the Big Hunch system as being favorable for the presence of stockwork molybdenum systems (fig. 55). As depicted, this favorable tract is bounded on the west by the trace of the Cliff Canyon fault and on the east by alteration in Mid Hills Adamellite in the general area of the Lighthouse Mine. Our failure to depict a favorable tract in the general area of Globe Canyon reflects our judgment that the occurrences there should not be ranked as equivalent to those at the Big Hunch system (see above).

#### **Porphyry copper and porphyry copper, skarn-related**

#### Known occurrences

There are no known occurrences of porphyry copper systems or porphyry copper, skarn-related systems in the EMNSA as defined by Cox and Singer (1986). In the exposed upper parts of many of these systems, the rocks commonly are intensely fractured and altered to various combinations of potassic, phyllitic, intermediate argillic, and argillic assemblages across wide areas, sometimes to as much as 20-30 km<sup>2</sup>. Many of these systems also include quartz stockwork veins that are also commonly widespread, and the systems also include distinctive pyritic halos, together with elevated abundances of many metals as discussed above. Many of these features are shared with stockwork molybdenum systems, and the features are present in the general area of the Big Hunch system (see above). In addition, the porphyry copper and the porphyry copper, skarn-related systems would show the same genetic relations to other types of mineral occurrences depicted for the stockwork molybdenum systems (fig. 52). In the general region of the EMNSA, porphyry copper systems have been inferred to be present in the area of Turquoise Mountain in the Halloran Hills (Hall, 1972), and in the Crescent Peak Mining District, Nevada, about 10 km

northeast of the EMNSA (D.M. Miller, oral commun., 1991). Near the south end of the Providence Mountains, north of the Horse Hills, Miller and others (1985) assigned a low potential for the presence of a gold-rich porphyry copper system in iron oxide-stained Jurassic igneous rocks. However, our field examination did not reveal the presence there of widespread altered and shattered rocks typical of the upper parts of many of these types of porphyry systems. In addition, the exposed iron oxides apparently are related to mineralized dilational fractures that opened in response to displacements along the regionally extensive Bighorn fault about 3 km to the east. Finally, examination of approximately 10 thin-sectioned rocks from this area failed to show the presence of any alteration phenomena characteristic of these systems.

#### Permissive terranes and favorable tract

All of the EMNSA underlain by Mesozoic igneous rocks is permissive for the presence of porphyry copper systems, and where these igneous rocks are near or in contact with sequences of Paleozoic carbonate rock, these latter areas are also permissive for the presence of porphyry copper, skarn-related systems. Excluding alteration associated with the Big Hunch system, the most likely porphyry-style alteration of igneous rocks noted during our study is in the general area of New Trail Canyon, in the northern part of the Ivanpah Mountains. Here, some outliers of the Ivanpah Granite, which crop out away from its major exposures farther to the south in the Ivanpah Mountains, are intensely fractured, iron-stained, and hydrothermally altered across several km<sup>2</sup>. The outlined favorable tract for porphyry copper and porphyry copper, skarn-related systems (fig. 56) coincides with one of the tracts also classified as favorable for the occurrence of various other types of skarn and polymetallic replacement occurrences in the EMNSA to be described below.

#### Skarn

Smirnov (1976) suggested that classification of skarns be based upon the composition of the original protolith of the skarn: calcareous, magnesian, or silicate. However, we follow the nongenetic definition of skarn proposed by Einaudi and others (1981): "replacement of carbonate [or other sedimentary or igneous rocks] by Ca-Fe-Mg-Mn silicates [resulting from] (1) metamorphic recrystallization of silica-carbonate rocks, (2) local exchange of components between unlike lithologies during high-grade regional or contact metamorphism, (3) local exchange at high temperatures of components between magmas and carbonate rocks, and (4) large-scale transfer of components over a broad temperature range between hydrothermal fluids \*\*\*and predominantly carbonate rocks." Most metallized skarns owe their genesis to processes largely involving the

fourth process. Thus we follow an overall classification of skarns based upon their sought-for metal content (see also Shimazaki, 1981 and Zharikov, 1970).

### Known Occurrences

We classify known metallized skarns in the EMNSA as polymetallic (18), zinc-lead (6), tungsten (3), iron (10), tin-tungsten (1), and copper (26)--the number of each shown parenthetically (table 8). Almost all of the skarns apparently formed during emplacement of either Jurassic or Cretaceous magmas into the carbonate sequences of Paleozoic rock that crop out in the EMNSA (pl. 1). A small number of relatively minor occurrences of skarn in the New York Mountains may be Proterozoic in age (see above). Examination of the regional distribution of the types of skarn in the EMNSA suggests that there is no readily apparent clustering by type of skarn in the immediate area of any particular type of granitoid body. Jurassic granitoids, however, seem to be associated preferentially with some of the largest and highest grade iron skarn deposits in the EMNSA such as those at the Vulcan Mine. Skarns are distributed widely across most of the exposed carbonate sequences of rocks in the EMNSA (pl. 2). Some of the most prominent skarns in the EMNSA are: (1) along the west flank of the Clark Mountains in the general area of the Mohawk and Copper World Mines--presumably Cretaceous in age; (2) in the Ivanpah Mountains in the general area of the Evening Star and Standard No. 2 Mines--presumably Jurassic in age; (3) near the central Providence Mountains at the Vulcan Iron Mine--Jurassic in age; and (4) in the general area of the Cowhole Mountains, the Little Cowhole Mountains, and Old Dad Mountain (pl. 2).

Of the 197 rock samples analyzed by the U.S. Bureau of Mines (1990a) that contain greater than 500 ppb gold, 36 are from mineralized skarns of all types in the EMNSA. As we described above, this particular data base does not include rocks from the Providence Mountains, which have been shown to host six skarn occurrences (pl. 2). Nonetheless, there is a small number of samples showing anomalous concentrations of gold in the RASS and PLUTO heavy-mineral-concentrate and rocks data bases obtained from the Providence Mountains (figs. 31, 32). All skarns regardless of type in the EMNSA can thus be characterized as being potential sites preferred for the deposition of at least some gold, and, in fact, significant concentrations of gold in some places. The highest concentration of gold reported by the U.S. Bureau of Mines (1990a) is from copper skarn at the New Trail Mine in the Ivanpah Mountains (51,700 ppb gold, map no. 163). In addition, our limited sample base collected during this study (tables 4, 5) includes a small number of samples from five occurrences of mineralized skarn in the EMNSA (Evening Star, Copper King, Vulcan, Mohawk, and Copper World). Four samples from the Evening Star Mine area show gold contents in the 26 to 450 ppb range (table 4, analysis nos. 1-4). The highest recorded gold in four select

samples from the Mohawk Mine area is 42 ppb (analysis no. 72); from the Vulcan Mine, 150 ppb (analysis no. 7). It is interesting to note that the highest content of gold we found at the Vulcan Mine is in marble somewhat less than 0.5 m beyond the magnetite front, suggesting a buildup of precious-metal content at the fringes of this iron-skarn system. Recently, the geologic environments of gold-bearing skarn world-wide have been examined by Theodore and others (1991b), Ray and others (1990), and Ray and Webster (1990). Korobeinikov (1991) lists the following criteria for granitoid intrusions that are associated with productive gold-bearing skarns, mostly in the Soviet Union: (1) sodium predominating over potassium by approximately 1 to 2 weight percent; (2) high chlorine/fluorine ratios in the evolved fluids; and (3) wide-ranging gold-bearing contact zones in the surrounding hornfels, marbles, and magnesian skarns.

As recognized by Meinert (1983, 1988a, b; 1989), many deposits referred to as gold-skarns in the literature have been classified, or could be classified, under skarn deposit models such as copper- and iron-skarns by their dominant base- or ferrous-metal contents. For these deposits, gold production may be considered a byproduct of base- or ferrous-metal mining. Furthermore, gold-bearing skarn deposits commonly may be gradational into skarn that contains no gold but does contain significant other metal(s) including the silver-rich skarns as defined by Ray and others (1986), sediment-hosted disseminated gold-silver deposits (also known as carbonate-hosted and Carlin-type), porphyry Cu or Cu-Mo deposits, or polymetallic replacement deposits (exemplified by the McCoy megasystem, Nev.) as well as other deposit types related to felsic intermediate plutonic emplacement or volcanic activity. Mineralized skarns show genetic linkages to a wide variety of deposit types, some of whose linkages are well-established by geologic relations in the EMNSA (fig. 52). The Cove deposit, McCoy Mining District, Nev., which has been shown to include proven and probable reserves of 48.7 million tonnes with an average grade of 1.85 g/tonne Au and 87.1 g/tonne Ag (Kuyper and others, 1991), has been classified recently as a distal disseminated Ag-Au deposit according to a scheme proposed by Cox and Singer (1990). Polymetallic veins, the most common type of deposit in the EMNSA, are one of the other deposit types that may be present on the fringes of gold-bearing skarn deposits (pl. 2; table 6). Other commodities produced by gold-bearing skarns include silver, copper, zinc, iron, lead, arsenic, bismuth, tungsten, and tin as principal or byproduct commodities and cobalt, cadmium, and sulfur as byproducts (Theodore and others, 1991b).

Gold-bearing skarns are generally calcic exoskarns with gold associated with intense retrograde hydrosilicate alteration, although gold-bearing magnesian skarns are known and in some areas are dominant. Some economically significant gold-bearing skarns (Hedley, British Columbia [2.986 million tonnes at 13.46 g/tonne Au, Theodore and others, 1991b], and Suijan, South Korea [0.53 million tonnes at 13.0 g/tonne Au, Theodore and others, 1991b]), however, are partly in endoskarn (Knopf, 1913; Pardee and Schrader, 1933). Significant concentrations of gold-bearing

endoskarn also are present at the Nambija, Ecuador, gold-skarn deposit (McKelvey and Hammarstrom, 1991). Gold bearing skarns can show diverse geometric relations to genetically associated intrusive rocks and nearby premetallization structures (Theodore and others, 1991b). Similar relations to these are present in some of the skarns in the EMNSA that have been shown above to contain some gold.

#### Permissive Terranes and Favorable Tracts

Permissive terranes and favorable tracts for the presence of metallized skarn of all types, including gold-bearing skarn, are considered by us to be coextensive and include all exposed areas of Paleozoic carbonate sequences in the EMNSA (fig. 56). In addition, some parts of the Proterozoic are also permissive for the presence of mineralized skarn, especially in the New York Mountains (see above). On figure 56, we delineate a favorable tract for iron skarn primarily on the basis of magnetic anomalies in the general area of the Vulcan iron skarn in the Providence Mountains and categorize the presence of magnetite-bearing skarn at two localities, the BC prospect and the Adams-Ikes Hope prospect, in the Colton Hills as being permissive for the presence of additional iron skarn occurrences (Goldfarb and others, 1988). However, the amplitude of the magnetic anomaly in the general area of these latter two occurrences, about 2,000 gammas, is somewhat lower than that in the general area of the Vulcan Mine, and Jurassic igneous rocks in the general area of the two prospects have a high magnetic susceptibility (Goldfarb and others, 1988). In addition, an extensive permissive terrane for iron skarn in the general area of Old Dad Mountain is delineated on the basis of wide-ranging positive magnetic anomalies that extend well into areas covered by unconsolidated gravels (fig. 56).

In established mining districts in the EMNSA zoned from mostly proximal copper-dominant deposits to distal precious-metal-dominant and base-metal-dominant veins, all stratigraphic sequences favorable for development of skarn in the zone of precious-metal deposits should be considered as permissive hosts for development of gold-bearing skarn. One area in the EMNSA that seems to show some of these zonal relations between a copper-enriched part and lead-zinc-enriched part is the general setting of the Mohawk and Copper World Mines in the southwestern part of the Clark Mountain Range. In another area, there is a gold-copper-iron zone distal to the iron skarn at the Vulcan Mine in the Providence Mountains (Goldfarb and others, 1988). In addition, Ray (1990) and Ray and Webster (1990) have included the Jurassic arc-related rocks in the EMNSA as being favorable hosts for the development of gold skarns. As pointed out by Ray and Webster (1990), some gold skarns develop in geologic settings that include primitive, oceanic crust-derived intrusions that are marked by diorite compositions, relatively high iron contents, and low to intermediate values for their  $^{87}\text{Sr}/^{86}\text{Sr}$  initial ratios. However, as noted by Theodore and

others (1991b), there are also world-class gold skarn deposits associated with felsic intrusions that are more highly evolved than those associated with the primitive intrusions associated with gold skarns found primarily in British Columbia. Polymetallic veins and polymetallic replacement deposits showing geochemical signatures and sulfide mineral assemblages similar to those at many gold-bearing skarns (for example, the Fe-As-Zn-Cu-Bi-Au- and Sb-bearing ores at the Matsuo Mine, Japan; Matsukuma, 1962) may be high-level or lateral reflections of gold-bearing skarn systems. Gold placers in regions permissive for the formation of skarn may also be suggestive of the presence of gold skarn (R.G. Russell, written commun., 1989), especially if the placer gold is intergrown with bismuth minerals, including bismuth oxides or bismuth tellurides (Theodore and others, 1987b; Theodore and others, 1989). However, only nine placer localities in the EMNSA show the presence of visible free gold (table 8). Even in some of the most heavily mineralized areas of the EMNSA, such as the northern parts of the Providence Mountains (pl. 2), only a small number of placer operations have examined extensively the gravels in drainages whose upper reaches head in the heavily mineralized areas (Moyle and others, 1986). Anomalous values of bismuth, tellurium, arsenic, selenium, and cobalt are useful geochemical signatures for some gold-bearing skarns (Brooks and Meinert, 1989). However, some economically important gold skarns are notably deficient in bismuth, arsenic, and tellurium (McKelvey and Hammarstrom, 1991). Metal ratios in jasperoids, which commonly are present in, or on the fringes of gold skarn systems, may also provide useful geochemical signatures for exploration (Theodore and Jones, 1991). Faults cutting skarns and intersecting structures are important pathways along which retrograde assemblages and associated ores are concentrated. R.G. Russell (written commun., 1989) distinguishes between barren, early, high temperature contact skarn formed adjacent to intrusive rocks and mineralized, fracture-enhanced exoskarn developed in gold-skarn systems.

#### **Polymetallic Replacement, Distal Disseminated Au-Ag, and Vein Magnesite**

##### **Known Occurrences**

There are 23 polymetallic replacement deposits, one distal disseminated Au-Ag occurrence, and one vein magnesite occurrence known in the EMNSA (table 8; pl. 2). Most of the polymetallic replacement deposits are in the western part of the Clark Mountain Range where some of them are present distal to well-developed lead-zinc skarn at the Mohawk Mine. Another notable concentration of polymetallic replacement deposits is near the south end of the Mescal Range--an area that is currently (1991) being evaluated for its mineral potential by private industry. Only one occurrence (U.S. Bureau of Mines, 1990a, map no. 161, pl. 1) has been classified by us tentatively as belonging to a distal-disseminated gold-silver type of occurrence. This particular

occurrence is in the Ivanpah Mountains and is described as a pyrite-bearing, iron-oxide stained jasperoid developed in dolomite (U.S. Bureau of Mines, 1990a). The magnesite vein occurrence is present in the New Trail Canyon area of the Ivanpah Mountains and it is near the copper and iron skarns at the New Trail Mine. These latter mineral occurrences are just to the north of a large mass of the Jurassic Ivanpah Granite which is a porphyritic monzogranite (pl. 1), and mineralization is presumably Jurassic in age in the general area of New Trail Canyon.

Polymetallic replacement deposits classified and analyzed in Cox and Singer (1986) show median tonnages of 1.8 million tonnes, and median grades of 5.2 weight percent lead, 3.9 weight percent zinc, and approximately 0.1 weight percent copper.

#### Permissive Terranes and Favorable Tracts

We designate all areas of the EMNSA that include outcrops of Paleozoic carbonate rock to be permissive for the presence of polymetallic replacement deposits, distal disseminated gold-silver occurrences, and magnesite vein occurrences (fig. 56). As such, the areas so designated are coextensive with those that we consider to be permissive for the presence of various types of skarn (see above). Our data are not refined to the point that we can confidently discriminate favorable tracts for skarn within the outlined permissive terrane. Figure 52 depicts graphically the genetic linkages among all these deposits.

#### **Polymetallic Vein, Polymetallic Fault, and Gold-Silver, Quartz-pyrite Vein**

##### Known Occurrences

There are 206 polymetallic vein occurrences, 79 polymetallic faults, and 80 occurrences classified as gold-silver, quartz pyrite veins in the EMNSA (table 8; pl. 2). All three of these types of occurrences are essentially cogenetic. The major differences between the polymetallic vein occurrences and the gold-silver, quartz-pyrite veins primarily include differences in the relative amounts of galena, sphalerite, and chalcopyrite that are present. Polymetallic veins generally show high concentrations of all of these minerals, even though they may have been exploited primarily for their precious metals. One of the most economically significant concentrations of polymetallic veins in the EMNSA is at the Morning Star Mine (U.S. Bureau of Mines, 1990a, map no. 178, pl. 1). As noted by Sheets and others (1989) and Ausburn (1988), proven reserves at this deposit included about 8 million tons of ore at a grade of 0.06 oz gold/ton in 1988. The deposit is hosted by the Jurassic Ivanpah granite and primarily is present along the hanging wall of a low-angle thrust related to the Mesozoic thrust belt (Sheets and others, 1989; Burchfiel and Davis, 1971). Early-stage quartz-carbonate veins in the deposit include pyrite, sericite, hematite, ilmenite, galena,

electrum, chalcopyrite, sphalerite, and tetrahedrite (Sheets and others, 1988; 1989; 1990). As pointed out by these authors, mineralization at the Morning Star Mine seemingly is associated spatially and genetically with fluids of metamorphic affinity. The tonnage of the mineralized system at the Morning Star Mine is larger than any of the deposits used in the base metal-silver category of polymetallic veins plotted by Bliss and Cox (1986). As pointed out by Bliss and Cox (1986), there are apparently two types of polymetallic veins: (1) base-metal-silver, and (2) gold-silver polymetallic veins that contain significant concentrations of copper, lead, and zinc. The Morning Star deposit probably belongs to the latter of these two categories. Some major mining districts elsewhere that show notable production from gold-bearing polymetallic vein have recently been described by Morris (1990), Fisher (1990), Shawe (1990), and Thompson (1990). Polymetallic veins in the EMNSA show elevated abundances of gold, silver, arsenic, antimony, and especially molybdenum (fig. 49).

The gold-silver, quartz-pyrite veins in the EMNSA typically do not show visible presence of galena, sphalerite, or chalcopyrite, and, as such, they commonly have low contents of lead, zinc, and copper. The classification scheme we adopted during our study of the EMNSA for those occurrences that we did not examine in the field and that do not report presence of galena, sphalerite, or chalcopyrite involves use of available analyses of mineralized rock reported by the U.S. Bureau of Mines (1990a). Those mineralized vein samples reported to contain in excess of several hundred ppm lead, zinc, or copper were included with the polymetallic veins. Analyses are available for 97 mineralized rocks from the sites of 47 gold-silver, quartz-pyrite veins in the EMNSA (table 13). In these 97 rocks, average contents are approximately 1,800 ppb gold; approximately 7 ppm silver; 17 ppm arsenic; 3 ppm antimony; and approximately 100 ppm zinc. The apparently low average contents of arsenic and antimony in these veins probably are a reflection of the emplacement of most of these veins in a mesothermal, essentially base-metal deficient environment. The polymetallic veins seem generally to contain more arsenic and antimony (fig. 49). The strongest elemental association of gold in these 97 rocks is for silver; calculation of Spearman's correlation coefficient yields a value of +0.4. In addition, some of the gold-silver, quartz-pyrite veins in the EMNSA may be Tertiary in age and epithermal rather than mesothermal (Lange, 1988). There are no models available for us to compare to gold-silver, quartz-pyrite veins in the EMNSA. Most likely these types of veins in the EMNSA are analogous to the gold-silver polymetallic veins of Bliss and Cox (1986). However, preliminary compilations by Bliss and Cox (1986) did not yield an adequate grade-tonnage sampling of gold-silver polymetallic veins, and they therefore present no plots showing their cumulative frequency distributions for grade and tonnage. There are some gold-bearing quartz veins elsewhere that bear some similarities to the gold-silver, quartz-pyrite veins we have delineated in the EMNSA. Gair (1989a), in a comprehensive evaluation of the mineral resources of the Charlotte  $1^{\circ} \times 2^{\circ}$

quadrangle, North Carolina and South Carolina, describes some gold-quartz and gold-pyrite-quartz veins that were important sources of gold there from about 1825 to 1910. As pointed by Gair (1989a), the gold-quartz and gold-pyrite-quartz veins he studied are epigenetic fissure fillings, many of which crosscut the foliation in the enclosing schists and gneisses. Many of the veins are in the upper parts of apparently subvolcanic intrusive rocks, and some of the gold grades in the mined veins apparently were as much as 11 oz Au/ton, but probably grades of 0.3 to 0.5 oz Au/ton were more prevalent at some of the more significant deposits (Gair, 1989a).

Polymetallic faults are mostly brittle-type gouge and fracture zones along structures of variable regional importance. Such mineralized fault zones typically do not include a silicate gangue mineralogy common to veins; quartz is not reported. Most of the brittle-type polymetallic faults in the EMNSA were exploited some time in the past primarily along their near-surface traces of gouge. Elsewhere, Wallace and Morris (1986) have documented the highly variable geometric relations between gouge and the trace of the associated fault zones (fig. 61). However, most importantly, these authors show the incredibly complex geometry that some mineralized faults may attain at relatively great depths below the present erosion surface (fig. 62). Similar relations also may be found at some future time along the seemingly geometrically simple East Providence fault in the EMNSA (pl. 1). Some of the mineralized strands of the East Providence fault may be as complex at depth as those depicted in the Coeur d'Alene Mining District, Idaho, by Wallace and Morris (1986), and, in fact, to this date we may not be able to decipher properly the massive fluid-flow patterns suggested by the presence of many small mineral occurrences in the general area of the fault.

All three of these types of mineralized occurrences may be related spatially and genetically to mineralized skarn, polymetallic replacement deposits and any centers of porphyry-type mineralization. We examined distribution patterns of polymetallic veins and gold-silver, quartz-pyrite veins in the EMNSA to determine whether or not their distribution may, in places, have followed the proximal-to-distal copper-gold (silver) -lead (zinc) zonation recognized in many porphyry-type metallization centers elsewhere in the southwestern United States. However, the spatial relations between these two types of vein occurrence in the EMNSA seem to be highly erratic (pl. 2).

#### Permissive Terranes and Favorable Tracts

We designate all areas of the EMNSA that mostly include outcrops of Proterozoic, Paleozoic, and Mesozoic rock (including both igneous and sedimentary protoliths) to be permissive for the presence of Mesozoic-age polymetallic veins, polymetallic faults, and gold-silver, quartz-pyrite

veins (pl. 1). We are not able to discriminate favorable tracts within the outlined permissive terranes based on the data available.

There are no grade-tonnage models available for the gold-silver, quartz-pyrite vein occurrences or the polymetallic fault-type of occurrences.

If the judgment is valid that some of the polymetallic veins in the EMNSA are analogous with the polymetallic-vein deposit model in Cox and Singer (1986), then some conclusions can be drawn regarding the probability of discovery of economic ore bodies. Grade-tonnage models based on data from 75 deposits in the United States and Canada classified as base metal-silver polymetallic veins indicate a 90 percent chance that any deposit newly discovered will contain at least a few hundred tonnes of ore, at average silver grades of around 140 g/tonne. Only a 10 percent chance exists that a new deposit will contain as much as 200,000 tonnes or more of ore, at grades as high as 4,700 g/tonne silver. Note again that these relations do not apply to the gold-silver polymetallic veins as classified by Bliss and Cox (1986), and to which the deposit at the Morning Star Mine apparently belongs as we discuss above.

## **Tertiary Deposits**

### **Volcanic-hosted Epithermal Gold Deposits**

#### **Known Occurrences**

Tertiary volcanic rocks in the Castle Mountains located near the California-Nevada border host one of the largest mineable reserves of gold in southern California (pl. 1). These gold deposits are located in the easternmost part of the EMNSA and are the most important economically of Tertiary-age deposits in the EMNSA. Development drilling in the Hart Mining District by Viceroy Gold Corporation from the mid 1980s to the present has delineated six individual ore bodies in the southernmost part of the Castle Mountains (Linder, 1989). Total combined reserves are 34 million metric tons of ore containing 2 million ounces of gold. The volcanic-hosted gold deposits in the Hart Mining District are similar to other economically important volcanic-hosted deposits being mined in Nevada such as Rawhide and Round Mountain; the latter with gold reserves of over 10 million ounces is the largest volcanic-hosted deposit in the United States. The large tonnage and grade of these ore bodies make them amenable to open pit and heap leach methods and this class of deposits constitutes a significant component of gold reserves in the United States. Gold was first located in the mining district in 1907 (Ausburn, 1991).

Similar age middle Miocene volcanic rocks are present elsewhere in and west of the EMNSA and, in the vicinity of the cities of Mojave and Lancaster, several rhyolite dome complexes host economically important gold deposits that are presently being mined. These deposits are

characterized by widespread acid-sulfate and argillic alteration. Closely associated in time and space with these gold deposits is the largest borate deposit in North America at Boron. It formed from hot spring systems that were active during this volcanic event. These hot springs vented into basins developed peripheral to the volcanic dome field. Based on this association, a model for the gold deposits in the Hart District must include the potential for boron, and other lithophile elements (Li, Mo, F, U) peripheral to the gold deposits.

Tertiary volcanic rocks in the Castle Mountains are middle Miocene in age and range from 18.5 to 14 Ma. The volcanic rocks unconformably overlie a Proterozoic metamorphic basement covered by a thin sequence of Paleozoic carbonate rocks (Capps and Moore, 1990) and Miocene sedimentary rocks (pl. 1). Volcanic rocks in the Castle Mountains have been divided into four units by Capps and Moore (1990) and from oldest to youngest they consist of: (1) Castle Mountains Tuff, a rhyolitic ash-flow tuff; (2) Jacks Well latite, basalt, and ash-flow tuff; (3) Linder Peak rhyolite flow-dome complex; and (4) Hart Peak basalt and intermediate flows and volcaniclastic rocks. The Linder Peak rhyolite flow-dome unit has an age of about 15.5 Ma and hosts the gold deposits which formed just after dome emplacement (Capps and Moore, 1990). These rhyolitic rocks also are present in a north-trending zone on the west side of the Castle Mountains to the north of the known ore bodies, and these rhyolitic rocks are potential hosts for volcanic-hosted gold deposits in addition to those already delineated.

Gold mineralization is present in structurally-controlled silicified fracture zones and more permeable lithologic sequences of rock which have also been silicified (Ausburn, 1991). Argillic alteration and local zones of advanced argillic alteration are associated with the ore bodies, and adularia and pyrite are present in close association with the gold. The ore minerals are native gold and electrum. The geochemical suite associated with the ore consists of arsenic, antimony, and mercury (Capps and Moore, 1990). Quartz-adularia alteration is associated with the main stage of gold mineralization.

We have shown 11 specific localities in the EMNSA as being volcanic-hosted epithermal gold occurrences (table 8; pl. 2). All of these are in the Castle Mountains. Although mineralized occurrences in the area of Hackberry Mountain have been classified as polymetallic fault, these occurrences are volcanic-hosted types of mineralization directly analogous with those in the Castle Mountains, but the mineralization at Hackberry Mountain may be confined to generally northeast-striking fault zones (see above).

Tertiary volcanic rocks of similar age to those hosting gold deposits in the Hart district are present in a large area in the south-central part of the EMNSA and are associated with the Woods Mountain volcanic center (McCurry, 1988). These volcanic rocks consist of regionally extensive ash-flow tuffs, and rhyolitic domes and flows. The ash-flow tuffs include the 15.8 Ma Wildhorse Mesa Tuff, a compositionally zoned metaluminous to mildly peralkaline tuff, and the possibly

younger Tortoise Shell Mountain Rhyolite, which may be a lava flow. Large amplitude circular gravity (about -30 mGal) and magnetic (about -600 nT) anomalies are centered over the Woods Mountain volcanic center and reflects a caldera and associated, buried felsic stock about 9 km in diameter. McCurry (1985, 1988) suggested the presence of a trap door style of collapse for a 10 km in diameter caldera, and the magnetic anomaly may reflect the outline of the caldera structure. However, the magnitude of the gravity anomaly and depth to pre-Tertiary basement, about 7 km, indicate a symmetrical zone of subsidence with a much larger component of collapse than previously postulated.

Equivalent age volcanic rocks at Hackberry Mountain to the east of the Woods Mountain volcanic center consist of ash-flow tuffs, flows, and domes. These volcanic rocks are altered over a large area in the southern part of Hackberry Mountain. The alteration pattern is coincident with an east-west trending magnetic low anomaly, which probably reflects the oxidation of magnetic minerals during alteration. In the alteration zone, drilling indicated the presence of disseminated native gold, as much as 0.088 ounces/ton, with stibnite and hematite in argillically altered and partly silicified ash-flow tuff cut by chalcedonic veinlets (Gottlieb and Friberg, 1984). Similar volcanic rocks are present around the northern and western margins of the Woods Mountain volcanic center and they have potential for volcanic-hosted gold deposits.

Volcanic-hosted gold deposits can be present in association with porphyry-type gold deposits (Rytuba and Cox, 1991). Most known porphyry gold deposits are characterized by a stockwork of quartz and pyrite veins in subvolcanic intrusive rocks. These deposits form at lower levels and laterally away from volcanic-hosted quartz-adularia and gold-alunite type deposits such as those in the Hart Mining District. The gold ore bodies are generally low grade, 1.5 to 2.5 grams of gold /ton but are known to contain a very large tonnages of ore, as much as several hundred million tons, elsewhere. The subvolcanic intrusive rocks associated with the flow dome complex in the Castle Mountains and the Woods Mountain volcanic center are permissive for porphyry gold deposits and those areas outlined below as being favorable for gold-alunite and gold-quartz adularia type deposits also have potential for porphyry gold deposits at depth.

#### Permissive Terranes

We delineate three terranes in the EMNSA as permissive for Tertiary, volcanic-hosted epithermal gold deposits of the quartz-alunite and(or) quartz-adularia variety (fig. 56). One is a north-northeast-trending terrane in the general area of the Castle Mountains. The northeastern boundary of this terrane is based upon the outer limit of small numbers of rhyolite and(or) latite intrusions emplaced into Proterozoic basement rock (pl. 1). The southern boundary of the permissive terrane is defined by our estimate of the southernmost extent of altered, demagnetized

volcanic rocks under the overlying Quaternary gravels (fig. 56). The overall configuration of these apparently demagnetized rocks under the gravels is inferred from the available magnetic data (pl. 5). The second of the two permissive terranes is a broadly ovoid one in the general area of Hackberry Mountain and the Woods Mountains, which includes the Miocene Hackberry Springs Volcanics and Wildhorse Mesa Tuff (units Ths, Tw, pl. 1) in the area of Hackberry Mountain and the mostly Miocene Tortoise Shell Mountain Rhyolite (map unit Tts, pl. 1) in the area of Woods Mountains. Relation of these rocks to a caldera is described above. The third terrane permissive for Tertiary, volcanic-hosted epithermal gold deposits is marked by sequences of ash-flow tuffs near the south-central edge of the EMNSA in the area of Van Winkle Mountain (fig. 56).

#### Favorable Tracts

We delineate a favorable tract for Tertiary, volcanic-hosted epithermal gold deposits of the quartz-adularia or quartz-alunite type within each of the first two above-outlined permissive terranes (fig. 56). These favorable tracts are outlined using the presence of magnetic lows, mineralized occurrences, and alteration anomalies detected by thematic mapper. Within these zones, deposits of boron and lithium, fluorine, and uranium may be present also.

### Speculative Associations

Some associations among known types of deposits in the EMNSA, as described above and depicted schematically in figure 52, nonetheless, apparently have still not been utilized fully in the search for additional exploration targets. Recognition of linkages among some deposits, including gold skarn and the association of boron and other lithophile elements with gold discussed above, might impact significantly exploration concepts in the Mesozoic and Tertiary magmatic-hydrothermal environments in the EMNSA. Application of an exploration concept based on linkages among deposit types is by no means a guarantee of an exploration success. Exploration failures far outnumber exploration successes. We recognize, furthermore, that no gold skarns, as defined by Theodore and others (1991b), are currently known in the EMNSA. As compiled, 39 gold skarns show median tonnages worldwide of 213,000 tonnes of ore, and median grades worldwide of 8.6 grams per tonne and include the 13.2 million tonne McCoy and the 5.1 million tonne Fortitude deposits in Nevada. Domestic primary gold production in 1989 was approximately 240 metric tonnes of contained gold (U.S. Bureau of Mines, 1990b).

Lastly, we examine two recently recognized deposit-type linkages as examples of how discoveries elsewhere that can impact future concepts of exploration that might be applied to the EMNSA. First, we will examine the possible linkage between distal sediment-hosted gold deposits and their proximal variants, including skarn of all types and porphyry stockwork systems,

and, second, we will examine the possible association between some possibly wrench-fault related Tertiary gold mineralization in the EMNSA and Mesquite-type gold deposits.

Local mineralized Mesozoic skarn environments in the EMNSA, as discussed above, should be examined from the perspective of (1) their being proximal to magma-equilibrated fluids exsolving from a progenitor intrusive complex, and (2) their being interior to sediment-hosted gold or Carlin-type systems in the surrounding sedimentary sequences of carbonate rock. Sillitoe and Bonham (1990) proposed that most gold in many sediment-hosted gold deposits originates in magma-derived fluids and may be deposited on the peripheries of base- and precious-metals mining districts as much as several km from the mineralizing plutons. Gold-bearing skarns, of which there are several in the EMNSA, can be viewed as "indicator" occurrences for sediment-hosted gold deposits, as described recently by Tingley and Bonham (1986). The schematic model proposed by Sillitoe and Bonham (1990) showing such linkages is applicable to some of the more shallow-seated magmatic hydrothermal pulses associated with emplacement of the Teutonia batholith (fig. 63). As noted by Sillitoe and Bonham (1990), the fringes in most carbonate sequences of rock beyond many intrusion-centered base- and precious-metal districts have been minimally explored for gold. Such conclusions are probably applicable also to the EMNSA. Perhaps the Navachab, Namibia, gold deposit that recently began production is an example of a type of mineralized system that might be present in the EMNSA. At Navachab, the gold ore contains 9.5 million tonnes at an average grade of 2.6 g/tonne and is hosted by steeply dipping marbles that include mottled dolomitic marble, biotite hornfels, and calc-silicate marble (Wyllie, 1991).

Gold-quartz veins at the Telegraph Mine in the north-central part of the EMNSA (Lange, 1988) apparently are related to wrench faults or strike-slip faults, suggesting that additional deposits of this type may be present elsewhere in the EMNSA. Mineralization at the Telegraph Mine is associated spatially with structures interpreted by Lange (1988) as Riedel shears (see Riedel, 1929; Tchalenko, 1970; Ramsay and Huber, 1987). These types of secondary shears are oriented generally at low angles to the general trace of a broad zone of shear. This type deposit at the Telegraph Mine in the EMNSA is particularly significant in terms of resource evaluation because a similar type occurrence in the Mesquite Mining District, Calif., is a world-class gold deposit.

The Mesquite Mining District is located in southeastern California about 150 km south-southeast of the south border of the EMNSA and 60 km east of the Salton Sea. Large-scale gold production from the mining district began in 1985 with announced reserves of 41 million short tons at an average grade of 0.056 troy ounces gold per short ton (Lindquist, 1987). By 1988, the mining district had become one of the largest producers of gold in California (Burnett, 1990), and continued exploration through 1989 increased the known reserves to 53 million short tons at an average grade of 0.043 troy ounces gold per short ton (Higgins, 1990).

Gold-bearing veins in the Mesquite Mining District formed in an epithermal setting within a few hundred meters of the surface (Willis and Holm, 1987; Manske and others, 1987; Willis, 1988; Manske and Einaudi, 1989; Manske, 1990). Gold-bearing quartz-adularia-sericite and ferroan carbonate veins are the mineralized structures in the various pits within the district (Willis, 1988; Manske, 1990). Quartz-cemented breccias are contemporaneous with the simple veins and are common in the parts of the pits with the highest economic grades. Younger, barren calcite and chalcedonic quartz veins are present locally. Vein deposition occurred by episodic open-space filling, evidenced by vuggy and comb quartz and carbonate minerals, multiple banding of chalcedonic quartz, and clasts of silica-matrix breccia within other breccias. Veins range from thin micro-cracks to breccias a meter or so thick. Little hydrothermal alteration of host lithologies accompanied mineralization (Manske and others, 1987; Willis, 1988). Weakly anomalous sporadic concentrations of Au, Ag, As, Sb, Hg, W, Zn, and Te were found in surface exposures of rock prior to mining (Tosdal and Smith, 1987).

The veins are steeply dipping and strongly controlled by right-lateral strike-slip faulting (Willis, 1988), as evidenced by the vein geometry in complex dilational jogs (Sibson, 1990), in negative and positive flower structures (Harding, 1985), and by limited kinematic evidence for strike-slip faulting along the major mineralized faults (Willis and others, 1989). All the mineralization in the mining district is hosted by gneissic rocks that were metamorphosed at amphibolite grade and, to a lesser extent, granite, pegmatite, and aplite that intrude the gneissic rocks (Willis, 1988). The ages of these rocks and their subsequent metamorphism have been established as Jurassic and Cretaceous respectively (R.M. Tosdal, unpub. data, 1987-1990). K-Ar and  $^{40}\text{Ar}/^{39}\text{Ar}$  geochronologic studies indicate a late Oligocene age of mineralization sometime between 37 and 27 Ma (Willis, 1988; D.L. Martin in Shafiqullah and others, 1990), or a minimum of 60 m.y. after the host rocks were formed. The apparent age of the ore bodies is, however, somewhat similar to the age of nearby volcanic and plutonic rocks in the Chocolate Mountains (Miller and Morton, 1977; Crowe and others, 1979). No Tertiary volcanic or plutonic rocks are known within the Mesquite Mining District, although they may have provided a heat-source to drive the hydrothermal system (Manske, 1990).

The large gold deposit in the Mesquite Mining District is a typical epithermal precious metal deposit similar to many of those hosted by volcanic rocks or by other rocks that are intruded by hypabyssal stocks elsewhere. Major distinctions between orebodies in the Mesquite Mining District and typical epithermal deposits include the gneissic host rocks, the large difference in age between the host rocks and the ore bodies, and the lack of volcanic or plutonic rocks of the appropriate age within the district. The strike-slip environment is not unique although it does provide a structural setting into which hydrothermal fluids could flow away from any associated heat source (Sibson, 1987).

Within the EMNSA, the Telegraph Mine appears to have an analogous setting to Mesquite. At this locality, gold-bearing epithermal veins and breccias, consisting of quartz-sericite-adularia-pyrite and quartz-carbonate, cut the Cretaceous Teutonia Adamellite (Lange, 1988). Veins in this mine are interpreted to have formed within a dextral strike-slip environment, which now strikes to the north-northeast at a high angle to trends of structures within the region. A single K-Ar age on adularia implies that the main stage of mineralization occurred in the Late Miocene, or about  $10.3 \pm 0.4$  Ma (Lange, 1988). There are no known Late Miocene volcanic rocks of this age in the immediate area of the Telegraph Mine (pl. 1), although Miocene felsic volcanism of similar age is present within the region, some 40 km to the east-southeast (see above), and Late Miocene to Pleistocene basaltic volcanism is present also in the Cima volcanic field to the immediate south (pl. 1). Some basaltic rocks elsewhere are known to host significant concentrations of gold. The Buckhorn deposit, the Mule Canyon deposit, and the Fire Creek occurrence, all in Nevada, apparently are hot-spring gold deposits in basaltic andesite above complexes of basaltic dikes associated with the middle Miocene northern Nevada rift (Cox and others, 1991). The Mule Canyon deposit includes approximately 850,000 oz Au at an average grade of 0.12 oz/ton Au (Consolidated Gold Fields Defense Document Against Minorco, Sept. 1989).

The tectonic setting of the Telegraph Mine is similar to that of the large Mesquite district, but the host rocks and age of mineralization are different. The question of mineral-resource potential for these types of gold-bearing epithermal deposits of Tertiary age within the EMNSA is difficult to address at this time. There is simply inadequate information available to us to outline reasonably-constrained permissive terranes, or favorable tracts, on the large pediments in the EMNSA. Select mineralized samples from gold-silver, quartz-pyrite veins that show high gold/silver ratios might be one method that could be used to discriminate mid-Miocene veins from others. Furthermore, surface expressions of the orebodies at Mesquite on the pediment prior to exploration were small and consisted of local high-grade gold-quartz-veins that had small amounts of reported production, and various small placer mines (Morton, 1977). There is also weak and very limited geochemical expression and no known geophysical expression associated with the ore bodies. Only thorough exploration around these small occurrences in the Mesquite Mining District could define the large ore bodies now identified there.

## SUMMARY

From our evaluations that largely used model-based criteria, we conclude that much of the EMNSA contains abundant indications of epigenetic mineralization of various types. It is possible that economically significant concentrations of many metals remain to be discovered in many parts of the EMNSA. We have discussed above specific types of deposits that are known to be present

in the EMNSA. Some of the mountain ranges that have widespread occurrences are the Providence Mountains, Clark Range, Ivanpah Mountains, and the New York Mountain; the area of Hackberry Mountain is included in a tract judged to be favorable for the discovery of epithermal, volcanic-hosted gold deposits (pl. 2). These ranges make up a broad, roughly north-south trending region in the central part of the EMNSA. Much less endowed with known occurrences of all of the various types of deposits considered above are the Granite Mountains, the central parts of the Piute Range, the Fenner Valley area, the general area of Cima Dome, the Cima volcanic field, and areas west to Soda Lake. We have attempted to make some judgments concerning the gravel-covered areas in the EMNSA (pl. 3), including the areal extent of bedrock apparently covered only by thin veneers of gravel. But there are few data available to us for the overwhelming bulk of the covered areas. The presence of any mineralization, the type of mineralization, and the extent and intensity of mineralization in the covered areas is essentially unknown. The likelihood is high, however, that those areas in the EMNSA covered only by a thin cap of gravels could host mineralization similar to that known in the adjoining mountain ranges. Most buried epigenetic mineral deposits do not respond to standard geophysical methods, particularly at the coarse spacing of the data-collection points available for our evaluation.

Restricting judgments concerning the presence of undiscovered metal resources in the EMNSA only to currently known types of deposits and to regionally representative tonnages for such deposits might yield small estimates for the volumes of many metals that might be exploited.

Metals from most newly discovered, base- and ferrous-metal deposits of the types presently known in the EMNSA probably would be insignificant from the standpoint of national needs. For example, copper from a newly discovered skarn deposit in the EMNSA would have roughly a 50 percent chance of being in excess of approximately 10,000 tonnes contained copper, if the grade-tonnage distribution curves of Jones and Menzie (1986b) for copper skarns are applicable to copper skarn the EMNSA. Most copper in the United States is produced in the southwest from much larger open-pit operations than those associated with the typical copper skarn. Historically, the EMNSA has been the site of minor production of many metals from a large number of sites. Recently, however, a small number of sites in the EMNSA, whose gold production and reserves are much greater than that of the preceding discoveries, have been developed (see U.S. Bureau of Mines, 1990a).

Nonetheless, widespread distribution of numerous types of deposit (including copper skarn, lead-zinc skarn, tin-tungsten skarn, polymetallic vein, gold-silver quartz-pyrite vein, low-fluorine porphyry molybdenum, gold breccia pipe, volcanic-hosted gold) petrogenetically associated with igneous rock in many parts of the EMNSA is indicative of a metallogenic environment that may be the site of future discoveries of types of mineral deposits that are not now recognized by the exploration community. Thus, a simple enumeration of contained metals in estimated numbers of

future discoveries in the EMNSA based only on some of the currently recognized deposits probably would not adequately represent the potential metal endowment of some areas in the EMNSA. The science, art, and luck of exploration methodologies continually evolve and this evolution is one of the most important aspects of currently employed methodologies of exploration (Bailly, 1981).

## REFERENCES CITED

Adrian, B.M., Friskin, J.G., Briggs, P.H., Bradley, L.A., and Crock, J.G., 1986a, Analytical results and sample locality map of heavy-mineral-concentrate and rock samples from the Fort Piute Wilderness Study Area (CDCA-267), San Bernardino County, California: U.S. Geological Survey Open-File Report 86-584, 15 p.

Adrian, B.M., Friskin, J.G., Malcolm, M.J., and Briggs, P.H., 1986b, Analytical results and sample locality map of heavy-mineral-concentrate and rock samples from the Cinder Cones Wilderness Study Area (CDCA-239), San Bernardino County, California: U.S. Geological Survey Open-File Report 86-403, 13 p.

Adrian, B.M., Friskin, J.G., Malcolm, M.J., and Crock, J.G., 1986c, Analytical results and sample locality map of heavy-mineral-concentrate and rock samples from the Castle Peaks Wilderness Study Area (CDCA-266), San Bernardino County, California: U.S. Geological Survey Open-File Report 86-416, 18 p.

Anderson, J.L., 1989, Proterozoic anorogenic granites of the southwestern United States, *in* Jenney, J.P., and Reynolds, S.J., eds., Geologic evolution of Arizona: Arizona Geological Society Digest 17, p. 211-238.

Anderson, J.L., Barth, A.P., Young, E.D., Bender, E.E., Davis, M.J., Farber, D.L., Hayes, E.M., and Johnson, K.A., 1991, Plutonism across the Tujunga - North American Terrane Boundary: A Middle to Upper Crustal View of two juxtaposed magmatic arcs, *in* Bartholomew, M.J., Hyndman, D.W., Mogk, D.V., and Mason R., eds., Characterization and Composition of Ancient (Precambrian to Mesozoic) Continental Margins: Holland, Reidel, D., Proceedings of the Eighth International Conference on Basement Tectonics (in press).

Anderson, J.L., and Bender, E.E., 1989, Nature and origin of Proterozoic A-type magmatism in the southwestern United States of America: *Lithos*, v. 23, p. 19-52.

Anderson, J.L., Barth, A.P., Young, E.D., Davis, M.J., Farber, D., Hayes, E.M., and Johnson, K.A., 1988, Contrasting depth of emplacement across the Tujunga-North America terrane boundary [abs.]: Geological Society of America Abstracts with Programs, v. 20, p. 139.

Anderson, J.L., Wooden, J.L., and Bender, E.E., 1990, Early and Middle Proterozoic crustal evolution of the western transitional zones: California-Nevada-Arizona: Geological Society of America DNAG Volume, Precambrian-Conterminous United States.

Anderson, J.L., Young, E.D., Barth, A.P., Wooden, J.L., Tosdal, R.M., and Morrison, Jean, 1991, Mesozoic batholiths of the Mojave [abs.]: Geological Society of America Abstracts with Programs, v. 23, no. 2, p. 3.

Anderson, J.L., Young, E.D., Clarke, H.S., Orrell, S.E., and Winn, M., 1985, The geology of the McCullough Range Wilderness area, Clark County, Nevada: Final Technical Report to the U.S. Geological Survey, Los Angeles, University of Southern California, 26 p., plate 1:24,000.

Anderson, P., and Guilbert, J.M., 1979, The Precambrian massive sulfide deposits of Arizona - a distinct metallogenic epoch and province: Nevada Bureau of Mines and Geology Report 33, Papers on mineral deposits of western North America, IAGOD V, v. 11, p. 39-48.

Aruscavage, P.J., and Crock, J.G., 1987, Atomic absorption methods, *in* Baedecker, P.A., ed., Methods for geochemical analysis: U.S. Geological Survey Bulletin 1770, p. C1-C6.

Ausburn, K.E., 1988, Tertiary volcanic hosted epithermal Au-mineralization at the Hart Mining District, Castle Mountains, northeastern San Bernardino County, California [abs.]: Geological Society of America Abstracts with Programs, v. 20, no. 3, p. .

-----1991, Ore-petrogenesis of Tertiary volcanic hosted epithermal gold mineralization at the Hart Mining District, Castle Mountains, NE San Bernardino County, California, *in* Raines, G.L., Lisle, R.E., Schafer, R.W., and Wilkinson, W.H., eds., Geology and ore deposits of the Great Basin Symposium Proceedings: Reno, Nevada, Geological Society of Nevada, p. 1147-1188.

Ayuso, R.A., and Shank, S.G., 1983, Quartz-molybdenite veins in the Priestly Lake granodiorite, north-central Maine: U.S. Geological Survey Open-File Report 83-800, 10 p.

Bagby, W.C., and Berger, B.R., 1985, Geologic characteristics of sediment-hosted, disseminated precious-metal deposits in the western United States, *in* Berger, B.R., and Bethke, P.M., eds., Geology and geochemistry of epithermal systems: Society of Economic Geologists Reviews in Economic Geology, v. 2, p. 169-202.

Bagby, W.C., and Cline, J.S., 1991, Constraints on the pressure of formation of the Getchell gold deposit, Humboldt County, as interpreted from secondary-fluid-inclusion data, *in* Raines, G.L., Lisle, R.E., Schafer, R.W., and Wilkinson, W.H., eds., Geology and ore deposits of the Great Basin, Symposium Proceedings: Reno, Nevada, Geological Society of Nevada, p. 793-804.

Bagby, W.C., Menzie, W.D., Mosier, D.I., and Singer, D.A., 1986, Grade and tonnage model carbonate-hosted Au-Ag, *in* Cox, D.P., and Singer, D.A., eds., Mineral deposit models: U.S. Geological Survey Bulletin 1693, p. 175-177.

Bailly, P.A., 1981, Today's resource status-tomorrow's resource problems: The need for research on mineral deposits, in National Research Council, Mineral Resources: Genetic understanding for practical applications: Washington, D.C., National Academy Press, p. 21-32.

Baker, E.M., and Andrew, A.S., 1991, Geologic, fluid inclusion, and stable isotope studies of the gold-bearing breccia pipe at Kidston, Queensland, Australia: *Economic Geology*, v. 86, no. 4, p. 810-830.

Ballhorn, R.K., 1989, Ore deposit genesis and characterization, *in* International Atomic Energy Agency, ed., *Uranium deposits in magmatic and metamorphic rocks*: Vienna, International Atomic Energy Agency Proceedings, Salamanca, 29 Sept.-30 Oct. 1986, p. 239-243.

Barnum, E.C., 1989, Lanthology: Applications of lanthanides and the development of Molycorp's Mountain Pass operations, *in* *The California desert mineral symposium, Compendium*: Sacramento, U.S. Bureau of Land Management, p. 245-249.

Barth, A.P., Tosdal, R.M., and Wooden, J.L., 1990, A petrologic comparison of Triassic plutonism in the San Gabriel and Mule Mountains, southern California: *Journal of Geophysical Research*, v. 95, no. B112, p. 20,075-20,096.

Barton, P.B., 1986, Commodity/geochemical index, *in* Cox, D.P., and Singer, D.A., eds., *Mineral deposit models*: U.S. Geological Survey Bulletin 1693, p. 303-317.

Beckerman, G.M., Robinson, J.P., and Anderson, J.L., 1982, The Teutonia batholith: A large intrusive complex of Jurassic and Cretaceous age in the eastern Mojave Desert, California, *in* Frost, E.G., and Martin, D.M., eds., *Mesozoic-Cenozoic tectonic evolution of the Colorado River region, California, Arizona, and Nevada*: San Diego, Cordilleran Publishers, p. 205-220.

Bender, E.E., and Miller, C.F., 1987, Petrology of the Fenner gneiss, a major Proterozoic metaplutonic unit in the eastern Mojave Desert, Calif. [abs.]: *Geological Society of America Abstracts with Programs*, v. 19, p. 358.

Bender, E.E., Anderson, J.L., Wooden, J.L., Howard, K.W., and Miller, C.F., 1988, Correlation of 1.7 Ga granitoid plutonism in the lower Colorado River region [abs.]: *Geological Society of America Abstracts with Programs*, v. 20, p. 142.

Bennett, V.C., and DePaolo, D.J., 1984, The definition of crustal provinces in the southern Rocky Mountain region using Sm-Nd isotopic characteristics [abs.]: *Geological Society of America Abstracts with Programs*, v. 16, p. 214.

----1987, Proterozoic crustal history of the western United States as determined by neodymium isotopic mapping: *Geological Society of America Bulletin*, v. 99, p. 674-685.

Berger, B.R., 1986, Descriptive model of carbonate-hosted Au-Ag, *in* Cox, D.P., and Singer, D.A., eds., *Mineral deposit models*: U.S. Geological Survey Bulletin 1693, p. 175.

Berger, B.R., and Henley, R.W., 1989, Advances in the understanding of epithermal gold-silver deposits, with special reference to the western United States, *in* Keays, R.R., Ramsay, W.R.H., and Groves, D.I., eds., *The geology of gold deposits: the perspective in 1988: Economic Geology Monograph 6*, p. 405-423.

Bergman, S.C., 1987, Lamproites and other potassium-rich rocks: a review of their occurrence, mineralogy, and geochemistry, *in* Fitton, J.G. & Upton, B.G. J. eds., Alkaline igneous rocks, Geological Society Special Publication no. 30, p. 103-190.

Bingler, E.C., and Bonham, H.F., Jr., 1972, Reconnaissance geologic map of the McCullough Range and adjacent areas, Clark County, Nevada: Nevada Bureau of Mines and Geology Map 45, scale 1:125,000.

Blakely, R.J., and Jachens, R.C., 1990, Concealed mineral deposits in Nevada: Insights from three-dimensional analysis of gravity and magnetic anomalies [abs.]: Geological Society of Nevada, Geology and Ore Deposits of the Great Basin, Program with Abstracts, p. 52-53.

Blanchard, Roland, 1968, Interpretation of leached outcrops: Nevada Bureau of Mines Bulletin 66, 196 p.

Bliss, J.D., ed., 1991, Developments in deposit modeling: U.S. Geological Survey Bulletin (in press).

Bliss, J.D., and Cox, D.P., 1986, Grade and tonnage model of polymetallic veins, *in* Cox, D.P., and Singer, D.A., eds., Mineral deposit models: U.S. Geological Survey Bulletin 1693, p. 125-129.

Bonura, C.J., 1984, Geology, stratigraphy, and origin of the Miocene volcanolacustrine rocks of Hackberry Mountain and Vontrigger Hills in the eastern Mojave desert, San Bernardino County, California: M.S. thesis, California State University, Los Angeles, 164 p.

Brooks, J.W., and Meinert, L.D., 1989, Mineralogy and petrology of the McCoy gold skarn, Lander County, Nev. [abs.]: Geological Society of America, Abstracts with Programs, v. 21, no. 5, p. 59-60.

Brown, H.J., 1986, Detailed geologic map of the eastern New York Mountains, San Bernardino County, Calif. [abs.]: Geological Society of America, Abstracts with Programs, v. 18, no. 2, p. 89.

Burchfiel, B.C., and Davis, G.A., 1971, Clark Mountain thrust complex in the Cordillera of southeastern California: geologic summary and field trip guide, *in* Elders, W.A., ed., Geological excursions in southern California: Campus Museum Contributions Number 1, Riverside, University of California, p. 1-28.

-----1977, Geology of the Sagamore Canyon-Slaughterhouse Spring area, New York Mounains, California: Geological Society of America Bulletin, v. 88, p. 1623-1640.

-----1981, Mojave Desert and environs, *in* Ernst, W.G., ed., The geotectonic development of California (Rubey Volume I): Englewood Cliffs, New Jersey, Prentice Hall, 217-252.

-----1988, Mesozoic thrust faults and Cenozoic low-angle normal faults, eastern Spring Mountains, Nevada, and Clark Mountains thrust complex, California, *in* Weide, D.L., and

Faber, M.L., eds., This extended land: Geological journeys in the southern Basin and Range: Geological Society of America Field Trip Guidebook, p. 87-106.

Burnett, J.L., 1990, 1989, California mining review: California Geology, v. 43, no. 10, p. 219-224.

Busby-Spera, C.J., 1988, Speculative tectonic model for the early Mesozoic arc of the southwest Cordilleran United States: Geology, v. 16, p. 1121-1125.

Busby-Spera, C.J., Schermer, E.R., and Mattinson, J., 1989, Volcano-tectonic controls on sedimentation in an extensional continental arc: A Jurassic example from the eastern Mohave Desert, California [abs.]: *in* Continental magmatism abstracts, International Association of Volcanology and Chemistry of the Earth's Interior, General Assembly, Santa Fe: New Mexico Bureau of Mines and Mineral Resources Bulletin 131, p. 34.

Capps, R.C., and Moore, J.A., 1990, Geologic setting of mid-Miocene gold deposits in the Castle Mountains, San Bernardino County, California, and Clark County, Nevada [abs.]: Geological Society of Nevada and U.S. Geological Survey Great Basin Symposium, Geology and ore deposits of the Great Basin, Program with Abstracts, p. 128.

----1991, Geologic setting of mid-Miocene gold deposits in the Castle Mountains, San Bernardino County, California, and Clark County, Nevada, *in* Raines, G.L., Lisle, R.E., Schafer, R.W., and Wilkinson, W.H., eds., Geology and ore deposits of the Great basin: Reno, Nevada, Geological Society of Nevada, Symposium Proceedings, p. 1,195-1,219.

Carlisle, D.L., Luyendyk, B.P., and McPherron, R.L., 1980, Geophysical survey in the Ivanpah Valley and vicinity eastern Mojave Desert, California, *in* Fife, D.E., and Brown, A.R., eds., Geology and Mineral Wealth of the California Desert, Southcoast Geological Society, p. 485-494.

Castor, S.B., Gleason, J.D., and COWPIE, 1989, Proterozoic ultrapotassic intrusive rocks in southeastern California [abs.]: Geological Society of America, Abstracts with Programs, v. 21, p. 64.

Chaffee, M.A., 1976, The zonal distribution of selected elements above the Kalamazoo porphyry copper deposit, San Manuel district, Pima County, Ariz.: Journal Geochemical Exploration, v. 5, p. 145-165.

Chamberlain, K.R., and Bowring, S.A., 1990, Proterozoic geochronologic and isotopic boundary in NW Arizona: Journal of Geology, v. 20, p. 149.

Chen, J.H., and Moore, J.G., 1979, Late Jurassic Independence dike swarm in eastern California: Geology, v. 7, p. 129-133.

Clark, W.B., 1970, Gold districts of California: California Division of Mines and Geology Bulletin 193, 186 p.

Clary, M.R., 1967, Geology of the eastern part of the Clark Mountain Range, San Bernardino County, California: California Division of Mines and Geology Map Sheet 6.

Conway, C.M., 1986, Field guide to Early Proterozoic strata that host massive sulfide deposits at Bagdad, Arizona, *in* Nations, J.D., Conway, C.M., and Swann, G.A., eds., Geology of central and northern Arizona, Geological Society of America, Rocky Mountain Section, field trip guidebook: Flagstaff, Northern Arizona University, p. 140-157.

-----1991, Tectonomagmatic settings of Proterozoic metallogenic provinces in the southwestern United States [abs.], *in* Goode, E.E., Slack, J.E., and Kotra, R.K., eds., USGS Research on Mineral Resources--1991 Program and Abstracts: U.S. Geological Survey Circular 1062, Seventh Annual McKelvey Forum on Mineral and Energy Resources, p.9-10.

Conway, C.M., Connelley, T.J., and Robison, L.C., 1986, An Early Proterozoic volcanic-hydrothermal-exhalative system at Bagdad, Arizona: Arizona Geological Society Digest, v. 16, p. 24-34.

Conway, C.M., Hassemer, J.R., Knepper, D.H., Jr., Pitkin, J.A., Jachens, R.C., and Chatman, M.L., 1991, Mineral resources of the Wabayuma Peak Wilderness Study Area, Mohave County, Arizona: U.S. Geological Survey Bulletin 1737-E (in press).

Cook, J.R., and Fay, W.M., 1982, Data report, western United States, hydrogeochemical and stream sediment reconnaissance: National Uranium Resource Evaluation Program, Savannah River from the Bristol/Granite Mountains (CDCA-256) Wilderness Study Area, San Bernardino County, California: U.S. Geological Survey Open-File Report 85-510, 8 p.

Cox, D.P., and Bagby, W.C., 1986, Descriptive model of W veins, *in* Cox, D.P., and Singer, D.A., eds., Mineral deposit models: U.S. Geological Survey Bulletin 1693, p. 64.

Cox, D.P., Barton, P.B., and Singer, D.A., 1986, Introduction *in* Cox, D.P., and Singer, D.A., eds., Mineral deposit models: U.S. Geological Survey Bulletin 1693, p. 1-10.

Cox, D.P., Ludington, Steve, Sherlock, M.G., and Singer, D.A., 1991, Delineation of resource assessment tracts and estimation of undiscovered deposits: U.S. Geological Survey Folio (in press).

Cox, D.P., and Singer, D.A., editors, 1986, Mineral deposit models: U.S. Geological Survey Bulletin 1693, 379 p.

Cox, D.P., and Singer, D.A., 1990, Descriptive and grade-tonnage models for distal disseminated Ag-Au deposits: A supplement to U.S. Geological Survey Bulletin 1693: U.S. Geological Survey Open-File Report 90-282, 7 p.

Crow, H.C., 1984, Geochemistry of shonkinites, syenites, and granites associated with the Sulfide Queen carbonatite body, Mountain Pass, California: Las Vegas, University of Nevada, M.S. thesis, 56 p.

Crowe, B.M., Crowell, J.C., and Krummenacher, D., 1979, Regional stratigraphy, K-Ar ages and tectonic implications of Cenozoic volcanic rocks, southeastern California: American Journal of Science, v. 279, p. 186-216.

Czechura, S.J., 1983, Vein paragenesis at Nevada Moly Hall deposit [abs.]: Geological Society of America Abstracts with Programs, v. 15, no. 5, p. 276.

Davis, J.C., 1986, Statistics and data analysis in geology: New York, John Wiley, 646 p.

Davis, J.F., and Anderson, T.P., 1980, Mineral resources of the California desert--an overview, *in* Fife, D.L., and Brown, A.R., eds., Geology and mineral wealth of the California desert: Santa Ana, South Coast Geological Society, p. 122-127.

Davis, W. M., 1933, Granitic domes of the Mohave Desert, California: San Diego Society Natural History Transactions, v. 7, p. 211-258.

Detra, D.E., and Kilburn, J.E., 1985, Analytical results and sample locality map of heavy-mineral-concentrate samples from the Bristol/Granite Mountains (CDCA-256) Wilderness Study Area, San Bernardino County, Calif.: U.S. Geological Survey Open-File Report 85-510, scale 1:62,500, 8 p.

Detra, D.E., Meier, A.L., Goldfarb, R.J., and Weaver, S.L., 1984, Analytical results and sample locality map of stream-sediment, panned-concentrate, and rock samples from the South Providence Mountains Wilderness Study Area, San Bernardino County, California: U.S. Geological Survey Open-File Report 84-118, 26 p.

DeWitt, E., 1987, Proterozoic ore deposits of the southwestern U.S.: Society of Economic Geologists Guidebook Series, v. 1, 189 p.

----1991, Base- and precious-metal concentrations of Early Proterozoic massive sulfide deposits in Arizona--crustal and thermochemical controls of ore deposition [abs.], *in* DeWitt, E., and Karlstrom, K.E., eds., Early Proterozoic geology of western Arizona: Arizona Geological Society Digest (in press).

DeWitt, E., Anderson, J.L., Barton, H.N., Jachens, R.C., Podwysocki, M.H., Brickey, D.W., and Close, T.J., 1989, Mineral resources of the South McCullough Mountains Wilderness Study Area, Clark County, Nevada: U.S. Geological Survey Bulletin 1730, 24 p.

DeWitt, E., Armstrong, E.L., Sutter, J.F., and Zartman, R.E., 1984, U-Th-Pb, Rb-Sr, and Ar-Ar mineral and whole-rock isotope systematics in a metamorphosed granitic terrane, southeastern California: Geological Society of America Bulletin, v. 95, p. 723-739.

DeWitt, E., Kwak, L.M., and Zartman, R.E., 1987, U-Th-Pb and  $^{40}\text{Ar}/^{39}\text{Ar}$  dating of the Mountain Pass carbonatite and alkalic igneous rocks, southeastern California: Geological Society of America Abstracts with Programs, v. 19, p. 642.

Dexter, J.J., Goodknight, C.S., Dayvault, R.D., and Dickson, R.E., 1983, Mineral evaluation of part of the Gold Butte district, Clark County, Nevada: U.S. Department of Energy Open-File Report GJBX-18, 31 p.

Dibblee, T.W., Jr., 1980, Pre-Cenozoic rock units of the Mojave Desert, in Fife, D.L., and Brown, A.R., eds., Geology and mineral wealth of the California desert: Santa Ana, South Coast Geological Society, p. 13-40.

Dohrenwend, J. C., 1987, Basin and Range, in Graf, W. L., ed., Geomorphic systems of North America: Boulder, Colorado, Geological Society of America, Centennial Special Volume 2, p. 303-342.

-----1988, Age of formation and evolution of pediment domes in the area of the Cima volcanic field, Mojave Desert, Calif., in Weide, D.L., and Faber, M.L., eds., This extended land, Geological journeys in the southern Basin and Range, Geological Society of America, Cordilleran Section, Field Trip Guidebook, p. 214-217.

Dohrenwend, J. C., McFadden, L. D., Turrin, B. D., and Wells, S. G., 1984, K-Ar dating of the Cima volcanic field, eastern Mojave Desert, California: late Cenozoic volcanic history and landscape evolution: *Geology*, v. 12, p. 163-167.

Dohrenwend, J. C., Wells, S. G., McFadden, L. D., and Turrin, B. D., 1987, Pediment dome evolution in the eastern Mojave Desert, California, in Gardiner, V., ed., International Geomorphology 1986 Part II: John Wiley & Sons, London, p. 1047-1062.

Donnelly, M.E., and Conway, C.M., 1988, Metallogenic map of volcanogenic massive-sulfide occurrences in Arizona, in Earhart, R.L., ed., Volcanogenic massive-sulfide map series: U.S. Geological Survey Miscellaneous Field Studies Map MF-1853-B, scale 1:100,000.

Dunne, G.C., 1972, Geology of the Devil's Playground area, eastern Mojave Desert, California: Houston, Rice University, Ph. D. thesis, 79 p.

-----1977, Geology and structural evolution of Old Dad Mountain, Mojave Desert, California: Geological Society of America Bulletin, v. 88, p. 737-748.

Duval, J.S., Cook, Beverly, and Adams, J.A.S., 1971, A study of the circle of investigation of an airborne gamma-ray spectrometer: *Journal of Geophysical Research*, v. 76, no. 35, p. 8466-8470.

Duval, J.S., Jones, W.J., Riggle, F.R., and Pitkin, J.A., 1989, Equivalent uranium map of conterminous United States: U.S. Geological Survey Open-File Report 89-478, 10 p., scale 1:2,500,000.

-----1990, Potassium and thorium maps of the conterminous United States: U.S. Geological Survey Open-File Report 90-338, 17 p., scale 1:2,500,000.

Eaton, G.P., 1984, The Miocene Great Basin of western North America as an extending back-arc region: *Tectonophysics*, v. 102, p. 275-295.

Einaudi, M.T., 1982, Skarns associated with porphyry copper plutons, I., Descriptions of deposits, southwestern U.S., II. General features and origin, *in* Titley, S.R., ed., Advances in the geology of the porphyry copper deposits, southwestern United States: Tucson, University of Arizona Press, p. 139-209.

Einaudi, M.T., and Burt, D.M., 1982, Introduction, terminology, classification, and composition of skarn deposits: *Economic Geology*, v. 77, no. 4, p. 745-754.

Einaudi, M.T., Meinert, L.D., and Newberry, R.J., 1981, Skarn deposits, *in* Skinner, B.J., ed., Seventy-fifth anniversary volume, 1905-1980, *Economic Geology*: New Haven, Conn., Economic Geology Publishing Company, p. 317-391.

Elliot, G.S., 1986, Early Proterozoic high-grade metamorphic rocks of Willow Wash, New York Mountains, southeastern California: San Jose, San Jose State University, M.S. thesis, 110 p.

Elliot, G.S., Wooden, J.L., Miller, D.M., and Miller, R.B., 1986, Lower-granulite grade Early Proterozoic supracrustal rocks, New York Mountains, SE California [abs.]: Geological Society of America Abstracts with Programs, v. 18, p. 353.

Farmer, G.L., Wilshire, H.G., Wooden, J.L., Glazner, A.F., and Katz, Marvin, 1991, Temporal variations in the sources of alkali basalts at the Cima volcanic field, SE California [abs.]: Geological Society of America Abstracts with Programs, v. 23, no. 2, p. 23.

Fisher, F.S., 1990, Gold deposits in the Sneffels-Telluride and Camp Bird Mining District, San Juan Mountains, Colo., *in* Shawe, D.R., Ashley, R.P., and Carter, L.M.H., eds., Gold-bearing polymetallic veins and replacement deposits--Part II: U.S. Geological Survey Bulletin 1857-F, p. F12-F18.

Fitzgibbon, T.T., Wentworth, C.M., and Showalter, P.K., 1990, Digital compilation of geologic maps and data bases using ALACARTE-ARC/INFO [abs.]: Geological Society of America Abstracts with Programs, v. 23, p. 25.

Folger, P.F., Detra, D.E., Goldfarb, R.J., Crock, J.G., Briggs, P.H., and Bradley, L.A., 1986, Analytical results and sample locality map of heavy-mineral-concentrate and rock samples from the Providence Mountains Wilderness Study Area (CDCA-263), San Bernardino County, California: U.S. Geological Survey Open-File Report 86-512, 58 p.

Fox, L.K., 1989, Albitization of Jurassic plutons in the southern Bristol Mountains, east-central Mojave Desert, southeastern California: Santa Barbara, University of California, Ph.D. dissertation, 324 p.

Fox, L.K., and Miller, D.M., 1990, Jurassic granitoids and related rocks of the southern Bristol Mountains, southern Providence Mountains, and Colton Hills, Mojave Desert, California: Geological Society of America Memoir 174, p. 111-132.

Franklin, J.M., Sangster, D.M., and Lydon, J.W., 1981, Volcanic-associated massive sulfide deposits, *in* Skinner, B.J., ed., Economic Geology Seventy-fifth Anniversary Volume: New Haven, Economic Geology Publishing Company, p. 485-627.

Friedrich, M.H., and Cuney, M., 1989, Uranium enrichment processes in peraluminous magmatism, *in* International Atomic Energy Agency, ed., Uranium deposits in magmatic and metamorphic rocks: Vienna, International Atomic Energy Agency, Proceedings Salamanca, 29 Sept. - 3 Oct., 1986, p. 11-35.

Gair, J.E., 1989a, Gold-quartz, and gold-pyrite-quartz veins, *in* Gair, J.E., ed., Mineral resources of the Charlotte 1° x 2° quadrangle, North Carolina and South Carolina: U.S. Geological Survey Professional Paper 1462, p. 61-64.

-----1989b, Criteria for assessment of mineral-resource potential, *in* Gair, J.E., ed., Mineral resources of the Charlotte 1° x 2° quadrangle North Carolina and South Carolina: U.S. Geological Survey Professional Paper 1462, p. 51-55.

Geodata International, Inc., 1977, Lake Mead dynamic test range for calibration of airborne gamma radiation measuring systems: U.S. Department of Energy Open-File Report GJBX-46(77), 83 p.

Gittins, J., 1989, The origin and evolution of carbonatite magmas, *in* Bell, K., ed., Carbonatites, genesis and evolution: London, Unwin Hyman, p. 580-600.

Glazner, A.F., and O'Neil, J.R., 1989, Crustal structure of the Mojave Desert, Calif.: Inferences from Sr and O isotope studies of Miocene volcanic rocks: Journal of Geophysical Research, v. 94, no. B6, p. 7861-7870.

Glazner, A.F., Bartley, J.M., and Walker, J.D., 1989, Magnitude and significance of Miocene crustal extension in the central Mojave Desert, California: Geology, v. 17, p. 50-53.

Glazner, A.F., Nielson, J.E., Howard, K.A., and Miller, D.J., 1986, Correlation of the Peach Springs Tuff, a large-volume Miocene ignimbrite sheet in California and Arizona: Geology, v. 14, p. 840-843.

Gleason, J.D., 1988, Petrology and geochemistry of the Barrel Spring pluton and related potassic rocks, Old Woman-Piute Range, southeastern California: Nashville, Vanderbilt University, M.S. thesis, 263 p.

Gleason, J.D., Miller, C.F., and Wooden, J.L., 1988, Barrel Spring alkalic complex: 1.4 Ga anorogenic plutonism in the Old Woman-Piute Range, eastern Mojave Desert, California [abs.]: Geological Society of America Abstracts With Programs, v. 20, p. 164.

Goldfarb, R.J., Miller, D.M., Simpson, R.W., Hoover, D.B., Moyle, P.R., Olson, J.E., and Gaps, R.S., 1988, Mineral resources of the Providence Mountains Wilderness Study Area, San Bernardino County, California: U.S. Geological Survey Bulletin 1712 Chap. D, 70 p.

Gottlieb, O.J., and Friberg, L.M., 1984, The geology and geochemistry of the Hackberry Mountain gold prospect, San Bernardino Co., Calif. [abs.]: Geological Society of America Abstracts with Programs, v. 16, no. 6, p. 522.

Grasty, R.L., and Darnley, A.G., 1971, The calibration of gamma-ray spectrometers for ground and airborne use: Geological Survey of Canada, Paper 71-17, 27 p.

Grimes, D.J., and Marranzino, A.P., 1968, Direct-current arc and alternating-current spark emission spectrographic field methods for the semiquantitative analysis of geologic materials: U.S. Geological Survey Circular 591, 6 p.

Grose, L.T., 1959, Structure and petrology of the northeast part of the Soda Mountains, San Bernardino County, California: Bulletin of the Geological Society of America, v. 70, p. 1509-1548.

Guilbert, J.M., and Park, C.F., Jr., 1986, The geology of ore deposits: New York, W.H. Freeman, 985 p.

Gunter, W.L., Hammitt, J.W., and Babcock, R.C., 1990, Geology of the Barneys Canyon gold deposit, Bingham Canyon, Utah [abs.]: 119th AIME Annual Meeting, Salt Lake City, February 1990, Abstracts with Programs, p. 38.

Hall, A., 1987, Igneous petrology, chapter 4, Nephelinites and carbonatites: Essex, Longman Scientific & Technical, p. 439-453.

Hall, D.K., 1972, Hydrothermal alteration and mineralization in the East Camp of the Turquoise District, San Bernardino Co., Calif.: Tucson, Ariz., University of Arizona, M.S. thesis.

Hamilton, D.L., Bedson, P., and Esson, J., 1989, The behaviour of trace elements in the evolution of carbonatites, in Bell, K., ed., Carbonatites, genesis and evolution: London, Unwin Hyman, p. 405-427.

Hammond, J.G., 1991, Middle Proterozoic diabase intrusions in the southwestern U.S.A. as indicators of limited extensional tectonism, in Mid-Proterozoic geology of the southern margin of ProtoLaurentia-Baltica: Geological Association of Canada Special Paper.

Harding, T.P., 1985, Seismic characteristics and identification of negative flower structures, positive flower structures, and positive structural inversion: American Association of Petroleum Geologists Bulletin, v. 69, p. 582-600.

Harland, W.B., Armstrong, R.L., Cox, A.V., Craig, L.E., Smith, A.G., and Smith, D.G., 1989, A geologic time scale 1989: Cambridge University Press, 247 p.

Harris, D.P., 1984, Mineral resource appraisal: Oxford, Clarendon Press, 445 p.

Haxel, G.B., Smith, D.B., Whittington, C.L., Griscom, A., Diveley-White, D.V., and Powell, R.E., Kreidler, T.J., 1988, Mineral resources of the Orocopia Mountains wilderness study area, Riverside County, California: U.S. Geological Survey Bulletin 1710, Chapter E, 18 p.

Hazzard, J.C., 1954, Rocks and structures of the northern Providence Mountains, San Bernardino County, California, *in* Jahns, R.H., ed., Geology of southern California: California Division of Mines Bulletin 170, chapter 4, p. 27-35.

Hazzard, J.C., and Dosch, E.F., 1936, Archean rocks in the Piute and Old Woman Mountains, San Bernardino County, California [abs]: Geological Society of America Program for 1936, 308-309.

Hedrick, J.B., 1990, Rare-earth metals: U.S. Bureau of Mines Mineral Commodity Summaries 1990, p. 134-135.

Heinrich, E.W., 1966, The geology of carbonatites: Chicago, Rand McNally, 555 p.

Hewitt, D.F., 1931, Geology and ore deposits of the Goodsprings quadrangle, Nevada: U.S. Geological Survey Professional Paper 162, 172 p.

-----1956, Geology and mineral resources of the Ivanpah quadrangle, California and Nevada: U.S. Geological Survey Professional Paper 275, 172 p.

Higgins, C.T., 1990, Mesquite Mine, A modern example of the quest for gold: California Geology, v. 43, no. 3, p. 51-56.

Hileman, G.E., Miller, C.F., and Knoll, M.A., 1990, Mid-Tertiary structural evolution of the Old Woman Mountains area: Implications for crustal extension across southeastern California: Journal of Geophysical Research, v. 95, no. B1, p. 581-599.

Hodges, C.A., and Ludington, Steve, eds., 1991, Quantitative assessment of undiscovered metallic mineral resources in the East Mojave National Scenic Area, southern California: U.S. Geological Survey Open-File Report 91-551, 18 p.

Hodgson, S.F., ed., 1980, Oil and gas prospect wells drilled in California through 1980: California Division of Oil and Gas, Publication TRO 1, 258 p.

Hollister, V.F., 1978, Geology of the porphyry copper deposits of the western Hemisphere: New York, Society of Mining Engineers of the American Institute of Mining, Metallurgical, and Petroleum Engineers, Inc., 219 p.

Hopson, C.A., 1988, Independence dike swarm: Origin and tectonic significance: EOS, v. 69, no. 44, p. 1479.

Howard, K.A., 1991, Intrusion of horizontal dikes: Tectonic significance of Middle Proterozoic diabase sheets widespread in the upper crust of the southwestern United States: Journal of Geophysical Research, v. 96, no. B7, p. 12,461-12,478.

Howard, K.A., Kilburn, J.E., Simpson, R.W., Fitzgibbon, T.T., Detra, D.E., Raines, G.L., and Sabine, C., 1987, Mineral resources of the Bristol/Granite Mountains wilderness study area, San Bernardino County, California: U.S. Geological Survey Bulletin 1712-C, 18 p.

Howard, K.A., Miller, C.F., and Stone, P., 1980, Mesozoic thrusting in the eastern Mojave Desert, Calif. [abs.]: Geological Society of America, v. 12, p. 112.

Howard, K.A., Nielson, J.E., Simpson, R.W., Hazlett, R.W., Alminas, H.V., Nakata, J.K., and McDonnell, J.R., Jr., 1988, Mineral resources of the Turtle Mountains Wilderness Study Area, San Bernardino County, California: U.S. Geological Survey Bulletin 1713, 28 p.

Jachens, R.C., and Griscom, Andrew, 1982, An isostatic residual gravity map of California: a residual map for interpretation of anomalies from intracrustal sources: Society of Exploration Geophysicists, Technical Program Abstracts and Biographies, Fifty-Second Annual International Meeting and Exposition, Dallas, Texas, October 17-21, 1982, p. 299-301.

Jachens, R.C., and Moring, B.C., 1990, Maps of the thickness of Cenozoic deposits and the isostatic residual gravity over basement for Nevada: U.S. Geological Survey Open-File Report 90-404, 15 p.

Jaffe, H.W., Meyrowitz, R., and Evans, Jr., H.T., 1953, Sahamalite, a new rare earth carbonate mineral: American Mineralogist, v. 38, p. 741-754.

James, E.W., 1989, Southern extension of the Independence dike swarm of eastern California: Geology, v. 17, p. 587-590.

Jennings, C.W., compiler, 1961, Geologic map of California, Kingman sheet: California Division of Mines and Geology, 1 sheet, scale 1:250,000.

John, D.A., Stewart, J.H., Kilburn, J.E., Silberling, N.J., and Rowan, L.C., 1991, Geology and mineral resources of the Reno 1° x 2° quadrangle, Nevada and California: U.S. Geological Survey Bulletin (in press).

Jones, A.P., and Wyllie, P.J., 1983, Low-temperature glass quenched from a synthetic, rare-earth carbonatite; implications for the origin of the Mountain Pass deposit, California: Economic Geology, v. 78, p. 1721-1723.

Jones, G.M., and Menzie, W.D., 1986a, Grade and tonnage model of W veins, *in* Cox, D.P., and Singer, D.A., eds., Mineral deposit models: U.S. Geological Survey Bulletin 1693, p. 65-66.

----1986b, Grade and tonnage model of Cu skarn deposits, *in* Cox, D.P., and Singer, D.A., eds., Mineral deposit models: U.S. Geological Survey Bulletin 1693, p. 86-89.

Joralemon, Peter, 1951, The occurrence of gold at the Getchell mine: Economic Geology, v.46, no. 3, p.267-310.

Kaiser, H.F., 1970, A second generation little jiffy: Psychometrika, v. 35, p. 401-415.

Karish, E.R., Miller, E.L., and Sutter, J.F., 1987, Mesozoic tectonic and magmatic history of the central Mojave Desert, *in* Dickinson, W.R., and Klute, M.A., eds., Mesozoic rocks of southern Arizona and adjacent areas: Arizona Geological Society Digest, v. 18, p. 15-32.

Kjarsgaard, B.A., and Hamilton, D.L., 1989, The genesis of carbonatites by immiscibility, *in* Bell, K., ed., Carbonatites, genesis and evolution: London, Unwin Hyman, p. 388-404.

Klovan, J.E., 1968, Selection of target areas by factor analysis: Proceedings, Symposium on decision-making in exploration, Vancouver, B.C., January 26, 1968, 9 p.

Knepper, D.H., Jr., and Simpson, S.L., 1991, Chapter VI. Remote Sensing, in Ludington, S.D., ed., Mineral resource evaluation of the Altiplano and Cordillera Oriental, Bolivia: U.S. Geological Survey Bulletin (in press).

Knopf, Adolph, 1913, Ore deposits of the Helena mining region, Montana: U.S. Geological Survey Bulletin 527, 143 p.

Kohler, S.L., 1984, Mineral land classification of the Lanfair Valley, Homer Mountain, and Davis Dam quadrangles, San Bernardino County, Calif.: California Division of Mines and Geology Open-File Report 84-30 SAC, 68 p.

Korobeinikov, A.F., 1991, Gold conduct in the contact-metasomatic processes of intrusions, *in* Aksyuk, A.M., and others, eds., Skarns-their genesis and metallogeny: Athens, Theophrastus Publications, S.A., p. 203-226.

Kuyper, B.A., Mach, L.E., Streiff, R.E., and Brown, W.A., 1991, Geology of the Cove gold-silver deposit: Society for Mining, Metallurgy, and Exploration, Inc., Preprint no. 91-125, 20 p.

Lange, P.C., 1988, Geology of the Telegraph Mine tectono-hydrothermal breccias, San Bernardino Co., Calif.: Fort Collins, Colo., Colorado State University, M.S. thesis, 190 p.

Lanphere, M.A., 1964, Geochronologic studies in the eastern Mohave Desert, California: Journal of Geology, v. 72, p. 381-399.

Laznicka, Peter, 1985, Empirical metallogeny, v. 1: Phanerozoic environments, associations and deposits, parts A and B: Amsterdam, Elsevier, 1,758 p.

LeBas, J.J., 1987, Nephelinites and carbonatites, *in* Fitton, J.G. & Upton, B.G.J., eds., Alkaline igneous rocks, Geological Society Special Publication no. 30, p. 53-83.

Lechler, P.J., 1988, A new platinum-group-element discovery at Crescent Peak, Clark County, Nevada: Nevada Bureau of Mines and Geology, Open-File Report 88-1, 5 p.

Levinson, A. A., 1980, Exploration Geochemistry, 2nd edition: Wilmette, Illin., Applied Publishing, 924 p.

Lichte, F.E., Golightly, D.W., and Lamothe, P.J., 1987, Inductively coupled plasma--atomic emission spectrometry, *in* Baedecker, P.A., ed., Methods for geochemical analysis: U.S. Geological Survey Bulletin 1770, p. B1-B10.

Linder, Harold, 1988, Geology of the Castle Mountains gold deposit, in Weide, D.L., and Faber, M.L., eds., This extended land: Geological journeys in the southern Basin and Range: Geological Society of America, Field Trip Guidebook, Cordilleran Section Meeting, Las Vegas, Nev., p. 78-80.

-----1989, Castle Mountains gold deposit, Hart Mining District: California Geology, v. 42, no. 6, p. 134-140.

Lindqvist, W.F., 1987, Discovery of the Mesquite gold deposit, Imperial County, California [abs.]: Abstracts American Institute of Mining Engineers, 116 Annual Meeting, p. 84.

Longwell, C.R., Pampeyan, E.H., Bowyer, B., and Roberts, R.J., 1965, Geology and mineral deposits of Clark County, Nevada: Nevada Bureau of Mines Bulletin 62, 218 p.

Ludington, S.D., 1981, Granite molydenite systems, *in* Erickson, R.L., ed., Characteristics of mineral deposit occurrences: U.S. Geological Survey Open-File Report 82-795, p. 43-46.

Manske, S.L., 1990, The relative timing and phase assemblages of vein controlled hypogene mineralization and alteration in the Mesquite deposit, Imperial County, California [abs.]: Geological Society of America Abstracts with Programs, v. 22, no. 3, p. 63.

Manske, S.L., and Einaudi, M.T., 1989, Relations of structure and rock fabric to alteration and mineralization in the Big Chief pit, Mesquite gold deposits, Imperial County, California, and implications for ore genesis [abs.]: Geological Society of America Abstracts with Programs, v. 21, no. 6, p. A295.

Manske, S.L., Matlack, W.F., Springett, M.W., Strakele, A.E., Jr., Watowich, S.N., Yoemans, B., Yeomans, E., 1987, Geology of the Mesquite deposit, Imperial County, Calif.: Society of Mining Engineers, no. 87-107, 9 p.

Mariano, A.N., 1989a, Nature of economic mineralization in carbonatites and related rocks, *in* Bell, K., ed., Carbonatites, genesis and evolution: London, Unwin Hyman, p. 149-176.

Mariano, A.N. 1989b, Economic geology of rare earth elements, *in* Lipin, B.R., McKay, G.A., eds., Geochemistry and mineralogy of rare earth elements: Mineralogical Society of America, Reviews in Mineralogy, v. 21, p. 309-337.

Mariano, John, Helferty, M.G., and Gage, T.B., 1986, Bouger and isostatic residual gravity maps of the Colorado River region, including the Kingman, Needles, Salton Sea, and El Centro quadrangles: U.S. Geological Survey Open-File Report 86-347, scales 1:750,000, and 1:250,000.

Marzolf, J.E., 1983, Early Mesozoic eolian transition from cratonal margin to orogenic-volcanic arc, *in* Gurgel, K.D., ed., Geologic excursions in stratigraphy and tectonics: From southeastern Idaho to the southern Inyo Mountains, California, via Canyonlands and Arches National Parks, Utah, Guidebook-Part II: Utah Geological and Mineral Survey, Special Studies 60, p. 39-46.

Marzolf, J.E., 1988, Reconstruction of Late Triassic and Early and Middle Jurassic sedimentary basins: Southwestern Colorado Plateau to the eastern Mojave Desert, *in* Weide, D.L., and Faber, M.L., eds., This extended land: Geological journeys in the southern Basin and Range: Geological Society of America, Field Trip Guidebook, Cordilleran Section Meeting, Las Vegas, Nev., p. 177-200.

Marzolf, J.E., 1991, Lower Jurassic unconformity (J-O) from the Colorado Plateau to the eastern Mojave Desert: Evidence of a major tectonic event at the close of the Triassic: *Geology*, v. 19, no. 4, p. 320-323.

Matsukuma, T., 1962, Gold and silver deposits and their ores in Kyushu, Japan, part 1: Akita University, Mining College Journal, Series A, v. 2, no. 2, p. 20-59.

McCulloh, T.H., 1954, Problems of the metamorphic and igneous rocks of the Mojave desert, California, *in* Jahns, R.H., ed., *Geology of Southern California*: California Division of Mines Bulletin 170, chapter 7, p. 13-24.

McCurry, M.O., 1985, The petrology of the Woods Mountains volcanic center, San Bernardino County, California: Los Angeles, California University, Ph.D. dissertation, 403 p.

-----1988, Geology and petrology of the Woods Mountains volcanic center, southeastern California: implications for the genesis of peralkaline rhyolite ash flow tuffs: *Journal of Geophysical Research*, v. 93, no. B12, p. 14835-14855.

McCurry, M.O., and Hensel, G., 1988, Structural petrological, and geophysical constraints on the Miocene-Recent crustal evolution of the eastern Mojave Desert [abs.] *Geological Society of America Abstracts with Programs*, v. 20, no. 3, p. 212.

McKelvey, G.E., and Hammarstrom, G.M., 1991, A reconnaissance study of gold mineralization associated with garnet skarn at Nambija, Zamora, Province, Ecuador [abs.], *in* Good, E.E., Slack, J.F., and Kotra, R.K., eds., *USGS Research on mineral resources --1991, Program and Abstracts*, U.S. Geological Survey Circular 1062, p. 55.

Meinert, L.D., 1983, Variability of skarn deposits-Guides to exploration, *in* Boardman, S.J., ed., *Revolution in the Earth Sciences*: Kendall-Hunt Publishing Co., p. 301-316.

-----1988a, Gold in skarn deposits--A preliminary overview, *in* Zachrisson, E., ed., *Proceedings of the Symposium of the 7th Quadrennial International Association of the Geochemistry of Ore Deposits*: Stuttgart, E. Schweizerbart'sche, p. 363-374.

-----1988b, Gold and silver in skarn deposits, *in* Goode, A.D.T., Smyth, E.L., Birch, W.D., and Bosma, L.I., compilers, *Bicentennial Gold 88, Extended Abstracts, Poster Programme*, v. 2: Geological Society of Australia, p. 614-616.

-----1989, Gold skarn deposits - Geology and exploration criteria, *in* Keays, Reid, Ramsay, Ross, and Groves, David, eds., *The geology of gold deposits: The perspective in 1988: Economic Geology Monograph*, 6 p.

Menges, C.M., and McFadden, L.D., 1981, Evidence for a latest Miocene to Pliocene transition from Basin-Range to post-tectonic landscape evolution in southeastern Arizona: *Arizona Geological Society Digest*, v. 13, p. 151-160.

Menzie, W.D., and Singer, D.A., 1990, A course on mineral resource assessment: Proceedings of International Symposium on Mineral Exploration: The Use of Artificial Intelligence, 1990, Tokyo, p. 172-182.

Miller, C.F., 1978, An early Mesozoic alkalic magmatic belt in western North America, *in* Howell, D.G., and McDougall, K.A., eds., Mesozoic Paleogeography of the Western United States: Pacific Section, Society Economic Paleontologists and Mineralogists, Pacific Coast Paleogeography Symposium 2, p. 163-187.

Miller, C.F., and Barton, M.D., 1990, Phanerozoic plutonism in the Cordilleran interior, U.S.A. *in* Kay, S.M., and Rapela, C.W., eds., Plutonism from Antarctica to Alaska: Geological Society of America Special Paper 241, p. 213-231.

Miller, D.M., Friskin, J.G., Jachens, R.C., and Gese, D.D., 1986, Mineral resources of the Castle Peaks Wilderness Study Area, San Bernardino County, California: U.S. Geological Survey Bulletin 1713-A, 17 p.

Miller, D.M., Glick, L.L., Goldfarb, R., Simpson, R.W., Hoover, D.B., Detra, D.E., Dohrenwend, J.C., and Munts, S.T., 1985, Mineral resources and resource potential map of the South Providence Mountains Wilderness Study Area, San Bernardino County, California: U.S. Geological Survey Miscellaneous Field Studies Map MF-1780-A, scale 1:62,500.

Miller, D.M., Howard, K.A., and John B.E., 1982, Preliminary geology of the Bristol Lake region, Mojave Desert, California, *in* Cooper J.D., compiler, Geologic excursions in the California desert (Geological Society of America Cordilleran Section meeting guidebook): Shoshone, California, Death Valley Publishing Company, p. 91-100.

Miller, D.M., Miller, R.J., Nielson, J.E., Wilshire, H.G., Howard, K.A., and Stone, Paul, comps., 1991, Preliminary geologic map of the East Mojave National Scenic Area, California: U.S. Geological Survey Open-File Report 91-435, 8 p.

Miller, D.M., and Wooden, J.L., 1988, An Early Proterozoic batholith in the northern New York Mountains area, California and Nevada [abs]: Geological Society of America Abstracts with Programs, v. 20, p. 215.

Miller, F.K., and Morton, D.M., 1977, Comparison of granitic intrusions in the Pelona and Orocopia Schists, southern California: U.S. Geological Survey Journal of Research, v. 5, no. 5, p. 643-649.

Miller, W.J., 1946, Crystalline rocks of southern California: Geological Society of America Bulletin, v. 57, p. 457-542.

Mitchell, R.H., 1973, Isotopic composition of lead in galena from the Mountain Pass carbonatite, California: Nature Physical Science, v. 241, p. 17-18.

Morris, H.T., 1990, Gold in the Tintic Mining District, Utah, *in* Shawe, D.R., Ashley, R.P., and Carter, L.M.H., eds., Gold-bearing polymetallic veins and replacement deposits--Part II: U.S. Geological Survey Bulletin 1857F, p. F1-F11.

Morton, P.K., 1977, Geology and mineral resources of Imperial County, Calif.: California Division of Mines and Geology County Report 7, 104 p.

Mootooka, J.M., 1988, An exploration geochemical technique for the determination of preconcentrated organometallic halides by ICP-AES: Applied Spectroscopy, v. 42, no. 7, p. 1,293-1,296.

Mootooka, J.M., and Grimes, D.J., 1976, Analytical precision of one-sixth order semiquantitative spectrographic analysis: U.S. Geological Survey Circular 738, 25 p.

Moyle, P.R., Olson, J.E., and Gaps, R.S., 1986, Mineral resources of the Providence Mountains study area, San Bernardino County, Calif.: U.S. Bureau of Mines Open-File Report MLA 47-86, 306 p.

Mueller, P.A., Ragland, P.C., Ranson, W.A., and Burchfiel, B.C., 1979, High-K calc-alkaline plutonic rocks from southeastern California: The Mountain Geologist, v. 16, p. 105-115.

Mutschler, F.E., Wright, E.G., Ludington, Steve, and Abbott, J.T., 1981, Granite molybdenite systems: Economic Geology, v. 76, no. 4, p. 874-897.

Myers, A.T., Havens, R.G., and Dunton, P.J., 1961, A spectrochemical method for the semiquantitative analysis of rocks, minerals and ores: U.S. Geological Survey Bulletin 1084, p.207-229.

Nielson J.E., Friskin, J.G., Jachens, R.C., and McDonnell, J.R., Jr., 1987, Mineral resources of the Fort Piute Wilderness Study Area, San Bernardino County, California: U.S. Geological Survey Bulletin 1713-C, 12 p.

Nielson, J.E., Lux, D.R., Dalrymple, G.B., and Glazner, A.F., 1990, Age of the Peach Springs Tuff, southeastern California and western Arizona: Journal of Geophysical Research, v. 95, no. B1, p. 571-581.

Nokleberg, W.J., Bundtzen, T.K., Berg, H.C., Brew, D.A., Grybeck, Donald, Robinson, M.S., Smith, T.E., and Yeend, Warren, 1987, Significant metalliferous lode deposits and placer districts of Alaska: U.S. Geological Survey Bulletin 1786, 104 p.

Novitsky-Evans, J.M., 1978, Geology of the Cowhole Mountains, southeastern California: Houston, Texas, Rice University, Ph.D. dissertation, 100 p.

Ntiamoah-Agyakwa, Yaw, 1987, Geology, hydrothermal mineralization, and geochemical exploration: New York Mountains and northern Mid Hills, San Bernardino County, California: Los Angeles, University of California, Ph.D. dissertation, 262 p.

O'Driscoll, M., 1988, Rare earths: Enter the dragon: Industrial Minerals, no. 254 (November, 1988), p. 21-55.

Oberlander, T. M., 1974, Landscape inheritance and the pediment problem in the Mojave Desert of southern California: *American Journal of Science*, v. 274, p. 849-875.

Oliver, H.W., Churchel, B.A., and Saltus, R.W., 1986, Aeromagnetic map of Nevada, Kingman sheet: Nevada Bureau of Mines and Geology, scale 1:250,000.

Olson, J.E., and Pray, L.C., 1954, The Mountain Pass rare-earth deposits, *in* Mineral deposits and mineral industry, chapter 8 of Jahns, R.H., ed., *Geology of southern California*: California Division of Mines Bulletin 170, p. 23-39.

Olson, J.E., Shawe, D.R., Pray, L.C., and Sharp, W.N., 1954, Rare-earth mineral deposits of the Mountain Pass district, San Bernardino County, California: U.S. Geological Survey Professional Paper 261, 75 p.

Ontoyev, D.O., 1990, The problem of the origin of the Bayan Obo complex iron-rare earth deposit, China: *International Geology Review*, v. 32, no. 10, p. 988-996.

Orrell, S.E., Anderson, J.L., Wooden, J.L., and Wright, J.E., 1987, Proterozoic crustal evolution of the lower Colorado River region: Rear arc orogenesis to anorogenic crustal remobilization [abs.]: *Geological Society of America Abstracts with Programs*, v. 19, p. 795.

Page, N.J., and Gray, Floyd, 1986, Descriptive model of Alaskan PGE, *in* Cox, D.P., and Singer, D.A. eds., *Mineral deposit models*: U.S. Geological Survey Bulletin 1693, p.49.

Page, N.J., Theodore, T.G., and Bradley, L.A., 1986, Discussion of ultramafic and mafic rocks and platinum-group element analyses from the Lost Basin mining district, northwestern Arizona: U.S. Geological Survey Open-File Report 86-33, 13 p.

Pardee, J.T., and Schrader, F.C., 1933, Metalliferous deposits of the greater Helena mining region, Montana: U.S. Geological Survey Bulletin 842, 318 p.

Peters, W.C., 1978, *Exploration and mining geology*: New York, John Wiley and Sons, 696 p.

Peterson, F., and Pipiringos, G.N., 1979, Stratigraphic relations of the Navajo Sandstone to Middle Jurassic Formations, southern Utah and northern Arizona: U.S. Geological Survey Professional Paper 1035-B, 43 p.

Peterson, J.A., Cox, D.P., and Gray, Floyd, 1983, Mineral resource assessment of the Ajo and Lukeville 1° x 2° quadrangles, Ariz.: U.S. Geological Survey Miscellaneous Field Studies Map MF-1834-B, scale 1:250,000.

Powell, J.L., Hurley, P.M., and Fairbain, H.W., 1966, The strontium isotopic composition and origin of carbonatites, *in* Tuttle, O.F., and Gittins, J., eds., *Carbonatites*: Interscience, p. 365-378.

Powell, R.E., 1981, Geology of the crystalline basement complex, eastern Transverse Ranges, southern California: Constraints on regional tectonic interpretations: Pasadena, California Institute of Technology, Ph.D. dissertation, 441 p.

Ramsay, J.G., and Huber, M.I., 1987, The techniques of modern structural geology; volume 2, folds and fractures: London, Academic Press Inc. (London), Ltd., p. 309-700.

Ransome, F.L., 1907, Preliminary account of Goldfield, Bullfrog, and other mining districts in southern Nevada: U.S. Geological Survey Bulletin 303, 98 p.

Ray, G.E., 1990, Precious metal enriched skarns of British Columbia: The Gangue, no. 30, January 1990, p. 2-4.

Ray, G.E., Ettlinger, A.D., and Meinert, L.D., 1990, Gold skarns: Their distribution, characteristics and problems in classification: British Columbia Ministry of Energy, Mines, and Petroleum Resources, Geological Fieldwork 1989, Paper 1990-1, p. 237-246.

Ray, G.E., McClintock, J., and Roberts, W., 1986, A comparison between the geochemistry of the gold-rich and silver-rich skarns in the Tillicum Mountain area, in Geological fieldwork, 1985: British Columbia Ministry of Energy, Mines and Petroleum Resources Paper 1986-1, p. 37-44.

Ray, G.E., and Webster, I.C.L., 1990, An overview of skarn deposits: Geological Association of Canada, Short Course Notes, Vancouver, 1990, p. 7-1; 7-55.

Reynolds, R.E., 1983, Jurassic trackways in the Mescal Range, San Bernardino County, California, in Gurgel, K.D., ed., Geologic excursions in stratigraphy and tectonics: From southeastern Idaho to the southern Inyo Mountains, California, via Canyonlands and Arches National Parks, Utah, Guidebook-Part II: Utah Geological and Mineral Survey, Special Studies 60, p. 46-48.

Reynolds, R.E., and Nance, M.A., 1988, Shadow Valley Basin: Late Tertiary deposition and gravity slides from the Mescal Range, in Weide, D.L., and Faber, M.L., eds., This extended land: Geological Journeys in the southern Basin and Range: Geological Society of America, Field Trip Guidebook, Cordilleran Section Meeting, Las Vegas, Nev., p. 207-209.

Richter, D.H., Singer, D.A., and Cox, D.P., 1975, Mineral resources map of the Nabesna quadrangle, Alaska: U.S. Geological Survey Miscellaneous Field Studies Map MF-655-K, scale 1:250,000.

Riedel, W., 1929, Zur Mechanik geologischer Brucherscheinungen: Neues Jahrbuch für Mineralogie, Geologie und Paläontologie, Monatschafte, v. 1929 B, p. 354-368.

Roberts, R.J., 1960, Alineaments of mining districts in north-central, Nevada: U.S. Geological Survey Professional Paper 400-B, p. B17-B19.

Roberts, R.J., 1986, The Carlin story, in Tingley, J.V., and Bonham, H.F., Jr., eds., Sediment-hosted precious-metal deposits of northern Nevada: Nevada Bureau of Mines and Geology Report 40, p. 71-80.

Roberts, R.J., and Arnold, D.C., 1965, Ore deposits of the Antler Peak quadrangle, Humboldt and Lander Counties, Nev.: U.S. Geological Survey Professional Paper 459-B, 94 p.

Rose, A.W., Hawkes, H.E., and Webb, J.S., 1979, Geochemistry in mineral exploration, second edition: New York, Academic Press, 657 p.

Rytuba, J.J., and Cox, D.P., 1991, Porphyry gold: a supplement to U.S. Geological Survey Bulletin 1693: U.S. Geological Survey Open-File Report 91-116, 7 p.

Sangster, D.F., 1980, Distribution and origin of Precambrian massive sulphide deposits of North America, *in* Strangway, D.W., ed., The continental crust and its mineral deposits: Geological Association of Canada Special Paper 20, p. 723-739.

Saunders, I., and Young, A., 1983, Rates of surface processes on slopes, slope retreat, and denudation: *Earth Surface Processes and Landforms*, v. 8, p. 473-501.

Schantz, Radford, Wetzel, Nicholas, Adams, Robert, and Raney, R.G., 1990, Minerals in the East Mojave National Scenic Area, Calif.: An economic analysis, volume II: U.S. Bureau of Mines Open-File Report MLA 6-90, 52 p.

Schmidt, K.W., Wotruba, P.R., and Johnson, S.D., 1988, Gold-copper skarn and related mineralization at Copper Basin, Nev.: *Geological Society of Nevada Field-trip Guidebook*, 1988, 6 p.

Schmidt, R.G., 1978, The potential for porphyry copper-molybdenum deposits in the Eastern United States: *U.S. Geological Survey Professional Paper* 907E, p. E1-E31.

Shafiqullah, Muhammad, Frost, E.G., Frost, D.L., and Damon, P.E., 1990, Regional extension and gold mineralization in the southern Chocolate Mountains, southeastern California - K-Ar constraints from fault rocks [abs.]: *Geological Society of America Abstracts with Programs*, v. 22, p. 82.

Shapiro, Leonard, 1975, Rapid analysis of silicate, carbonate, and phosphate rocks (revised edition): *U.S. Geological Survey Bulletin* 1401, 76 p.

Sharp, J.E., 1984, A gold mineralized breccia pipe complex in the Clark Mountains, San Bernardino County, Calif., *in* Wilkins, Joe, Jr., ed., *Gold and silver deposits of the Basin and Range province, western U.S.A.*: *Arizona Geological Society Digest*, v. 15, p. 119-139.

Sharp, R.E., 1957, Geomorphology of Cima Dome, Mojave Desert, California: *Geological Society of America Bulletin*, v. 68, p. 273-290.

Shawe, D.R., 1988, The case for gold--An introduction to geology and resources of gold in the United States, *in* Shawe, D.R., Ashley, R.P., and Carter, L.M.H., eds., *Introduction to geology and resources of gold, and geochemistry of gold: U.S. Geological Survey Bulletin 1857A*, p. A1-A8.

----1990, Gold in the Alma Mining District, Colo., *in* Shawe, D.R., Ashley, R.P., and Carter, L.M.H., eds., *Gold-bearing polymetallic veins and replacement deposits--part II: U.S. Geological Survey Bulletin 1857-F*, p. F19-F31.

Sheets, R.W., Ausburn, Kent, Bodnar, R.J., and Craig, J.R., 1990, Fault-related gold mineralization: Ore petrology and geochemistry of the Morning Star Deposit, Calif. [abs.], *in* Geology and ore deposits of the Great Basin, Great Basin Symposium, Program with Abstracts: Reno, Nev., Geological Society of Nevada and U.S. Geological Survey, April, 1990, p. 109-110.

Sheets, R.W., Ausburn, Kent, Bodnar, R.J., Craig, J.R., and Law, R.D., 1989, Geology and precious metal mineralization at the Morning Star deposit, San Bernardino Co., Calif.: U.S. Bureau of Land Management Compendium, The California Desert Mineral Symposium, March, 1989, p. 219-231.

Sheets, R.W., Bodnar, R.J., Craig, J.R., and Ausburn, K.E., 1988, Precious-metal mineralization at the Morning Star deposit, San Bernardino Co., Calif. [abs.]: Geological Society of America Abstracts with Programs, v. 20, no. 7, p. A142.

Sheridan, D.M., and Raymond, W.H., 1982, Stratabound Precambrian sulfide deposits, Colorado and Wyoming, *in* Erickson, R.L., Characteristics of mineral deposits: U.S. Geological Survey Open-File Report 82-795, p. 92-99.

Shimazaki, Hideiko, 1981, Skarn deposits and related acid igneous activities: State of Sonora [Mexico], Special Publication, Director of Minerals, Geology, and Energy, Hermosillo, 50 p.

Sibson, R.H., 1987, Earthquake rupturing as a mineralizing agent in hydrothermal systems: Geology, v. 15, no. 8, p. 701-704.

Sibson, R.H., 1990, Faulting and fluid flow, *in* Nesbitt, B.E., ed., Fluids in tectonically active regimes of the continental crust: Mineralogical association of Canada Short Course, v. 18, p. 93-132.

Sillitoe, R.H., 1979, Some thoughts on gold-rich porphyry copper deposits: Mineralium Deposita, v. 14, p. 161-174.

-----1980, Types of porphyry molybdenum deposits: Mining Magazine, v. 142, p. 550-551, 553.

-----1991, Intrusion-related gold deposits, *in* Foster, R.P., ed., Gold metallogeny and exploration: Glasgow and London, Blackie and Son Ltd., p. 165-209.

Sillitoe, R.H., and Bonham, H.F., Jr., 1990, Sediment-hosted gold deposits: Distal products of magmatic-hydrothermal systems: Geology, v. 18, p. 157-161.

Silver, L.T., McKinney, C.R., and Wright L.A., 1961, Some Precambrian ages in the Panamint Range, Death Valley, California [abs.]: Geological Society of America Special Paper 68, p. 55.

Singer, D.A., 1975, Mineral resource models and the Alaskan mineral resource assessment program, *in* Vogley, W.A., ed., Mineral materials modeling: A state-of-the-art review: Baltimore, The Johns Hopkins University Press, p. 370-382.

----1990, Development of grade and tonnage models for different deposit types [abs.]: Toronto, 8th IAGOD Symposium, Program with Abstracts, p. A99-A100.

----1991, Development of grade and tonnage models for different deposit types: Geological Association of Canada Special Paper (in press).

Singer, D.A., and Cox, D.P., 1988, Applications of mineral deposit models to resource assessment: U.S. Geological Survey Yearbook 1987, p. 55-57.

Singer, D.A., and Mosier, D.L., 1986, Grade and tonnage model of Cyprus massive sulfide, *in* Cox, D.P., and Singer, D.A., eds., Mineral deposit models: U.S. Geological Survey Bulletin 1693, p. 131-135.

Singer, D.A., Page, N.J., Smith, J.G., Blakely, R.J., and Johnson, M.G., 1983, Mineral resource assessment maps of the Medford 1° by 2° quadrangle, Oregon-California: U.S. Geological Survey Miscellaneous Field Studies Map MF-1383-C, scale 1:250,000.

Smirnov, V.I., 1976, Geology of mineral deposits: Moscow, Mir Publishers, 520 p.

Snoke, A.W., and Miller, D.M., 1988, Metamorphic and tectonic history of the northeastern Great Basin, *in* Ernst, W.G., ed., Metamorphism and crustal evolution of the western United States, Rukey Volume 7: Englewood Cliffs, New Jersey, Prentice-Hall, p. 606-648.

Snyder, D.G., Roberts, C.W., Saltus, R.W., and Sikora, R.F., 1982, A magnetic tape containing the principal facts of 64,026 gravity stations in the state of California: U.S. Geological Survey NTIS PB-82-168287 (available from U.S. Department of Commerce, National Technical Information Service, Springfield, Va., 22152).

Spencer, J.E., 1985, Miocene low-angle normal faulting and dike emplacement, Homer Mountain and surrounding areas, southeastern California and southernmost Nevada: Geological Society of America Bulletin, v. 96, p. 1140-1155.

Spencer, J.E., and Turner, R.D., 1985, Geologic map of Homer Mountain and the southern Piute Range, southeastern California: U.S. Geological Survey Miscellaneous Field Studies Map MF-1709, scale 1:24,000.

Stensrud, H.L., and More, S., 1980, Precambrian geology and massive sulfide environments of the west-central Hualapai Mountains, Mohave County, Ariz.; a preliminary report, *in* Jenney, J.P., ed., Studies in western Arizona: Arizona Geological Digest, v. 12, p. 155-164.

Stewart, J.H., 1970, Upper Precambrian and Lower Cambrian strata in the southern Great Basin, California and Nevada: U.S. Geological Survey Professional Paper 620, 206 p.

Stewart, J.H., Poole, F.G., 1975, Extension of the Cordilleran miogeosynclinal belt to the San Andreas fault, southern California: Geological Society of America Bulletin, v. 86, p. 205-212.

Stone, P., Howard, K.A., and Hamilton, W., 1983, Correlation of metamorphosed Paleozoic strata of the southeastern Mojave Desert region, California and Arizona: Geological Society of America Bulletin, v. 94, p. 1135-1147.

Streckeisen, A.L., and others, 1973, Plutonic rocks; classification and nomenclature recommended by the IUGS Subcommission on the Systematics of Igneous Rocks: *Geotimes*, v. 18, no. 10, 26-30.

Sutter, J.F., 1968, Geochronology of major thrusts, southern Great Basin, California: Houston, Texas, Rice University, M.S. Thesis, 32 p.

Taylor, S.R., and McLennan, S.M., 1985, The continental crust: its composition and evolution. An examination of the geochemical record preserved in sedimentary rocks: Blackwell, 312 p.

Tchalenko, J.S., 1970, Similarities between shear zones of different magnitudes: *Geological Society of America Bulletin*, v. 81, p. 1625-1640.

Theodore, T.G., Blair, W.N., and Nash, J.T., 1987a, Geology and gold mineralization of the Gold Basin-Lost Basin mining districts, Mohave County, Arizona: U.S. Geological Survey Professional Paper 1361, 167 p.

Theodore, T.G., Blake, D.W., Loucks, T.A., and Johnson, C.A., 1991a, Geology of the Buckingham stockwork molybdenum deposit and surrounding area, Lander County, Nevada, *with a section on* Potassium-argon and  $^{40}\text{Ar}/^{39}\text{Ar}$  geochronology of selected plutons in the Buckingham area, *by* E.H. McKee, *and a section on* Economic geology, *by* T.A. Loucks and C.A. Johnson, *and a section on* Supergene copper deposits at Copper Basin *by* D.W. Blake, *and a section on* Mineral chemistry of Late Cretaceous and Tertiary skarns *by* J.M. Hammarstrom: U.S. Geological Survey Professional Paper 798-D [in press].

Theodore, T.G., Czamanske, G.K., and Keith, T.E.C., 1987b, Sillenite and other bismuth minerals associated with placer gold, Battle Mountain mining district, Nevada [abs.]: *Geological Society of America Abstracts with Programs*, v. 20, no. 3, p. 237.

Theodore, T.G., Czamanske, G.K., Keith, T.E.C., and Oscarson, R.L., 1989, Bismuth minerals associated with placer gold, Battle Mountain Mining District, Nevada [abs.], *in* Shindler, K.S., ed., USGS Research on Mineral Resources, 1989, Program and Abstracts: U.S. Geological Survey Circular 1035, p. 72-74.

Theodore, T.G., and Jones, G.M., 1991, Geochemistry and geology of gold in jasperoid, Elephant Head area, Lander County, Nev.: U.S. Geological Survey Bulletin (in press).

Theodore, T.G., and Menzie, W.D., 1984, Fluorine-deficient porphyry molybdenum deposits in the cordillera of western North America, *in* Janelidze, T.V., and Tvalchrelidze, A.G., eds., *Proceedings of the Sixth Quadrennial IAGOD Symposium*, Tbilisi, U.S.S.R., September 6-12, 1982, v. 1, E. Schweizerbart'sche Verlagsbuchhandlung, Stuttgart, p. 463-470.

Theodore, T.G., Orris, G.M., Hammarstrom, J.M., and Bliss, J.D., 1991b, Gold-bearing skarns: U.S. Geological Survey Bulletin 1930, 61 p.

Thomas, W.M., Clarke, H.S., Young, E.D., Orrell, S.E., and Anderson, J.L., 1988, Proterozoic high-grade metamorphism in the Colorado River region, Nevada, Arizona, and California, *in*

Ernst, W.G., ed., Metamorphism and crustal evolution of the western United States, Rubey Volume VII: Englewood Cliffs, Prentice Hall, p. 526-537.

Thompson, T.B., 1982, Classification and genesis of stockwork molybdenum deposits: Discussion: *Economic Geology*, v. 77, no. 3, p. 709-710.

-----1990, Precious metals in the Leadville Mining District, Colo., *in* Shawe, D.R., Ashley, R.P., and Carter, L.M.H., eds., Gold-bearing polymetallic veins and replacement deposits--Part II: U.S. Geological Survey Bulletin 1857-F, p. F32-F49.

Tingley, J.V., and Bonham, H.F., Jr., 1986, eds., 1986, Sediment-hosted precious-metal deposits of northern Nevada: Nevada Bureau of Mines and Geology Report 40, 103 p.

Tooker, E.W., 1990, Gold in the Bingham District, Utah, *in* Shawe, D.R., Ashley, R.P., and Carter, L.M.H., eds., Geology and resources of gold in the United States: U.S. Geological Survey Bulletin 1857-E, p. E1-E16.

Tosdal, R.M., and Smith, D.B., 1987, Some characteristics of gneiss-hosted gold deposits of southeastern Calif. [abs.]: U.S. Geological Survey Circular 995, p. 71.

Tosdal, R.M., Haxel, G.B., and Wright, J.E., 1989, Jurassic geology of the Sonoran Desert region, southern Arizona, southeastern California, and northernmost Sonora: Construction of a continental-margin magmatic arc, *in* Jenney, J.P., and Reynolds, S.J., eds., Geologic evolution of Arizona: Arizona Geological Society Digest 17, p. 397-434.

Turner, R.D., 1985, Magma mixing and fractional crystallization of Miocene volcanic rocks in the Castle Mountains, northeastern Mojave desert [abs.]: Geological Society of America Abstracts with Programs, v. 17, no. 6, p. 414.

Turner, R.D., and Glazner, A.F., 1990, Miocene volcanism, folding and faulting in the Castle Mountains, southern Nevada and eastern California, *in* Wernicke, B.P., ed., Cenozoic tectonics of the Basin and Range Province at the latitude of Las Vegas: Geological Society of America Memoir 176, p. 23-25.

Turner, R.D., Huntoon, J.E., and Spencer, J.E., 1983, Miocene volcanism, sedimentation and folding in the northeastern Castle Mountains, California and Nevada [abs.]: Geological Society of America Abstracts with Programs, v. 15, no. 5, p. 433.

Turrin, B.D., Dohrenwend, J.C., Drake, R.E., and Curtis, G.H., 1985, K-Ar ages from the Cima volcanic field, eastern Mojave Desert, California: Isochron West, no 44, p. 9 - 16.

Turrin, B.D., Dohrenwend, J.C., Wells, S.G., and McFadden, L.D., 1984, Geochronology and eruptive history of the Cima volcanic field, eastern Mojave desert, California, in Dohrenwend, J.C., Surficial geology of the eastern Mojave Desert, California: Geological Society of America 1984 Annual Meeting Guidebook, Reno, Nevada, p.88-100.]

Twyman, J.D., and Gittins, J., 1987, Alkalic carbonatite magmas: parental or derivative, in Fitton, J.G. & Upton, B.G.J. eds., Alkaline igneous rocks, Geological Society Special Publication no. 30, p. 85-94.

U.S. Bureau of Land Management, 1980, The California desert conservation area plan: U.S. Bureau of Land Management, 173 p.

-----1982, Final environmental impact statement and proposed plan California Desert Conservation Area, Appendix 14, volume G (revised) Geology--Energy-Minerals: U.S. Bureau of Land Management, p. 1-202.

U.S. Bureau of Mines, 1990a, Minerals in the East Mojave National Scenic Area, Calif.: A minerals investigation, v. 1: U.S. Bureau of Mines Open-File Report MLA 6-90, 356 p.

U.S. Bureau of Mines, 1990b, Copper, gold: U.S. Bureau of Mines Mineral Commodity Summaries, 1990, p. 52-53, p. 70-71.

U.S. Bureau of Mines and U.S. Geological Survey, 1980, Principles of a resource/reserve classification for minerals: U.S. Geological Survey Circular 831, 5 p.

U.S. Department of Energy, 1979a, Aerial radiometric and magnetic survey, Trona National Topographic Map, California: U.S. Department of Energy Open-File Report GJBX-64 (79), 204 p.

-----1979b, Airborne gamma-ray spectrometer and magnetometer survey, Las Vegas quadrangle (Arizona, California, Nevada), William quadrangle (Arizona), Prescott quadrangle (Arizona), and Kingman quadrangle (Arizona, California, Nevada): U.S. Department of Energy Open-File Report GJBX-59(79), 993 p.

-----1979c, Aerial radiometric and magnetic survey, Needles National Topographic Map, California and Nevada: U.S. Department of Energy Open-File Report GJBX-114(79), v. I, 189 p., v. II, 88 p.

-----1980, Airborne gamma-ray spectrometer and magnetic survey, Los Angeles quadrangle, San Bernardino quadrangle, Santa Ana quadrangle, Calif.: U.S. Department of Energy Open-File Report GJBX-214(80), 5 v., 640 p.

U.S. Geological Survey, 1981, Aeromagnetic map of the Needles 1° x 2° quadrangle, California and Arizona: U.S. Geological Survey Open-File Report 81-85, scale 1:250,000.

-----1983, Aeromagnetic map of the Kingman-Trona area, California: U.S. Geological Survey Open-File Report 83-663, scale 1:250,000.

VanTrump, George, Jr., and Miesch, A.T., 1977, The U.S. Geological Survey RASS-STATPAC system for management and statistical reduction of geochemical data: Computers and Geosciences, v. 3, p. 475-488.

Volborth, A., 1962, Allanite pegmatites, Red Rock, Nevada, compared with allanite pegmatites in southern Nevada and California: Economic Geology, v. 57, p. 209-216.

Walker, J.D., 1987, Permian to Middle Triassic rocks of the Mojave Desert, *in* Dickinson, W.R., and Klute, M. A., eds., Mesozoic rocks of southern Arizona and adjacent areas: Arizona Geological Society Digest, v. 18, p. 1-14.

Wallace, R.E., 1978, Geometry and rates of change of fault-generated range fronts, north-central Nevada: U. S. Geological Survey Journal of Research, v. 6, p. 637-650.

Wallace, R.E., and Morris, H.T., 1986, Characteristics of faults and shear zones in deep mines: Pure and Applied Geophysics, v. 124, no. 1-2, p. 107-125.

Ward, D.L., 1978, Construction of calibration pads facility, Walker Field, Grand Junction, Colorado: U.S. Department of Energy Open-File Report GJBX-37(78), 57 p.

Warnke, D.A., 1969, Pediment evolution in the Halloran Hills, central Mojave Desert, California: *Zeitschrift fur Geomorphologie*, v. 13, p. 357-389.

Wasserburg, G.J., Wetherill, G.W., and Wright, L.A., 1959, Ages in the Precambrian terrane of Death Valley, California: *Journal of Geology*, v. 67, p. 702-708.

Watson, K.D., Morton, D.M., and Baird, A.K., 1974, Shonkinite-syenite plutons, Mountain Pass, San Bernardino County, California [abs.]: Geological Society of America Abstracts with Programs, v. 6, p. 273.

Weldin, R.D., 1991, The California Desert-Protect it or develop it?: U.S. Bureau of Mines, Minerals Today, January, 1991, p. 12-17.

Westra, Gerhard, and Keith, S.B., 1981, Classification and genesis of stockwork molybdenum deposits: *Economic Geology*, v. 76, no. 4, p. 844-873.

White, W.H., Bookstrom, A.A., Kamilli, R.J., Ganster, M.W., Smith, R.P., Ranta, D.E., and Steininger, R.C., 1981, Character and origin of Climax-type molybdenum deposits, *in* Skinner, B.J., ed., *Economic Geology, 75th anniversary volume, 1905-1980*: New Haven Conn., Economic Geology Publishing Co., p. 270-316.

Willis, G.F., 1988, Geology and mineralization of the Mesquite open pit gold mine, *in* Schafer, R.W., Cooper, J.J., and Vikre, P.G., eds., Bulk mineable precious metal deposits of the Western United States: Geological Society of Nevada, Symposium Proceedings, 1987, p. 473-486.

Willis, G.F., and Holm, V.T., 1987, Geology and mineralization of the Mesquite open pit gold mine, *in* Johnson, J.L., Bulk mineable, Guidebook for field trips: Geological Society of Nevada, Symposium, 1987, p. 52-56.

Willis, G.F., Tosdal, R.M., and Manske, S.L., 1989, Structural control on epithermal gold veins and breccias in the Mesquite district, southeastern California [abs.]: U.S. Geological Survey Circular 1035, p. 78.

Wilshire, H.G., 1987, Multistage generation of alkalic basalt in the mantle: The Cima volcanic field, California [abs.]: Geological Society of America Abstracts with Programs, v. 19, no. 7, p. 892.

-----1988, Geology of the Cima volcanic field, San Bernardino County, Calif., *in* Weide, D.L., and Faber, M.L., eds., This extended land: Geological Journeys in the Southern Basin and Range: Geological Society of America, Field Trip Guidebook, Cordilleran Section Meeting, Las Vegas, Nev., p. 210-213.

Wilshire, H.G., Frisken, J.G., Jachens, R.C., Prose, D.V., Rumsey, C.M., and McMahan, A.B., 1987, Mineral resources of the Cinder Cones Wilderness Study Area, San Bernardino County, California: U.S. Geological Survey Bulletin 1712-B, 13 p.

Wilshire, H.G., McGuire, A.V., Noller, J.S., and Turrin, B.D., 1989, Petrology of lower crustal and upper mantle xenoliths from the Cima volcanic field, California: *Journal of Petrology* (in press).

Wilson, S.A., Kane, J.S., Crock, J.G., and Hatfield, D.B., 1987, Chemical methods of separation for optical emission, atomic absorption spectrometry, and colorimetry, *in* Baedecker, P.A., ed., Methods for geochemical analysis: U.S. Geological Survey Bulletin 1770, D1-D14.

Woodcock, J.R., and Hollister, V.F., 1978, Porphyry molybdenite deposits of the North American Cordilleran: Minerals, Science, and Engineering (Johannesburg), v. 10, p. 3-18.

Wooden, J.L., and Miller, D.M., 1990, Chronologic and isotopic framework for Early Proterozoic crustal evolution in the eastern Mojave Desert region, southeastern California: *Journal of Geophysical Research*, v. 95, no. B12, p. 20, 133-20, 146.

Wooden, J.L., Stacey, J.S., Howard, K.A., Doe, B.R., and Miller, D.M., 1988, Pb isotopic evidence for the formation of Proterozoic crust in the southwestern United States, *in* Ernst, W.G., ed., Metamorphism and crustal evolution of the western United States, Rubey Volume VII: Englewood Cliffs, Prentic Hall, p. 69-86.

Woolley, A.R., and Kempe, D.R.C., 1989, Carbonatites: Nomenclature, average chemical composition, and element distribution, *in* Bell, K., ed., Carbonatites, genesis and evolution: London, Unwin Hyman, p. 1-14.

Wotrub, P.R., Benson, R.G., and Schmidt, K.W., 1986, Battle Mountain describes the geology of its Fortitude gold-silver deposit at Copper Canyon: *Mining Engineering*, July, 1986, v. 38, no. 7, p. 495-499.

Woyski, M.S., 1980, Petrology of the Mountain Pass carbonatite complex—A review, *in* Fife, D.L., and Brown, A.R., eds., Geology and mineral wealth of the California desert: Santa Ana, South Coast Geological Society, p. 367-378.

Wright, J.E., and Howard, K.A., and Anderson, J.L., 1987, Isotopic systematics of zircons from Late Cretaceous intrusive rocks, southeastern California: Implications for a vertically stratified crustal column: Geological Society of America Abstracts with Programs, v. 19, p. 898.

Wright, L.A., 1968, Talc deposits of the southern Death Valley-Kingston Range region, California: California Division of Mines and Geology Special Report 95, 79 p.

Wright, L.A., Troxel, B.W., Williams, E.G., Roberts, M.T., and Diehl, P.E., 1976, Precambrian sedimentary environments of the Death Valley region, eastern California: California Division of Mines and Geology Special Report 106, p. 7-15.

Wrucke, C.T., Otton, J.K., and Desborough, G.A., 1986, Summary and origin of the mineral commodities in the Middle Proterozoic Apache Group in central Arizona, in Beatty, B., and Wilkinson, P.A.K., eds., Frontiers in Geology and ore deposits of Arizona and the southwest: Arizona Geological Society Digest, v. 16, p. 12-17.

Wyllie, P.J., 1989, Origin of carbonatites: evidence from phase equilibrium studies, in Bell, K., ed., Carbonatites, genesis and evolution: London, Unwin Hyman, p. 500-545.

Wyllie, R.J.M., 1991, Navachab, Namibia's new mine: Engineering and Mining Journal, January, 1991, p. 28-31.

Yeend, Warren, Dohrenwend, J.C., Smith, R.S.U., Goldfarb, R.J., Simpson, R.W., Jr., and Munts, S.R., 1984, Mineral resources and mineral resource potential of the Kelso Dunes Wilderness Study Area (CDCA-250), San Bernardino County, California: U.S. Geological Survey Open-File Report 84-647, 19 p.

Young, E.D., 1989, Petrology of biotite-cordierite-garnet gneiss of the McCullough Range, Nevada II.  $P-T-aH_2O$  path and growth of cordierite during late stages of Low- $P$  granulite-grade metamorphism: Journal of Petrology, v. 30, pt. 1, p. 61-78.

Young, E.D., Anderson, J.L., Clarke, H.S., and Thomas, W.M., 1989, Petrology of biotite-cordierite-garnet gneiss of the McCullough Range, Nevada I. Evidence for Proterozoic low-pressure fluid-absent granulite-grade metamorphism in the southern Cordillera: Journal of Petrology, v. 30, pt. 1, p. 39-60.

Young, R.A., and Brennan, W.J., 1974, Peach Springs Tuff: Its bearing on structural evolution of the Colorado Plateau and development of Cenozoic drainage in Mohave County, Arizona: U.S. Geological Survey Bulletin, v. 85, p. 83-90.

Zharikov, V.A., 1970, Skarns: International Geology Review, v. 12, p. 541-559, 619-647, 760-775.

Table 1. Listing of the estimated average concentrations of potassium, uranium, and thorium for various geologic units in the East Mojave National Scenic area

Estimated Concentration values			
Geologic Unit	Potassium percent K	Uranium ppm eU	Thorium ppm eTh
Qaf	2.9	3.2	13.0
Qaf2	2.6	3.0	10.9
Qes1	2.2	2.0	4.4
Qes2	2.9	3.9	18.5
Qp	2.4	4.2	18.5
Qtb1	1.6	2.5	8.0
QTg	2.6	2.7	8.3
Td	2.2	3.0	10.9
Tdr	2.1	3.9	19.5
Tg	2.7	2.4	13.0
Tts	3.5	4.4	15.4
Tv1	3.0	3.9	14.3
Tw	3.0	3.5	15.0
Kg1	2.4	2.4	10.1
Klo	2.7	2.9	7.3
Kmh	3.0	2.4	13.3
Kpm	2.0	3.4	12.0
Krs	2.3	2.6	12.0
Kt	2.8	3.4	18.9
KJg	2.4	3.4	14.5
Jd	2.3	2.5	9.5
Jfc	2.6	1.9	12.0
Jg	2.1	3.1	11.5
Jgo	3.0	2.9	11.5
Jig	3.2	3.4	31.0
Jmc	1.9	2.8	9.0
Js	2.8	2.1	6.5
Mvz	2.3	4.0	11.3
Czs	1.9	1.6	6.5
Cd	0.5	1.5	3.0
Xg	2.5	2.8	15.2
Xg1	2.4	2.5	12.4
Xg2	3.2	3.4	14.0
Xm	2.0	2.1	17.5

Table 2. Summary of resultant colors of alteration minerals and vegetation on a color-ratio composite image prepared with TM channels 5/7 in red, TM channels 3/1 in green, and TM channels 3/4 in blue (After Knepper and Simpson, unpub. data, 1991)

Material	TM5/7 (red)	TM3/1 (green)	TM3/4 (blue)	Resultant color
Carbonate and hydroxyl-bearing minerals	High	Low	Moderate to Low	Magenta
Limonite (hematite, goethite)	Low	High	Moderate to high	Green to cyan
Limonite (Jarosite)	High	High	Moderate to high	Yellow to white
Carbonate, Hydroxyl-bearing and limonite	High	High	Moderate to high	Yellow to white
Vegetation	High	Low	Very low	Red

Table 3. Listing of areas in the East Mojave National Scenic Area, California, with references to interpretive geochemical reports and releases of raw geochemical data  
[---, status unknown]

Area on figure 23	Interpretive report	Raw geochemical data
Soda Mountains	--	--
Little Cowhole Mountain	--	--
Cowhole Mountain	--	--
Cinder Cone	Wilshire and others, 1987	Adrian and others, 1986b
Marl Mountains	--	--
Old Dad Mountain	--	--
Kelso Mountains	--	--
Bristol Mountains	--	--
Clark Mountain Range	--	--
Mescal Range	--	--
Ivanpah Mountains	--	--
Cima Dome	--	--
New York Mountains	Miller and others, 1986	Adrian and others, 1986c
Mid Hills	--	--
Providence Mountains	Goldfarb and others, 1988 Miller and others, 1985	Folger and others, 1986 Detra and others, 1984
Granite Mountains	Howard and others, 1987 Yeend and others, 1984	Detra and Kilburn, 1985
Van Winkle Mountain	--	--
Grotto Hills	--	--
Pinto Mountain	--	--
Table Mountain	--	--
Woods Mountains	--	--
Hackberry Mountain	--	--
VonTrigger Hills	--	--
Piute Range	Nielson and others, 1987	Adrian and others, 1986a
Castle Mountains	--	--
Homer Mountain	--	--

Table 4. Analyses of select rock samples from some mineralized areas in the East Mojave National Scenic Area, California

[Analyses numbers same as table 5. Semiquantitative and quantitative optical spectroscopic analyses by inductively coupled-plasmas methods of Lichte and others (1987) and Motooka (1988); analyses, D.L. Fey and J.M. Motooka. Looked for but not found, at detection levels shown in parentheses: 110 (4), 114 (40), and U (100). Precision for concentration higher than 10 times the detection limit is better than  $\pm 10$ -percent relative standard deviation; instrumental precision of the scanning instrument is  $\pm 2$ -percent relative standard deviation. Au determined by combined graphite furnace and atomic absorption spectroscopy method; W, was determined colorimetrically; 11g was determined by a cold vapor-atomic absorption method, and As was determined by a hydride-generation atomic absorption spectrometry method (Wilson and others, 1987; Aruscavage and Crock, 1987); analysts, A.H. Love, E.P. Welsch, P.L. Hagerman, and B.H. Roush; -, not detected.]

Analysis No.	Field No. 90TT	Ag	Ba	Be	Bi	Cd	Co	Cr	Cu	Eu	Ga	La	Li	Mn	Mo	Nb	Nd	Ni	Pb	Sc		
Inductively coupled plasma-atomic emission spectroscopy (total) (parts per million)																						
1	015	99	28	<1	440	<2	8	7	12	30,100	<2	5	12	5	2,200	<2	7	18	<2	49	<2	
2	016	147	188	<1	1,140	<2	10	7	5	57,700	<2	<4	13	4	1,490	2	11	13	<2	86	<2	
3	019	15	8	<1	70	7	<4	12	5	10,600	<2	6	4	11	2,970	<2	<4	11	<2	15	<2	
4	020	3	13	1	50	3	<4	5	5	2,330	<2	9	7	11	4,890	6	<4	13	3	10	<2	
5	027	9	7	2	20	3	6	58	118	13,500	<2	20	5	11	5,130	<2	5	4	18	18	<2	
6	030	<2	4	<1	<10	3	4	227	1	151	<2	26	5	5	465	<2	<4	<4	165	13	<2	
7	031	<2	3	<1	<10	<2	<4	2	<1	40	<2	<4	3	3	506	<2	<4	9	<2	5	<2	
8	032	<2	347	3	<10	<2	117	1	<1	30	<2	15	56	3	99	<2	39	47	<2	8	3	
9	035	<2	44	<1	<10	3	<4	126	5	224	<2	18	3	41	327	<2	<4	36	7	<2		
10	038	17	234	<1	220	<2	11	40	10	10,800	<2	4	7	6	802	4	<4	7	15	58	2	
11	040	<2	1,270	1	<10	<2	33	3	<1	16	<2	8	23	3	57	<2	10	11	<2	10	<2	
12	041	8	453	2	10	<2	13	4	4	4	637	<2	6	6	75	28	12	<4	6	4	18,600	2
13	042	6	505	2	10	<2	34	5	5	1,510	<2	5	21	6	46	<2	<4	17	<2	66	2	
14	043	20	66	<1	70	<2	<4	1	<1	5,690	<2	<4	<2	5	7	2	<4	<2	28	<2		
15	045	6	356	<1	70	<2	34	9	10	464	<2	5	28	12	553	4	<4	16	6	425	4	
16	046	<2	673	2	<10	<2	88	3	<1	55	<2	14	58	2	54	<2	20	37	2	10	2	
17	047	<2	185	<1	<10	<2	<4	12	5	130	<2	<4	3	3	21	17	<4	<4	10	5	<2	
18	049	<2	338	3	<10	<2	120	1	<1	22	<2	14	57	3	98	<2	42	48	<2	10	3	
19	050	<2	34	1	<10	<2	61	<1	<1	6	<2	14	33	<2	19	<2	20	22	<2	<4	<2	
20	051	<2	262	1	40	<2	26	<1	<1	5	<2	9	16	3	31	5	6	10	<2	13	<2	
21	052	<2	30	1	<10	<2	56	<1	<1	3	<2	14	33	2	15	3	13	19	<2	<4	<2	
22	053	<2	20	2	<10	<2	86	<1	<1	7	<2	15	50	2	12	<2	11	29	<2	<4	<2	
23	054	<2	11	<1	<10	<2	24	<1	<1	2	<2	11	18	2	7	<2	5	13	<2	<4	<2	
24	055	<2	494	1	10	<2	115	4	1	218	<2	13	66	3	9	16	<4	44	<2	21	4	
25	056	6	220	1	30	<2	167	2	25	520	<2	17	78	6	55	<2	7	72	<2	15	13	
26	058	<2	23	2	<10	<2	99	<1	<1	15	<2	16	65	2	11	2	<4	36	<2	6	<2	
27	059	<2	371	3	<10	<2	152	<1	<1	6	<2	13	100	2	23	16	8	56	<2	10	2	
28	060	<2	27	2	<10	<2	115	<1	<1	23	<2	15	61	2	21	4	13	42	<2	<4	3	
29	061	178	125	<1	<10	<2	11	<1	<1	411	<2	4	7	6	44	17	<4	5	<2	6,060	<2	
30	062	13	29	<1	<10	<2	<4	1	1	2,120	<2	<4	<2	4	64	66	<4	<2	2,670	<2		
31	063	<2	485	2	<10	<2	137	2	<1	7	<2	14	76	4	80	<2	10	49	2	11	4	
32	065	<2	293	2	<10	<2	47	13	44	3	<2	12	28	18	385	<2	<4	17	19	21	4	
33	066	150	101	<1	250	8	24	9	9	1,830	<2	6	14	12	55	<2	<4	11	<2	3,070	5	
34	067	<2	114	2	<10	<2	137	30	67	192	<3	21	80	38	2,460	<2	11	61	37	55	16	
35	068	<2	690	2	<10	<2	101	13	28	62	<2	19	55	27	1,040	<2	12	48	11	32	16	
36	069	25	54	<1	20	14	7	6	2	969	<2	<4	4	11	14	<2	<4	<4	<2	6,100	<2	
37	070	33	<1	140	3	6	<1	464	5	1	<2	5	4	22	48	26	<4	4	<2	3,010	<2	
38	071	103	29	<1	210	4	6	1	1	1,070	<2	6	4	19	49	4	<4	<4	<2	1,960	<2	
39	072	4	86	1	<10	<2	44	12	20	65	<2	15	24	9	72	<2	4	19	7	177	10	
40	073	<2	757	2	<10	<2	132	<1	13	9	<2	29	70	8	77	22	<4	64	<2	19	10	
41	074	198	91	3	520	<2	13	23	73	96	2	<4	28	8	1,080	14	<4	36	36	5,810	7	
42	075	2	87	<1	<10	<2	42	4	<1	15	<2	<4	18	34	132	3	<4	31	2	29	<2	
43	076	<2	706	2	<10	<2	46	1	13	5	<2	37	28	13	104	69	4	21	3	8	10	
44	077	<2	606	2	<10	<2	61	<1	13	6	<2	37	35	11	72	24	4	25	<2	4	11	
45	078	<2	445	1	<10	<2	49	<1	22	3	<2	24	26	5	65	49	<4	23	<2	<4	9	
46	079	<2	269	3	<10	<2	66	7	11	30	<2	14	57	39	102	664	<4	14	18	56	7	
47	080	9	46	1	<10	<2	<4	<1	<1	41	<2	<4	<2	88	16	15	<4	4	65	<2		
48	081	4	65	2	<10	<2	14	1	2	101	<2	7	8	62	48	27	<4	7	<2	136	2	
49	082	57	59	2	30	13	8	<1	<1	175	<2	7	5	68	260	126	<4	5	<2	3,730	<2	
50	083	385	282	<1	60	18	<4	<1	<1	2,560	<2	<4	<2	19	14	11	<4	<2	4,800	<2		
51	084	15	91	<1	<10	<2	<4	<1	<1	162	<2	<4	2	41	18	5	<4	<4	<2	138	<2	
52	085	37	120	2	30	9	7	<1	<1	289	<2	7	4	21	455	7	<4	<4	<2	1,130	<2	
53	086	13	149	<1	<10	5	<4	<1	<1	99	<2	<4	<2	16	4,820	<2	<4	<4	<2	324	<2	
54	088	7	143	<1	20	4	5	1	1	632	<2	<4	3	9	2,620	<2	<4	<4	<2	60	<2	
55	089	7	115	2	140	<2	19	1	1	44	<2	<4	16	10	8	23	12	<4	7	<2	178	<2
56	090	<2	1,070	1	<10	2	8	2	<1	7	<2	5	9	3	5,640	4	<4	20	<2	224	<2	
57	091	<2	557	2	<10	<2	32	2	<1	5	<2	6	21	18	3,480	2	<4	24	6	123	<2	
58	092	407	459	3	<10	85	<4	1	1	4,690	<2	<4	3	112	57	112	<4	<2	20,100	<2		
59	093	7	393	6	200	<2	7	3	<1	20	<2	6	4	51	1,570	70	<4	5	221	<2		
60	094	30	46	1	<10	<2	<4	<1	<1	98	<2	<4	<2	89	36	56	<4	<4	539	<2		
61	096	593	63	<1	490	13	<4	3	1	12,800	<2	<4	2	12	10	39	8	<4	14	<2	12,500	<2

Analysis No.	Field No. 90TT	Inductively coupled plasma-atomic emission spectroscopy (total) (parts per million)							Inductively coupled plasma-atomic emission spectroscopy (partial) (parts per million)							Chemical Analyses (ppm; except Au, ppb)							
		Sn	Sr	Th	V	Y	Yb	Zn	Ag	As	Au	Bi	Cd	Cu	Mo	Pb	Sb	Zn	As	Hg	W	Au	
1	015	130	24	<4	47	20	1	141	87	--	--	360	--	25,000	--	72	--	28	16	.38	--	450	
2	016	40	20	<4	39	14	<1	117	130	--	--	920	--	45,000	--	88	46	15	7.8	.14	--	400	
3	019	10	32	<4	13	10	<1	1,540	14	46	--	73	7.7	10,000	--	14	7.9	1,300	37	.04	2	50	
4	020	430	32	<4	15	15	<1	792	2	52	--	51	3.1	2,400	1.3	--	--	720	39	--	--	26	
5	027	40	16	8	42	7	<1	378	0.86	--	--	--	.8	7,300	--	--	--	--	31	.04	2	24	
6	030	<10	54	5	168	<2	<1	82	--	22	--	--	--	170	--	1.1	--	1.6	26	--	--	<2	
7	031	<10	61	<4	<2	<2	<1	6	--	--	--	--	--	44.0	--	--	--	1.6	2.1	--	--	150	
8	032	<10	119	20	5	51	6	14	--	--	--	--	--	28.0	--	7.8	--	2.9	0.5	--	--	--	
9	035	<10	64	<4	41	<2	<1	44	--	13	--	--	--	230	--	--	--	8.8	30	--	--	--	
10	038	<10	62	<4	22	4	<1	54	16	--	--	270	1.2	12,000	2.6	79	11	44	1.2	8.6	--	450	
11	040	<10	135	37	3	8	2	3	--	--	--	--	--	9.1	--	6.8	--	0.6	--	--	--	2	
12	041	<10	94	<4	32	3	<1	13	5.8	--	--	--	--	680	13	25,000	8.3	--	2.4	.04	--	100	
13	042	<10	15	9	23	6	<1	16	6.5	15	--	9.7	--	1,800	--	42	--	9.4	13	.18	2	1,700	
14	043	<10	<10	<4	<2	<2	<1	9	18	9.3	--	76	--	6,300	1.5	35	16	6.4	15	.78	--	2,800	
15	045	<10	<10	<4	50	5	<1	14	5.8	--	22	74	--	510	4.1	490	--	7.5	8	.1	--	25,000	
16	046	<10	<10	31	5	25	3	8	--	--	--	--	--	51	2	6	--	1.4	0.3	--	--	--	
17	047	<10	<10	<4	115	<2	<1	24	--	--	--	--	--	140	18	6.6	--	22	1.6	.02	15	4	
18	049	<10	<10	29	5	55	6	12	--	--	--	--	--	21	--	--	--	3.4	0.5	--	--	--	
19	050	<10	<10	24	3	9	2	3	--	--	--	--	--	0.74	--	--	--	--	0.2	--	--	--	
20	051	<10	<10	4	12	<2	<1	9	--	--	--	41	--	--	4.2	--	--	--	0.4	--	2	28	
21	052	<10	<10	6	3	3	<1	<2	--	--	--	--	--	--	2.2	--	--	--	0.2	--	1	2	
22	053	<10	<10	39	3	13	2	<2	--	--	--	--	--	5.3	--	--	--	--	0.5	--	--	2	
23	054	<10	<10	20	3	5	1	2	--	--	--	--	--	--	--	--	--	<0.2	--	--	--	--	
24	055	<10	<10	17	23	<2	<1	7	--	--	--	6.4	--	210	15	7.8	--	--	1.8	.04	--	4	
25	056	<10	<10	6	138	4	<1	5	6.7	--	--	--	--	510	1.2	--	--	--	0.8	.16	7	6	
26	058	<10	<10	14	6	8	1	4	--	--	--	--	--	8.8	1.6	--	--	--	<0.2	--	--	--	
27	059	<10	<10	25	4	27	3	5	--	--	--	--	--	2.5	18	--	--	--	0.2	--	--	--	
28	060	<10	<10	19	7	15	2	9	--	--	--	--	--	18.0	3.4	--	--	--	0.3	--	--	--	
29	061	<10	<10	<4	5	<2	<1	51	200	--	1.7	--	1.9	490	18	8,100	--	40	1.5	.28	--	3,600	
30	062	<10	<10	<4	<2	<2	<1	9	10	--	--	--	.81	2,300	58	3,300	--	4	<0.2	.02	--	500	
31	063	<10	<10	24	19	19	3	9	--	--	--	--	--	0.92	--	11	--	5.6	0.7	--	--	--	
32	065	<10	<10	22	21	6	<1	45	--	--	--	--	--	1.7	--	22	--	41	1.1	--	--	2	
33	066	<10	<10	<4	16	3	<1	1,180	190	--	5.6	290	9.7	2,100	--	4,400	--	1,000	14	.34	--	7,600	
34	067	<10	<10	13	105	26	2	385	--	--	--	--	--	1.6	210	--	41	--	390	2.5	--	1	6
35	068	<10	<10	15	52	33	3	175	--	--	--	--	--	73	--	20	--	180	0.6	--	2	--	
36	069	<10	<10	<4	<2	<2	<1	1,910	26	--	--	18	17	1,100	--	8,100	--	1,800	3.2	.08	--	450	
37	070	<10	<10	<4	9	<2	<1	495	210	--	7.1	160	3	540	29	4,100	--	370	5.2	.28	--	5,100	
38	071	<10	<10	<4	9	<2	<1	1,220	110	11	2.3	240	5.2	1,200	3.7	2,600	--	1,200	13	.32	--	3,150	
39	072	<10	<10	9	39	5	<1	70	4.4	--	--	--	--	72	1.4	240	--	31	4.1	.02	--	100	
40	073	<10	28	29	47	16	<1	13	--	--	--	--	--	0.38	24	12	--	6.3	4	.02	4	2	
41	074	<10	125	<4	44	29	2	328	250	68	--	620	.78	110	16	9,600	--	300	50	.06	3	45	
42	075	<10	33	<4	3	121	9	13	0.55	6.7	--	--	--	13	2.7	21	--	6.8	6.6	.02	--	800	
43	076	<10	41	8	94	4	<1	8	--	--	--	--	--	2.8	66	--	--	--	0.4	--	4	--	
44	077	<10	64	7	104	5	<1	7	--	--	--	--	--	1.4	19	--	--	--	0.5	--	4	--	
45	078	<10	24	9	60	4	<1	6	--	--	--	--	--	53	--	--	--	--	0.5	--	3	--	
46	079	<10	849	9	155	8	1	64	--	22	--	--	--	32	730	63	--	70	23	.02	4	6	
47	080	<10	10	<4	9	<2	<1	55	2.4	96	--	--	--	37	13	83	--	52	78	.36	--	300	
48	081	<10	24	5	26	<2	<1	162	2.4	140	--	--	--	110	30	180	14	160	100	.32	4	150	
49	082	<10	17	<4	280	<2	<1	136	71	260	--	42	11	190	160	5,500	760	120	260	9	.38	50	
50	083	<10	15	<4	119	<2	<1	428	520	360	--	260	23	3,000	11	7,100	1,800	440	270	17.1	12	1,450	
51	084	<10	7	<4	11	<2	<1	15	12	--	--	--	1	160	4.5	160	160	8.9	13	1.2	3	4	
52	085	<10	49	<4	52	<2	<1	232	42	150	--	22	5.1	340	8.7	1,500	790	240	190	10.5	.56	100	
53	086	<10	14	4	5	2	<1	47	12	77	--	--	1.1	110	2.7	430	220	46	86	1	1,700	30	
54	088	<10	19	<4	6	3	<1	284	5.7	68	--	13	3.4	710	2	90	190	310	66	3.9	1,080	4	
55	089	<10	39	<4	41	<2	<1	68	2.1	27	--	130	--	44	8.8	220	110	65	26	1.2	13	12	
56	090	<10	422	<4	20	36	3	26	--	--	--	--	--	2.7	4.7	3.6	310	--	23	9.9	.12	67	2
57	091	<10	240	<4	16	24	2	18	--	--	--	--	--	1.5	3.8	2.5	170	--	14	8.7	.02	85	4
58	092	<10	76	<4	760	4	<1	663	500	760	1.9	41	96	--	5,400	180	29,000	4,700	530	490	>34	9	4,150
59	093	<10	30	<4	11	5	<1	91	12	--	--	210	.32	18	25	380	14	81	6.4	.28	28	54	
60	094	<10	9	<4	54	<2	<1	3,640	28	--	--	--	--	110	51	670	20	3,600	7.1	.26	8	50	
61	096	<10	196	<4	115	<2	<1	1,840	620	--	--	500	14	12,000	28	16,000	320	1,200	51	19.2	8	800	
62	100	<10	303	<4	56	19	2	77	0.62	150	--	--	--	33	--	660	--	87	110	.04	--	2	
63	101	<10	660	<4	54	8	<1	48	--	--	--	--	--	5.4	--	10	--	51	2	.04	--	--	
64	102	<10	468	<4	65	10	1	60	2.1	--	--	8.8	.35	8,500	--	190	--	64	5.4	.08	1	4,050	
65	103	<10	333	<4	58	6	<1	51	--	9.2	--	--	--	1,000	--	330	--	54	18	--	--	300	
66	104	<10	<10	<4	17	<2	<1	9	12	--	13	--	--	29	1	240	--	--</					

Table 5. Descriptions of select rock samples collected from some East Mojave National Scenic Area, California  
 [Diop, diopside; trem, tremolite; mal, malachite; py, pyrite; px, pyroxene; sph, sphalerite; qtz, quartz; cp, chalcopyrite; mag, magnetic; gn, galena; hm, hematite; cc, calcite; bx, breccia; cov, covellite; chrys, chrysocolla; bio, biotite; chl, chlorite; wm, white mica; pg, plagioclase; wolf, wolframite; epi, epidote; fs, feldspar; kfs, K-feldspar; asp, arsenopyrite]

Analysis No. (Same as table 4)	Field No. (90TT...)	Location	Latitude	Longitude	Description	
1	015	Evening Star Mine	35°21'39"	115°32'32"	Massive diop skarn retrograded to trem; two generations diop; mal and iron oxidized after py.	
2	016	Do.	Do.	Do.	Do.	
3	019	Do.	Do.	Do.	Px hfs developed in sulfidized marble.	
4	020	Do.	Do.	Do.	Calc-silicate hfs, trem and sph, replacement of marble.	
5	027	Copper King Mine	35°21'06"	115°32'38"	Cp-mag skarn, includes retrograde chl and zois.	
6	030	Vulcan Mine	34°55'23.91"	115°33'54.75"	Mag skarn, py-bearing.	
7	031	Do.	Do.	Do.	Marble, less than 0.5 m from skarn front.	
8	032	Do.	Do.	Do.	Mag skarn, py-bearing.	
9	035	Do.	Do.	Do.	Mag skarn.	
10	038	Big Horn Mine	34°50'28.7"	115°32'24.76"	Qtz-cp-py vein; late stage cc fills fractures.	
11	040	Do.	34°50'32.10"	115°32'23.47"	Rhyolite breccia.	
12	041	Do.	Do.	Do.	Qtz-gn-cp veins; multiple qtz generations.	
13	042	Do.	34°48'28.66"	115°32'42.36"	Qtz-cp <th>hm veins; comb qtz, open-cavity fillings.</th>	hm veins; comb qtz, open-cavity fillings.
14	043	Do.	34°48'32.5"	115°32'55.21"	Qtz-cp-base metal veins.	
15	045	Do.	34°48'41.71"	115°32'50.74"	Qtz-py (trace)-cc along fault; sparse wm.	
16	046	Vic. Quail Spring Wash	34°49'46.92"	115°33'40.97"	—	
17	047	Do.	34°49'55.33"	115°33'40.44"	Qtz-py veins associated with syenogranite of Quail Spring (Miller and others, 1985).	
18	049	Do.	34°50'2.77"	115°33'31.91"	Syenogranite of Quail Spring.	
19	050	Do.	34°49'59.83"	115°33'24.36"	Do.	
20	051	Do.	34°49'50.09"	115°33'17.02"	Qtz-py vein; brick red associated iron oxide(s).	
21	052	Do.	34°49'40.45"	115°33'19.18"	Py along east-west fractures in syenogranite of Quail Spring.	
22	053	Do.	54°49'38.12"	115°33'26.16"	Clay-altered syenogranite of Quail Spring.	
23	054	Do.	34°49'38.71"	115°33'30.97"	Syenogranite of Quail Spring.	
24	055	Do.	34°48'59.95"	115°33'11.59"	Fault bx, abundant gossan.	
25	056	Do.	—	—	Iron-oxide-stained metavolcanic.	

26	Do.	34°49'40.48"	115°33'54.7"	
27	Do.	Do.	Do.	
28	Do.	Do.	Do.	
29	Okaw Mine	35°2'45.22"	115°33'12.74"	Porphyritic felsite dike. Hornblende-biotite monzodiorite.
30	Do.	35°2'41.61"	115°33'5.21"	Do.
31	Do.	35°2'42.48"	115°33'1.13"	Qtz-gn-cp-py vein; secondary cov. Qtz-gn-cp vein; secondary chrys.
32	Globe Canyon	35°3'6.75"	115°31'00"	Porphyritic leucogranite dike; primary bio altered
33	South Star Mine	35°3'5.42"	115°29'33.69"	to chl, spare w m alteration of pg.
34	Do.	Do.	Do.	Fault bx and gossan.
35	Do.	Do.	Do.	Qtz-py vein, including some w m.
36	Do.	35°3'6.65"	115°29'31.44"	Qtz-cc veined and chl-altered dacite(?) dike.
37	S.S. nos. 17-19, north	35°3'6.78"	115°29'46.97"	Qtz-py vein.
38	Do.	Do.	Do.	Qtz-py veins; brecciated, multiple
39	South Star Mine	35°3'12.89"	115°29'33.7"	generations of qtz.
40	S.S. no. 17	35°2'58.16"	115°29'55.04"	Fault bx; silicified.
41	Globe Mine	35°2'39.9"	115°29'8.23"	Gossan; along fault breccia.
42	Do.	Do.	Do.	Qtz vein; py impregnated, abundant brick-red
43	S.S. no. 17	35°2'58.16"	115°29'55.04"	iron oxide.
44	Do.	Do.	Do.	Qtz-vein massive outcrop, sericitically altered
45	Do.	Do.	Do.	granitoid fragments.
46	Do.	Do.	Do.	Gossan reddish orange-brown.
47	Tungsten Flat	35°3'23.46"	115°2'50.74"	Qtz-fluorite-py vein; abundant gossan.
48	Do.	Do.	Do.	Qtz-wm-altered bio granite.
49	Do.	35°3'8.76"	115°2'50.41"	Do; heavily qtz-veined and iron oxide-stained.
50	Do.	35°3'8.76"	115°2'45.32"	Gossan; brick red to brownish maroon.
51	Do.	35°3'8.96"	115°2'37.23"	Qtz-py vein; moderate amounts fine-grained w m.
52	Do.	35°2'53.85"	115°2'44.68"	Gossan; ochre.
53	Do.	35°2'55.76"	115°2'49.63"	Qtz-py-stibiconite (trace) gn vein.
54	Do.	35°2'47.19"	115°2'48.08"	Do; includes some secondary chrys.
55	Do.	35°2'42.33"	115°2'31.1"	Qtz-py veins.
56	Do.	35°2'30.43"	115°2'40.8"	Do.
57	Do.	35°2'11.66"	115°2'47.39"	Qtz-wolf-gn (tr)-stibiconite (tr)-py vein.
58	Do.	Do.	Do.	Do.
				Manganiferous cc vein; coarsely crystalline;
				streaked with iron oxide.
				Qtz-manganiferous cc vein.
				Qtz-chrys-grn-stibiconite vein; coarsely
				crystalline qtz.

59	093	Do.	35°2'7.33"	115°2'54.81"	crystalline qtz.
60	094	Do.	35°2'10.23"	115°2'55.87"	Gossan; reddish-brown.
61	096	Leiser Rag Mine	35°1'33.22"	115°2'13.67"	Qtz-sph vein; multiple generations qtz. Qtz-cp-gn-sph vein; brecciated; multiple generations qtz.
62	100	True Blue Mine	35°5'2.04"	115°9'6.47"	Qtz vein; cuts chloritized gneissic granite; wm and epi alteration.
63	101	Do.	Do.	Do.	Chloritized gneissic granite; relict bio; phyllonitic, strained fs porphyroclasts. Qtz-chrys veins; open-cavity fillings. Qtz-py-cp (trace) vein; some secondary Mn-bearing minerals.
64	102	Do.	35°4'54.14"	115°8'57.37"	Qtz-py-gn (trace) vein.
65	103	Do.	Do.	Do.	Qtz-kf <sub>2</sub> iron oxide (trace) vein; locally mylonitic fabric.
66	104	American Flag	35°4'35.89"	115°7'27.84"	Gossan; ochre to maroon; narrow seams in granite.
67	105	Rattlesnake Mine	35°6'7.72"	115°4'48.12"	Silicified fault zone.
68	106	Do.	35°5'50.12"	115°4'51.82"	Qtz-py vein.
69	107	Do.	35°5'40.93"	115°50.37"	Silicified granite; clay altered.
70	108	Do.	35°5'43.83"	115°57.71"	Sulfidized (gn, asp, sph) shear zone;
71	109	Do.	35°5'39.74"	115°455.97"	oxidized; some vein qtz.
72	110	Mohawk Mine	35°28'43"	115°3701"	Oxidized gn, asp, and sph in vein qtz; some cp and py.
73	113	Do.	Do.	Do.	Gar-px skarn; late-stage wm and qtz.
74	115	Do.	35°30'20.49"	115°36'9.78"	Gossan.
75	118	Copper World Mine	35°31'23.8"	115°38'34.02"	Qtz-py (altered to buff-colored vein oxide)
76	128	Conquistador No. 2			vein; chl- and wm-altered fragments
77	130	Emperor Mine	35°31'26.25"	115°37'51.45"	Gn-sph-cc along fault zone.
78	131	Do.	Do.	Do.	Do.

Table 6. Geochemical statistics for selected elements in samples of stream sediment, heavy-mineral concentrate, rock, and soil from the East Mojave National Scenic Area and surrounding area from 34°30' to 35°45' North latitude and 114°45' to 116°15' West longitude, California and Nevada

[Concentrations in RASS and PLUTO samples determined by emission spectrographic methods; concentrations in NURE samples determined by neutron activation. Ppm, parts per million; 50th percentile, concentrations in one-half of samples are equal to or lower than this number; N, not detected at lower limit of determination; G, greater than upper limit of determination; L, detected below lower limit of determination; <, less than value shown or less than lower limit of determination if no value shown; >, greater than value shown; ---, no data. Threshold: PM, Providence Mountains Wilderness Study Area (Goldfarb and others, 1988, table 3); SPM, South Providence Mountains Wilderness Study Area (Miller and others, 1985, tables 1,2)]

Element	Limits of determination (ppm)		Concentration (ppm)					Number of samples analyzed	Number of anomalous samples		
	Lower	Upper	Minimum	Maximum	50 th percentile	Threshold					
					This study	PM	SPM				
RASS and PLUTO stream sediment (figs. 26, 31, 34) <sup>a,b</sup>											
Silver (Ag)	0.5-1	5,000	N	>20	<0.5	0.7	---	<0.5	368	22	
Boron (B)	5-10	2,000	N	>100	10	50	---	---	368	16	
Barium (Ba)	20	5,000	70	5,000	700	1,500	---	---	368	11	
Beryllium (Be)	1-5	1,000	N	15	2	7	---	---	368	7	
Cobalt (Co)	1-5	2,000	L	100	10	30	---	---	368	30	
Copper (Cu)	2-5	20,000	<5	1,200	20	70	---	100	368	18	
Manganese (Mn)	50	5,000	<50	7,000	700	2,000	---	---	368	17	
Molybdenum (Mo)	1-5	2,000	N	100	3	10	---	---	368	54	
Lead (Pb)	5-10	20,000	N	5,000	20	7C	---	---	368	22	
Tin (Sn)	2-10	1,000	N	30	<5	<10	---	---	368	15	
Tungsten (W)	20-100	10,000	N	70	<50	<50	---	---	368	5	
Zinc (Zn)	5-200	10,000	N	7,000	50	N(200) or 100	---	---	367	78	
RASS nonmagnetic heavy-mineral concentrates (figs. 27, 29, 32, 35, 37)											
Silver (Ag)	1	10,000	N	1,000	N	L	L	3	498	69	
Arsenic (As)	500	20,000	N	3,000	N	N	N	---	498	3	
Gold (Au)	20	1,000	N	G	N	N	N	N	498	11	
Boron (B)	20	5,000	N	700	20	70	---	---	498	28	
Barium (Ba)	50	10,000	N	G	1,000	5,000	7,000	3,000	498	102	
Beryllium (Be)	2	2,000	N	200	L	3	---	---	498	23	
Bismuth (Bi)	20	2,000	N	G	N	N	N	30	498	34	
Cobalt (Co)	10-20	5,000	N	300	N	15	---	---	498	39	
Copper (Cu)	10	50,000	N	10,000	N	70	30	70	498	39	
Lanthanum (La)	50-100	2,000	N	G	300	1,500	---	---	498	15	
Manganese (Mn)	20	10,000	N	10,000	500	1,000	---	---	498	45	
Molybdenum (Mo)	10	5,000	N	5,000	N	10	150	N	498	77	
Niobium (Nb)	50	5,000	N	700	L	150	---	---	498	19	
Lead (Pb)	20	50,000	N	G	70	700	1,500	100	498	92	
Antimony (Sb)	200	20,000	N	3,000	N	N	N	---	498	9	
Tin (Sn)	20	2,000	N	2,000	N	30	---	---	498	87	
Thorium (Th)	200	5,000	N	G	L	2,000	---	---	480	26	
Tungsten (W)	50-100	20,000	N	10,000	N	100	300	---	498	83	
Zinc (Zn)	500	20,000	N	G	N	N	N	---	498	19	

Table 6. Geochemical statistics for selected elements in samples of stream sediment, heavy-mineral concentrate, rock, and soil from the East Mojave National Scenic Area and surrounding area from 34°30' to 35°45' North latitude and 114°45' to 116°15' West longitude, California and Nevada--Continued.

Element	Limits of determination (ppm)		Concentration (ppm)				Threshold		Number of samples analyzed	Number of anomalous samples
	Lower	Upper	Minimum	Maximum	50 th percentile	This study	PM	SPM		
PLUTO heavy-mineral concentrates (figs. 27, 29, 32, 35, 37) <sup>c</sup>										
Silver (Ag)	1	---	<1	70	<1	1.5	---	---	262	58
Gold (Au)	20	---	<10	20	<10	10	---	---	262	3
Boron (B)	20	---	<10	>200	50	100	---	---	262	18
Barium (Ba)	2	---	100	>10,000	700	1,500	---	---	262	25
Beryllium (Be)	1	---	<2	70	3	7	---	---	262	15
Bismuth (Bi)	10	---	<20	200	<20	<d	---	---	262	22
Cobalt (Co)	5	---	3	200	50	70	---	---	262	33
Copper (Cu)	1	---	3	7,000	70	100	---	---	262	51
Lanthanum (La)	20	---	20	>2,000	500	1,500	---	---	262	39
Manganese (Mn)	2	---	200	>20,000	3,000	10,000	---	---	262	21
Molybdenum (Mo)	5	---	<2	300	15	20	---	---	262	63
Niobium (Nb)	10	---	5	3,000	150	700	---	---	262	9
Lead (Pb)	10	---	<5	2,000	70	300	---	---	262	17
Tin (Sn)	10	---	<5	>10,000	10	20	---	---	262	39
Thorium (Th)	200	---	<500	3,000	<500	500	---	---	262	19
Tungsten (W)	100	---	<100	2,000	<100	<d	---	---	262	9
Zinc (Zn)	200	---	30	5,000	200	300	---	---	262	53
PLUTO heavy-mineral concentrates (figs. 40, 43)										
Cerium (Ce)	200 <sup>c</sup>	---	<200	10,000	700	2,000	---	---	262	29
Dysprosium (Dy)	50 <sup>c</sup>	---	<20	1,000	<20	<d	---	---	262	20
Europium (Eu)	2-15 <sup>e</sup>	---	<2	100	10	30	---	---	262	10
Neodymium (Nd)	100 <sup>c</sup>	---	<100	>2,000	300	1,000	---	---	262	26
Samarium (Sm)	100 <sup>c</sup>	---	<100	1,000	100	200	---	---	262	21
Terbium (Tb)	50 <sup>e</sup>	---	<50	300	<50	<50	---	---	262	35
Ytterbium (Yb)	5 <sup>c</sup>	---	1.5	700	30	100	---	---	262	21
RASS and PLUTO rocks (figs. 28, 30, 33, 36, 38) <sup>a,b</sup>										
Silver (Ag)	0.5-1	5,000	N	1,000	<0.5	0.7	---	---	943	249
Arsenic (As)	100-500	10,000	N	G	<700	<d	---	---	943	19
Gold (Au)	5-10	500	N	150	<15	<d	---	---	943	21
Boron (B)	2-10	2,000	N	500	<10	20	---	---	937	111
Barium (Ba)	2-30	5,000	N	G	300	1,500	---	---	943	80
Beryllium (Be)	1-5	1,000	N	150	1	5	---	---	944	30
Bismuth (Bi)	10-20	1,000	N	3,000	<10	<d	---	---	944	107
Cobalt (Co)	0.5-10	2,000	N	1,000	5	30	---	---	944	85
Copper (Cu)	0.2-5	20,000	N	G	15	100	---	---	944	203
Lanthanum (La)	5-30	1,000	N	1,000	30	150	---	---	944	29
Manganese (Mn)	10	5,000	N	G	300	2,000	---	---	943	53
Molybdenum (Mo)	1-10	2,000	N	2,000	<5	7	---	---	942	125
Niobium (Nb)	5-20	2,000	N	100	<20	30	---	---	944	11
Lead (Pb)	3-10	20,000	N	G	20	50	---	---	944	233
Antimony (SB)	20-100	10,000	N	7,000	<100	<d	---	---	944	27
Tin (Sn)	5-10	1,000	N	G	<10	<d	---	---	933	34

Table 6. Geochemical statistics for selected elements in samples of stream sediment, heavy-mineral concentrate, rock, and soil from the East Mojave National Scenic Area and surrounding area from 34°30' to 35°45' North latitude and 114°45' to 116°15' West longitude, California and Nevada--Continued.

Element	Limits of determination (ppm)		Concentration (ppm)					Number of samples analyzed	Numbers of anomalous samples	
	Lower	Upper	Minimum	Maximum	50 th percentile	This study	Threshold PM			
RASS and PLUTO rocks (figs. 28, 30, 33, 36, 38) <sup>a,b</sup> --Continued										
Thorium (Th)	100-500	2,000	N	300	<200	<d	---	---	944	3
Tungsten (W)	20-100	10,000	N	5,000	<50	<d	---	---	944	46
Zinc (Zn)	5-200	10,000	N	G	<200	N(200) or 100	---	---	944	176
PLUTO rocks (figs. 41, 44) <sup>c</sup>										
Cerium (Ce)	200 <sup>c</sup>	---	<20	300	70	150	---	---	155	8
Dysprosium (Dy)	50 <sup>c</sup>	---	<10	20	<10	<d	---	---	155	11
Europium (Eu)	1-2 <sup>e</sup>	---	<1	5	2	3	---	---	155	9
Neodymium (Nd)	100 <sup>c</sup>	---	<50	150	<100	70	---	---	155	14
Terbium (Tb)	20-50 <sup>c</sup>	---	<20	30	<20	<d	---	---	155	10
Ytterbium (Yb)	5 <sup>c</sup>	---	<0.5	10	1	3	---	---	155	6
NURE stream-sediment and soil (figs. 39, 42, 45) <sup>e</sup>										
Cerium (Ce)	10-20	---	<10	930	70	169	---	---	1,136	61
Dysprosium (Dy)	0.1-3.8	---	<1	45	2.7	7.9	---	---	911	85
Europium (Eu)	0.1-3	---	<0.1	7.6	0.6	1.6	---	---	1,009	169
Lanthanum (La)	1-20	---	<1	1,900	36	169	---	---	1,157	108
Lutetium (Lu)	0.1-0.6	---	<0.1	7.8	0.4	1.1	---	---	804	34
Samarium (Sm)	1-2	---	<1	130	6	16	---	---	963	48
Terbium (Tb)	---	---	0.13	2.3	0.9	1.6	---	---	28	3
Thorium (Th)	2	---	<2	320	13	39	---	---	1,153	67
Uranium (U)	---	---	0.10	30	2.4	5.9	---	---	1,259	42
Ytterbium (Yb)	1-2	---	<1	55	1.8	5.9	---	---	942	52

<sup>a</sup>Variable lower limits of determination

<sup>b</sup>Upper limits are the customary ones for RASS samples

<sup>c</sup>Lower limits from Myers and others, 1961, table 2

<sup>d</sup>Variable lower limits of determination; any detectable concentration is anomalous

<sup>e</sup>Lower limits are from the data

Table 7. Summary of geochemical anomalies in the East Mojave National Scenic Area, California

[NS, no samples. Based on emission spectrographic analyses of RASS and PLUTO samples and neutron activation analyses of NURE samples. Determination of whether or not an area is geochemically anomalous with respect to a given element is based on (1) presence and proportion of samples with anomalous concentrations, (2) proportion of samples with high, but not necessarily anomalous concentrations, and (3) comparison of area with the entire East Mojave National Scenic Area and surrounding area from latitude 34°30' to 35°45' and longitude 114°45' to 116°15']

Area on figure 23	Sample type and data base				
	RASS and PLUTO stream sediment	RASS concentrate	PLUTO concentrate	RASS and PLUTO rock	NURE stream sediment and soil
Soda Mountains	Zn, Sn, B, Mo	NS	Cu, Mn, Pb, Ag, Zn, Au, Bi, Sn, Mo, Be, Th, Nb, La, Ce, Tb, Yb, Dy	NS	Eu, Lu
Little Cowhole Mountain		NS	Cu, Bi, Sn, Mo, Be, Th, Tb	NS	
Cowhole Mountain		NS	Mo	NS	
Cinder Cone	Zn, Mo, Co, B	Mn, Co, Sn, Mo, B, Th, Nb	Cu, Mn, Ag, Zn, Bi, Sn, Mo, Be, B, Th, Tb, Yb	Cu, Pb, Ag, Zn, As, Sb, Mn, Bi, Sn, Mo, W	Th, Ce, Eu
Marl Mountains	Pb, Ag, Zn, Mo	NS	Cu, Ag, Zn, Au, Bi, Sn, Mo, Th, La, Ce, Nd, Sm, Tb, Yb, Dy	NS	Th, La, Eu, Dy
Old Dad Mountain		Cu, Pb, Ag, Bi, Sn, Th	Tb	Cu, Pb, Zn, Ag, Au, Cd, Bi, Mo, B, Be	Eu
Kelso Mountains		NS	Cu, Ag, Au, W, La, Ce, Nd, Sm, Tb, Dy	NS	La, Dy
Bristol Mountains	Mn, Pb, Zn, Sn, Mo, B	NS	Cu, Mn, Ag, Zn, Sn, Be, Nb, La, Nd, Sm, Eu, Yb, Dy	NS	Yb, Eu
Clark Mountain Range	Pb, Ag, Zn, Be, Sb	Cu, Pb, Ag, Zn, As, Sb, Ba, Bi, Sn, Mo, W, B, Th, Nb, La	Cu, Pb, Ag, Co, Ba, W, Be, Th, La, Ce, Nd, Sm, Eu, Tb, Nb	Ag, Sn, Mo, W, Be	Th, La, Ce, Lu, Sm, Yb, Dy
Mescal Range		NS	Pb, Zn, Tb	NS	
Ivanpah Mountains	Cu, Ag, Zn, Mo, Sn, W	Cu, Pb, Ag, Au, Bi, Mn, Co, Sn, Mo, W, Th, La	Cu, Mn, Pb, Ag, Co, Mo, W, Be, Th, La, Ce, Nd, Sm, Tb, Dy	Mn, Pb, Ag, As, Sb, Cu, Zn, Co, Ba, Bi, Sn, Mo, Be, B	Th, U, La, Ce, Lu, Sm, Eu, Tb, Yb, Dy
Cima Dome	NS	NS	NS	Tb	NS

Table 7. Summary of geochemical anomalies in the East Mojave National Scenic Area, California--Continued

Area on figure 23	Sample type and data base					
	RASS and PLUTO stream sediment	RASS concentrate	PLUTO concentrate	RASS and PLUTO rock	NURE stream sediment and soil	
New York Mountains	Cu, Mn, Pb, Ag, Zn, Co, Mo, W, B, Be	Cu, Pb, Zn, Ba, Mn, Ag, Co, B, Sn, Mo, W	Cu, Mn, Pb, Ag, Zn, Co, Ba, Bi, Sn, Mo, W, Be, B, Th, Nb, La, Ce, Nd, Sm, Eu, Tb, Yb, Dy	Cu, Pb, Ag, Zn, Au, As, Co, Sb, Ba, Bi, Sn, B, La, Mo	Th, U, La, Ce, Lu, Eu	Yb
Mid Hills	Zn, Mo, Be, B	Mn, Bi, Mo, W, B, Th, Nb	Ag, Ba, Bi, Th, La, Ce, Nd	Cu, Mn, Pb, Ag, As, Ba, Co, Bi, Sn, W, Mo	Ce	
Providence Mountains	Cu, Mn, Pb, Ag, Zn, Co, Ba, Sn, Mo, Bi, B	Cu, Mn, Pb, Ag, Zn, Co, Bi, Sn, Mo, Au, As, Co, Sb, Ba, Bi, Sn, Mo, W, B, Th, Nb, La	Cu, Pb, Ag, Zn, Co, Bi, Sn, Mo, W, Th, La, Ce, Nd, Sm, Eu, Tb	Cu, Mn, Pb, Ag, Zn, Au, Co, As, Sp, Ba, Bi, Sn, Mo, W, Be, B, Th, Nb, Nd, Eu, Tb	Th, U, La, Lu	Sm, Eu, Yb, Dy, Ce
Granite Mountains						Yb, Dy, La, Ce
Van Winkle Mountain	NS	NS	NS	NS	Cu, Mn, Ag, Zn, Ba, Co, Bi, Mo, B, Nb, Ge, Nd, Tb, Yb, Dy, Ce, As, Pb, Sn	La, Sm, Eu
Grotto Hills	Ag, Zn, Mo	NS	Cu, Mn, Zn, Co, Mo	NS	Cu, Mn, Ag, Zn, Ba, Co, Bi, Mo, B, Nb, Ge, Nd, Tb, Yb, Dy, Ce, As, Pb, Sn	La
Pinto Mountain		NS	Mo	NS		
Table Mountain	Zn, Mo	NS	Ag	NS		
Woods Mountains			Ag, La	NS		
Hackberry Mountain	Ba	NS	Mn, Ag, Zn, Ba, Mo	NS		
VonTrigger Hills		NS	Cu, Mn, Ag, Zn, Ba, Mo, Nb, La, Ce, Yb	Cu, Mn, Pb, Zn, Ag, As, Sb, Bi, Mo, Bc, B, Nb	Eu	
Piute Range	Zn, Co, Mo, Be, B	Cu, Pb, Zn, Ag, Ba, B, Bi, Sn, Mo, W, Be, La	Ag, Ba, Mo, La, Sm, Tb	Cu, Pb, Ag, Zn, Au, Sb, Bi, Mo, W, Be	La, Cc, Lu, Sm, Eu, Yb, Dy, Th	
Castle Mountains	Mn, Pb, Zn, Co, Mo	Cu, Ba, Mn, Co	Cu, Mn, Zn, Co, Ba, Bi, Mo, B, Th, La, Ce, Nd, Sm, Eu, Yb, Dy	Mn, Ag, Pb, Sb, Ba, Mo, Be, Nb, Tb, B, Ce, Eu	Dy, Eu	
Homer Mountain	Ag, Zn, Mo, Be, B	NS	Zn, Sn, Mo	Nb		Eu, Dy

Table 8. Types and number of mineral occurrences identified as being present in the East Mojave National Scenic Area as of February, 1991  
[--, not available]

U.S. Geological Survey Model <sup>2</sup>				Example of typical deposit or occurrence <sup>1</sup>		
Name	Model no.	Number identified <sup>3</sup>	Name	Principal commodities		
				Amount <sup>4</sup>	Type	Additional elements present
Carbonatite, rare-earth element	10	5	Esperanza Group	--	Ce, La, Sm	U, Th
Polymetallic vein	22c	206	Morningstar	480,000 oz (M)	Au	Ag, Pb, Zn, Cu
Low sulfide, Au-quartz vein	36a	5	Conquistador No. 2	--	Au	--
Polymetallic replacement	19a	23	Iron Horse	400 tons ore (M)	Pb, Zn	Fe, Cu, Au, Ag
Distal disseminated Au-Ag	--	1	Unnamed prospect	--	Au, Ag	Zn
Au breccia pipe	--	2	Colosseum	10,500,000 tons ore	Au, Ag	Cu, Pb, Zn
Ag-Cu brecciated dolostone	--	25	Beatrice Mine	--	Ag, Cu	Au, V
Fluorite vein	--	16	Pacific Fluorite	--	F	Sb, Ag, Pb, Zn
Tungsten vein	15a	18	Mojave Tungsten	38,400 lb (M)	WO <sub>3</sub>	Ba, F
Au-Ag, quartz-pyrite vein <sup>5</sup>	--	80	Little Dove	--	Au, Ag	--
Polymetallic fault	--	79	Billy Boy	--	Au	Zn, Cu, Ag
Polymetallic skarn	--	18	Copper Commander	--	Cu, Pb, Zn	Au, Sb, As, Ag
Zn-Pb skarn	18c	6	Mohawk Mine area	1,793,422 lb (M)	Zn	Cu, Pb, Ag, As
W skarn	14a	3	Silverado-Tungstate	Small tonnage (M)	W	Au, Ag, Cu, Pb, Zn
Fe skarn	18d	10	Vulcan	2,643,000 tons ore (M)	Fe	--
Sn (W) skarn	14b	1	Evening Star Tin	3,200 lb (M)	Sn	W, Au, Ag, Zn, Cu
Cu Skarn	18b	26	Copper World	5,321,184 lb (M)	Cu	Pb, Ag, Au, Zn
Vein barite	--	6	Susan's Peak	--	Ba	--
Vein magnesite	--	1	New Trail Magnesite	~300 tons ore (M)	Mg	--
Porphyry Mo, low F	21b	3	Big Hunch	800,000,000 lbs MoS <sub>2</sub>	Mo	Ag
Epithermal qtz-adularia (alunite) (Au)	25e	11	Castle Mountains (Hart)	2,020,000 oz	Au	Ag
Placer Au-PGE <sup>6</sup>	39a	34	Terry	--	Au	--
Placer Fe±Ti	--	2	Kelso Dunes	1,000 tons Fe <sub>3</sub> O <sub>4</sub> (M)	Fe	Ti, Au

<sup>1</sup>Additional mineral occurrences, by type, in EMNSA include sand and gravel (4), cinder (3), sandstone (1), marble (3), slate (1), limestone (6), dolomite (4), graphite (1), talc (1), mica (2), gemstone (1), decorative and dimension stone (5), silica (1), pyrophyllite (1), clay (9), perlite (3), and pumice (2). Numbers of occurrences shown parenthetically.

<sup>2</sup>Numbered models from Cox and Singer (1986); others from geologic literature (see text).

<sup>3</sup>Occurrence types assigned provisionally in this report to 587 of 701 occurrences reported in EMNSA by U.S. Bureau of Mines (1990a, table 2). Small number of localities assigned more than one deposit type.

<sup>4</sup>Contained metal or ore in place prior to onset of mining; (M), amount of metal or ore mined.

<sup>5</sup>Mostly Mesozoic in age, but includes some Tertiary, gold-silver vein occurrences, exemplified by the Telegraph Mine, that are epithermal and apparently related to wrench-style tectonics (see Lange, 1988).

<sup>6</sup>PGE (platinum group elements) retained in name of model type to maintain consistency with previous usage by Cox and Singer (1986). However, presence of PGE elements apparently has not been established in placers of EMNSA (U.S. Bureau of Mines, 1990a). Of 34 apparent placer Au-PGE occurrences in EMNSA, field examinations (U.S. Bureau of Mines, 1990a) indicate presence of visible, alluvial free gold at only nine localities and production from placers at no localities.

Table 9. Summary statistics for 20 elements in 1,050 samples of rock analyzed from the East Mojave National Scenic Area [From U.S. Bureau of Mines, 1990, tables 2A, B; in ppm, except Au and Fe, which are in ppb and weight percent, respectively; --, not applicable]

Total No. of undetermined concentrations	"Less-than" concentrations		"Greater-than" concentrations		Data matrix including substituted values					Log-transformed data			
	No.	Value substituted (ppm)	No.	Value substituted	Min.	Max.	Mean	Geometric mean	50th percentile	Mode	Standard deviation	Kurtosis	Skewness
Au <sup>2</sup>	253	253	1.0 ppb	0	--	1.0	51,700	973	20.5	1.0	3,380	-0.778	0.456
Ag	481	481	1	0	--	1	3,080	70.6	6.1	1	238	-.387	.883
As	24	23	.5	1	10,000	.5	120,000	664	22.5	.5	4,790	-.453	.811
Ba	369	369	25	0	--	25	184,000	1,150	151	25	8,900	.478	.598
Ce	402	402	2.5	0	--	2.5	7,200	51.3	14.4	17	2.5	268	-1.13
Co	642	642	2.5	0	--	2.5	859	20	6	2.5	66.8	1.28	1.36
Cr	209	209	10	0	--	10	3,990	181	99.5	160	10	2.8	-.661
Cs	549	549	.5	0	--	.5	138	2.6	.5	.5	6.2	.113	1.01
Fe <sup>3</sup>	83	83	.1 (%)	0	--	.1	62	4.9	2	.1	8	-.185	-.209
La	181	181	1	0	--	1	52,600	71.1	8.8	10	1	1,620	.444
Mo	376	376	.5	0	--	.5	2,080	34.3	4	3	.5	135	-.618
Ni	801	801	5	0	--	.5	560	15.7	7.8	.5	39	3.63	2.04
Sb	18	18	.05	0	--	.05	122,000	346	5.9	3.2	.2	3,890	-.249
Sc	185	185	.1	0	--	.1	123	4.2	1.4	1.8	.1	7.4	.647
Sm	91	91	.05	0	--	.05	6,360	9.5	1.3	1.7	.05	196	.161
Ta	687	687	.25	0	--	.25	10	.6	.42	.25	.9	.887	1.34
Th	154	154	.1	0	--	.1	26,300	40.3	2.6	3.5	.1	22	-.054
U	69	69	.1	0	--	.1	1,590	9.3	2.7	3.1	.1	70	1.06
W	256	256	.5	0	--	.5	165,000	93	5.2	4	.5	6,050	1.74
Zn	477	477	.50	0	--	.50	325,000	4,080	254	130	.50	17,400	.608

<sup>1</sup>Substituted values are 50 percent of the minimum detection limit.

<sup>2</sup>Concentration values in parts per billion (ppb).

<sup>3</sup>Concentrations values in weight percent.

Table 10. Array of Spearman correlation coefficients for 1,050 rock samples from the East Mojave National Scenic Area  
 [Calculated from data in U.S. Bureau of Mines (1990)]

	Log (Au)	Log (Ag)	Log (As)	Log (Ba)	Log (Cc)	Log (Co)	Log (Cr)	Log (Cs)	Log (Fc)	Log (La)	Log (Mo)	Log (Ni)	Log (Sb)	Log (Se)	Log (Sm)	Log (Th)	Log (U)	Log (W)	Log (Zn)
Log (Au)	1.0																		
Log (Ag)	.323	1.0																	
Log (As)	.136	.485	1.0																
Log (Ba)	-.139	-.349	-.285	1.0															
Log (Cc)	-.152	-.473	-.341	.614	1.0														
Log (Co)	.241	.01	.046	.089	.108	1.0													
Log (Cr)	.177	-.218	-.343	.222	.15	-.016	1.0												
Log (Cs)	-.181	-.305	-.092	.519	.54	.156	-.012	1.0											
Log (Fe)	.319	.013	.167	.133	.149	.691	.019	.14	1.0										
Log (La)	-.101	-.345	-.221	.627	.883	.147	.085	.525	.22	1.0									
Log (Mo)	.292	.367	.294	-.185	-.328	.053	.142	-.22	.166	-.271	1.0								
Log (Ni)	.082	-.041	.077	.087	.089	.356	.042	.12	.313	.111	-.004	1.0							
Log (Sb)	-.009	.552	.751	-.258	-.363	-.129	-.358	-.09	-.08	-.244	.248	.029	1.0						
Log (Se)	-.097	-.449	-.271	.579	.724	.417	.11	.555	.454	.714	-.279	.244							
Log (Sm)	-.17	-.429	-.278	.621	.879	.177	.113	.554	.2	.896	-.341	.11	.312	.777	1.0				
Log (Ta)	-.184	-.349	-.3	.448	.649	.02	.054	.452	.07	.621	-.259	.034	-.278	-.535	.65	1.0			
Log (Th)	-.091	-.459	-.334	.593	.838	.089	.206	.523	.182	.804	-.274	.053	-.387	.705	.813	.674	1.0		
Log (U)	.24	.108	.205	.001	.166	.261	-.007	.149	.435	.216	.242	.102	.067	.177	.109	.184	.252	1.0	
Log (W)	.165	.146	.163	.02	-.071	.19	.017	.147	.278	-.024	.316	.07	.141	.057	.022	-.023	.204	1.0	
Log (Zn)	.226	.559	.47	-.216	-.241	.217	-.322	-.049	.297	-.129	.289	.08	.442	-.13	-.199	-.17	-.233	.26	.196

Table 11. Characteristics of permissive terranes and favorable tracts for Proterozoic carbonatite-related, rare-earth-element deposits; Mesozoic gold-bearing breccia pipes; Mesozoic stockwork molybdenum systems, and other types of deposits in the East Mojave National Scenic Area, California [--, not available; n.a., not applicable (see text)]

Deposit type	Permissive terrane	Favorable tract	Criteria used to delineate favorable tract <sup>1</sup>	Age	Median tonnage <sup>2</sup> (million tonnes)	Median grade
Proterozoic carbonatite-related, REE deposit	All Early Proterozoic rocks	Belt of metaplastics rocks and carbonatite	1, 2, 3	1.4 (Ga)	60	30.58 percent Nb205
Mesozoic						
Gold-bearing breccia pipes	Shallow-seated magmatic-hydrothermal environment	Area delineated by petrogenetically linked veins	1, 4, 5, 6, 9	~100 Ma	--	--
Stockwork molybdenum deposits	Area underlain by Midd Hills adamellite of Beckerman and others (1982)	Widespread alteration	1, 4, 5, 7, 8	~59-71 Ma	94	0.085 percent Mo
Copper skarns	Sequences of Paleozoic carbonate rocks <sup>4</sup>	Sequence of Paleozoic carbonate rocks <sup>4</sup>	1, 4, 5, 9, 10	Jurassic and Cretaceous	0.56	1.7 percent Cu
Lead-zinc skarn	Do.	Do.	Do.	Do.	1.4	5.9 percent Zn 2.8 percent Pb
Tungsten skarn	Do.	Do.	Do.	Do.	1.1	0.67 percent WO <sub>3</sub>
Tin (tungsten) skarn	Do.	Do.	Do.	Do.	59.4	50.31 percent Sn
Iron skarn	Do.	Do.	1, 4, 5, 9, 10, 11	Do.	7.2	50 percent Fe
Gold skarn	Do.	Do.	4, 5, 9, 10	Do.	60.213	68.6 g/tonne Au
Polymetallic replacement	Do.	Do.	1, 4, 5, 9, 10	Do.	1.8	5.2 percent Pb 3.9 percent Zn
Polymetallic veins	All Mesozoic and older rocks	All Mesozoic and other rocks	1, 4, 5, 6, 12 <sup>5</sup>	Do.	n.a.	n.a.
Tertiary						
Epithermal volcanic-hosted gold	Rhyolitic flow domes and caldera	Altered hydrothermal and demagnetized	1, 4, 5, 7, 11, 12	15.5 Ma	71.6	78.4 g/tonne Au
Notes						
11. Presence of mines and prospects; 2, presence of ultrapotassic and carbonatite rocks; 3, anomalous concentrations of REE in rock geochemistry, concentrate sample, and NURE samples; 4, geochemical anomalies of base- and precious metals in various sample media; 5, presence of petrogenetically linked metal occurrences; 6, presence of major pre-mineral structure; 7, widespread hydrothermal alteration of host igneous phase; 8, widespread presence of quartz-sulfide stockworks; 9, presence of reactive, pre-mineralization rocks; 10, widespread alteration in carbonatite rock together with widespread occurrences of polymetallic veins, polymetallic faults, and gold-silver, quartz-pyrite veins; 11, aeromagnetic data; 12, widespread alteration detected using thematic-mapper image.						
2From Cox and Singer (1986).						
3World-class REE deposits at Mountain Pass, just outside the EMNSA, include sparse Nb and extraordinary contents of LREE (see text).						
4Includes copper, lead-zinc, iron, tungsten, tin (tungsten) and gold skarns in all the EMNSA (see text).						
5Based on only grade and tonnage information from four deposits.						
6From Theodore and others (1991).						
7From epithermal quartz-alumic vein deposit model in Cox and Singer (1986).						

Table 12. Analyses of rocks in the general area of the Big Hunch, New York Mountains, stockwork molybdenum system  
 [-, not detected; Semiquantitative emission spectrographic analyses by J. Harris and B. Spillare. Results are reported with a relative standard deviation for each value of plus 50 percent and minus 33 percent.  
 Looked for but not found, at the part-per-million detection levels shown in parentheses: As (150), Au (10), Cd (32), Dy (22), Er (10), Eu (10), In (6.8), Ho (15), Hf (15), Ge (1.5), Ir (15), Lu (15), Os (22), Pd (1), Pr (68), Pt (4.6), Re (10), Rh (2.2), Ru (2.2), Sb (32), Sm (10), Ta (460), Tb (32), Tm (4.6), U (320), W (10). Partial chemical analyses by E. Campbell and D. Kobilis using standard methods of Shapiro (1975).]

Analysis	Sample 81TT	Semiquantitative emission spectrographic analyses (parts per million)																				
		Ag	B	Ba	Be	Ce	Co	Cr	Cu	Ga	La	Li	Mn	Mo	Nb	Nd	Ni	Pb	Sc	Sn	Te	
1	40	—	—	860	—	—	—	—	19	10	—	—	33	13	—	—	6.9	1.7	—	310	—	
2	41	—	9.6	320	2	—	—	—	32	13	24	75	95	84	7.5	—	—	4.6	4.5	410	—	
3	42	0.096	—	1,000	3	—	—	—	70	25	25	—	130	190	4.9	—	—	24	4.1	8.3	340	
4	43	1.3	—	600	—	2.3	—	—	8.6	29	29	—	77	4.3	41	—	9	3.1	3.1	300	—	
5	44	—	5.7	320	—	—	—	—	32	10	10	—	110	1.2	10	—	18	4.4	—	300	—	
6	45B	0.38	—	540	—	—	—	—	7.6	18	18	—	65	50	—	—	9.3	1.9	—	260	—	
7	46	1.4	31	440	—	—	—	—	73	22	22	—	50	82	6.9	—	16	2.4	1.6	200	—	
8	47	0.18	24	870	1.5	—	—	—	32	49	49	—	66	81	52	—	15	3	2.4	350	—	
9	48	—	—	600	—	—	—	—	190	19	19	—	60	5.1	4.2	—	7.7	2.8	3.1	210	—	
10	49	—	—	1,000	2.3	—	—	—	32	27	27	—	75	7	4.8	—	13	3.3	4.4	390	—	
11	50	—	—	570	1.7	—	—	—	17	21	21	—	140	7.5	3.3	—	—	3.1	1.9	250	—	
12	51	—	—	640	1.2	—	—	—	32	20	20	—	78	81	3.3	—	—	3.2	2.4	250	—	
13	52	—	—	620	1.8	—	—	—	1.3	570	31	31	73	90	260	4.2	—	9.1	5.5	3	250	
14	53	—	49	1,100	3.2	—	—	1.5	—	2,400	29	29	89	43	14	5.7	46	—	22	3.4	580	
15	54	—	—	830	2.4	—	—	1.4	230	21	21	—	67	—	4.7	40	—	12	3.1	3.3	450	
16	55	—	—	730	2.3	—	—	1.4	—	220	29	29	—	97	—	6.4	53	—	12	4	3.1	460
17	56	—	—	740	2.4	—	—	1.7	—	44	12	26	—	99	—	44	40	—	1.5	1.3	2.7	490
18	57	—	—	720	2.3	—	—	1.2	—	48	15	22	—	81	—	4.2	—	—	18	2.5	5.5	510
19	58	0.17	7.7	480	4.3	56	2	—	210	18	40	—	160	9.6	7.2	50	—	26	4.1	3.4	200	
20	59	4.6	—	120	1.3	—	—	—	43	12	—	—	110	460	—	—	2.1	170	2.6	3.1	34	
21	60	0.33	9.7	820	2.7	—	—	—	41	21	16	—	74	87	4.2	32	—	9.6	4	4	300	
22	61	—	—	360	—	—	—	1.3	—	42	15	15	—	110	—	4.9	—	—	32	2.4	2.7	260
23	62	—	—	720	1.8	—	—	1.1	—	70	18	17	—	110	—	6	—	—	25	3	2.5	400
24	63	—	—	300	—	—	—	—	9.5	—	6.7	—	29	21	6.7	—	1.8	1.7	4.1	1.50	—	
25	64	0.15	38	420	3.6	—	—	—	60	13	28	—	84	81	86	6	36	—	11	3.9	2.6	290
26	65	—	5.3	580	3	—	—	1.6	—	4,000	19	25	—	210	2.3	6.2	—	—	17	3.8	4	280
27	73	—	41.0	310	2.5	—	—	—	41	21	25	—	94	150	4.3	44	—	28	3.3	2.4	730	
28	76	0.66	—	1,100	5.1	—	—	—	140	25	54	—	260	—	6.1	83	2	2.1	31	4	3	440
29	77	0.9	—	700	4.8	—	—	—	1.6	99	23	19	—	280	—	8.	—	—	1.6	12	4.8	390
30	78	—	—	—	—	—	—	—	1.1	2.2	21	20	—	110	—	6.1	32	—	4.1	1.7	3.9	270
31	79	—	0.16	—	910	37	—	—	1.8	7	22	—	220	—	7.2	—	—	25	5	3.8	640	
32	80	—	20	1,000	2.4	—	—	2.3	1.3	67	19	33	—	78	—	5.6	55	1.8	14	4.8	3.3	560
33	70	—	32	200	200	—	—	—	22	24	14	14	4.5	23	—	1.6	24	—	16	4.7	3.7	540
34	71	—	6.6	1,100	1,100	—	—	2.1	—	13	19	38	38	21	5.6	—	—	28	3.2	—	80	
35	72	—	210	210	—	—	—	—	32	17	—	—	30	—	—	—	—	2	12	4.6	1.8	210
36	81	—	6.0	190	190	—	—	—	32	26	—	—	—	—	—	—	—	—	—	—	—	—

Table 12. Analyses of rocks in the general area of the Big Hunch, New York Mountains, stockwork molybdenum system.—Continued

Analysis	Sample	Semi-quantitative emission spectrographic analyses (parts per million)						Chemical analyses (parts per million)			
		V	Y	Yb	Zn	Zr	F	Cl	W		
1	40	5.7	3	.32	—	41	700	22	2.7		
2	41	14	6.8	.5	23	88	2,500	13	7		
3	42	20	4.3	.54	—	71	2,200	13	7.9		
4	43	12	4.6	.51	18	34	1,000	13	4.6		
5	44	5.9	7.9	.92	—	23	1,000	17	2.8		
6	45B	6.5	2.2	—	—	31	800	16	2.5		
7	46	5.1	8.3	.87	—	34	1,400	—	4.1		
8	47	12	5.5	.36	15	39	1,100	—	3.1		
9	48	9.6	4.9	.5	2	42	1,200	—	3.3		
10	49	19	7.8	.68	18	82	1,300	—	3.7		
11	50	21	3.7	.5	19	59	1,400	13	5.2		
12	51	14	7.2	.77	17	44	900	24	4.1		
13	52	22	14	1.1	—	73	1,800	—	3		
14	53	13	5.9	.86	32	110	1,200	—	3.9		
15	54	11	5.5	.53	27	73	1,200	18	1.1		
16	55	14	8.5	.78	39	49	1,400	24	1.8		
17	56	12	3.1	.12	25	54	900	31	.56		
18	57	12	3.9	.19	23	68	1,100	16	.5		
19	58	19	7.9	.18	24	96	880	15	8.8		
20	59	18	2.1	.29	17	12	1,000	—	3.5		
21	60	29	5.9	4.8	—	100	2,100	17	3.9		
22	61	4.8	10	.25	17	36	400	19	.26		
23	62	8.5	7.6	.85	45	64	1,000	26	.96		
24	63	3.9	4.1	.39	17	15	500	14	1.3		
25	64	6.8	17	6.8	26	74	1,400	16	3.8		
26	65	7.5	15	7.5	56	98	1,000	67	1.7		
27	73	15	6.8	15	23	59	2,100	—	4		
28	76	23	5.4	.23	—	130	5,800	—	7.9		
29	77	20	4.8	.20	56	65	900	18	2.2		
30	78	27	2.3	.27	—	74	2,500	—	12		
31	79	20	3	.38	—	65	4,000	—	57		
32	80	13	7.5	.82	—	93	1,800	19	4		
33	70	3.7	12	1.2	17	17	1,300	20	2.3		
34	71	16	9.4	1	—	—	2,000	25	3.6		
35	72	4.7	6.9	.64	19	19	2,000	—	.5		
36	81	2.5	9.2	1.1	18	18	1,000	18	2.2		

1-4 Variably quartz veined, gneissic Mid Hills Adamellite of Beckerman and others (1982).

5 Rhyodacite dike.

6-19 Variably quartz veined, gneissic Mid Hills Adamellite.

20-21 Variably quartz veined, gneissic Mid Hills Adamellite.

22 Teuonia monzogranite.

23-26 Variably quartz veined, gneissic Mid Hills Adamellite.

27-31 Variably altered, very weakly quartz veined, gneissic Mid Hills Adamellite.

32 Surface grab sample; quartz veined, gneissic Mid Hills Adamellite.

33 Drill core. Serrically altered, porphyritic rhyodacite.

34 DDH York-5-1,364 ft. Potassically-altered Mid Hills Adamellite.

35 Surface grab sample; gneissic Mid Hills Adamellite.

36 DDH York-5-1,364 ft. Argillite-altered Mid Hills Adamellite.

Av. Age quartile: 65 years (87 samples)

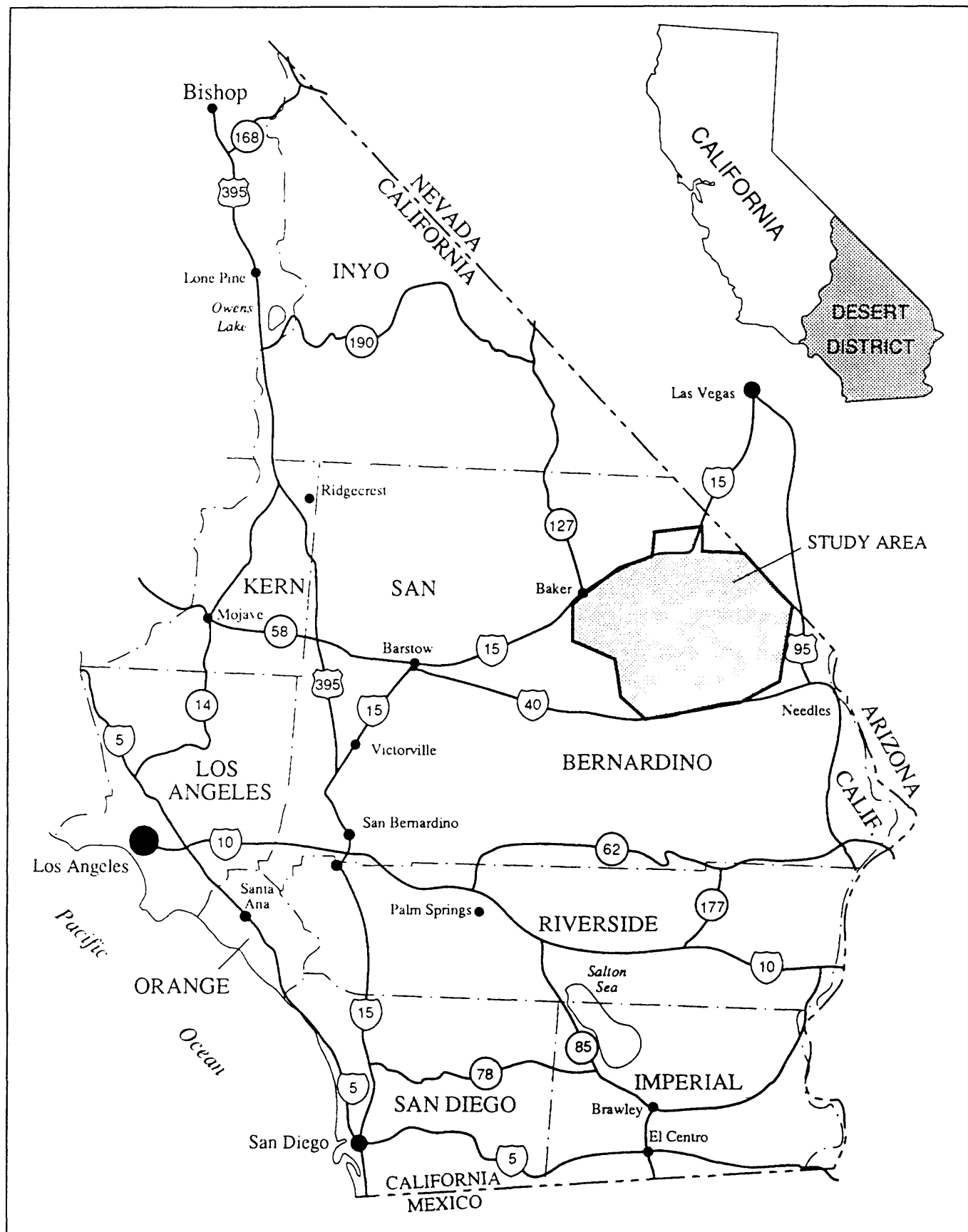


Figure 1. Location map of the study area of the East Mojave National Scenic Area, San Bernardino County, California.

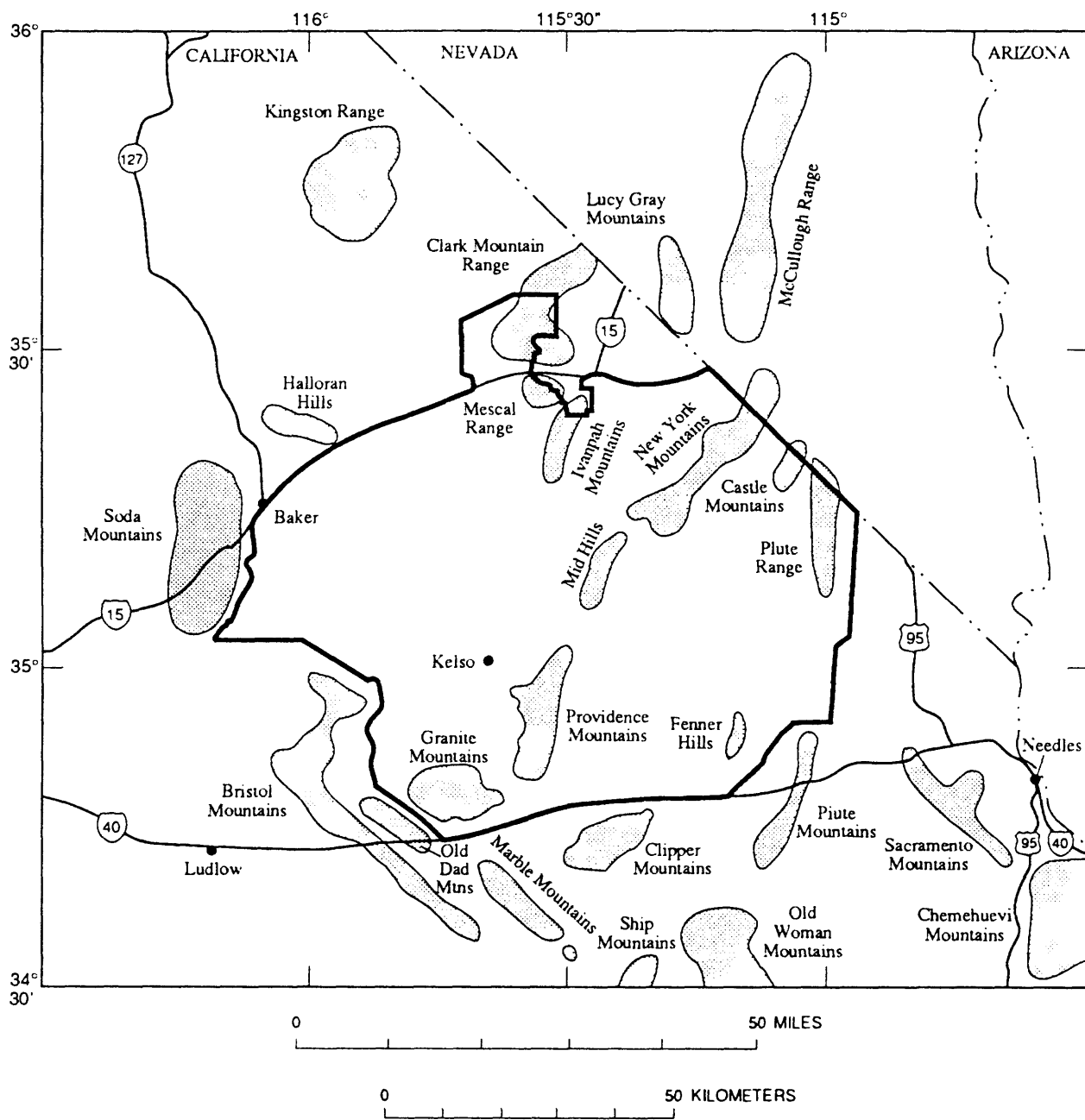


Figure 2. Map of the East Mojave National Scenic Area showing locations of some of the major mountain ranges.

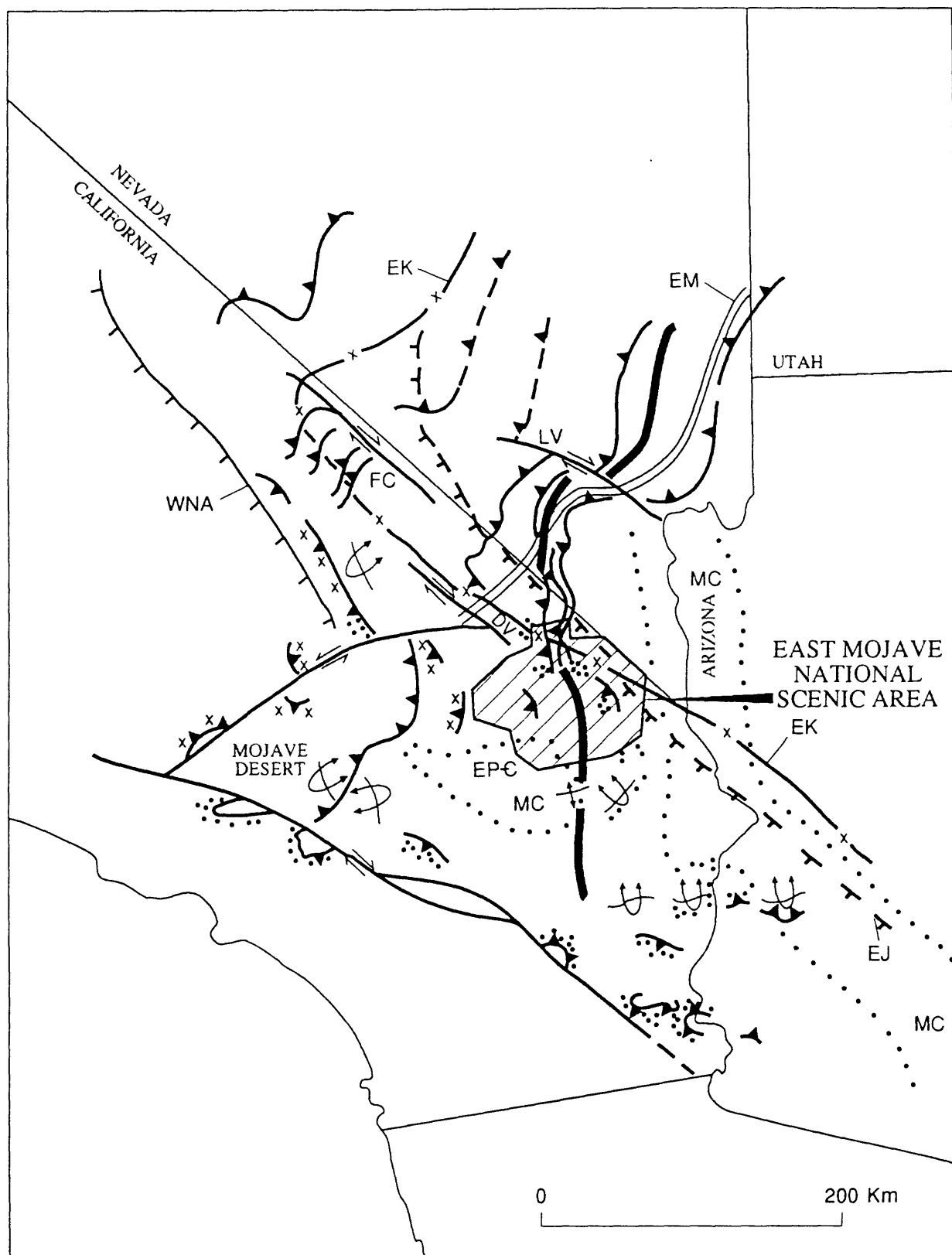


Figure 3. Schematic tectonic map of southeastern California and adjoining regions showing relations among major structural and paleographic elements. Stippled, structures that involve Proterozoic crystalline rocks; cross pattern, structures that involve Mesozoic plutonic rocks; WNA, western limit of the North American Proterozoic crystalline basement; EM, eastern limit of the Paleozoic miogeocline; EPC, eastern limit of Late Proterozoic sedimentary rocks; FC, Furnace Creek fault, LV; Las Vegas shear zone; EK, eastern limit large Cretaceous plutons; MC, areas of metamorphic core complexes, outer limit indicated by dotted lines. Vergence of major overturned folds also shown. Modified from Burchfiel and Davis (1981, 1988) and Brown (1986).

FIGURE - GENERALIZED GEOLOGY OF THE  
THE EAST MOJAVE NATIONAL SCENIC AREA

EXPLANATION

- Quaternary and Tertiary sedimentary rocks
- Quaternary and Tertiary volcanic rocks
- Mesozoic plutonic rocks
- Paleozoic and L. Proterozoic carbonate rocks
- Proterozoic plutonic and metamorphic rocks
- Mesozoic to Proterozoic volcanic and sedimentary rocks, undivided

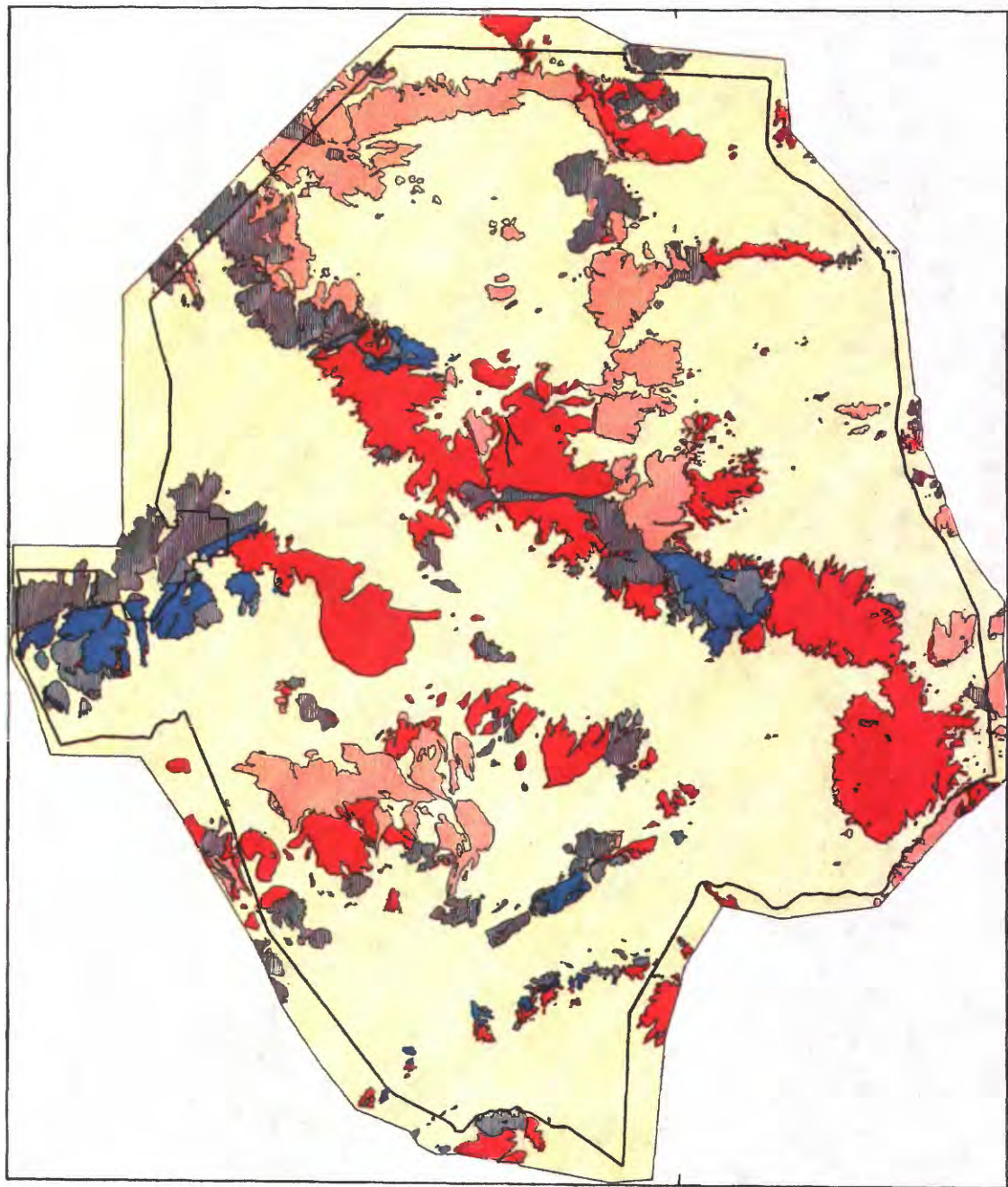
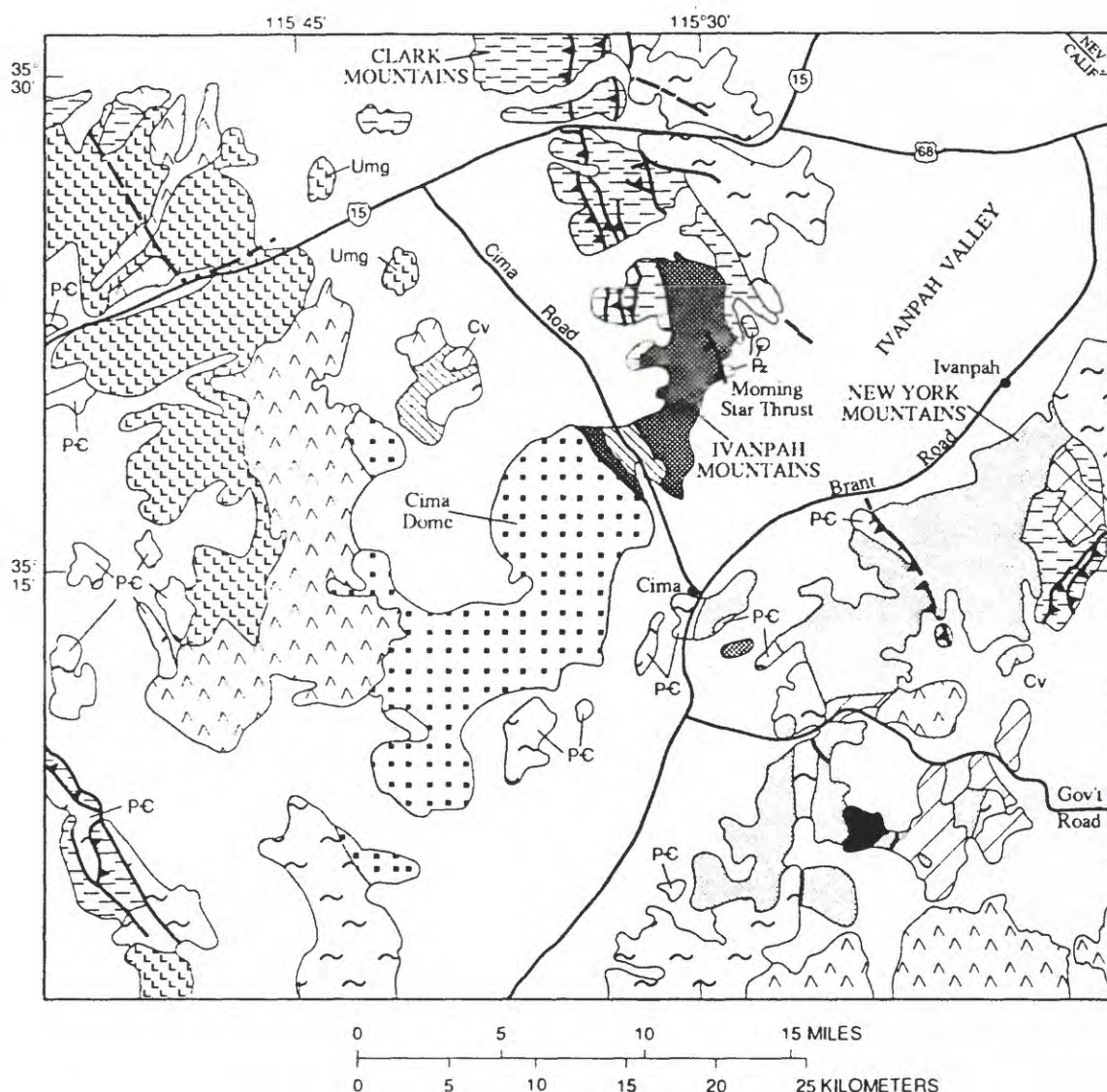


Figure 4. Generalized geologic map of the East Mojave National Scenic area. Modified from plate 1.



#### EXPLANATION

- Quaternary alluvium (Qal)
- ▨ Cenozoic volcanic rocks (Cv)
- TEUTONIA BATHOLITH OF BECKMAN AND OTHERS (1982)
- Black Canyon horblende gabbro (Kbc)
- ▨ Live Oak Canyon granodiorite (Klo)
- ▨ Mid Hills adamellite (Kmh)
- ▨ Ivanpah granite (Jig)
- ▨ Rock Spring monzodiorite (Krs)
- ▨ Undifferentiated granitic rocks of the batholith (Umg)
- ▨ Kessler Springs adamellite (Kks)
- ▨ Teutonia adamellite (Kt)
- ▨ Paleozoic sedimentary rocks (Pz)
- ▨ Proterozoic banded and quartzofeldspathic gneisses (P-C)

Figure 5. Geologic sketch map of the north-central part of the East Mojave National Scenic Area showing the distribution of the various phases of the Teutonia Batholith. Modified from Beckerman and others (1982).

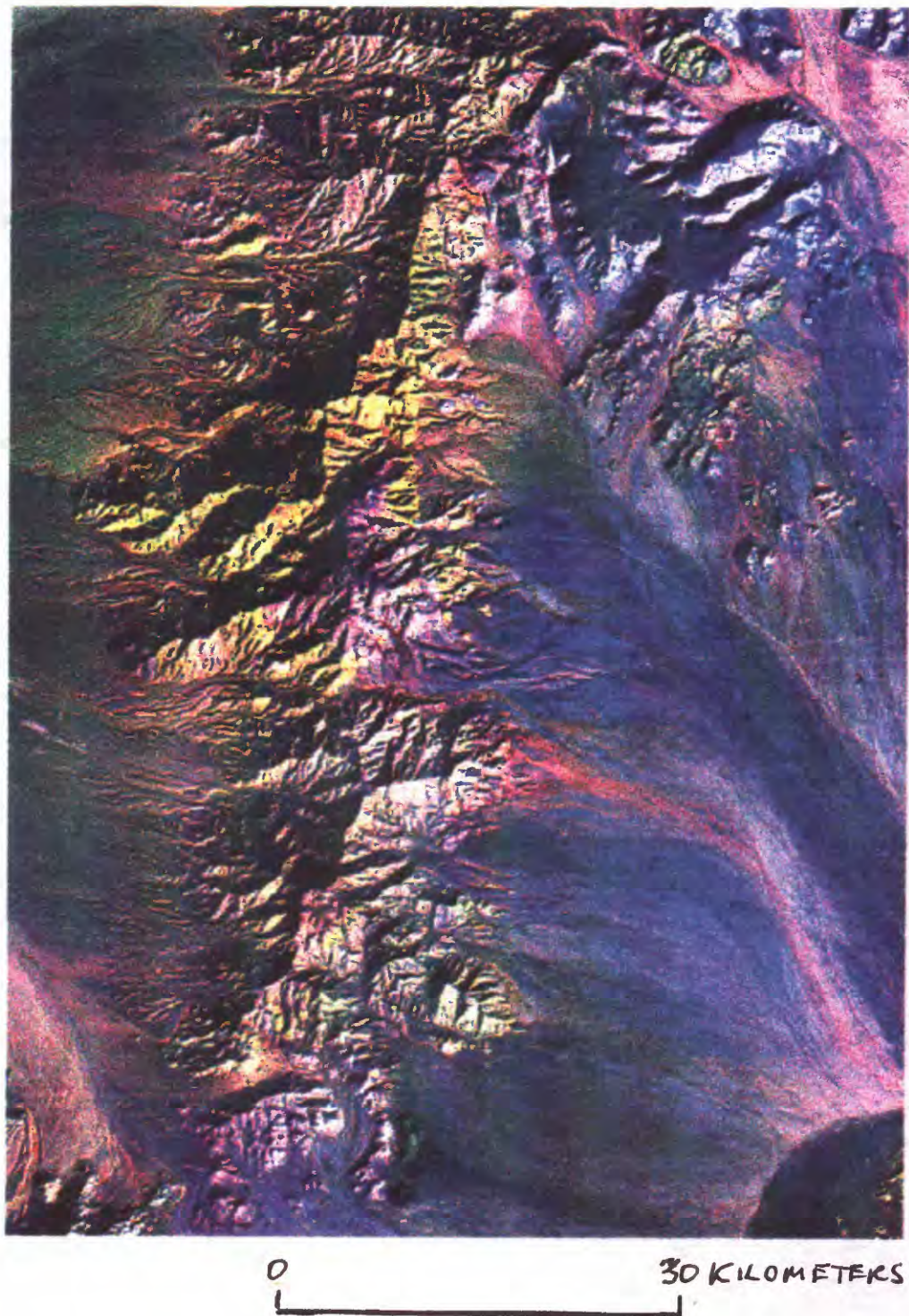
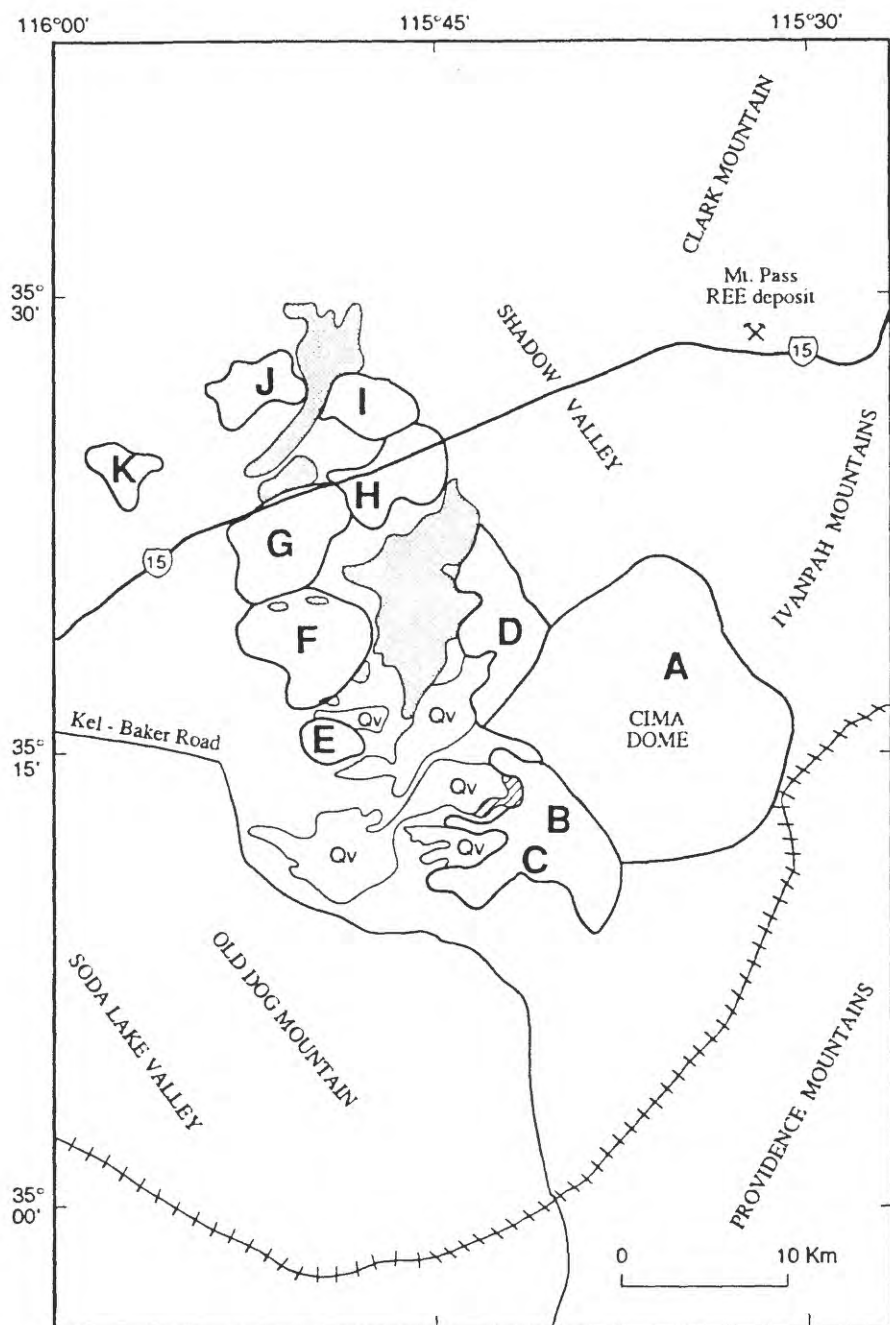


Figure 6. Satellite image of the Providence Mountains and adjacent piedmonts, East Mojave National Scenic Area, California (Landsat 4 Thematic Mapper scene 40149-17441, 12 December 1984 (path 39, row 36)). This image has been enhanced to emphasize the spatial relations between piedmont deposits and the source areas from which these deposits were derived. Image enhancement was done with an inexpensive desktop image processing system. Individual spectral bands were corrected for atmospheric absorption and scattering and for variations in scanner sensitivity. Differences between spectral bands were then calculated and presented as a false color composite where: red=band 5 - band 7, green=band 5 - band 4 (high-pass filtered), and blue=band 3 - band 1 (median filtered). Image scale=1:125,000.



#### EXPLANATION

[Qv]	Quaternary vents and flows	Letters mark the locations of pediment domes:
[Hatched]	Late Miocene vents and flows	A-Chima dome
[Solid]	Latest Miocene and Early Pliocene vents and flows	G-Marl Mountain dome
		H-Solomons Knob dome
		I-Squaw Mountain dome
		J-Turquoise Mountain dome
		K-Yucca Grove dome

Figure 7. Generalized map of the Cima volcanic field showing the locations of major pediment domes: Tv1 - late Miocene vents and flows; Tv2 - latest Miocene and early Pliocene vents and flows; Qv - Quaternary vents and flows. Letters mark the locations of pediment domes: A - Cima dome; B - Cimacita dome; C - Cow Cove dome; D - Granite Springs dome; E - Halloran Wash dome; F - Indian Springs dome; G - Marl Mountain dome; H - Solomons Knob dome; I - Squaw Mountain dome; J - Turquoise Mountain dome, K - Yucca Grove dome. From Dohrenwend (1988).

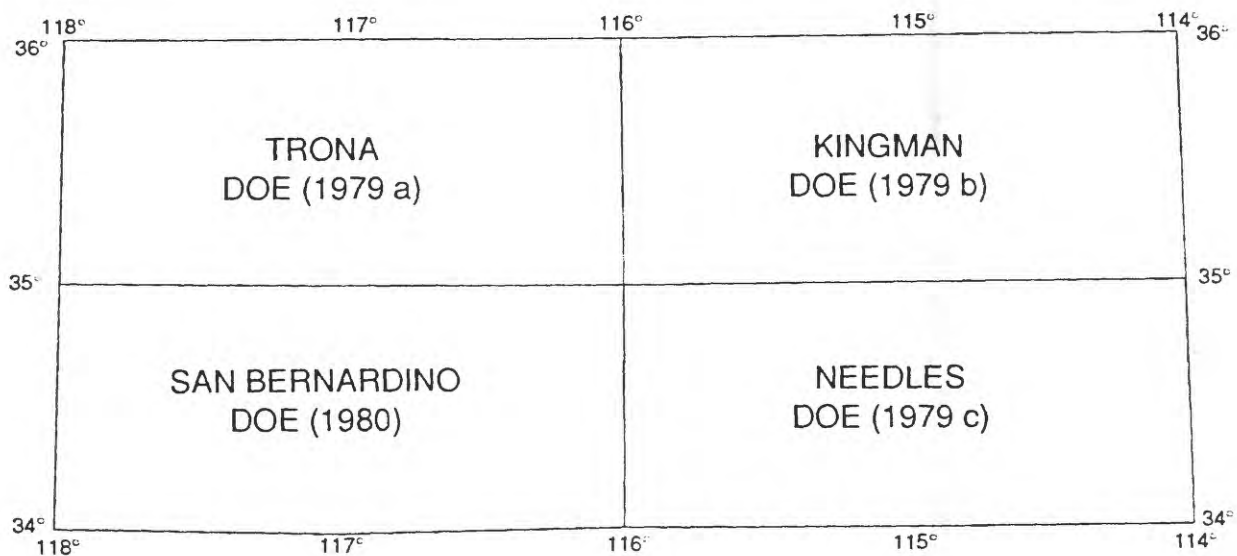


Figure 8. Index map showing the  $1^{\circ} \times 2^{\circ}$  quadrangles in the general area of the East Mojave National Scenic Area from which the NURE aerial gamma-ray data were taken for this study.

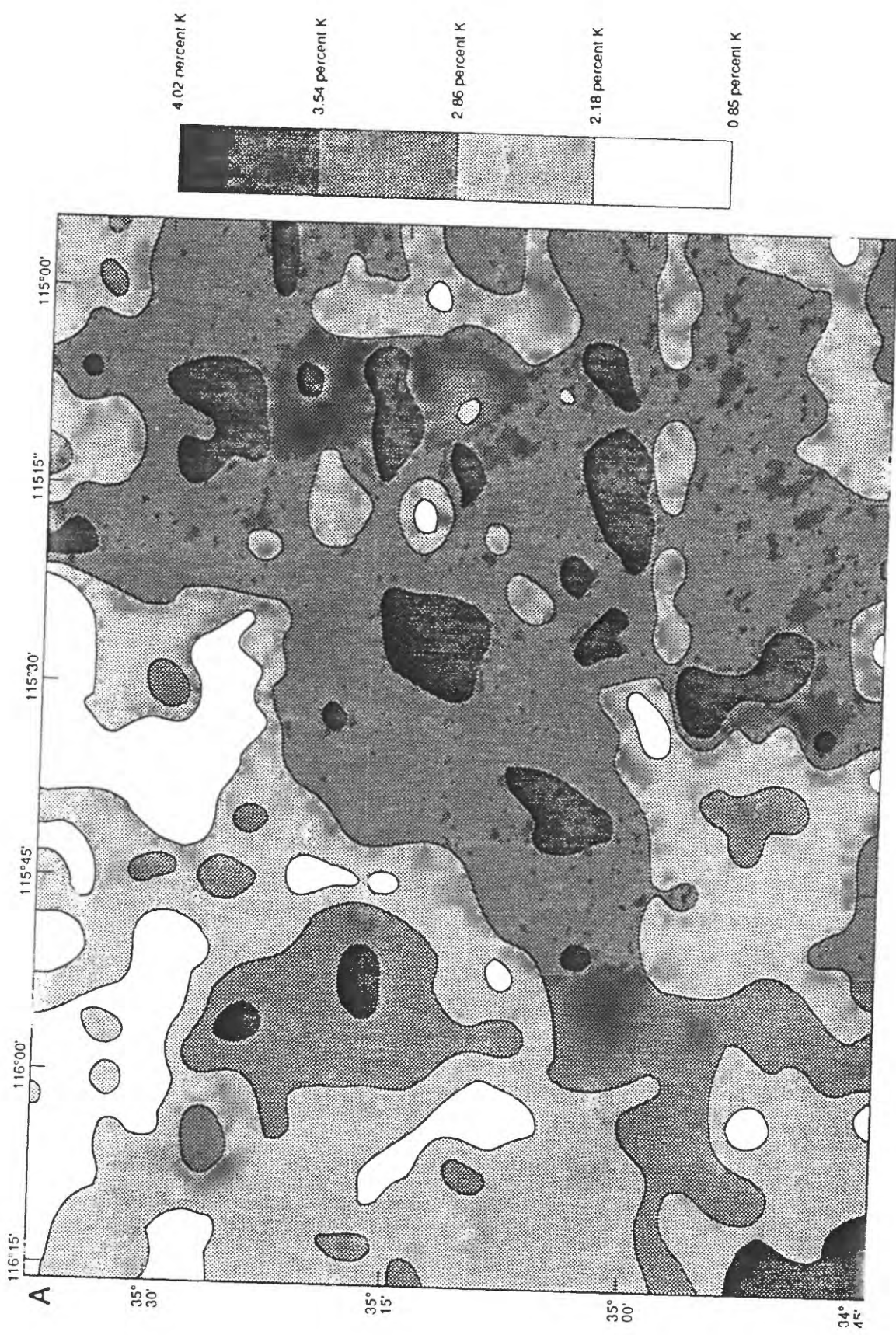


Figure 9. Contoured plots of percent potassium (A), thorium as parts per million equivalent (B), and uranium as parts per million equivalent (C).

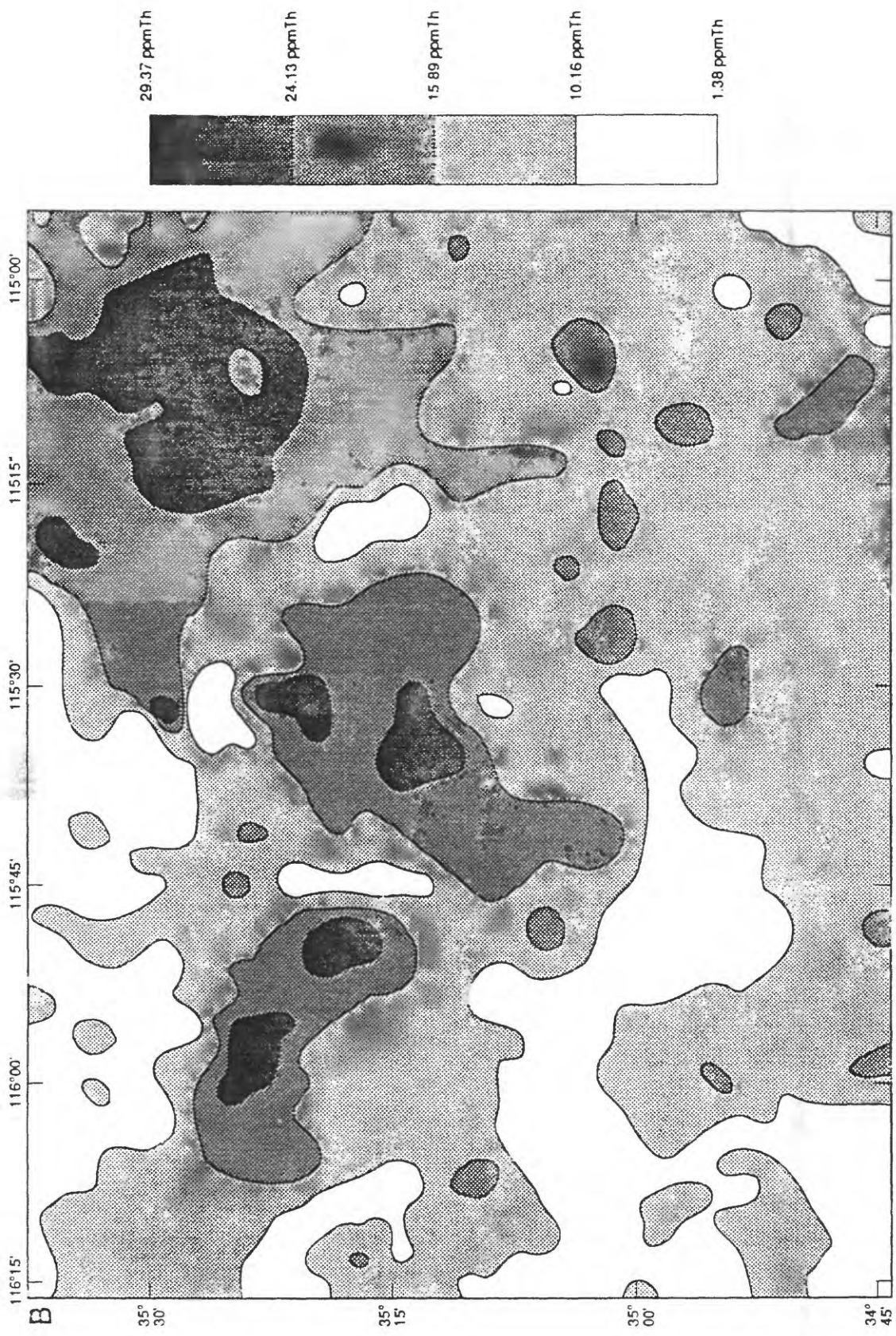


Figure 9 (cont.)

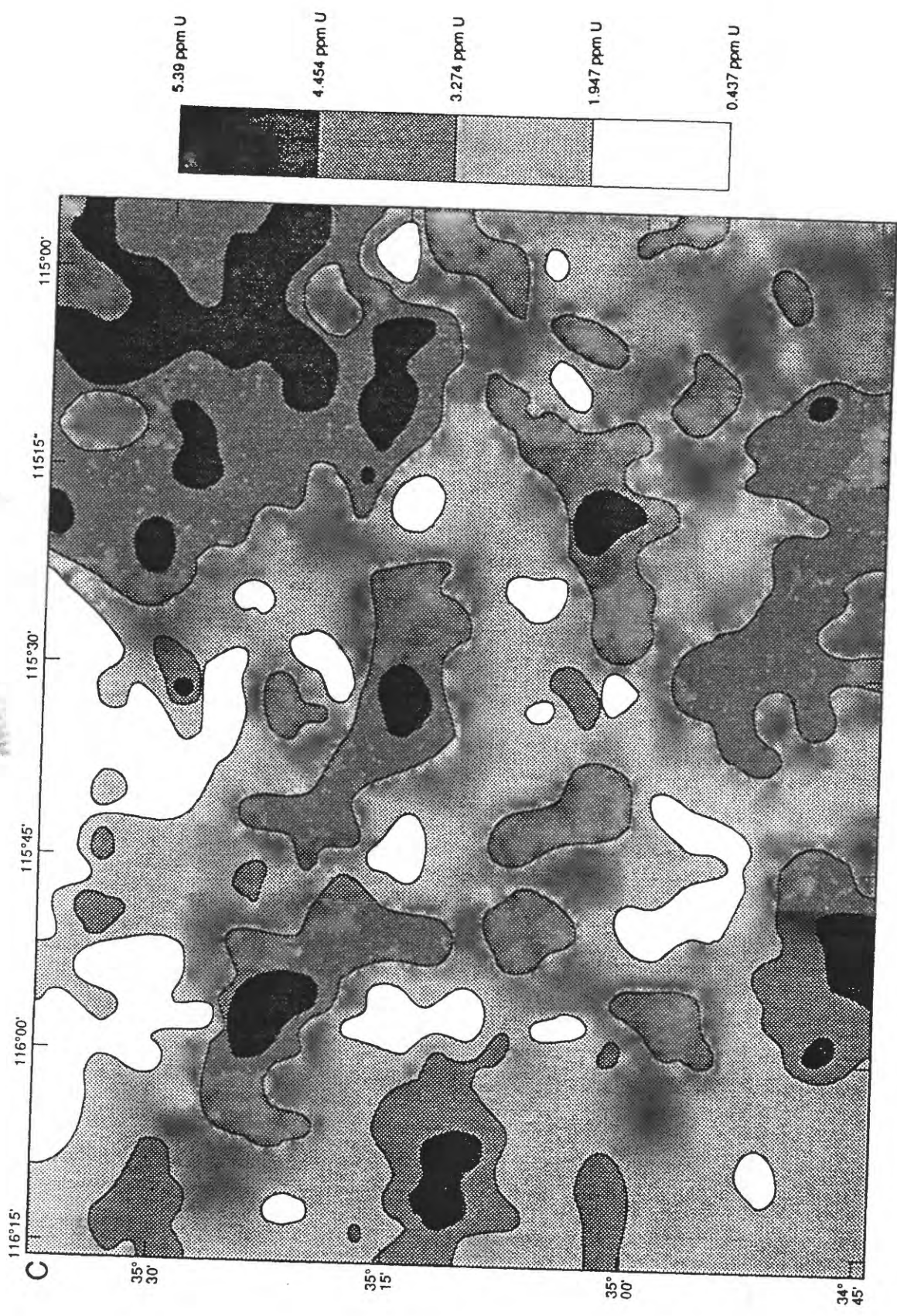




Figure 10. Color-ratio composite produced by digital image processing of a quarter Landsat Thematic Mapper scene (50 8271 73 95) that includes a large part of the East Mojave National Scenic Area.

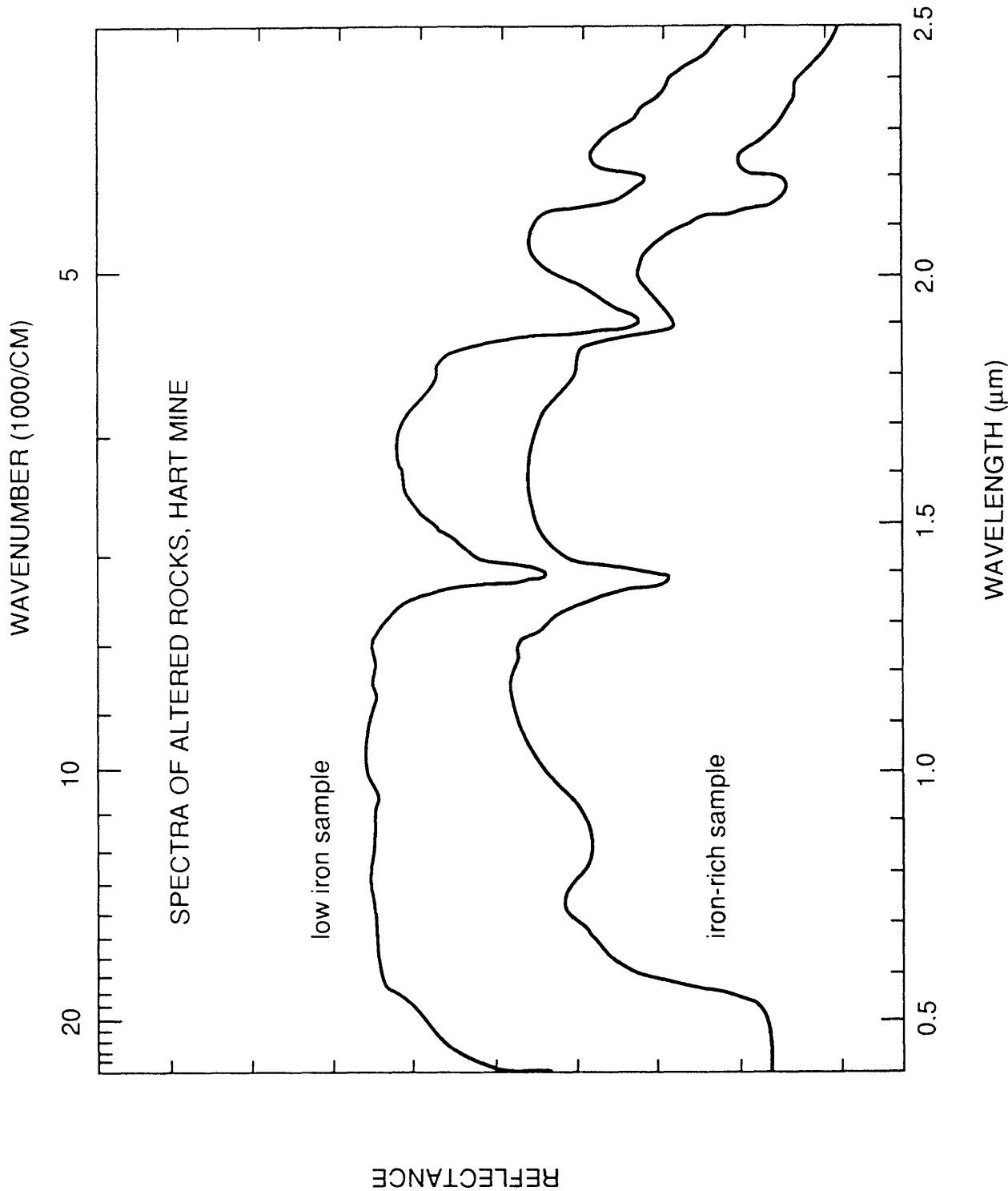


Figure 11. Spectra of highly altered dacite-rhyolite samples collected at Hart Mine, Castle Mountains. (unit  $T_{dr}$ , pl. 1). For both these samples, TM 7 will have a low value, resulting in a high TM 5/7 (red). TM 3/1 (green) will be high for the iron-rich sample, moderate for the other sample, and TM 3/4 (blue) will be low/moderate for the iron-rich sample, low for the low iron sample. This will produce a white to yellow color response on the image.

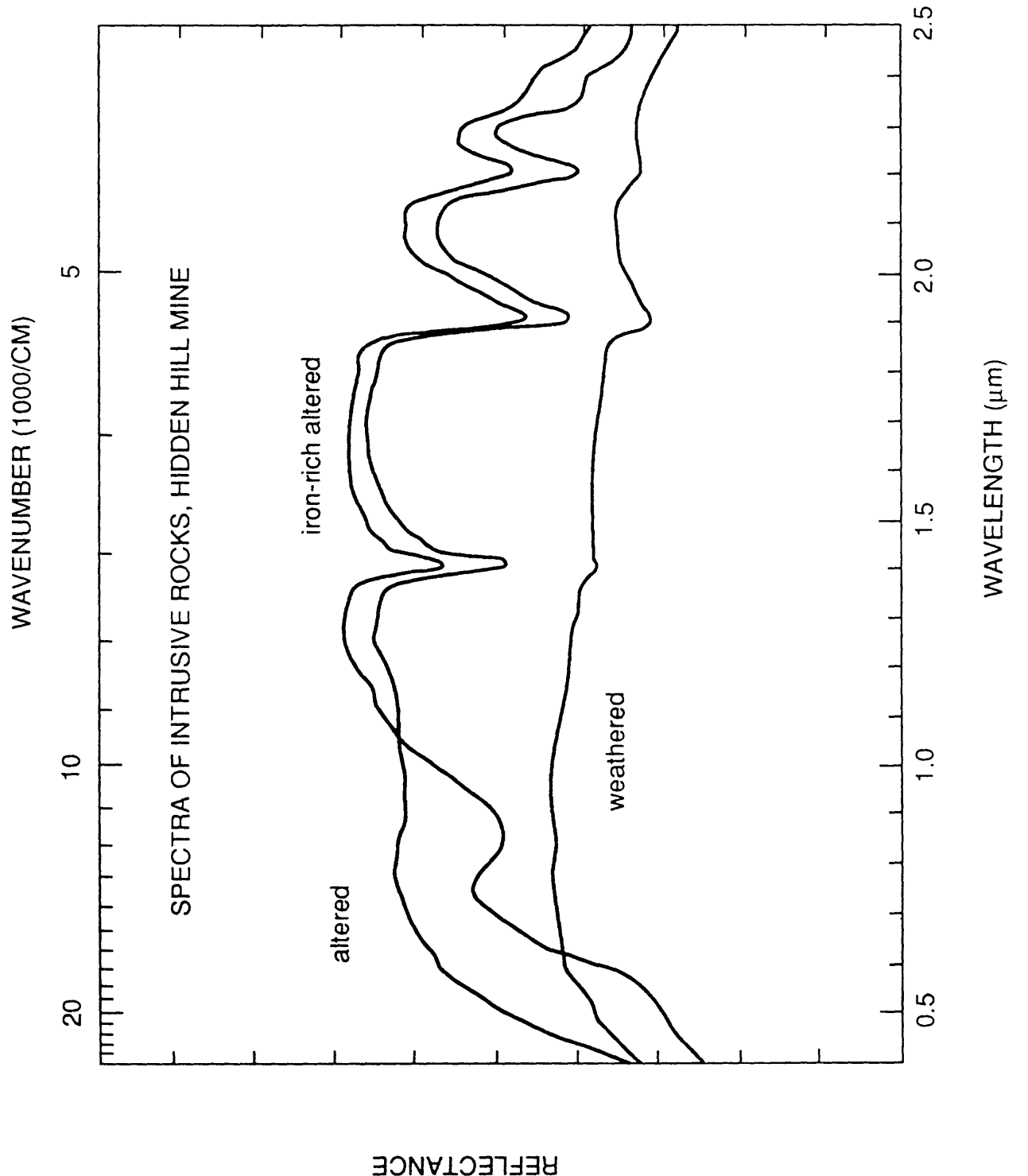
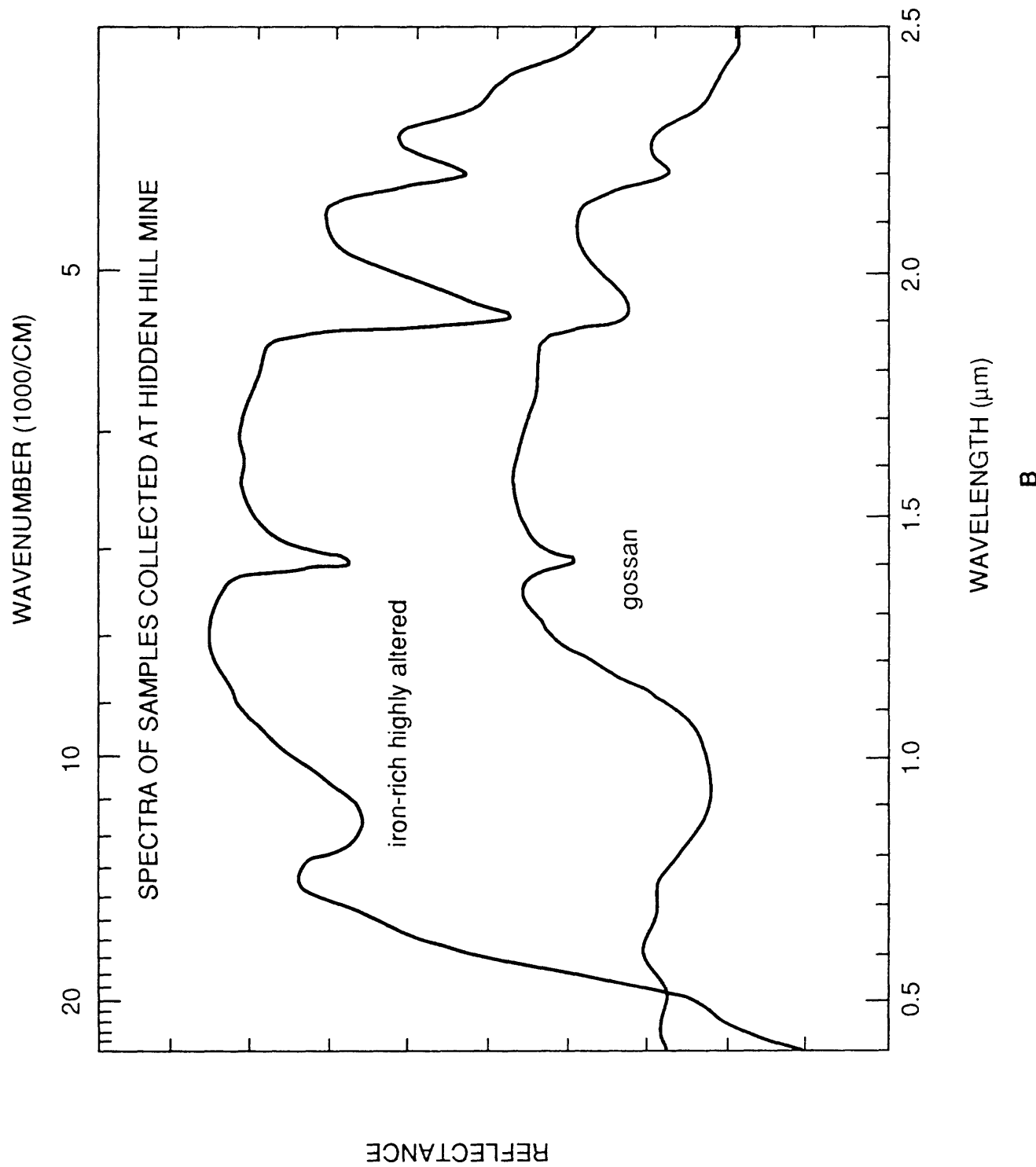


Figure 12. Spectra of weathered sample of quartz monzonite (unit Jgo, pl. 1) (A) and of altered samples, including gossan, (B) all collected at Hidden Hill Mine site. The altered rocks will produce a yellow to white color on the image as the rocks of figure 9. Color response of the weathered rock will be blue to slight magenta. TM 3/1 will not be as high for the gossan sample reducing the green component.

Figure 12 (cont.)



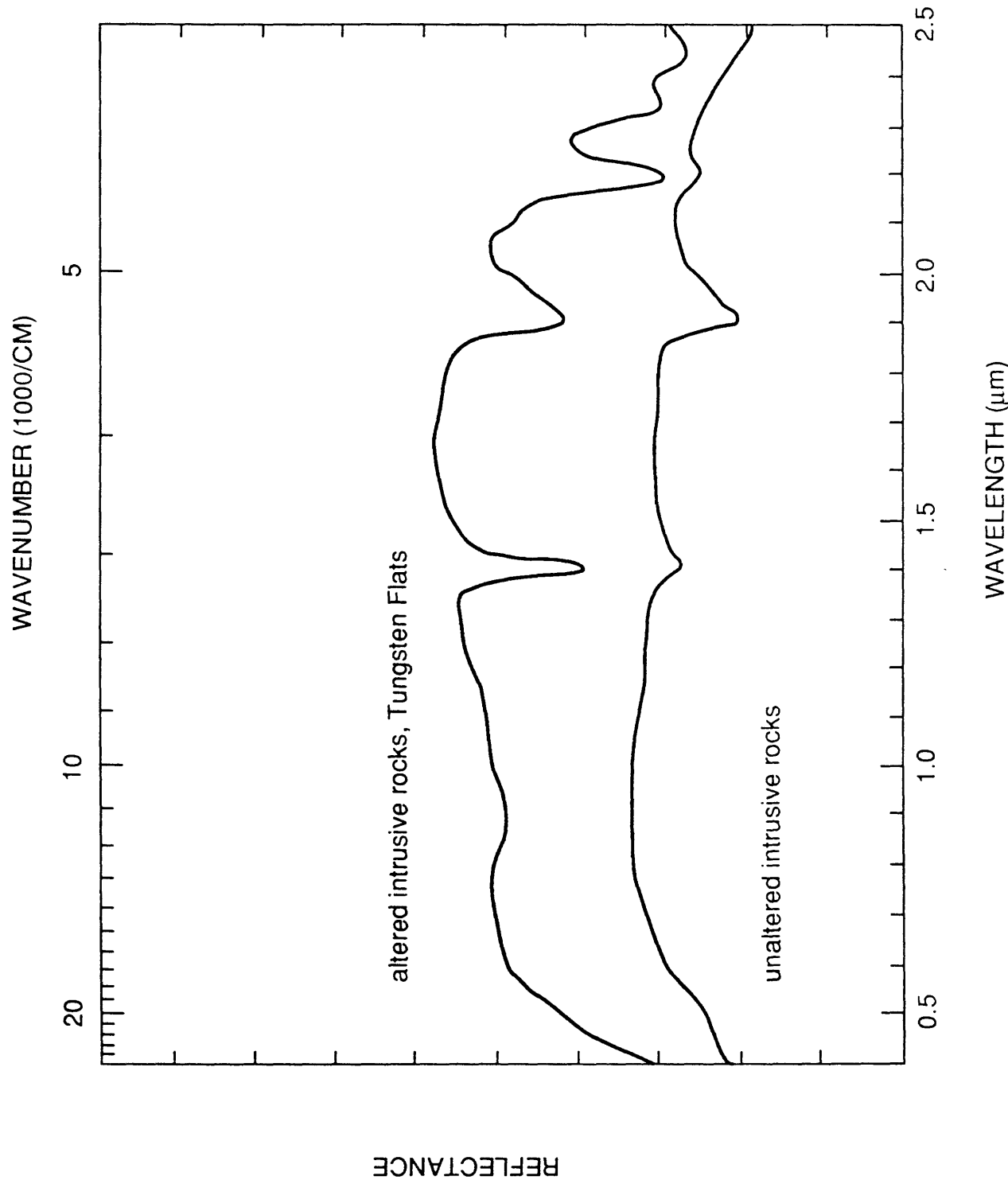


Figure 13. Spectra of monzogranite (unit Kg1, pl. 1) including altered sample, both collected at open shaft, in general area of Tungsten Flats. The TM color response of the altered sample, white; the unaltered intrusive, blue to slight red.

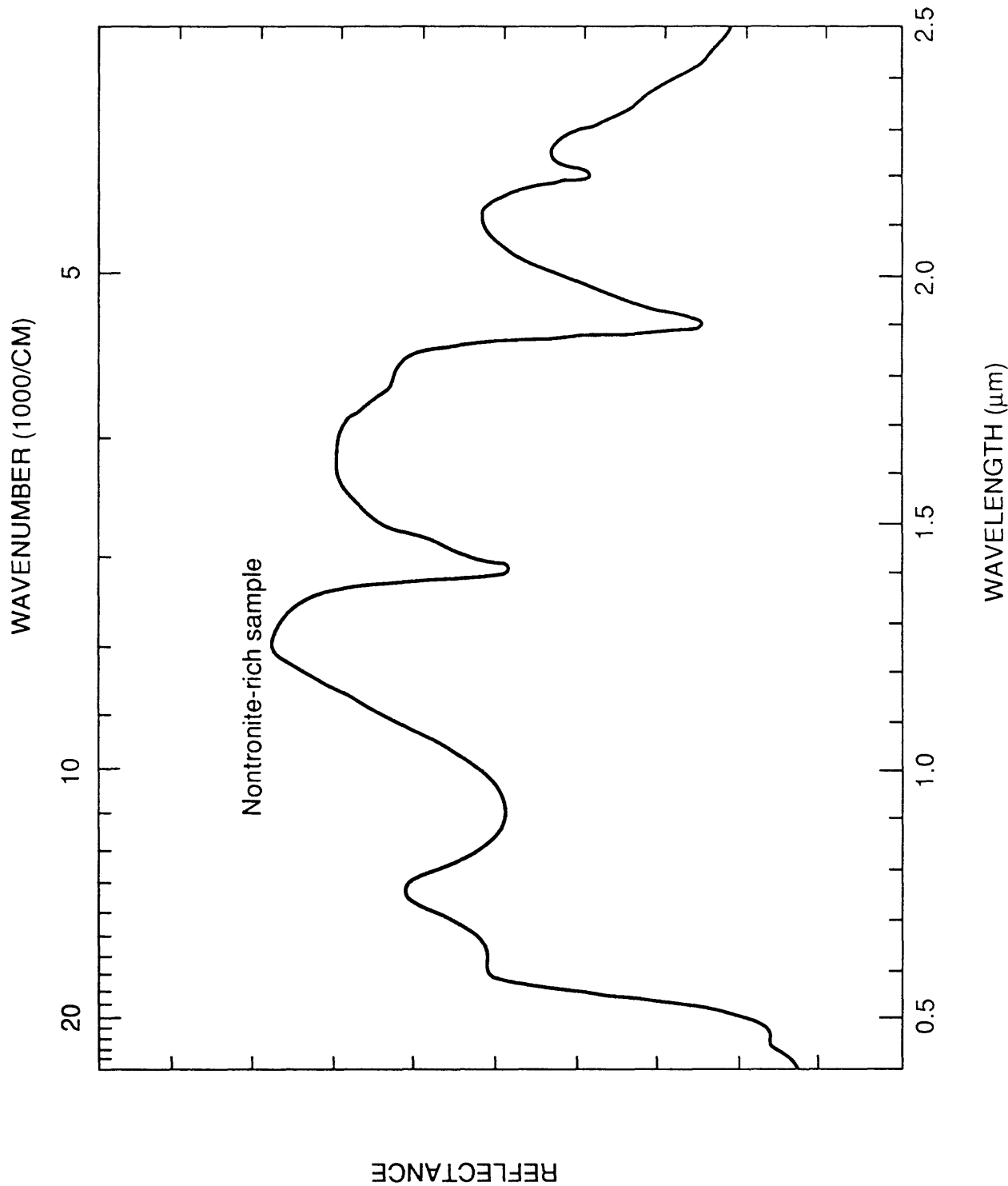


Figure 14. Spectrum of highly altered Rock Springs monzodiorite (unit Krs, pl. 1) sample. Mafic minerals have been altered to nontronite, which dominates the spectrum. The TM color response will be white.

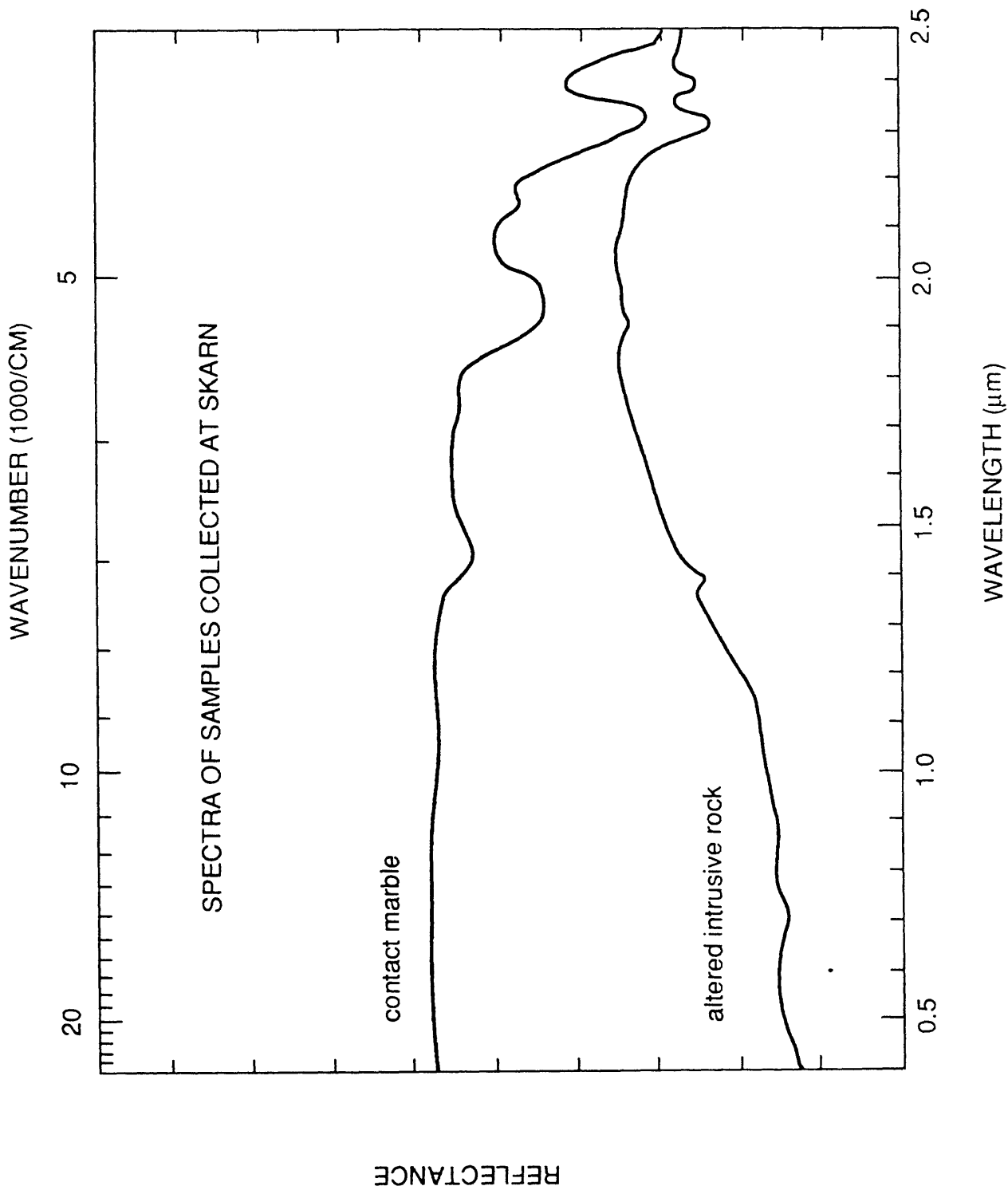


Figure 15. Spectra of dolomitic marble (altered Bird Springs Dolomite?) (unit Pd1, pl. 1) and of garnet-calc-silicate rock derived from the Moenkopi Formation (Trm) collected near skarn deposit. TM 5/7 (red) for marble will be high, less so for the intrusive rock. The color response of TM 3/1 (green) and 3/4 (blue) will be low for both samples. The resultant colors on the TM image are similar but a deeper red response for the carbonate-bearing rock.

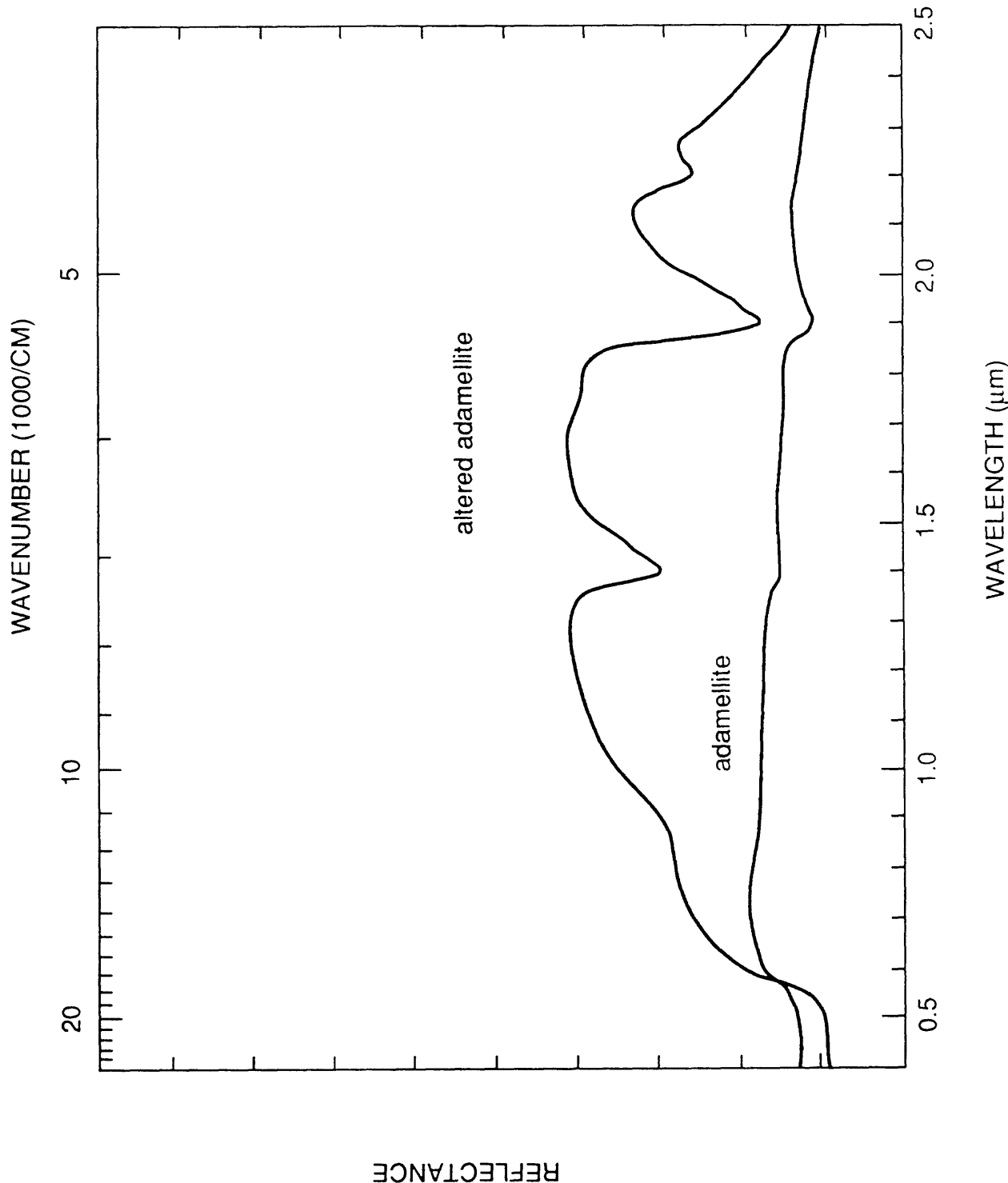


Figure 16. Spectra of monzogranite samples (unit Kgl, pl. 1) (adamellite?), one altered, collected from road cut (old railroad grade) in New York Mountains. TM white color response for the altered rock. TM 3/1 will be high due to ferric iron absorption of the adamellite, so the otherwise flat spectrum will result in a slight cyan color on the TM image.

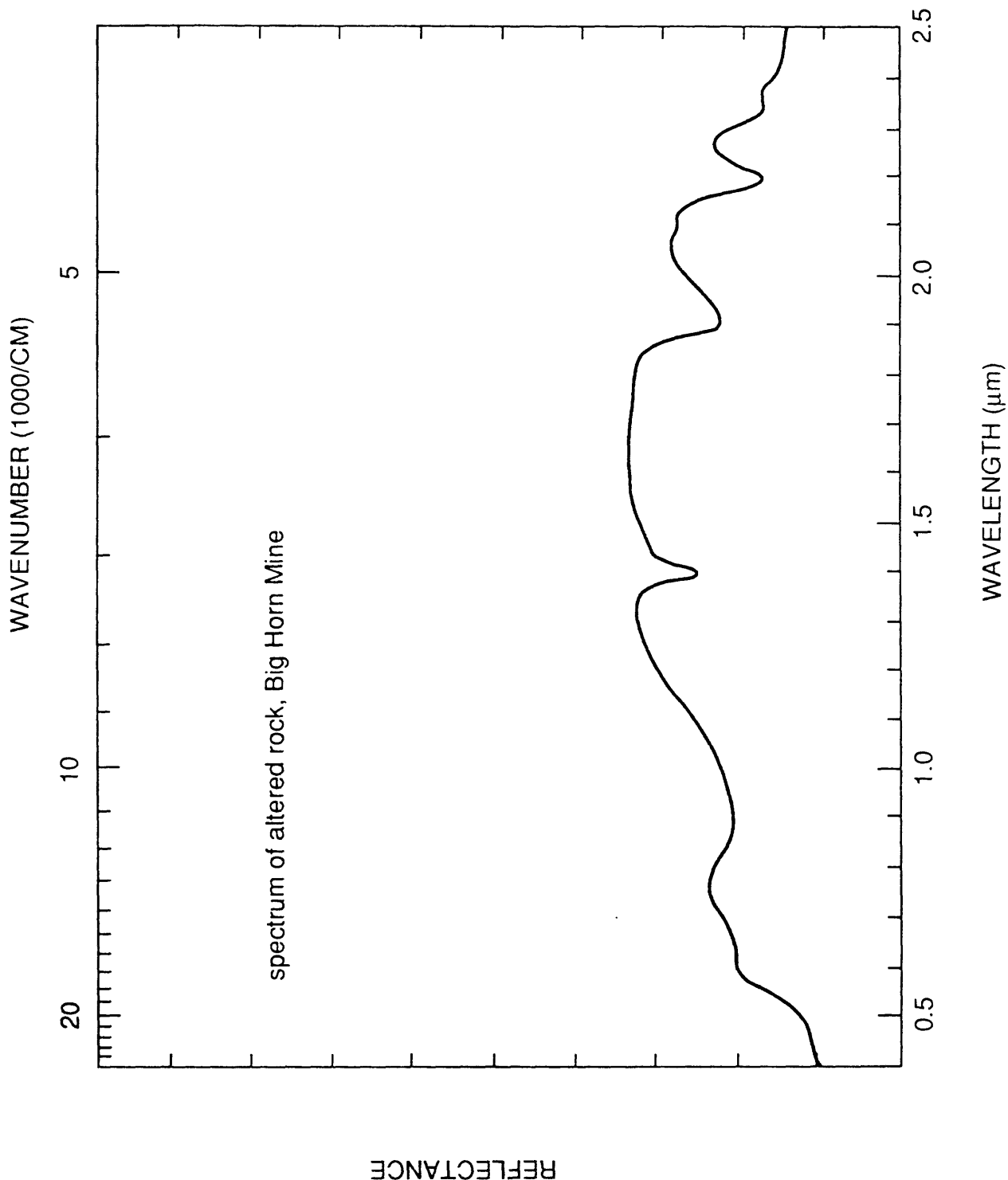


Figure 17. Spectra of altered quartz monzonite (unit Jgo, pl. 1) collected at the Big Horn Mine. Resultant color on the TM image will be white to yellow but as the spectral reflectance is low relative to spectra exhibited on figure 9, these rocks would not be as bright on the image.

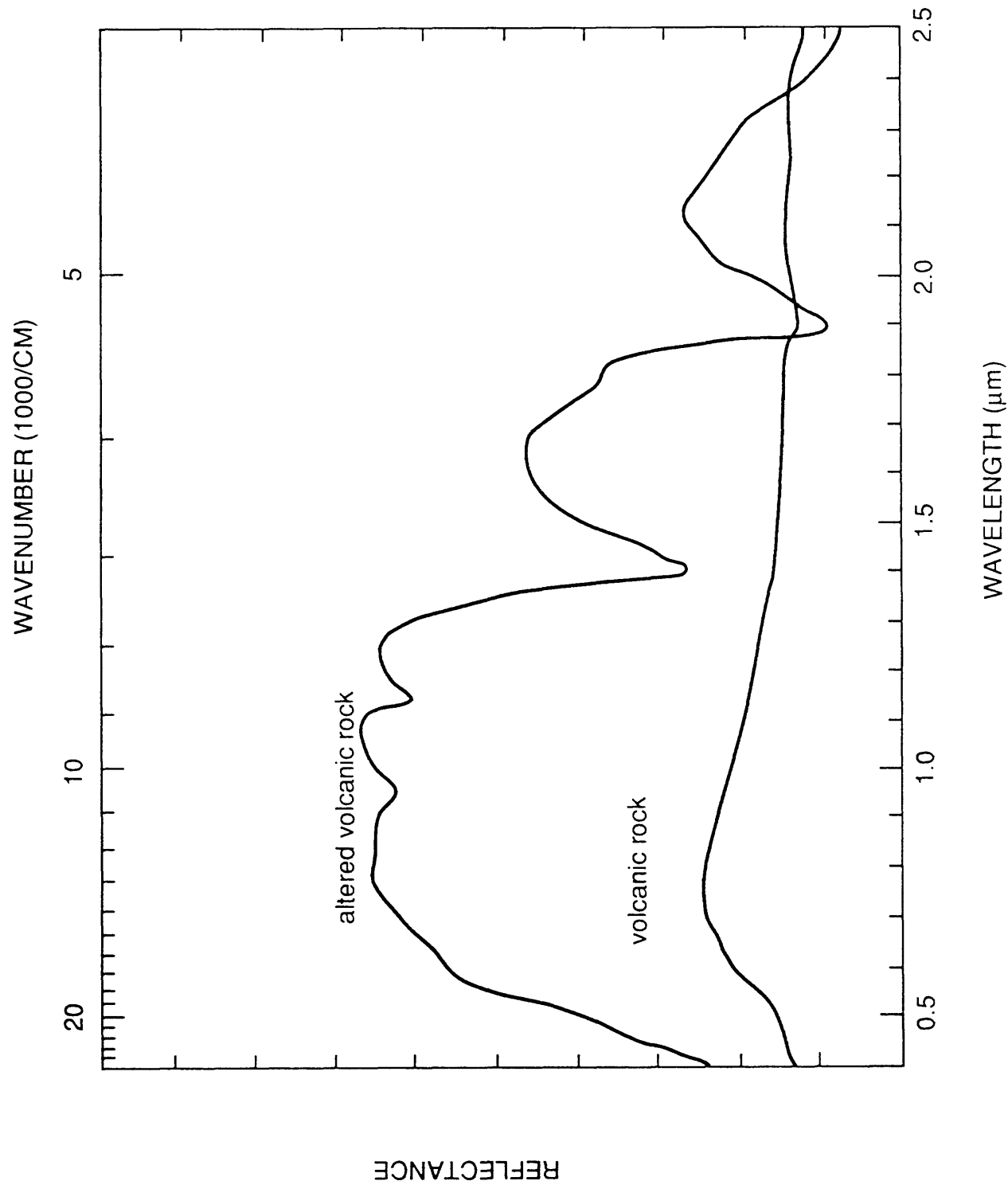


Figure 18. Spectra of Tertiary volcanic rocks (Peach Springs Tuff?, unit Tps, pl. 1), including altered sample collected north of Hackberry Mountains. The altered volcanic rocks should be very bright white but actually appear yellow on the image, possibly because of thin vegetation cover. Unaltered volcanic rocks are blue to slight magenta.

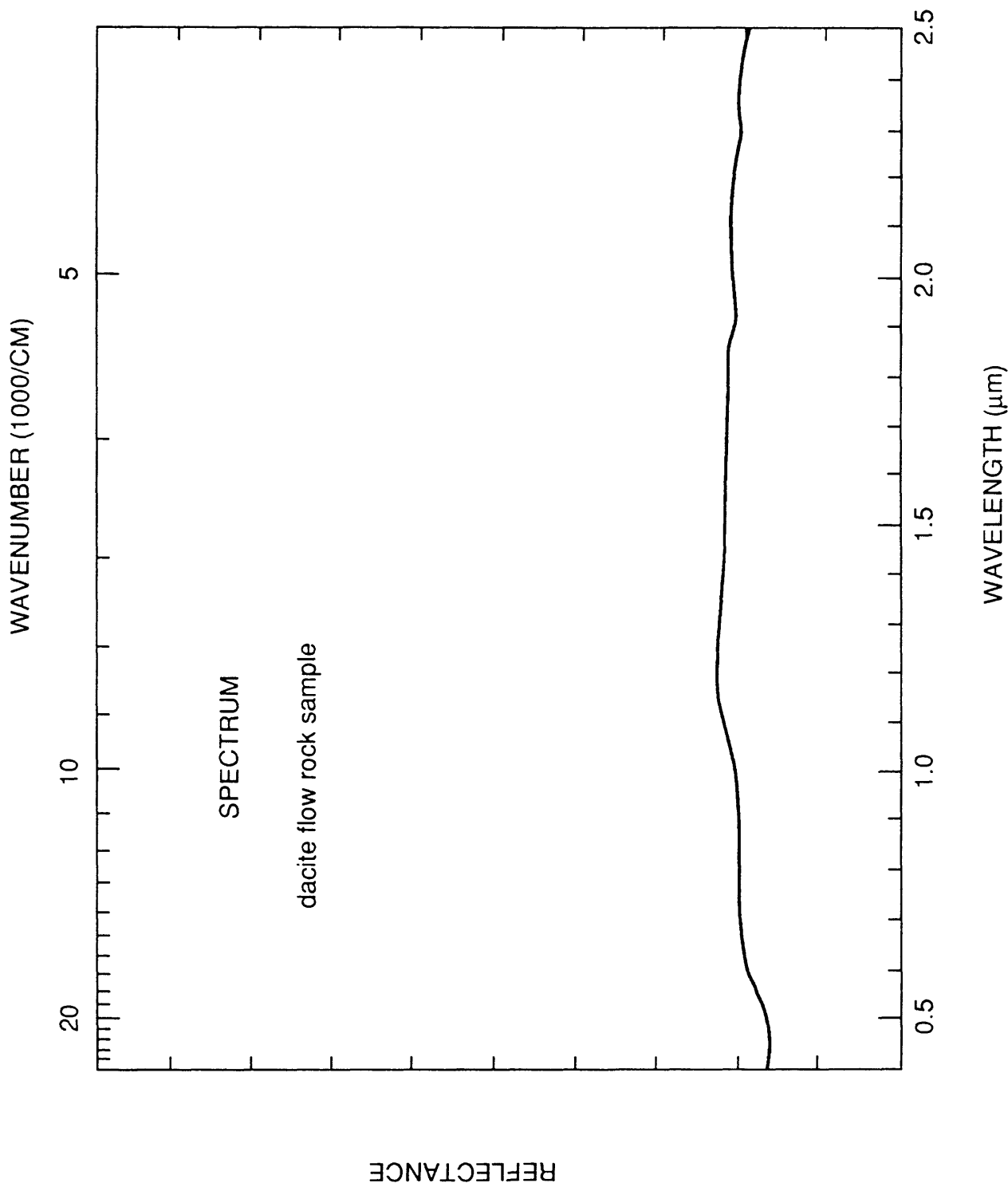


Figure 19. Spectrum of dacite (unit Td, pl. 1) collected in Piute Hills, near old Mohave road. Spectrally flat producing a blue color in this CRC color combination.

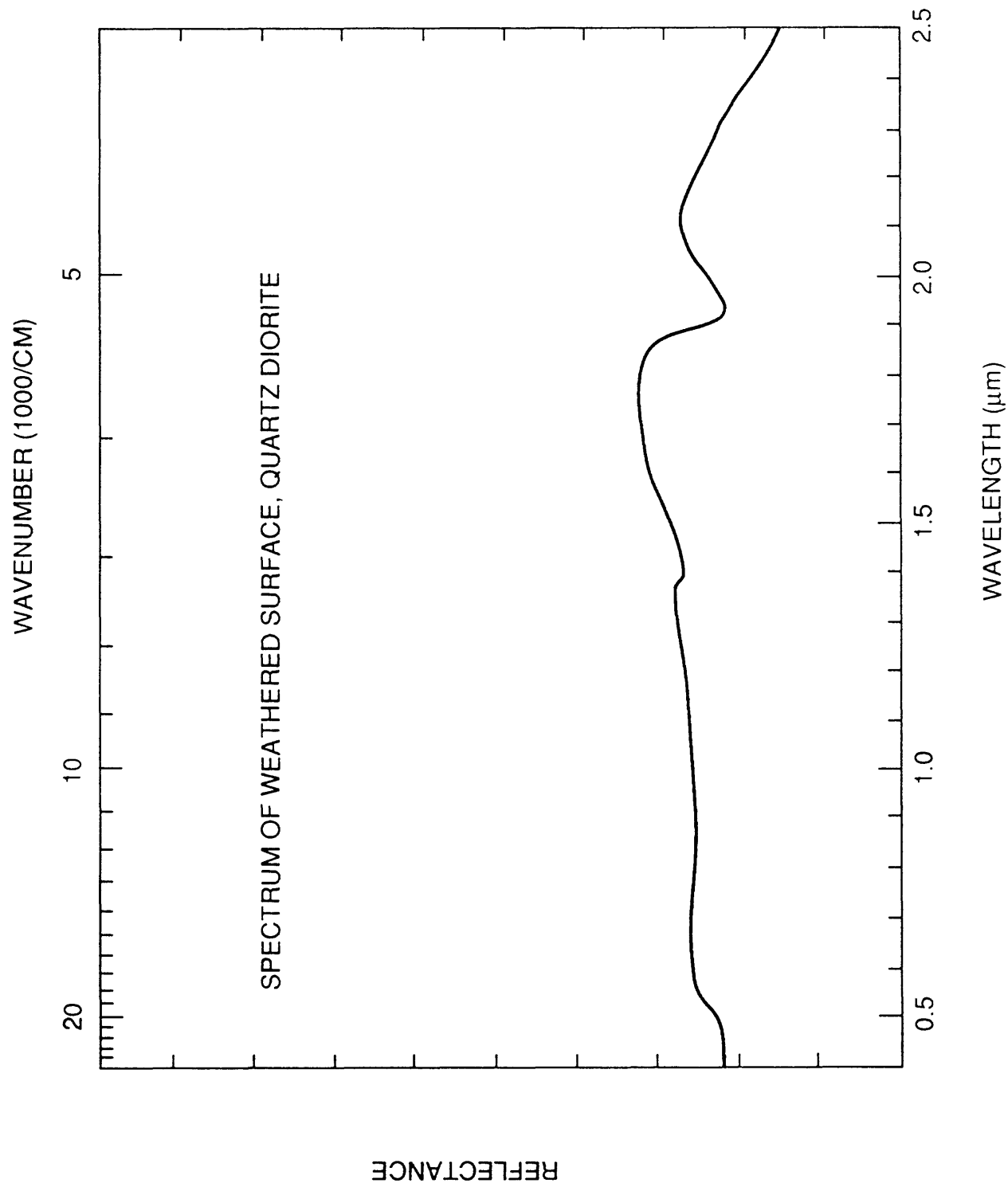


Figure 20. Spectrum of Proterozoic quartz diorite (unit Xg1, pl. 1) weathered surface, collected near True Blue Mine. Sample does not appear to be altered. Spectrally flat except for a slight absorption in the short wavelengths (TM channel 1) due to ferric iron on the weathered surface. TM color response will be blue with a very slight green component.

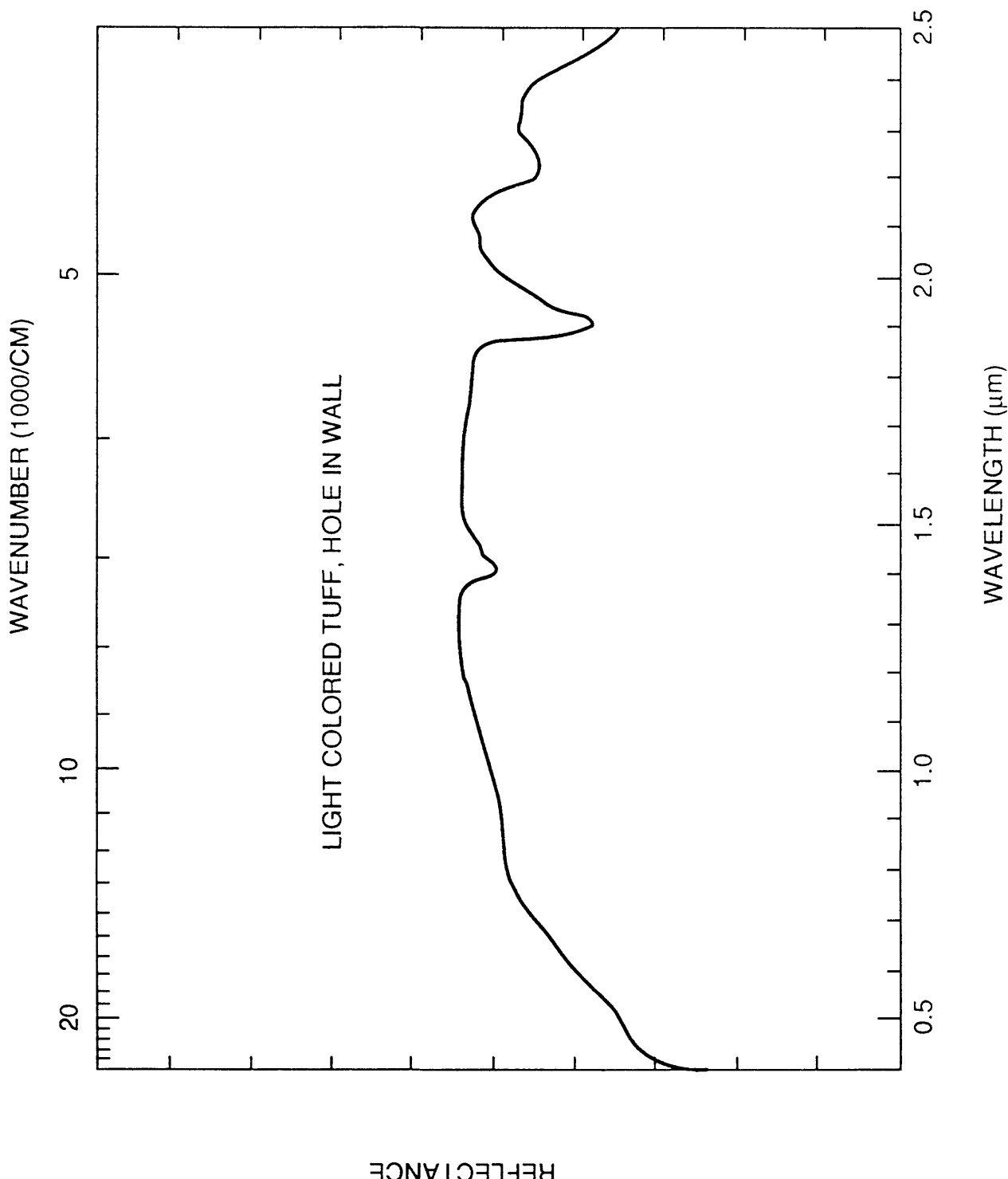


Figure 21. Spectrum of rhyolite ash flow tuff, (White Horse Mesa Tuff unit, TW, pl. 1) which appears to be slightly altered; collected near Hole-in-the-Wall campground. The spectrum of this very bright tuff does display an absorption band near 2.2 mm resulting in a high TM 5/7 (red) as well as moderately high TM 3/1 and 3/4. The unaltered rock can be confused with altered rocks because of the resulting white to yellow color response on TM imagery.

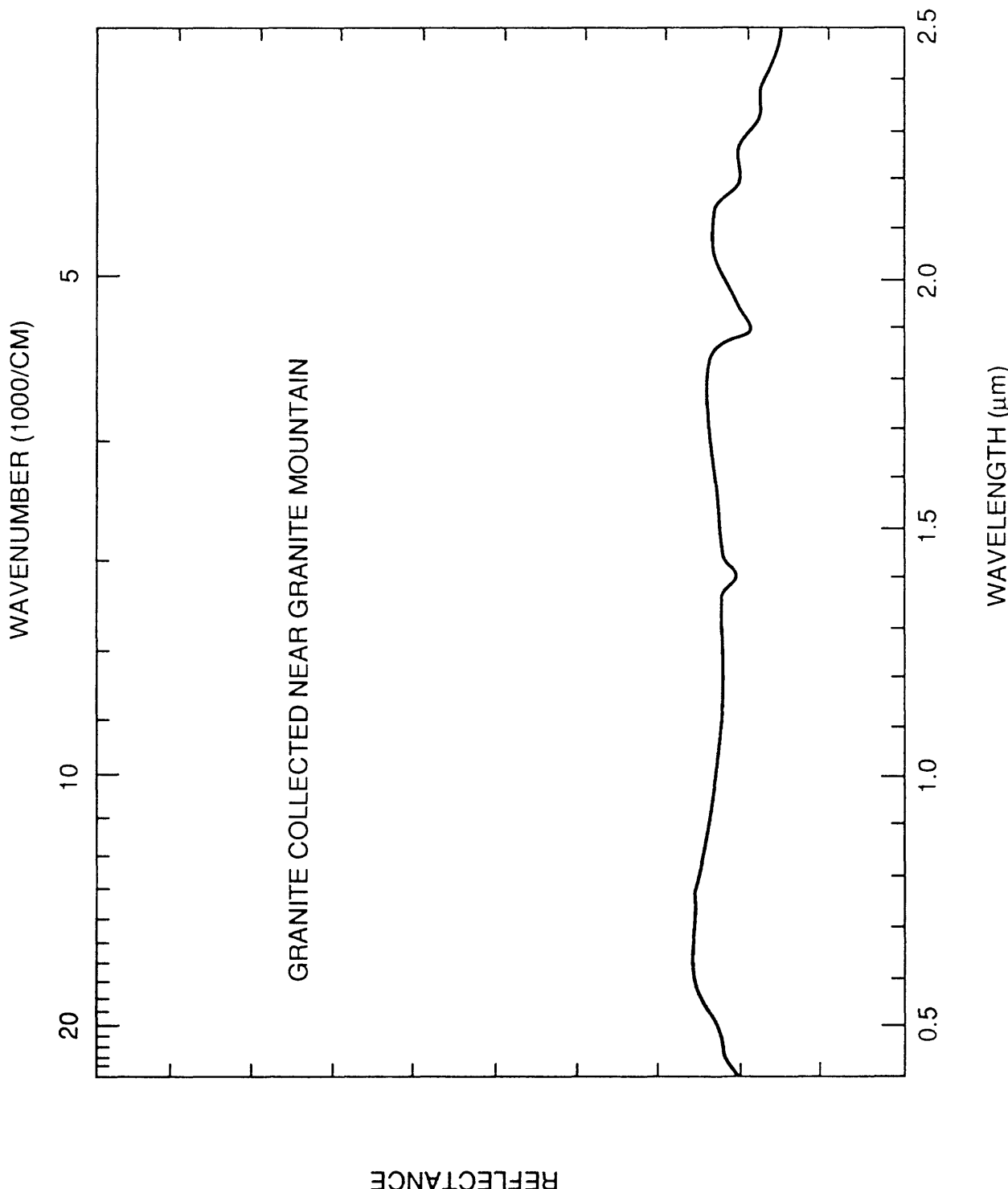


Figure 22. Spectrum of granite unit (Jqs, pl. 1) collected at Granite Pass. Because of the 2.2 mm and 2.34 mm absorption due to micaceous minerals, TM 5/7 (red) will be high. Weathering of biotite results in ferric iron absorption (TM 3/1 high) and should produce a green component. The ferric iron band is relatively weak for most of the exposed granite in the image resulting in a blue color.

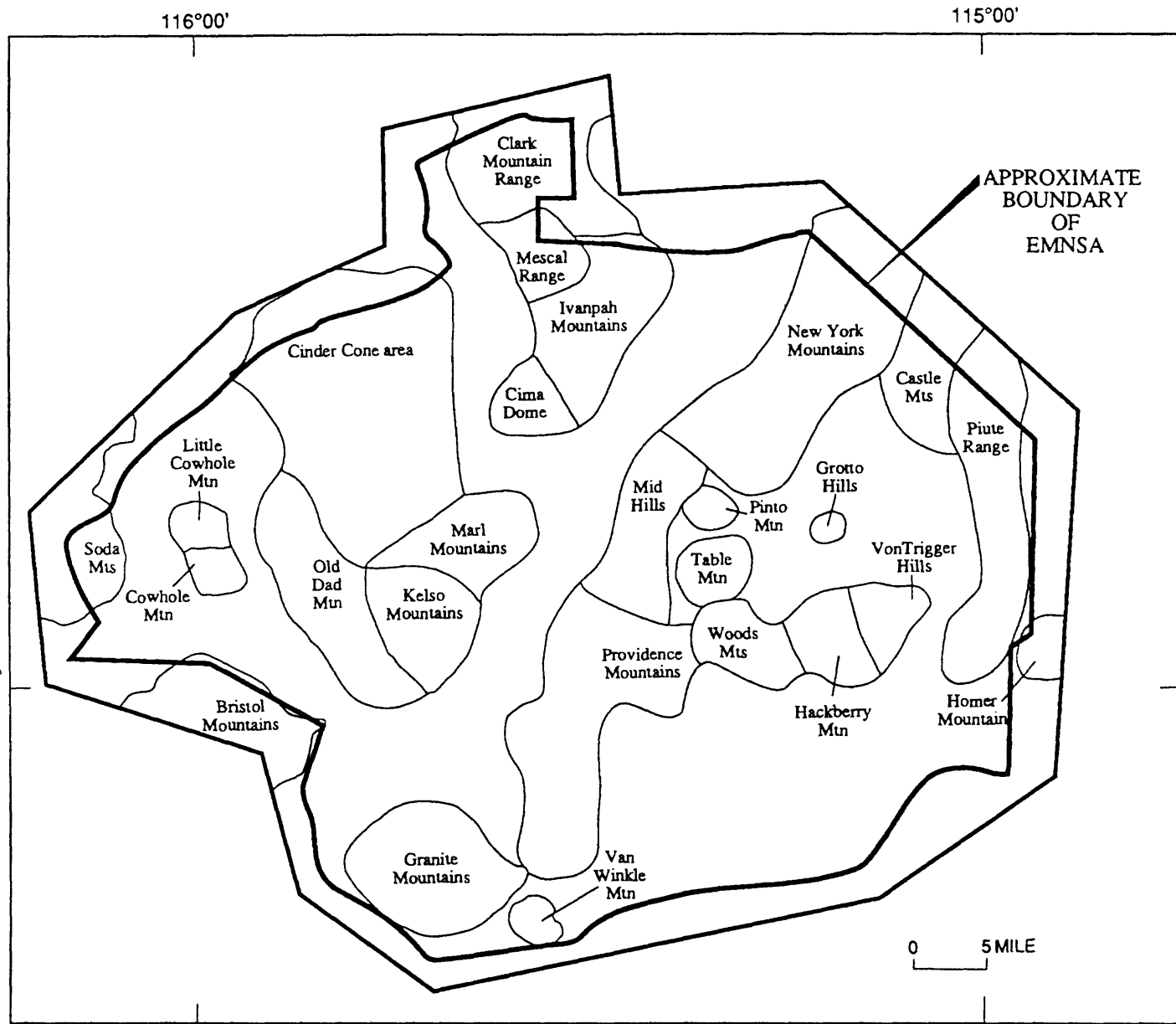


Figure 23. Map of the East Mojave National Scenic Area, Calif., showing geographic areas discussed in section on geochemistry of RASS, PLUTO, and NURE data bases.

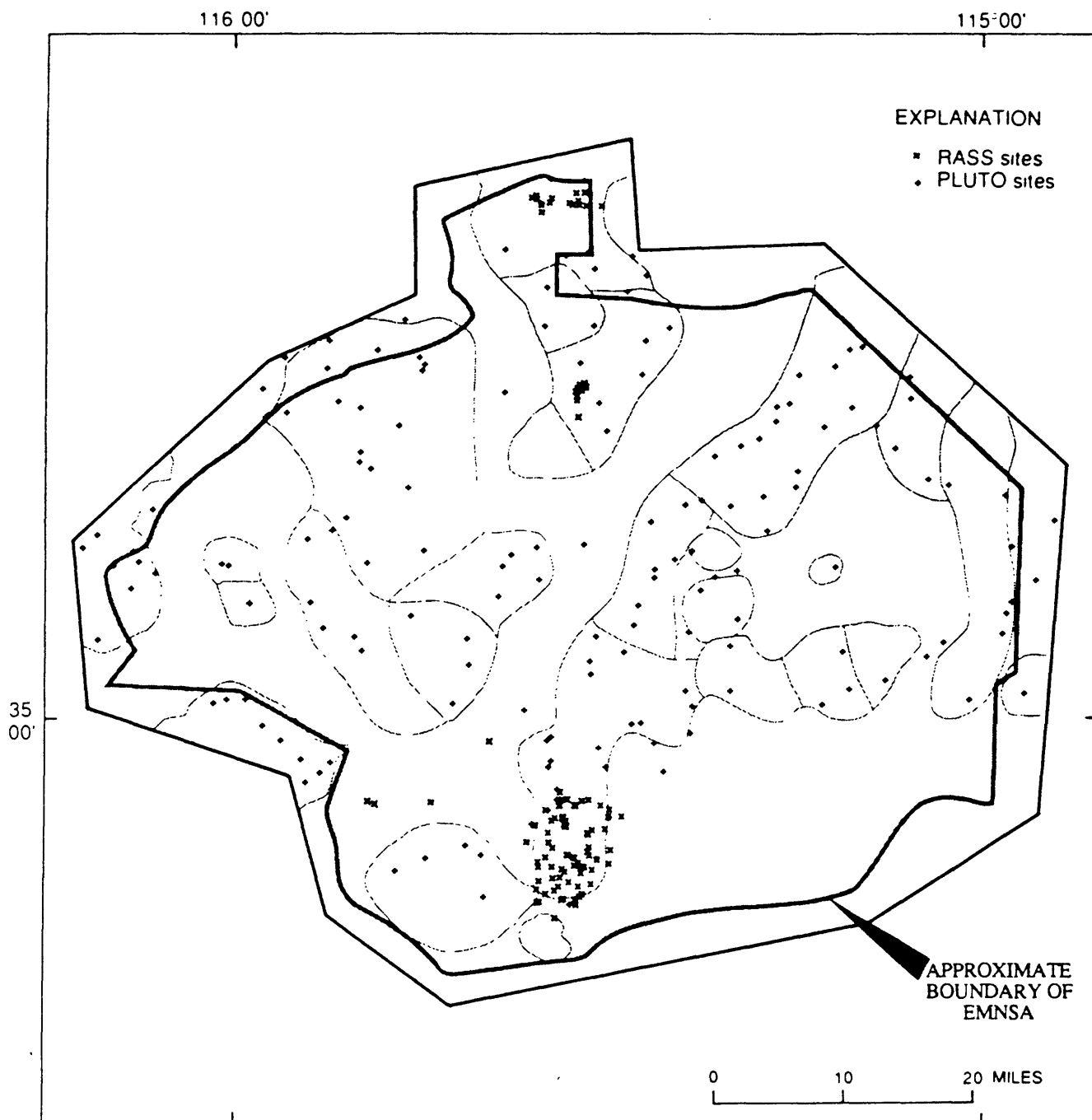


Figure 24. Sampling sites for RASS and PLUTO stream-sediment samples from the East Mojave National Scenic Area, Calif.

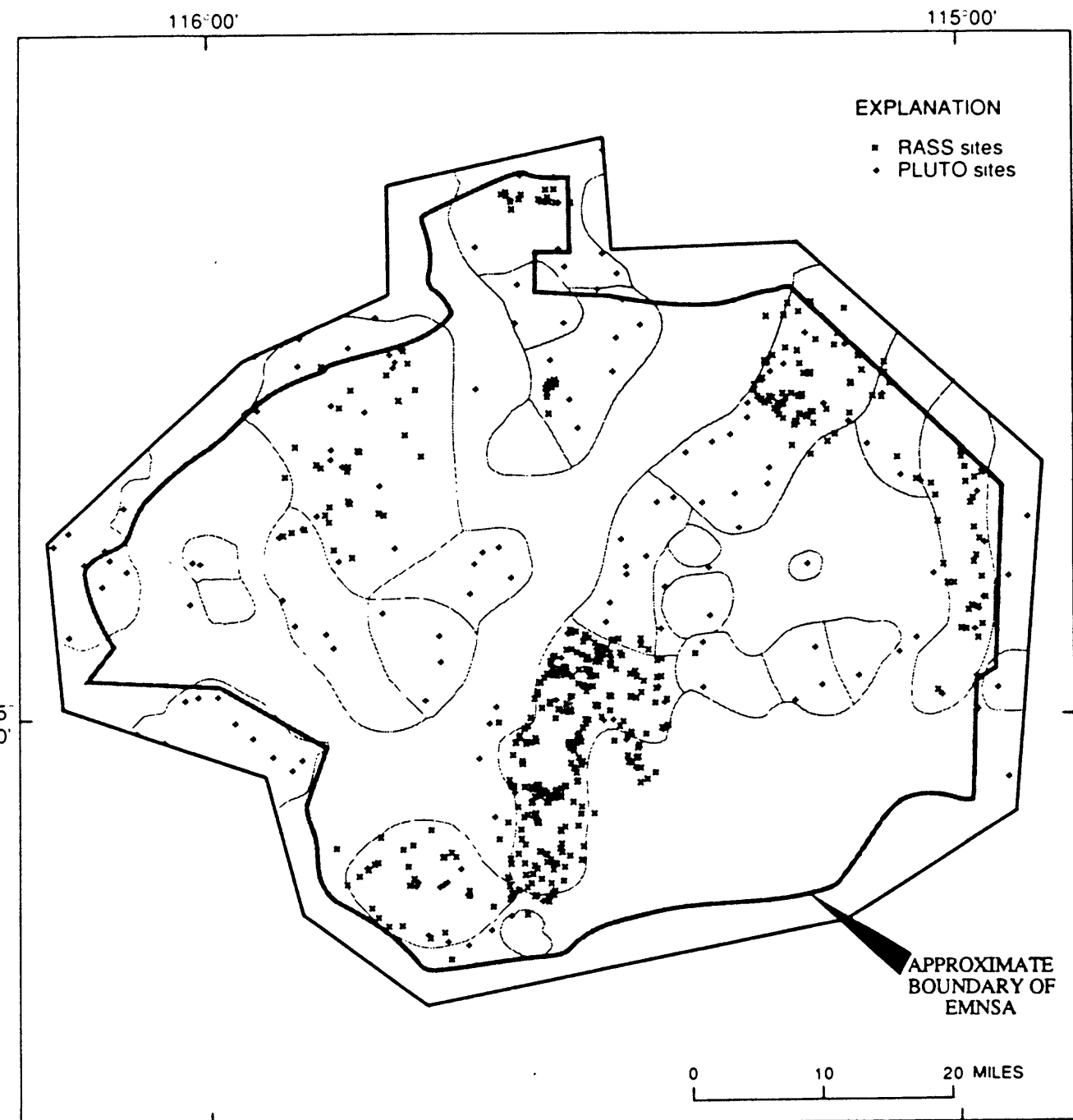


Figure 25. Sampling sites for RASS and PLUTO heavy-mineral-concentrate samples from the East Mojave National Scenic Area, Calif.

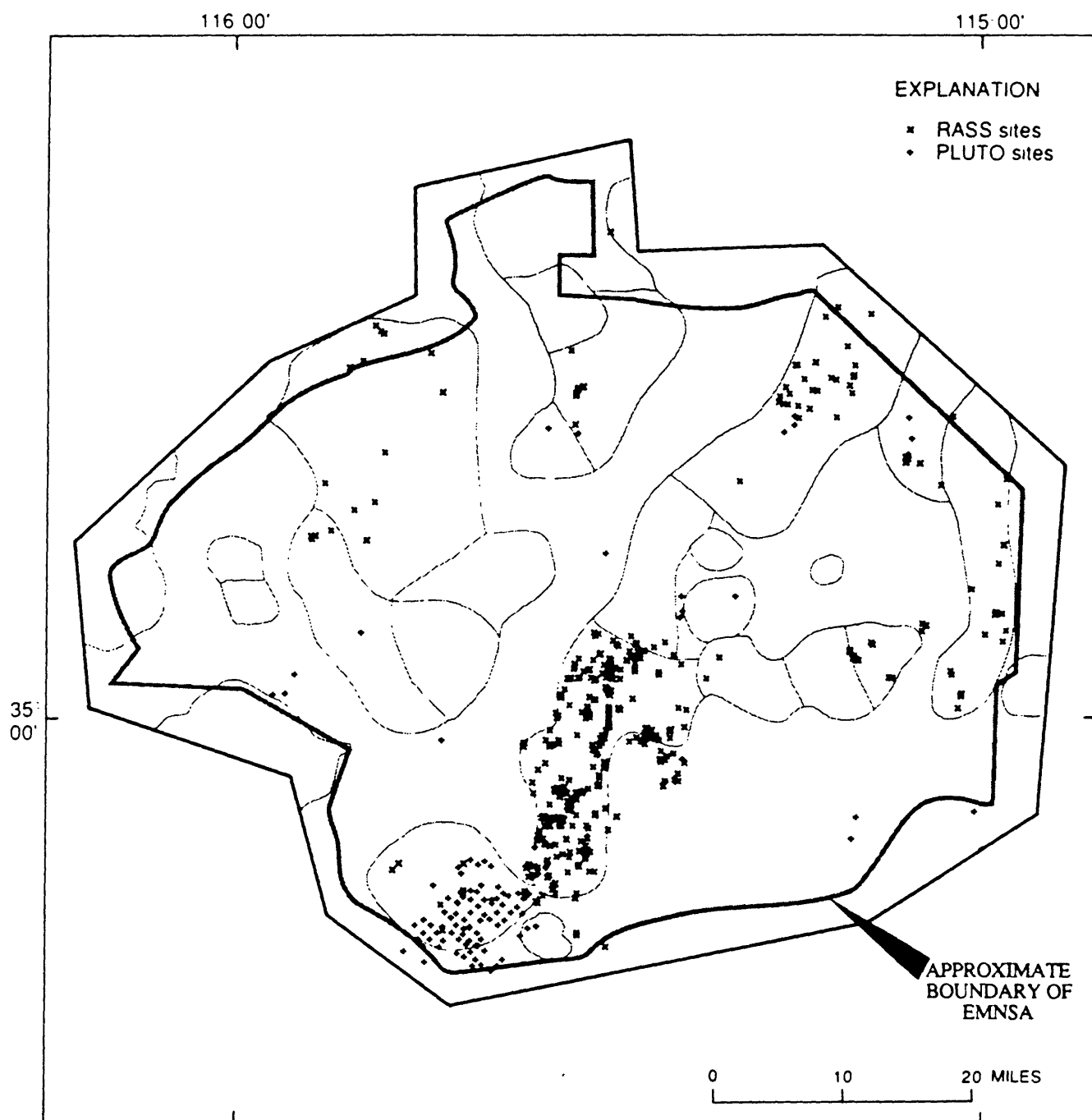


Figure 26. Sampling sites for RASS and PLUTO rock samples from the East Mojave National Scenic Area, Calif.

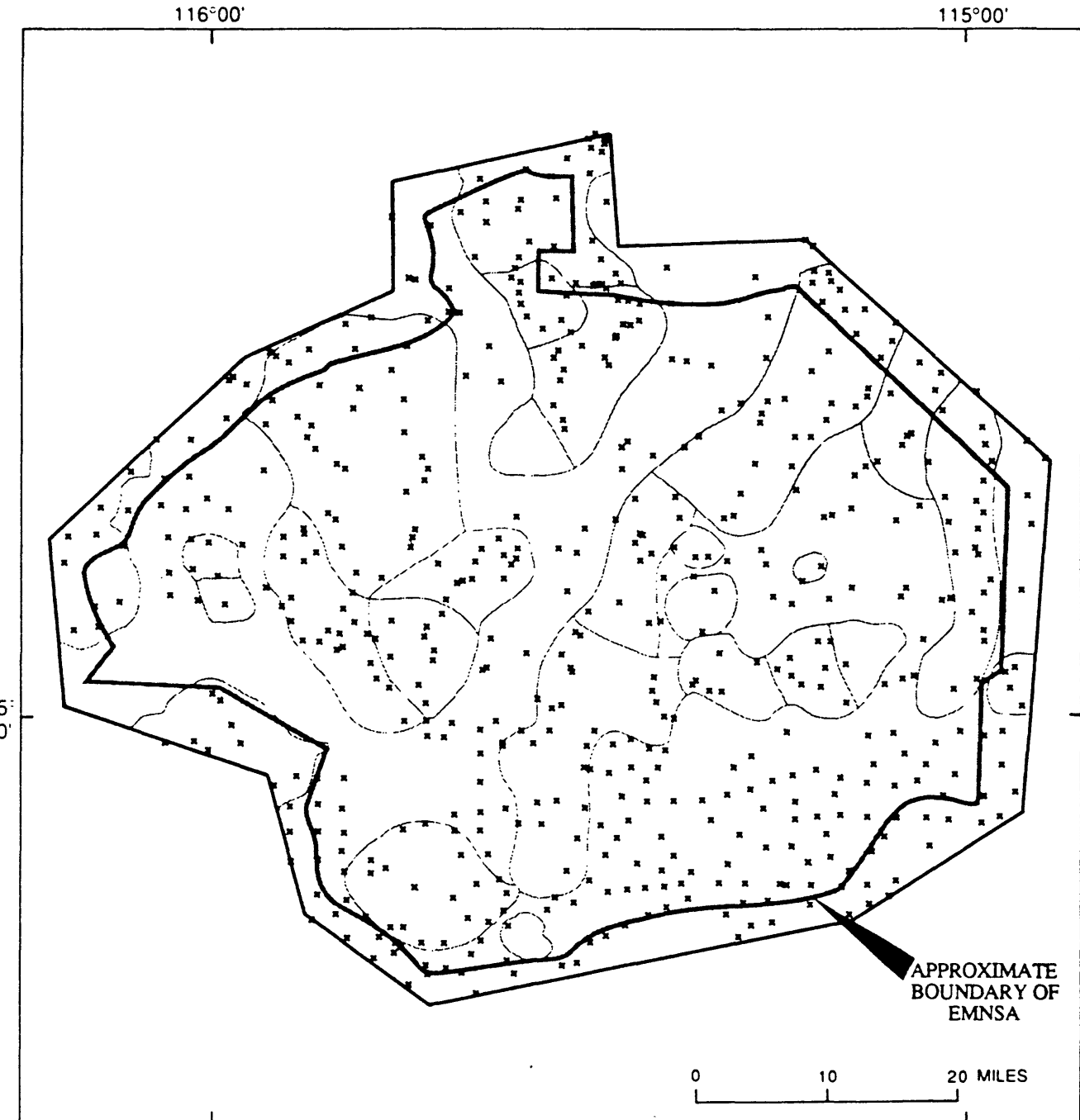


Figure 27. Sampling sites for NURE stream-sediment and soil samples from the East Mojave National Scenic Area, Calif.

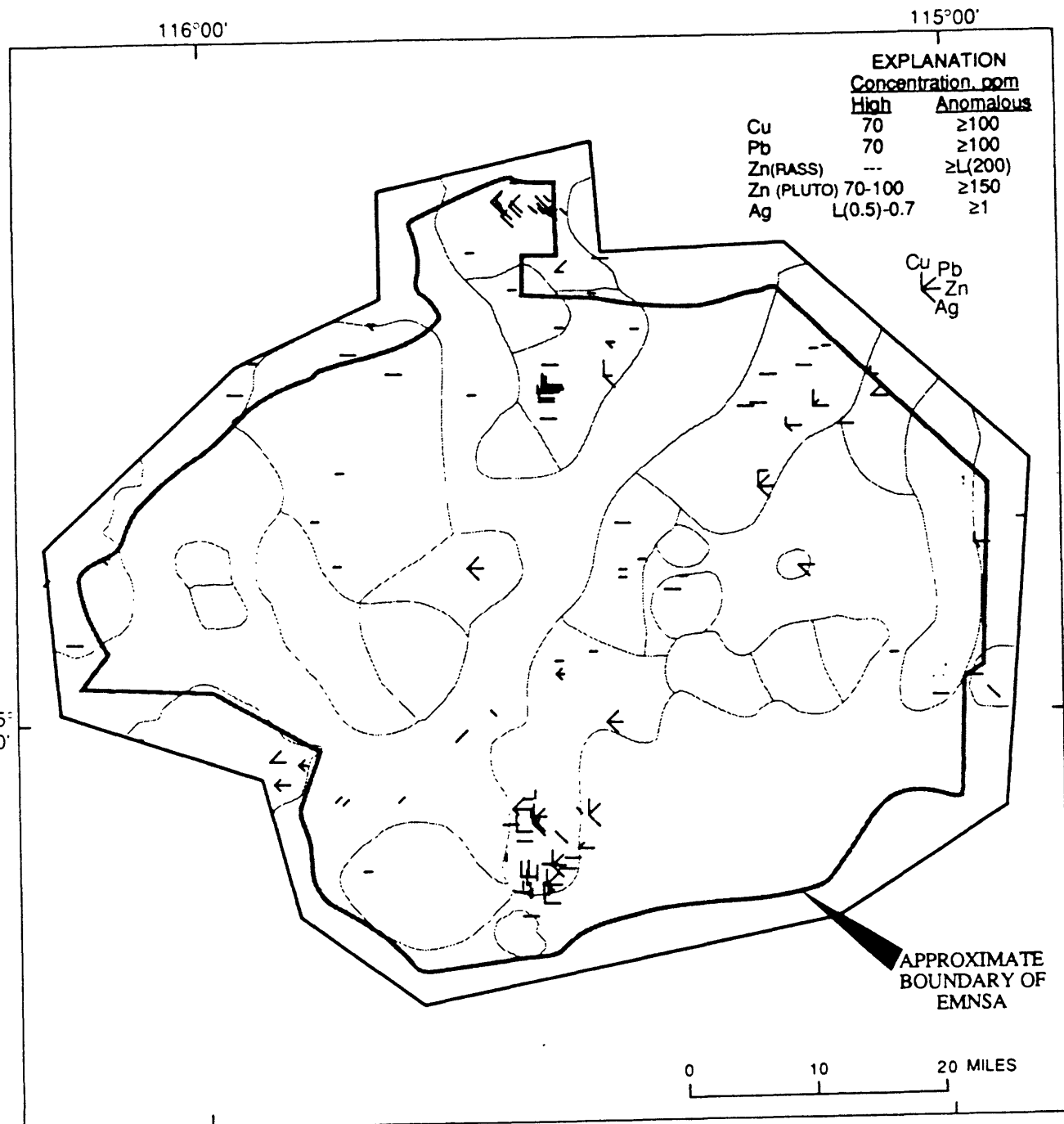


Figure 28. Distribution of anomalous and high concentrations of Cu, Pb, Zn, and Ag in RASS and PLUTO stream-sediment samples from the East Mojave National Scenic Area, Calif. If symbols show more than one length, longer length indicates anomalous value present above threshold values given in table 6; shorter length indicates value of element approximately equivalent to 90th percentile up to threshold, defined as highest background.

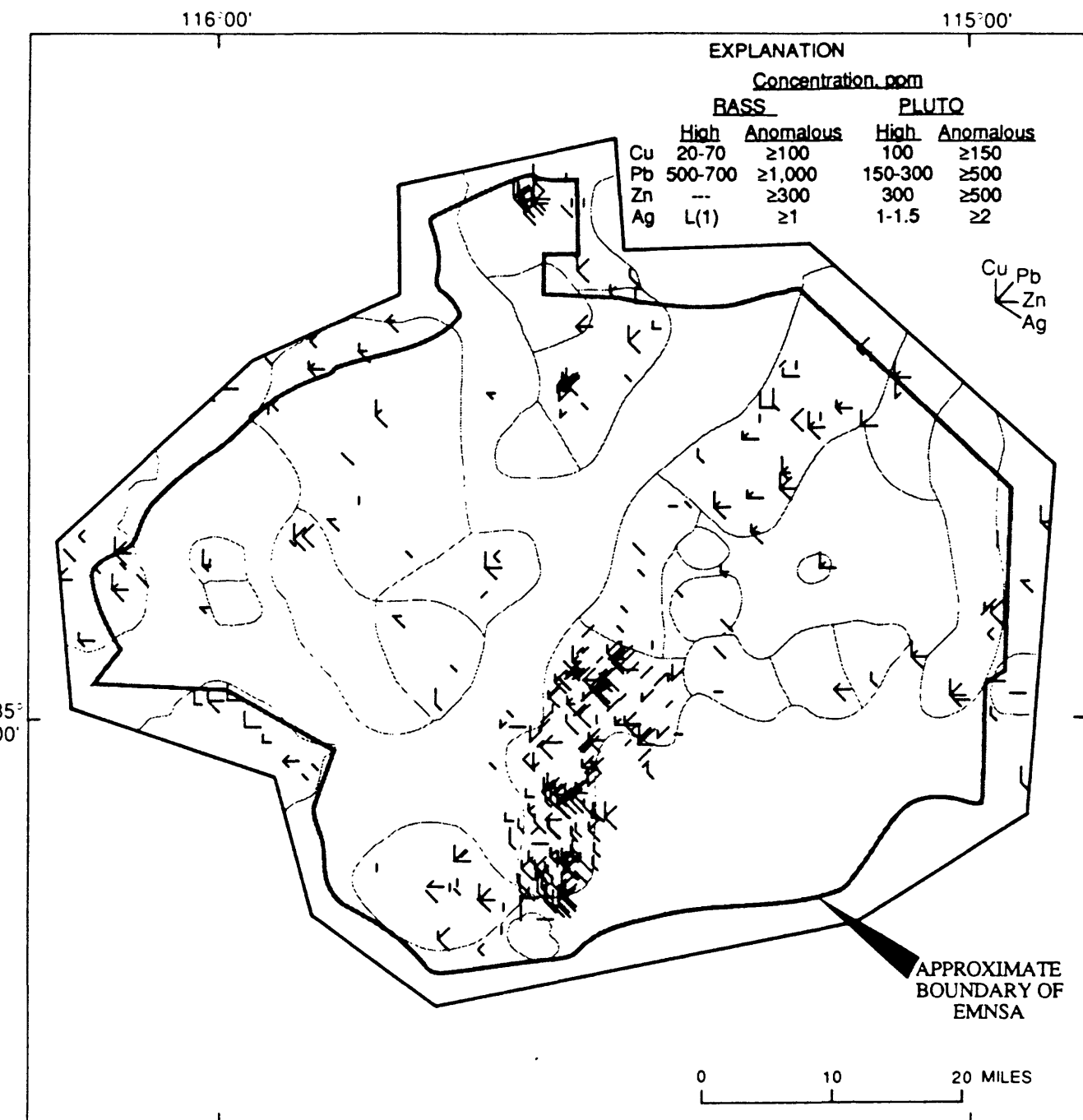


Figure 29. Distribution of anomalous and high concentrations of Cu, Pb, Zn, and Ag in RASS and PLUTO heavy-mineral-concentrate samples from the East Mojave National Scenic Area, Calif. Symbols explained on figure 28.

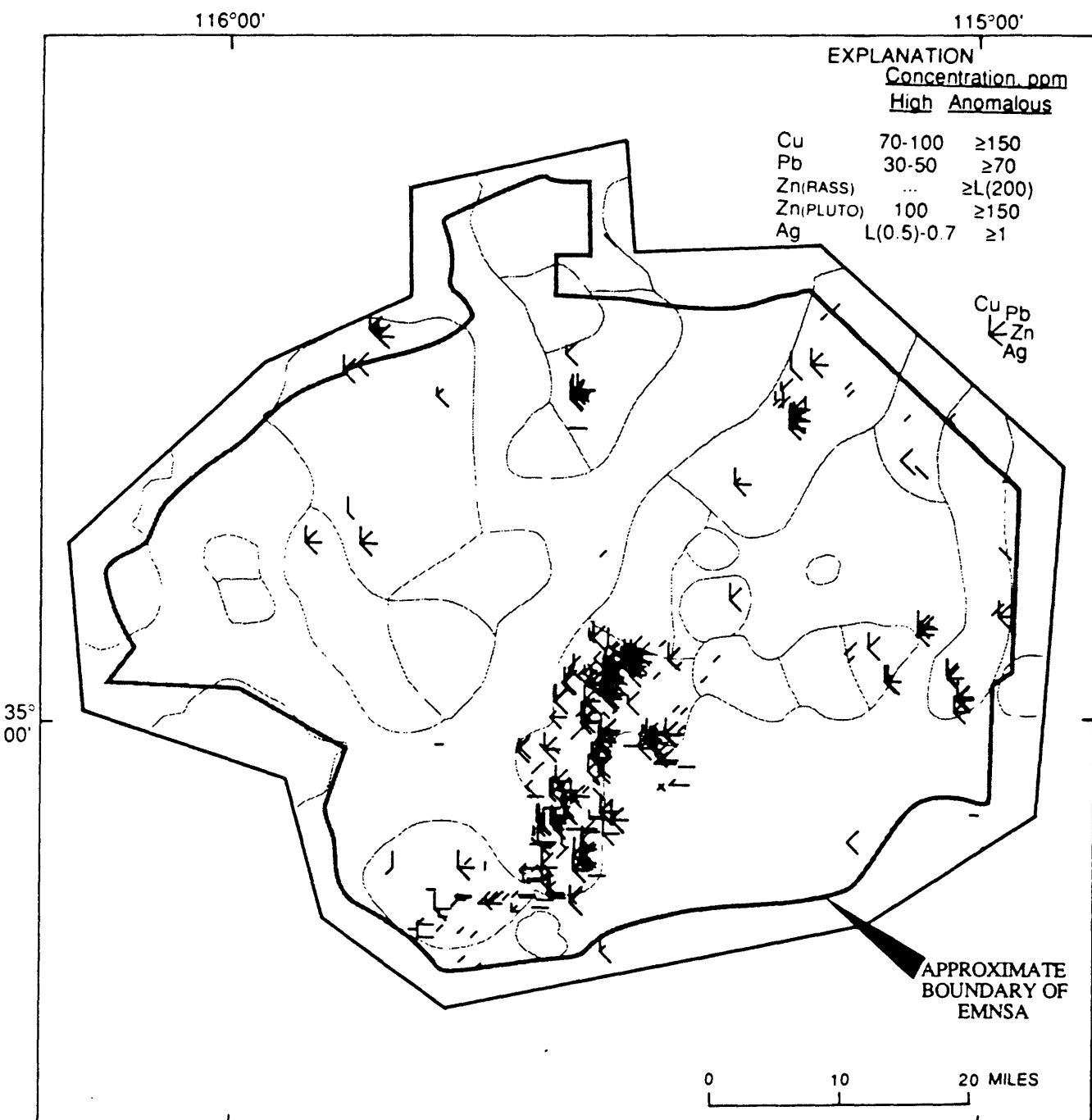


Figure 30. Distribution of anomalous and high concentrations of Cu, Pb, Zn, and Ag in RASS and PLUTO rock samples from the East Mojave National Scenic Area, Calif. Symbols explained on figure 28.

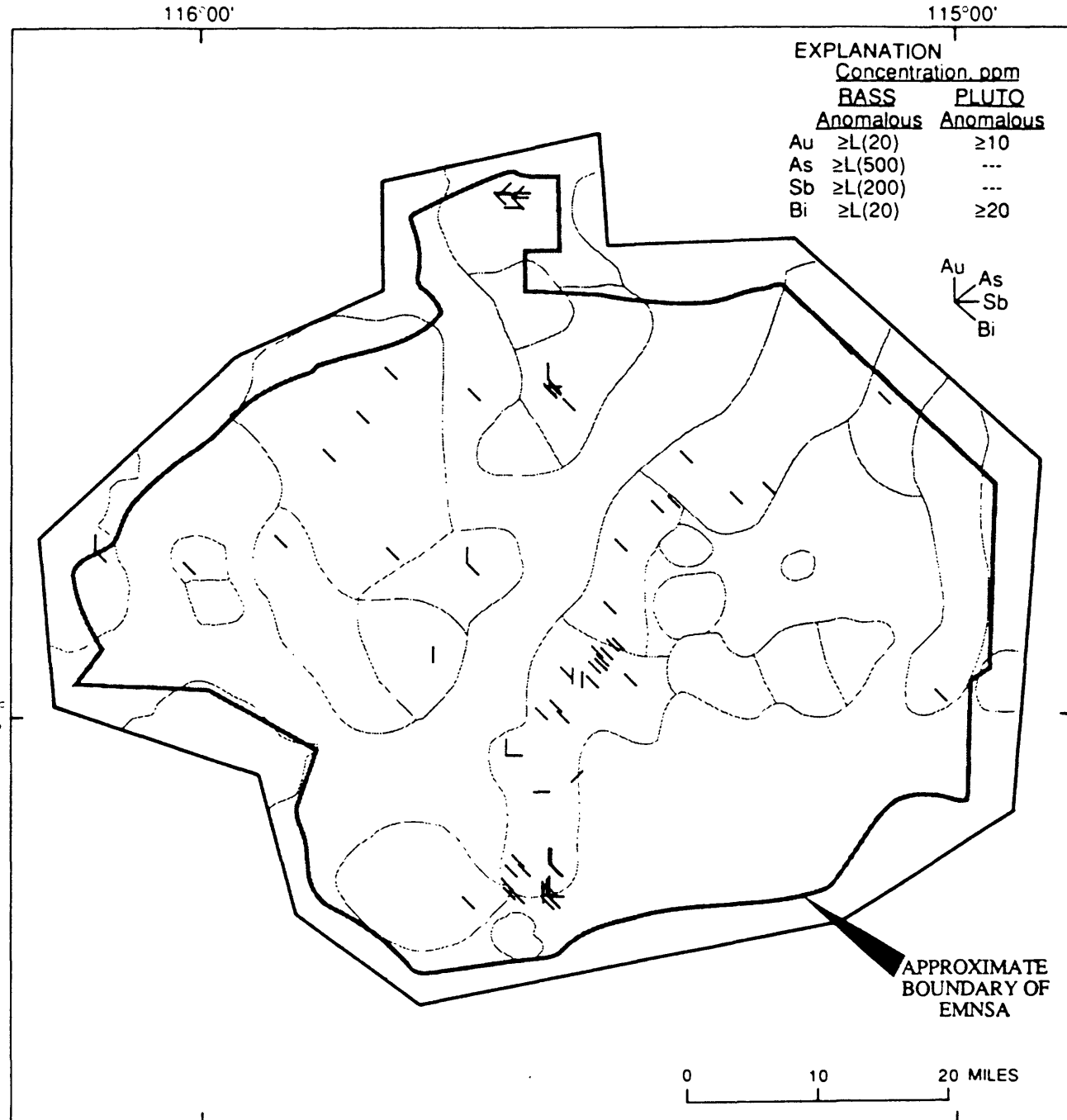


Figure 31. Distribution of anomalous concentrations of Au, As, Sb, and Bi in RASS and PLUTO heavy-mineral-concentrate samples from the East Mojave National Scenic Area, Calif. Symbols explained on figure 28.

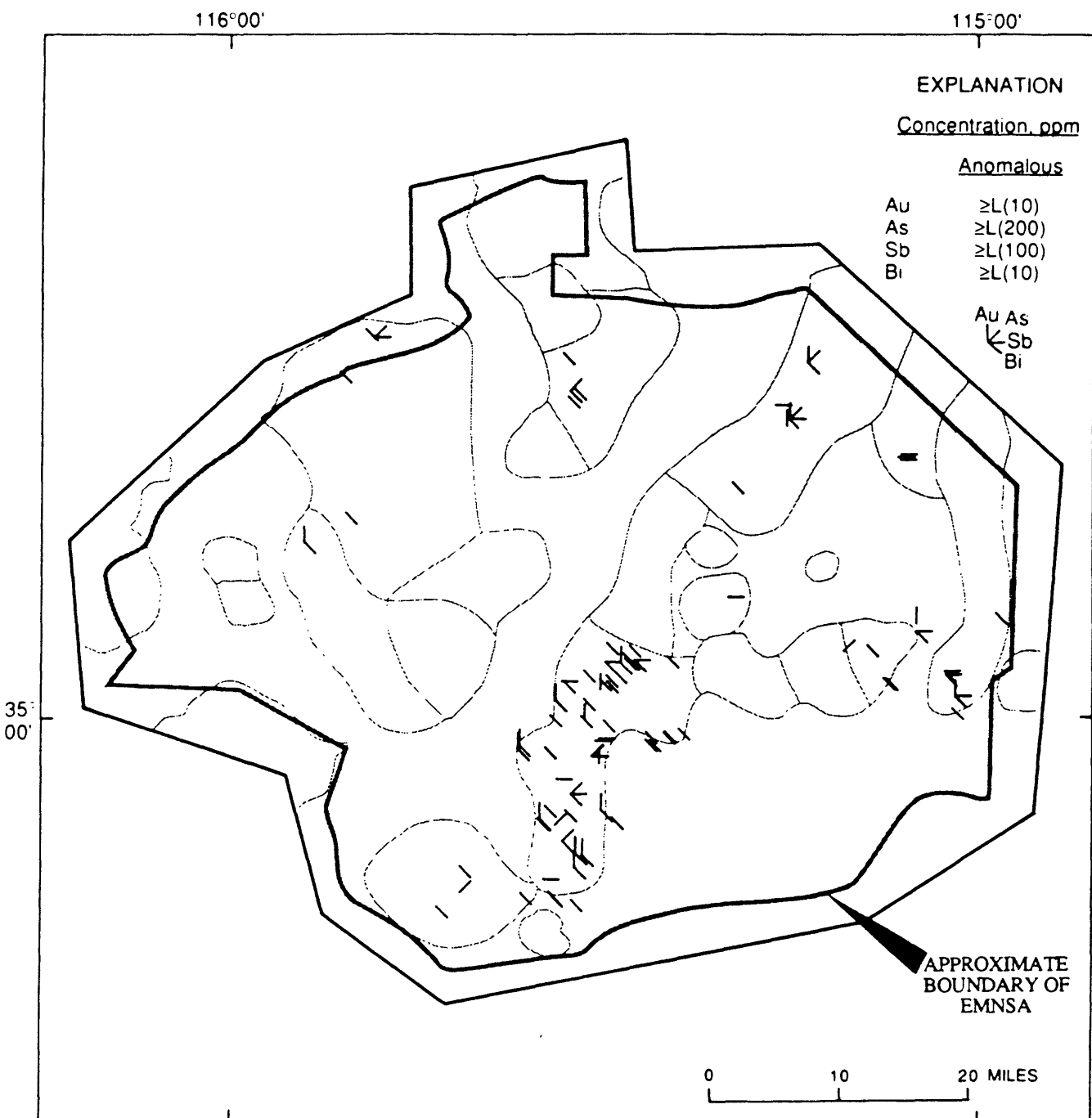


Figure 32. Distribution of anomalous concentrations of Au, As, Sb, and Bi in RASS and PLUTO rock samples from the East Mojave National Scenic Area, Calif. Symbols explained on figure 28.

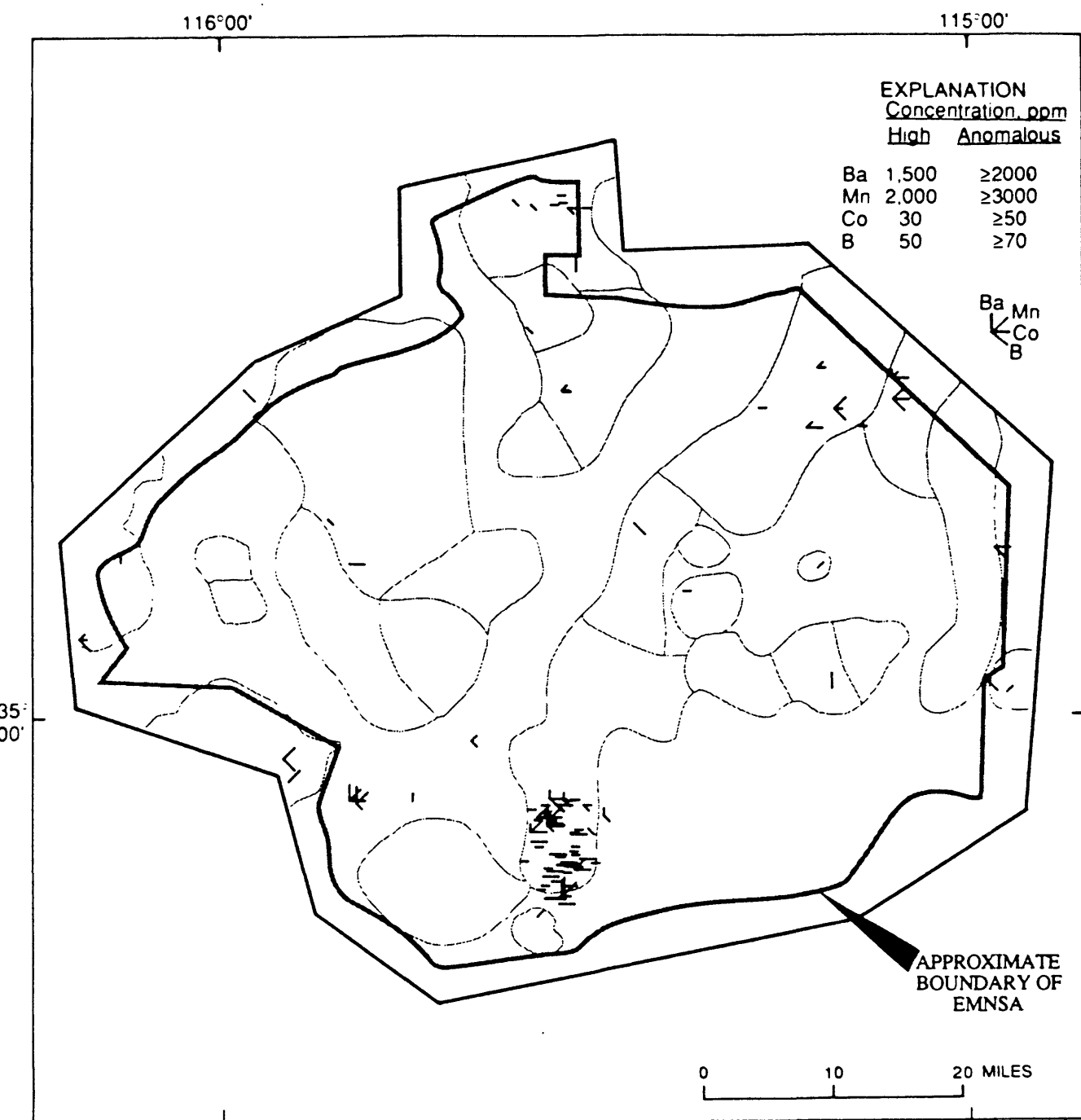


Figure 33. Distribution of anomalous and high concentrations of Ba, Mn, Co, and B in RASS and PLUTO stream-sediment samples from the East Mojave National Scenic Area, Calif. Symbols explained on figure 28.

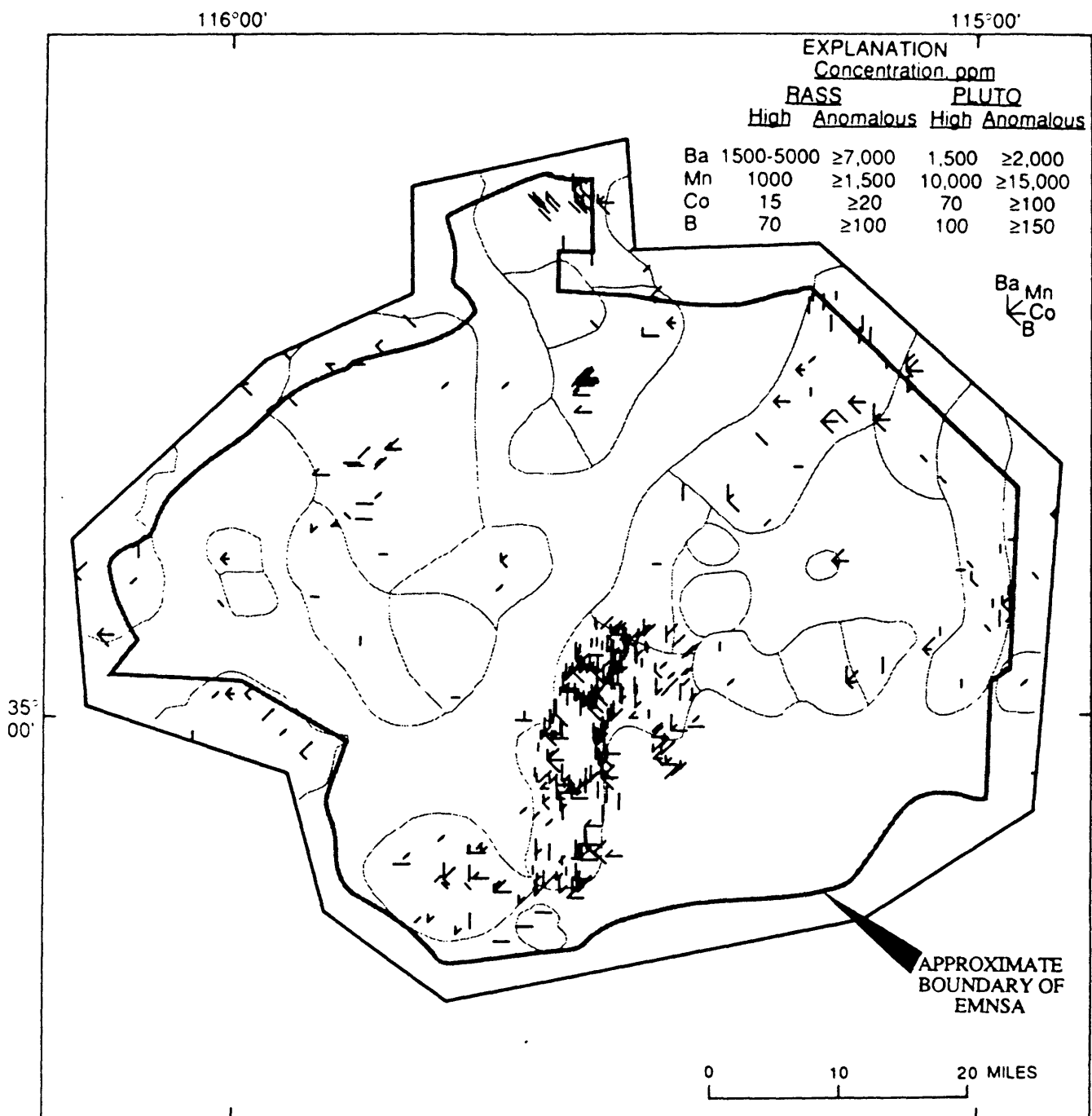


Figure 34. Distribution of anomalous and high concentrations of Ba, Mn, Co, and B in RASS and PLUTO heavy-mineral-concentrate samples from the East Mojave National Scenic Area, Calif. Symbols explained on figure 28.

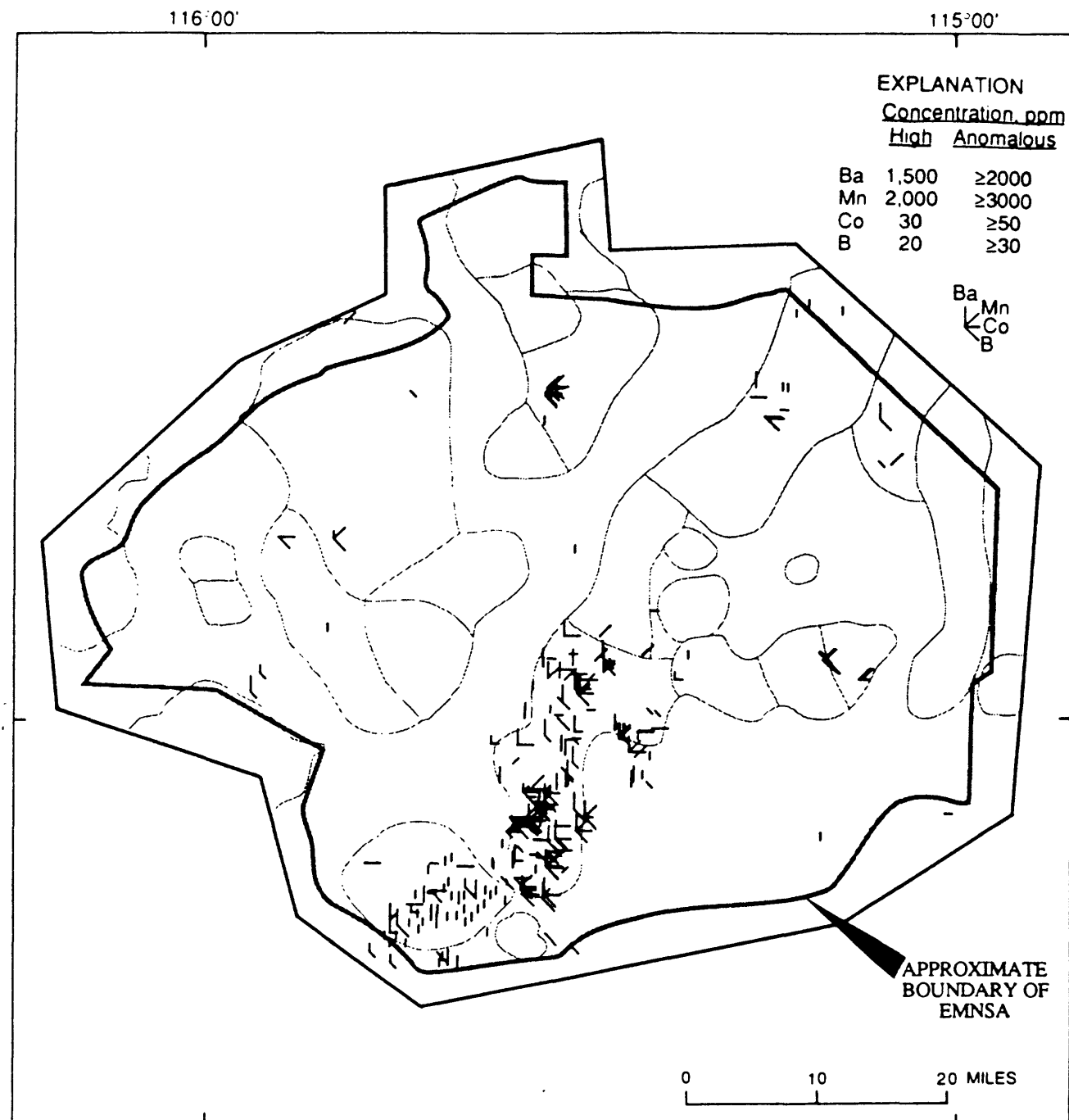


Figure 35. Distribution of anomalous and high concentrations of Ba, Mn, Co, and B in RASS and PLUTO rock samples from the East Mojave National Scenic Area, Calif. Symbols explained on figure 28.

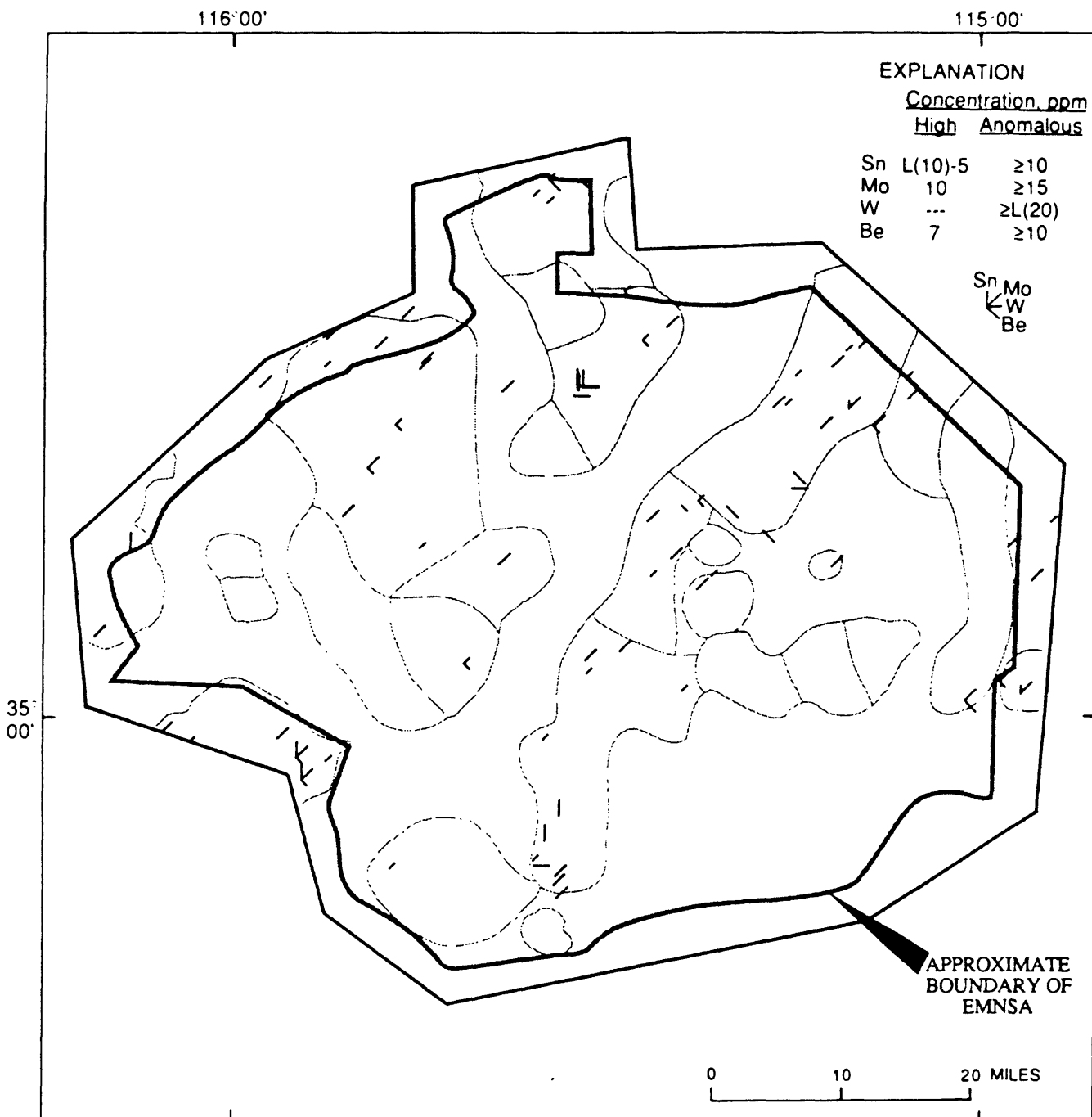


Figure 36. Distribution of anomalous and high concentrations of Sn, Mo, W, and Be in RASS and PLUTO stream-sediment samples from the East Mojave National Scenic Area, Calif. Symbols explained on figure 28.

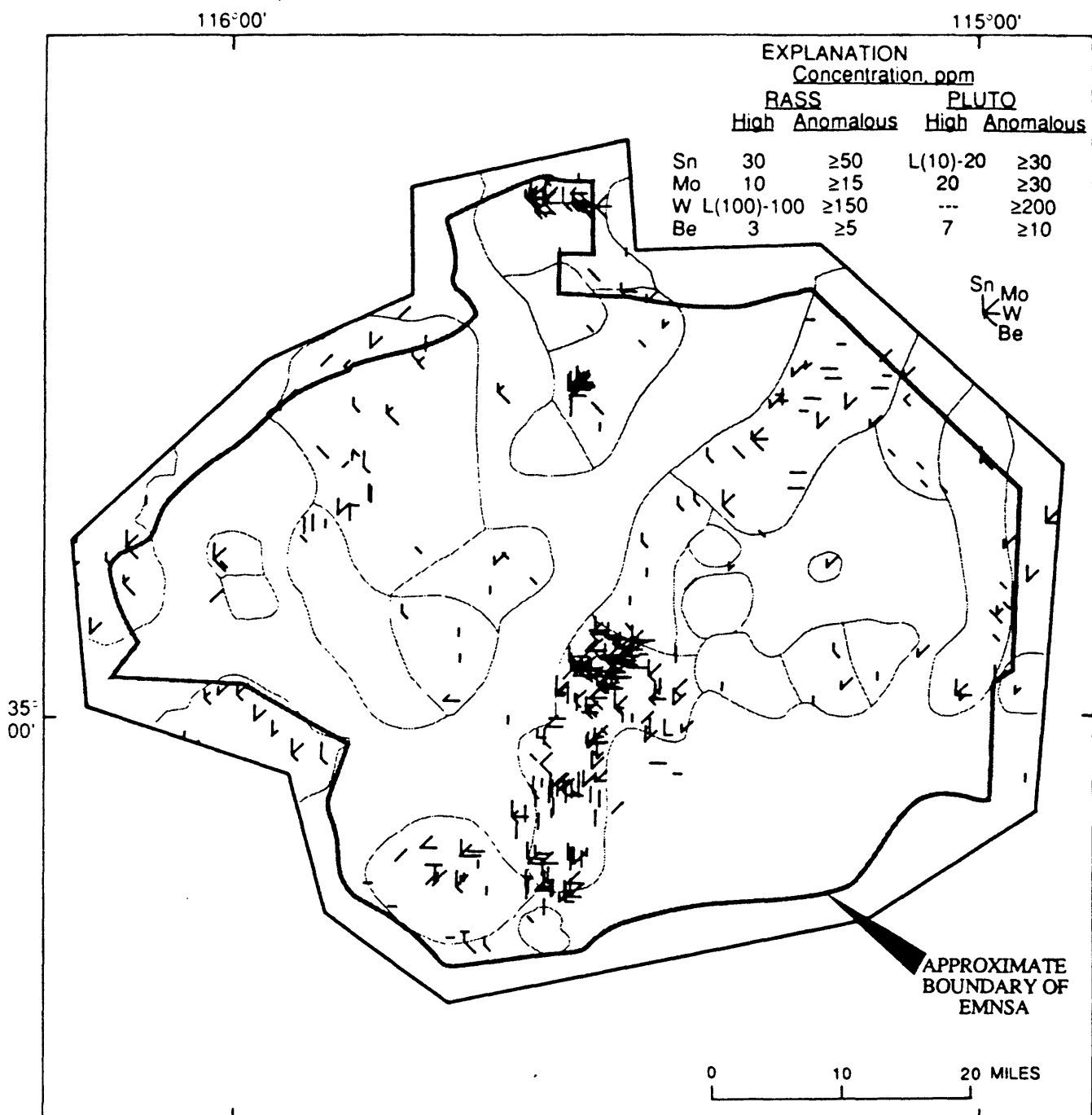


Figure 37. Distribution of anomalous and high concentrations of Sn, Mo, W, and Be in RASS and PLUTO heavy-mineral-concentrate samples from the East Mojave National Scenic Area, Calif. Symbols explained on figure 28.

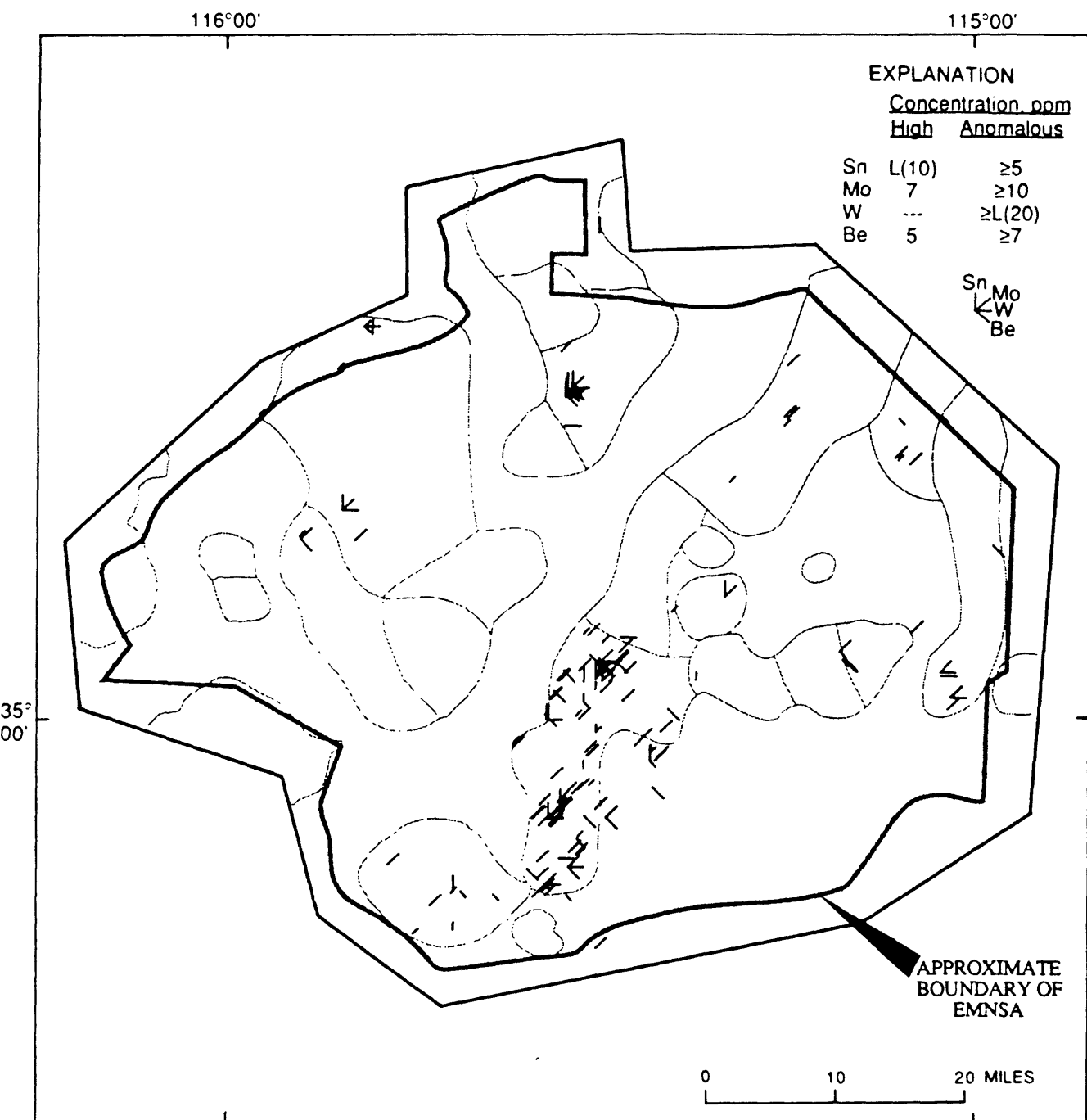


Figure 38. Distribution of anomalous and high concentrations of Sn, Mo, W, and Be in RASS and PLUTO rock samples from the East Mojave National Scenic Area, Calif. Symbols explained on figure 28.

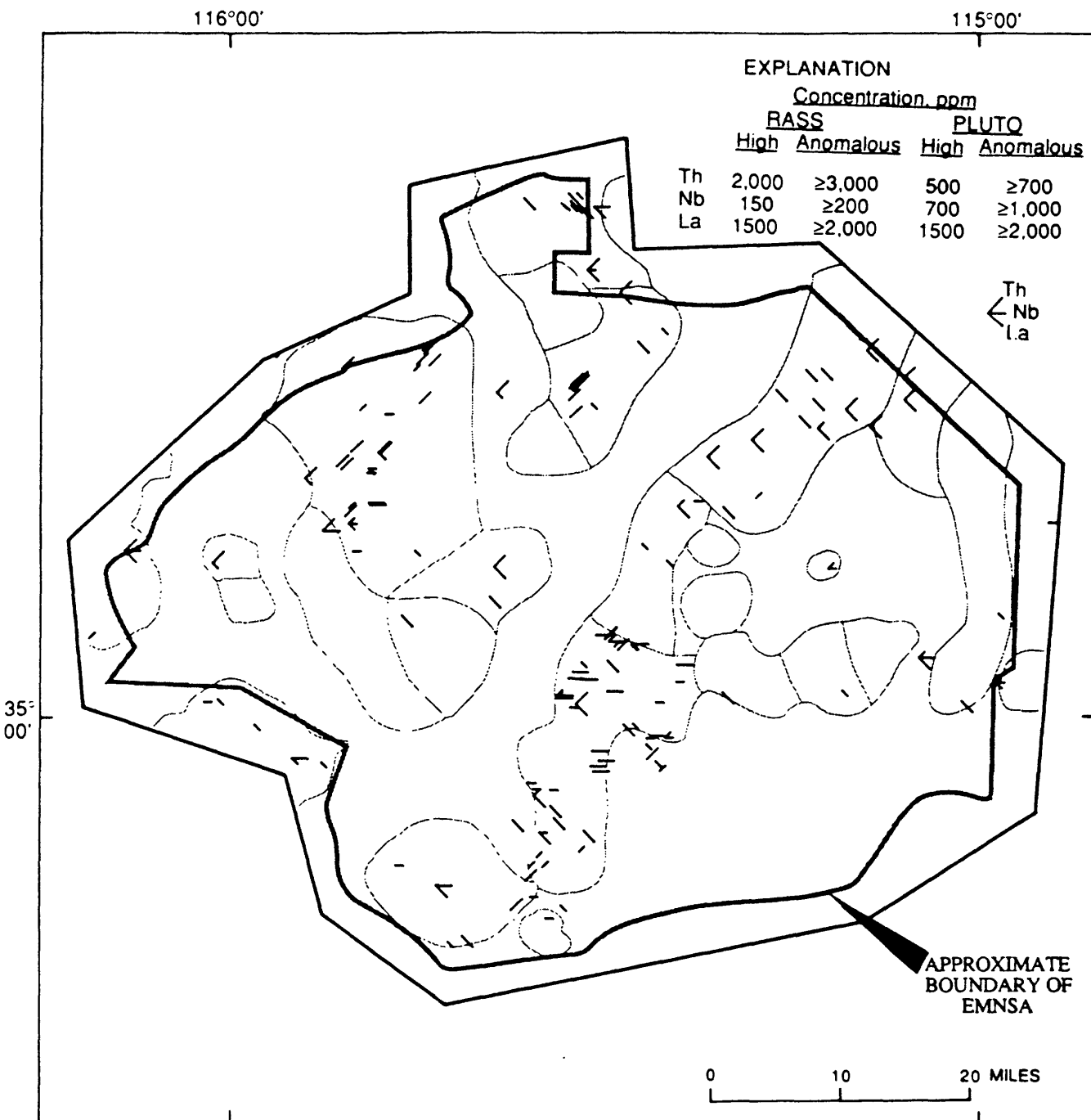


Figure 39. Distribution of anomalous and high concentrations of Th, Nb, and La in RASS and PLUTO heavy-mineral-concentrate samples from the East Mojave National Scenic Area, Calif. Symbols explained on figure 28.

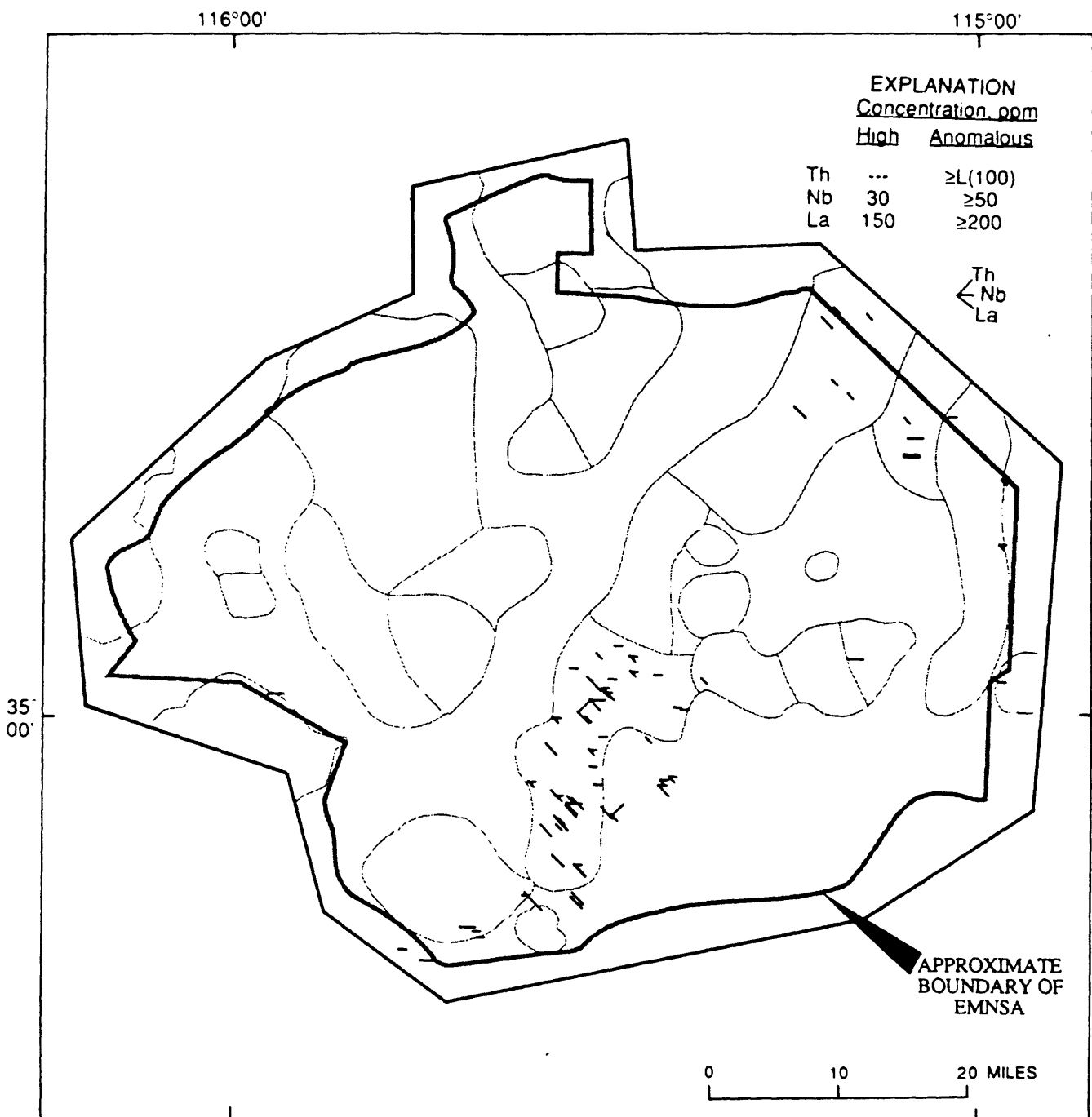


Figure 40. Distribution of anomalous and high concentration of Th, Nb, and La in RASS and PLUTO rock samples from the East Mojave National Scenic Area, Calif. Symbols explained on figure 28.

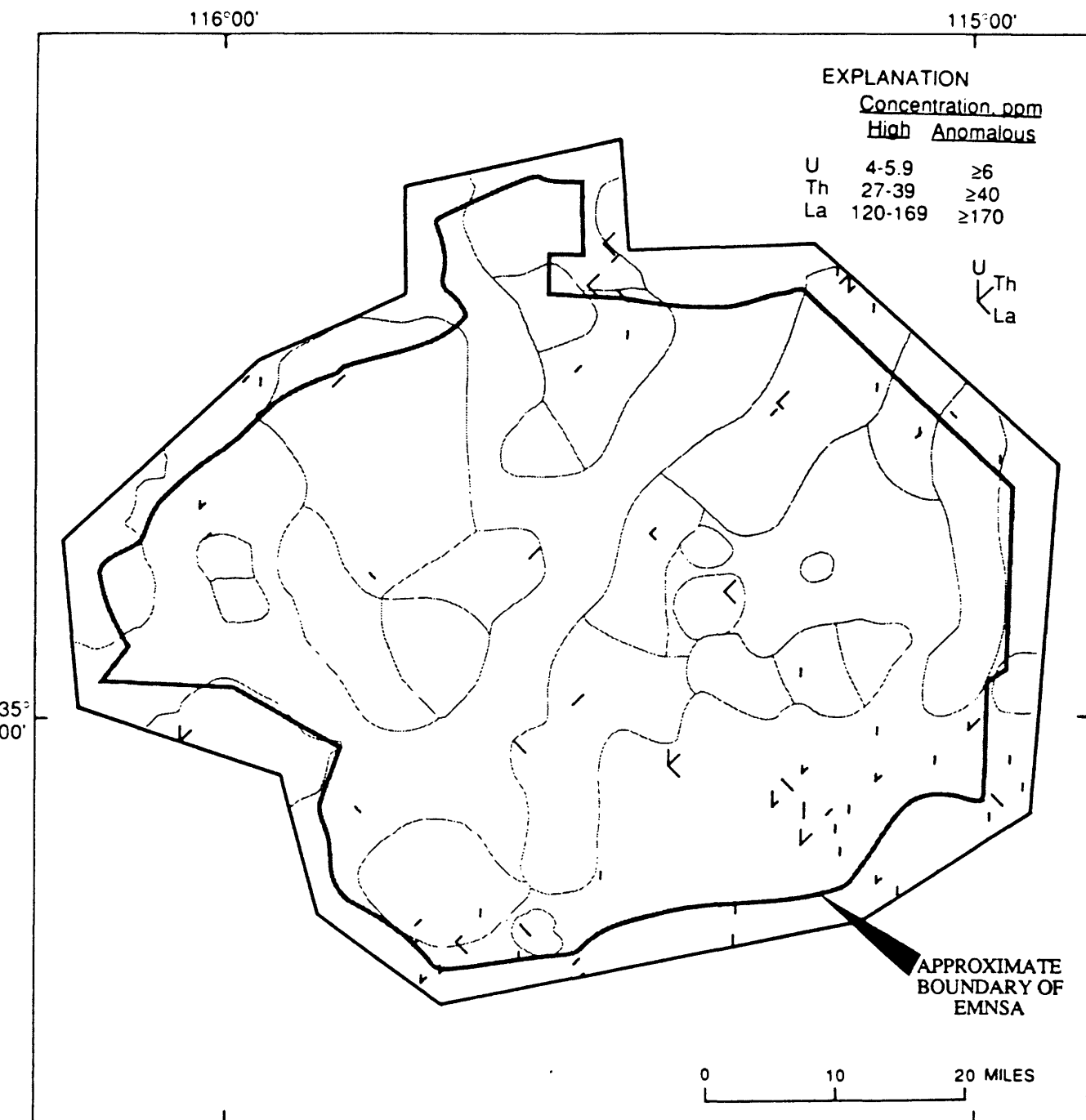


Figure 41. Distribution of anomalous and high concentrations of U, Th, and La in NURE stream-sediment and soil samples from the East Mojave National Scenic Area, Calif. Symbols explained on figure 28.

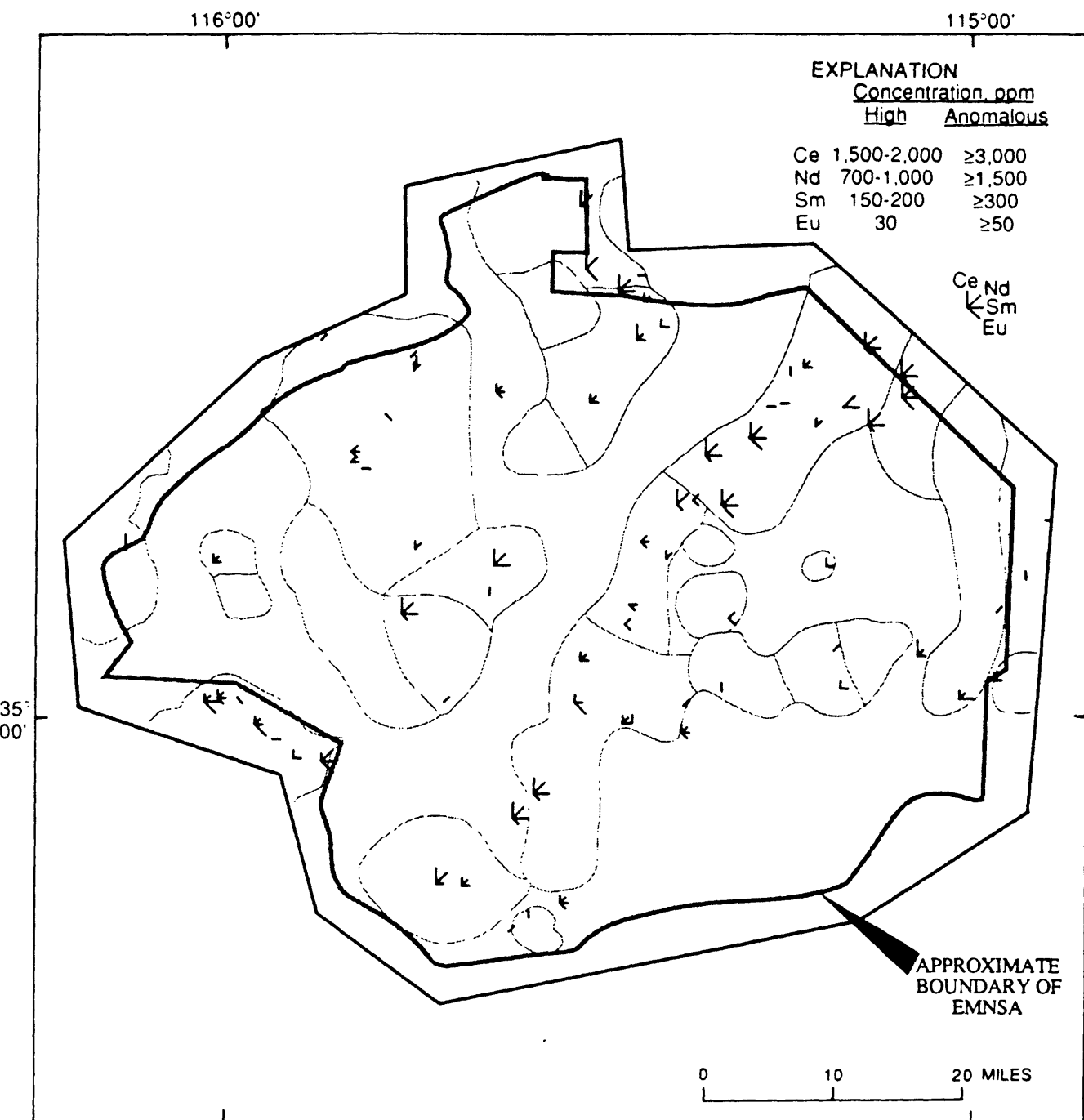


Figure 42. Distribution of anomalous and high concentrations of Ce, Nd, Sm, and Eu in PLUTO heavy-mineral concentrate samples from the East Mojave National Scenic Area, Calif. Symbols explained on figure 28.

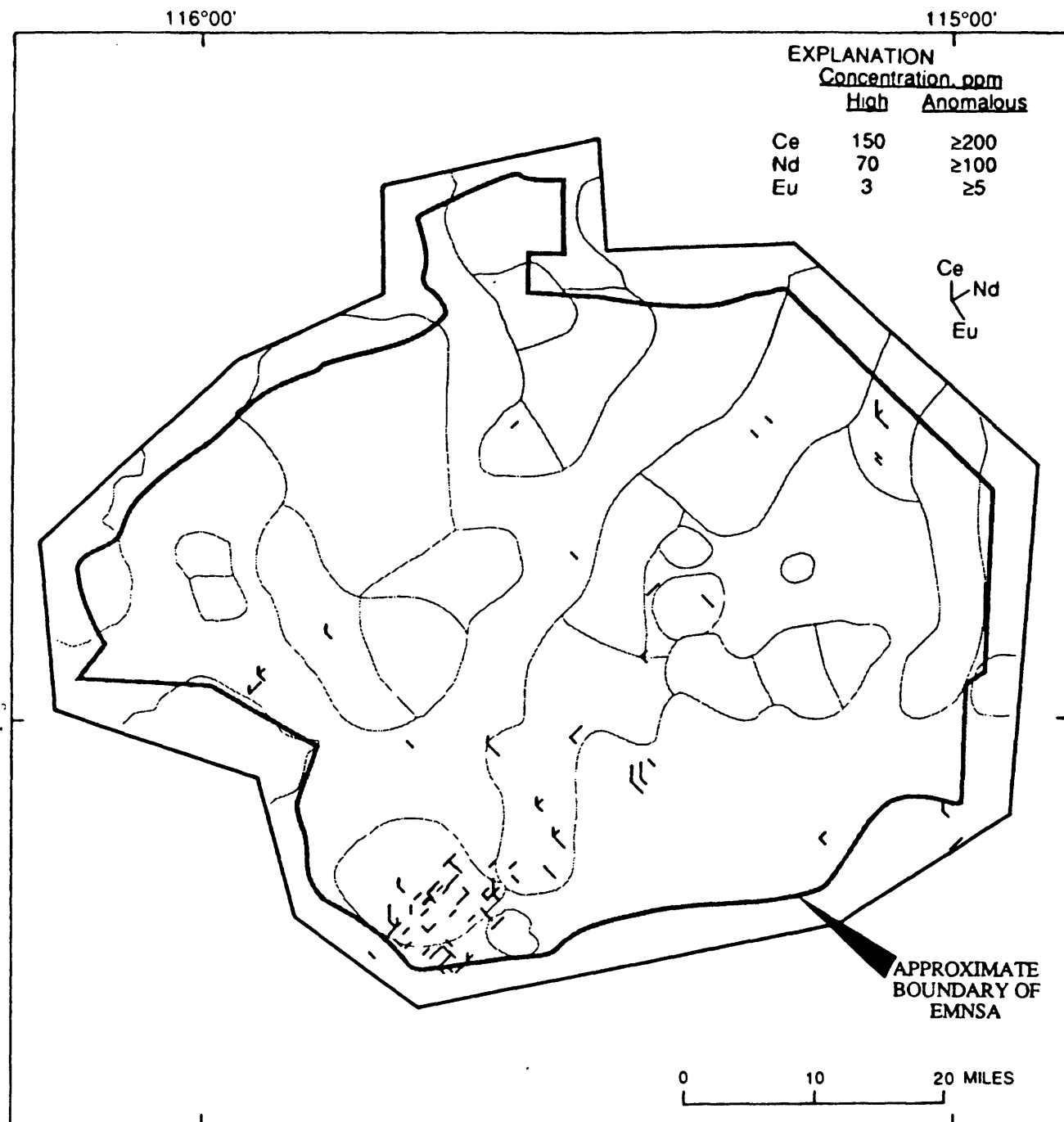


Figure 43. Distribution of anomalous and high concentrations of Ce, Nd, Sm, and Eu in PLUTO rock samples from the East Mojave National Scenic Area, Calif. Symbols explained on figure 28.

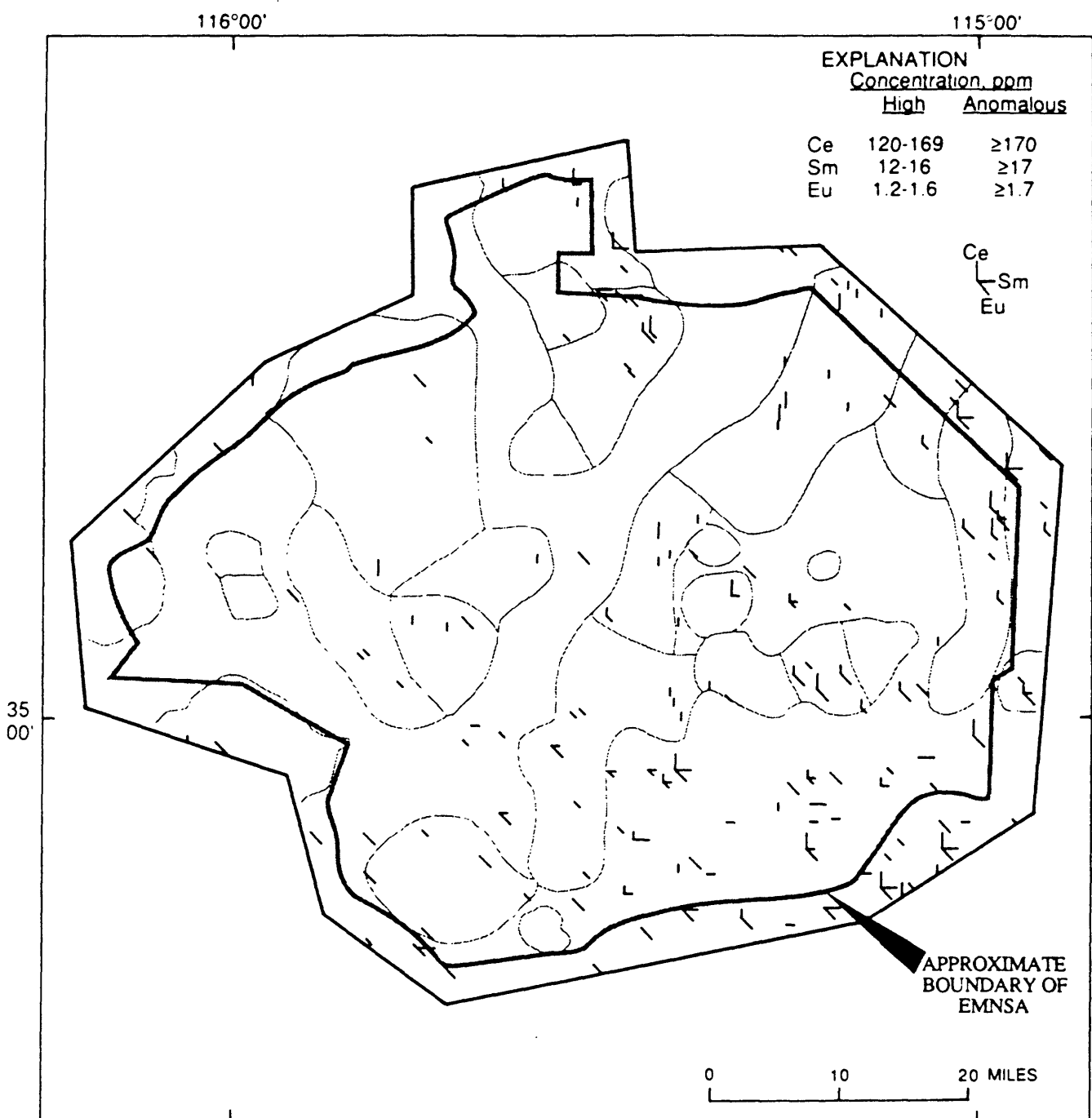


Figure 44. Distribution of anomalous and high concentrations of Ce, Sm, and Eu in NURE stream-sediment and soil samples from the East Mojave National Scenic Area, Calif. Symbols explained on figure 28.

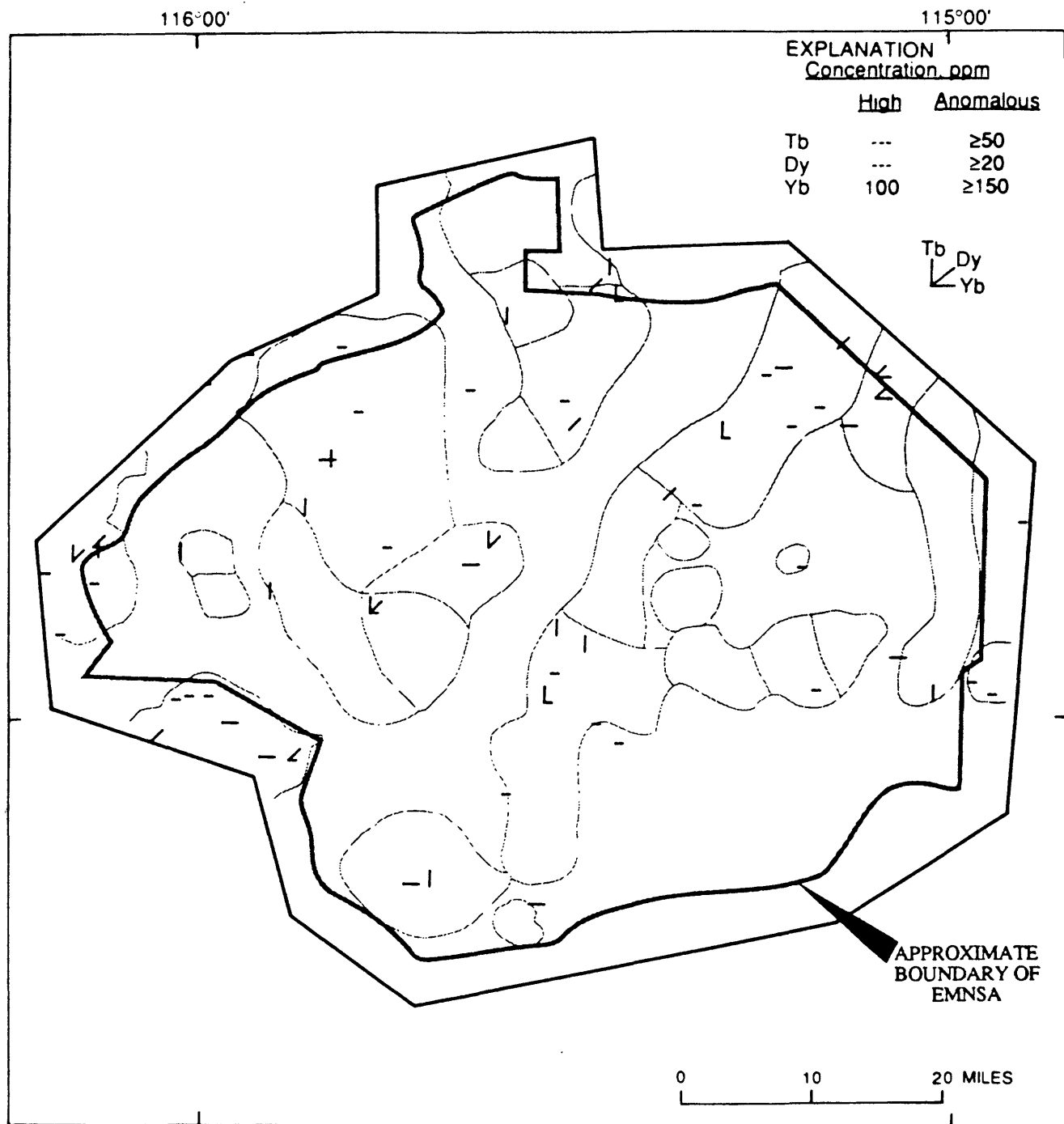


Figure 45. Distribution of anomalous and high concentrations of Tb, Dy, and Yb in PLUTO heavy-mineral-concentrate samples from the East Mojave National Scenic Area, Calif. Symbols explained on figure 28.

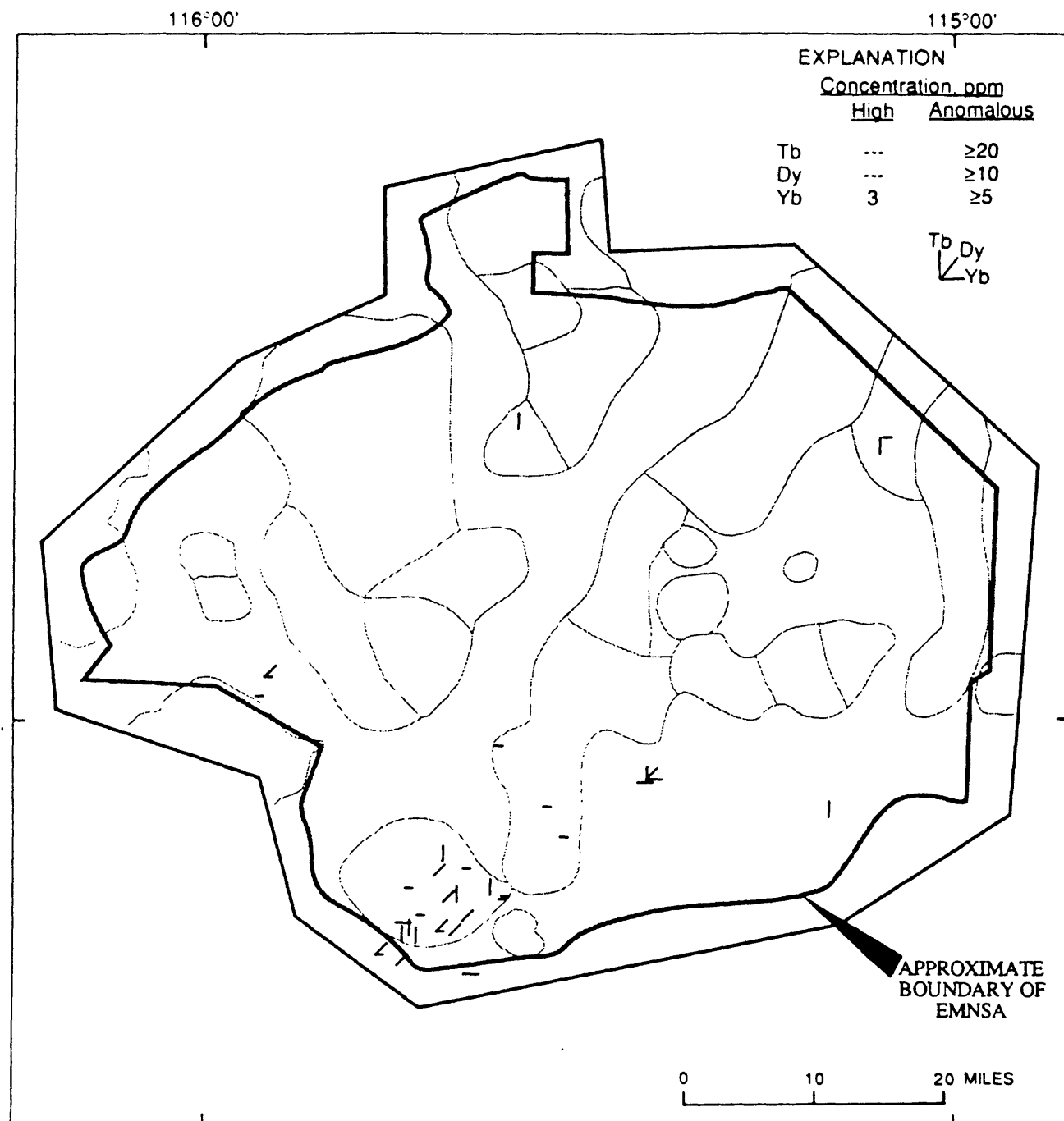


Figure 46. Distribution of anomalous and high concentrations of Tb, Dy, and Yb in PLUTO rock samples from the East Mojave National Scenic Area, Calif. Symbols explained on figure 28.

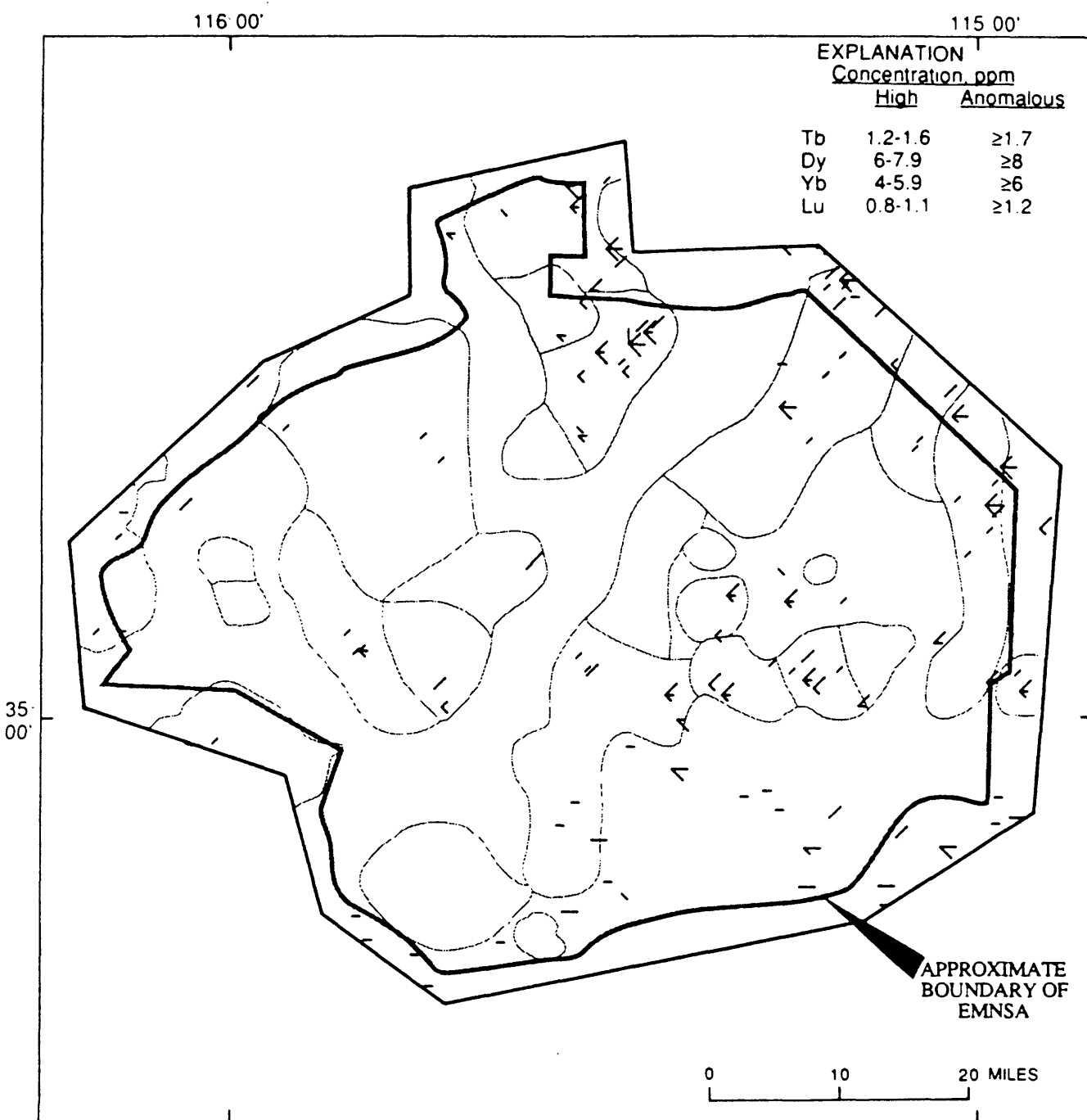
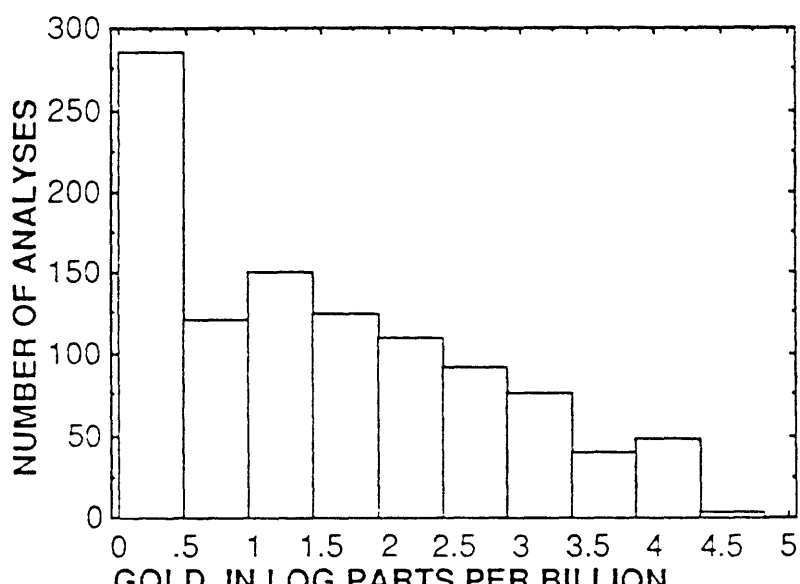
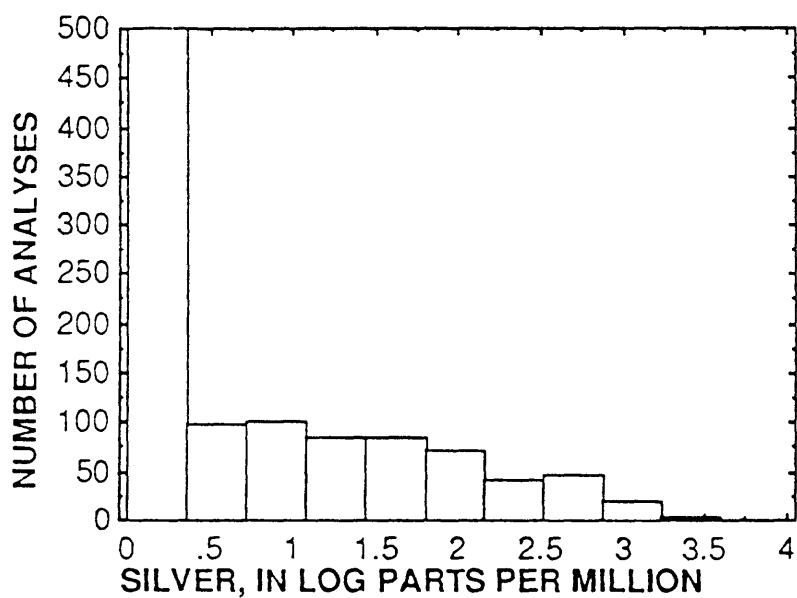


Figure 47. Distribution of anomalous and high concentrations of Tb, Dy, Yb, and Lu in NURE stream-sediment and soil samples from the East Mojave National Scenic Area, Calif. Symbols explained on figure 28.



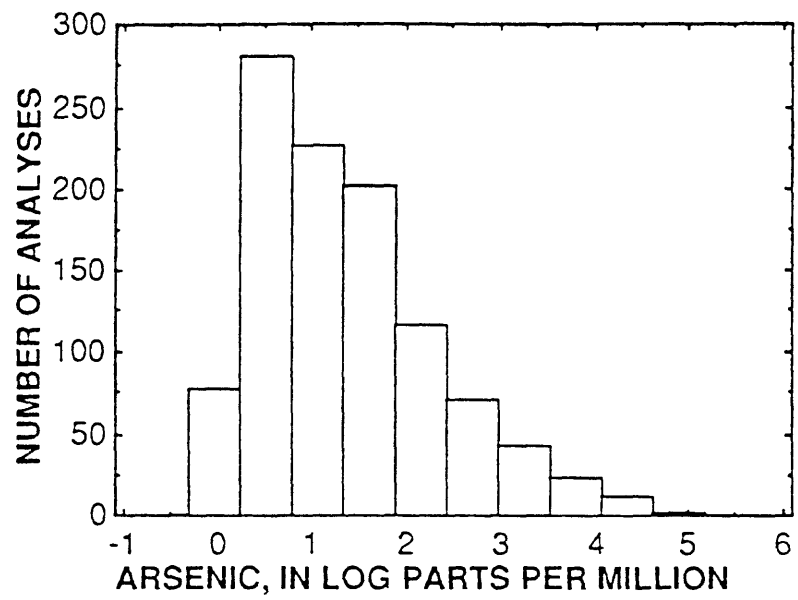
**A**



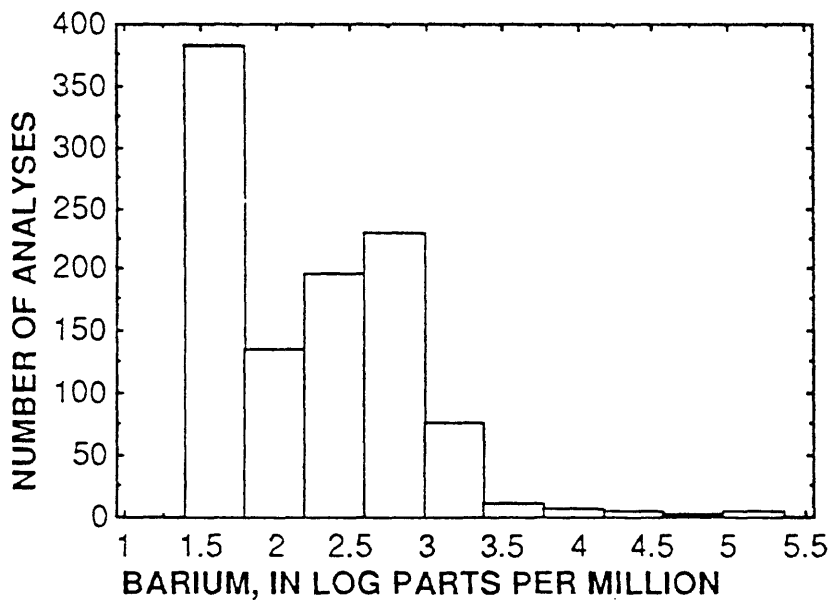
**B**

Figure 48. Plots showing frequency distribution (A-U) for Au, Ag, As, Ba, Ce, Co, Cr, Cs, Fe, La, Mo, Ni, Sb, Sc, Sm, Ta, Th, U, W, and Zn in 1,050 rocks from the East Mojave National Scenic Area analyzed by the U.S. Bureau of Mines (1990a).

Figure 48 (cont.)



**C**



**D**

Figure 48 (cont.)

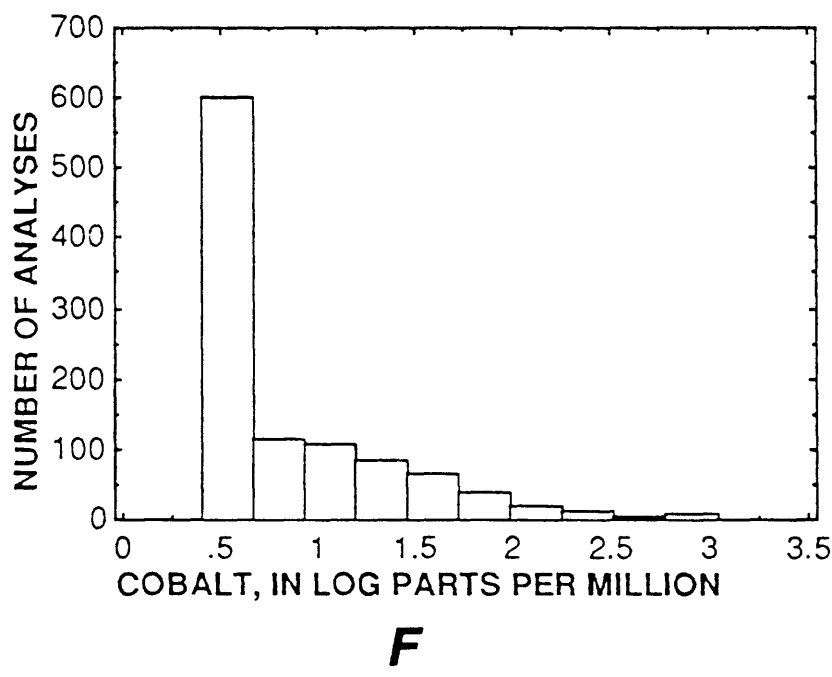
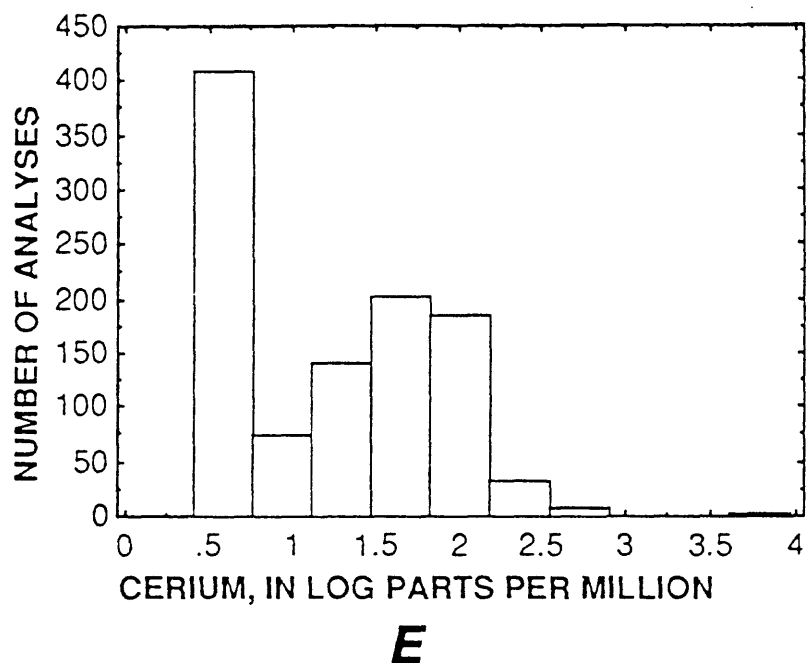
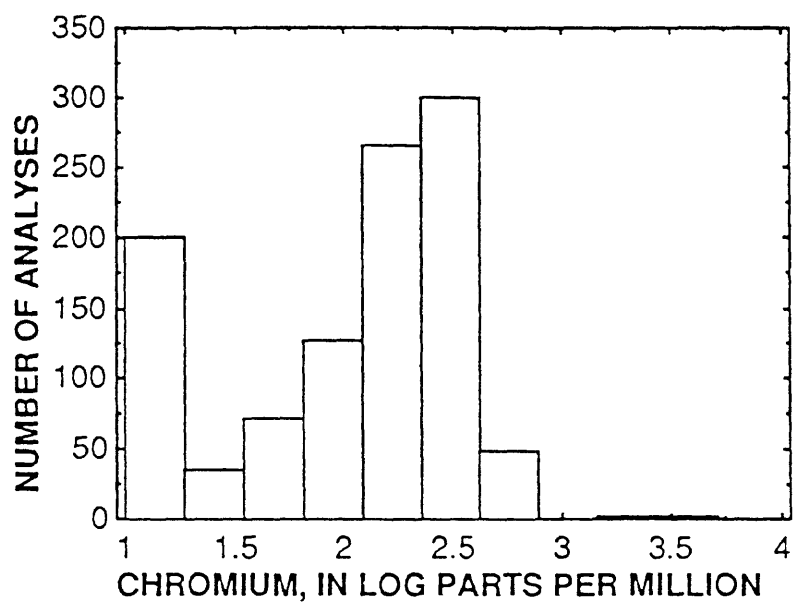
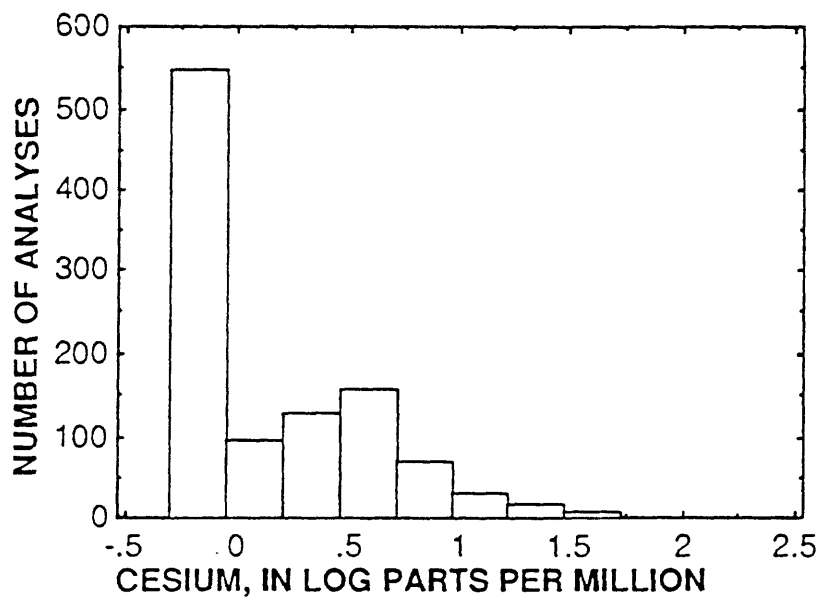


Figure 48 (cont.)

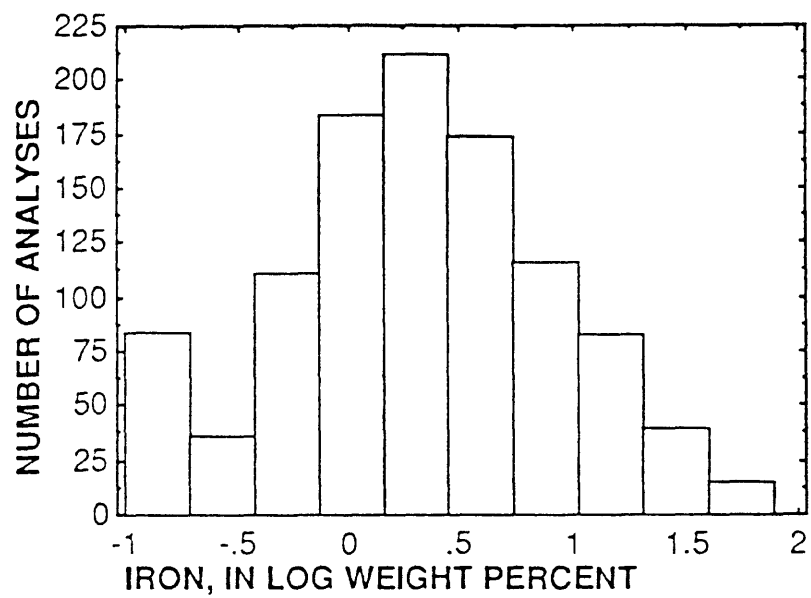


**G**

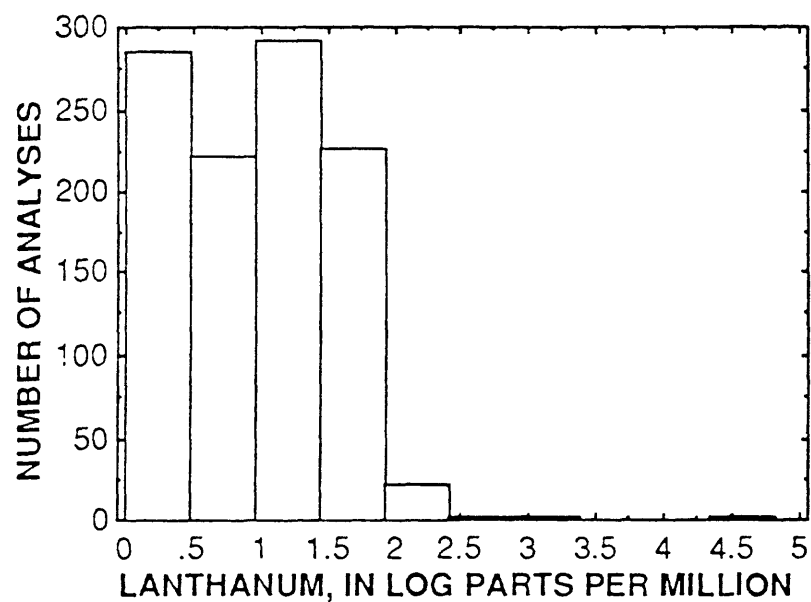


**H**

Figure 48 (cont.)

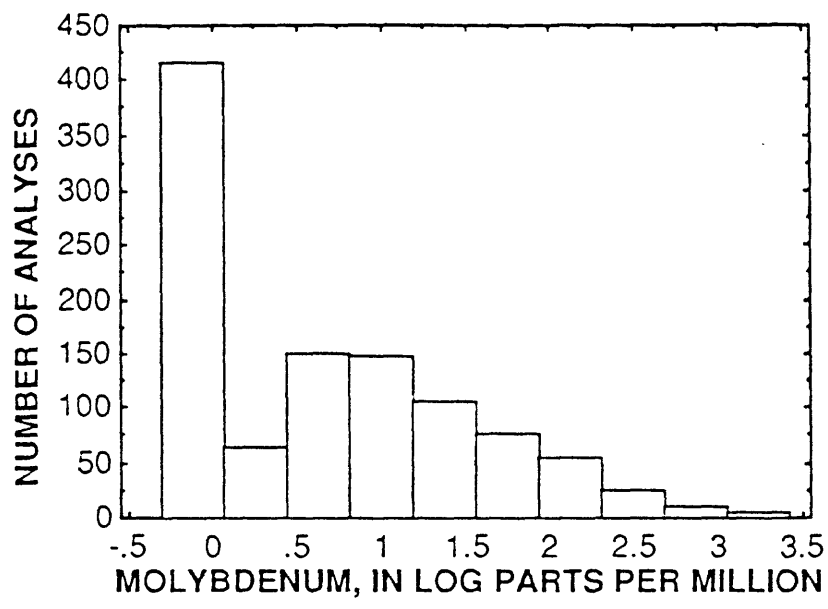


I

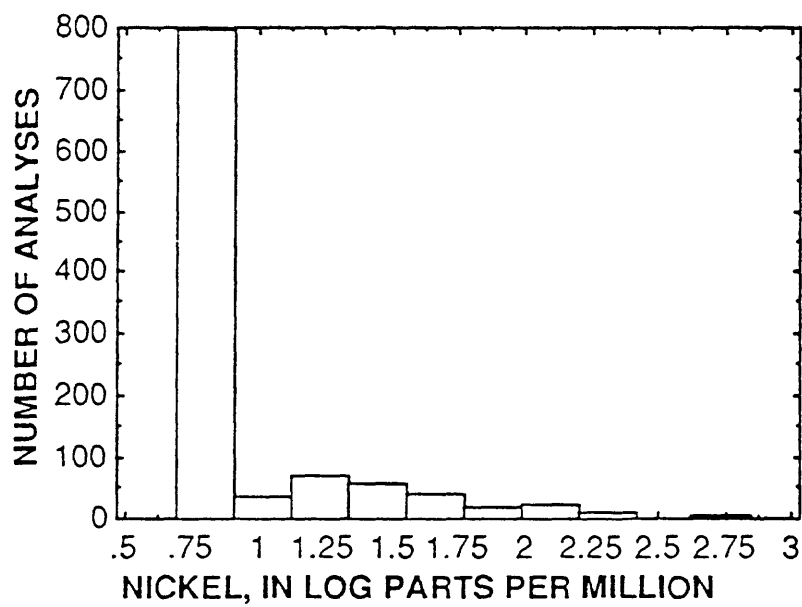


J

Figure 48 (cont.)

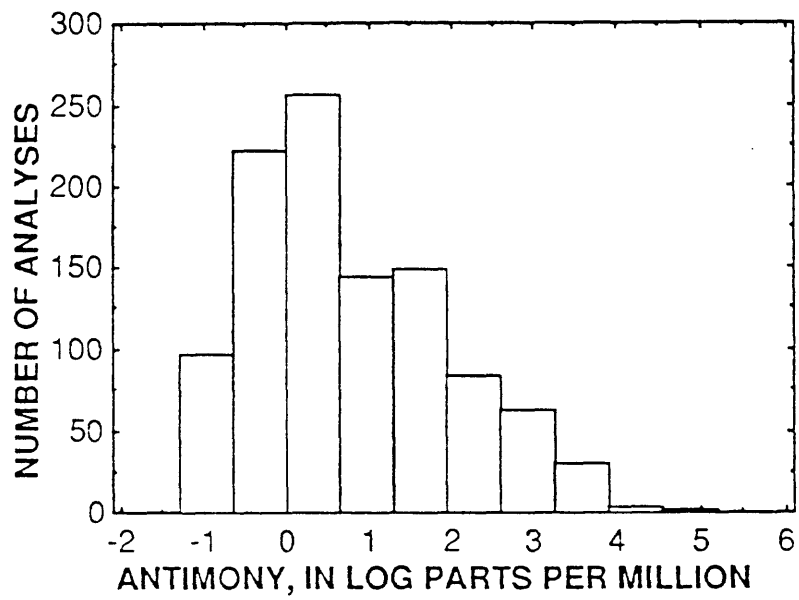


**K**

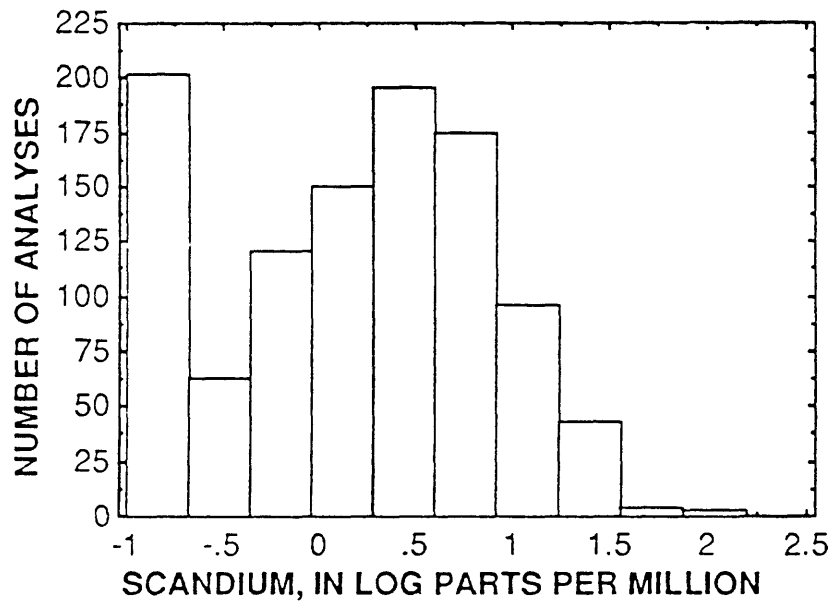


**L**

Figure 48 (cont.)

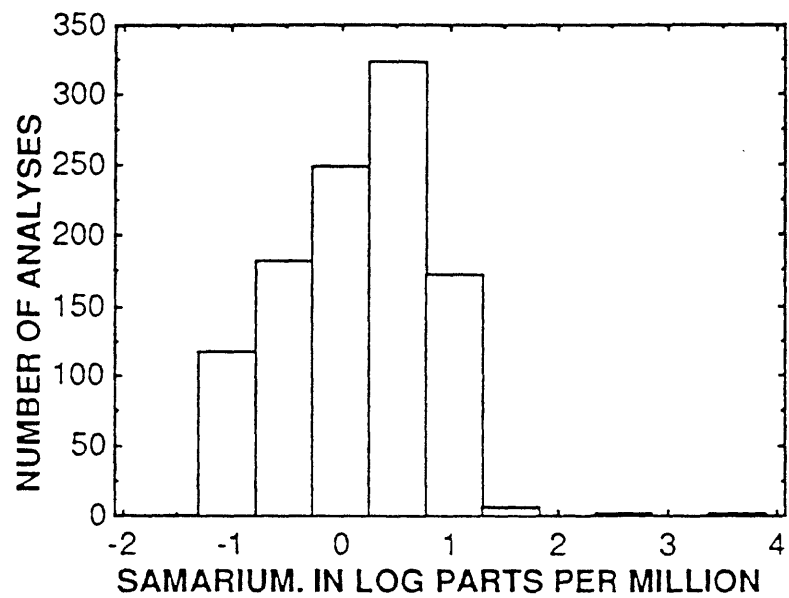


**M**

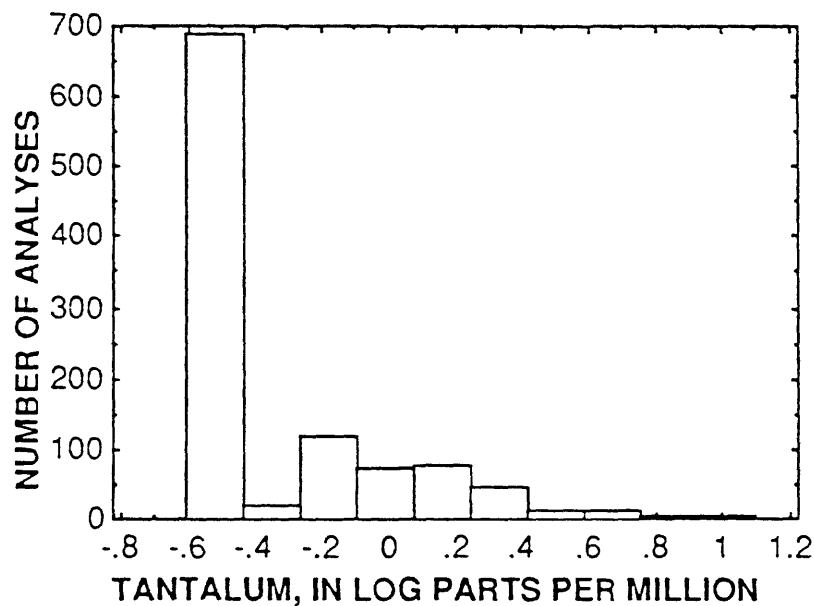


**N**

Figure 48 (cont.)

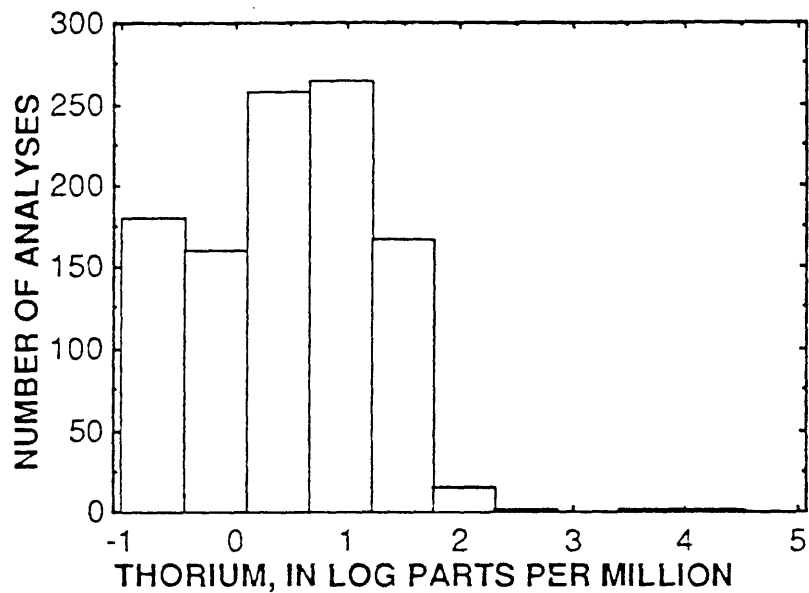


**O**

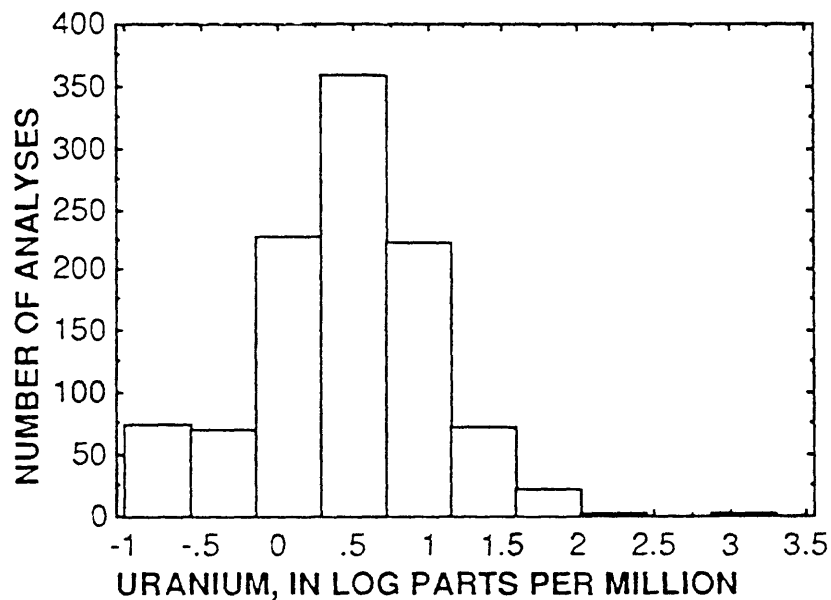


**P**

Figure 48 (cont.)

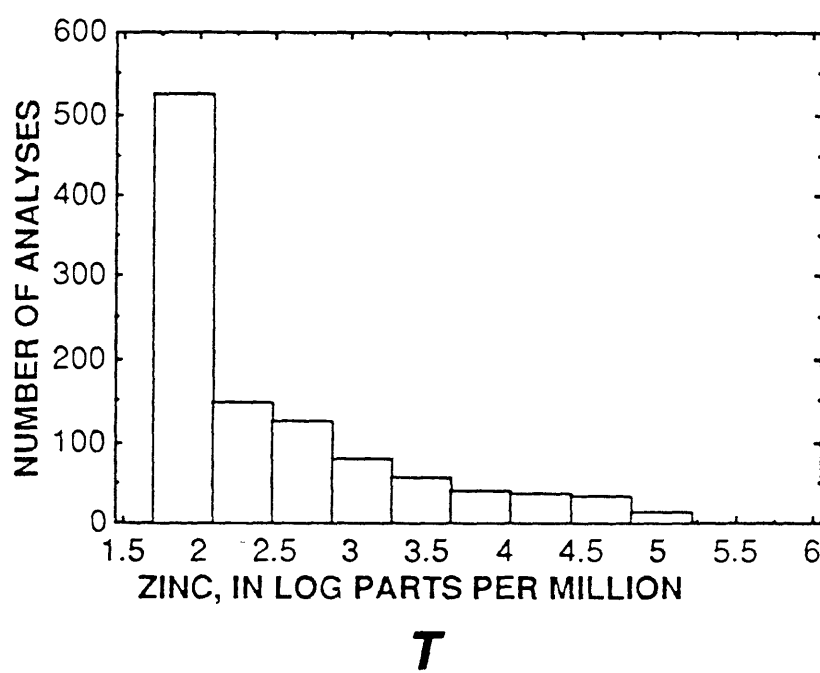
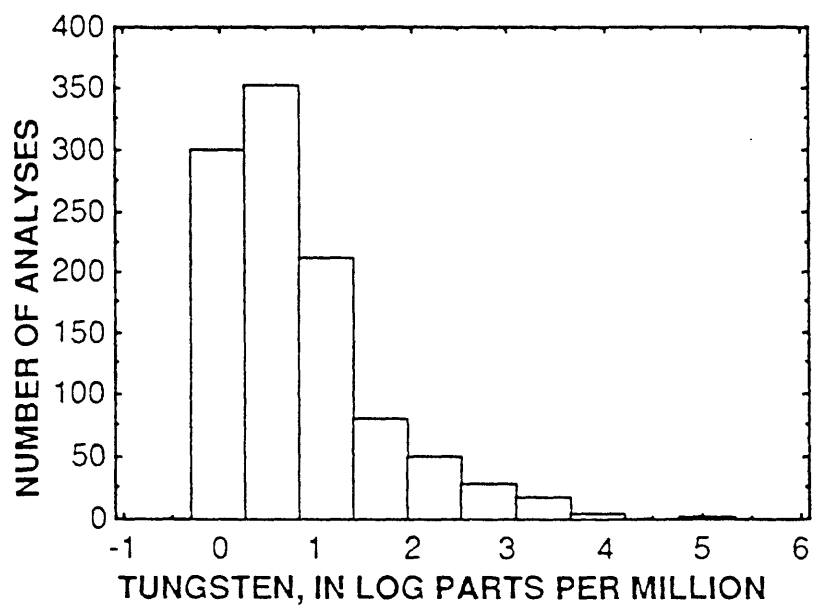


**Q**



**R**

Figure 48 (cont.)



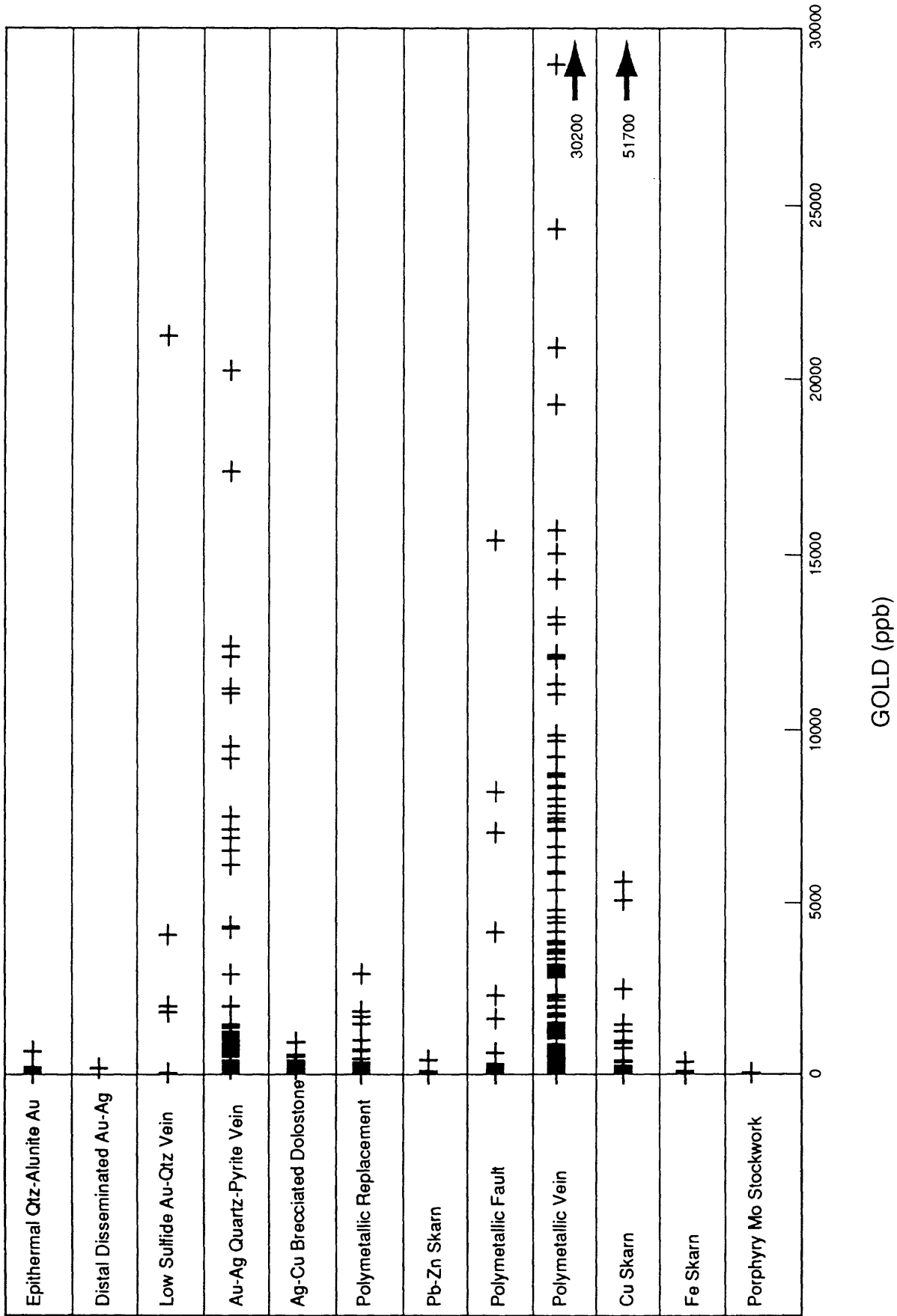


Figure 49. Concentrations of gold (A), silver (B), arsenic (C), antimony (D), molybdenum (E), and zinc (F) in mineralized rocks analyzed by the U.S. Bureau of Mines (1990a), grouped by deposit type in the East Mojave National Scenic Area.

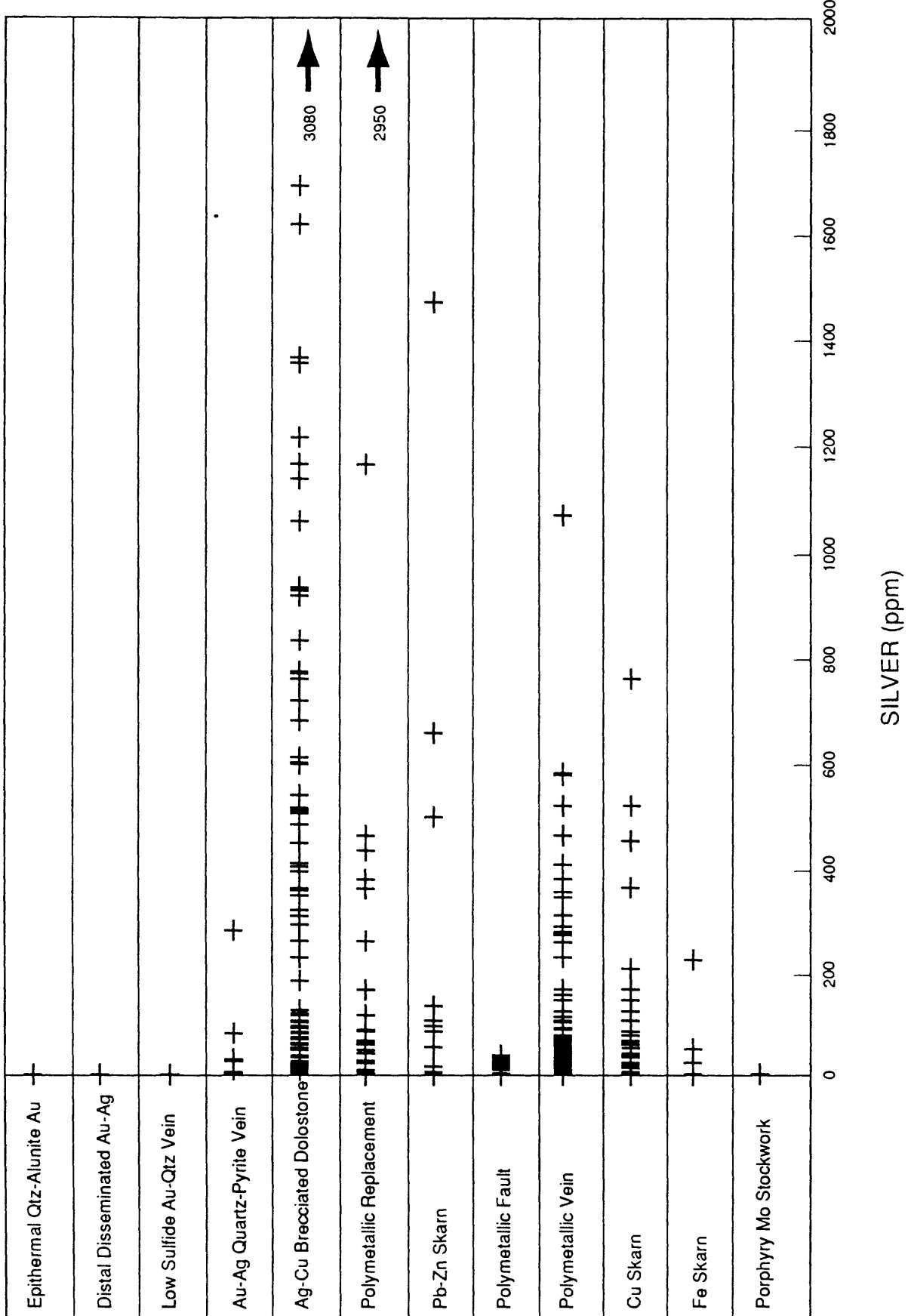
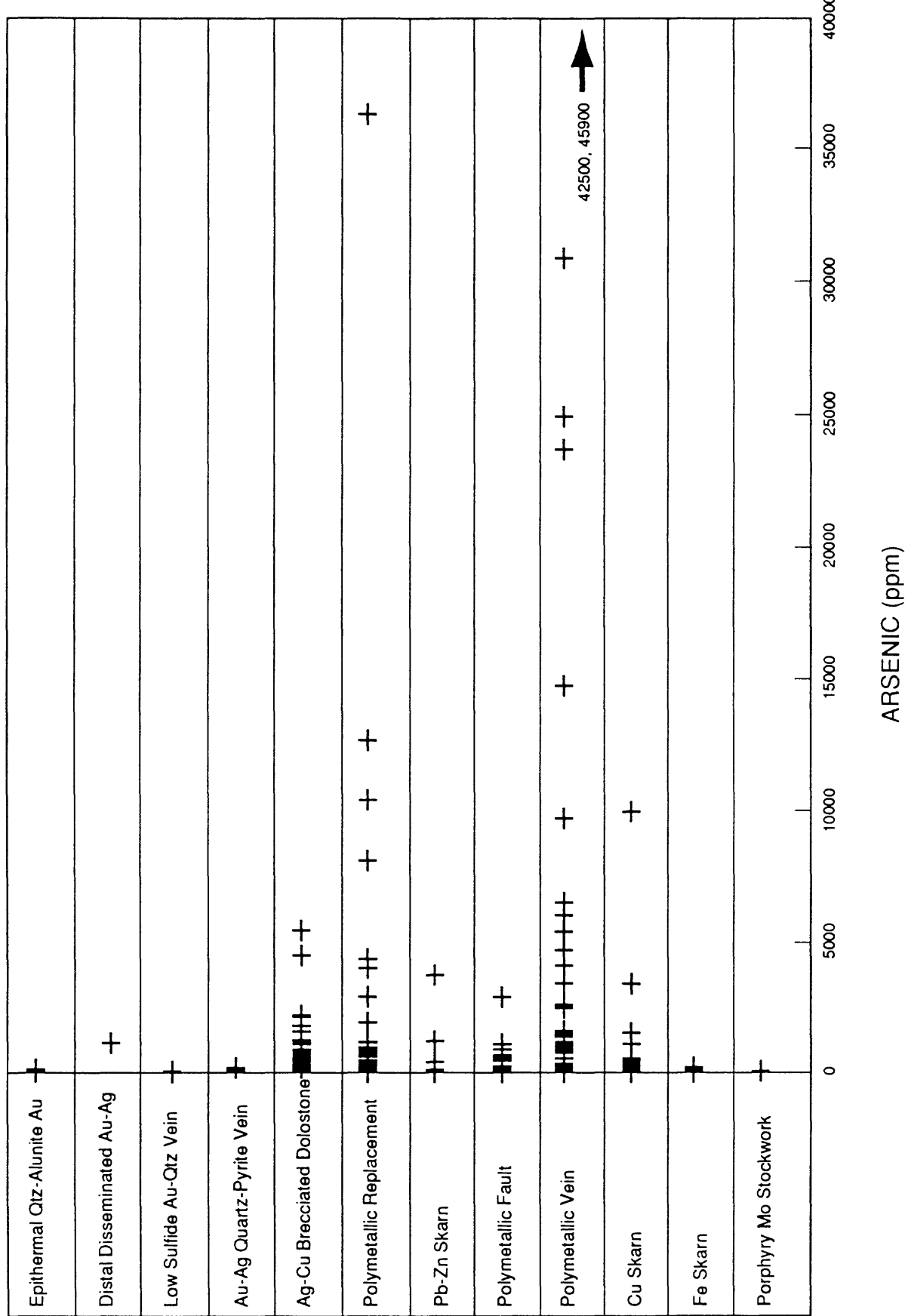
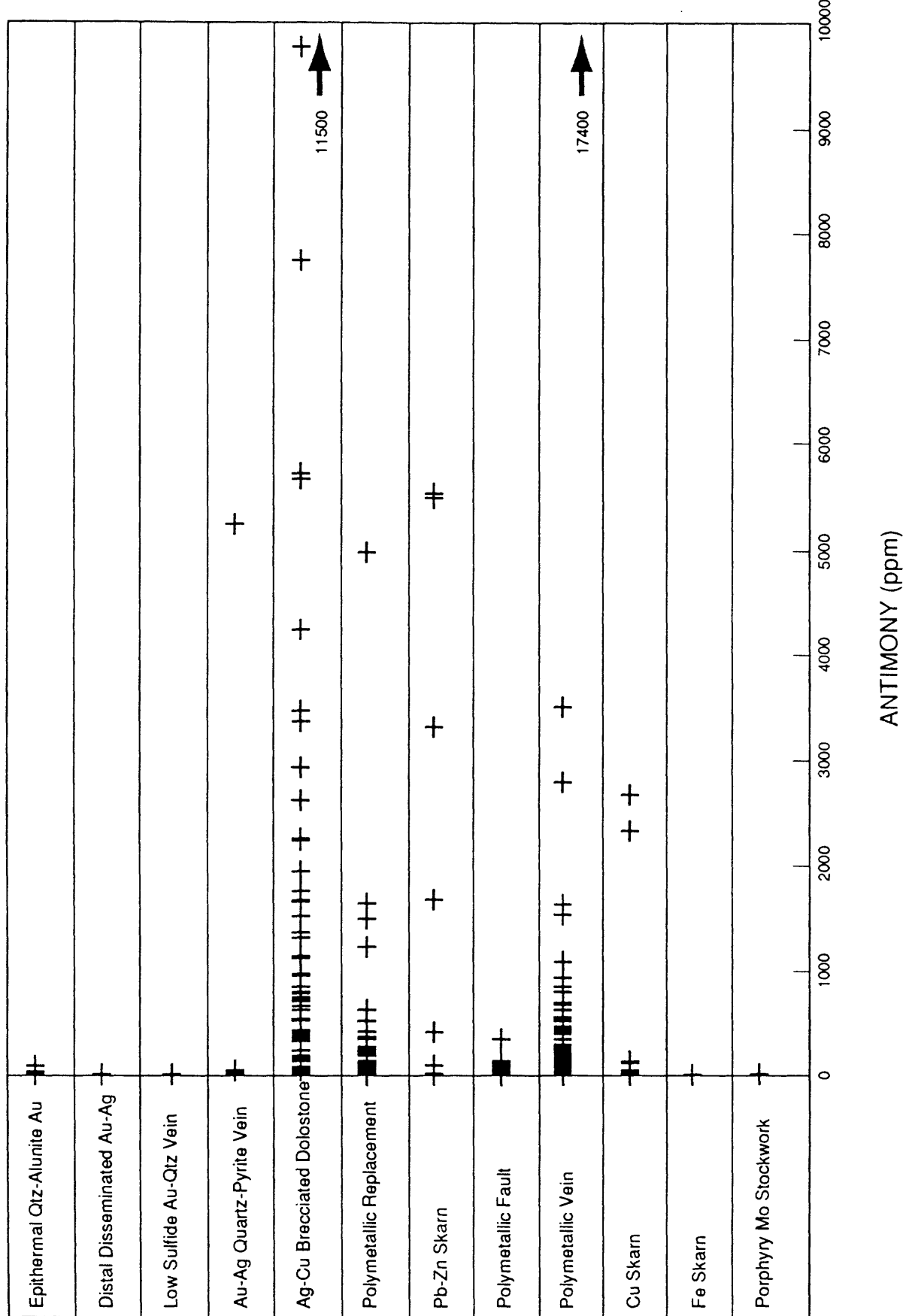


Figure 49 (cont.)





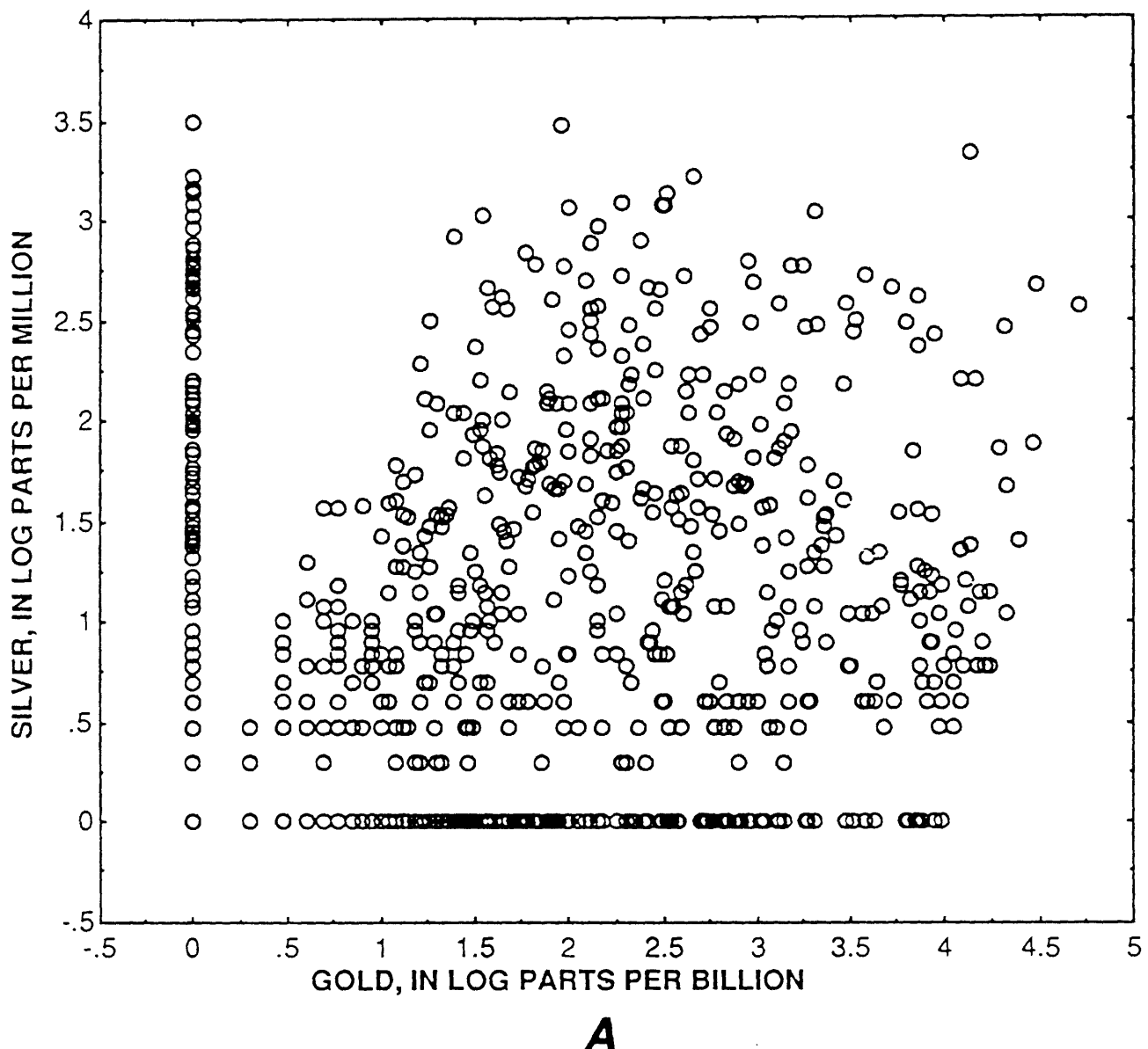


Figure 50. Scatter plots for gold versus silver (A), gold versus iron (B), lanthanum versus samarium (C), silver versus antimony (D), cobalt versus iron (E), and barium versus uranium (F), for 1,050 rocks from the East Mojave National Scenic Area analyzed by the U.S. Bureau of Mines (1990a).

Figure 50 (cont.)

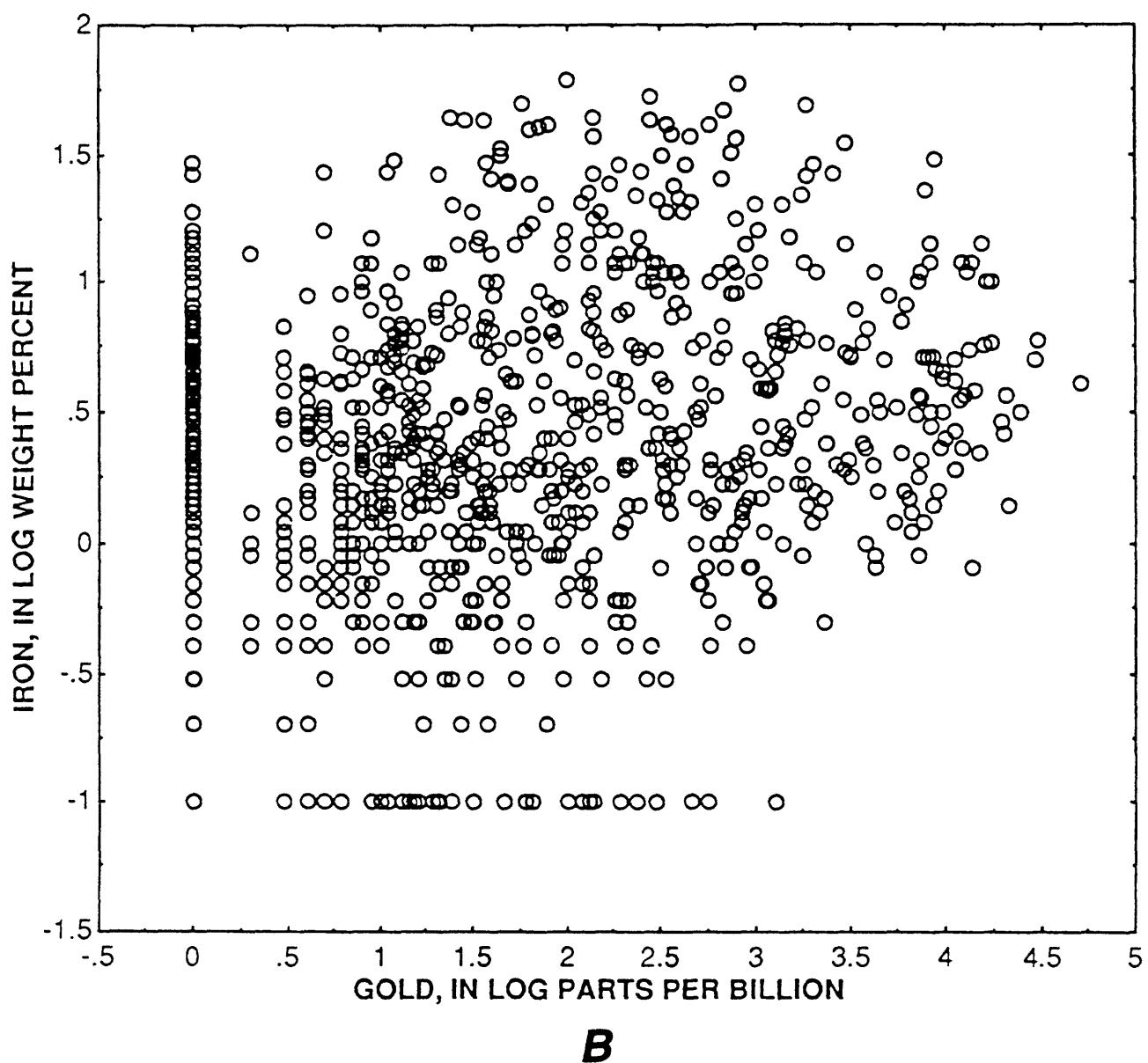


Figure 50 (cont.)

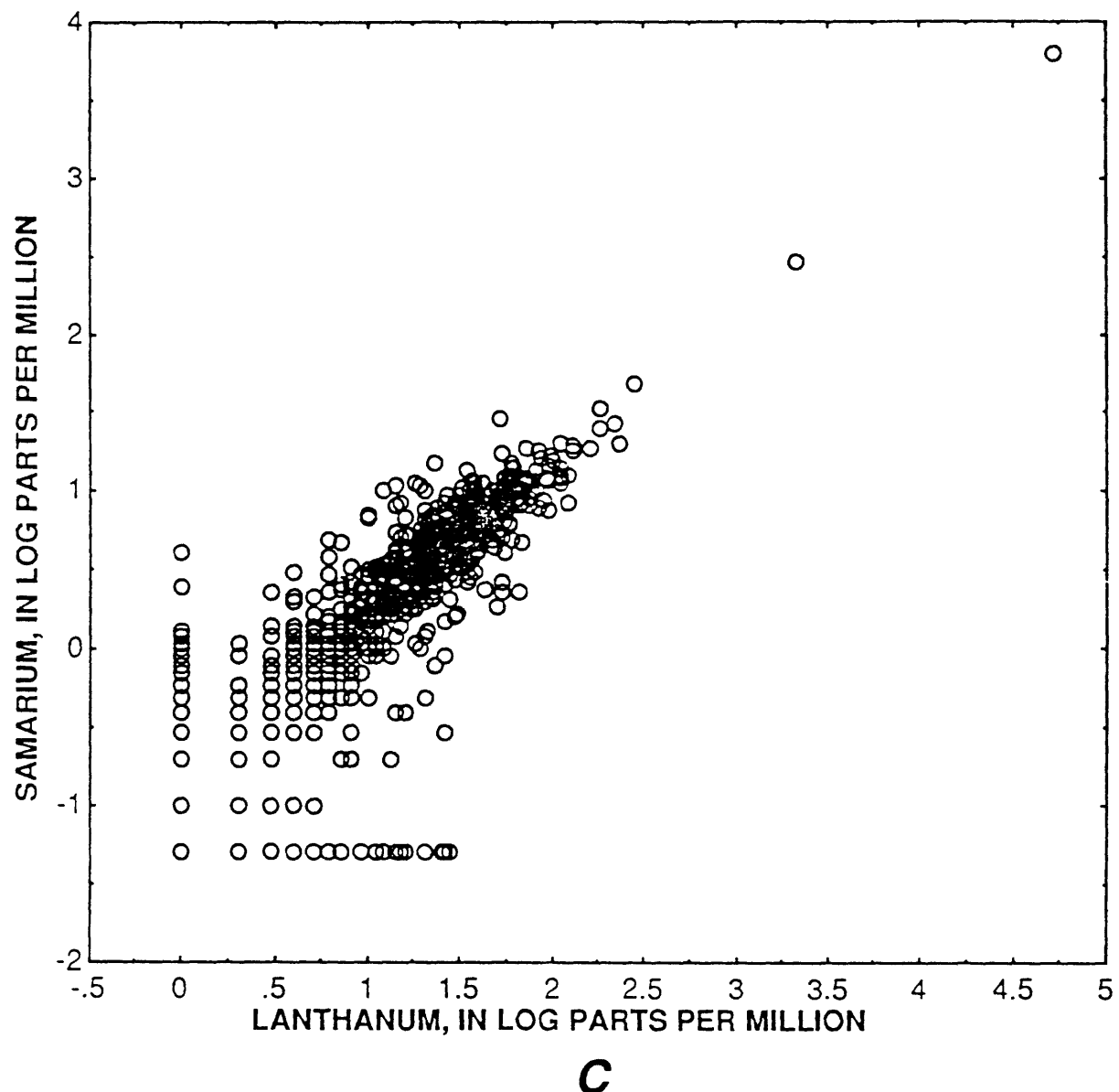


Figure 50 (cont.)

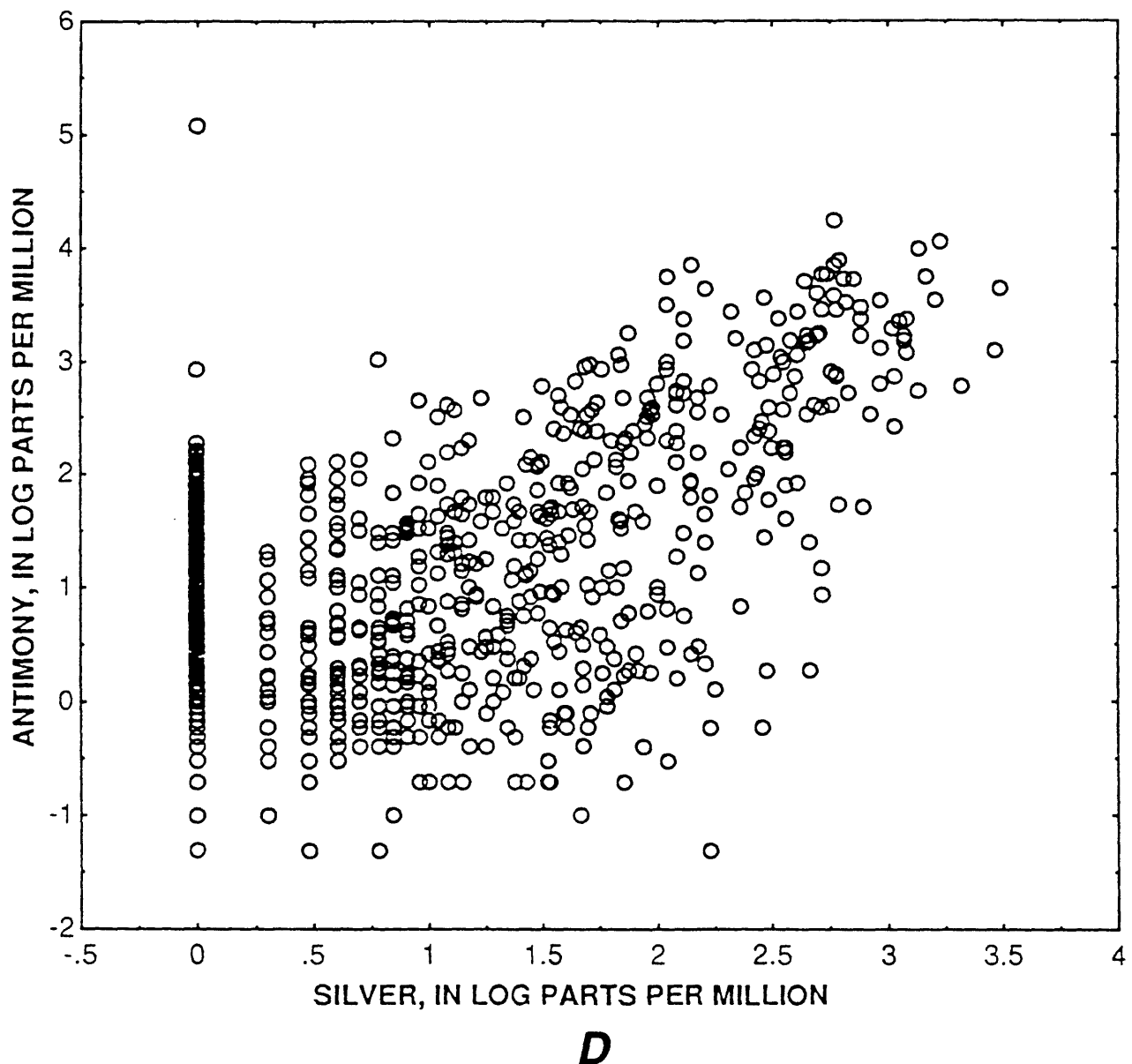


Figure 50 (cont.).

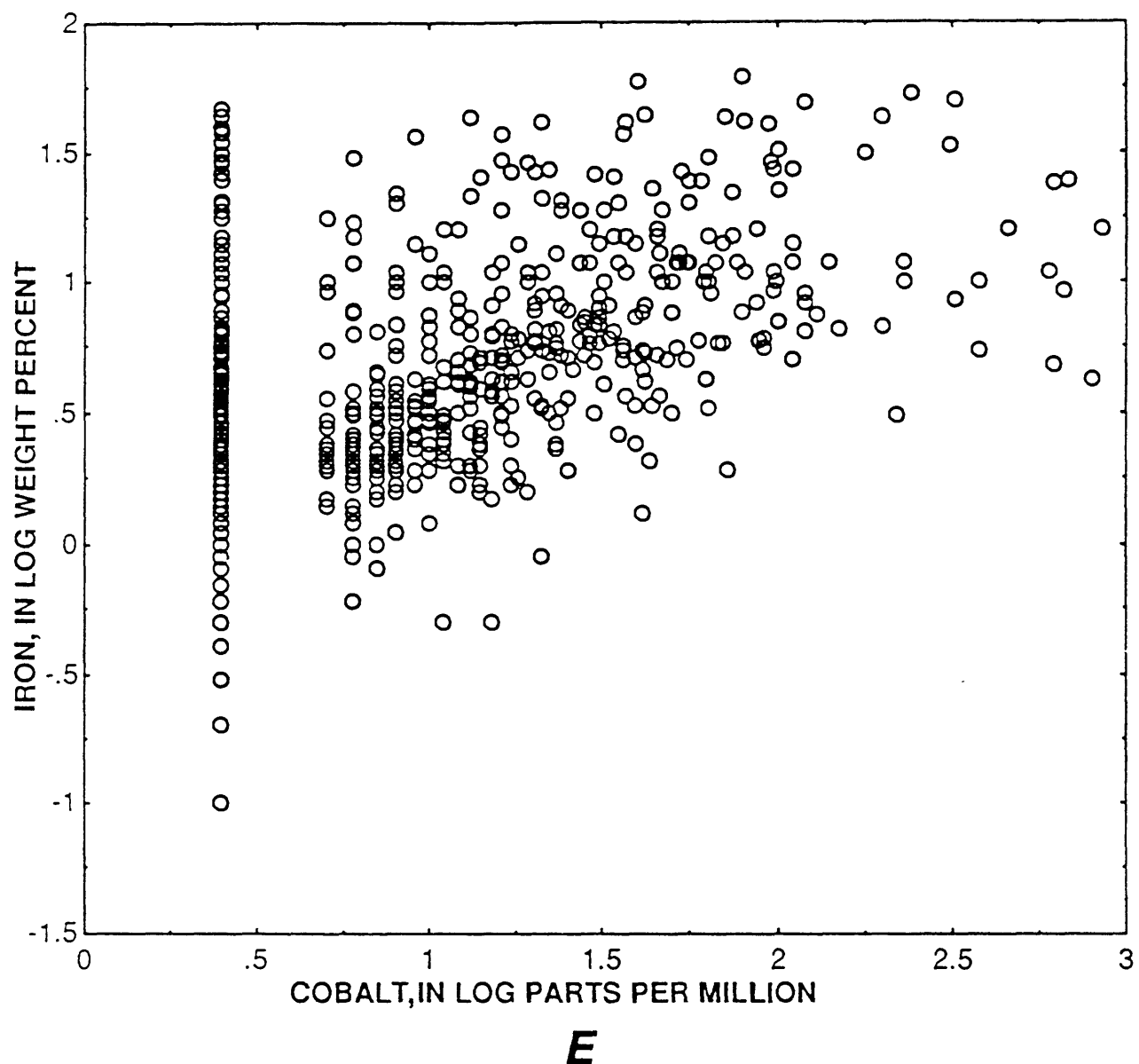
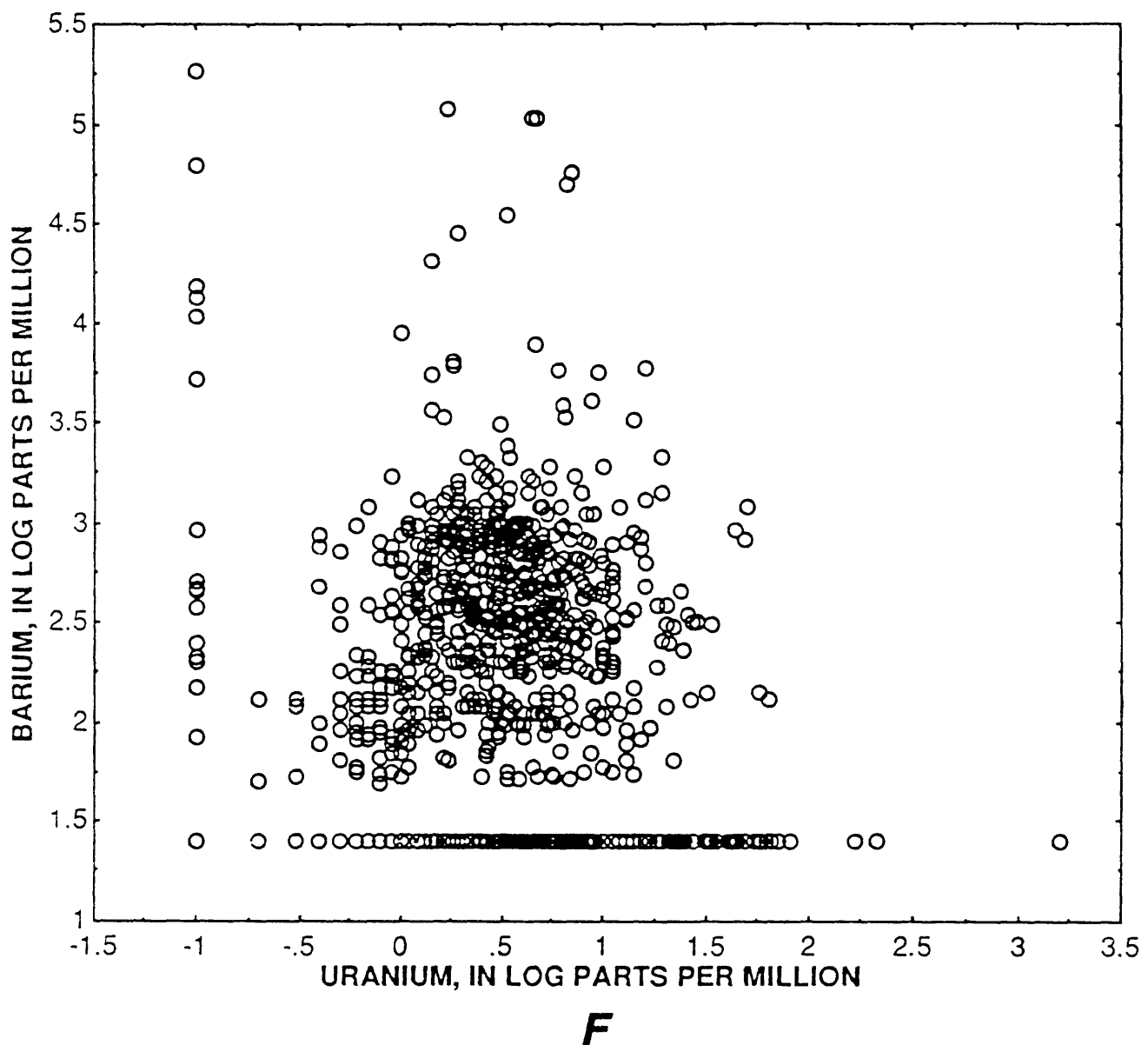


Figure 50 (cont.)



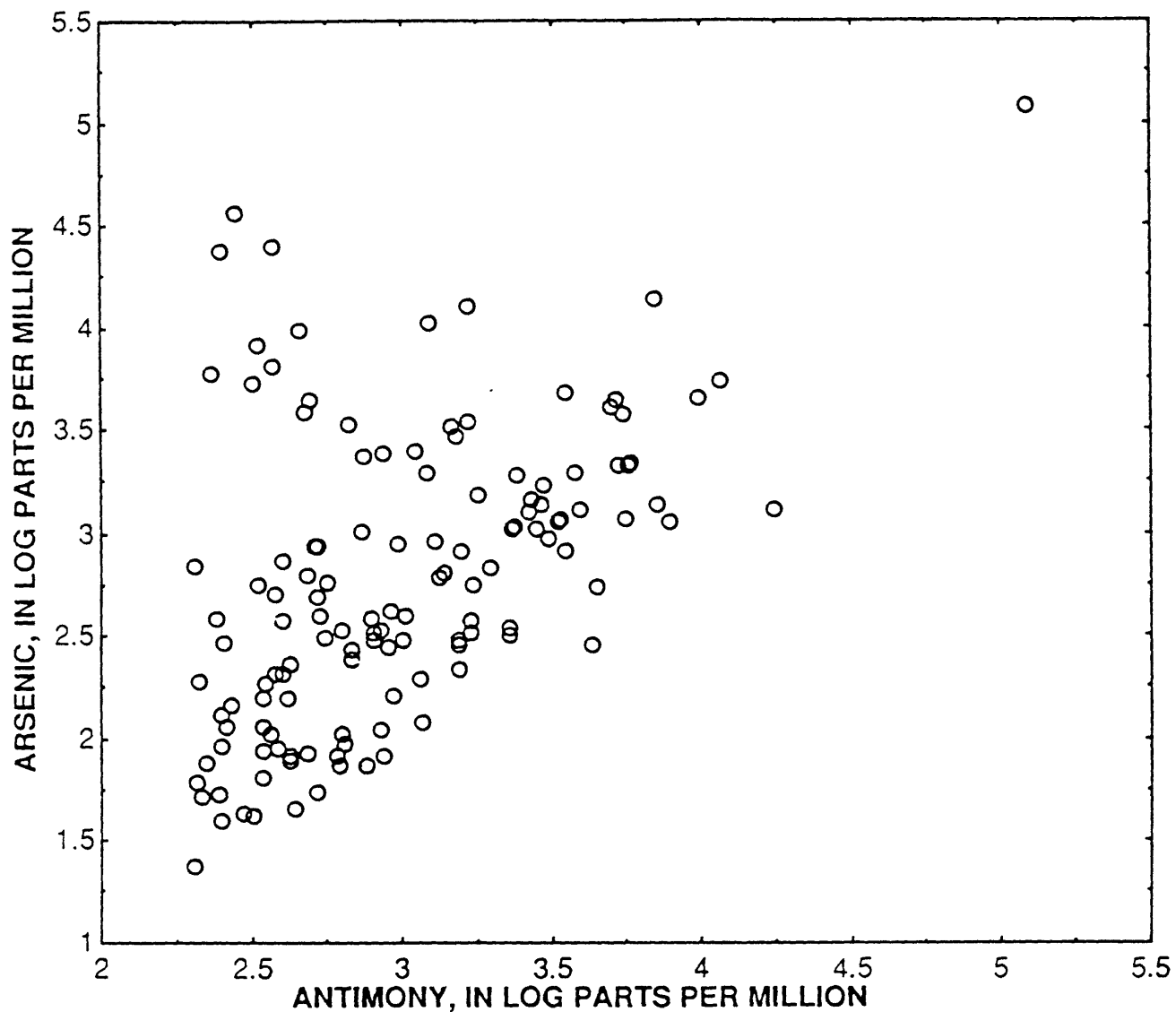
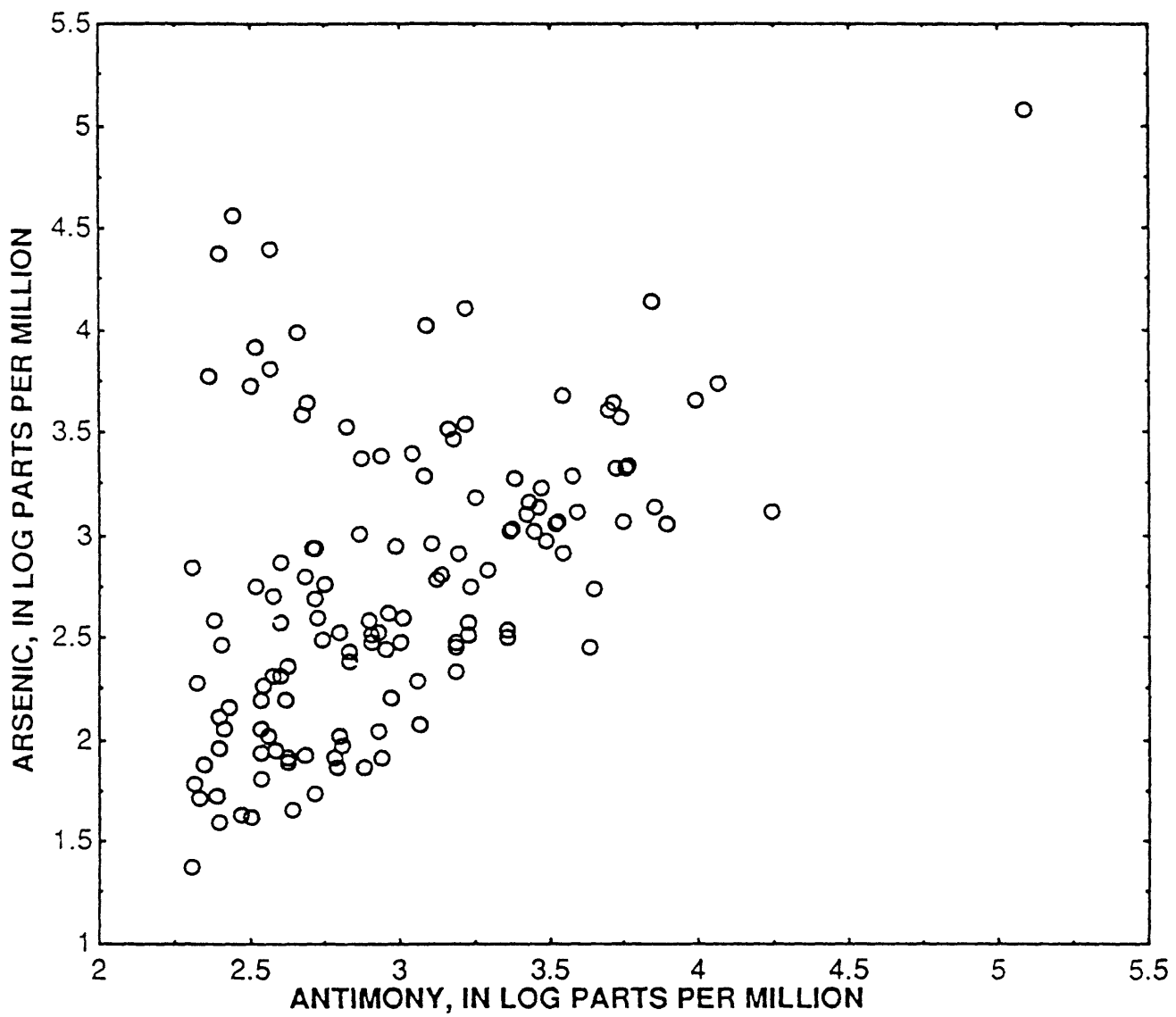


Figure 51. Plot showing antimony compared with arsenic in 131 samples containing greater than 200 ppm antimony selected from the 1,050 rock-data base from the East Mojave National Scenic Area (see text).

Figure 51 (cont.)



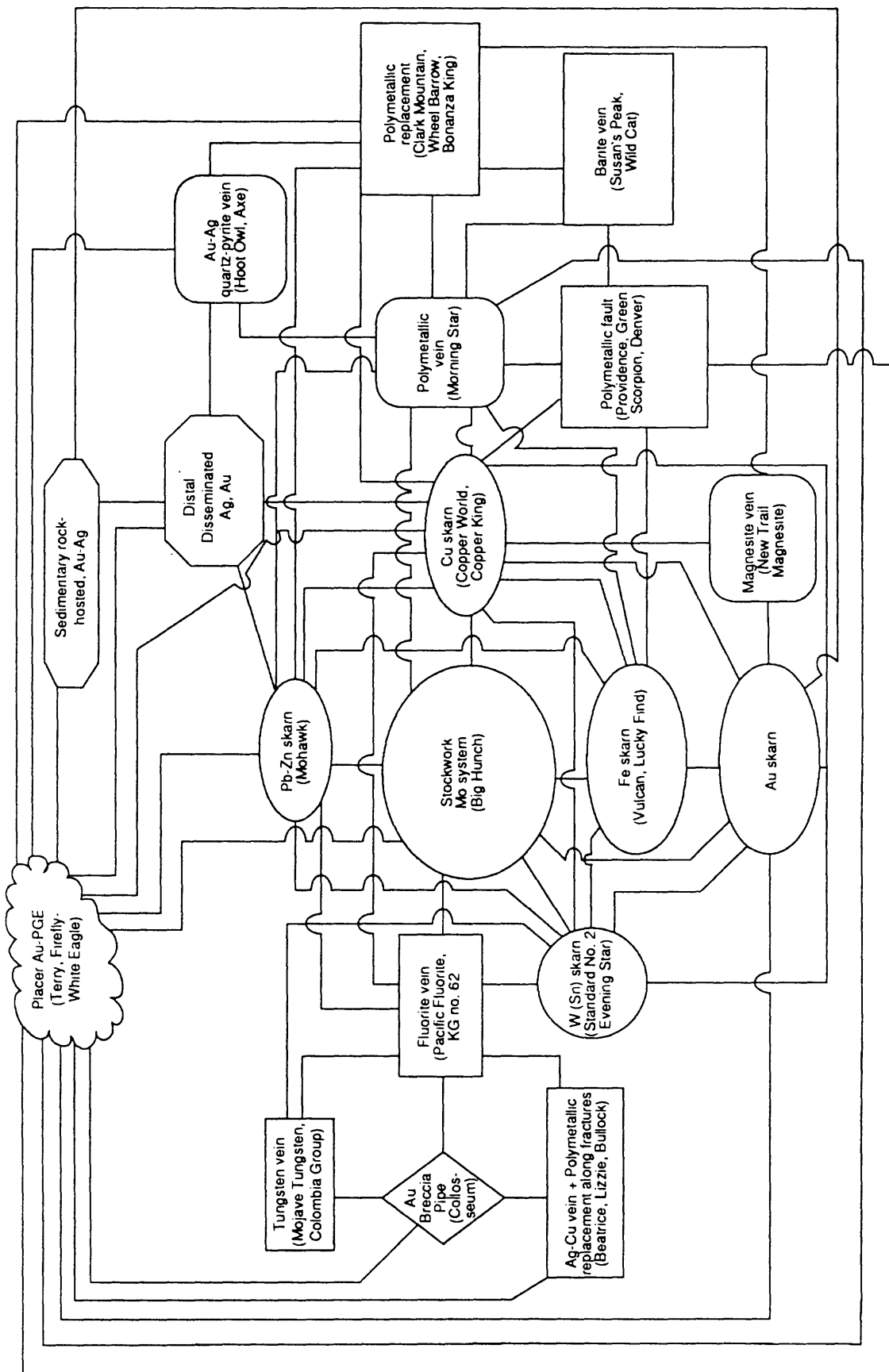


Figure S2. Possible linkages among some types of mineral occurrences in the East Mojave National Scenic Area associated with felsic intrusive rocks. Most linkages are inferred from mineral zonations established in mining districts elsewhere. Example of mineral occurrence in the East Mojave National Scenic Area shown parenthetically.

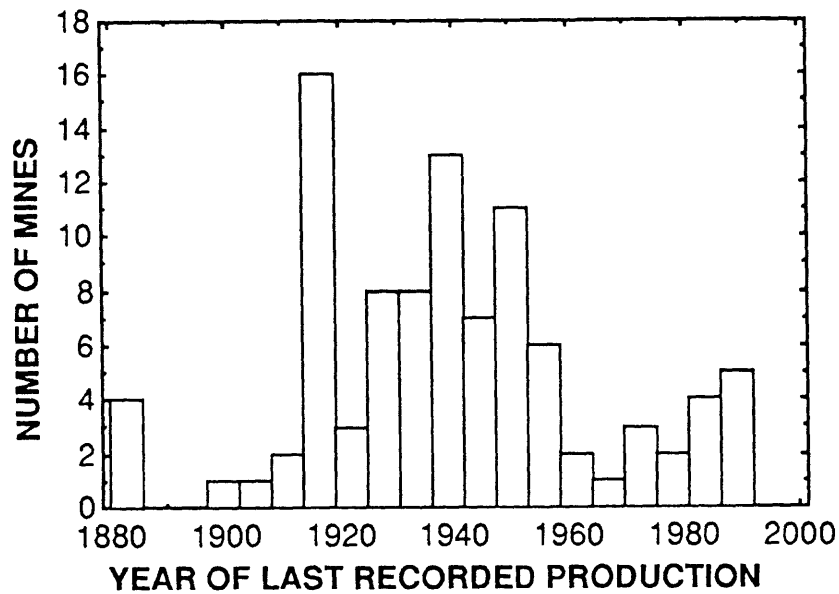


Figure 53. Graph showing number of mines in the East Mojave National Scenic Area plotted against the year of their last recorded production. Data available for 97 mines in U.S. Bureau of Mines (1990a).

## CALIFORNIA MINERAL LAND CLASSIFICATION DIAGRAM

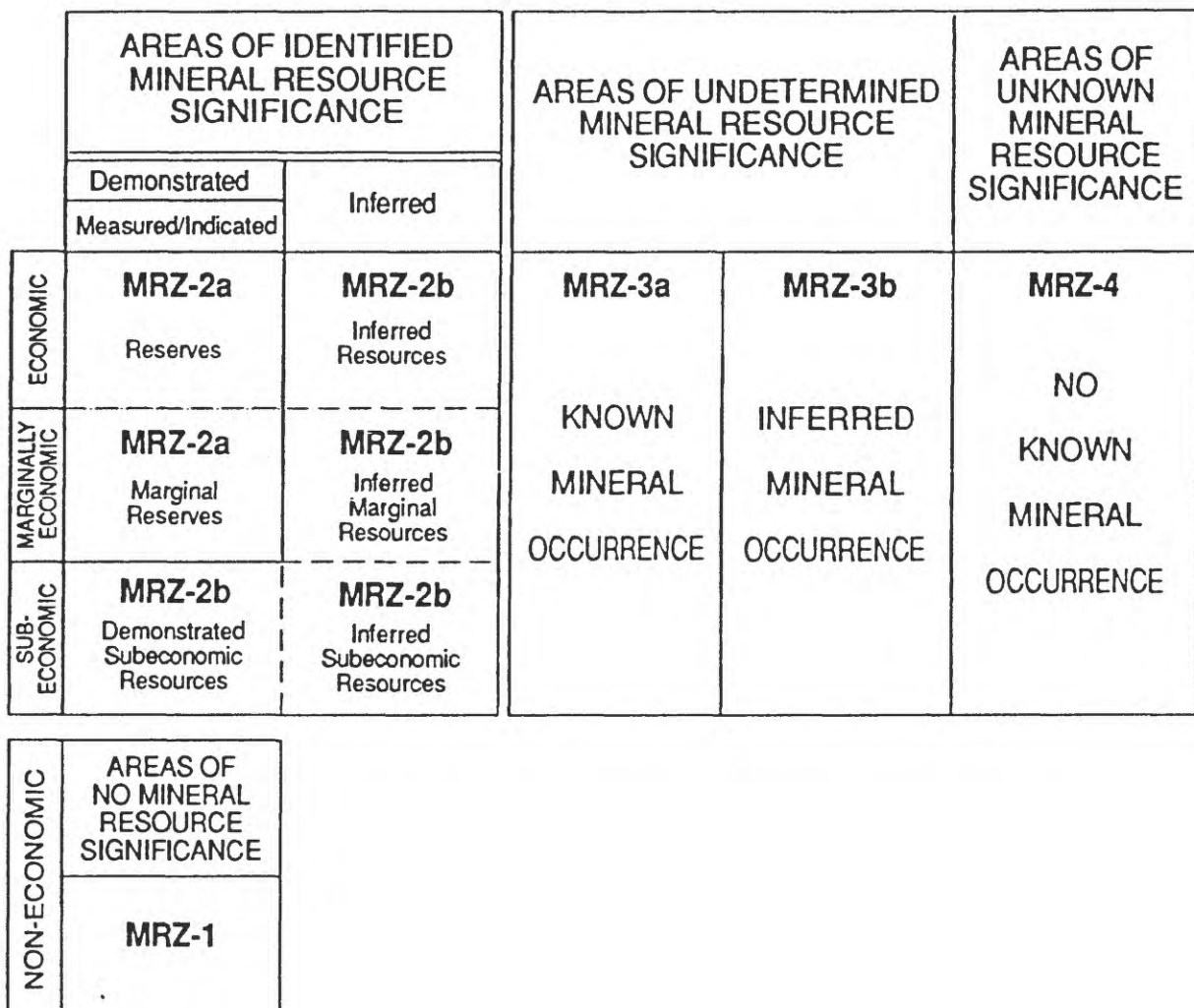


Figure 54. Mineral land classification diagram adopted by the State of California showing a diagrammatic relationship of mineral-resource-zone categories to the resource-reserve classification system. From D.O. Shumway (written commun., 1991).

Figure 55. Sketch map showing permissive terranes and favorable tracts for (1) Proterozoic carbonatite-related, REE occurrences; (2) Mesozoic gold-bearing breccia pipes; (3) Mesozoic tungsten veins; and (4) Mesozoic stockwork molybdenum systems in the East Mojave National Scenic Area.

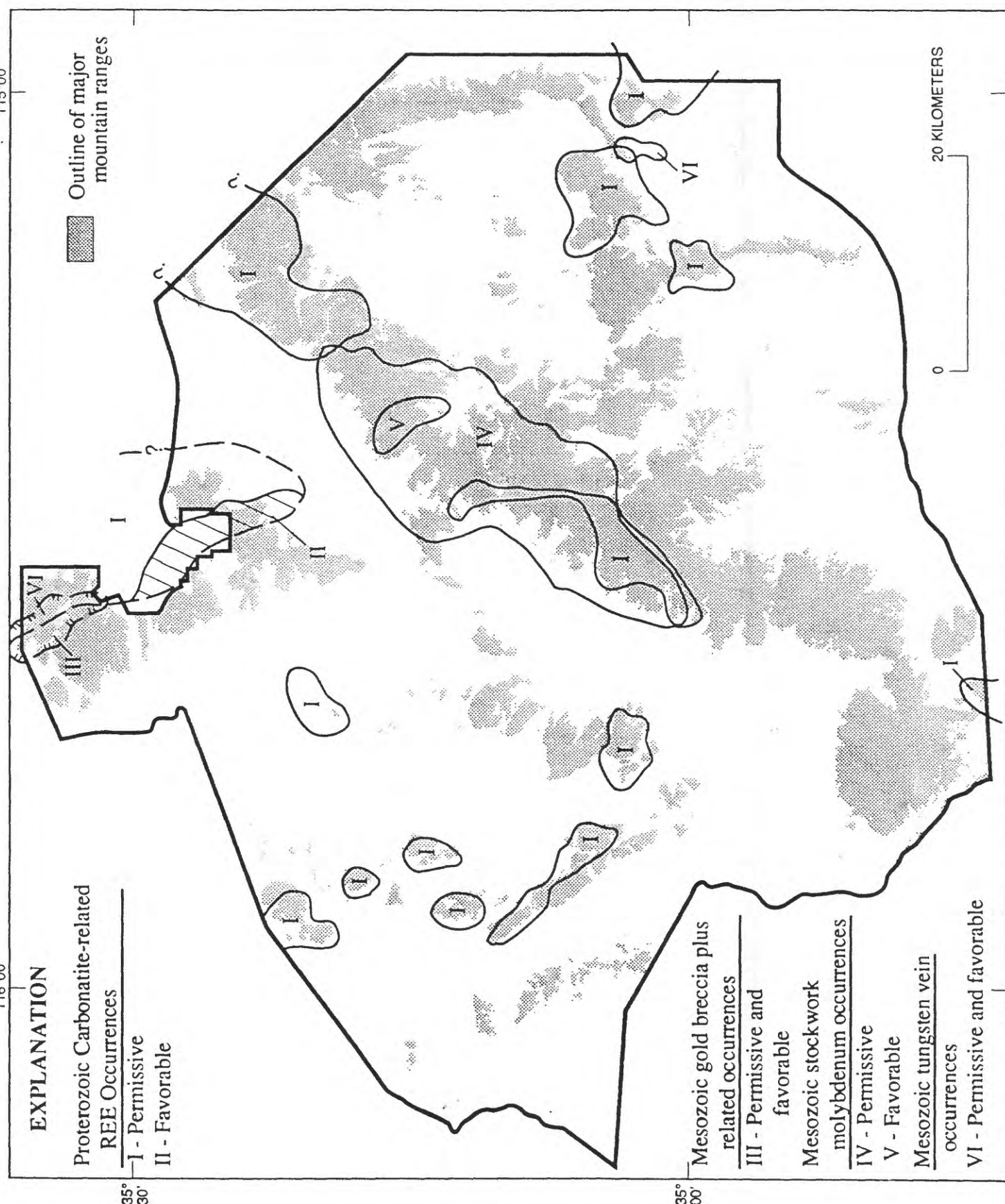
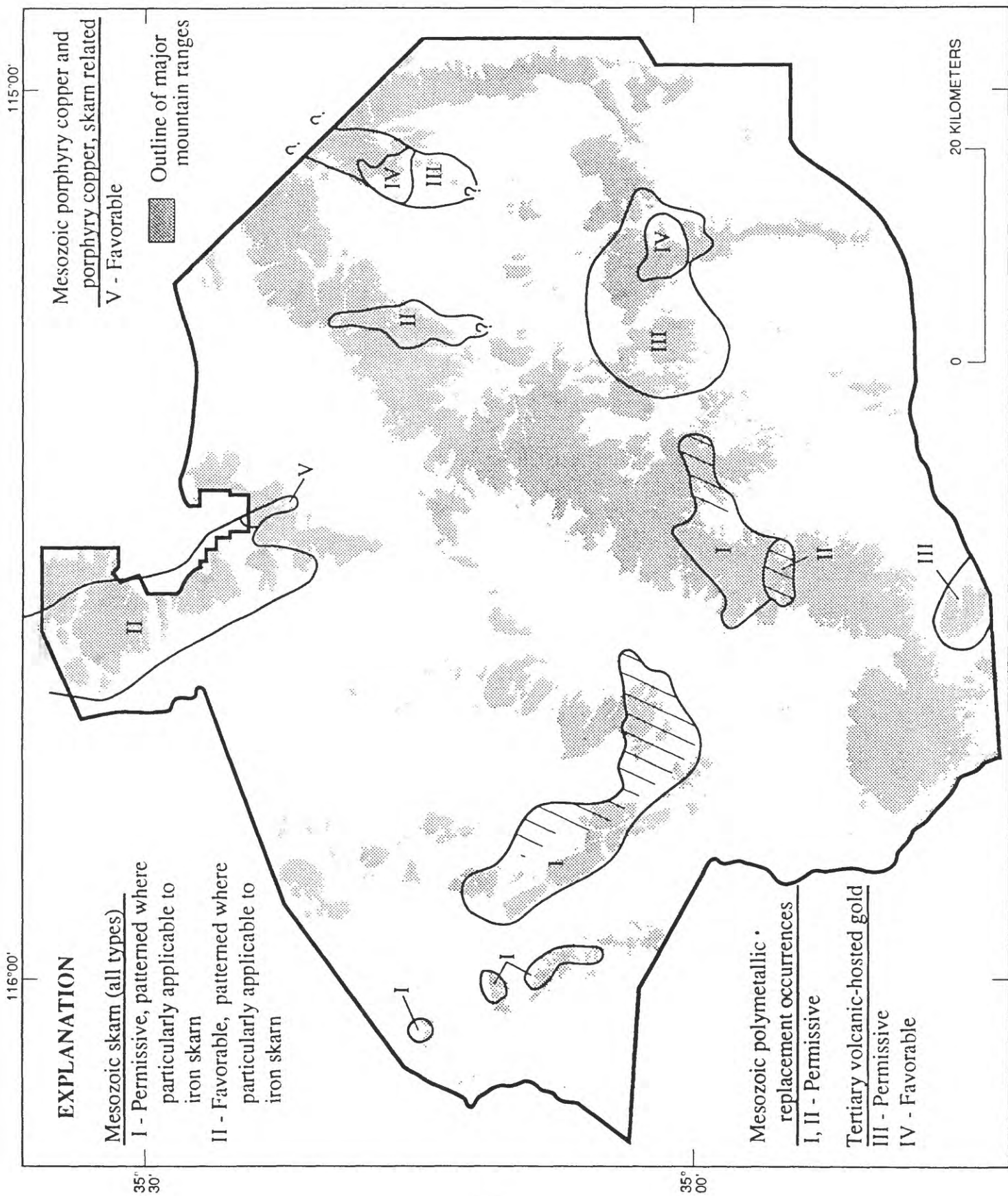


Figure 56. Sketch map showing major permissive terranes and favorable tracts for (1) Mesozoic mineralized skarns of all types and iron skarns in particular, (2) Mesozoic porphyry copper and porphyry copper, skarn-related systems; (3) Mesozoic polymetallic replacement occurrences; and (4) Tertiary volcanic hosted, epithermal gold-silver occurrences in the East Mojave National Scenic Area.



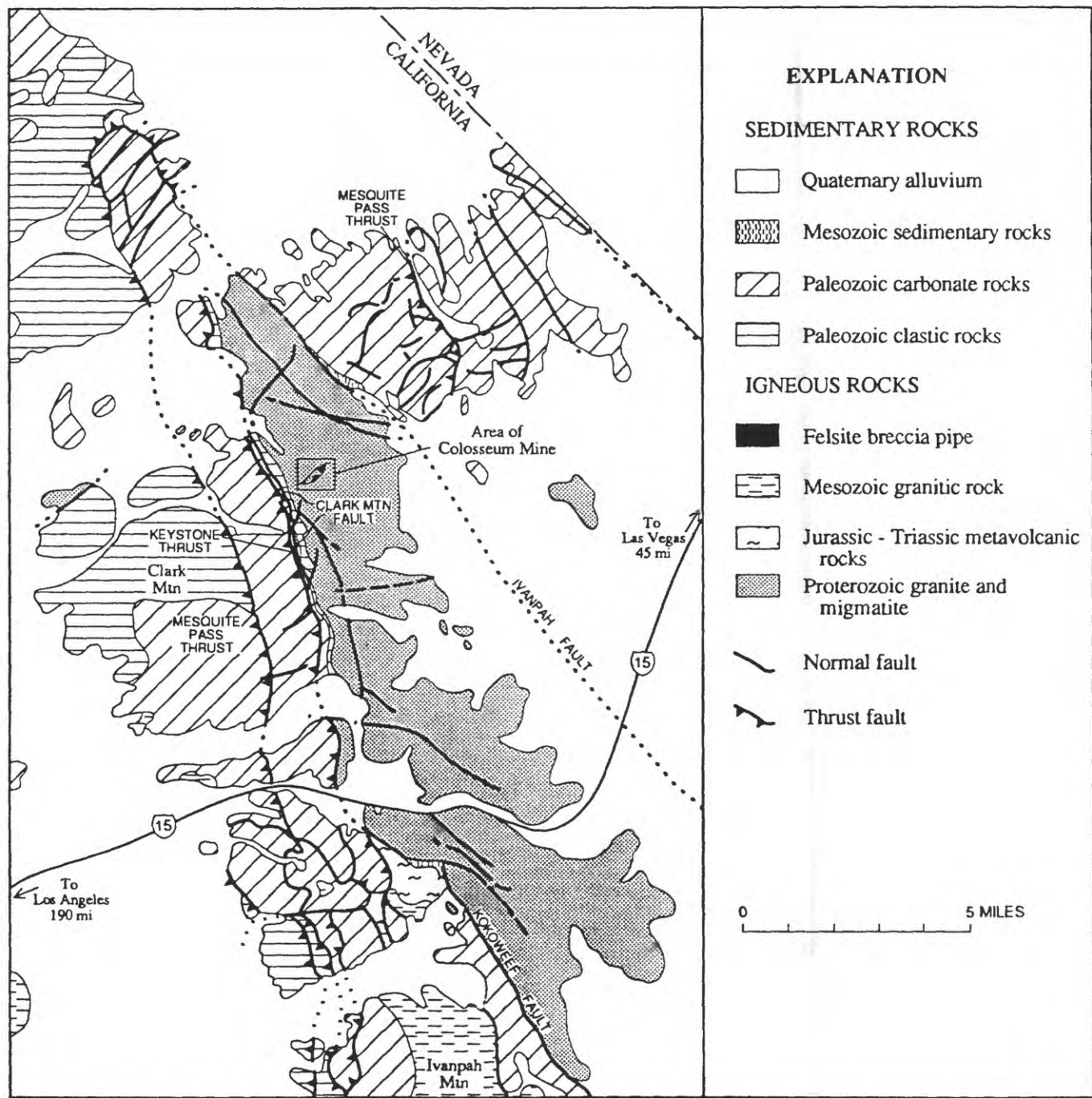


Figure 57. Geologic sketch map of the area surrounding the gold-bearing, Cretaceous breccia pipes at the Colosseum Mine in the north-central part of the East Mojave National Scenic Area. Modified from Sharp (1984).

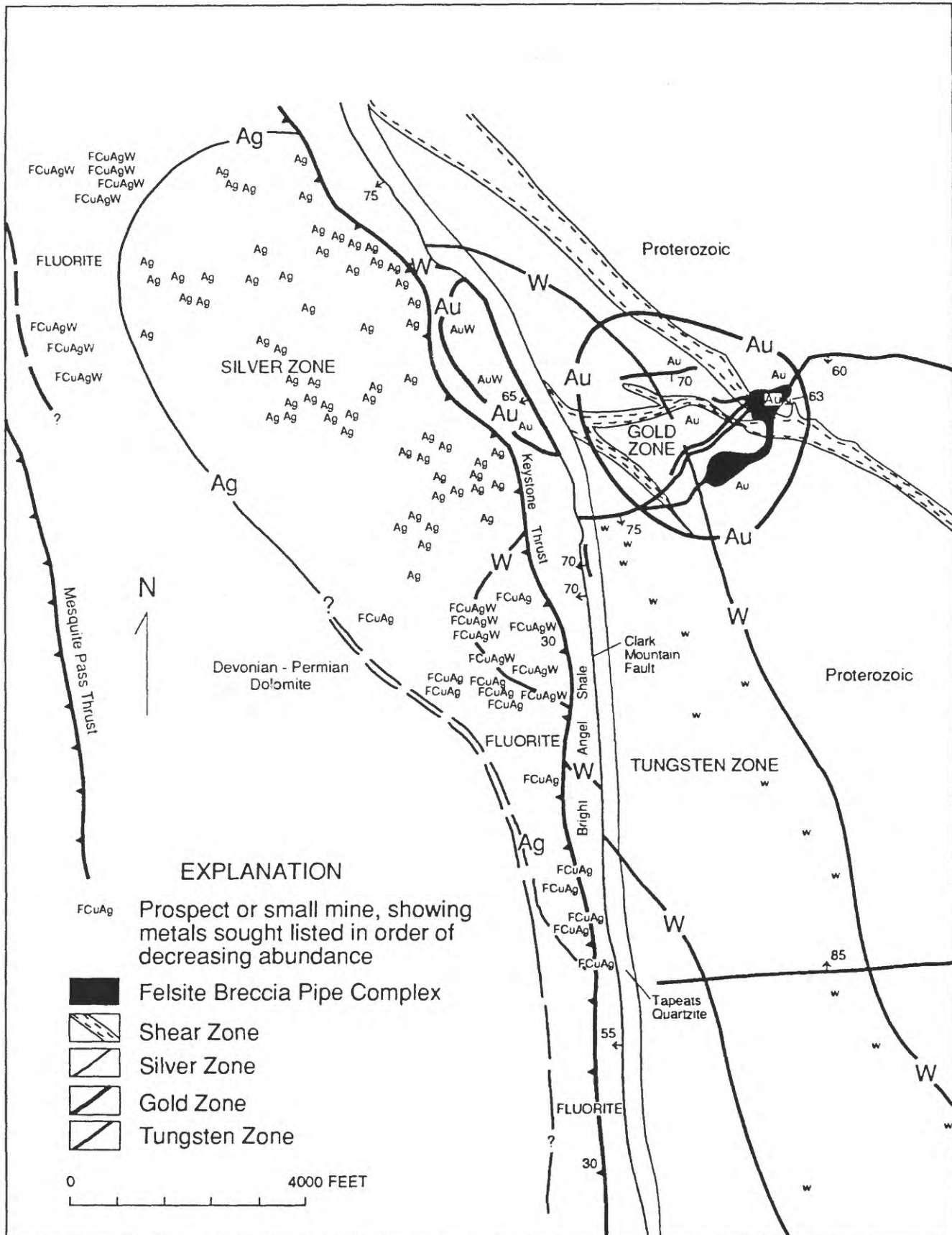
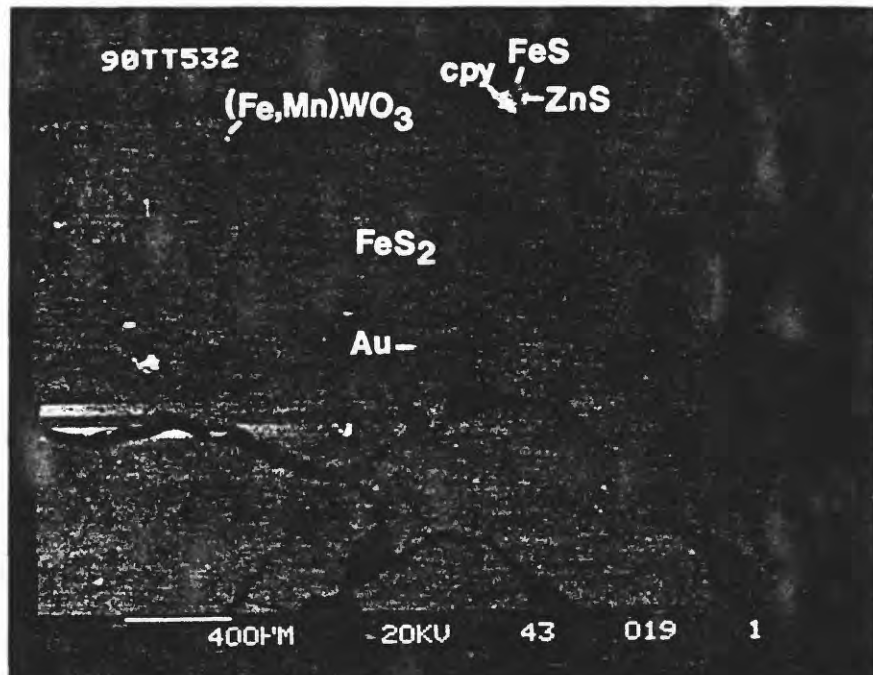
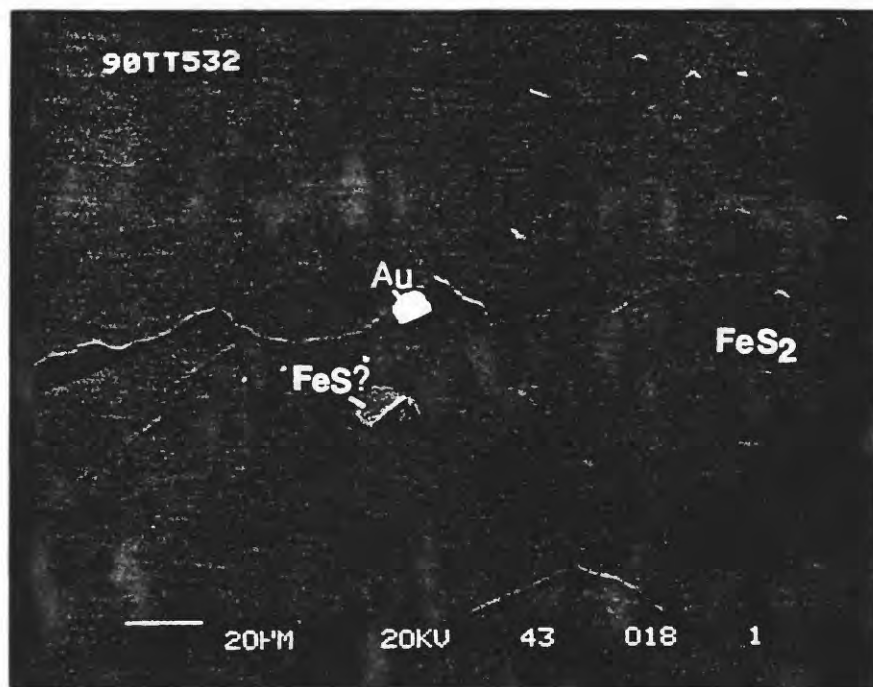


Figure 58. Metal zoning in the northeast part of the Clark Mountain Mining District, north-central East Mojave National Scenic Area. Modified from Sharp (1984).



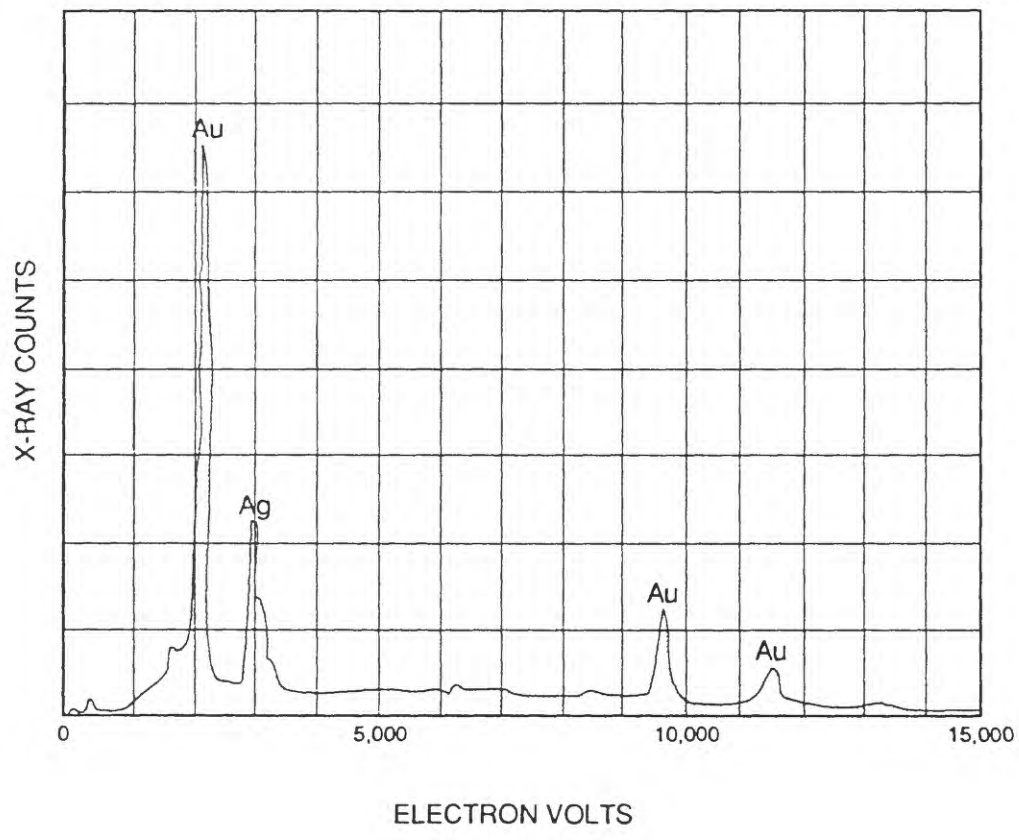
A



B

Figure 59. Scanning electron micrographs of a selected sample from the gold-bearing breccia pipe at the Colosseum Mine. Py or  $\text{FeS}_2$ , pyrite; Au, gold; ZnS, sphalerite; FeS, pyrrhotite;  $(\text{Fe},\text{Mn})\text{WO}_3$ , wolframite;  $(\text{Ce},\text{La},\text{Nd})\text{PO}_4$ , monazite;  $\text{SiO}_2$ , quartz; Kf, K-feldspar; CuS, covellite; Cpy, chalcopyrite. A, general morphology of pyrite hosting various minerals including gold; B, gold along a microcrack in pyrite; some possible pyrrhotite is also in the field of view; C, X-ray spectrogram of argentiferous gold grain in figure 56B; D, gold associated with pyrrhotite in pyrite; E, euhedral outlines of pyrite crystals common throughout the sample; monazite crystals along margins between pyrite crystals; F, enlargement of part of D; G, silver tellurides ( $\text{AgTe}$ ) and bismuth tellurides ( $\text{BiTe}$ ) in pyrite; H, clot of chalcopyrite, pyrrhotite, and sphalerite in pyrite; I, sphalerite surrounded by covellite in K-feldspar.

Figure 59 (cont.)



1C

Figure 59 (cont.)

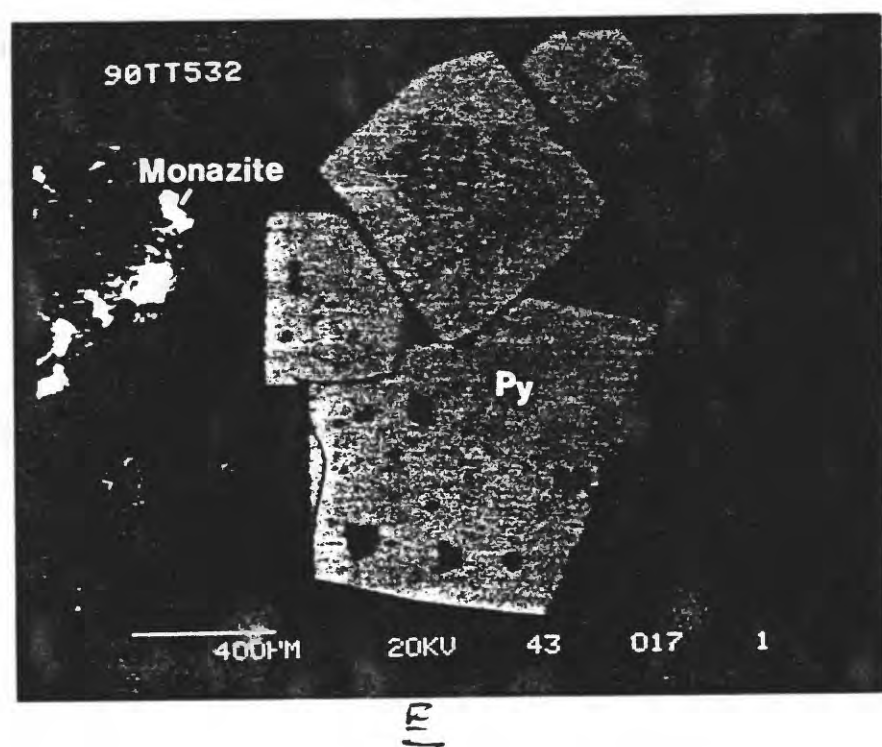
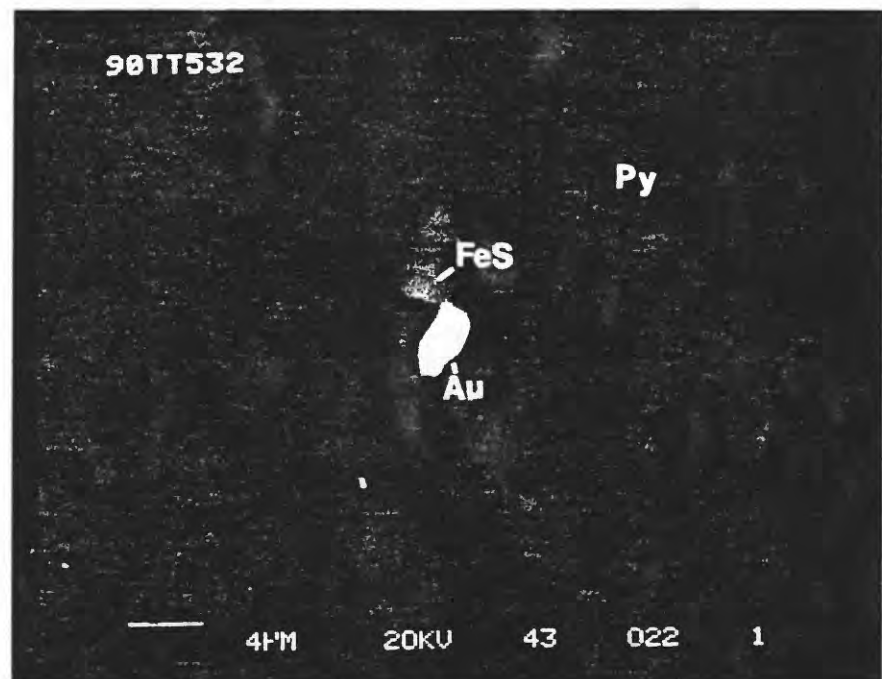


Figure 59 (cont.)

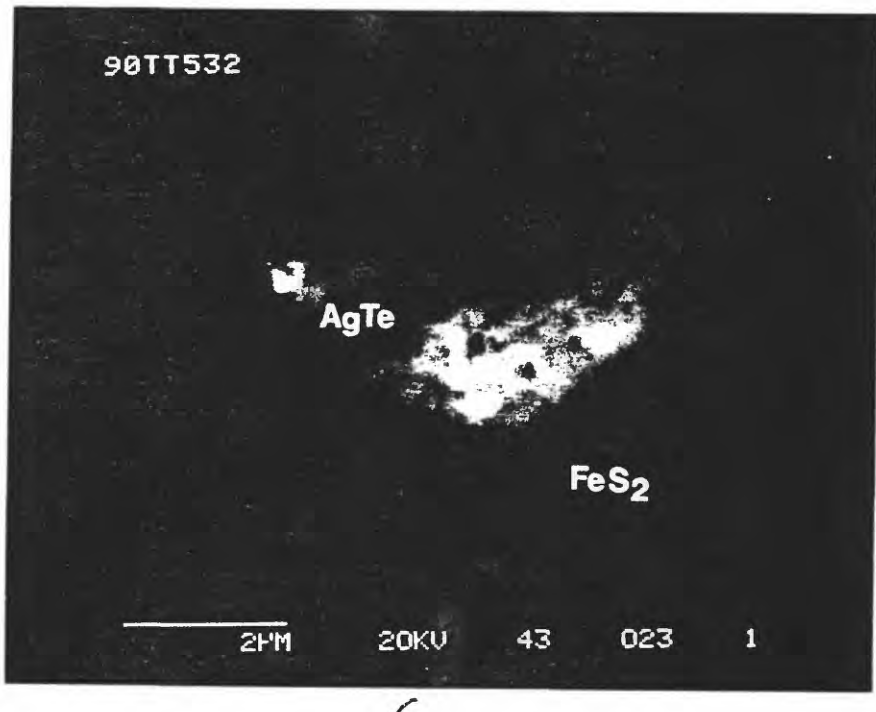
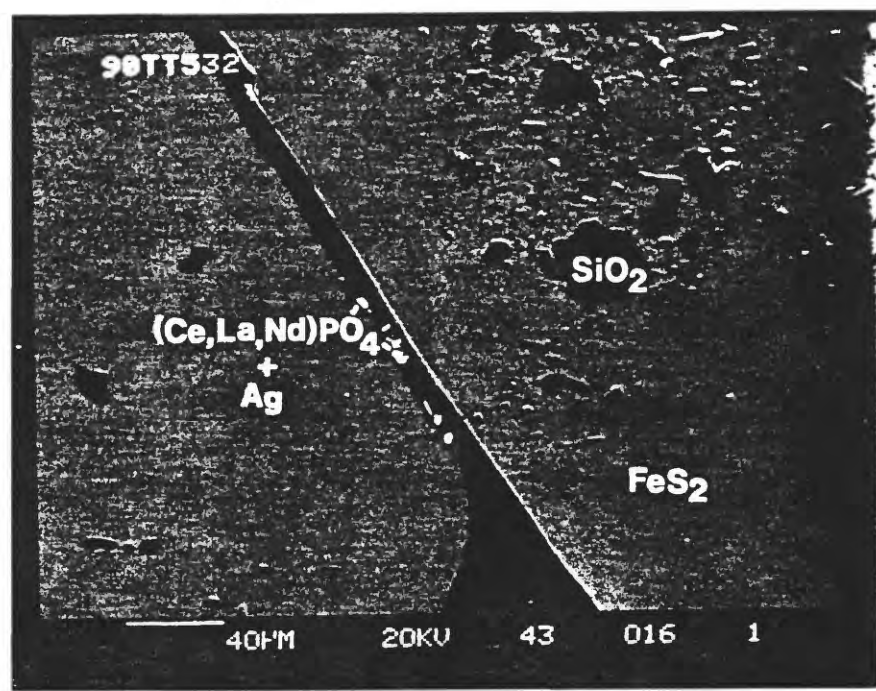
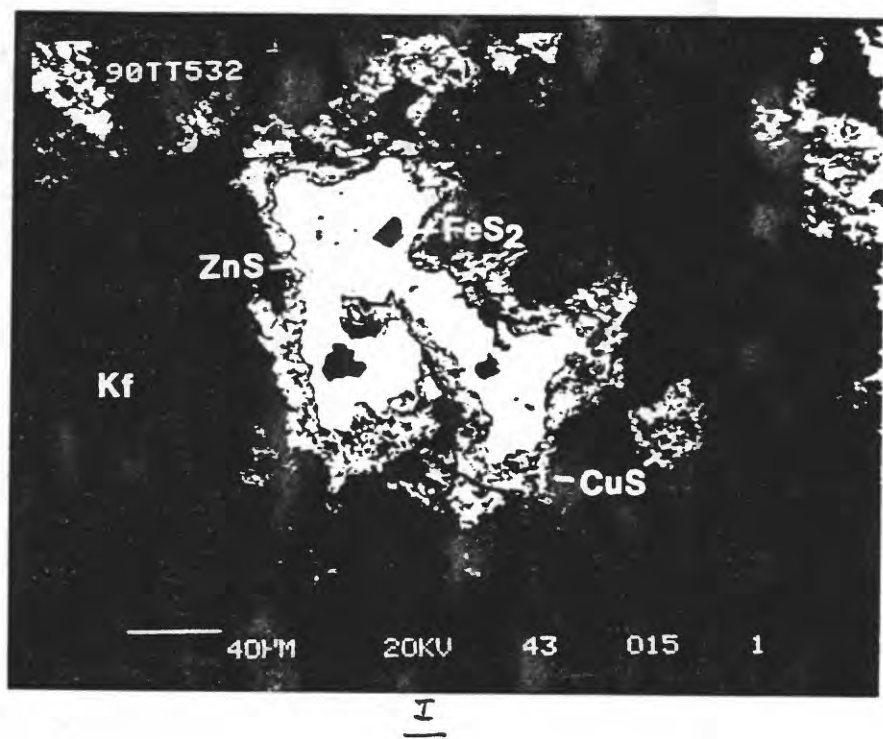
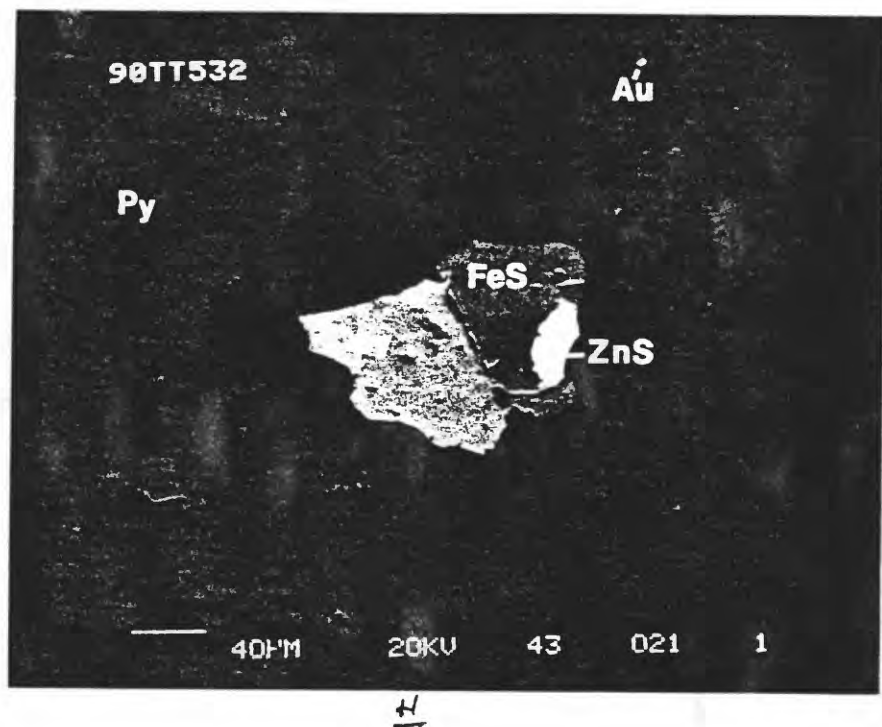


Figure 59 (cont.)



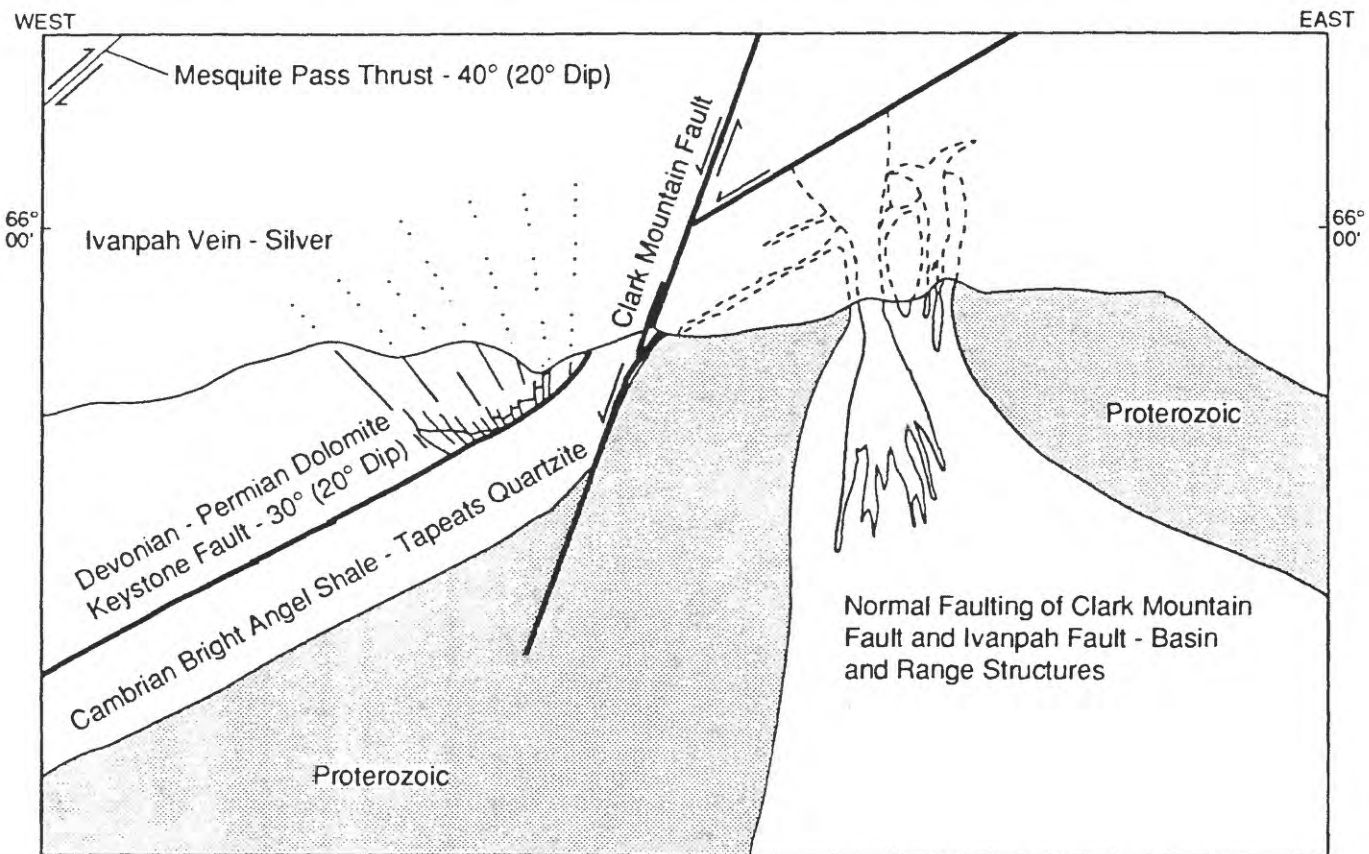


Figure 60. Schematic representation in cross-section of the displacement to the west of the silver-copper brecciated dolostone vein-type occurrences from their initial positions at the top of the gold-bearing breccia pipes at the Colosseum Mine. From Sharp (1984).

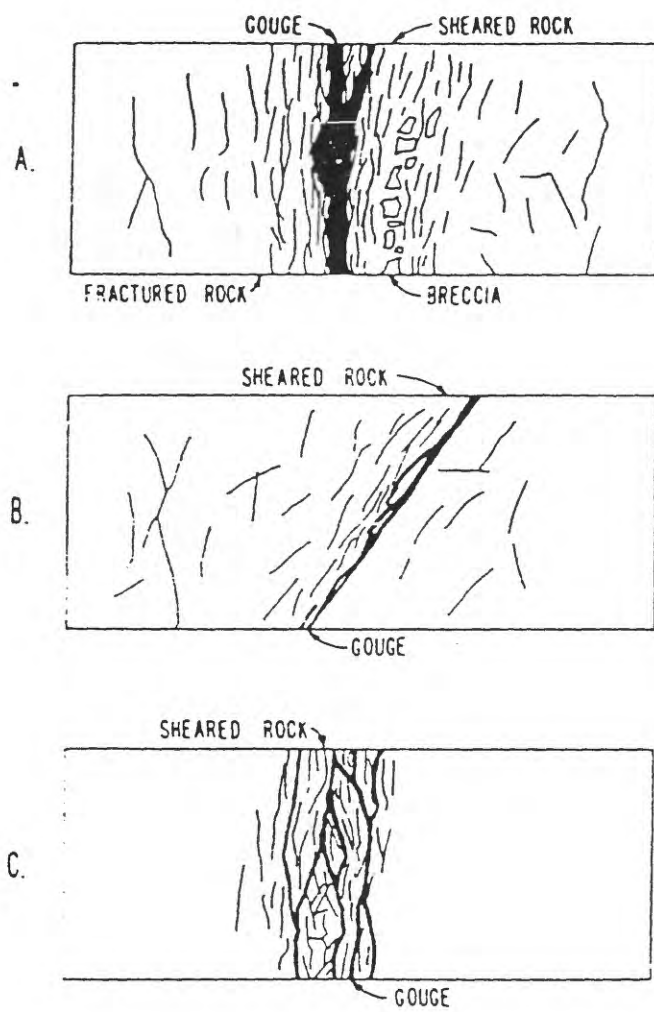


Figure 61. Schematic diagrams showing various relations of gouge within a fault zone: **A**, gouge zone near center of trace of a fault zone; **B**, gouge zone preferentially located near one boundary of a fault zone; and **C**, thin seams of gouge developed throughout the zone of sheared rock defining the overall width of a fault zone. From Wallace and Morris (1986).

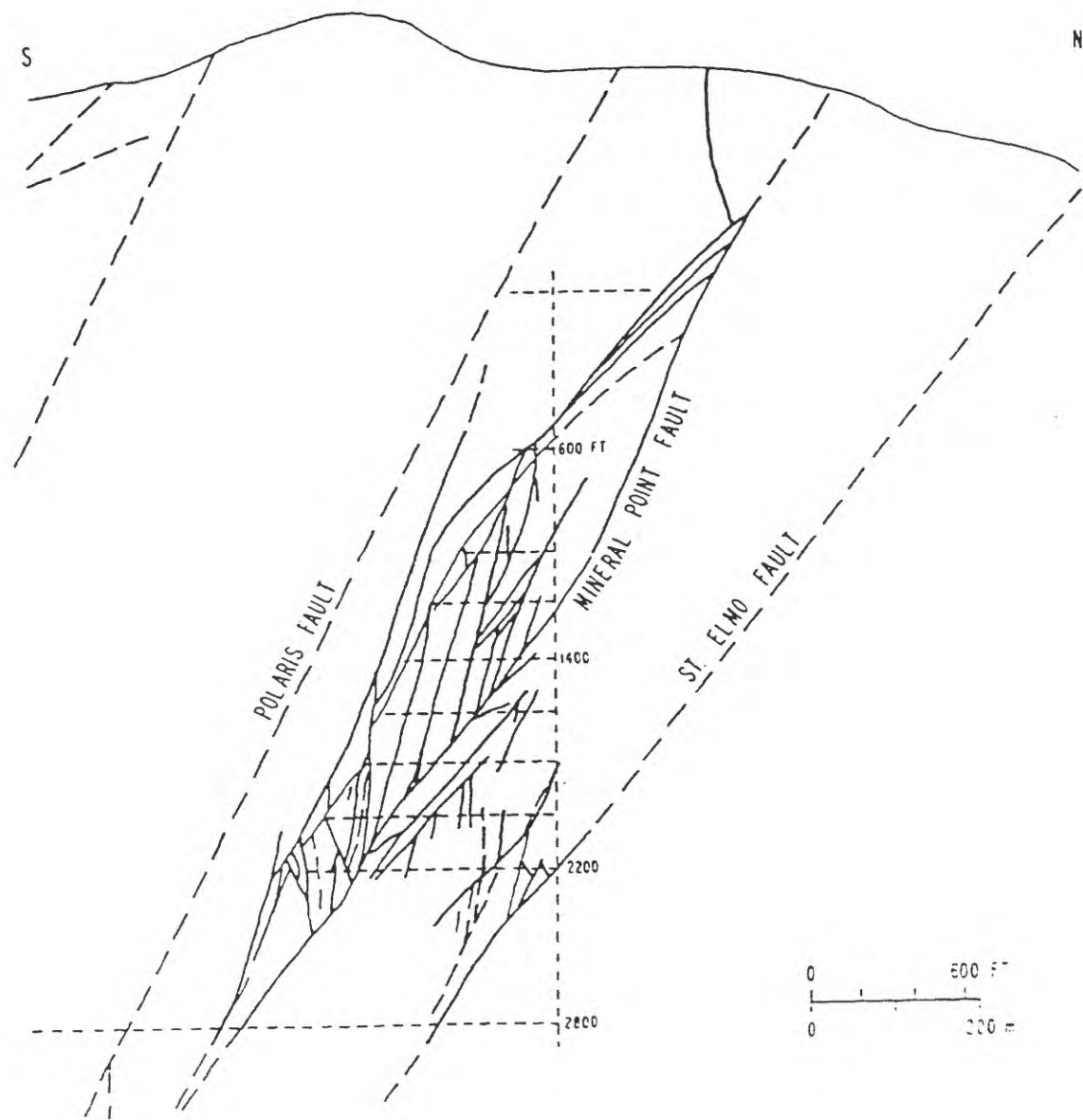


Figure 62. Cross section through the Coeur d'Alene Mine, Idaho, showing complex anastomosing pattern of traces of fault found in 200-ft intervals of underground mine workings. From Wallace and Morris (1986).

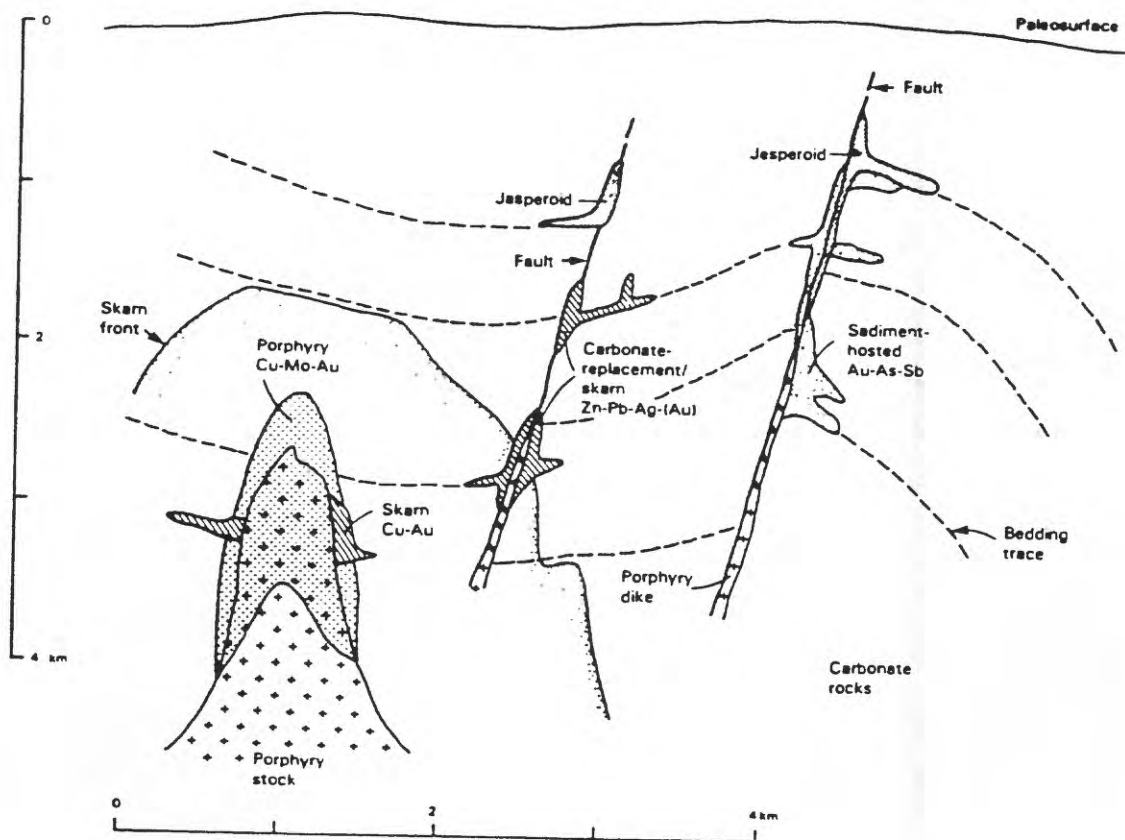


Figure 63. Schematic cross-section showing the general relationship of sediment-hosted gold deposits on the fringes of base- and precious-metal mining districts. From Sillitoe and Bonham (1990).